Hydrogen Bonding Phase-Transfer Catalysis with Alkali Metal Fluorides: Enantioselective Synthesis of β-Fluoroamines from Reaction Development to Scale-up

Anna Chiara Vicini

A thesis submitted to the Board of the Faculty of Physical Sciences,

in partial fulfilment of the requirements for the degree of Doctor of Philosophy

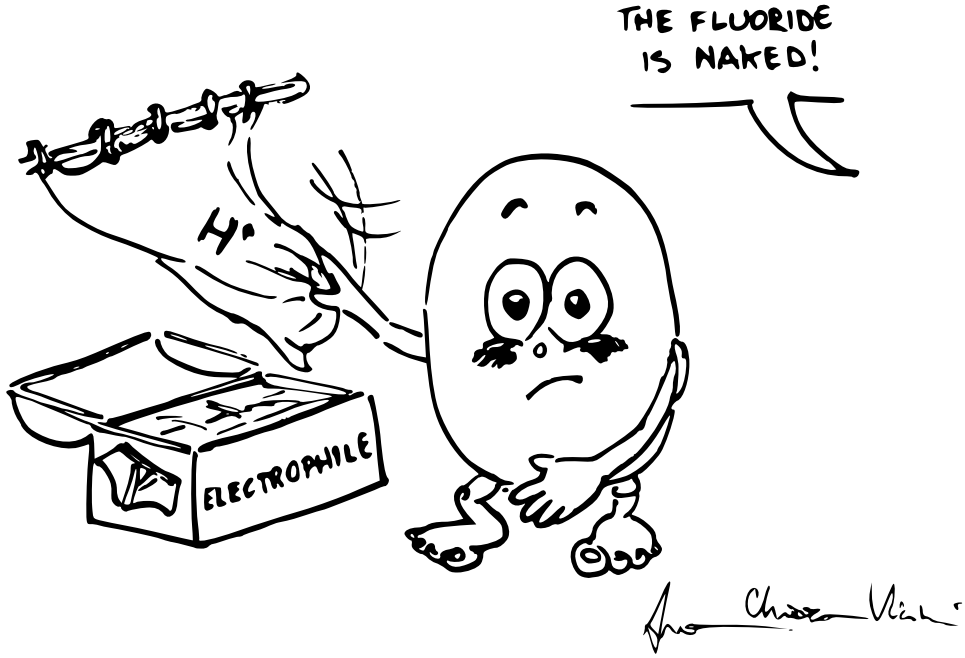
at the University of Oxford.



Oriel College

Michaelmas Term 2020

Intentionally left blank


THE FLUORIDE IS NAKED!
ELECTROPHILE

Intentionally left blank

Author's Declaration

The work presented in this thesis was conducted at the Chemistry Research Laboratory at the University of Oxford under the supervision of Professor Véronique Gouverneur, between Michaelmas Term 2016 and Trinity Term 2020. All the work is my own, except where otherwise stated, and has not been submitted for any other degree at this or any other university.



Anna Chiara Vicini

October 2020

Intentionally left blank

Table of Contents

Abstract vii
Acknowledgements ix
Abbreviations and Acronyms (Alphabetical) xiii

Chapter 1: Introduction
1.1 Enantioselective Nucleophilic Fluorination with Alkali Metal Fluorides 2
1.1.1 The Production Chain of Fluorinated Compounds 2
1.1.2 Challenges in the Use of Alkali Metal Fluorides in Synthesis 5
1.1.3 Fluoride Activation *via* Phase-Transfer Catalysis (PTC) 8
1.1.4 Asymmetric PTC for Enantioselective Fluorination 12
1.1.5 Hydrogen Bonding for Nucleophilic Fluorination 19
1.1.6 Asymmetric Hydrogen Bonding Phase-Transfer Catalysis (HB-PTC) 27
1.2 β-Fluoroamines 28
1.2.1 Fluorine for Molecular Editing 28
1.2.2 β-Fluoroamines Applications 36
1.2.3 Enantioselective Synthesis of β-Fluoroamines 39
1.3 Conclusions and Thesis Outline 44
1.4 References 45

Chapter 2: Enantioselective Fluorination of Aziridinium Ions with Alkali Metal Fluorides under Hydrogen Bonding Phase-Transfer Catalysis (HB-PTC)
2.1 Hydrogen Bonding Phase-Transfer Catalysis (HB-PTC) 54
2.2 Project Aim 60
2.3 Fluorination of Aziridinium Ions with MF Catalysed by Achiral Schreiner's Urea 62
2.4 Optimisation of the Enantioselective Fluorination with CsF 65
2.4.1 Synthesis of Chiral BINAM-Derived bis-Urea Organocatalysts 65
2.4.2 Fluorination of Stilbene-Derived β-Chloro-*N*,*N*-Dibenzylamine 69
2.4.3 Fluorination of Stilbene-Derived β-Chloro-*N*,*N*-Diallylamine 76
2.5 Optimisation of the Enantioselective Fluorination with KF 80
2.6 Enantioselective Fluorination of Stilbene-Derived β-Chloroamines 83
2.6.1 Substrate Scope 83
2.6.2 Derivatisation of Enantioenriched β-Fluoroamines 86
2.7 Enantioselective Fluorination with KF on 50 g Scale 88
2.8 Enantioselective Fluorination of Aliphatic β-Haloamines 90
2.8.1 Reaction Optimisation 90
2.8.2 Substrate Scope 96
2.9 Experimental and Computational Insights into the Reaction Mechanism 98
2.9.1 Experimental Evidence for the Phase-Transfer Role of (*S*)-2.78 99
2.9.2 Computational Investigations 101
2.10 Conclusions 103
2.11 References 104

Chapter 3: Scale-up of the Synthesis of Mono-N-Alkyl Bis-Ureas for HB-PTC
3.1 Project Aim 109
3.2 Scale-up of the Synthesis of Catalyst (*S*)-2.3 110
3.3 Scale-up of the Synthesis of Catalyst (*S*)-2.78 112
3.3.1 Urea Synthesis *via in situ* Formation of the Isocyanate: Limitations 112
3.3.2 Overview of Alternative Synthesis of Catalyst (*S*)-2.78 120
3.3.3 Route 1: Published Procedure 121
3.3.4 Route 2: The Quadruple Suzuki-Miyaura Cross-Coupling Route 122
3.3.5 Route 3: The Isocyanate Route 128

3.4 Conclusions 139
3.5 References 142

Chapter 4: Scale-up of Enantioselective Fluorination under HB-PTC in a Mechanically Stirred 1 L Glass Reactor
4.1 Mixing in Industrial Reactors 145
4.2 Calorimetry in Process Safety 149
4.2.1 Differential Scanning Calorimetry (DSC) 149
4.2.2 Reaction Calorimetry (RC) 150
4.3 Project Aim 154
4.4 *Trans*-2-fluorocyclohexan-1-amine 155
4.5 Optimisation of the Reaction Conditions 158
4.5.1 Substrate Selection 158
4.5.2 Fluoride Source 164
4.6 Scale-up in Round-bottom Flasks 176
4.7 Optimisation of the Isolation and Work-up Conditions 178
4.8 Optimisation of the Recrystallisation 180
4.9 Scale-up in a Mechanically Stirred 1 L Reactor 183
4.9.1 Fluorination on 200 g of *rac*-2.108 183
4.9.2 Preliminary Results on Mixing Parameters 185
4.9.3 Calorimetric Experiments 189
4.10 Catalyst Recovery and Degradation 194
4.11 Conclusions 201
4.12 References 203

Chapter 5: Experimental
5.1 General Experimental 207
5.2 Additional Data from Chapter 2 209
5.2.1 Additional Screening Reactions from Chapter 2 209
5.2.2 Experimental Procedures and Characterisation of Compounds in Chapter 2 216
5.3 Additional Data from Chapter 3 294
5.3.1 Procedures for the Multigram Synthesis of Catalyst (*S*)-2.3 and (*S*)-2.78 294
5.3.2 Optimisation of the Recrystallisation of Catalyst (*S*)-2.78 301
5.3.3 Experimental Procedures and Characterisation of Compounds from Chapter 3 303
5.3.4 Copy of the NMR Spectra Used in the Assignment of (*S*)-3.14-3.16 314
5.4 Additional Data from Chapter 4 323
5.4.1 Experimental procedures and Characterisation of Compounds from Chapter 4 323
5.4.2 Experimental Procedure for the Asymmetric Fluorination under HB-PTC in a Mechanically Stirred Reactor 335
5.4.3 Optimisation of the Recrystallisation 337
5.4.4 HPLC Trace of (*R*,*R*)-2.109 343
5.4.5 Characterization of 4.23 344
5.5 References 345

Abstract

This thesis reports the development of hydrogen bonding phase-transfer catalysis (HB-PTC) for asymmetric fluorination with alkali metal fluorides. This catalytic manifold harnesses the ability of fluoride to engage in hydrogen bonding to promote solubilisation of the inorganic fluoride salt, with concomitant formation of a reactive chiral catalyst-fluoride complex. Herein, HB-PTC has been applied to the synthesis of enantioenriched β-fluoroamines, with a focus on the industrial application of the methodology.

Chapter 1 introduces the challenges associated with enantioselective nucleophilic fluorination with alkali metal fluorides and the strategies reported in the literature for fluoride activation. An overview of properties and applications of β-fluoroamines is also included. ***Chapter 2*** opens with a summary of the previous work on HB-PTC. Next, the chapter is devoted to describing the development of the asymmetric synthesis of β-fluoroamines with KF and CsF *via* HB-PTC. Computational modelling is used to rationalise the observed selectivity and scope. ***Chapter 3*** describes the development of a practical and scalable (> 10 g) synthesis of the novel *N*-alkyl bis-urea introduced in Chapter 2. Different synthetic routes are explored, and advantages and drawbacks of each are compared. ***Chapter 4*** reports the study of the scale up (200 g) of the enantioselective fluorination in a mechanically stirred 1 L reactor, representing the proof of principle that HB-PTC can be applied in industrial settings. Thermal safety tests and preliminary calculations on the mixing requirements are included. The chapter concludes with the analysis of the recyclability of the catalyst and of its degradation products. ***Chapter 5*** contains additional screening tables, synthetic procedures, and characterisation data from compounds of Chapters 2–4.

Intentionally left blank

Acknowledgements

First and foremost, I would like to thank my DPhil supervisor, Véronique, for the opportunity to join her group and to work on such an exciting project. Her passion and determination are a great source of inspiration, which I will remember in the years to come. I am grateful for the discussions we had and her advice, which made me grow as a scientist and as a person.

This research was funded by the European project ISOTOPICS, and my thanks goes to the members of the consortium for their insightful suggestions and the training provided in the past years. A special "thank you" goes to Sébastien and Cathy, who welcomed me in SANOFI and without whom this thesis would have been very different. I am extremely thankful for the experience in process chemistry, and for all the help received while I was in France. Philippe and Diké, thank you for all the practical help, the advice, and the coffee. I certainly won't forget my time in Guy Lussac trying to find the perfect reactor!

All the way through these years in Oxford, I was extremely lucky to collaborate with some brilliant scientists. Thank you to the amazing "Hydrogen-Bonding team", especially Francesco, Gabriele and David, with whom I started my first project and enormously contributed to this work. To Gabriele, the postdoc who guided me through the beginning and taught me so much on asymmetric catalysis; to David, who has the wonderful gift to explain computational chemistry in a way that makes it sound extremely simple; and to Francesco, an excellent scientist, and an even better friend: thank you! *Grazie*! My thanks go also to Dr. Paolo Ricci, who left the group shortly after I joined, but who was the first to introduce me to HB-PTC. Many thanks also to Giulia, Jimmy and Konstantinos for sharing their catalysts and substrates, and to Alex, for the insightful discussions.

Thank you to all the rest of the VG group, for the support, suggestions, and laughs. Thank you to those of you who first welcomed me and taught me all the practical tricks when I was still a liability for the laboratory glassware, especially Nick, who has always been extremely patient. Thank you to those who started after me and to whom I hope I have been equally helpful, especially Joe and James, who might did not succeed in improving my English pronunciation, but certainly improved my music knowledge. Thank you to the F12 crew, who made the days feel shorter and the columns less tedious. Thank you to all the VG members who made the nights outs on Friday unforgettable.



Nick, thank you for having been the first to welcome me in the group, the diners before coming back to the laboratory, and the help in proof-reading. Thank you for your advice as a mature PhD student, and being such a good listener and friend. Jeroen, we started this PhD together, and together we grow as scientists. Thank you for your enthusiasm, the chats, the burritos/pad thai and all the support you gave me these four years. Most of all, thank you for your friendship. Francesco, you welcomed me as I started in the group and you have always been there, through the good and the hard times. Thank you for all the lunches

together, educating my musical tastes and all your wise words when I most needed them. Thank you for being such a good friend! Rob, since the first time we “properly met”, when you were looking for somebody crazy enough to join you for a winter mountaineering course in Scotland (who would ever pay for being in the cold the whole day?), you always pushed me to take up new challenges and believe in myself. Thank you for introducing me to climbing, the deep discussion and the light ones, your positive attitude and always taking the best out of me. Thank you, dear friend!

My warmest thanks go to my housemates, Rob, Ben and Jonny, who have been extremely supportive in these last months of uncertainty. Thank you for the good times together, from the movie nights to the Friday evenings and the interminable chats in the kitchen. Thank you to the member of the OUMC for the great time climbing and at the pub, especially to Anne, even though we didn’t climb or drink that much together. Thank you to Mateusz, who during the ISOTOPICS meetings was my loyal companion for city exploration. Thank you to Simone and Rachele, who encouraged me to apply to Oxford and supported me from a distance all the way through the PhD.

Finally, my warmest thank you goes to my family who have always encouraged and sustained me. Thank you to my mum, Annamaria, who has allowed innumerable experiments to be performed on the kitchen table bearing with the inevitable mess, and has been a strenuous advocate of European projects, encouraging me to apply to ISOTOPICS. Thank you to my dad, Sergio, who answered my countless “why?” childish questions and was not afraid to listen to the technicism of my PhD project. Thank you to my little sister, Laura, who I deeply admire for her determination and inspired me to take up the challenge of moving abroad for so long. She is one of the toughest persons I know, yet she doesn’t realise it. And she is one of my best allies. Thank you! *Grazie!*

Intentionally left blank

Abbreviations and Acronyms (Alphabetical)

1,2-DFB	1,2-Difluorobenzene
3F-NMDA	3-Fluoro-*N*-methyl-D-aspartate
5'-FDA	5'-Fluoro-5'-deoxyadenosine
18-Crown-6	1,4,7,10,13,16-Hexaoxacyclooctadecane
Aliquat® 336	Trioctylmethylammonium chloride
APCI	Atmospheric-pressure chemical ionisation
Asp	Aspartate
BACE	Beta-site amyloid precursor protein cleaving enzyme
BARF	Tetrakis(3,5-bis(trifluoromethyl)phenyl)borate
BDE	Bond dissociation energy
BINAM	[1,1'-Binaphthalene]-2,2'-diamine
BINOL	1,1′-Bi-2-naphthol
Boc	*tert*-Butoxycarbonyl
BP	Boiling point
BRSM	Based on recovered starting material
Bzh	Benzhydryl
CAM	Cerium ammonium molybdate
Cbz	Benzyloxycarbonyl
CC	Cross-coupling
CDI	1,1′-Carbonyldiimidazole
CNS	Central nervous system
DABCO	1,4-Diazabicyclo[2.2.2]octane
DAST	Diethylaminosulfur trifluoride
DCE	1,2-Dichloroethane
DDQ	2,3-Dichloro-5,6-dicyano-1,4-benzoquinone
Deoxo-fluor®	Bis(2-methoxyethyl)aminosulfur trifluoride
Dfp	(2*S*)-4,4-Difluoroproline
DFT	Density functional theory
DIC	*N,N′*-Diisopropylcarbodiimide
DIPEA	*N*,*N*-Diisopropylethylamine
DMAP	4-(Dimethylamino)pyridine
DMPU	*N*,*N′*-Dimethylpropyleneurea
DMSO	Dimethyl sulfoxide
DPP	Dipetidyl peptidase
Dppb	1,4-Bis(diphenylphosphino)butane
E^+	Electrophile
e.r.	enantiomeric ratio
ESI	Electrospray ionisation
FCC	Flash column chromatography
[^{18}F]FCNT	2β-Carbomethoxy-3β-(4-chlorophenyl)-8-(2-[^{18}F]-fluoroethyl)-nortropane
FGI	Functional group interconversion
Flp	(2*S*,4*R*)-4-Fluoroproline
flp	(2*S*,4*S*)-4-Fluoroproline
Gly	Glycine
H_8-BINAM	5,5',6,6',7,7',8,8'-Octahydro-[1,1'-binaphthalene-2,2'-diamine]
HB	Hydrogen bonding
HBD	Hydrogen bond donor

HB-PTC	Hydrogen bonding phase-transfer catalysis
HFIP	Hexafluoro isopropanol
HIV	Human immunodeficiency virus
HRMS	High resolution mass spectrometry
Hyd	*Trans*-4-hydroxy-L-proline
IUPAC	International Union of Pure and Applied Chemistry
KSP	*Kinesin* spindle protein
LLS	Longest linear sequence
*m*CPBA	*meta*-Chloroperbenzoic acid
MD	Molecular dynamics
ML	Mother liquor
MP	Melting point
MS	Molecular sieves
MTBE	Methyl *tert*-buthyl ether
MTSR	Maximum temperature of the synthesis reaction
MTT	Maximum technical temperature
NBS	*N*-Bromosuccinimmide
NFSI	*N*-Fluorosulfonimide
N_{js}	Rotational speed of "just suspension"
NMDA	*N*-Methyl-D-aspartate
NMM	*N*-Methylmorpholine
NMR	Nuclear magnetic resonance
Nu	Nucleophile
O/N	Overnight
P_0	Power number
PBT	Pitched-blade turbine
PEG	Poly(ethylene glycol)
PET	Positron emission tomography
PIM	Proviral integration site
PLP	Pyridoxal 5′-phosphate
PMA	Phosphomolybdic acid
PMB	*para*-Methoxybenzyl
PMNT	Phenylethanolamine-*N*-methyl transferase
PNP	Purine nucleoside phosphorylase
PTFE	Polytetrafluoroethylene
Pro	Proline
PTC	Phase-transfer catalysis
PyBOX	Pyridine bis(oxazoline)
RBF	Round-bottom flask
Re	Reynolds numbers
rpm	Round per minute
rt	Room temperature
Salen	*N*,*N*′-Bis(salicylidene)ethylenediamine
SAM	*S*-Adenosylmethionine
SAR	Structure activity relationship
Selectfluor®	1-Chloromethyl-4-fluoro-1,4-diazoniabicyclo[2.2.2]octane bis(tetrafluoroborate)
SEM	Scanning electron microscopy
Ser	Serine
(*S*)-*N*-Et-BINAM	(*S*)-N^2-Ethyl-[1,1'-binaphthalene]-2,2'-diamine

(*S*)-*N*-^{i}Pr-BINAM	(*S*)-N^2-Isopropyl-[1,1'-binaphthalene]-2,2'-diamine
SPhos	2-Dicyclohexylphosphino-2′,6′-dimethoxybiphenyl
TBABr	Tetra *n*-butyl ammonium bromide
TBAF	Tetra *n*-butyl ammonium fluoride
TBAI	Tetra *n*-butyl ammonium iodide
TFA	Trifluoroacetic acid
THF	Tetrahydrofuran
Thr	Threonine
TMS	Trimethyl-silyl
TRIP	3,3′-Bis(2,4,6-triisopropylphenyl)-1,1′-binaphthyl-2,2′-diyl hydrogenphosphate
Triphosgene	Bis(trichloromethyl) carbonate
TS	Transition state
Tyr	Tyrosine

Symbols and Units of Measurement

From Chapter 1

$\AA$	Ångström, 10^{-10} m
K_{X^-/Y^-}^{sel}	Selectivity Constant: a measurement of the catalyst relative selectivity for the nucleophile (X^-) and the leaving group (Y^-)
$[QX]_{org}$	Concentration of the catalyst (Q) -nucleophile (X^-) ion-pair in the organic phase
$[QY]_{org}$	Concentration of the catalyst (Q) -leaving group (Y^-) ion-pair in the organic phase
$[X^-]_{aq}$	Concentration of the nucleophile (X^-) in the aqueous phase
$[Y^-]_{aq}$	Concentration of the leaving group (Y^-) in the aqueous phase

From Chapter 4

Fluid dynamic parameters

D	Impeller diameter, expressed in m
γ_{imp}	Impeller average turbulent shear rate, expressed in s^{-1}
ε_{max}	Local maximum energy dissipation rate at the impeller region, expressed in $W*Kg^{-1}$
N	Impeller rotational speed, expressed in s^{-1}
μ	Dynamic viscosity, expressed in $N*s*m^{-2}$
P_0	Impeller power number, expressed in W
P	Power input, expressed in W
V_{imp}	Volume at the bottom of the impeller zone, expressed in m^3

A	Wetted heat transfer area, expressed in m^2
C_p	Specific heat of the reaction mass, expressed in $J*K^{-1}*g^{-1}$
C_{pc}	Specific heat of the cooling fluid used in the condenser, expressed in $J*K^{-1}*g^{-1}$
C_{pf}	Specific heat of the feed stream, expressed in $J*K^{-1}*g^{-1}$
ΔH	Reaction molar enthalpy, expressed in $J*mol^{-1}$
ΔT_{ad}	Temperature variation of the reaction mass in adiabatic conditions, expressed in K
K_{loss}	Heat transfer coefficient towards the ambient $W*K^{-1}$
m	Total Mass inside the reactor, expressed in g
m_c	Mass of the cooling fluid used in the condenser, expressed in g
m_f	Mass of the feed stream, expressed in g
Q_r	Heat flow, expressed in W
U	Heat transfer coefficient, expressed in $W*K^{-1}*m^{-2}$
t	Time, expressed in s
T_{amb}	Temperature of the laboratory, expressed in K
$T_{c\ in}$	Temperature of the cooling fluid at the inlet of the condenser, expressed in K
$T_{c\ out}$	Temperature of the cooling fluid at the outlet of the condenser, expressed in K
T_j	Temperature of the jacket fluid, expressed in K
T_r	Temperature inside the reactor, expressed in K

Chapter 1:
Introduction

1.1 Enantioselective Nucleophilic Fluorination with Alkali Metal Fluorides

1.1.1 The Production Chain of Fluorinated Compounds

Fluorine is one of the most abundant elements in the Earth crust (0.065% by mass, 13th most abundant),[1] yet its isolation in the elemental form was announced only in 1886,[2] significatively later than its neighbours in the periodic table, excluding the noble gases (1772: Nitrogen;[3] 1774: Oxygen;[4] 1810: Chlorine;[5] 1811: Iodine;[6] 1825: Bromine[7]). The hypothesis of the existence of a missing halogen, lighter than chlorine, was formulated as early as 1809 in the epistolary correspondence between the French chemist A.-M. Ampère and the British H. Davy.[2] Ampère had already suggested that electrolysis could be used to isolate fluorine gas (F_2) from anhydrous hydrogen fluoride (HF). Yet, for more than seventy years the challenge seemed insurmountable: the toxicity and corrosiveness of both compounds caused numerous injuries and fatalities among the experimenters. Finally, on June 28th, 1886, the French chemist H. Moissan succeeded in synthesising an extremely reactive yellow-green gas: the existence of fluorine was confirmed! Moissan's process consisted of the electrolysis of anhydrous HF in the presence of molten potassium hydrogen difluoride (KHF_2), added to improve the medium conductivity. Modern industrial production of F_2 is still based on this early process.

Moissan's discovery, for which he was awarded the Nobel prize in 1906, was a first step towards the synthesis of fluorinated compounds, whose unique properties have favoured the advancement of fields far beyond the realm of pure chemistry. Nowadays, many fluorinating reagents are available, their development spurred by the need for safer alternatives to anhydrous HF and F_2.[8] These reagents are classified either as nucleophilic

(source of "F^-") or electrophilic (source of "F^+") fluorinating reagents. In spite of their differing reactivity, ultimately they all derive from the same natural sources (Figure 1.1).[9] Fluorine is found in the minerals Cryolite (AlF_3,NaF), Fluorite (CaF_2) and Fluorapatite ($Ca_5(PO_4)_3F$), which is currently used for the production of phosphoric acid. Cryolite mines were exhausted as early as 1980 and no commercial process has been developed for the recovery of fluorine from aqueous fluorosilicic acid (H_2SiF_6), a by-product in the manufacture of phosphoric acid, leaving Fluorite as the sole natural fluorine source exploited today. With an estimate global reserve of about 310 million metric tonnes,[10] located mainly in South Africa, Mexico and China, and an increasing annual consumption currently around 7 million metric tonnes, models predict that these deposits will last less than a century. This has urged the implementation of a feasible process to produce fluorine from Fluorapatite, reserves of which are estimated to be in the range of hundreds of billions of tonnes.

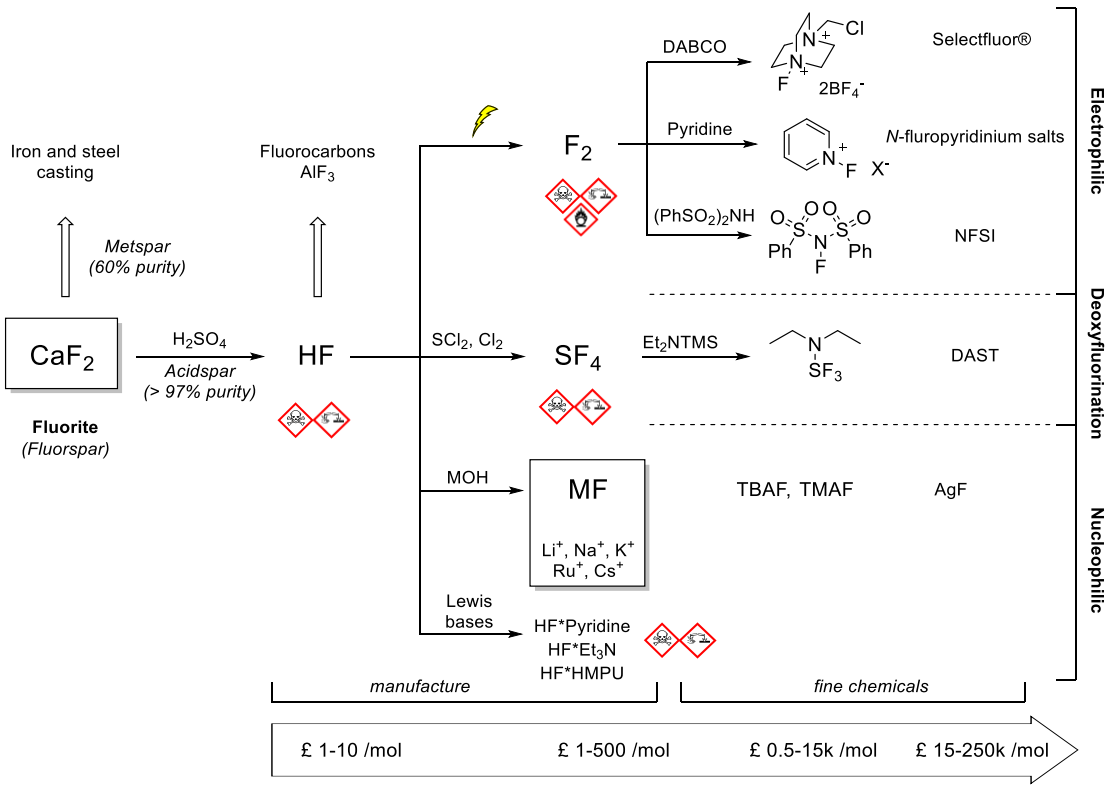


Figure 1.1: The production chain of fluorinated compounds.[9]

About half of the mined calcium fluoride (purity ~60%) is used by the steel industry, while the purest fraction (>97% purity) is dissolved in concentrated sulfuric acid to obtain anhydrous HF.[11] The majority of this is employed in the manufacture of fluorocarbons (42%), which are used as foaming agents, refrigerants and monomers for fluoropolymers. Anhydrous HF is also used in the production of synthetic cryolite (AlF_3) for the aluminium industry (33%) and of metal fluorides (16%).[11] Direct use of HF as a catalyst for olefin alkylation (2%) and synthesis of F_2 (1.8%) have a minor but significant role in HF consumption.

Nucleophilic fluorinating reagents for the fine chemical industry are obtained directly from HF, by complexation with pyridine, amines or ureas (Olah's reagent = HF*Pyridine, Et_3N*3HF, HF*DMPU,[12] Figure 1.1) or from its neutralisation with an appropriate base (e.g. alkali metal fluorides, TBAF, ...). Electrophilic and deoxyfluorinating reagents are also derived from HF *via* the synthesis of toxic and corrosive F_2 and sulfur tetrafluoride (SF_4) gases (Figure 1.1). Direct application of F_2 for fluorination is convenient only for large production volumes, while its conversion into electrophilic *N*–F reagents (Selectfluor®= 1-chloromethyl-4-fluoro-1,4-diazoniabicyclo[2.2.2]octane bis(tetrafluoro-borate), *N*-fluoropyridinium salts, NFSI = *N*-Fluorosulfonimide) has found application on laboratory scale. SF_4 is the precursor of SF_6, which is used as an electrical insulator, and of various deoxyfluorinating reagents (*e.g.* DAST = diethylaminosulfur trifluoride, Deoxo-fluor® = bis(2-methoxyethyl)aminosulfur trifluoride, *etc.*).

The higher number of transformations required to access these latter classes of chemicals, as well as the need to build specialised plants to handle the hazardous gaseous precursors, is reflected in the higher price of electrophilic and deoxyfluorinating reagents (£ 500-250 000 /mol) compared to nucleophilic reagents (£ 1-15 000 /mol). Moreover, their synthesis requires a significantly higher amount of energy and generates more waste

compared to reagents directly derived from HF, resulting in a better economic and ecological profile for nucleophilic sources of fluorine. This is particularly true for alkali metal fluorides, especially potassium fluoride (KF), which are abundant, cheap (£ 6-56 /mol) and easy-to-handle solids. Despite these attractive features, several challenges must be addressed to use these reagents in asymmetric fluorination.

1.1.2 Challenges in the Use of Alkali Metal Fluorides in Synthesis

Alkali metal fluorides are ionic salts of general structure MF, where M is a monovalent cation of the first group IA. The spatial arrangement of the ions within the crystal is typical for alkali halides and consists of two face-centered cubic lattices, where the cations occupy the octahedral holes of the fluoride lattice (Figure 1.2A).[13]

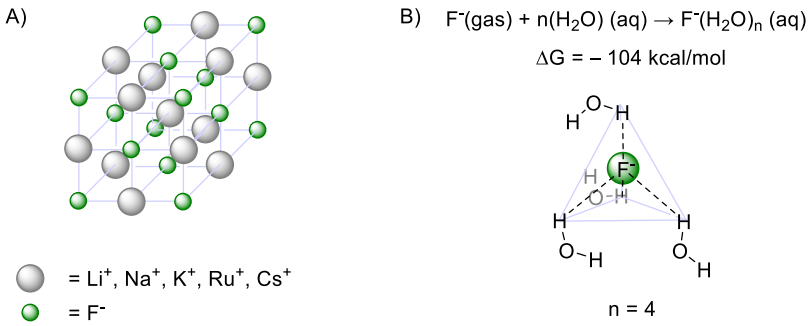


Figure 1.2: A) Crystal lattice of alkali metal fluorides. B) Hydration energy of fluoride and tetrahedral structure of the most stable $F^{-}(H_2O)_4$ cluster.[14]

As the cation radius increases within the group, with consequent reduction in charge density, the lattice energy decreases accordingly. This impacts the physical properties of the salts, such as melting point and solubility (Table 1.1), as well as hygroscopicity. For instance, while CsF is highly soluble in water (573 g/ 100 g H_2O at 25°C)[15] and methanol, as well as partially soluble in polar organic solvents, water is unable to fully solubilise LiF at room temperature (0.134 g/ 100 g H_2O at 25 °C).[15] Solubility of alkali metal fluorides other than CsF in organic solvents, either polar aprotic or protic, is likewise poor,[16] a feature

that has hindered their application in organic synthesis. Similarly, the hygroscopicity of these salts can be correlated with their lattice energy, explaining why CsF will absorb moisture from the atmosphere within a few minutes if left uncapped, while LiF will stay indefinitely solid under the same conditions.

Table 1.1: Selected properties of alkali metal fluorides.[15]

MF	*M^+ radius (Å)*	*M^+ charge density (C/mm^3)*	*Lattice energy (kcal/mol)*	*Melting point (° C)*	*Solubility (g/ 100 g H_2O)*
LiF	0.79	52	251	845	0.134
NaF	1.02	24	222	993	4.13
KF	1.38	11	198	858	102
RuF	1.52	8	190	795	300
CsF	1.67	6	181	682	573

Water solubility and hygroscopicity are the result of the fluoride ion's ability to engage in strong hydrogen bonds with protic donors. The hydration energy of fluoride has been calculated to be –104.2 $\pm$ 0.7 kcal/mol at 25 °C.[14] In the smallest $F^-(H_2O)_n$ cluster (n = 4), fluoride engages in four hydrogen bonds with four water molecules, which occupy the vertexes of a distorted tetrahedron (Figure 1.2B). The preference for this structure is reinforced in clusters of bigger size (n= 8, 12, 16), where the additional water molecules are hydrogen bonded to those constituting the primary solvation shell. Hydration of fluoride results in its diminished basicity and nucleophilicity, because the negative charge is attenuated by the formation of hydrogen bonds. Hydrogen bonding has thus historically been regarded as detrimental for fluoride reactivity. In some cases, particularly with carboxylic acids and phenols, hydrogen bonding with fluoride increases the nucleophilicity of the hydrogen bond donor to the extent that the latter acts as a nucleophile in place of fluoride. [17]

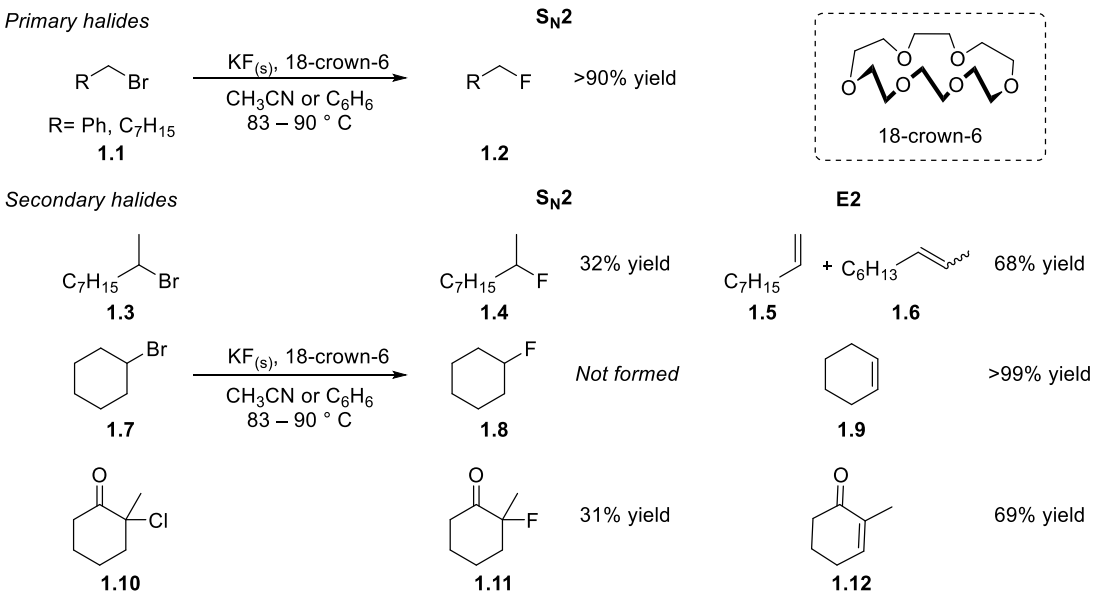
Fluoride's small radius makes it one of the hardest anion (charge density = 24 C/mm^3) and the tendency of unsolvated or "naked" fluoride to act as a base is well documented.[18] The

basicity of fluoride is strongly dependent on the solvent, the counter-cation and the presence of protic donors (*e.g.* anhydrous conditions or not). Diluted aqueous HF is a weak acid (pK_a=3.2),[19] while fluoride in anhydrous polar aprotic solvents is a base strong enough to deprotonate fluorene (pK_a ~ 22,[20] DMSO), acetonitrile (pK_a = 31.3,[20] DMSO) and dimethyl sulfoxide (DMSO; pK_a = 35.1,[20] DMSO). [18]

To overcome the poor solubility of alkali metal fluorides, quaternary ammonium salts have been introduced. These are highly hygroscopic, due to the reduced interaction between the cation and fluoride. For this reason, tetrabutylammonium fluoride (TBAF) is commercialised as the stable trihydrate. Attempts to remove the coordination water by heating this reagent under vacuum cause its decomposition *via* Hofmann elimination.[21] Thus, if anhydrous conditions are required, alkali metal fluorides are usually preferred. Alternatively, TBAF can be generated *in situ via* nucleophilic aromatic substitution of hexafluorobenzene with cyanide, according to the protocol developed by DiMagno.[22]

1.1.3 Fluoride Activation *via* Phase-Transfer Catalysis (PTC)

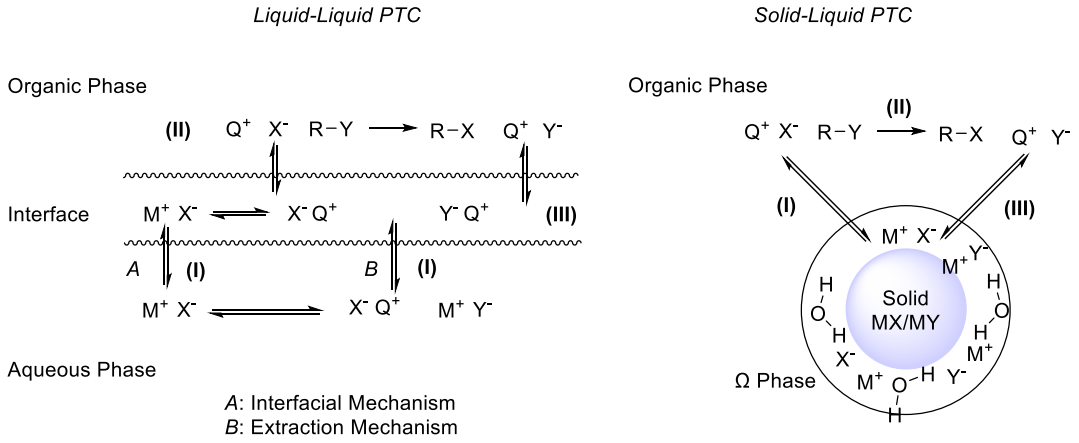
In 1974, Liotta *et. al* reported the use of catalytic 18-crown-6 (19-68 mol%) to improve KF solubility in acetonitrile and benzene.[23] Beside increasing the lipophilicity of the ion-pair, complexation of the metal cation by the crown ether had the effect to create a very reactive, unsolvated – "naked" in the authors' words – anion, which behaved either as a nucleophile or as a base depending on the structure of the electrophile (Scheme 1.1).



Scheme 1.1**:** 18-Crown-6 as phase transfer catalyst for nucleophilic fluorination with alkali metal fluorides.[23]

Since this early report, cationic phase-transfer catalysis (PTC), both across a solid-liquid interface (solid-liquid PTC), and between an aqueous solution and an organic phase (liquid-liquid PTC), has been recognised as a powerful strategy to promote nucleophilic fluorinations. The catalysts traditionally employed are either organic molecules able to complex the cation through Lewis basic sites (*e.g.* crown ethers, cryptands, PEGs), or quaternary ammonium or phosphonium salts which replace the alkali metal. The reactivity of fluoride is tremendously increased under PTC conditions, but this often comes at the price of reduced selectivity.

PTC has been applied to a broader range of nucleophiles besides fluoride. In general, all PTC reactions involve multiple steps, namely the translocation of one of the reactants across the interface (**I**, Scheme 1.2), the reaction(s) in the organic phase (**II**), and the regeneration of the active catalyst (**III**), which involves translocation of the leaving-group into the aqueous phase or its precipitation as inorganic salt.[24] All these steps have to be fast in order to create an efficient catalytic cycle, and indeed, in cationic PTC, the role of the catalyst is dual: to promote the phase transfer and to activate the nucleophile *via* formation of a less tight ion-pair.



Scheme 1.2: A) Simplified mechanism of liquid-liquid PTC. B) Simplified mechanism of solid-liquid PTC.[24]

In liquid-liquid PTC, interaction with the organocatalyst also promotes dehydration of the anion, enhancing its nucleophilicity. In this type of PTC, an important aspect is the relative affinity of the catalyst for the nucleophile (X^-) and the leaving group (Y^-), which is expressed as a selectivity constant $K^{sel}_{X^-/Y^-}$ (Equation 1.1). When $K^{sel}_{X^-/Y^-}$>1, the cationic catalyst pairs preferentially with the nucleophile, ensuring catalytic turnover; while when $K^{sel}_{X^-/Y^-}$< 1, and even more so for $K^{sel}_{X^-/Y^-}$< 0.1, the reaction stops without reaching full conversion, because the built-up of the anionic leaving group poisons the catalyst.[25] Fluoride is a notoriously difficult anion to engage in cationic liquid-liquid PTC due to its high charge to volume ratio, which results in a high degree of hydration and a lower affinity

for the catalyst compared to the more lipophilic leaving group (which is usually one of the heavier halogens).

$$K_{X^-/Y^-}^{sel} = \frac{[QX]_{org}[Y^-]_{aq}}{[QY]_{org}[X^-]_{aq}} \qquad \text{Eq. 1.1}$$

In solid-liquid PTC the interface between different phases is the surface of the solid itself. Well-dispersed, small particles will maximise the surface area and in turn guarantee more efficient phase-transfer. More subtly, the presence of defects in the crystal lattice in proximity of the surface will aid in its breakage and the establishment of new interactions with the phase-transfer catalyst. This might be mediated by molecules of water capable of solvating the ions. Systematic studies by Sasson and Dermeik revealed that up to ~5% water content of the inorganic salt (expressed as the ratio of water and solid weights, w/w) had a positive impact on the rate of nucleophilic substitutions catalysed by quaternary ammonium cations, while further additions were detrimental (Figure 1.3).[26] The authors explained this trend in terms of the opposite effect that water had on mass transfer, favoured by its adsorption on the surface of the hygroscopic salt, and nucleophilicity of the anion, which is reduced when hydrated.

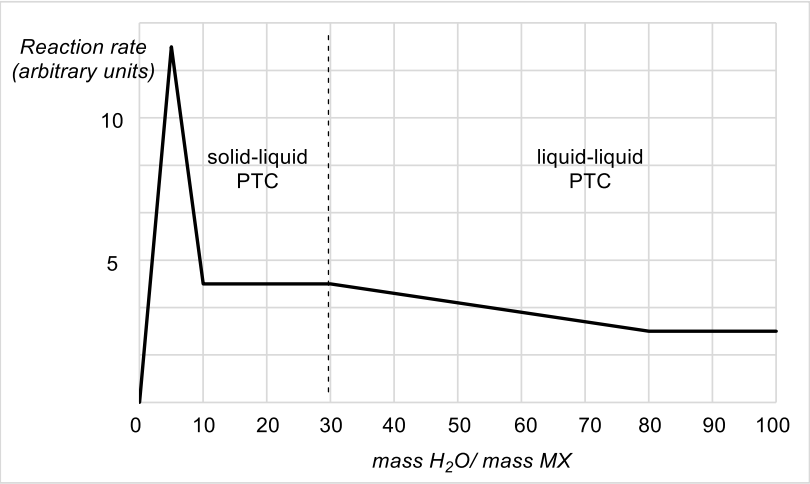
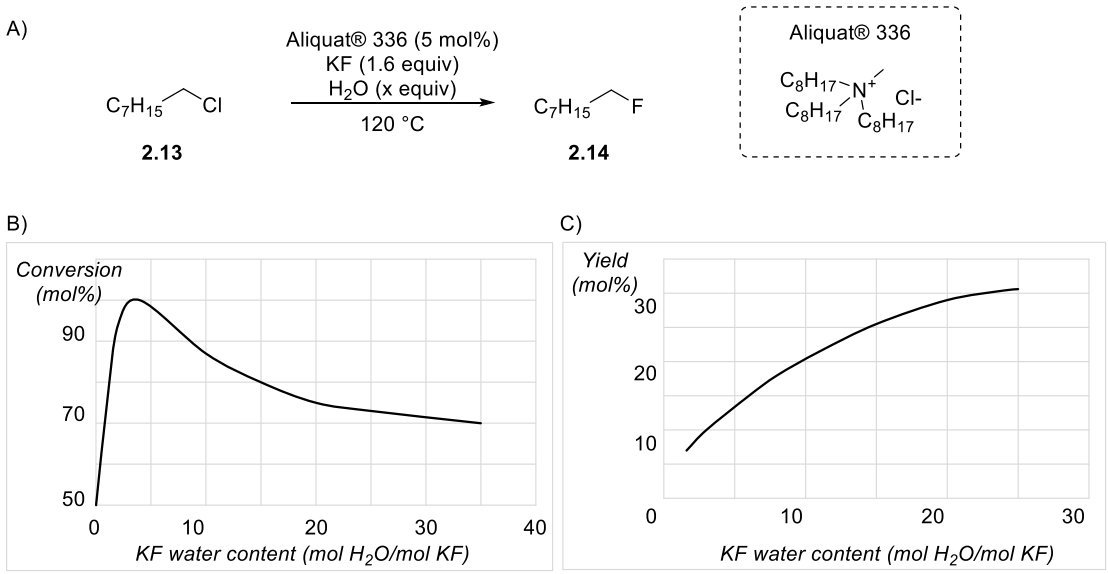


Figure 1.3: General trend of reaction rate *versus* water content in nucleophilic substitution under solid-liquid PTC catalysed by quaternary ammonium salts. Adapted from reference 26.

The reaction of KF with *n*-octyl chloride in the presence of 5 mol% of Aliquat® 336 **(**trioctylmethylammonium chloride) as phase-transfer catalyst follows the general trend described, with water affecting both yield and reaction rate (Scheme 1.3).[27,28] A similar trend was observed by Liotta and co-workers in solid-liquid PTC nucleophilic substitutions catalysed by crown ethers.[29] The authors noticed that when water was present, most of the catalyst (>97%) was extracted from the organic phase and adsorbed onto the solid. They called this new region the *Omega phase* and they suggested it aided complexation of the inorganic cation with the catalyst.[29,30]



Scheme 1.3: Effect of water in solid-liquid PTC with quaternary ammonium salts A) Reaction conditions for the fluorination of *n*-octyl chloride with KF catalysed by Aliquat® 336. B) Effect of water content on conversion (120 h).[27] B) Effect of water content on the reaction rate (4 h).[28]

1.1.4 Asymmetric PTC for Enantioselective Fluorination

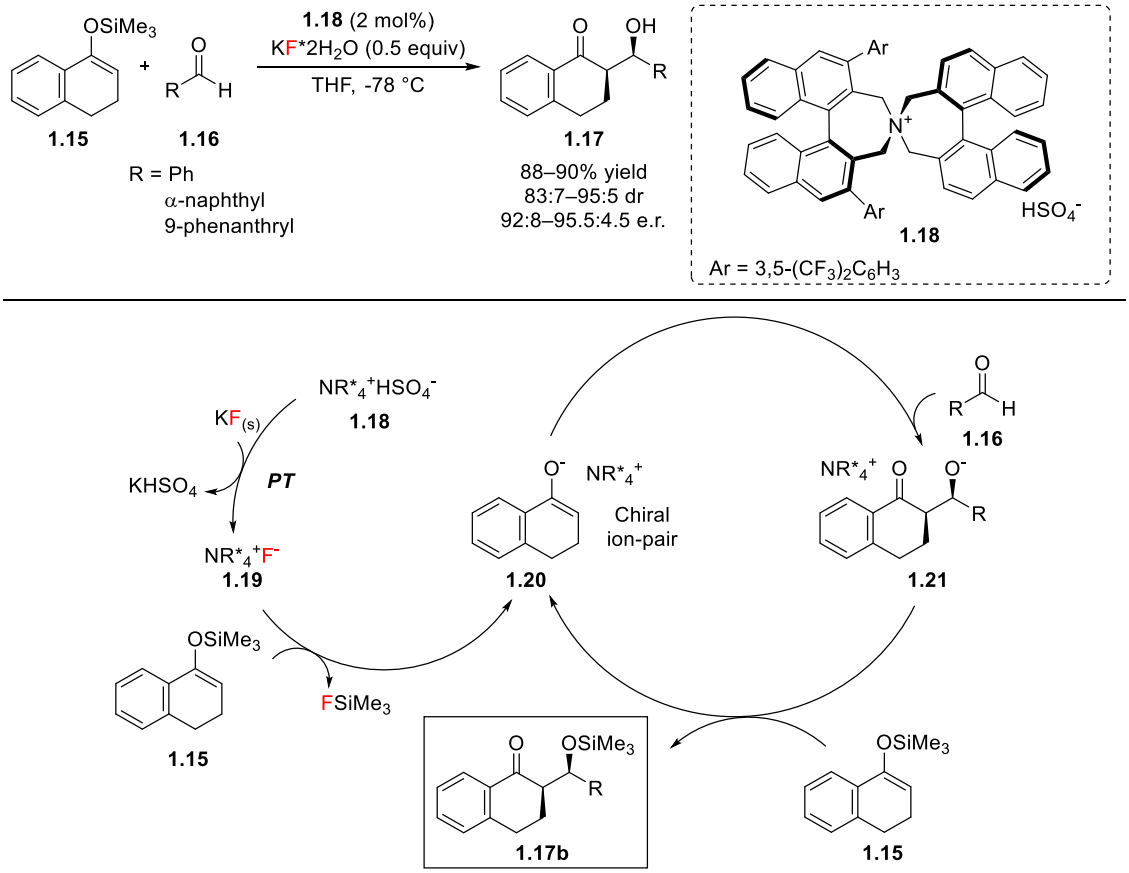
When PTC reactions are catalysed by chiral non-racemic molecules, an enantioenriched product could in principle be obtained, provided that the catalyst exerts sufficient control in the enantiodetermining step. The main interaction exploited in PTC is electrostatic in nature, making it a special case of asymmetric ion-pairing catalysis taking place in a biphasic system.[31] This is maximised in solvents of low dielectric constant and in the presence of densely charged ions tightly interacting. Additional weaker but usually more directional secondary interactions, either attractive or repulsive, are exploited to differentiate the diastereomeric transition states, in a manner akin to that observed in enzymes. Four types of ion-pair catalysis can be distinguished: 1) chiral cation-directed catalysis (section 1.1.4.1) and 2) cation-binding catalysis (section 1.1.4.2) —pairing with anionic reactants— and 3) chiral anion-directed catalysis (section 1.1.4.3), and 4) anion-binding catalysis (section 1.1.4.4) —pairing with cationic reactants.[31] Application of these catalytic manifolds in combination with fluorine sources is described in the following sections. The examples are not limited to fluorinations but also include transformations where fluoride acts as desilylating reagent.

1.1.4.1 Chiral Cation-Directed PTC

Chiral cation-directed PTC is one of the oldest forms of asymmetric PCT, building on the work of the late ‘60s on PTC for the activation of anionic reactants. The organocatalysts employed are charged chiral quaternary ammonium and phosphonium cations. In 1980, Merck scientists reported the highly enantioselective *C*-methylation of indanones in the presence of a chiral quaternary ammonium phase-transfer catalyst derived from cinchona alkaloids.[32] Subsequently the field grew steadily to the point that nowadays this technology is applied to processes on multi-kilogram scale involving enolate intermediates

(e.g. *Letermovir*, PTC-aza-Michael addition; *Fingolimod* analogue, PTC-enolate alkylation, *MK-3207*, PTC-enolate alkylation).[33]

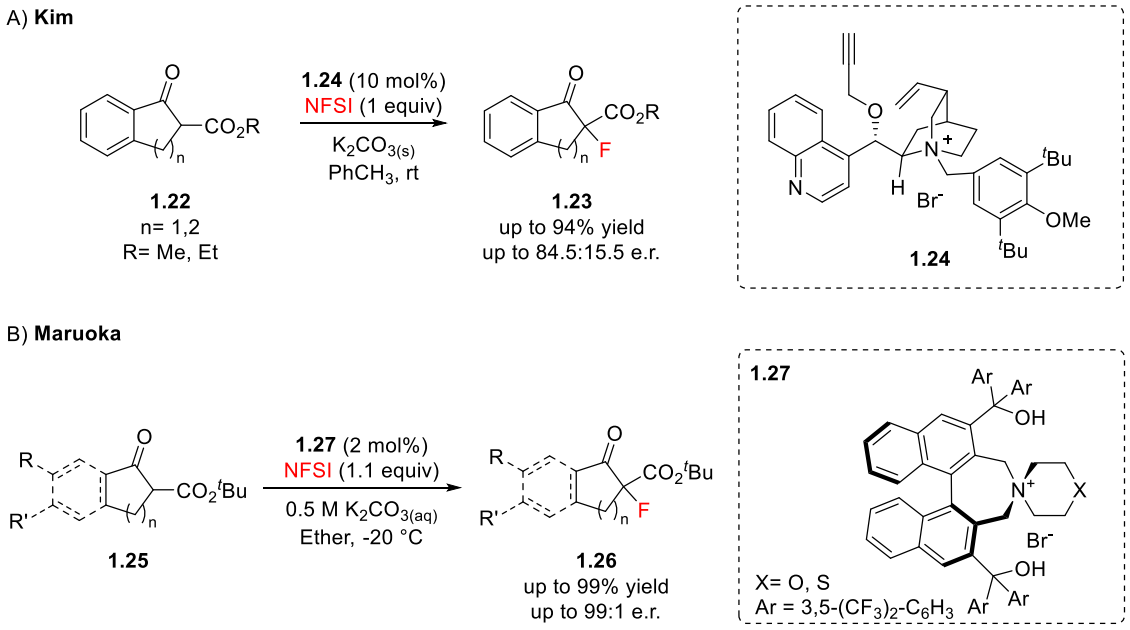
The application of chiral cation-directed PTC to enantioselective nucleophilic fluorination with alkali metal fluorides is unknown. The only example in which a chiral quaternary ammonium salt acts as phase transfer catalyst towards KF is a Mukaiyama-type aldol reaction reported by Maruoka (Scheme 1.4).[34] KF is used in substochiometric amounts, its role being to activate the silyl enol ether in the first catalytic cycle.



Scheme 1.4: Mukaiyama-type aldol reaction promoted by KF under solid-liquid PTC conditions.[34]

On the contrary, enantioselective electrophilic fluorination of the chiral ammonium cation-enolate ion-pair has been reported by different groups.[35,36] The fluoride source is soluble in the reaction media and the ammonium salt acts as a phase-transfer catalyst towards the inorganic base used to generate the enolate. The first example was reported by Kim *et al.* using NFSI for the α-fluorination of β-ketoesters in the presence of solid potassium

carbonate (K_2CO_3) and a quaternary ammonium cation derived from cinchona alkaloids (Scheme 1.5A).[35] The level of enantioinduction was moderate (up to 84.5:15.5 e.r., e.r. = enantiomeric ratio) and improvement of the reaction by the Maruoka group (up to 99:1 e.r.) was possible employing a bifunctional catalyst based on the C_2-symmetric binaphthyl scaffold (Scheme 1.5B).[36]



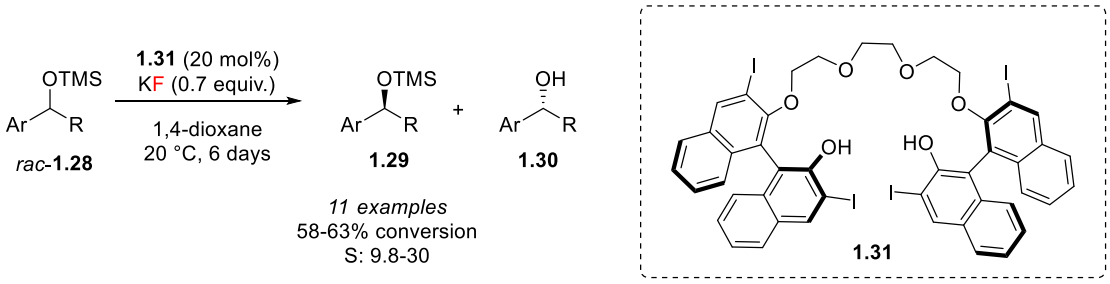
Scheme 1.5: Enantioselective electrophilic fluorination under cationic PTC.[35,36] The ammonium salts acts as phase-transfer catalyst towards the inorganic base, while the fluorine source is soluble in the reaction media.

1.1.4.2 Cation-Binding PTC

Cation-binding is an alternative method for the activation of anionic species exploited since the early applications of PTC. The organocatalyst is a neutral species able to interact with the metal counter-cation of the anionic reactant, enhancing the lipophilicity of the ion-pair. This promotes transfer of the ion-pair into the organic phase.

Chiral crown ethers have been described for the activation of alkali metal fluorides for desilylation reactions, but their application to the asymmetric construction of C–F bonds remains elusive. Asymmetric cation-binding catalysis has been successfully applied to the

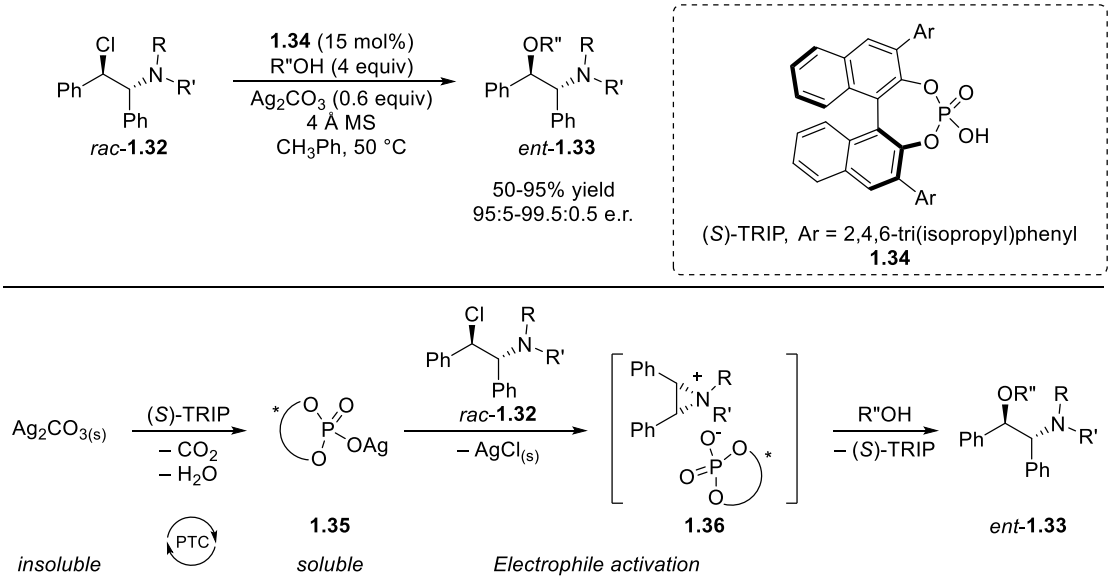
activation of KF for the kinetic resolution of secondary silyl alcohols by Song *et al.* using a chiral ether **1.31** consisting of two 1,1'-bi-2-naphthol (BINOL) units connected by a triethylene glycol chain (Scheme 1.6).[37] While the cation (K^+) interacted primarily with the polyether chain, the authors pointed out that secondary interactions were essential to achieve high level of reactivity and enantiocontrol. In fact, it was noted that no reaction was taking place unless the BINOL 3,3' substituents were halogens, and a positive correlation existed between the halogen polarisability and the reactivity and enantioselectivity observed. X-ray diffraction of the **1.31**-KF complex revealed the existence of an interaction between the metallic cation and the halogen, which was deemed responsible for the reduced $K^+ F^-$ attraction and consequent enhanced reactivity. Moreover, methylation of the BINOL OHs resulted in reaction suppression, thus suggesting that hydrogen bonding between the catalyst and fluoride played a crucial role (see also 1.1.5).



Scheme 1.6: Kinetic resolution of secondary silyl alcohols with solid KF *via* cation binding catalysis.[37]

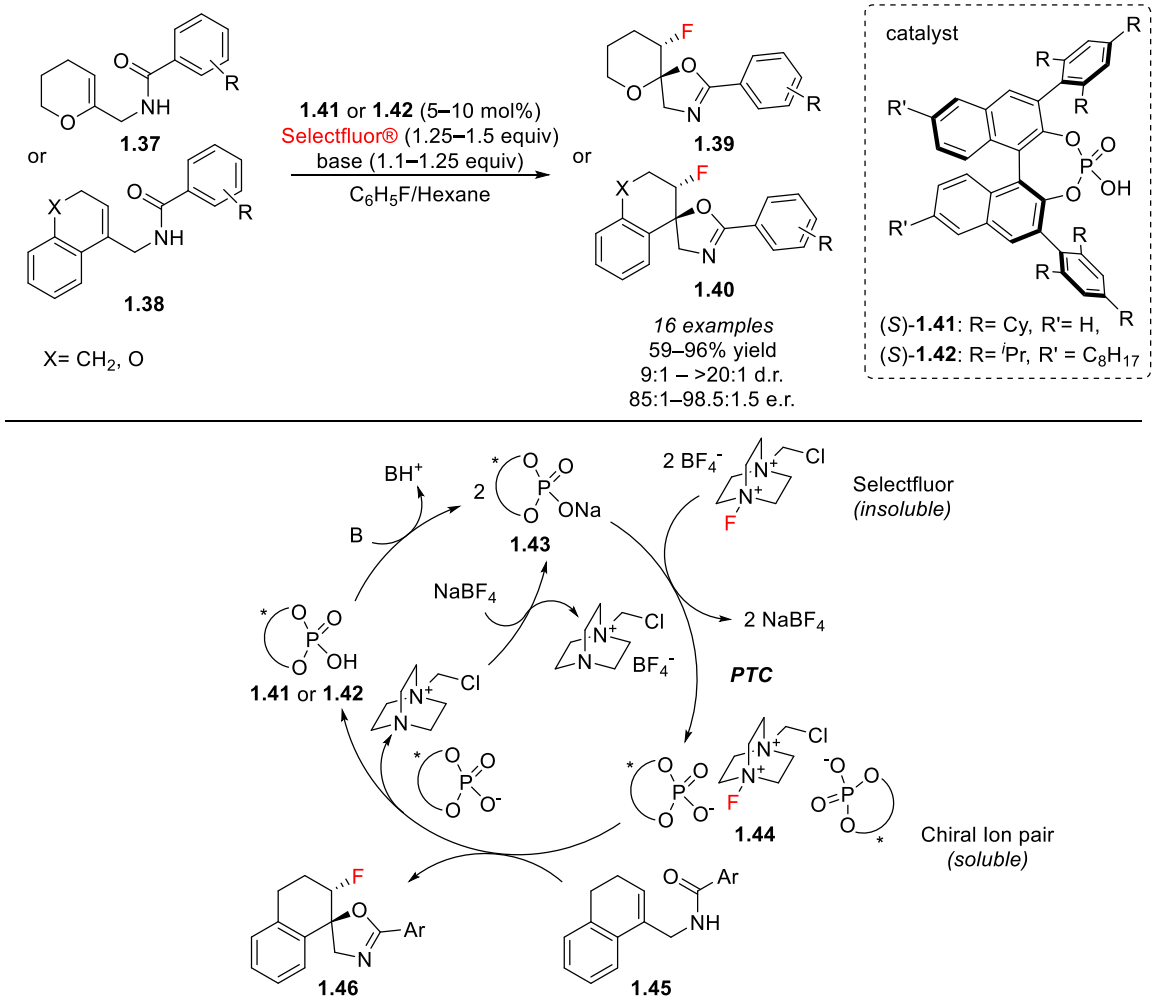
1.1.4.3 Chiral Anion-Directed PTC

Chiral anion-directed PTC is the charge-inverted process of the well-established PTC with chiral cations, but its successful application is comparatively more recent (early 2000s). Pioneering studies with chiral borate anions and preformed cationic electrophiles were conducted in the early 2000s, obtaining low levels of enantioinduction.[38] Subsequently, insoluble silver carbonate (Ag_2CO_3) and a chiral phosphoric acid as phase transfer catalyst were used by the Toste group for the activation of aziridinium precursors in the first example of highly enantioselective anionic PTC (Scheme 1.7).[39]



Scheme 1.7: Anionic PTC applied to the enantioselective desymmetrisation of *meso* aziridinium ions.

Asymmetric anionic PTC has been successfully applied to enantioselective electrophilic fluorination, taking advantage of the poor solubility of the doubly cationic Selectfluor® in apolar media, which supresses background reaction in absence of the phase-transfer catalyst. In the presence of a chiral phosphate anion, high levels of enantioselectivity were achieved in the fluorocyclisation of alkenes with Selectfluor® (up to 98.5:1.5 e.r., Scheme 1.8).[40] A negative non-linear effect was observed, supporting a mechanism wherein both tetrafluoroborate (BF_4^-) anions were exchanged with the chiral phosphate.

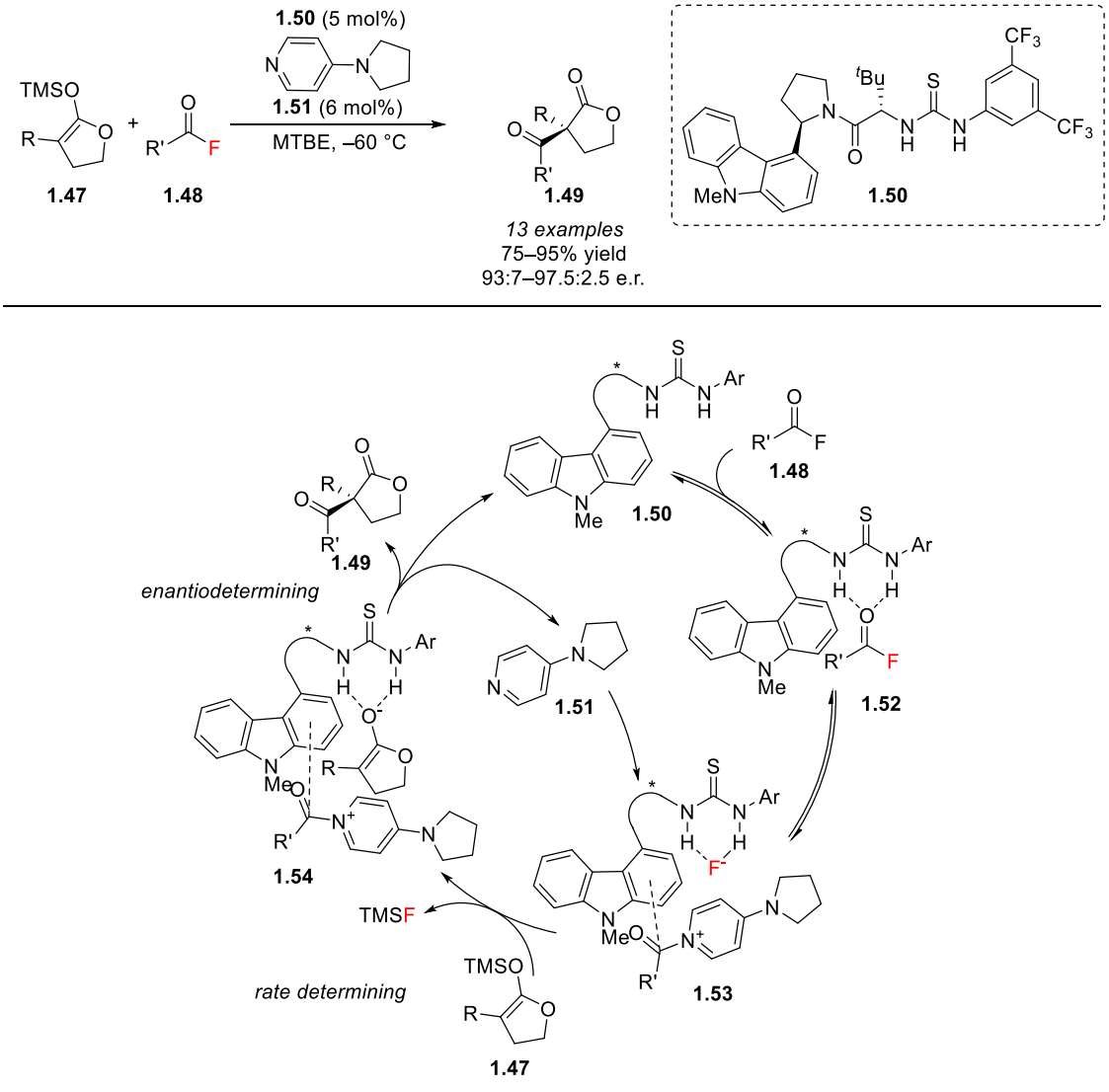


Scheme 1.8: Enantioselective electrophilic fluorination under anionic PTC.[40]

1.1.4.4 Anion-Binding Catalysis

Asymmetric anion-binding catalysis under homogeneous conditions has been pioneered by the Jacobsen group and relies on the interaction of a chiral neutral hydrogen bond donor with an anionic species.[31] Halide anions usually have a spectator role, the ion-pair being formed concomitantly with electrophile activation by anion abstraction.[31,41] The reactivity and the selectivity are markedly dependent on the nature of the leaving group, and due to the strength of the C–F bond, fluoride does not feature in anion-abstraction catalysis. A rare exception of anion-biding catalysis with fluoride involves the use of acyl fluorides in the

acylation of silyl ketene acetals under dual nucleophilic and hydrogen bonding catalysis (Scheme 1.9).[42] While experimental results suggested the involvement of the hydrogen bonded fluoride-thiourea complex **1.53** in the rate-determining step (desilylation), it is believed that a different complex (**1.54**) participated in the enantiodetermining step. According to the proposed mechanism, anion metathesis resulting from desilylation of the silyl ketene acetal forms the reactive ion-pair that ultimately delivers the enantioenriched 1,3-ketoester.



Scheme 1.9: Enantioselective acylation of silyl ketene acetals involving fluoride anion-binding catalysis.[42]

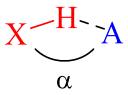
Anion-binding catalysis was not applied to PTC prior to the seminal publication from the Gouverneur group which constitutes the basis of this thesis (section 1.1.6).

1.1.5 Hydrogen Bonding for Nucleophilic Fluorination

1.1.5.1 Definition of Hydrogen Bonding

The IUPAC defines the hydrogen bond as "*an attractive interaction between a hydrogen atom from a molecule or a molecular fragment X–H in which X is more electronegative than H, and an atom or a group of atoms in the same or a different molecule, in which there is evidence of bond formation*".[43] According to the strength of the interaction, hydrogen bonds can be divided into three classes (Table 1.2):[44] "strong hydrogen bonds", mostly covalent in character, characterised by bond dissociation energies (BDE) between 14 and 40 kcal/mol, short bond lengths (1.2–1.5 Å) and almost linear geometries (bond angles α between 170–180 °); "moderate hydrogen bonds", mostly electrostatic, with BDE between 4 and 15 kcal/mol, bond lengths between 1.5–2.2 Å and bond angles α between 130 ° and 180 °; "weak hydrogen bonds", where the force holding the fragments together is purely electrostatic (BDE < 4 kcal/mol), resulting in longer bonds (2.2–3.2 Å). In this latter case substantial deviation from linearity is observed (bond angles α: 90–150 °).

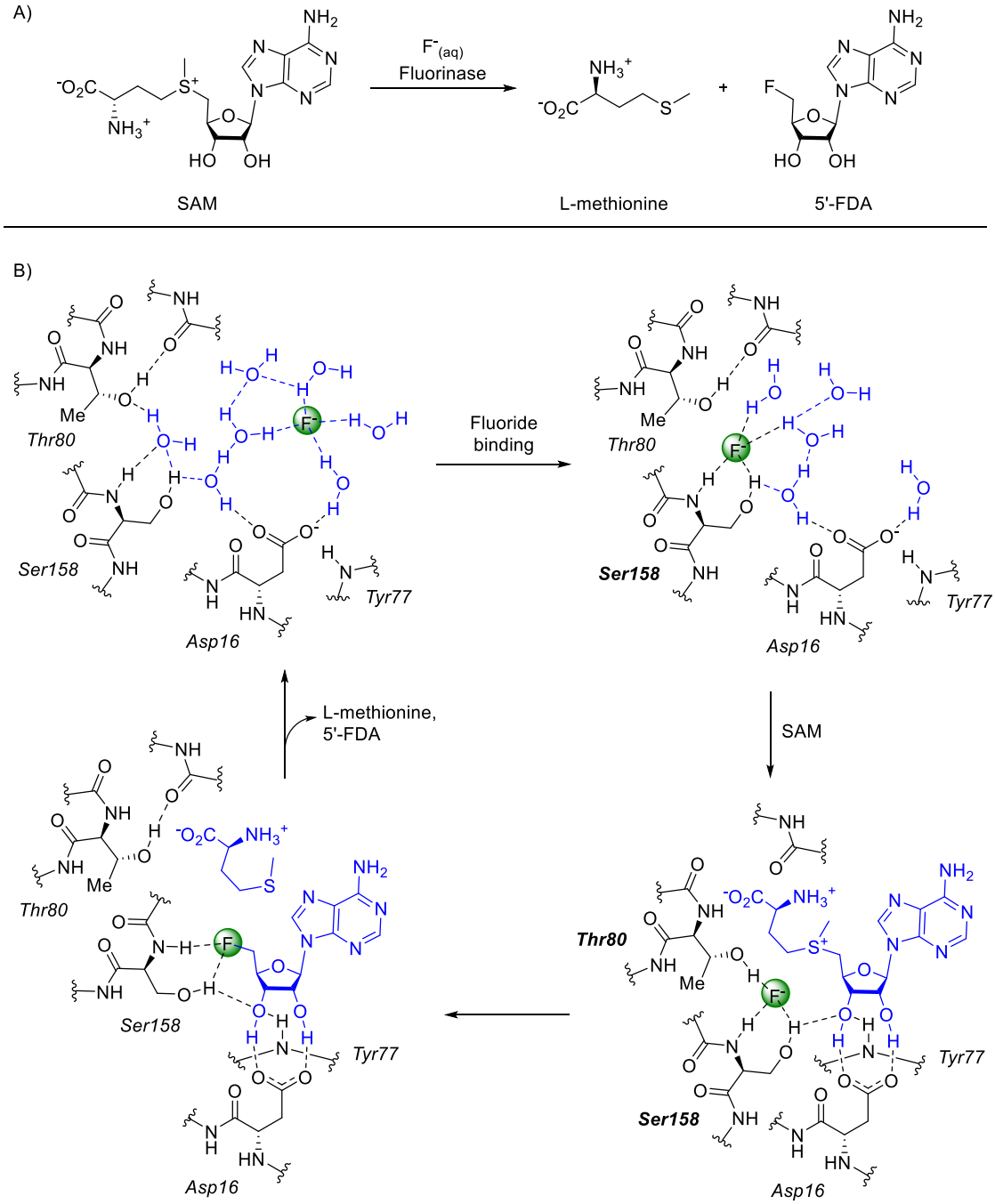
Table 1.2: Classification of hydrogen bonds.[44]

Donor (Hydrogen-bond donor)  **Acceptor** (Hydrogen-bond acceptor)

	Strong	*Moderate*	*Weak*
BDE (kcal/mol)	14–40	4–15	< 4
H---A Bond length (Å)	1.2–1.5	1.5–2.2	2.2–3.2
Bond angle α (°)	170–180	130–180	90–150
Example	F–H---F^-	HO–H---OH_2	O–H---F–C

1.1.5.2 The Fluorinase Enzyme

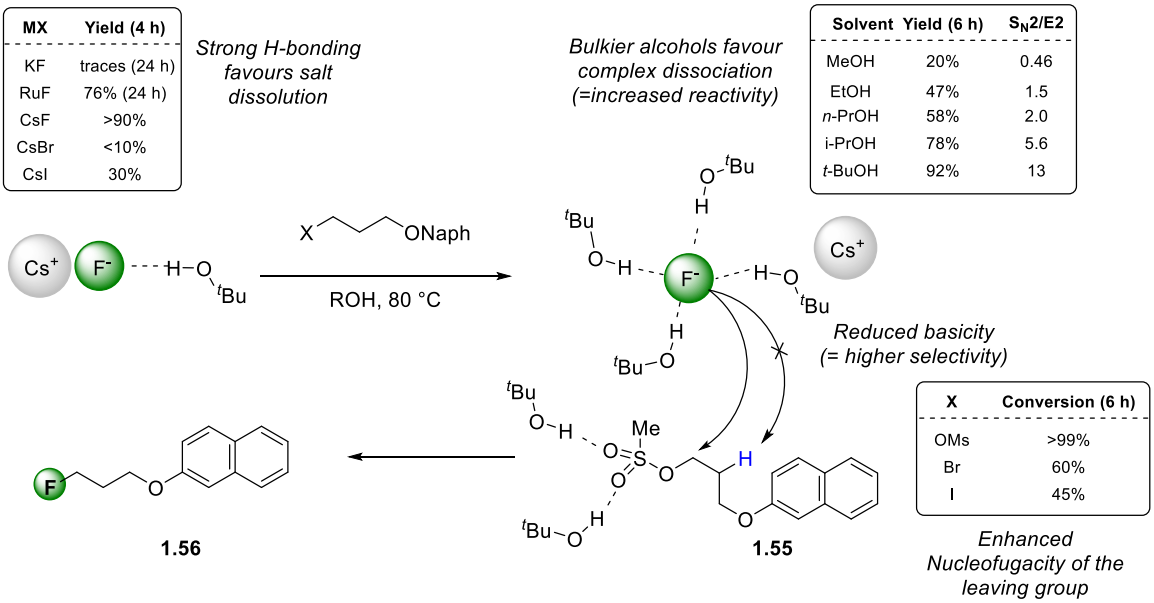
In 2002, the O'Hagan group reported that a partially purified protein extracted from the bacterium *Streptomyces Cattleya* was able to catalyse the nucleophilic fluorination of *S*-adenosylmethionine (SAM) to 5'-fluoro-5'-deoxyadenosine (5'-FDA) (Scheme 1.10A).[45] This is a remarkable transformation considering the challenges in activating aqueous fluoride described in section 1.1.2, therefore extensive investigations were undertaken to fully elucidate the mechanism of the sole fluorinase enzyme known to date.[46–49] On the basis of experimental and computational results, the authors concluded that three hydrogen bonds donors within the catalytic pocket (the side chain and backbone of Serine 158 and side chain of Threonine 80) played a key role in desolvating aqueous fluoride and pre-organising the reactants, leading to the proposal of the mechanism depicted in Scheme 1.10B. Fluoride binds first, but weakly, to the enzyme in an open conformation, with formation of bifurcate hydrogen bonding with Serine 158 (Ser158) and partial dehydration. Upon binding SAM, the enzyme undergoes a conformational change which favours full dehydration of the anion. A further hydrogen bonding of fluoride with threonine 80 (Thr80) is then established, and the fluoride is now trapped into a small hydrophobic pocket of fluoride size. The reactants are thus aligned favourably for S_N2 substitution, the ribose ring being preorganised in a high-energy conformation which favours the approach of the nucleophile and the cleavage of the C–S bond. Labelling experiments and computational calculations further supported this substitution pathway, the latter suggesting that the positively charged sulfonium ion plays a key role in stabilising the transition state.[49,50] Release of L-methionine and 5'-FDA completes the catalytic cycle.



Scheme 1.10: The fluorinase enzyme. A) Catalytic reaction. B) Mechanism of the fluorination.

1.1.5.3 Fluoride Activation via Hydrogen Bonding

Host-guest interactions based on the hydrogen bond acceptor ability of fluoride have long been explored in the field of anion sensing.[51,52] On the other hand, the stability of these complexes (up to $K_a = 10^7\ M^{-1}$) was regarded as detrimental for their application as fluorinating reagents, until the discovery of the fluorinase enzyme prompted the scientific community to challenge the paradigm that protic solvents are detrimental for substitution reactions. Indeed, Kim and co-workers demonstrated that CsF could be conveniently used in bulky tertiary alcohols with dramatic acceleration of the S_N2 rate over competitive elimination.[53] The reaction protocol was successfully extended to the radio-fluorination of PET (Positron Emission Tomography) tracers which were under clinical trials at the time. It was proposed that the solvent activated both the nucleophile, promoting the solubilisation of inorganic CsF and subsequent separation of the ion-pair, and the electrophile, *via* hydrogen bonding to the sulfonate leaving group (Scheme 1.11).[54] Moreover, solvation of fluoride drastically reduced its basicity, leading to almost complete suppression of the elimination product, thus resulting in enhanced yield compared to reactions carried out in polar aprotic solvents.

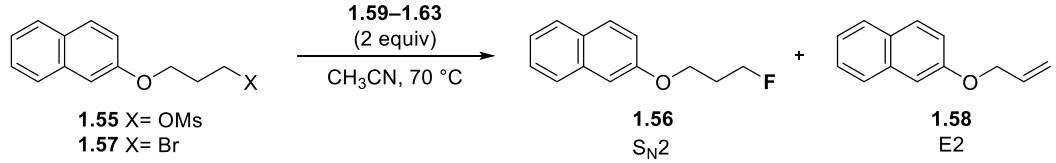


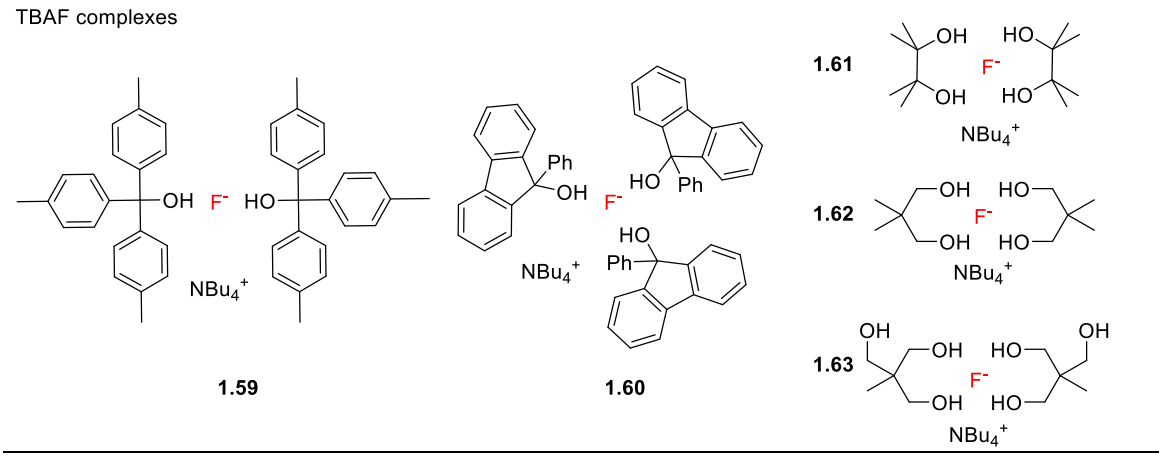
Scheme 1.11: Nucleophilic fluorination promoted by hydrogen bonding.[54]

Building on these findings, the authors and others introduced a novel class of phase-transfer catalysts for the activation of alkali metal fluorides, combining Lewis basic functionalities, able to chelate metal cations, with hydrogen bonds donor moieties, to interact with fluoride.[55,56,57] Compared to traditional crown-ethers, these bifunctional organocatalysts were more chemoselective and could be used with base-sensitive substrates.

The same research group introduced tetrabutylammonium tetra(*tert*-butyl alcohol)fluoride (TBAF*(^{t}BuOH)$_4$) as a stable, anhydrous and non-hygroscopic fluoride source.[58] The observation that this was a superior fluorinating reagent in the Tsuji-Trost type fluorination of allylic *p*-nitrobenzoate and carbonates under both palladium and iridium catalysis,[59,60] prompted the Gouverneur group to conduct more systematic research on the structure and reactivity of a series of homoleptic fluoride-alcohol complexes **1.59–1.63**.[61] Single-crystal X-ray diffraction revealed that fluoride engaged in two to four hydrogen bonds with the alcohol donors, the number of interactions decreasing with increased steric bulk (Table 1.3).

Table 1.3: Solid-state structure and reactivity of homoleptic fluoride-alcohol complexes.[61]





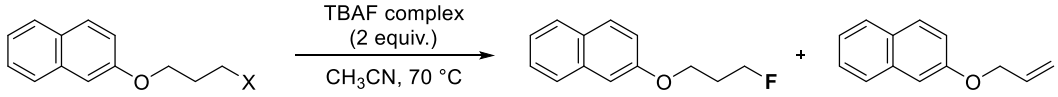
Entry	*Complex*	*Complex concentration (M)*	*K_2 (rel)*	*$S_N2/E2$*
1	**1.59**	0.50	4.1	2.1
2	**1.59**	0.13	14	1.03
3	**1.59**	0.05	20	0.74
4	**1.60**	0.50	0.52	3.5
5	TBAF*$(H_2O)_3$	0.50	1	1.6
6	TBAF*$(^tBuOH)_4$	0.50	2.1	2.0
7	**1.61**	0.50	0.35	2.8
8	**1.62**	0.50	0.066	3.1
9	**1.63**	0.50	0.037	4.2

Evaluation of reactivity and selectivity ($S_N2/E2$) was performed using either 3-(naphthalen-2-yloxy)propyl methanesulfonate **1.55** or 2-(3-bromopropoxy)naphthalene **1.57** as model substrates (Table 1.3). Both reactivity and selectivity showed a marked dependence on concentration (entries 1–3). The observed trend of increased reactivity and decreased $S_N2/E2$ selectivity upon dilution suggested that dissociation was responsible for the formation of a more reactive but less selective ($S_N2/E2$) species. The same dependency of fluoride reactivity and selectivity on the number of hydrogen bond interactions was found comparing different complexes: those with the highest number of hydrogen bonds were the most selective but the least reactive (entries 2, 4–9).

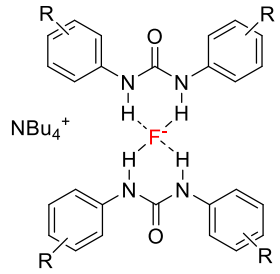
Next, the Gouverneur group synthesised a series of aromatic urea-TBAF complexes to study the effect of the electronic properties of the hydrogen bond donor on fluoride reactivity and selectivity.[62] The complexes were characterised by X-ray and neutron diffraction. In the presence of the bulky tetrabutylammonium cation, fluoride engaged preferentially in four hydrogen bond interactions: besides the $[U_2F]^-$ structure A (U= urea, Table 1.4) reported in the literature,[63] supramolecular adducts $[U_4F_2]^{2-}$ (structure B) and systems including bridging water $[U_2(H_2O)_2F_2]^{2-}$ (structure C) were observed.[62] Tetracoordination was also preferred with squaramides as hydrogen bond donors.[62] When smaller tetraethylammonium or tetramethylammonium cations were used, three ureas coordinated the fluoride with six hydrogen bonding interactions, in a distorted paddle-wheel structure (structure D).[62]

The fluoride-urea complexes were tested in the fluorination of the same model substrates **1.55** and **1.57** employed in the precedent study with fluoride-alcohol complexes.[61] The urea-fluoride complexes were found to be significantly more selective (S_N2/E2, Table 1.4), albeit less reactive, than the alcohol-fluoride complexes previously reported (Table 1.3). Dilution increased the reactivity, suggesting that a partially dissociated 1:1 urea-fluoride complex was the active fluorinating reagent. The presence of the 1:1 species was confirmed by UV-vis and NMR titration, and the binding strength of the urea-fluoride complexes was correlated to the electronic properties of the donors. Electron-withdrawing substituents on the aromatic ring increased the acidity of the urea protons, resulting in more stable and thus more S_N2/E2 selective complexes.

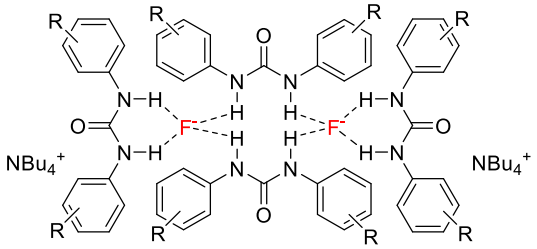
Table 1.4: Solid-state structure and reactivity of homoleptic fluoride-diarylurea complexes.[62]



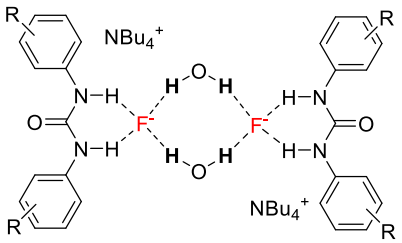
TBAF complexes



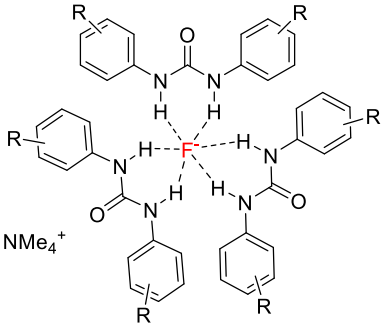
A



B



C



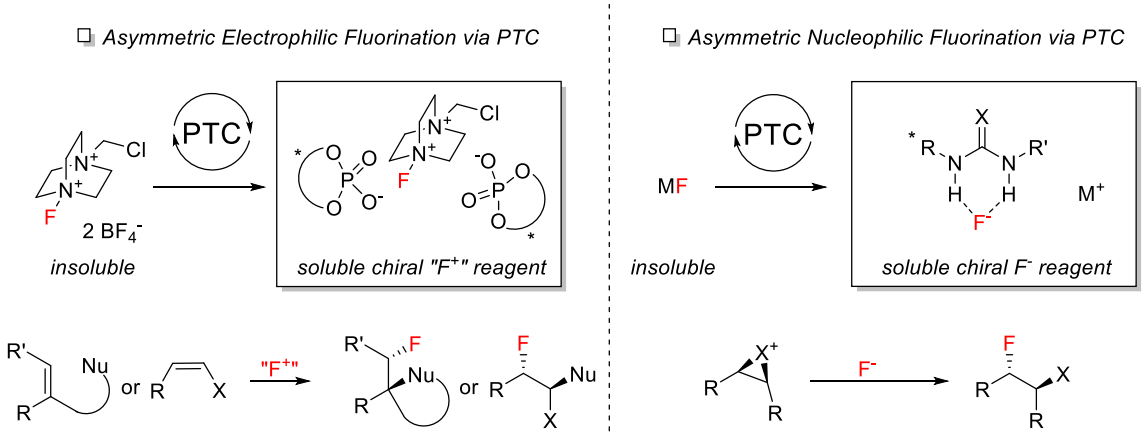
D

Entry	*R*	*Complex type*	*k_2 (S_N2)/ 10^{-5} $M^{-1}s^{-1}$*	*k_2 (S_N2)/ k_2'(E2)*
1	4-OMe	A	12.7	5.2
2	4-Me	A	9.8	5.7
3	3-Me	A	5.95	5.6
4	H	A	5.76	6.8
5	4-F	B	5.67	7.1
6	4-Cl	A	5.83	6.9
7	4-NO_2	A	3.2	8.4
8	4-CF_3	A	1.65	8.7
9	–	TBAF*$(H_2O)_3$	375	1.6

1.1.6 Asymmetric Hydrogen Bonding Phase-Transfer Catalysis (HB-PTC)

The possibility of fine-tuning fluoride reactivity *via* hydrogen bonding (section 1.1.5) offered an exciting opportunity for the development of enantioselective organocatalytic nucleophilic fluorination. The paucity of methodologies based on nucleophilic fluorinating reagents, compared to the vast literature covering the use of electrophilic fluorinating reagents in asymmetric catalysis,[64,65] is testament to the inherent challenges of this transformation.

The modular nature of chiral (thio)ureas is well-suited for catalyst design and this class of organocatalysts has been successfully employed in a variety of transformations.[66] Thus we envisaged that a chiral (thio)urea-fluoride complex could provide the desired level of enantioselectivity in the reaction with an appropriate electrophile. Moreover, the demonstrated ability of hydrogen bond donors to activate solid CsF (section 1.1.5.3) prompted us to merge hydrogen bonding with solid-liquid PTC, with the aim to develop a general catalytic manifold for the activation of insoluble inorganic salts. This approach is complementary to the enantioselective PTC protocols with electrophilic fluorinating reagents previously reported (sections 1.1.4.1 and 1.1.4.3) and offers the advantage of employing safe and economical alkali metal fluorides (Scheme 1.12).



Scheme 1.12: PTC for the activation of the fluorinating reagent in asymmetric catalysis.

1.2 β-Fluoroamines

This thesis focuses on the desymmetrisation of aziridinium ions to access β-fluoroamines, but application of enantioselective nucleophilic fluorination under HB-PTC has not been limited to these electrophiles.[67,68] β-Fluoroamines have found application in drug discovery (section 1.2.2.1) and catalyst design (section 1.2.2.2) because of the unique properties imparted by the presence of the fluorine substituent (section 1.2.1).

1.2.1 Fluorine for Molecular Editing

Due to its unique combination of small size (Van der Waals radius = 1.47 Å) and high electronegativity (χ_P = 3.98, Pauli), fluorine incorporation has a profound effect on the bio- and physicochemical properties of an organic molecule, making it an excellent tool for molecular editing.[69] The high electron-density of the fluorine atom is the cause of its low polarisability and of the low energy of its valence orbitals ($2s_{(F)}$: –40.1 eV, $2p_{(F)}$: –18.9 eV), not dissimilar to those of carbon ($2s_{(C)}$: –19.4 eV, $2p_{(C)}$: –10.7 eV).[70] This ensues the formation of a strong and highly polarised C–F bond (Bond dissociation energy, BDE: 115 kcal/mol; bond dipole moment: 1.41 D) and a low lying $\sigma^*_{(C–F)}$.

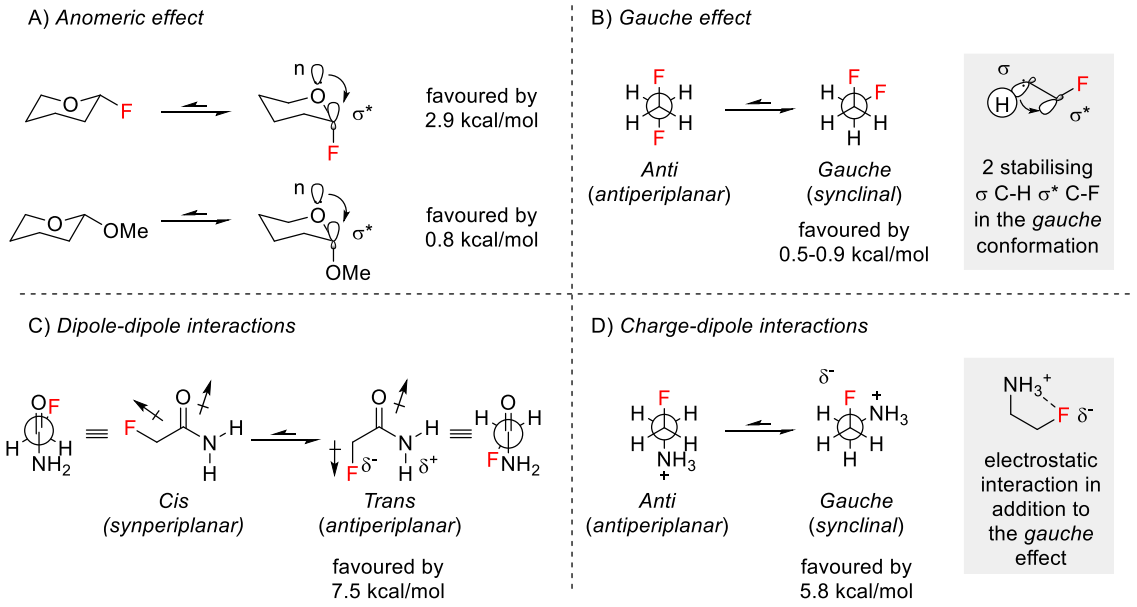
Table 1.5: Selected properties of several 2nd row elements and halogens and corresponding C–X bonds.[15,71,72]

Element (X)	*H*	*C*	*N*	*O*	***F***	*Cl*	*Br*	*I*
Van der Waals radius (Å)	1.20	1.70	1.55	1.52	**1.47**	1.75	1.85	1.98
Pauli electronegativity χ_P	2.20	2.55	3.04	3.44	**3.98**	3.16	2.96	2.66
Polarisability α ($Å^3$)	0.67	1.76	1.10	0.82	**0.56**	2.18	3.05	4.7
C–X BDE (kcal/mol)	98.0	83.1	69.7	84.0	**115**	78.5	64.3	50.7
C–X Bond length (Å)	1.09	1.54	1.47	1.43	**1.35**	1.77	1.94	2.13
C–X Bond dipole moment (D)	0.4	0.0	Substitution dependent		**1.41**	1.46	1.38	1.19

Collectively, these properties rationalise the unique behaviour of fluorinated compounds, such as increased lipophilicity of heavily fluorinated molecules, or the reduction in the pK_a of neighbouring functionalities (section 1.2.1.2). The strength of the C–F bond is exploited in medicinal chemistry to enhance metabolic stability, particularly towards enzymatic oxidation, while the stereoelectronic effects arising from fluorine substitution have found application both in medicinal and synthetic chemistry (section 1.2.1.1).[73–77]

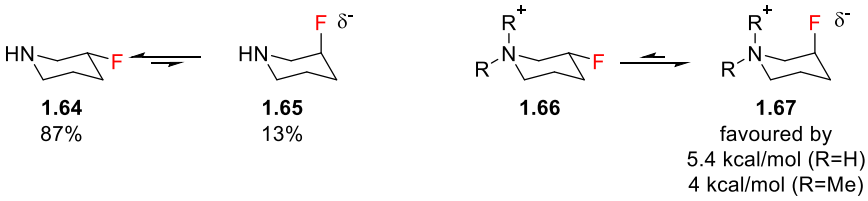
1.2.1.1 Conformational Bias

Scheme 1.13 summarises the factors responsible for conformational bias in molecules containing aliphatic C–F bonds.[69] Hyperconjugation, arising from the preferential interaction of the low lying $\sigma^*_{(C–F)}$ with electron-rich $\sigma_{(C–R)}$ (R= H, C) or $\pi_{(C–C)}$ orbitals, gives rise to the anomeric (Scheme 1.13A)[78] and the *gauche* effect (Scheme 1.13B). Minimisation of the overall dipole moment determines the preferred conformation in the presence of dipole-dipole interactions, as in the case of α-fluoroamides, where the two dipoles point in opposite directions (*trans*, Scheme 1.13C). The preference for this conformation is reinforced by an attractive electrostatic interaction ($N–H^{\delta+}---F^{\delta-}–C$).[79] Finally, electrostatic interaction with a positive charge favours the *gauche* conformer (Scheme 1.13D).



Scheme 1.13: Interactions determining conformational bias in fluorinated molecules. A) Anomeric effect.[78] B) *Gauche* effect. C) Dipole-dipole interactions. D) Charge-dipole interactions. [69]

Charge-dipole interactions are of particular importance for protonated β-fluoroamines. For instance, while in the neutral 3-fluoropiperidine in D_2O fluorine is found prevalently in the equatorial position, 3-fluoropiperidinium cations exist preferentially as the conformers with axial fluorine (Scheme 1.14).[80,81] Similarly, protonated 4-, 5- and 8-membered fluorinated nitrogen heterocycles, as well as acyclic β-fluoroammonium species were found to be strongly biased towards the conformer which maximises charge-dipole (N^+–H---$C^{\delta+}$–$F^{\delta-}$) interaction.[82–84]



Scheme 1.14: Preferred conformation of 3-fluoropiperidine and 3-fluoropiperidinium cations in D_2O. [80,81]

A stunning example illustrating the power of fluorination for molecular editing has been reported by Seebach and Jaun, who showed that a single fluorine substitution in the central amino acid of a β-heptapeptide dramatically affected its folding depending on stereochemistry.[85,86] The two epimers led either to the formation of a $3_{1,4}$ helix, where the

fluorine occupied an axial position (Figure 1.4, left), or to a structure presenting a central 10-membered hydrogen bonded ring (Figure 1.4, right). In both cases, the preferred structure arose from a combination of dipole-dipole interaction between the C–F bond and the neighbouring amide (in the box) and the *gauche* effect between the C–F bond and the C–N bond in the β position (in blue).

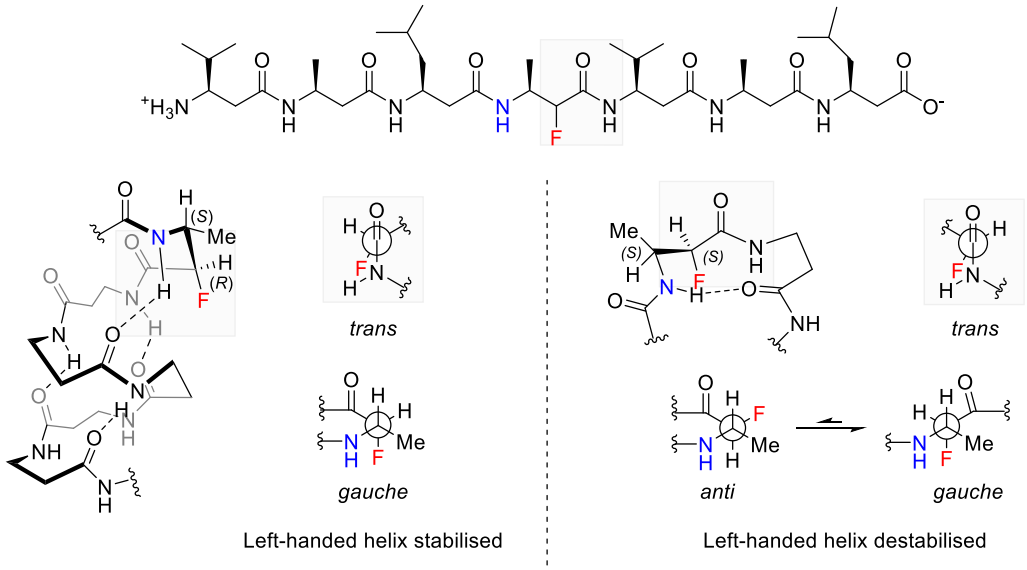
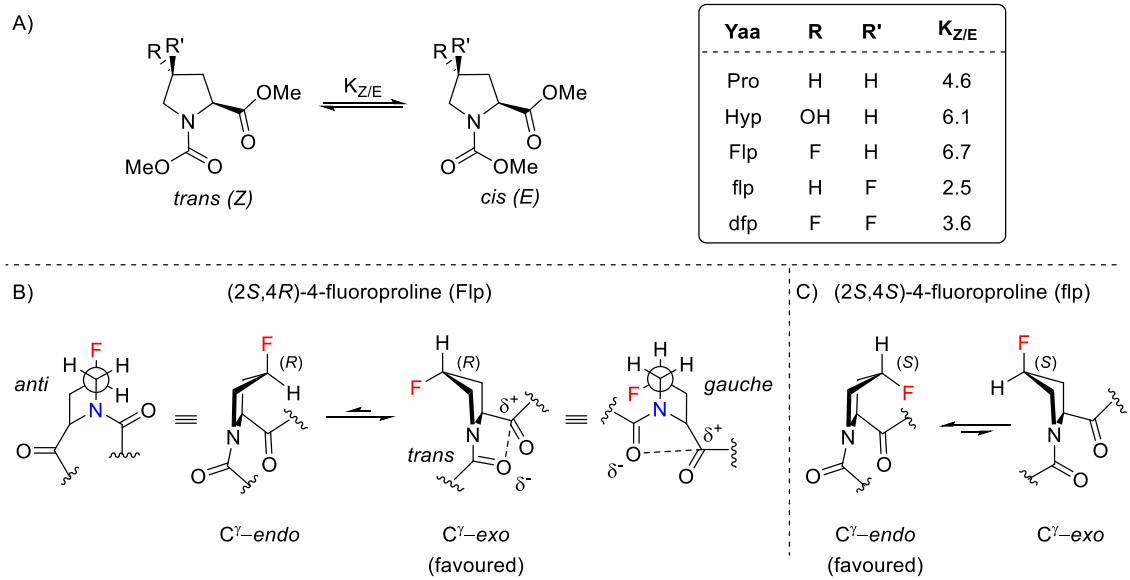


Figure 1.4: Influence of fluorine substitution on peptide folding. Additional substituents on the peptide chain in the 3D structures removed for clarity. [85,86]

Stereoselective fluorination has been used by the Reines group to shed light on the role of *trans*-4-hydroxy-L-proline (Hyd) in the formation and stability of the triple helix of collagen.[87] This fibrous protein is composed of three polypeptide chains where the sequence Gly-Xaa-Yaa (Gly = glycine) is repeated about 300 times. Xaa is usually L-Proline (Pro), while Yaa is more often Hyd. Substitution of either the Xaa or Yaa residues with (2*S*,4*R*)-4-fluoroproline (Flp), (2*S*,4*S*)-4-fluoroproline (flp) or (2*S*)-4,4-difluoroproline (Dfp) revealed that: i) Flp, but not flp stabilises collagen when introduced in the Yaa position;[87] ii) the reverse happens when the substitution occurs at the Xaa position;[88] iii) Dfp reduces the stability of triple helix regardless of the substitution pattern.[89] Taken together, these observations suggest that stereoelectronic effects rather than hydrogen bonding determine the tertiary structure of collagen. The final observation

was used by the authors to exclude the possibility that the enhanced stability imparted by 4-fluoroproline is due to the hydrophobic effect. In fact, the authors argued, if the main drive for collagen folding was the segregation of hydrophobic residues away from water, the lipophilic 4-fluoroproline and 4,4-difluoroproline should have been equally stabilising.

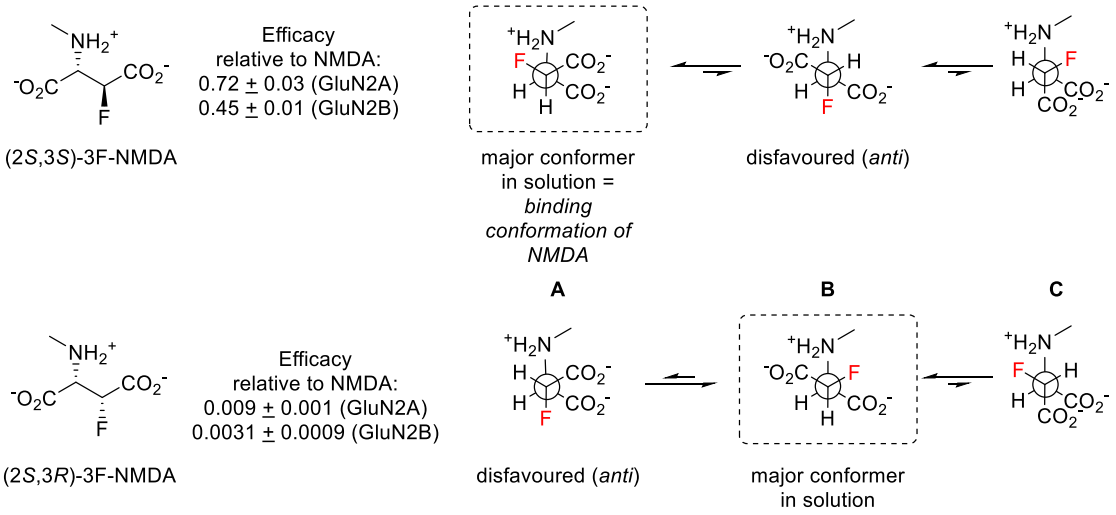
More specifically, a *gauche* effect between fluorine and the β-nitrogen is observed in both Flp and flp, but due to the opposite stereochemistry at C4 (= Cγ) Flp and flp adopt different puckered conformations (Flp: C^{γ} *exo* puckered, Scheme 1.15B; flp: C^{γ} *endo* puckered, Scheme 1.15C).[90] These are the preferred conformations adopted by Pro in the Yaa and Xaa positions, respectively. When part of a peptide bond, the *trans* (*Z*) configuration is favoured for Flp, because it allows a favourable interaction between the oxygen of the carbonyl$^{(i-1)}$ and the carbon of Flp carbonyl$^{(i)}$ (Scheme 1.15B). This corresponds of a dihedral angle ψ =141 °, which is close to ψ =150 ° required for the formation of the right-handed triple helix of collagen, thus reducing the entropic penalty paid by the protein upon folding.



Yaa	R	R'	$K_{Z/E}$
Pro	H	H	4.6
Hyp	OH	H	6.1
Flp	F	H	6.7
flp	H	F	2.5
dfp	F	F	3.6

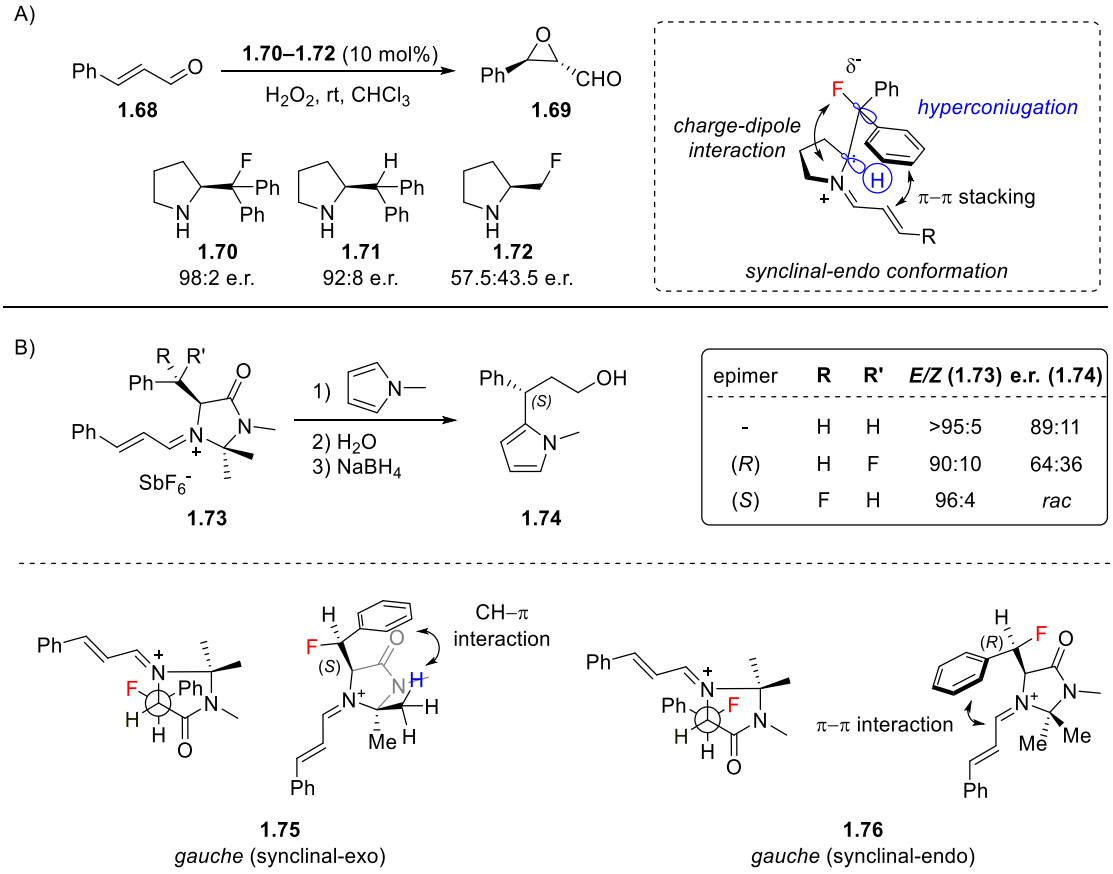
Scheme 1.15: Preferred conformation of C4-substituted proline. A) Effect of substitution on the geometry of the peptide bond (*E*/*Z*).[87] B) Conformational equilibrium of (2*S*,4*R*)-4-fluoroproline (Flp). C) Conformational equilibrium of (2*S*,4*S*)-4-fluoroproline (flp).

The potency of a protein ligand can be greatly enhanced by preorganisation, making stereoselective fluorination invaluable for biological studies and medicinal chemistry. For example, the two diastereoisomers of 3F-NMDA (3-fluoro-*N*-methyl-D-aspartate), epimeric at the fluorinated C3, showed a remarkable difference in potency against both GluN2A and GluN2B receptors, though neither outcompeted the parent NMDA (*N*-methyl-D-aspartate) as receptor agonist.[91] These probes are zwitterionic species and adopt distinctive conformations in solution, due to a stabilising charge-dipole interaction (Scheme 1.16). Conformation **A**, required for binding to the target protein, is disfavoured for (2*S*,3*R*)-3F-NMDA, due to the antiperiplanar arrangement of the C–F and C–N^+ bonds.



Scheme 1.16: 3F-NMDA conformations and their efficacy relative to NMDA.[91]

Preorganisation also plays an important role in asymmetric catalysis. As part of their systematic investigation of fluorine as stereocontrol element in catalyst design,[92] the Gilmour group has studied β-fluoroamines in iminium ion organocatalysis, using the epoxidation of α,β-unsaturated aldehydes as model reaction.[93] They proposed that a combination of the fluorine-iminium ion *gauche* effect and secondary π-stacking interactions favours the *synclinal-endo* conformation in the transition state (Scheme 1.17A), resulting in enhanced selectivity compared to the non-fluorinated catalyst (98:2 e.r. *versus* 92:8 e.r.).



Scheme 1.17: β-Fluoroamines in iminium ion organocatalysis. A) Effect of fluorine substitution in the asymmetric epoxidation of α,β-unsaturated aldehydes.[93] B) Conformer equivalents of McMillan's imidazolidinone, and evaluation of their selectivity in Michael addition to cinnamaldehyde.[94]

Moreover, selective fluorination allowed the same group to confirm the stereochemical model proposed for the enantioselective Michael additions catalysed by MacMillan's first generation imidazolidinone. Based on solid state data and computations, Seebach and Grimme had proposed a "windshield wiper model" wherein the freely-rotating benzyl group can move from a conformation where the phenyl ring rests on top of the heterocycle (*synclinal-exo*, Scheme 1.17B) to the one in which it shields the *Re* face of the iminium π-system (*synclinal-endo*, Scheme 1.17B).[95] Two "conformer equivalents" of these species were synthesised by selective fluorination at the benzylic position.[94] Both epimers exhibited a strong *gauche* effect, which allowed to lock the iminium ion in the desired conformation *synclinal-exo* and *synclinal-endo* (Scheme 1.17B). The better enantioselectivity observed in the presence of the *synclinal-endo* conformer (64:36 e.r.

versus 50:50 e.r.), where the phenyl ring is shielding the *Re* face, supports the validity of this model.

1.2.1.2 pK_a Modulation

Basic nitrogen atoms are ubiquitous in biological active molecules. The value of their pK_a influences not only the binding affinity at the target, but also the drug biodistribution and its off-target interactions, making its fine-tuning an important aspect in lead optimisation.[96] It is well-known that electron-negative atoms, such as fluorine and oxygen, reduce the pK_a of neighbouring functionalities *via* inductive effect through the connecting bonds. This can be easily predicted for acyclic amines where each fluorine atom introduced in the β-position contributes to a decrease of the pK_a of 1.6–1.7 units. This effect decreases rapidly as the number of bonds separating the two functionalities increases (γ-fluorination: $\Delta pK_a = –0.7$; δ-fluorination: $\Delta pK_a = –0.3$; ε-fluorination: $\Delta pK_a = –0.1$, Figure 1.5).

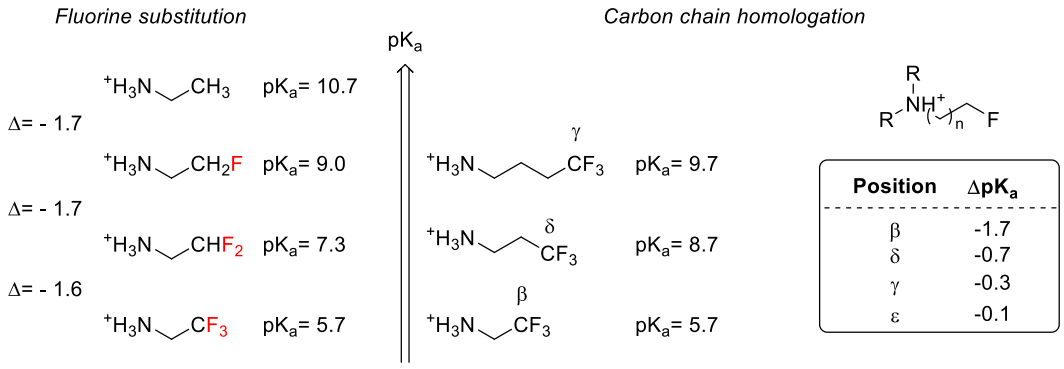


Figure 1.5: Effect of fluorine substitution and carbon chain homologation on amines pK_a.[96]

Reasonable predictions can be obtained for unconstrained cyclic systems, too, remembering that fluorine acts as σ-acceptor *via* all the interconnecting bonds (Figure 1.6A). However, conformational effects depending on C–F stereochemistry, as well as the presence of through-space interactions in rigid (poly)cyclic systems might result in deviation from predicted values (Figure 1.6B).

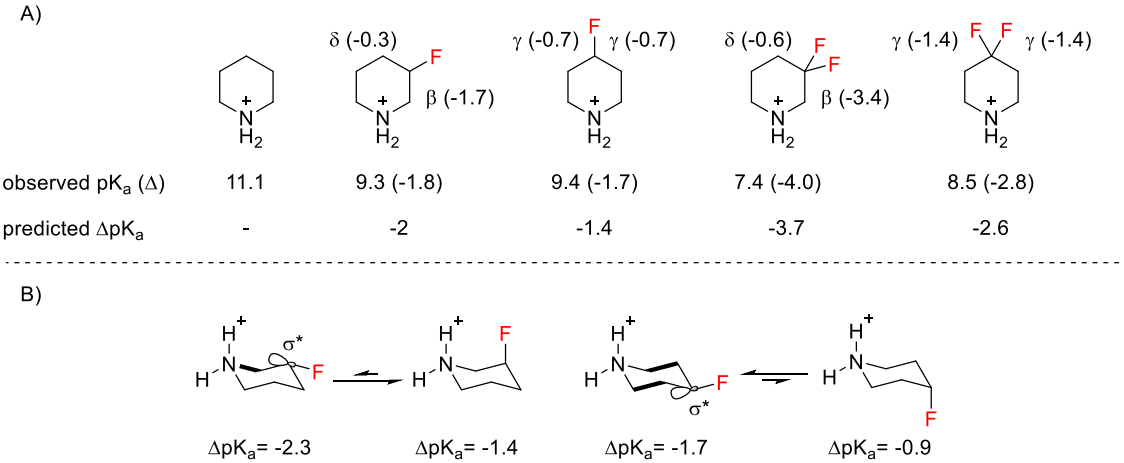


Figure 1.6: Influence of fluorination on the pK_a of cyclic amines.[96] A) Prediction for cyclic amines. B) Influence of stereochemistry.

1.2.2 β-Fluoroamines Applications

1.2.2.1 β-Fluoroamines in Drug Discovery

β-Fluoroamines have found application in many therapeutic areas, including but not limited to cancer, diabetes, CNS pathologies, HIV, and other viral diseases. A couple of radiotracers for brain imaging have been reported containing the radioactive isotope of fluorine (^{18}F) as part of a β-fluoroamino motif (Figure 1.9). Figures 1.7–1.9 report a survey of drug candidates at different stages of development, from lead optimisation to commercialisation. They have been divided into three categories based on the structure of the β-fluoroamino motif: a) cyclic, where at least one nitrogen is not part of the cycle (Figure 1.7); b) fluorinated *N*-heterocycles, (Figure 1.8); and c) linear, (Figure 1.9). From a structural point of view, the majority of β-fluoroamines are found either on a heterocycle, such as pyrrolidine, piperidine or a furanose ring (Figure 1.7), which constitutes the core of many antiviral drugs, or as a modification of the heterocycle itself (Figure 1.8). Regarding the acyclic structures, the most prominent example consists of modified α-amino acids that have been reported as suicide substrates for PLP-dependent enzymes

(Figure 1.9).[97] When it is not part of a cyclic structure, the nitrogen is predominantly in the form of a free primary amine or substituted with an electron-withdrawing group.

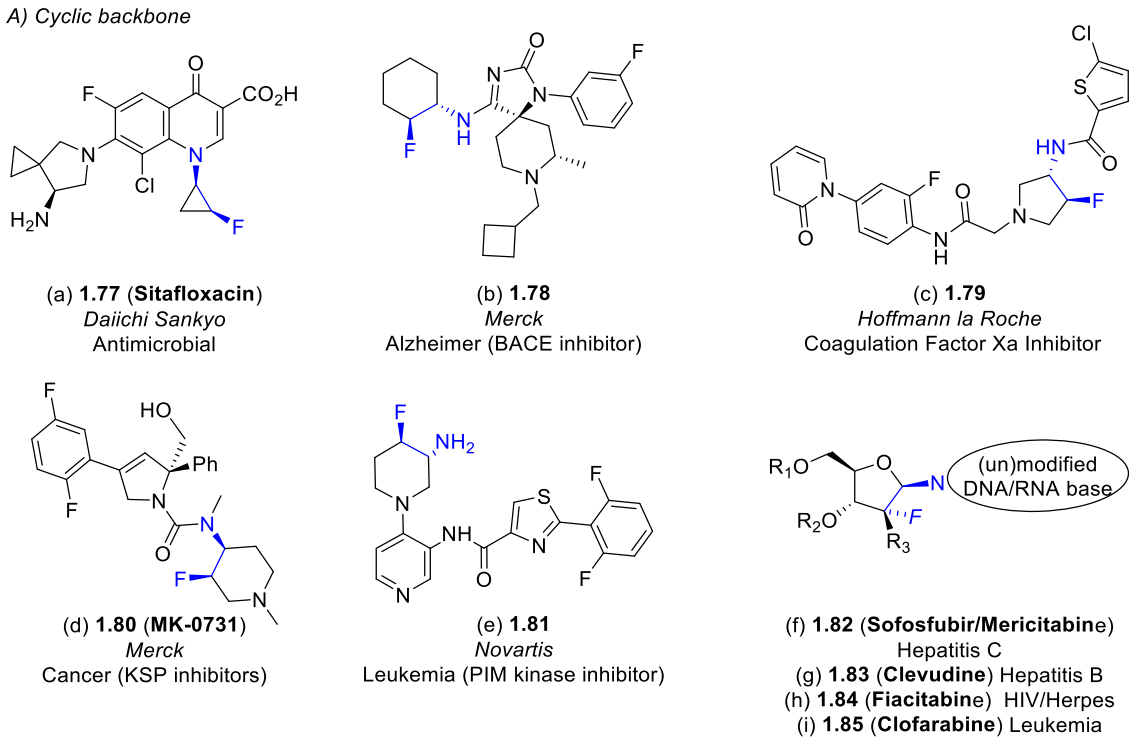


Figure 1.7: β-Fluoroamines in drug discovery with cyclic scaffolds: (a)[98] (b)[99] (c)[100] (d)[101] (e)[102,103] (f)[104] (g)[105] (h)[106] (i)[107].

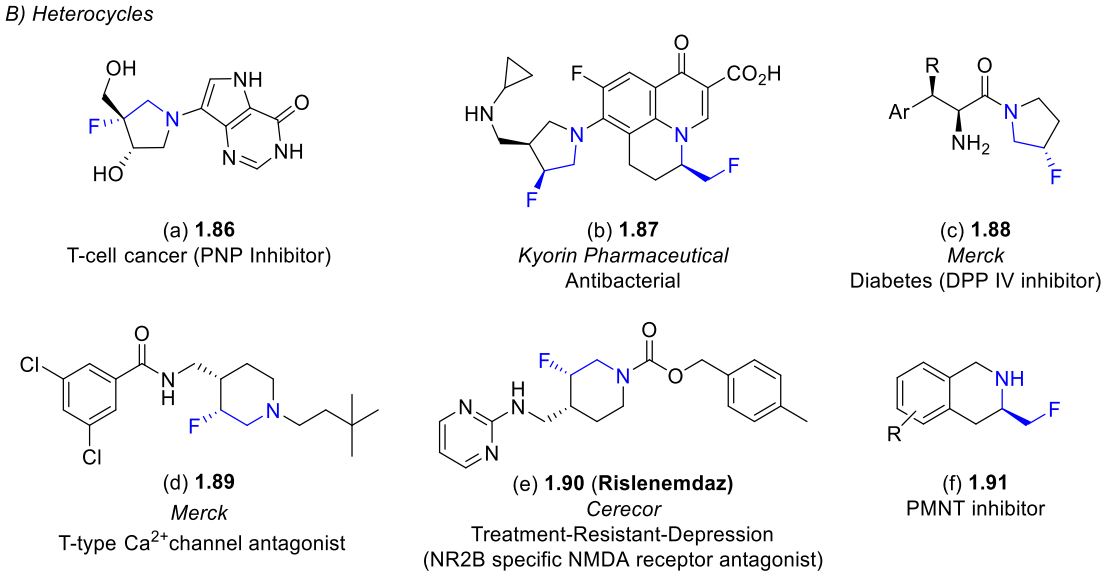


Figure 1.8: Cyclic β-fluoroamines in drug discovery: (a)[108] (b)[109] (c)[110] (d)[111] (e)[112] (f)[113].

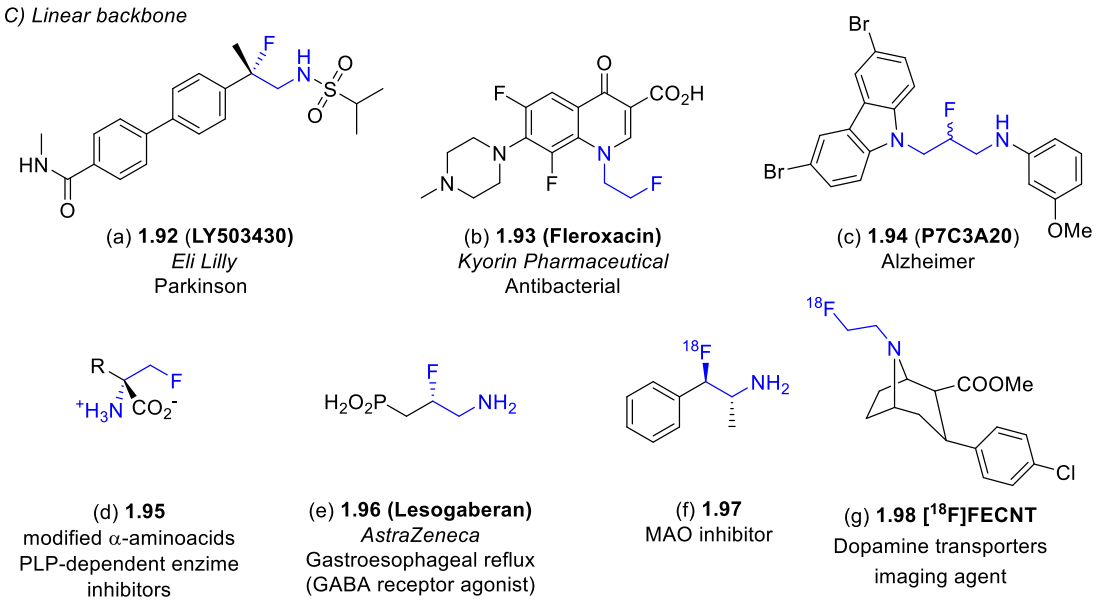


Figure 1.9: β-Fluoroamines in drug discovery: linear scaffold: (a)[114] (b)[115] (c)[116] (d)[97] (e)[117] (f)[118] (g)[119].

1.2.2.2 β-Fluoroamines in Catalyst Design for Asymmetric Synthesis

As detailed in the previous section (section 1.2.1.1), fluorine is an excellent tool for molecular editing, and as such, it has found application in the design of organocatalysts for asymmetric transformations.[76,77,92] Figure 1.10 offers an overview of the organocatalysts containing the β-fluoroamino motif developed to date.

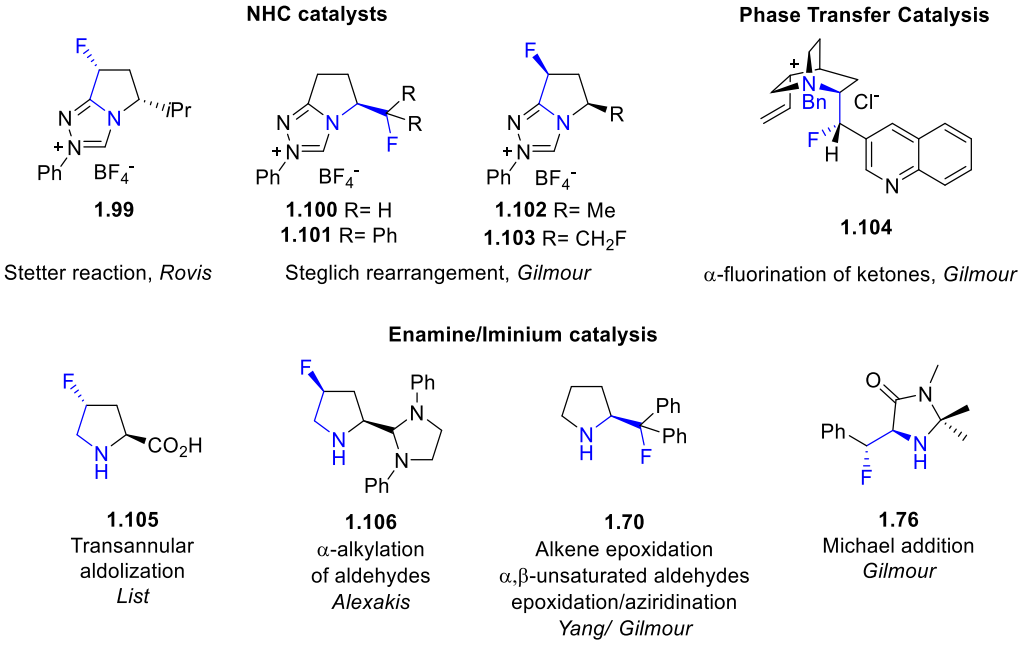
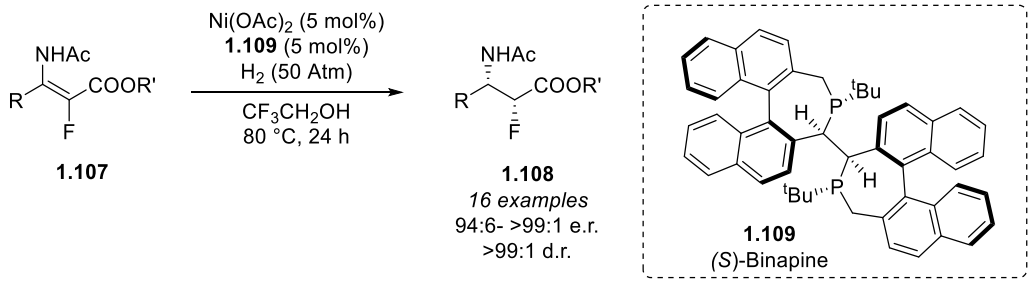


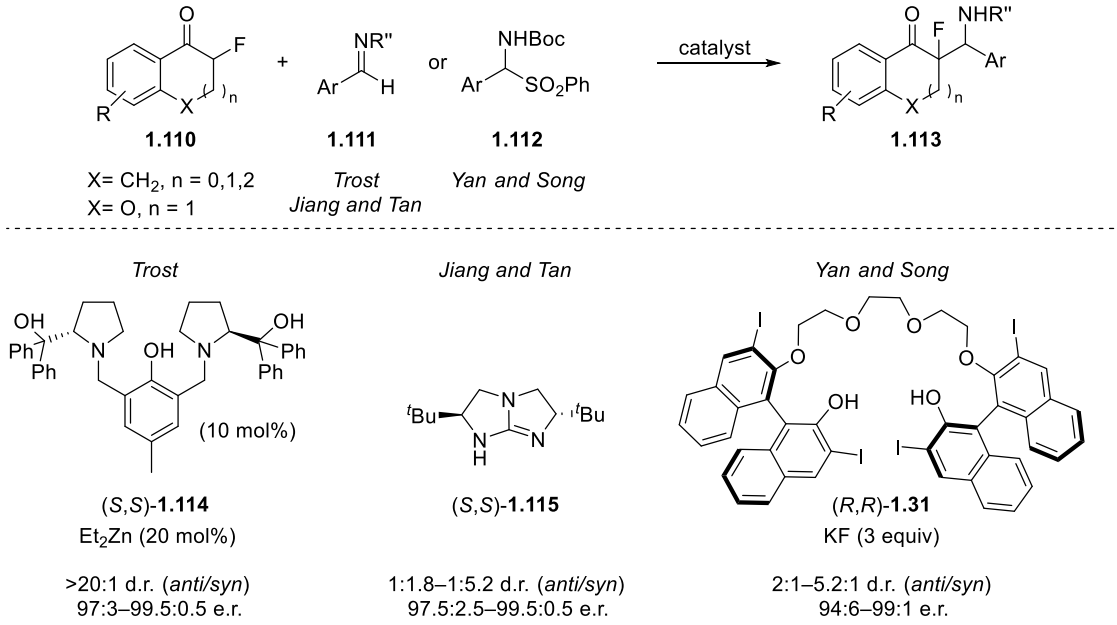
Figure 1.10: Organocatalysts containing the β-fluoroamino motif. [92,120]

1.2.3 Enantioselective Synthesis of β-Fluoroamines

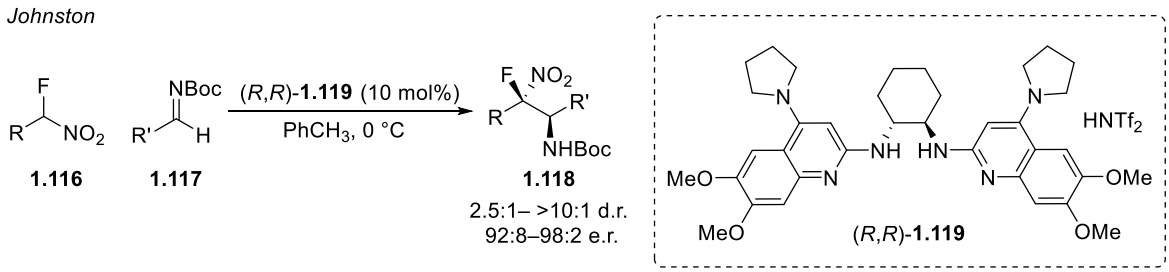
Enantioselective methodologies have been reported for the synthesis of β-fluoroamine based on fluorinated building-blocks. These involve either nickel-catalysed hydrogenation of fluoroenamides (Scheme 1.18),[121] or Mannich reactions to form the central C–C bond (Schemes 1.19–1.20).[122–126] In the latter case, an activating group is needed to generate the nucleophile, thus limiting the scope to enolizable substrates.



Scheme 1.18: Enantioselective synthesis of β-fluoroamine *via* catalytic hydrogenation.[121]



Scheme 1.19: Enantioselective Mannich reaction under Lewis acid (Trost),[122] Brønsted base (Jiang and Tan),[123] and cation-binding (Yan and Song)[124] catalysis.

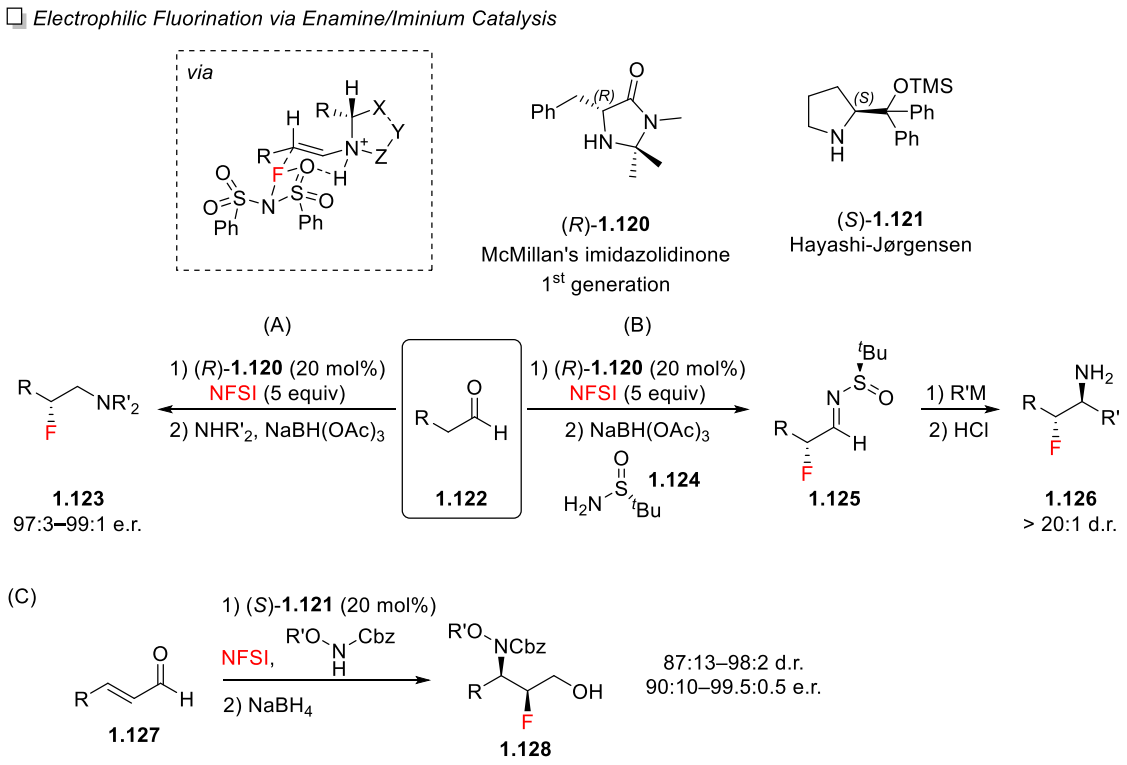


Scheme 1.20: Enantioselective aza-Henry reaction.[126]

1.2.3.1 Enantioselective Electrophilic Fluorination

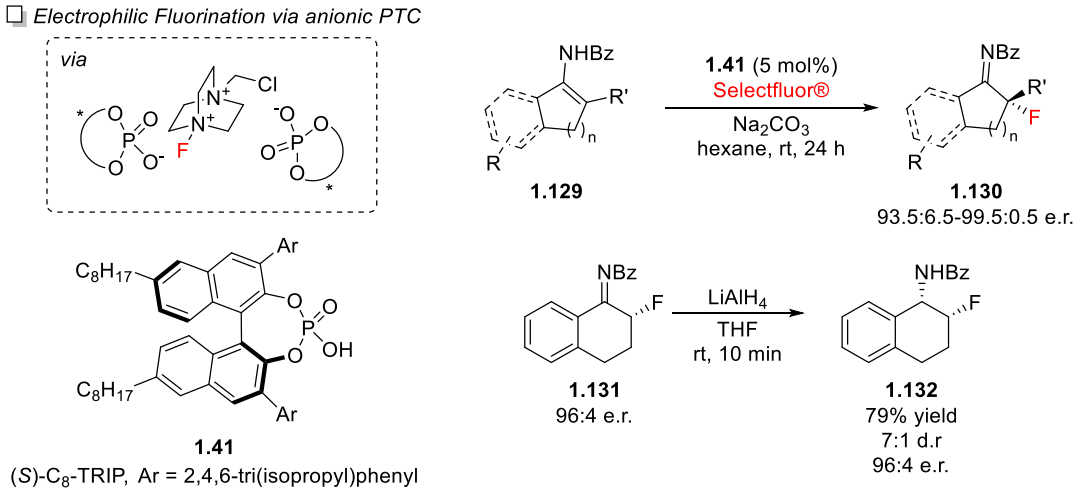
An alternative approach relies on the enantioselective construction of the C–F bond. Enamine and phase-transfer catalysis in combination with electrophilic fluorinating reagents have been used to access β-fluoroamine precursors in high enantiomeric ratio. Subsequent reduction affords the desired β-fluoroamines.

The highly enantioselective (up to 99.5:0.5 e.r.) α-fluorination of aldehydes with NFSI catalysed by secondary amines was independently reported by McMillan, Jørgensen and Barbas III in 2005.[127–129] Lindsley *et al.* have adapted this procedure to the synthesis of β-fluoroamines, developing a one-pot-two-step protocol based on enantioselective fluorination catalysed by McMillan's imidazolidinone, followed by reductive amination (Scheme 1.21A).[130,131] Since, at the time, ketones were poor substrates for the asymmetric fluorination,[132] the use of a chiral auxiliary was envisaged to access branched β-fluoroamines with high control of both diastereo and enantioselectivity (Scheme 1.21B).[133] The Hayashi-Jørgensen organocatalyst was found optimal instead for the one-pot aminofluorination of α,β-unsaturated aldehydes proceeding *via* an iminium-enamine organocascade (Scheme 1.21C).[134] The corresponding primary β-fluoroamine could be accessed *via* catalytic hydrogenation (R' =Bn).[135]



Scheme 1.21: Synthesis of β-fluoroamines *via* enamine/iminium catalysis. A) One-pot organocatalytic enantioselective α-fluorination/reductive amination of aldehydes.[130] B) Enantioselective synthesis of branched β-fluoroamines.[133] C) One-pot aminofluorination of α,β-unsaturated aldehydes *via* iminium ion-enamine organocascade.[134]

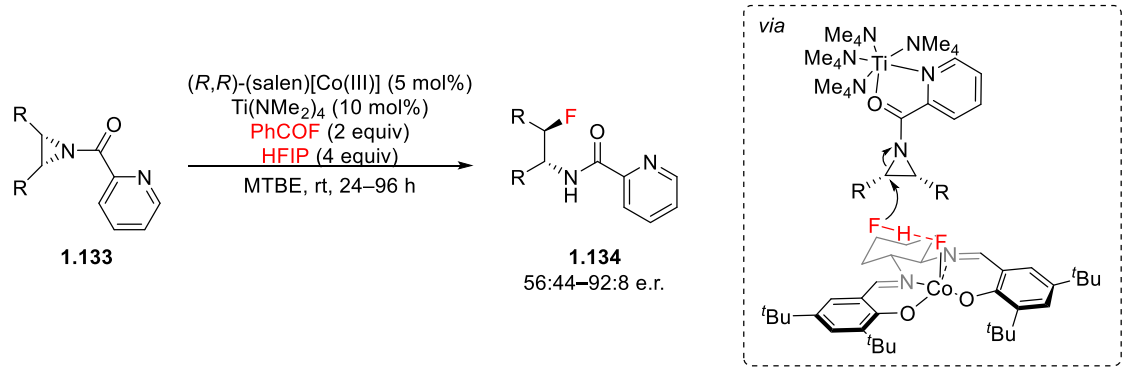
The Toste group applied anionic PTC (section 1.1.4.3) to the synthesis of enantioenriched α-fluoroimines (93.5:6.5–99.5:0.5 e.r.) with Selectfluor® in the presence of a chiral phosphoric acid (Scheme 1.22).[136] These products can be stereoselectively reduced to access *syn* β-fluoroamines.



Scheme 1.22: Electrophilic α-fluorination of enamides under asymmetric anionic PTC. [136]

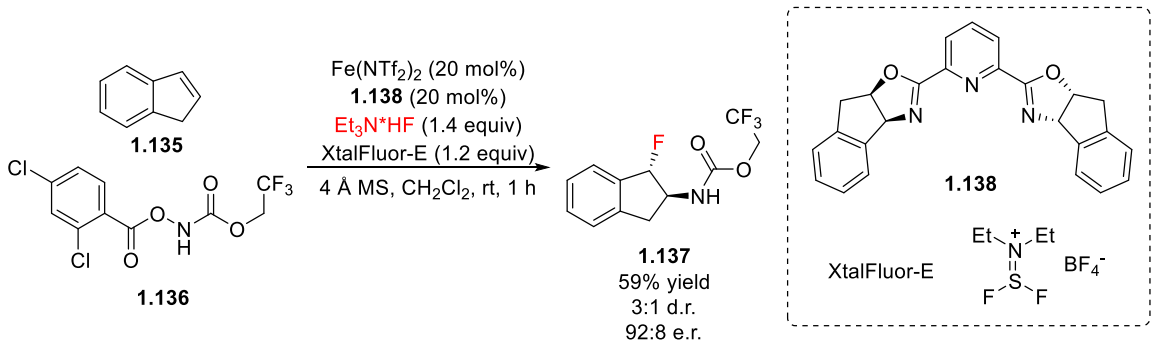
1.2.3.2 Enantioselective Nucleophilic Fluorination

Reported synthesis of β-fluoroamines *via* asymmetric nucleophilic fluorination employ hydrogen fluoride (HF), directly or by *in situ* generation, as fluoride source. Moderate to good enantioselectivities (up to 92:8 e.r.) were obtained by Doyle and Kalow in the desymmetrisation of activated *meso* azetidines under cooperative Lewis acid catalysis (Scheme 1.23).[137] A chelating protecting group derived from picolinamide was found to be crucial to activate the aziridine through coordination of the achiral Ti(IV) cocatalyst. The nucleophile was proposed to be delivered in an asymmetric fashion by the chiral cobalt (III) bifluoride [(*R*,*R*)-(salen)Co(III)F(HF)] generated *in situ* from hexafluoro isopropanol (HFIP) and benzoyl fluoride.



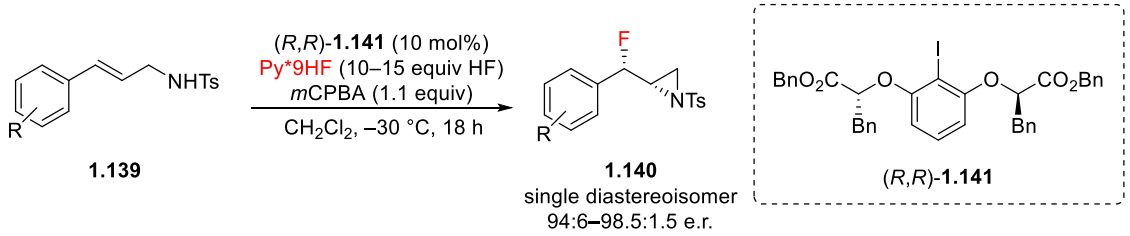
Scheme 1.23: Desymmetrisation of activated azetidines with HF under cooperative Lewis acid catalysis.[137]

Numerous transition metal-catalysed (Pd, Ag, Au, Cu, Fe) protocols have been reported for the aminofluorination of olefins using achiral catalysts.[138] The Xu group investigated the use of earth-abundant Iron (II) pre-catalysts in combination with Et_3N*3HF and XtalFluor-E.[139,140] As a proof of principle, the reaction of indene was carried out in the presence of a chiral PyBOX ligand (Scheme 1.24). A good level of enantioselectivity (92:8 e.r. for both diastereoisomers) was obtained, albeit at the expense of both reactivity and diastereoselectivity (59% yield, 3:1 d.r. = diastereomeric ratio).[140]



Scheme 1.24: Iron-catalysed asymmetric aminofluorination of unfunctionalised alkenes. [140]

In 2013, Nevado *et al.* reported the metal-free regio- and enantioselective aminofluorination of alkenes in the presence of stoichiometric chiral non-racemic aryliododifluoride.[141] Using *meta*-chloroperbenzoic acid (*m*CPBA) as stoichiometric oxidant, Shibata and co-workers succeeded in making the reaction catalytic in aryl iodide.[142] Both protocols suffered from moderate enantiocontrol (Nevado: 80.5:19.5–94:6 e.r.; Shibata: 72.5:27.5–85:15 e.r.) and it was only recently that the Jacobsen group improved the methodology to access β-fluoroaziridines with high selectivity (94:6–98.5:1.5 e.r., Scheme 1.25)[143] These fluorinated building-blocks could be treated with a variety of nucleophiles to access highly functionalised β-fluoroamines.



Scheme 1.25: Diastereo- and enantioselective organocatalytic aminofluorination of alkenes.[143]

1.3 Conclusions and Thesis Outline

β-Fluoroamines are an important motif in medicinal chemistry, where the introduction of fluorine in proximity to the basic nitrogen is a well-known strategy for pK_a fine-tuning during drug discovery campaigns. Moreover, stereocontrolled introduction of fluorine into peptide chains or chiral secondary amine-organocatalysts has proved useful to induce conformational bias. Thus, methodologies that allow the enantio- and diastereoselective construction of vicinal fluoroamines are in high demand and ideally should employ safe and inexpensive fluorinating reagents. This thesis describes the development of hydrogen bonding phase-transfer catalysis (HB-PTC) for asymmetric fluorination with alkali metal fluorides. HB-PTC has been applied to the synthesis of enantioenriched β-fluoroamines with a focus on the industrial application of the methodology.

Chapter 2 introduces HB-PTC and describes the development of the methodology for the asymmetric synthesis of β-fluoroamines using KF. The scope of the transformation is reported and rationalised *via* computational modelling performed by Dr. David Ascough, while the experimental work is my own. Contributions of other synthetic chemists (Dr. Gabriele Pupo and Dr. Francesco Ibba) with whom I closely collaborated during this project are clearly stated. Chapter 3 focuses on the development of a practical and scalable synthesis of the novel class of *N*-alkyl bis-urea developed in Chapter 2. Different synthetic routes were explored, and the advantages and drawbacks of each are compared. Finally, Chapter 4 reports the study of the scale up (200 g) of the enantioselective fluorination in a mechanically stirred 1 L reactor, representing a proof of principle that HB-PTC can be applied in industrial setting. Thermal safety tests and preliminary calculations on the mixing requirements are included.

1.4 References

(1) Reuss, G.; Disteldorf, W.; Gamer, A. O.; Hilt, A. "Fluorine." *Ullmann's Encycl. Ind. Chem.* **2012**, *15*, 735–768.

(2) Tressaud, A. "Henri Moissan: Winner of the Nobel Prize for Chemistry 1906." *Angew. Chemie - Int. Ed.* **2006**, *45*, 6792–6796.

(3) Dobbin, L. "Daniel Rutherford's Inaugural Dissertation." *J. Chem. Educ.* **1935**, 370.

(4) "Joseph Priestley and the Discovery of Oxygen" http://www.acs.org/content/acs/en/education/whatischemistry/landmarks/josephpriestleyoxygen.html (accessed Jul 2, 2020).

(5) Emsley, J. "Chlorine" https://edu.rsc.org/elements/chlorine/2000019.article (accessed Jul 2, 2020).

(6) Dronsfield, A.; Ellis, P.; Swain, P. "Discovering Iodine" https://edu.rsc.org/feature/discovering-iodine/2020126.article (accessed Jul 2, 2020).

(7) "Periodic Table: Bromine" https://www.rsc.org/periodic-table/element/35/bromine (accessed Jul 2, 2020).

(8) Champagne, P. A.; Desroches, J.; Hamel, J. D.; Vandamme, M.; Paquin, J. F. "Monofluorination of Organic Compounds: 10 Years of Innovation." *Chem. Rev.* **2015**, *115*, 9073–9174.

(9) Harsanyi, A.; Sandford, G. "Organofluorine Chemistry: Applications, Sources and Sustainability." *Green Chem.* **2015**, *17*, 2081–2086.

(10) US Geological Survey. *Mineral Commodity Summary 2020: Fluorspar*.

(11) Villalba, G.; Ayres, R. U.; Schroder, H. "Accounting for Fluorine: Production, Use and Loss." *J. Ind. Ecol.* **2007**, *11*, 85–101.

(12) Liang, S.; Hammond, G. B.; Xu, B. "Hydrogen Bonding: Regulator for Nucleophilic Fluorination." *Chem. - A Eur. J.* **2017**, *23*, 17850–17861.

(13) Baldochi, S. L.; Ranieri, I. M. "Alkali Halide Crystals Growth." *Ref. Modul. Mater. Sci. Mater. Eng.* **2016**, 1–6.

(14) Zhan, C. G.; Dixon, D. A. "Hydration of the Fluoride Anion: Structures and Absolute Hydration Free Energy from First-Principles Electronic Structure Calculations." *J. Phys. Chem. A* **2004**, *108*, 2020–2029.

(15) *CRC Handbook of Chemistry and Physics*, 85th ed.; Lide, D. R., Ed.; CRC Press: Boca Raton, FL, 2004.

(16) Wynn, D. A.; Roth, M. M.; Pollard, B. D. "The Solubility of Alkali-Metal Fluorides in Non-Aqueous Solvents with and without Crown Ethers, as Determined by Flame Emission Spectrometry." *Talanta* **1984**, *31*, 1036–1040.

(17) Sasson, Y.; Mushkin, N.; Abu, E.; Negussie, S.; Dermeik, S.; Zoran, A. "Fluoride Anion as a Base and a Nucleophile in Phase-Transfer Catalysis of Uncharged Species." *ACS Symp. Ser.* **1997**, *659*, 148–162.

(18) Clark, J. H. "Fluoride Ion as a Base in Organic Synthesis." *Chem. Rev.* **1980**, *80*, 429–452.

(19) Bordwell, F. G. "Equilibrium Acidities in Dimethyl Sulfoxide Solution." *Acc. Chem. Res.* **1988**, *21*, 456–463.

(20) Matthews, W. S.; Bares, J. E.; Bartmess, J. E.; Bordwell, F. G.; Cornforth, F. J.; Drucker, G. E.; Margolin, Z.; Mccallum, R. J.; Mccollum, G. J.; Vanier, N. R. "Equilibrium Acidities of Carbon Acids . VI . Establishment of an Absolute Scale of Acidities in Dimethyl Sulfoxide Solution." *J. Am. Chem. Soc.* **1972**, *97*, 7006–7014.

(21) Sharma, R. K.; Fry, J. L. "Instability of Anhydrous Tetra-*N*-Alkylammonium Fluorides." *J. Org.*

Chem. **1983**, *48*, 2112–2114.

(22) Sun, H.; DiMagno, S. G. "Anhydrous Tetrabutylammonium Fluoride." *J. Am. Chem. Soc.* **2005**, *127*, 2050–2051.

(23) Liotta, C. L.; Harris, H. P. "The Chemistry of 'Naked' Anions. I. Reactions of the 18-Crown-6 Complex of Potassium Fluoride with Organic Substrates in Aprotic Organic Solvents." *J. Am. Chem. Soc.* **1974**, *96*, 2250–2252.

(24) Starks, C. M.; Liotta, C. L.; Halpern, M. *Phase-Transfer Catalysis Fundamentals, Applications and Industrial Perspectives*; Chapmann & Hall: London, UK, 1994.

(25) Sasson, Y.; Zahalka, H. A. "Catalyst Poisoning Phenomenon in Phase Transfer Catalysis: Effect of Aqueous Phase Concentration." *J. Chem. Soc. Chem. Commun.* **1983**, 1347–1349.

(26) Sasson, Y.; Arrad, O.; Dermeik, S.; Zahalka, H. A.; Weiss, M.; Wiener, H. "The Role of Water in Phase Transfer Catalysis." *Mol. Cryst. Liq. Cryst. Inc. Nonlinear Opt.* **1988**, *161*, 495–516.

(27) Dermeik, S.; Sasson, Y. "Effect of Water on the Extraction and Reactions of Fluoride Anion by Quaternary Ammonium Phase-Transfer Catalysts." *J. Org. Chem.* **1985**, *50*, 879–882.

(28) Dermiek, S.; Sasson, Y. "Darstellung von Primaren Alkylfluoriden Unter Einsatz Der Phasen Transfer Katalyse." *J. Fluor. Chem.* **1983**, *22*, 431–437.

(29) Liotta, C. L.; Burgess, E. M.; Ray, C. C.; Black, E. D.; Fair, B. E. "Mechanism of Phase-Transfer Catalysis: The Omega Phase." *ACS Symp. Ser.* **1987**, 15–23.

(30) Liotta, C. L.; Berkner, J.; Wright, J.; Fair, B. "Mechanisms and Applications of Solid-Liquid Phase-Transfer Catalysis." *ACS Symp. Ser.* **1997**, 29–40.

(31) Brak, K.; Jacobsen, E. N. "Asymmetric Ion-Pairing Catalysis." *Angew. Chemie - Int. Ed.* **2013**, *52*, 534–561.

(32) Dolling, U. H.; Davis, P.; Grabowski, E. J. J. "Efficient Catalytic Asymmetric Alkylations. 1. Enantioselective Synthesis of (+)-Indacrinone *via* Chiral Phase-Transfer Catalysis." *J. Am. Chem. Soc.* **1984**, *106*, 446–447.

(33) Burke, A. J.; Marques, C. S.; Turner, N. J.; Hermann, G. J. *Active Pharmaceutical Ingredients in Synthesis, Catalytic Processes in Research and Development*; Wiley-VCH: Weinheim, Germany, 2018.

(34) Ooi, T.; Doda, K.; Maruoka, K. "Distinct Advantage of the *in Situ* Generation of Quaternary Ammonium Fluorides under Phase-Transfer Conditions toward Catalytic Asymmetric Synthesis." *Org. Lett.* **2001**, *3*, 1273–1276.

(35) Kim, D. Y.; Park, E. J. "Catalytic Enantioselective Fluorination of β-Keto Esters by Phase-Transfer Catalysis Using Chiral Quaternary Ammonium Salts." *Org. Lett.* **2002**, *4*, 545–547.

(36) Wang, X.; Lan, Q.; Shirakawa, S.; Maruoka, K. "Chiral Bifunctional Phase Transfer Catalysts for Asymmetric Fluorination of β-Keto Esters." *Chem. Commun.* **2010**, *46*, 321–323.

(37) Yan, H.; Jang, H. Bin; Lee, J. W.; Kim, H. K.; Lee, S. W.; Yang, J. W.; Song, C. E. "A Chiral-Anion Generator: Application to Catalytic Desilylative Kinetic Resolution of Silyl-Protected Secondary Alcohols." *Angew. Chemie - Int. Ed.* **2010**, *49*, 8915–8917.

(38) Carter, C.; Fletcher, S.; Nelson, A. "Towards Phase-Transfer Catalysts with a Chiral Anion: Inducing Asymmetry in the Reactions of Cations." *Tetrahedron Asymmetry* **2003**, *14*, 1995–2004.

(39) Hamilton, G. L.; Kanai, T.; Toste, F. D. "Chiral Anion-Mediated Asymmetric Ring Opening of *Meso*-Aziridinium and Episulfonium Ions." *J. Am. Chem. Soc.* **2008**, *130*, 14984–14986.

(40) Rauniyar, V.; Lackner, A. D.; Hamilton, G. L.; Toste, F. D. "Asymmetric Electrophilic Fluorination Using an Anionic Chiral Phase-Transfer Catalyst." *Science* **2011**, *334*, 1681–1684.

(41) Ford, D. D.; Lehnherr, D.; Kennedy, C. R.; Jacobsen, E. N. "Anion-Abstraction Catalysis: The Cooperative Mechanism of α-Chloroether Activation by Dual Hydrogen-Bond Donors." *ACS Catal.*

2016, *6*, 4616–4620.

(42) Birrell, J. A.; Desrosiers, J. N.; Jacobsen, E. N. "Enantioselective Acylation of Silyl Ketene Acetals through Fluoride Anion-Binding Catalysis." *J. Am. Chem. Soc.* **2011**, *133*, 13872–13875.

(43) Arunan, E.; Desiraju, G. R.; Klein, R. A.; Sadlej, J.; Scheiner, S.; Alkorta, I.; Clary, D. C.; Crabtree, R. H.; Dannenber, J. J.; Hobza, P.; Kjaergaard, H. G.; Legon, A. C.; Mennucci, B.; Nesbitt, D. J. "Definition of the Hydrogen Bond (IUPAC Recommendations 2011)." *Pure Appl. Chem.* **2011**, *83*, 1637–1641.

(44) Steiner, T. "The Hydrogen Bond in the Solid State." *Angew. Chemie - Int. Ed.* **2002**, *41*, 48–76.

(45) O'Hagan, D.; Schaffrath, C.; Cobb, S. L.; Hamilton, J. T. G.; Murphy, C. D. "Biosynthesis of an Organofluorine Molecule." *Nature* **2002**, *416*, 279–279.

(46) Dong, C.; Huang, F.; Deng, H.; Schaffrath, C.; Spencer, J. B.; O'Hagan, D.; Naismith, J. H. "Crystal Structure and Mechanism of a Bacterial Fluorinating Enzyme." *Nature* **2004**, *427*, 561–565.

(47) Cadicamo, C. D.; Courtieu, J.; Deng, H.; Meddour, A.; O'Hagan, D. "Enzymatic Fluorination in *Streptomyces Cattleya* Takes Place with an Inversion of Configuration Consistent with an S_N2 Reaction Mechanism." *ChemBioChem* **2004**, *5*, 685–690.

(48) Senn, H. M.; O'Hagan, D.; Thiel, W. "Insight into Enzymatic C–F Bond Formation from QM and QM/MM Calculations." *J. Am. Chem. Soc.* **2005**, *127*, 13643–13655.

(49) Zhu, X.; Robinson, D. A.; McEwan, A. R.; O'Hagan, D.; Naismith, J. H. "Mechanism of Enzymatic Fluorination in *Streptomyces Cattleya*." *J. Am. Chem. Soc.* **2007**, *129*, 14597–14604.

(50) Vincent, M. A.; Hillier, I. H. "The Solvated Fluoride Anion Can Be a Good Nucleophile." *Chem. Commun.* **2005**, 5902–5903.

(51) Cametti, M.; Rissanen, K. "Recognition and Sensing of Fluoride Anion." *Chem. Commun.* **2009**, 2809–2829.

(52) Zhou, Y.; Zhang, J. F.; Yoon, J. "Fluorescence and Colorimetric Chemosensors for Fluoride-Ion Detection." *Chem. Rev.* **2014**, *114*, 5511–5571.

(53) Kim, D. W.; Ahn, D. S.; Oh, Y. H.; Lee, S.; Kil, H. S.; Oh, S. J.; Lee, S. J.; Kim, J. S.; Ryu, J. S.; Moon, D. H.; Chi, D. Y. "A New Class of S_N2 Reactions Catalyzed by Protic Solvents: Facile Fluorination for Isotopic Labeling of Diagnostic Molecules." *J. Am. Chem. Soc.* **2006**, *128*, 16394–16397.

(54) Dong, W. K.; Jeong, H. J.; Seok, T. L.; Sohn, M. H.; Katzenellenbogen, J. A.; Dae, Y. C. "Facile Nucleophilic Fluorination Reactions Using Tert-Alcohols as a Reaction Medium: Significantly Enhanced Reactivity of Alkali Metal Fluorides and Improved Selectivity." *J. Org. Chem.* **2008**, *73*, 957–962.

(55) Lee, J. W.; Yan, H.; Jang, H. Bin; Kim, H. K.; Park, S. W.; Lee, S.; Chi, D. Y.; Song, C. E. "Bis-Terminal Hydroxy Polyethers as All-Purpose, Multifunctional Organic Promoters: A Mechanistic Investigation and Applications." *Angew. Chemie - Int. Ed.* **2009**, *48*, 7683–7686.

(56) Jadhav, V. H.; Choi, W.; Lee, S. S.; Lee, S.; Kim, D. W. "Bis-Tert-Alcohol-Functionalized Crown-6-Calix[4]Arene: An Organic Promoter for Nucleophilic Fluorination." *Chem. - A Eur. J.* **2016**, *22*, 4515–4520.

(57) Kang, S. M.; Kim, C. H.; Lee, K. C.; Kim, D. W. "Bis-Triethylene Glycolic Crown-5-Calix[4]Arene: A Promoter of Nucleophilic Fluorination Using Potassium Fluoride." *Org. Lett.* **2019**, *21*, 3062–3066.

(58) Kim, D. W.; Jeong, H. J.; Lim, S. T.; Sohn, M. H. "Tetrabutylammonium Tetra(Tert-Butyl Alcohol)-Coordinated Fluoride as a Facile Fluoride Source." *Angew. Chemie - Int. Ed.* **2008**, *47*, 8404–8406.

(59) Hollingworth, C.; Hazari, A.; Hopkinson, M. N.; Tredwell, M.; Benedetto, E.; Huiban, M.; Gee, A. D.; Brown, J. M.; Gouverneur, V. "Palladium-Catalyzed Allylic Fluorination." *Angew. Chemie - Int. Ed.* **2011**, *50*, 2613–2617.

(60) Benedetto, E.; Tredwell, M.; Hollingworth, C.; Khotavivattana, T.; Brown, J. M.; Gouverneur, V. "Regio- and Stereoretentive Synthesis of Branched, Linear (*E*)- and (*Z*)-Allyl Fluorides from Allyl Carbonates under Ir-Catalysis." *Chem. Sci.* **2013**, *4*, 89–96.

(61) Engle, K. M.; Pfeifer, L.; Pidgeon, G. W.; Giuffredi, G. T.; Thompson, A. L.; Paton, R. S.; Brown, J. M.; Gouverneur, V. "Coordination Diversity in Hydrogen-Bonded Homoleptic Fluoride-Alcohol Complexes Modulates Reactivity." *Chem. Sci.* **2015**, *6*, 5293–5302.

(62) Pfeifer, L.; Engle, K. M.; Pidgeon, G. W.; Sparkes, H. A.; Thompson, A. L.; Brown, J. M.; Gouverneur, V. "Hydrogen-Bonded Homoleptic Fluoride–Diarylurea Complexes: Structure, Reactivity and Coordinating Power." *J. Am. Chem. Soc.* **2016**, *138*, 13314–13325.

(63) Kirby, I. L.; Brightwell, M.; Pitak, M. B.; Wilson, C.; Coles, S. J.; Gale, P. A. "Systematic Experimental Charge Density Analysis of Anion Receptor Complexes." *Phys. Chem. Chem. Phys.* **2014**, *16*, 10943–10958.

(64) Yang, X.; Wu, T.; Phipps, R. J.; Toste, F. D. "Advances in Catalytic Enantioselective Fluorination, Mono-, Di-, and Trifluoromethylation, and Trifluoromethylthiolation Reactions." *Chem. Rev.* **2015**, *115*, 826–870.

(65) Zhu, Y.; Han, J.; Wang, J.; Shibata, N.; Sodeoka, M.; Soloshonok, V. A.; Coelho, J. A. S.; Toste, F. D. "Modern Approaches for Asymmetric Construction of Carbon-Fluorine Quaternary Stereogenic Centers: Synthetic Challenges and Pharmaceutical Needs." *Chem. Rev.* **2018**, *118*, 3887–3964.

(66) Doyle, A. G.; Jacobsen, E. N. "Small-Molecule H-Bond Donors in Asymmetric Catalysis." *Chem. Rev.* **2007**, *107*, 5713–5743.

(67) Pupo, G.; Ibba, F.; Ascough, D. M. H.; Vicini, A. C.; Ricci, P.; Christensen, K. E.; Pfeifer, L.; Morphy, J. R.; Brown, J. M.; Paton, R. S.; Gouverneur, V. "Asymmetric Nucleophilic Fluorination under Hydrogen Bonding Phase-Transfer Catalysis." *Science* **2018**, *360*, 638–642.

(68) Roagna, G.; Ascough, D. M. H.; Ibba, F.; Vicini, A. C.; Christensen, K. E.; Peschiulli, A.; Oehlrich, D.; Misale, A.; Trabanco, A. A.; Paton, R. S.; Pupo, G.; Gouverneur, V. "Hydrogen Bonding Phase-Transfer Catalysis with Ionic Reactants : Enantioselective Synthesis of γ-Fluoroamines." *J. Am. Chem. Soc.* **2020**, *142*, 14045–14051.

(69) O'Hagan, D. "Understanding Organofluorine Chemistry. An Introduction to the C–F Bond." *Chem. Soc. Rev.* **2008**, *37*, 308–319.

(70) Fleming, I. *Molecular Orbitals and Organic Chemical Reactions*; John Wiley & Sons, Ltd: Chichester, UK, 2010.

(71) Pauli, L. *The Nature of the Chemical Bond and the Structure of Molecules and Crystals*; Cornell University Press: Itacha, 1939.

(72) Bondi, A. "Van Der Waals Volumes and Radii." *J. Phys. Chem.* **1964**, *68*, 441–451.

(73) Gillis, E. P.; Eastman, K. J.; Hill, M. D.; Donnelly, D. J.; Meanwell, N. A. "Applications of Fluorine in Medicinal Chemistry." *J. Med. Chem.* **2015**, *58*, 8315–8359.

(74) *Fluorine in Medicinal Chemistry and Chemical Biology*; Ojima, I., Ed.; Wiley-Blackwell: Chichester, UK, 2009.

(75) *Fluorine in Pharmaceutical and Medicinal Chemistry*; Gouverneur, V., Muller, K., Eds.; Imperial College Press: London, 2012.

(76) Zimmer, L. E.; Sparr, C.; Gilmour, R. "Fluorine Conformational Effects in Organocatalysis: An Emerging Strategy for Molecular Design." *Angew. Chemie - Int. Ed.* **2011**, *50*, 11860–11871.

(77) Cahard, D.; Bizet, V. "The Influence of Fluorine in Asymmetric Catalysis." *Chem. Soc. Rev.* **2014**, *43*, 135–147.

(78) Trapp, M. L.; Watts, J. K.; Weinberg, N.; Pinto, B. M. "Component Analysis of the X–C–Y Anomeric Effect (X = O, S; Y = F, OMe, NHMe) by DFT Molecular Orbital Calculations and Natural Bond Orbital Analysis." *Can. J. Chem.* **2006**, *701*, 692–701.

(79) W. Banks, J.; S. Batsanov, A.; A. K. Howard, J.; O'Hagan, D.; S. Rzepa, H.; Martin-Santamaria, S. "The Preferred Conformation of α-Fluoroamides." *J. Chem. Soc. Perkin Trans. 2* **1999**, 2409–2411.

(80) Lankin, D. C.; Chandrakumar, N. S.; Rao, S. N.; Spangler, D. P.; Snyder, J. P. "Protonated 3-Fluoropiperidines: An Unusual Fluoro Directing Effect and a Test for Quantitative Theories of Solvation." *J. Am. Chem. Soc.* **1993**, *115*, 3356–3357.

(81) Sun, A.; Lankin, D. C.; Hardcastle, K.; Snyder, J. P. "3-Fluoropiperidines and *N*-Methyl-3-Fluoropiperidinium Salts: The Persistence of Axial Fluorine." *Chem. - A Eur. J.* **2005**, *11*, 1579–1591.

(82) Gooseman, N. E. J.; O'Hagan, D.; Slawin, A. M. Z.; Teale, A. M.; Tozer, D. J.; Young, R. J. "The Intramolecular β-Fluorine···Ammonium Interaction in 4- and 8-Membered Rings." *Chem. Commun.* **2006**, 3190–3192.

(83) Gerig, J. T.; Mcleod, R. S. "Conformations of *Cis*- and *Trans*-4-Fluoro-L-Proline in Aqueous Solution." *J. Am. Chem. Soc.* **1973**, *95*, 5725–5729.

(84) Briggs, C. R. S.; Allen, M. J.; O'Hagan, D.; Tozer, D. J.; Slawin, A. M. Z.; Goeta, A. E.; Howard, J. A. K. "The Observation of a Large *Gauche* Preference When 2-Fluoroethylamine and 2-Fluoroethanol Become Protonated." *Org. Biomol. Chem.* **2004**, *2*, 732–740.

(85) Mathad, R. I.; Gessier, F.; Seebach, D.; Jaun, B. "The Effect of Backbone-Heteroatom Substitution on the Folding of Peptides – A Single Fluorine Substituent Prevents a β-Heptapeptide from Folding into a 3_{14}-Helix (NMR Analysis)." *Helv. Chim. Acta* **2005**, *88*, 266–280.

(86) Jaun, B.; Seebach, D.; Mathad, R. I. "*Note:* Helix or No Helix of β-Peptides Containing β^3hAla(αF) Residues?" *Helv. Chim. Acta* **2011**, *94*, 355–361.

(87) Bretscher, L. E.; Jenkins, C. L.; Taylor, K. M.; DeRider, M. L.; Raines, R. T. "Conformational Stability of Collagen Relies on a Stereoelectronic Effect." *J. Am. Chem. Soc.* **2001**, *123*, 777–778.

(88) Hodgest, J. A.; Raines, R. T. "Stereoelectronic Effects on Collagen Stability: The Dichotomy of 4-Fluoroproline Diastereomers." *J. Am. Chem. Soc.* **2003**, *125*, 9262–9263.

(89) Shoulders, M. D.; Kamer, K. J.; Raines, R. T. "Origin of the Stability Conferred upon Collagen by Fluorination." *Bioorganic Med. Chem. Lett.* **2009**, *19*, 3859–3862.

(90) Eberhardt, E. S.; Panasik, N.; Raines, R. T. "Inductive Effects on the Energetics of Prolyl Peptide Bond Isomerization: Implications for Collagen Folding and Stability." *J. Am. Chem. Soc.* **1996**, *118*, 12261–12266.

(91) Chia, P. W.; Livesey, M. R.; Slawin, A. M. Z.; Van Mourik, T.; Wyllie, D. J. A.; O'Hagan, D. "3-Fluoro-*N*-Methyl-D-Aspartic Acid (3F-NMDA) Stereoisomers as Conformational Probes for Exploring Agonist Binding at NMDA Receptors." *Chem. - A Eur. J.* **2012**, *18*, 8813–8819.

(92) Aufiero, M.; Gilmour, R. "Informing Molecular Design by Stereoelectronic Theory: The Fluorine *Gauche* Effect in Catalysis." *Acc. Chem. Res.* **2018**, *51*, 1701–1710.

(93) Tanzer, E. M.; Zimmer, L. E.; Schweizer, W. B.; Gilmour, R. "Fluorinated Organocatalysts for the Enantioselective Epoxidation of Enals: Molecular Preorganisation by the Fluorine-Iminium Ion Gauche Effect." *Chem. - A Eur. J.* **2012**, *18*, 11334–11342.

(94) Holland, M. C.; Paul, S.; Schweizer, W. B.; Bergander, K.; Mück-Lichtenfeld, C.; Lakhdar, S.; Mayr, H.; Gilmour, R. "Noncovalent Interactions in Organocatalysis: Modulating Conformational Diversity and Reactivity in the MacMillan Catalyst." *Angew. Chemie - Int. Ed.* **2013**, *52*, 7967–7971.

(95) Seebach, D.; Schweizer, W. B. "Experimental and Theoretical Conformational Analysis of 5-Benzylimidazolidin-4-One Derivatives – a Playground for Studying Dispersion Interactions and a Windshield-Wiper Effect in Organocatalysis." *Helv. Chim. Acta* **2010**, *93*, 1–16.

(96) Morgenthaler, M.; Schweizer, E.; Hoffmann-Röder, A.; Fischer, H.; Bendels, S.; Zimmerli, D.; Schneider, J. "Predicting and Tuning Physicochemical Properties in Lead Optimization: Amine Basicities." *ChemMedChem* **2007**, *2*, 1100–1115.

(97) Kollonitsch, J.; Patchett, A. A.; Marburg, S.; Maycock, A. L.; Perkins, L. M.; Doldouras, G. A.;

Duggan, D. E.; Aster, S. D. “Selective Inhibitors of Biosynthesis of Aminergic Neurotransmitters.” *Nature* **1978**, *274*, 906–908.

(98) Sato, K.; Hoshino, K.; Tanaka, M.; Hayakawa, I.; Osada, Y. “Antimicrobial Activity of DU-6859, a New Potent Fluoroquinolone, against Clinical Isolates.” *Antimicrob. Agents Chemother.* **1992**, *36*, 1491–1498.

(99) Coburn, C. A.; Egbertson, M. S.; Graham, S. L.; McGaughey, G. B.; Stauffer, S. R.; Rajapakse, H. A.; Nantermet, P. G.; Stachel, S. R.; Yang, W.; Lu, W.; Fahr, B. “Spiropiperidine Beta-Secretase Inhibitors for the Treatment of Alzheimer’s Disease.” WO 011833, 2007.

(100) Groebke Zbinden, K.; Haap, W.; Hilpert, H.; Panday, N.; Ricklin, F.; Wirz, B. “Cyclic Amines.” US7820699, 2006.

(101) Cox, C. D.; Coleman, P. J.; Breslin, M. J.; Whitman, D. B.; Garbaccio, R. M.; Fraley, M. E.; Buser, C. A.; Walsh, E. S.; Hamilton, K.; Schaber, M. D.; Lobell, R. B.; Tao, W.; Davide, J. P.; Diehl, R. E.; Abrams, M. T.; South, V. J.; Huber, H. E.; Torrent, M.; Prueksaritanont, T.; Li, C.; Slaughter, D. E.; Mahan, E.; Fernandez-Metzler, C.; Yan, Y.; Kuo, L. C.; Kohl, Na. E.; Hartman, G. D. “Kinesin Spindle Protein (KSP) Inhibitors. 9. Discovery of (2*S*)-4-(2,5-Difluorophenyl)-*N*-[(3*R*,4*S*)-3-fluoro-1-methylpiperidin-4-yl]-2-(hydroxymethyl)-*N*-methyl-2-phenyl-2,5-dihydro-1H-pyrrole-1-carboxamide (MK-0731) for the Treatment of Taxane-Refractory C.” *J. Med. Chem.* **2008**, *51*, 4239–4252.

(102) Burger, M.; Lan, J.; Lindvall, M.; Nishiguchi, G.; Tetalman, M. “PIM Kinase Inhibitors and Methods of Their Use.” PCT Int. Patent. Appl. EP2009/052506, 2009.

(103) Gentile, I.; Coppola, N.; Buonomo, A. R.; Zappulo, E.; Borgia, G. “Investigational Nucleoside and Nucleotide Polymerase Inhibitors and Their Use in Treating Hepatitis C Virus.” *Expert Opin Investig Drugs* **2014**, *23*, 1211–1223.

(104) Sofia, M. J.; Bao, D.; Chang, W.; Du, J.; Nagarathnam, D.; Rachakonda, S.; Reddy, P. G.; Ross, B. S.; Wang, P.; Zhang, H.; Bansal, S.; Espiritu, C.; Keilman, M.; Lam, A. M.; Steuer, H. M. M.; Niu, C.; Otto, M. J.; Furman, P. A. “Discovery of a β-D-2’-Deoxy-2’-α-fluoro-2’-β-*C*-methyluridine Nucleotide Prodrug (PSI-7977) for the Treatment of Hepatitis C Virus.” *J. Med. Chem.* **2010**, *53*, 7202–7218.

(105) Niu, C.; Murakami, E.; Furman, P. A. “Clevudine Is Efficiently Phosphorylated to the Active Triphosphate Form in Primary Human Hepatocytes.” *Antivir. Ther.* **2008**, *13*, 263–269.

(106) Watanabe, K. A.; Reichman, U.; Hirota, K.; Lopez, C.; Fox, J. J. “Nucleosides. 110. Synthesis and Antiherpes Virus Activity of Some 2′-Fluoro-2′-deoxyarabinofuranosylpyrimidine Nucleosides.” *J. Med. Chem.* **1979**, *22*, 21–24.

(107) Bonate, P. L.; Arthaud, L.; Cantrell, W. R.; Stephenson, K.; Secrist, J. A.; Weitman, S. “Discovery and Development of Clofarabine: A Nucleoside Analogue for Treating Cancer.” *Nat. Rev. Drug Discov.* **2006**, *5*, 855–863.

(108) Mason, J. M.; Murkin, A. S.; Li, L.; Schramm, V. L.; Gainsford, G. J.; Skelton, B. W. “A β-Fluoroamine Inhibitor of Purine Nucleoside Phosphorylase.” *J. Med. Chem.* **2008**, *51*, 5880–5884.

(109) Asahina, Y.; Takei, M.; Kimura, T.; Fukuda, Y. “Synthesis and Antibacterial Activity of Novel Pyrido[1,2,3-*de*][1,4]Benzoxazine-6-Carboxylic Acid Derivatives Carrying the 3-Cyclopropylaminomethyl-4-Substituted-1-Pyrrolidinyl Group as a C-10 Substituent.” *J. Med. Chem.* **2008**, *51*, 3238–3249.

(110) Edmondson, S. D.; Mastracchio, A.; Duffy, J. L.; Eiermann, G. J.; He, H.; Ita, I.; Leiting, B.; Leone, J. F.; Lyons, K. A.; Makarewicz, A. M.; Patel, R. A.; Petrov, A.; Wu, J. K.; Thornberry, N. A.; Weber, A. E. “Discovery of Potent and Selective Orally Bioavailable β-Substituted Phenylalanine Derived Dipeptidyl Peptidase IV Inhibitors.” *Bioorganic Med. Chem. Lett.* **2005**, *15*, 3048–3052.

(111) Yang, Z.; Barrow, J. C.; Shipe, W. D.; Schlegel, K. S.; Shu, Y.; Yang, F. V.; Lindsley, C. W.; Rittle, K. E.; Bock, M. G.; Hartman, G. D.; Uebele, V. N.; Nuss, C. E.; Fox, S. V; Kraus, R. L.; Doran, S. M.; Connolly, T. M.; Tang, C.; Ballard, J. E.; Kuo, Y.; Adarayan, E. D.; Prueksaritanont, T.; Zrada, M. M.; Marino, M. J.; Graufelds, V. K.; Dilella, A. G.; Reynolds, I. J.; Vargas, H. M.; Bunting, P.

B.; Woltmann, R. F.; Magee, M. M.; Koblan, K. S.; Renger, J. J. “Discovery of 1,4-Substituted Piperidines as Potent and Selective Inhibitors of T-Type Calcium Channels.” *J. Med. Chem.* **2008**, *51*, 6471–6477.

(112) Garner, R.; Gopalakrishnan, S.; Mccauley, J. A.; Bednar, R. A.; Gaul, S. L.; Mosser, S. D.; Kiss, L.; Lynch, J. J.; Patel, S.; Fandozzi, C.; Lagrutta, A.; Briscoe, R.; Liverton, N. J.; Paterson, B. M.; Vornov, J. J.; Mazhari, R. “Preclinical Pharmacology and Pharmacokinetics of CERC-301, a GluN2B-Selective *N*-Methyl-D-Aspartate Receptor Antagonist.” *Pharmacol. Res. Perspect.* **2015**, *3*, 1–12.

(113) Grunewald, G. L.; Caldwell, T. M.; Li, Q.; Criscione, K. R. “Synthesis and Evaluation of 4-Fluoro-8-Substituted-2,3,4,5-Tetrahydro-1*H*-2-Benzazapines as Selective Inhibitors of Phenylethanolamine *N*-Methyltransferase *versus* the A2-Adrenoceptor.” *J. Med. Chem.* **2001**, *44*, 2849–2856.

(114) Murray, T. K.; Whalley, K.; Robinson, C. S.; Ward, M. A.; Hicks, C. A.; Lodge, D.; Vandergriff, J. L.; Baumbarger, P.; Siuda, E.; Gates, M.; Ogden, A. M.; Skolnick, P.; Zimmerman, D. M.; Nisenbaum, E. S.; Bleakman, D.; O’Neill, M. J. “LY503430, a Novel α-Amino-3-Hydroxy-5-Methylisoxazole-4-Propionic Acid Receptor Potentiator with Functional, Neuroprotective and Neurotrophic Effects in Rodent Models of Parkinson’s Disease.” *J. Pharmacol. Exp. Ther.* **2003**, *306*, 752–762.

(115) Balfour, J. A.; Todd, P. A.; Peters, D. H. “Fleroxacin. A Review of its Pharmacology and Therapeutic Efficacy in Various Infections.” *Drugs* **1995**, *49*, 794–850.

(116) de Jesús-cortés, H.; Xu, P.; Drawbridge, J.; Estill, S. J.; Huntington, P.; Tran, S.; Britt, J.; Tesla, R.; Morlock, L.; Naidoo, J.; Melito, L. M.; Wang, G.; Williams, N. S.; Ready, J. M.; McKnight, S. L.; Pieper, A. A. “Neuroprotective Efficacy of Aminopropyl Carbazoles in a Mouse Model of Parkinson Disease.” *Proc. Natl. Acad. Sci.* **2012**, *109*, 17010–17015.

(117) Alstermark, C.; Amin, K.; Dinn, S. R.; Elebring, T.; Fjellström, O.; Fitzpatrick, K.; Geiss, W. B.; Gottfries, J.; Guzzo, P. R.; Harding, J. P.; Holmén, A.; Kothare, M.; Lehmann, A.; Mattsson, J. P.; Nilsson, K.; Sundén, G.; Swanson, M.; von Unge, S.; Woo, A. M.; Wyle, M. J.; Zheng, X. “Synthesis and Pharmacological Evaluation of Novel γ-Aminobutyric Acid Type B (GABAB) Receptor Agonists as Gastroesophageal Reflux Inhibitors.” *J. Med. Chem.* **2008**, *51*, 4315.

(118) Lehmann, L.; Thiele, A.; Heinrich, T.; Brumby, T.; Halldin, C.; Gulyas, B.; Nag, S. “Compounds for Use in Imaging, Diagnosing, and/or Treatment of Diseases of the Central Nervous System or of Tumors.” Patent WO2009052970A2, 2007.

(119) Davis, M. R.; Votaw, J. R.; Bremner, J. D.; Byas-Smith, M. G.; Faber, T. L.; Voll, R. J.; Hoffman, J. M.; Grafton, S. T.; Kilts, C. D.; Goodman, M. M. “Initial Human PET Imaging Studies with the Dopamine Transporter Ligand ^{18}F-FECNT.” *J. Nucl. Med.* **2003**, *44*, 855–861.

(120) Rey, Y. P.; Gilmour, R. “Modulating NHC Catalysis with Fluorine.” *Beilstein J. Org. Chem.* **2013**, *9*, 2812–2820.

(121) Guan, Y. Q.; Han, Z.; Li, X.; You, C.; Tan, X.; Lv, H.; Zhang, X. “A Cheap Metal for a Challenging Task: Nickel-Catalyzed Highly Diastereo- and Enantioselective Hydrogenation of Tetrasubstituted Fluorinated Enamides.” *Chem. Sci.* **2019**, *10*, 252–256.

(122) Trost, B. M.; Saget, T.; Lerchen, A.; Hung, C. J. “Catalytic Asymmetric Mannich Reactions with Fluorinated Aromatic Ketones: Efficient Access to Chiral β-Fluoroamines.” *Angew. Chemie* **2016**, *128*, 791–794.

(123) Zhao, Y.; Pan, Y.; Liu, H.; Yang, Y. “Fluorinated Aromatic Ketones as Nucleophiles in the Asymmetric Organocatalytic Formation of C–C and C–N Bonds : A Facile Route to the Construction of Fluorinated Quaternary Stereogenic Centers.” *Chem. - A Eur. J.* **2011**, *17*, 3571–3574.

(124) Vaithiyanathan, V.; Kim, J.; Liu, Y.; Yan, H. “Direct Access to Chiral β-Fluoroamines with Quaternary Stereogenic Center through Cooperative Cation-Binding Catalysis.” *Chem. - A Eur. J.* **2017**, *23*, 1268–1272.

(125) Paladhi, S.; Park, S. Y.; Yang, J. W.; Song, C. E. “Asymmetric Synthesis of α-Fluoro-β-Amino-Oxindoles with Tetrasubstituted C–F Stereogenic Centers *via* Cooperative Cation-Binding

Catalysis." *Org. Lett.* **2017**, *19*, 5336–5339.

(126) Vara, B. A.; Johnston, J. N. "Enantioselective Synthesis of β-Fluoro Amines *via* β-Amino α-Fluoro Nitroalkanes and a Traceless Activating Group Strategy." *J. Am. Chem. Soc.* **2016**, *138*, 13794–13797.

(127) Beeson, T. D.; MacMillan, D. W. C. "Enantioselective Organocatalytic α-Fluorination of Aldehydes." *J. Am. Chem. Soc.* **2005**, *127*, 8826–8828.

(128) Marigo, M.; Fielenbach, D.; Braunton, A.; Kjærsgaard, A.; Jørgensen, K. A. "Enantioselective Formation of Stereogenic Carbon–Fluorine Centers by a Simple Catalytic Method." *Angew. Chemie - Int. Ed.* **2005**, *44*, 3703–3706.

(129) Steiner, D. D.; Mase, N.; Barbas III, C. F. "Direct Asymmetric α-Fluorination of Aldehydes." *Angew. Chemie - Int. Ed.* **2005**, *44*, 3706–3710.

(130) Fadeyi, O. O.; Lindsley, C. W. "Rapid, General Access to Chiral β-Fluoroamines and β,β-Difluoroamines *via* Organocatalysis." *Org. Lett.* **2009**, *11*, 943–946.

(131) O'Reilly, M. C.; Lindsley, C. W. "A General, Enantioselective Synthesis of β- And γ-Fluoroamines." *Tetrahedron Lett.* **2013**, *54*, 3627–3629.

(132) Kwiatkowski, P.; Beeson, T. D.; Conrad, J. C.; MacMillan, D. W. C. "Enantioselective Organocatalytic α-Fluorination of Cyclic Ketones." *J. Am. Chem. Soc.* **2011**, *133*, 1738–1741.

(133) Schulte, M. L.; Lindsley, C. W. "Highly Diastereoselective and General Synthesis of Primary β-Fluoroamines." *Org. Lett.* **2011**, *13*, 5684–5687.

(134) Appayee, C.; Brenner-Moyer, S. E. "Organocatalytic Enantioselective Olefin Aminofluorination." *Org. Lett.* **2010**, *12*, 3356–3359.

(135) Jones, J. H.; Appayee, C.; Brenner-Moyer, S. E. "One-Pot Preparation of Enantiopure Fluorinated β-Amino Acid Precursors." *European J. Org. Chem.* **2014**, *2014*, 5273–5280.

(136) Phipps, R. J.; Hiramatsu, K.; Toste, F. D. "Asymmetric Fluorination of Enamides: Access to α-Fluoroimines Using an Anionic Chiral Phase-Transfer Catalyst." *J. Am. Chem. Soc.* **2012**, *134*, 8376–8379.

(137) Kalow, J. A.; Doyle, A. G. "Enantioselective Fluoride Ring Opening of Aziridines Enabled by Cooperative Lewis Acid Catalysis." *Tetrahedron* **2013**, *69*, 5702–5709.

(138) Chen, P.; Liu, G. "Advancements in Aminofluorination of Alkenes and Alkynes: Convenient Access to β-Fluoroamines." *European J. Org. Chem.* **2015**, 4295–4309.

(139) Lu, D.; Liu, G.; Zhu, C.; Yuan, B.; Xu, H. "Iron(II)-Catalyzed Intramolecular Olefin Aminofluorination." *Org. Lett.* **2014**, *16*, 2912–2915.

(140) Lu, D.; Zhu, C.; Xu, H. "Iron(II)-Catalyzed Intermolecular Aminofluorination of Unfunctionalized Olefins Using Fluoride Ion." *J. Am. Chem. Soc.* **2016**, *138*, 11360–11367.

(141) Kong, W.; Feige, P.; de Haro, T.; Nevado, C. "Regio- and Enantioselective Aminofluorination of Alkenes." *Angew. Chemie - Int. Ed.* **2013**, *52*, 2469–2473.

(142) Suzuki, S.; Kamo, T.; Fukushi, K.; Hiramatsu, T.; Tokunaga, E.; Dohi, T.; Kita, Y.; Shibata, N. "Iodoarene-Catalyzed Fluorination and Aminofluorination by an Ar-I/HF·pyridine/*m*CPBA System." *Chem. Sci.* **2014**, *5*, 2754–2760.

(143) Mennie, K. M.; Banik, S. M.; Reichert, E. C.; Jacobsen, E. N. "Catalytic Diastereo- and Enantioselective Fluoroamination of Alkenes." *J. Am. Chem. Soc.* **2018**, *140*, 4797–4802.

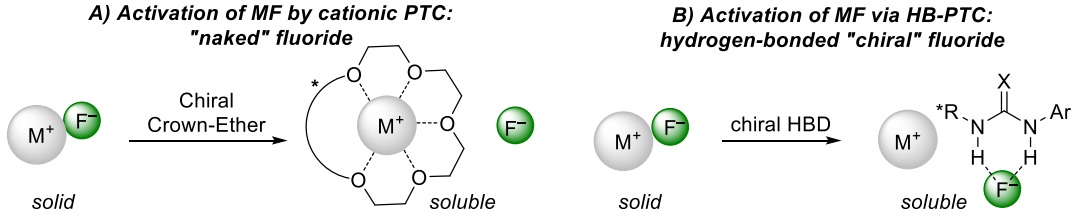
Chapter 2:
Enantioselective Fluorination of Aziridinium Ions with Alkali Metal Fluorides under Hydrogen Bonding Phase-Transfer Catalysis (HB-PTC)

The work described in this chapter was carried out in collaboration with Dr. David Ascough, Dr. Gabriele Pupo and Dr. Francesco Ibba. Dr. David Ascough performed all the computational work. Dr. Gabriele Pupo carried out the 50 g scale fluorination reported in section 2.7 following the reaction optimisation that I performed. Dr. Francesco Ibba executed the NMR experiments reported in section 2.9.1. Their contribution is clearly stated within the chapter and when no specific attribution is given, it is implied that the work described is my own experimental work. The work reported in this chapter features in the publication *Hydrogen Bonding Phase-Transfer Catalysis with Potassium Fluoride: Enantioselective Synthesis of β-Fluoroamines,* G. Pupo*, A. C. Vicini*, D. M. H. Ascough, F. Ibba, K. E. Christensen, A. L. Thompson, J. M. Brown, R. S. Paton, V. Gouverneur *J. Am. Chem. Soc.* **2019**, *141*, 2878–2883.[1] This work has been reused in accordance with the ACS Author Choice Creative Commons Attribution (CCBY) License, Copyright 2019 American Chemical Society.

2.1 Hydrogen Bonding Phase-Transfer Catalysis (HB-PTC)

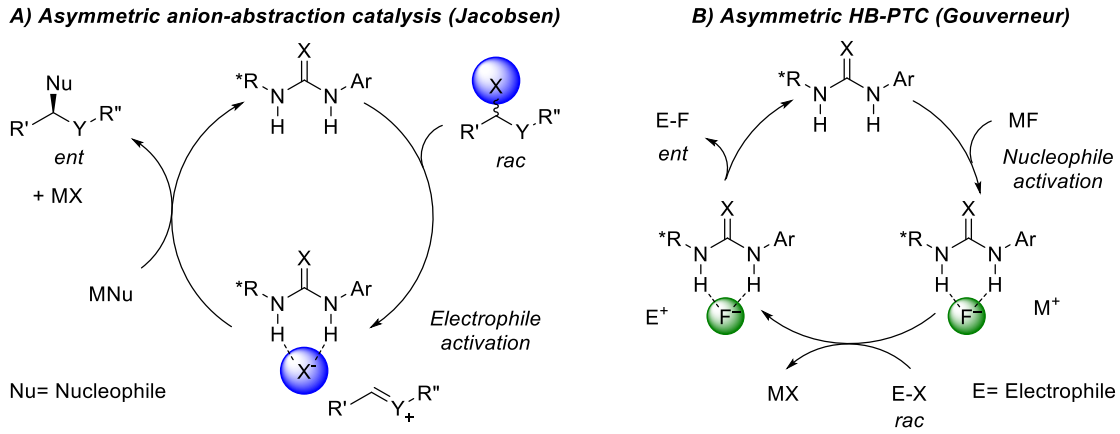
As discussed in Chapter 1, achiral cationic phase-transfer catalysts, such as ammonium ions and crown ethers that are able to interact with metal cations, have been extensively used for the solubilisation of solid alkali metal fluorides (1.1.3).[2] The corresponding chiral phase-transfer catalysts have been applied to asymmetric transformations involving a fluoride-mediated desilylation step (sections 1.1.4.1 and 1.1.4.2).[3,4] However, asymmetric cationic PTC so far has been unsuccessful in the enantioselective construction of C–F bonds. This is presumably due to the difficulties in controlling the selectivity of the uncoordinated ("naked") fluoride generated with this approach, because the chiral element is located on the ion-paired cation, relying on non-directional electrostatic interactions to influence fluoride enantioselectivity (Scheme 2.1A). Our group demonstrated that urea-

fluoride complexes are competent nucleophiles in fluorination reactions (1.1.5.3),[5] thus we envisioned that an enantioselective fluorinating reagent could be obtained by complexation of the fluoride ion by a chiral hydrogen bond donor (HBD, Scheme 2.1B), with concomitant solubilisation of the alkali metal fluoride salt. The poor solubility of the inorganic salt in organic solvents was advantageous, preventing the unselective background reaction of unbound fluoride. To describe this catalytic manifold, we coined the term Hydrogen Bonding Phase-Transfer Catalysis (HB-PTC).



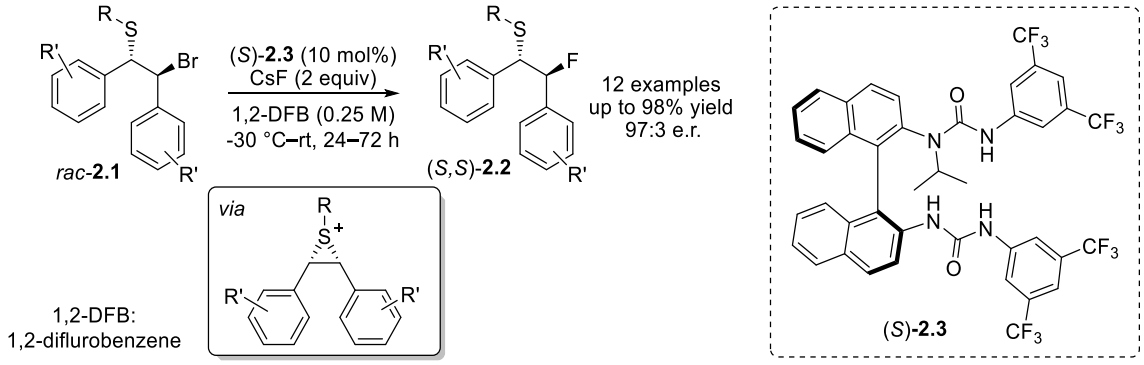
Scheme 2.1: A) Activation of MF by cationic PTC. This results in a "naked" fluoride, whose reactivity, chemo- and enantioselectivity are difficult to control. B) Activation of MF *via* hydrogen bonding complexation of fluoride. In the presence of a chiral HBD this results in a "chiral" fluoride.

Even though they are both based on interaction of a chiral HBD with an anionic species, HB-PTC is distinct from asymmetric anion-abstraction catalysis, whereby hydrogen bonding to halides has been exploited for electrophile activation. In this latter scenario, the chiral ion-pair formed by anion-abstraction reacts with an external nucleophile (Scheme 2.2A).[6,7] In contrast, in HB-PTC the organocatalyst activates an insoluble salt with formation of a hydrogen bonded chiral nucleophile (Scheme 2.2B).



Scheme 2.2: A) General mechanism of anion-abstraction catalysis for electrophile activation. B) Schematic representation of HB-PTC for nucleophile activation.

The research that validated HB-PTC as a novel catalytic manifold took place concomitantly with the work described in this thesis, and while the main contributors to the seminal report were Dr. Gabriele Pupo, Dr. Francesco Ibba and Dr. David Ascough, I actively participated in its development. The proof of principle of HB-PTC was demonstrated employing CsF in the enantioselective desymmetrisation of *meso*-episulfonium ions, generated *in situ* from the corresponding β-bromosulfides *rac*-**2.1**, (Scheme 2.3), obtaining β-fluorosulfides (*S*,*S*)-**2.2** in up to 98% yield and 97:3 e.r. (e.r.= enantiomeric ratio).[8]



Scheme 2.3: HB-PTC with CsF for the enantioselective desymmetrisation of *meso*-episulfonium ions.[8]

High levels of enantioselectivity were observed in the presence of a novel class of *N*-alkyl bis-urea organocatalysts, such as **2.3**, which bind fluoride *via* three hydrogen bonds. This binding mode was first predicted computationally. Molecular dynamics simulations of the interaction of non-alkylated urea **2.4** with CsF at 373 K revealed that complexation of fluoride with four hydrogen bonds accounted for 58% of the population of binding modes (Figure 2.1A). In the remaining 42%, urea rotation from the *anti-anti* to the *syn-anti* isomer gave rise to a tricoordinate fluoride-urea complex (Figure 2.1B). Bidentate cooperative binding, where one urea acts as hydrogen bond donor to fluoride and acceptor to the second urea, was not observed (Figure 2.1C). Subsequent DFT calculations revealed that a transition state displaying tridentate binding was energetically favoured by 24 kJ/mol compared to tetradentate binding.

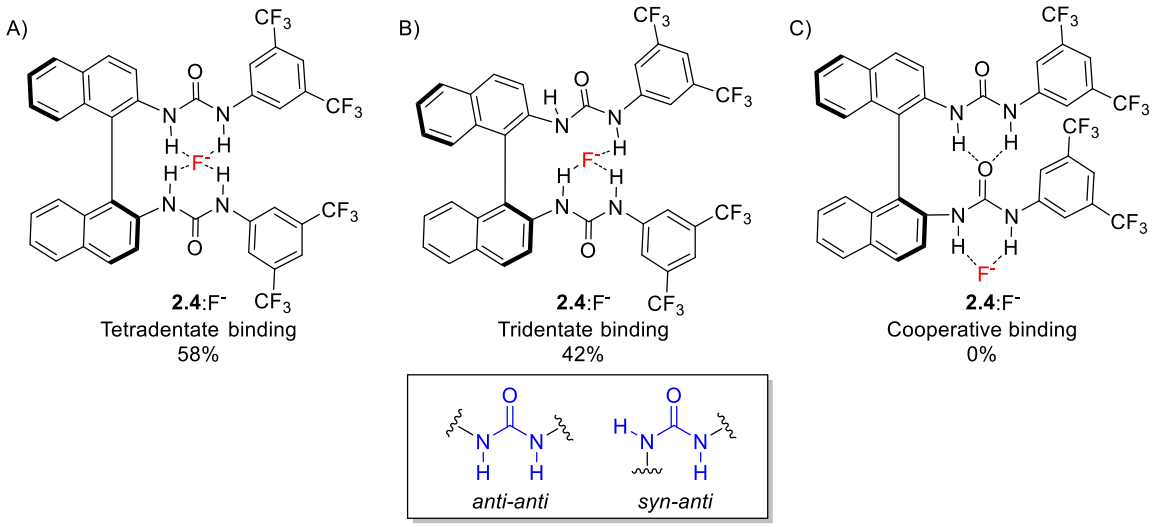
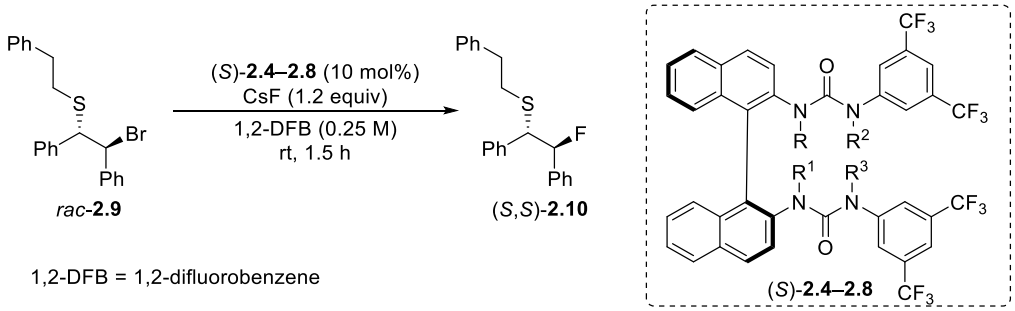


Figure 2.1: Molecular dynamics simulations of **2.4**:F⁻ binding modes (373 K) reporting the percentage of population of each binding mode.[8]

The requirement for only three hydrogen bonding interactions was subsequently validated experimentally with the synthesis of mono- and bis-methyl bis-ureas **2.5-2.8**. The catalytic activity was entirely suppressed in the presence of bis-methyl **2.5** and **2.6** (entries 2–3, Table 2.1). The introduction of a single methyl group on the urea nitrogen proximal to the 3,5-bis(trifluoromethyl)phenyl ring (**2.7**, entry 4) reduced reactivity, while reactivity was retained for the other mono-methyl isomer (**2.8**). The latter was also more enantioselective than non-alkylated **2.4** (88:12 e.r. *versus* 86:14 e.r., entry 5 *versus* 1).

Table 2.1: Effect of bis-urea *N*-alkylation on the enantioselective fluorination of β-bromosulfides.



Entry	*Catalyst*	*R*	*R*^{1}	*R*^{2}	*R*^{3}	*Yield*	*e.r.*
1	(*S*)-**2.4**	H	H	H	H	>95%	86:14
2	(*S*)-**2.5**	H	H	Me	Me	No reaction	–
3	(*S*)-**2.6**	Me	Me	H	H	No reaction	–
4	(*S*)-**2.7**	H	H	Me	H	15%	53:47
5	(*S*)-**2.8**	Me	H	H	H	>95%	88:12

To validate the proposed HB-PTC mechanism, further computational and experimental studies were undertaken. Based on the retention of relative configuration of β-fluorosulfides compared to the corresponding β-bromosulfides, the reaction is proposed to proceed *via* a *meso*-episulfonium ion. Computational experiments revealed that self-ionisation of β-bromosulfides and Schreiner's urea-mediated ionisation are equally favoured at room temperature. On the other hand, the hydrogen bond donor plays an important role in stabilising fluoride in solution.[8] This does not exclude anion-abstraction from being operative but suggests it is unlikely to be the main source of catalysis. Instead, the lack of reaction in the absence of the hydrogen bond donor points towards its role as phase-transfer catalyst.

The ability of *N*-alkyl bis-ureas to solubilise CsF was later demonstrated by sonicating (*S*)-**2.3** with solid CsF in a sealed NMR tube in CD_2Cl_2. This led to the formation of 1:1 and 2:1 urea-fluoride complexes in 85:15 ratio at room temperature.[9] Both complexes — (*S*)-**2.3**:CsF and Cs[((*S*)-**2.3**)$_2$:F]—were characterised in solution using a combination of NMR experiments. These data, together with the crystal structures of the 1:1 (*S*)-**2.3**:TBAF complex (Figure 2.2A) and the related 1:1 (*S*)-**2.11**:CsF complex (Figure 2.2B), confirmed the preference of this class of catalysts for tridentate binding of fluoride in solution and in the solid state.[9]

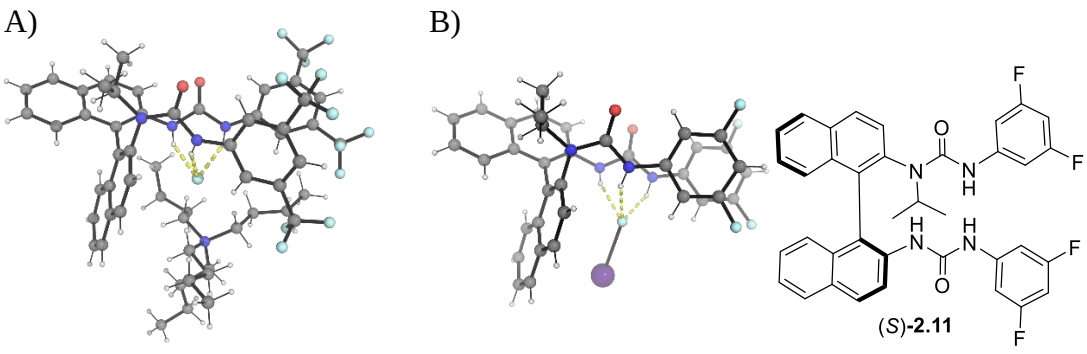
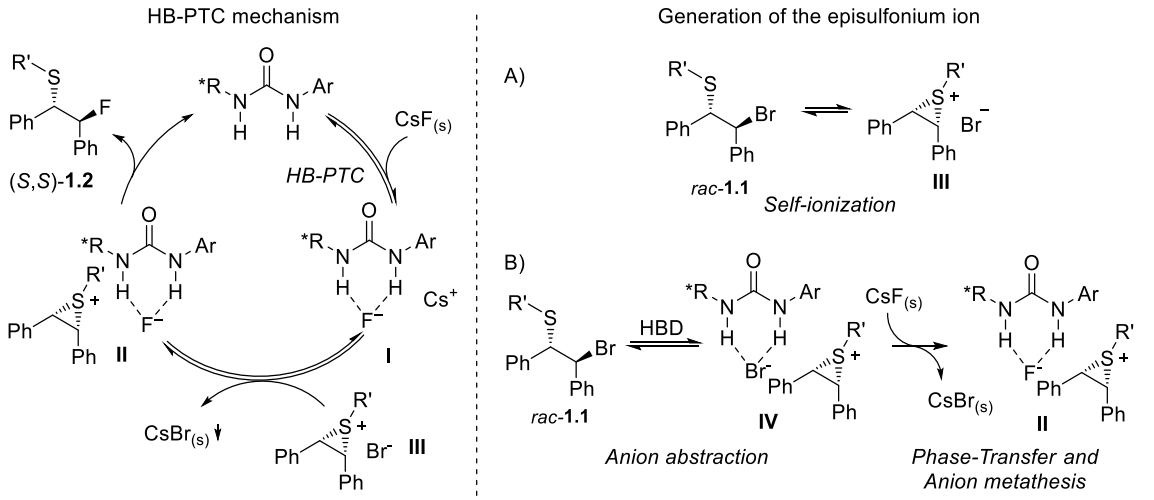


Figure 2.2: A) Solid state structure of **2.3**:TBAF from single crystal X-ray diffraction compared to B) solid state structure of **2.11**:CsF (solvent omitted for clarity).

Addition of racemic (2-bromo-1,2-diphenylethyl)(phenethyl)sulfane **2.9** to the solution of (*S*)-**2.3**:CsF/Cs[((*S*)-**2.3**)$_2$:F] caused immediate precipitation of a solid, presumably CsBr, and formation of the corresponding β-fluorosulfide **2.10** in 86.5:13.5 e.r., which is in line with the value measured in the catalytic reaction (88:12 e.r.).[9] This suggests that the proposed hydrogen bonded fluoride complex is active in fluorination. The absence of non-linear effects in the fluorination conducted with scalemic mixtures of catalyst **2.3**, and the independence of the enantiomeric ratio on the nature of the leaving group further support the presence of a 1:1 urea-fluoride complex in the enantiodetermining step.[8]

Based on these insights, a catalytic cycle is proposed in Scheme 2.4 (left). Phase-transfer of solid CsF mediated by the hydrogen bond donor generates a soluble chiral fluoride paired with the Cs^+ cation (**I**). Cation exchange with the *in situ* formed episulfonium ion causes precipitation of CsBr and generates the reactive ion pair **II** from which irreversible fluorination affords the enantioenriched product with concomitant release of the catalyst.



Scheme 2.4: Left: Proposed mechanism for the asymmetric fluorination of β-bromosulfides with CsF. Right: Generation of the *meso*-episulfonium intermediate, either *via* self-ionisation (A) or by anion abstraction (B).

The charged episulfonium ion could be formed either by self-ionisation (A) of the β-bromosulfide precursor with formation of **III**, or this process might be mediated by the urea (B), with formation of ion pair **IV** (Scheme 2.4, right). In our proposal, **IV** would

undergo anion metathesis with CsF, generating again the ion pair **II** and insoluble CsBr. Regardless of how the episulfonium is generated, the hydrogen bond donor is bound to the nucleophile in the enantiodetermining step (irreversible fluorination) and not to the leaving group, a striking difference from Jacobsen's anion abstraction mechanism.[6]

2.2 Project Aim

Our initial studies focused on episulfonium ions inspired by the Fluorinase natural substrate: *S*-adenosylmethionine, a sulfonium ion.[10] In both the enzymatic and the HB-PTC reaction, the positive charge of the reactant played a crucial role.[11,8] This prompted us to evaluate aziridinium ions as an electrophilic partner for enantioselective fluorination under HB-PTC, because their fluorination affords highly valuable enantioenriched β-fluoroamines. As reported in Chapter 1, this motif has important applications in medicinal chemistry (1.2.2.1) and has been exploited in catalyst design (1.2.2.2).

Moreover, as our goal was to develop a practical methodology that could be translated to industrial settings, we were interested in applying HB-PTC to the activation of KF. KF is economical (£ 6/mol, Table 2.2), abundant, and easy-to-handle.

Table 2.2: Prices per mole of different fluorine sources.[1]

Fluorine source	*Price (£/mol)*
KF	6
CsF	56
AgF	749
TBAF	53
NFSI	86
Selectfluor®	526

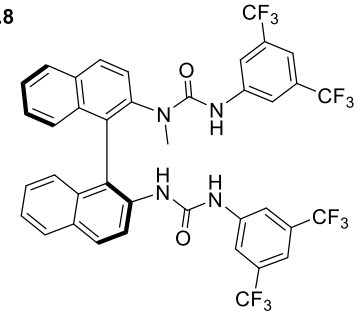
We anticipated that its activation *via* HB-PTC would have been more challenging than that of CsF, due to the increased lattice energy (KF: 829 kJ/mol *versus* CsF: 759 kJ/mol).[12] Preliminary calculations performed by Dr. David Ascough revealed that interaction of KF with a hydrogen bond donor in CH_2Cl_2 makes the thermodynamic of phase transfer significantly more favourable (Table 2.3, entry 6 *versus* entry 10).[1] These calculations also confirmed the challenges associated with the use of KF in HB-PTC compared to CsF. The Gibbs free energy change for solvation of CsF in the presence of urea **2.8** is only 0.4 kJ/mol (Table 2.3, entry 9), significantly smaller than the 33.0 kJ/mol for the analogous process with KF (Table 2.3, entry 10).

Table 2.3: Derived Gibbs free energies at 298.15 K for MF solubilisation. Calculations performed by Dr. D. Ascough.[1]

Entry	*Process*	*ΔG (kJ/mol)*
1	$CsF_{(s)} \rightarrow CsF_{(g)}$	152
2	$KF_{(s)} \rightarrow KF_{(g)}$	194
3	$CsF_{(g)} \rightarrow CsF_{(CH_2Cl_2)}$	–116
4	$KF_{(g)} \rightarrow KF_{(CH_2Cl_2)}$	–124
5	$CsF_{(s)} \rightarrow CsF_{(CH_2Cl_2)}$	35.8
6	$KF_{(s)} \rightarrow KF_{(CH_2Cl_2)}$	70.2
7	$CsF_{(CH_2Cl_2)} + \mathbf{2.8}_{(CH_2Cl_2)} \rightarrow CsF * \mathbf{2.8}_{(CH_2Cl_2)}$	–35.4
8	$KF_{(CH_2Cl_2)} + \mathbf{2.8}_{(CH_2Cl_2)} \rightarrow KF * \mathbf{2.8}_{(CH_2Cl_2)}$	–37.2
9	$CsF_{(s)} + \mathbf{2.8}_{(CH_2Cl_2)} \rightarrow CsF * \mathbf{2.8}_{(CH_2Cl_2)}$	0.4
10	$KF_{(s)} + \mathbf{2.8}_{(CH_2Cl_2)} \rightarrow KF * \mathbf{2.8}_{(CH_2Cl_2)}$	33.0

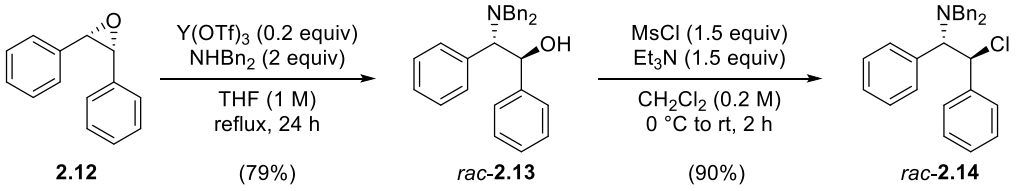
MF refers to a giant ionic lattice in solid state and an ion paired formula unit in gas and solution phases.

(*S*)-**2.8**



2.3 Fluorination of Aziridinium Ions with MF Catalysed by Achiral Schreiner's Urea

For this study, we selected the stilbene-derived β-chloro *N*-dibenzylamine *rac*-**2.14** as stable aziridinium ion precursor, by analogy with the previously investigated stilbene-derived β-bromosulfides. The choice of *N*-substitution was guided by the requirement for facile deprotection following fluorination. *Rac*-**2.14** was obtained from the ring-opening of *cis*-stilbene oxide with dibenzylamine under Lewis acid catalysis, followed by chlorination with methanesulfonyl chloride (MsCl) (Scheme 2.5). The chlorinated product is formed with retention of configuration, due to the anchimeric assistance of the neighbouring amine.[13,14] Since both epoxide ring-opening and chlorination are stereospecific, the synthesis affords *rac*-**2.14** as a single diastereoisomer. Attempts to isolate the corresponding bromide or mesylate failed due to the instability of these compounds in the aqueous work-up required to remove the co-products.



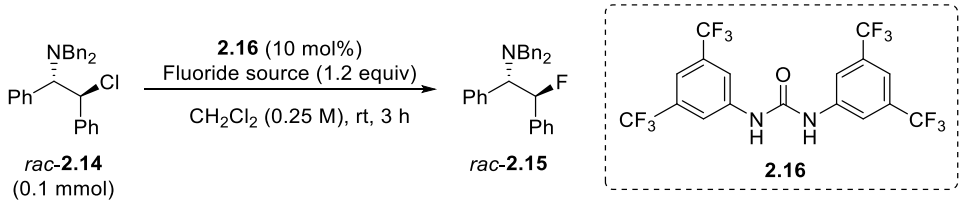
2.12 (79%) *rac*-**2.13** (90%) *rac*-**2.14**

Scheme 2.5: Synthesis of the starting material *rac*-**2.14**.

We firstly tested *rac*-**2.14** in the presence of achiral Schreiner's urea **2.16** as phase-transfer catalyst (10 mol% loading) in combination with 1.2 equivalents of alkali metal fluorides (MF, Table 2.4). The only product obtained was β-fluoroamine *rac*-**2.15**, as determined by ^{1}H NMR analysis of the crude reaction mixture. CsF gave the highest yield (61%, entry 7, Table 2.4), but RbF (40%, entry 5) and KF (15%, entry 3) were also suitable fluoride sources for the fluorination under HB-PTC. The trend in reactivity can be inversely correlated with the lattice energy of the salts, consistent with our mechanistic hypothesis. Control experiments in the absence of the urea confirmed its role in promoting phase-

transfer, as only traces of *rac*-**2.15** were formed after 24 h with CsF (entry 8), and no product was obtained with either RbF or KF (entries 4 and 6). The fluorination with TBAF*3H_2O in the absence of Schreiner's urea (entry 9) was also tested for comparison. The reaction afforded *rac*-**2.15** in lower yield (16%) than the fluorination under HB-PTC with CsF. Lack of reactivity accounted for the low yield observed, as no other species besides the product and the starting material were detected in the ^{1}H NMR spectrum. Notably alcohol *rac*-**2.13** was not formed, even if TBAF*3H_2O was used in this test.

Table 2.4: Screening of MF for the fluorination of *rac*-**2.14** with achiral Schreiner's urea



Entry	*Fluoride source*	*Lattice energy (kJ/mol)*[12]	***2.16** (mol%)*	*Yield* [a]
1	LiF	1049	10	No reaction
2	NaF	930	10	No reaction
3	KF	829	10	15%
4[b]	KF	829	–	No reaction
5	RbF	795	10	40%
6[b]	RbF	795	–	No reaction
7	CsF	759	10	61%
8[b]	CsF	759	–	3%
9	TBAF*3H_2O	–	–	16%

Reaction conditions: *rac*-**2.14** (0.1 mmol), MF (1.2 equiv), **2.16** (10 mol%), CH_2Cl_2 (0.25 M), rt, stirring at 1200 rpm, 3 h. [a] Yield determined by ^{19}F NMR using 4-fluoroanisole as internal standard. [b] 24 h.

Rac-**2.15** used as reference for HPLC separation on a chiral non-racemic stationary phase was synthesised under HB-PTC conditions using Schreiner's urea **2.16** (10 mol%) and CsF (1.2 equiv). As the reaction proceeded, precipitation of a solid that was assigned to the CsBr co-product was observed. The product was purified by flash column chromatography on silica gel and characterised by ^{1}H and ^{19}F NMR. The ^{19}F NMR spectrum shows the presence of a double doublet at –181.42 ppm ($^2J_{HF}$ = 47.8 Hz and $^3J_{HF}$ = 18.5 Hz), at the

characteristic chemical shift interval for aliphatic single C–F bonds. The same coupling constants can be identified in the ^{1}H NMR spectrum for the signals at 6.01 ppm and 4.12 ppm, which can be attributed to the protons geminal and vicinal to the fluorine, respectively (Figure 2.3A). The coupling constant between the two protons ($^{3}J_{HH}$) is 7.5 Hz. These values are similar to those reported for β-fluorosulfides obtained by desymmetrisation of episulfonium ions (Figure 2.3B), for which the retention of configuration was confirmed by single crystal X-ray diffraction of (1*S*,2*S*)-2-fluoro-1,2-di-m-tolylethyl)(phenethyl)sulfane **2.17**. Net retention of configuration is consistent with the proposed mechanism involving desymmetrisation of an intermediate aziridinium ion.

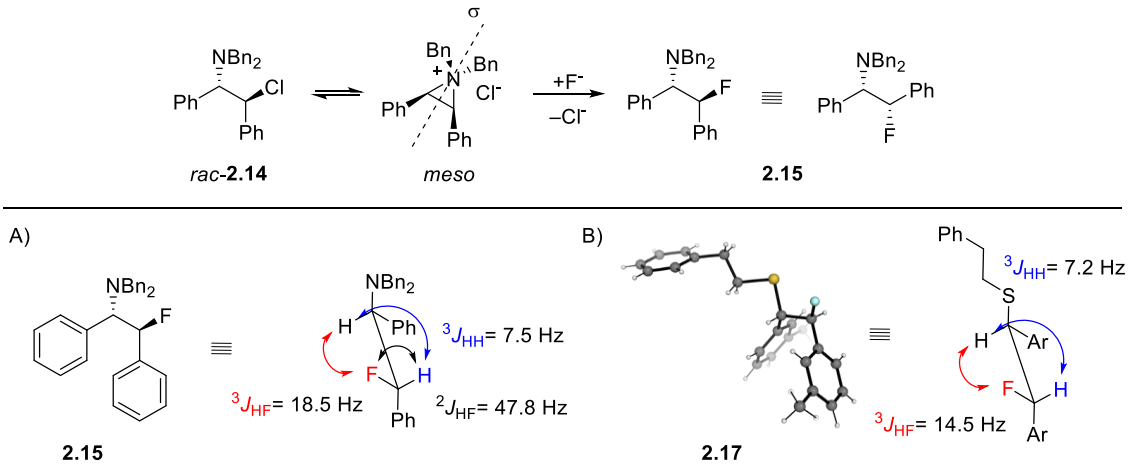


Figure 2.3: Top: β-fluoroamine **2.15** is obtained by fluoride ring opening of a *meso*-aziridinium ion, resulting in retention of configuration. Bottom: Comparison of the coupling constant observed in β-fluoroamine **2.15** (A) and β-flurosulfide **2.17** (B), for which relative and absolute configuration were confirmed by single crystal X-ray diffraction. **2.17** is depicted in the conformation observed in the solid state, which might not correspond to the most stable conformer in solution. **2.15** is depicted in the same conformation to aid comparison of the two structures.

2.4 Optimisation of the Enantioselective Fluorination with CsF

2.4.1 Synthesis of Chiral BINAM-Derived bis-Urea Organocatalysts

Some of the catalysts reported in the following sections were available in the laboratory. The remaining catalysts were synthesised by Dr. Gabriele Pupo and myself. To accelerate the synthesis, I prepared the chiral anilines and Dr. Gabriele Pupo performed the final urea coupling. Catalysts (*S*)-**2.38,** (*S*)-**2.60,** (*S*)-**2.66,** (*S*)-**2.73,** (*S*)-**2.74,** (*S*)-**2.119** and (*S*)-**2.120** were entirely synthesised by myself.

Preliminary screening of chiral hydrogen bond donors, including ureas, thioureas and squaramides, revealed that only ureas were competent catalysts in the fluorination under HB-PTC (see Chapter 5, Scheme 5.1). Among the ureas tested, the axially chiral C_2 H_8-BINAM (5,5',6,6',7,7',8,8'-octahydro-[1,1'-binaphthalene-2,2'-diamine]) derivative (*S*)-**2.18** gave the highest e.r. and was therefore chosen as the lead candidate to design a superior organocatalyst. BINAM ([1,1'-binaphthalene]-2,2'-diamine) is commercially available in enantiopure form and this chiral scaffold can be easily modified through partial reduction of the binaphthyl rings, and 3,3'- or 6,6'-substitution.[15,16] Additionally, structural diversity can be introduced by variation of the isocyanate coupling partner and *via* urea *N*-alkylation (Figure 2.4).

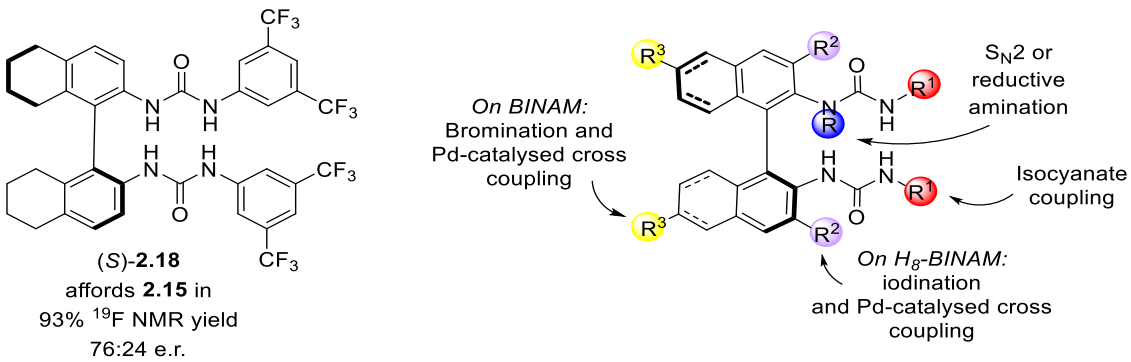
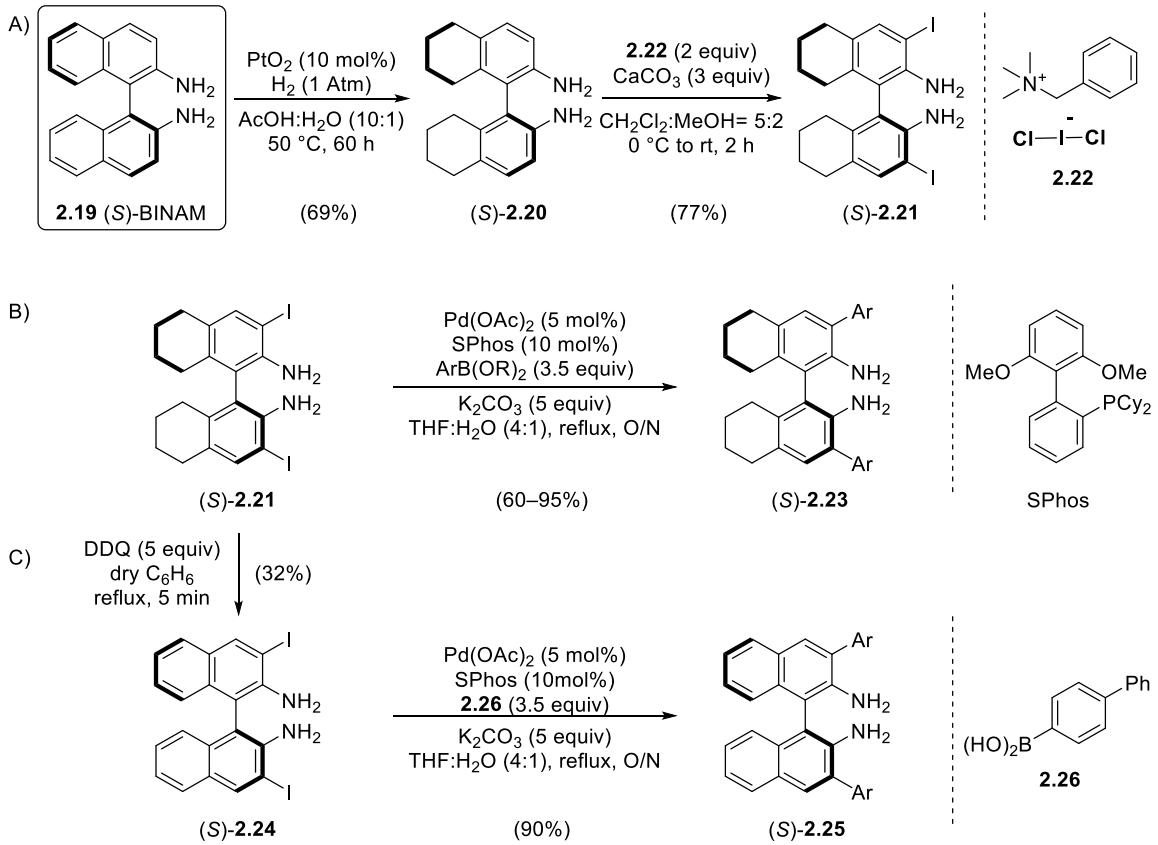


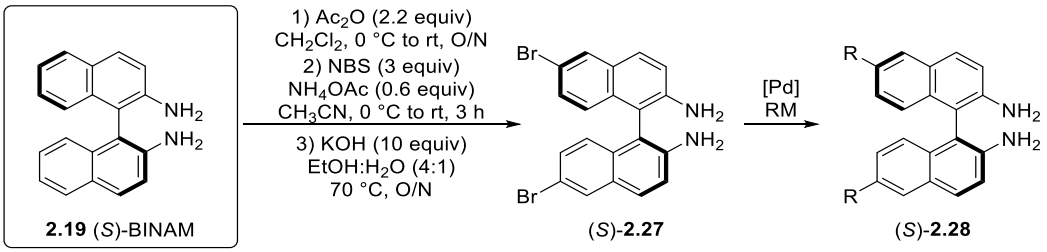
Figure 2.4: Structural modification of the BINAM-derived bis-urea organocatalyst.

Unsaturated 3,3'-substituted bis-anilines (*S*)-**2.23** were synthesised in a three-step sequence (Scheme 2.6). Reduction of commercially available (*S*)-BINAM **2.19**,[17] followed by iodination of the 3,3' positions afforded the common precursor bis-iodoaniline (*S*)-**2.21** (Scheme 2.6A).[18] Partial hydrogenation was necessary to avoid competitive halogenation of the more reactive 6,6' positions. Generation of a library of 3,3'-substituted catalysts was achieved coupling (*S*)-**2.21** with the appropriate boronic acid/ester under Pd-catalysis prior to the formation of the urea in the final step (Scheme 2.6B). Attempts to perform the Suzuki-Miyaura cross-coupling on the preformed urea failed, presumably due to the increased steric hindrance. Oxidation of bis-iodoaniline (*S*)-**2.21** to afford the corresponding unsaturated (*S*)-**2.24** was accomplished with 2,3-dichloro-5,6-dicyano-1,4-benzoquinone (DDQ, Scheme 2.6C).[18] From (*S*)-**2.24**, different aromatic substituents could be introduced in the 3,3'-positions of the BINAM scaffold *via* Pd-catalysed cross-coupling.



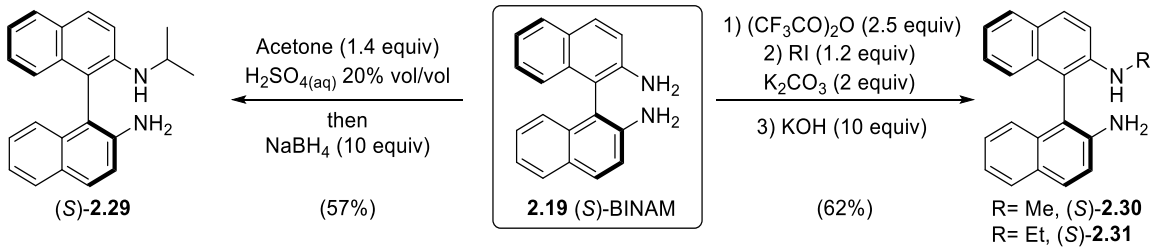
Scheme 2.6: Synthesis of 3,3'-substituted H_8-BINAM- and BINAM-derived anilines. O/N = overnight.

Pd-catalysed cross-coupling was also used for the functionalisation of the 6,6'-positions starting from the corresponding 6,6'-bis-bromo-derivative (*S*)-**2.27**, obtained by treating acetylated (*S*)-BINAM with *N*-bromosuccinimide (NBS) and ammonium acetate (Scheme 2.7), followed by hydrolysis.[19]



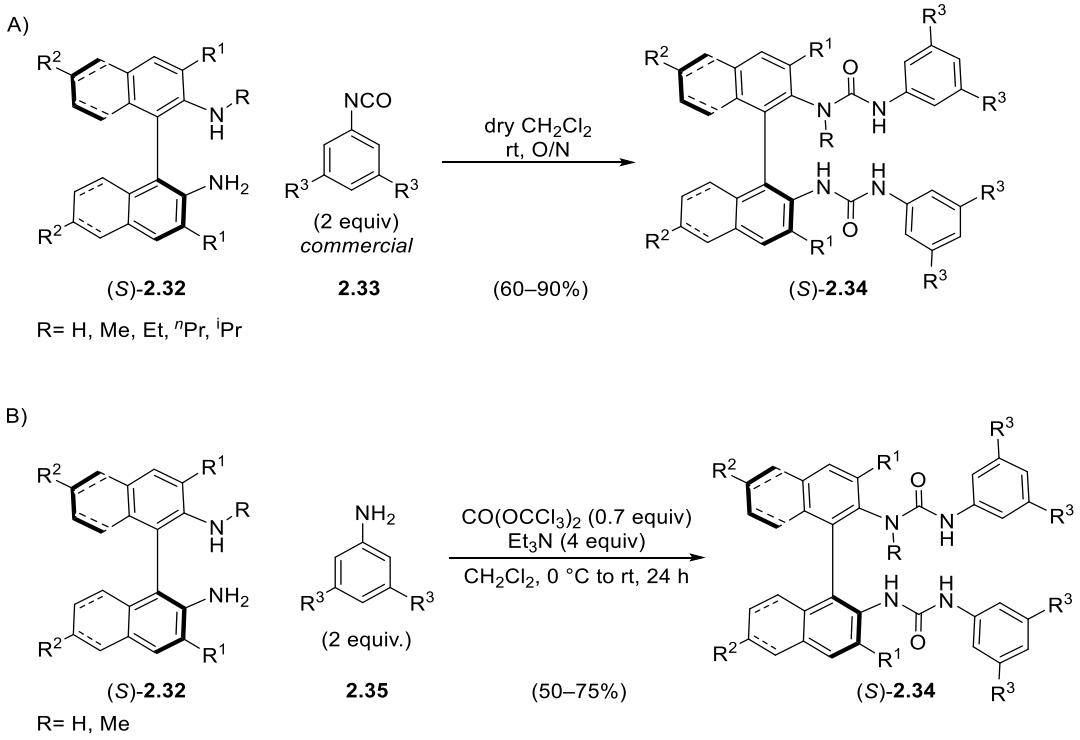
Scheme 2.7: Synthesis of 6,6'-substituted BINAM-derived anilines *via* bromination of the 6 and 6' positions followed by Pd-catalysed cross-coupling. O/N = overnight.

Finally, alkylation was performed either on unprotected (*S*)-BINAM *via* reductive amination (Scheme 2.8, left) or on the corresponding trifluoroacetamide with the appropriate alkylating agent (MeI or EtI), followed by basic hydrolysis, to afford the unprotected anilines (*S*)-**2.30** (R =Me) and (*S*)-**2.31** (R =Et) (Scheme 2.8, right).[8]



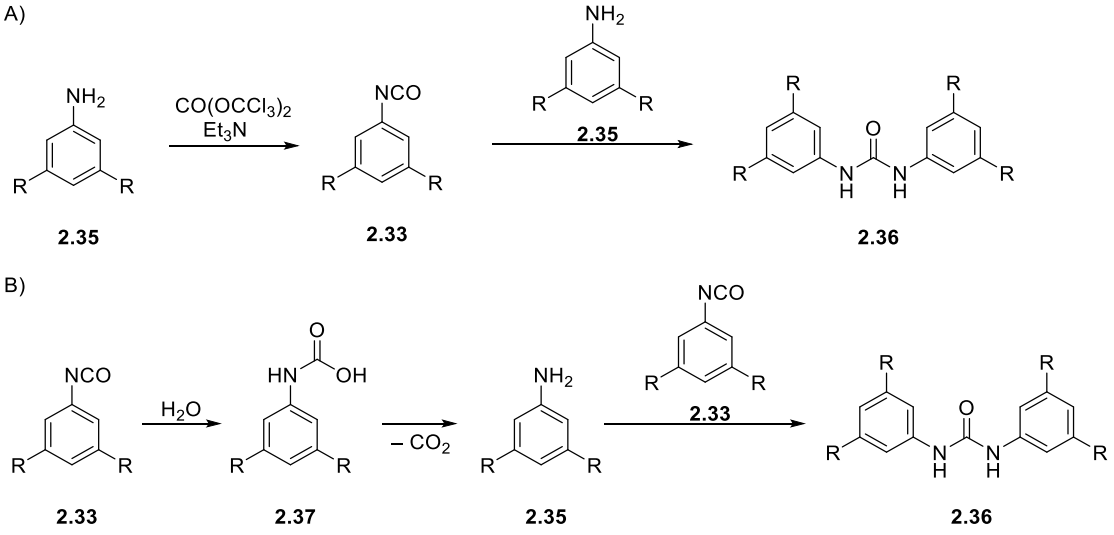
Scheme 2.8: Mono *N*-alkylation of (*S*)-BINAM **2.19** *via* reductive amination (left) or S_N2 substitution (right).[8]

The bis-urea organocatalysts (*S*)-**2.34** were synthesised by coupling the BINAM-derived chiral aniline (*S*)-**2.32** with the desired isocyanate **2.33**, which was either obtained from commercial suppliers (Scheme 2.9A) or generated *in situ* from the corresponding achiral aniline **2.35** in the presence of bis(trichloromethyl) carbonate (triphosgene) and triethylamine (Scheme 2.9B).



Scheme 2.9: Urea coupling using commercial isocyanates (A) or generating the isocyanate *in situ* with triphosgene and Et_3N (B).

An unwanted side-product of both procedures was the achiral urea of general structure **2.36**, derived from homocoupling of the achiral aniline (Scheme 2.10A). When commercial isocyanates were employed, aniline **2.35** was formed by isocyanate hydrolysis followed by decarboxylation (Scheme 2.10B).



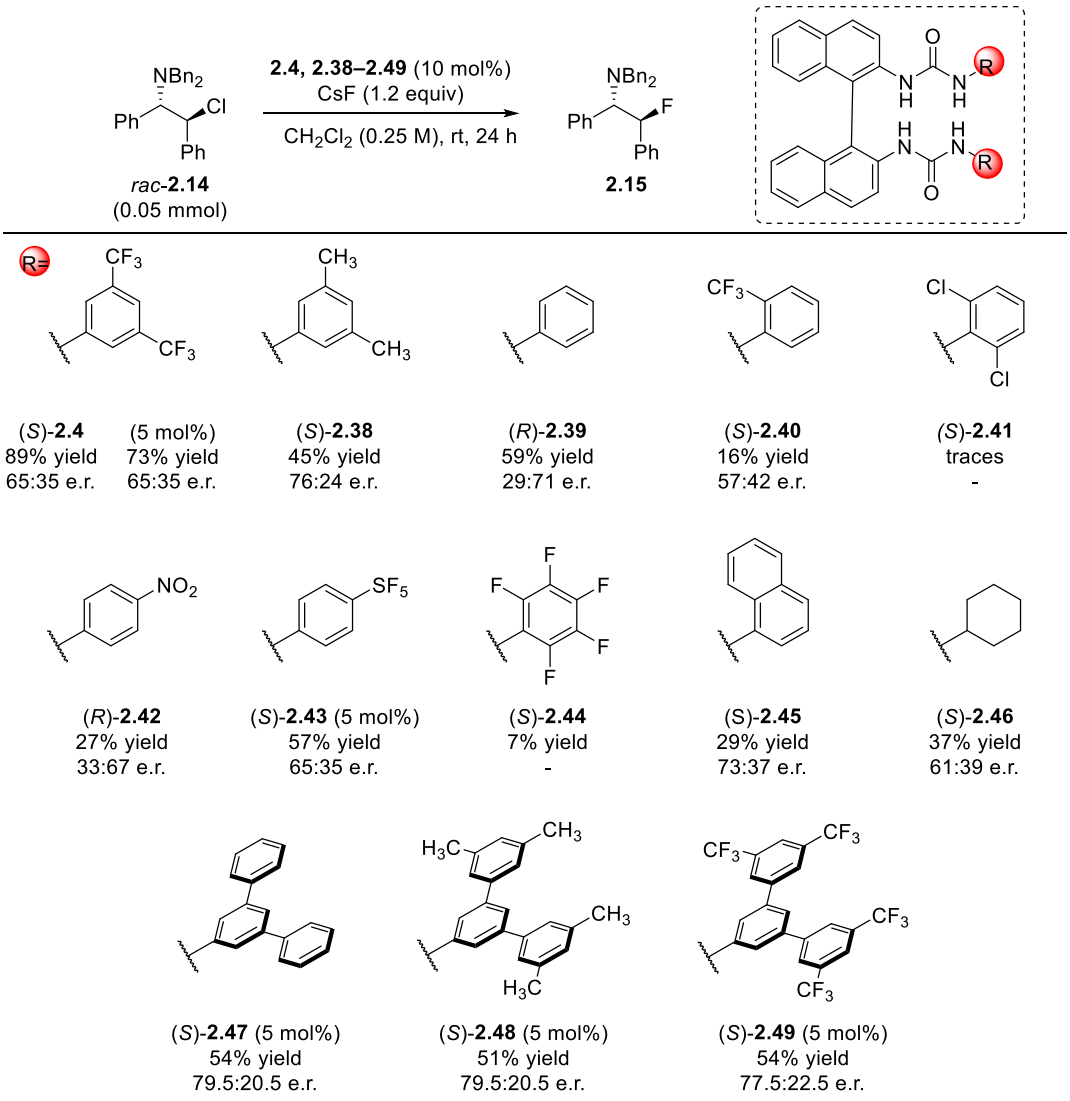
Scheme 2.10: Generation of achiral urea **2.36** *via* homocoupling. A) Reaction of the isocyanate generated *in situ* with unreacted aniline **2.35**. B) Reaction of the commercial isocyanate and the aniline formed by isocyanate decomposition *via* hydrolysis followed by decarboxylation.

Careful chromatographic purification was required to remove achiral **2.36** from the chiral bis-urea. This was important because the achiral urea **2.36** could act as phase-transfer catalyst in a competitive non-enantioselective fluorination. To limit its formation during work-up, methanol was added at the end of the reaction to quench unreacted isocyanate.

2.4.2 Fluorination of Stilbene-Derived β-Chloro-*N*,*N*-Dibenzylamine

The parent bis-urea (*S*)-**2.4**, and the C_2-symmetric hydrogen bond donors originally screened (see Chapter 5, Scheme 5.1) bear 3,5-bis(trifluoromethyl)phenyl substituents, introduced by reaction of the chiral bis-aniline with 3,5-bis(trifluoromethyl)phenyl isocyanate. This motif is commonly encountered in the design of (thio)urea organocatalysts. The electron withdrawing trifluoromethyl groups increase the acidity of the hydrogen bond donor and of the neighbouring ortho-protons, two effects that are considered responsible of improved catalysis.[20,21] It has been suggested that the highly polar ortho protons might play a role in catalyst activation *via* an intramolecular hydrogen bonding with the (thio)carbonyl group, decreasing its basicity and thus disfavouring intermolecular aggregation. Such an interaction would also contribute to further decreasing the pK_a of the (thio)urea N–Hs.[22,23] Finally, the relatively acidic ortho protons might be involved in additional non-covalent interactions with the substrate. Replacement of this motif with either alkyl (cyclohexyl) or other aromatic groups on the BINAM-derived bis-urea scaffold **2.38–2.49** resulted in less active catalysts, regardless of the electronic properties of the isocyanate substituents (Scheme 2.11). Ortho-substituted aromatic rings were extremely detrimental for both reactivity and enantioselectivity, probably due to the increased steric hindrance in proximity of the urea motif. The enantioselectivity was improved with introduction of an extended terphenyl unit in place of the phenyl ring (up to 79.5:20.5 e.r., catalysts (*S*)-**2.47–2.49**). Within this series, slightly better enantiocontrol was obtained with more electron rich substituents ((*S*)-**2.47**, (*S*)-**2.48** 79.5:20.5 e.r. *versus*

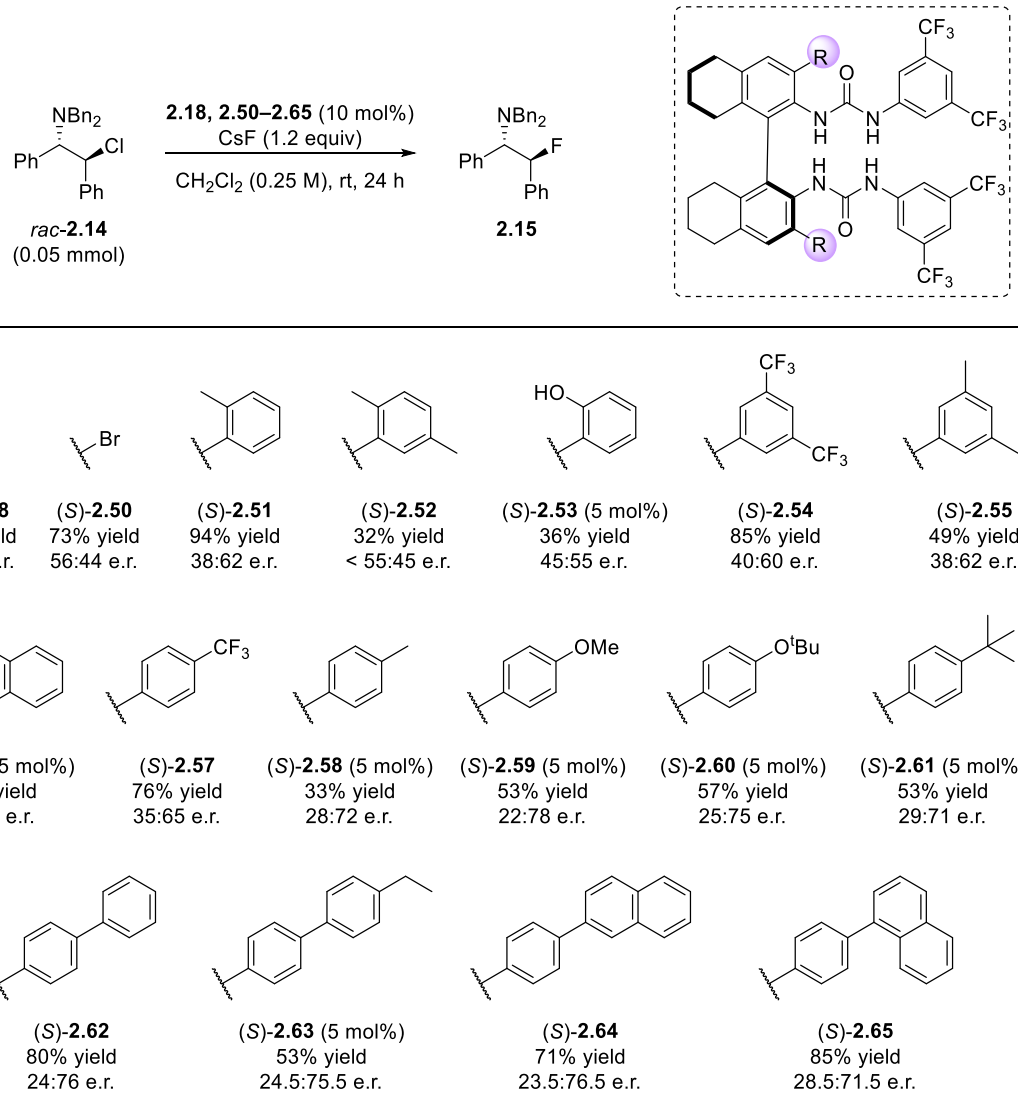
(*S*)-**2.49**, 77.5:22.5 e.r.). On the other hand, polyfluorination improved the solubility of (*S*)-**2.49** compared to the non-fluorinated analogues (*S*)-**2.47** and (*S*)-**2.48**.



Scheme 2.11: Effect of structural variation on the achiral side of the urea organocatalyst on the outcome of the enantioselective fluorination of *rac*-**2.14** with CsF. Yield determined by ^{19}F NMR using 4-fluoroanisole as internal standard. e. r. determined by HPLC using a chiral non-racemic stationary phase.

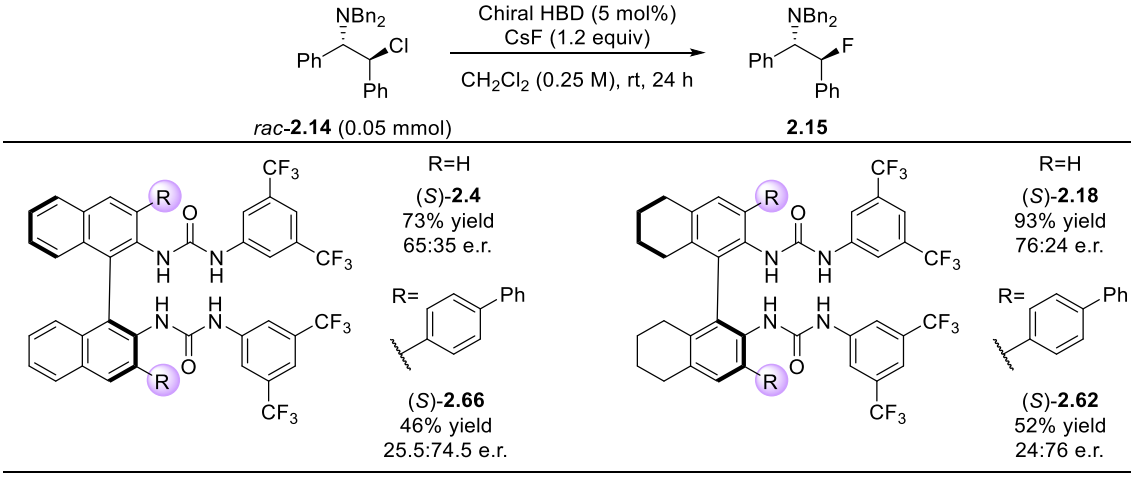
Next, we evaluated the effect of substituents in the 3 and 3' positions of the BINAM scaffold (Scheme 2.12). Except for (*S*)-**2.18** (R =H) and (*S*)-**2.50** (R =Br), all the catalysts within this series afforded **2.15** with opposite enantioselectivity than those previously screened (Scheme 2.11). While almost all the ureas tested afforded **2.15** in good yield, the steric and electronic properties of the 3,3'-substituents proved to be crucial in influencing enantioselectivity. The catalyst bearing ortho- ((*S*)-**2.51–2.53**, up to 38:62 e.r., Scheme

2.12) and meta-substituted aryl rings ((*S*)-**2.54–2.55**, up to 38:62 e.r.) gave poorer results than unsubstituted (*S*)-**2.18** (76:24 e.r.). For *para*-substituted aryl rings ((*S*)-**2.57–2.65**), enantioselectivity increased with the electron donating ability of the para substituent (*p*-CF_3 35:65 e.r., *p*-CH_3 28:72 e.r., *p*-OMe: 22:78 e.r.), with urea (*S*)-**2.59** bearing 4-OMe(phenyl) groups giving the highest e.r.. Finally, the steric requirements of the para substituent had a major effect on enantioselectivity, which decreased with bulkier substituents ((*S*)-**2.59**, R = 4-OMe(phenyl) 22:78 e.r. *versus* (*S*)-**2.60**, R = 4-O^{t}Bu(phenyl), 25:75 e.r. and (*S*)-**2.62**, R = 4-biphenyl 24:76 e.r. *versus* (*S*)-**2.61**, R = 4-^{t}Bu(phenyl), 29:71 e.r.).



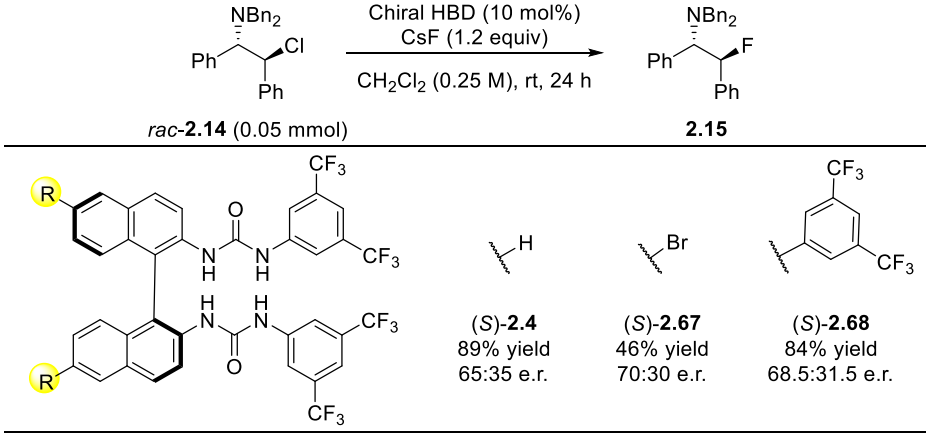
Scheme 2.12: Effect of 3,3' substitution of the bis-urea scaffold on the outcome of the enantioselective fluorination of *rac*-**2.14** with CsF. Yield determined by ^{19}F NMR using 4-fluoroanisole as internal standard. e. r. determined by HPLC using a chiral non-racemic stationary phase.

Unsubstituted (*S*)-**2.4** and (*S*)-**2.18**, derived from BINAM and H_8-BINAM respectively, exhibited remarkably different selectivity ((*S*)-**2.4**: 65:35 e.r. and (*S*)-**2.18**: 76:24 e.r.). On the contrary, 3,3'substituted BINAM-derived (*S*)-**2.66** and H_8-BINAM-derived (*S*)-**2.62** afforded **2.15** in comparable yield and e.r. (Scheme 2.13). Since the synthesis of (*S*)-**2.66** involved an extra step (oxidation), which was low-yielding, and the catalyst did not offer any improvement compared to (*S*)-**2.62**, this class was not further evaluated.



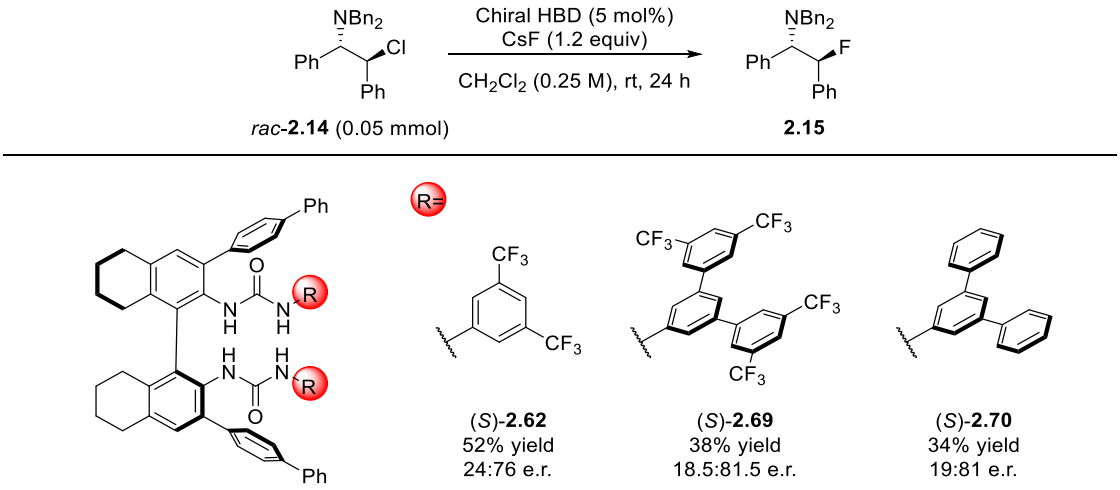
Scheme 2.13: Effect of the oxidation state of the BINAM scaffold on the outcome of the enantioselective fluorination of *rac*-**2.14** with CsF. Yield determined by ^{19}F NMR using 4-fluoroanisole as internal standard. e. r. determined by HPLC using a chiral non-racemic stationary phase.

Finally, 6,6'-substitution had only a marginal positive effect on enantioselectivity (Scheme 2.14), inferior to that obtained with 3,3'-substitution (Scheme 2.12).



Scheme 2.14: Effect of 6,6' substitution of the bis-urea scaffold on the outcome of the enantioselective fluorination of *rac*-**2.14** with CsF. Yield determined by ^{19}F NMR using 4-fluoroanisole as internal standard. e. r. determined by HPLC using a chiral non-racemic stationary phase.

Since both extension of the achiral side of the urea (Scheme 2.11) and 3,3'-substitution (Scheme 2.12) had a positive impact on enantioselectivity, we next combined these features (Scheme 2.15). Catalyst (*S*)-**2.69**, bearing 3,3'-biphenyl substituents and a polyfluorinated terphenyl unit, afforded **2.15** in 18.5:81.5 e.r., which is superior to the enantiomeric ratio obtained with either (*S*)-**2.49** (77.5:22.5 e.r., Scheme 2.11), which lacked 3,3'-substitution, or (*S*)-**2.62** (24:76 e.r., Scheme 2.15), bearing the 3,5-bis(trifluoromethyl)phenyl unit. Similar enantioselectivity was obtained with the non-fluorinated analogue (*S*)-**2.70** (19:81 e.r.). It is worth noting that (*S*)-**2.49** and (*S*)-**2.62** afforded **2.15** with opposite enantioselectivity, which might explain the small gain in selectivity observed upon combining their key structural elements.

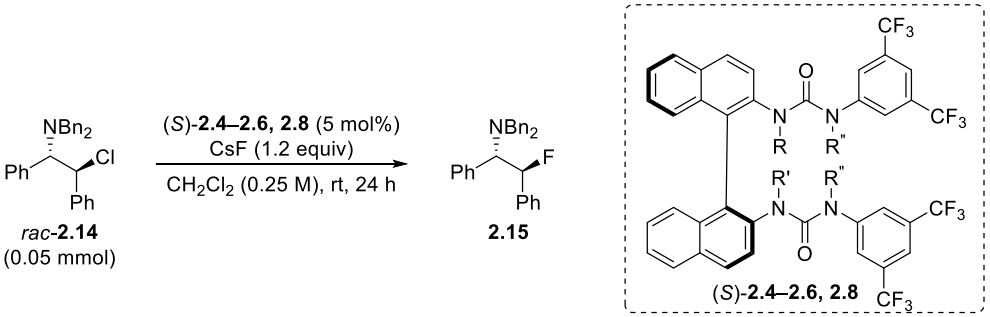


Scheme 2.15: Combination of the features of the most enantioselective bis-ureas in a single catalyst structure and evaluation of this novel class in the enantioselective fluorination of *rac*-**2.14** with CsF. Yield determined by ^{19}F NMR using 4-fluoroanisole as internal standard. e. r. determined by HPLC using a chiral non-racemic stationary phase.

While these catalysts represented a significant improvement, the level of enantioselectivity achieved (up to 81.5:18.5 e.r.) was still unsatisfactory. At this stage of the project, parallel studies on the episulfonium system led to the discovery that urea alkylation had a beneficial impact on enantioselectivity (section 2.1). The same methylated bis-urea organocatalysts were tested in the fluorination of *rac*-**2.14** (Table 2.5). As observed in the desymmetrisation

of episulfonium ions, only mono *N*-methylation on the BINAM side ((*S*)-**2.8**) retained reactivity (54% yield, entry 4), while improving enantiocontrol (72:28 e.r. *versus* 65:35 e.r for non-alkylated (*S*)-**2.4**).

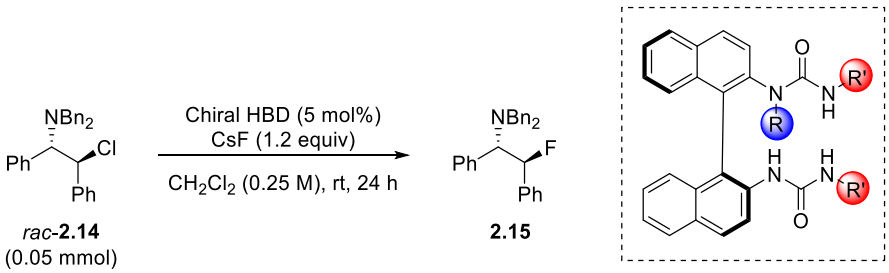
Table 2.5: Effect of urea *N*-methylation on the outcome of the enantioselective fluorination of *rac*-**2.14** with CsF.

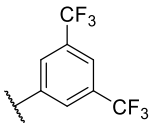
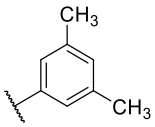
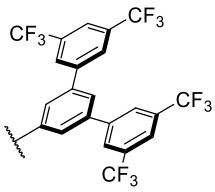
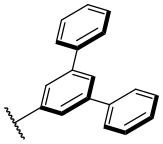


Entry	*Catalyst*	*R*	*R'*	*R"*	*Yield*[a]	*e.r.*[b]
1	**2.4**	H	H	H	73%	65:35
2	**2.5**	H	H	Me	No reaction	–
3	**2.6**	Me	Me	H	No reaction	–
4	**2.8**	Me	H	H	54%	72:28

Reaction conditions: *rac*-**2.14** (0.05 mmol), 1.2 equiv of CsF, 5 mol% of catalyst, CH_2Cl_2 (0.25 M), stirring at 900 rpm at rt for 24 h. [a] Yield determined by ^{19}F NMR using 4-fluoroanisole as internal standard. [b] e. r. determined by HPLC using a chiral non-racemic stationary phase.

Organocatalysts (*S*)-**2.71**, (*S*)-**2.72** and (*S*)-**2.3**, bearing bulkier *N*-substituents were tested next (Scheme 2.16, entry 1). In the case of the episulfonium system, increasing the size of the alkyl chain from methyl to isopropyl led to increased selectivity.[8] On the contrary, for the aziridinium ion derived from *rac*-**2.14**, catalysts with bulkier side-chains showed substantially reduced enantiocontrol than methylated (*S*)-**2.8** (between 59:41 e.r. and 64.5:35.5 e.r. *versus* (*S*)-**2.8**: 72:28 e.r.) similar to that of non-alkylated (*S*)-**2.4** (65:35 e.r.). In general, alkylated catalysts were less reactive than the parent non-alkylated urea. The methylated analogue of (*S*)-**2.49** afforded β-fluoroamine **2.15** in 85.5:14.5 e.r., (entry 3), the highest enantiomeric ratio obtained up to this point.



	R'=	R= H	R= Me	R= Et	R= Pr	R= ^{i}Pr
1		(*S*)-**2.4** 73% yield 65:35 e.r.	(*S*)-**2.8** 54% yield 72:28 e.r.	(*S*)-**2.71** 57% yield 63:37 e.r.	(*S*)-**2.72** 77% yield 64.5:35.5 e.r.	(*S*)-**2.3** 75% yield 59:41 e.r
2		(*S*)-**2.38** 45% yield 76:24 e.r.	(*S*)-**2.73** 25% yield 82.5:17.5 e.r.	–	–	–
3		(*S*)-**2.49** 54% yield 77.5:22.5 e.r.	(*S*)-**2.74** 34% yield 85.5:14.5 e.r.	–	–	–
4		(*S*)-**2.47** 54% yield 79.5:20.5 e.r.	(*S*)-**2.75** 34% yield 76:24 e.r.	–	–	–

Scheme 2.16: Effect of urea *N*-alkylation on the outcome of the enantioselective fluorination of *rac*-**2.14** with CsF. Yield determined by ^{19}F NMR using 4-fluoroanisole as internal standard. e. r. determined by HPLC using a chiral non-racemic stationary phase.

Figure 2.5 summarises the effect that structural modifications of BINAM-derived bis-ureas have on the asymmetric fluorination of model β-chloroamine *rac*-**2.14**. Extension of the π-system of the achiral side of the urea increased the enantiomeric ratio up to 79.5:20.5 e.r. from 65:35 e.r. ((*S*)-**2.4**). Similar enantiocontrol, but in the opposite direction, was exerted by the best 3,3'-substituted catalysts (up to 22:78 e.r.). Among this class, the best results were obtained by introducing electron rich para-substituted aromatic rings (e.g. 4-methoxy phenyl). These effects were not additive: their combination only marginally improved the enantiocontrol compared to the parent catalysts (19:81 e.r. *versus* 24:76 e.r. and

77.5:22.5 e.r.), probably due to the opposite enantioinduction of the two classes. *N*-Methylation of (*S*)-**2.4** was beneficial (72:28 e.r.). Combining *N*-methylation with the extended terphenyl unit furnished the most selective catalyst tested with *rac*-**2.14**, but the enantiocontrol was only moderate (85.5:14.5 e.r.). The most enantioselective BINAM-derived bis-ureas afforded **2.15** in low to moderate yields (34-54%) after 24 h. Both these results were unsatisfactory.

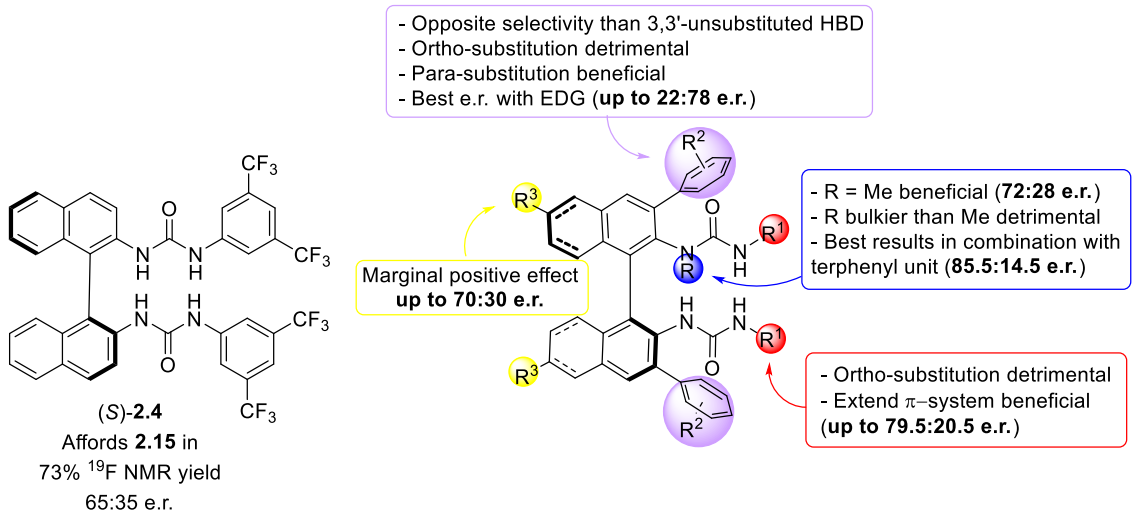
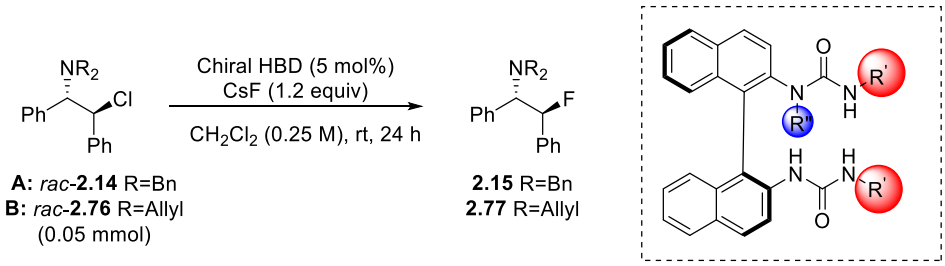


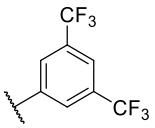
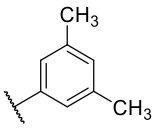
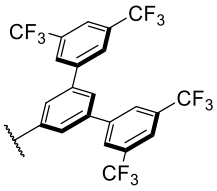
Figure 2.5: Summary of the effect of bis-urea structural modifications on the enantioselectivity of the fluorination of β-chloroamine *rac*-**2.14**.

2.4.3 Fluorination of Stilbene-Derived β-Chloro-*N*,*N*-Diallylamine

N-Methyl bis-urea (*S*)-**2.74**, bearing the polyfluorinated terphenyl unit, was the most selective catalyst synthesised for the enantioselective fluorination of *rac*-**2.14**, but neither the yield, nor the selectivity obtained were satisfactory (34% yield, 85.5:14.5 e.r). We thus turned to evaluating the effect of *N*-substitution on the β-chloroamine precursor, selecting racemic β-chloro *N*-diallylamine **2.76** for further investigation. The choice of *N*-allyl substitution was dictated by the possibility to access the corresponding primary amine *via* Pd-catalysed deallylation post-fluorination.[24] This substrate was evaluated in the enantioselective fluorination with CsF in the presence of a selected number of catalysts

(Scheme 2.17). *Rac*-**2.76** was more reactive than *rac*-**2.14**, affording the corresponding β-fluoroamine **2.77** in >80% yield with all catalysts tested. While enantiocontrol in the presence of the non-alkylated catalysts was poor, this was greatly improved upon urea methylation (e.g. (*S*)-**2.8**, R'=Me, 85:15 e.r. *versus* (*S*)-**2.4**, R' =H, 60:40 e.r., entry 1, Scheme 2.17). The selectivity was unvaried upon increasing the size of the *N*-alkyl chain on the catalysts (entry 1). The positive impact of *N*-methylation was retained in the series bearing the terphenyl units (entry 3) and (*S*)-**2.74** confirmed its superior performance, affording **2.77** in >95% yield and 89:11 e.r..

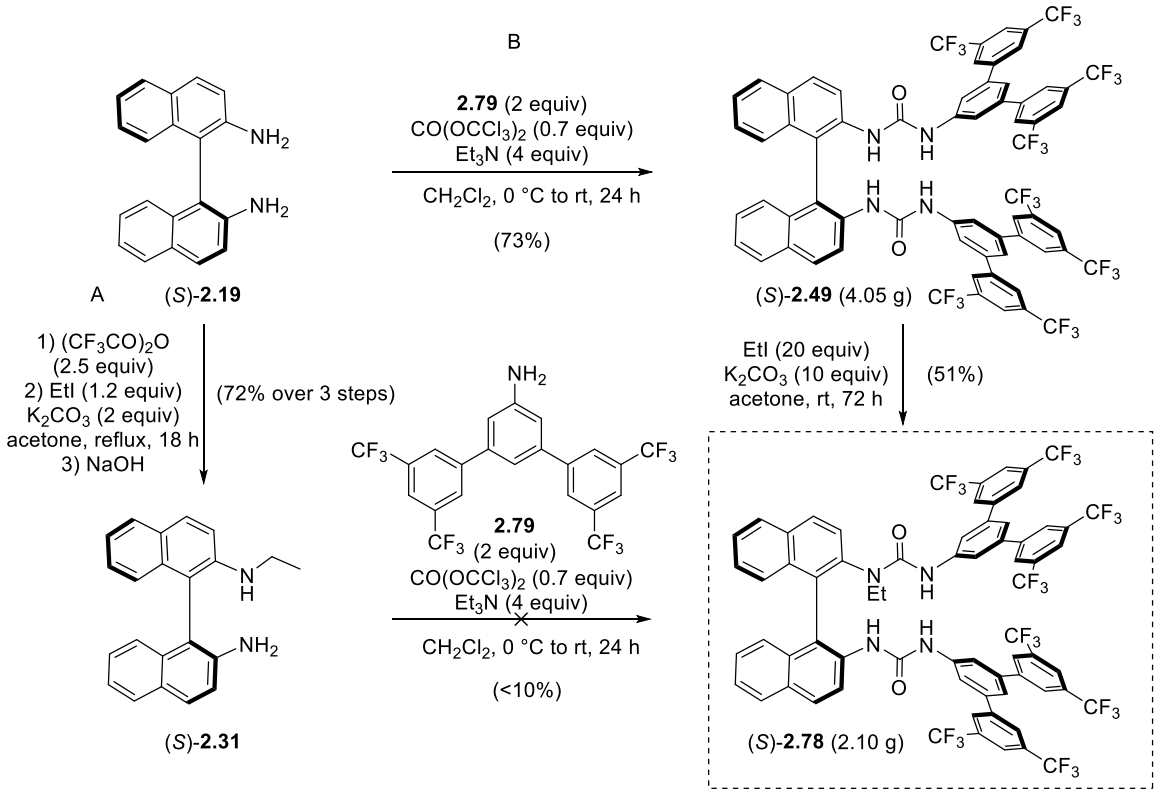


	R" =	R= H	R= Me	R= Et	R= Pr	R= ^{i}Pr
1		(*S*)-**2.4** **A:** 73% yield 65:35 e.r. **B:** >95% yield 60:40 e.r.	(*S*)-**2.8** **A:** 54% yield 72:28 e.r. **B:** >95% yield 85:15 e.r.	(*S*)-**2.71** **A:** 57% yield 63:37 e.r. **B:** >95% yield 86:14 e.r.	(*S*)-**2.72** **A:** 77% yield 65.5:35.5 e.r. **B:** >95% yield 86:14 e.r.	(*S*)-**2.3** **A:** 75% yield 59:41 e.r. **B:** >95% yield 84:16 e.r.
2		(*S*)-**2.38** **A:** 45% yield 76:24 e.r. **B:** >95% yield 65:35 e.r.	(*S*)-**2.73** **A:** 25% yield 82.5:17.5 e.r. **B:** >95% yield 80:20 e.r.	–	–	–
3		(*S*)-**2.49** **A:** 54% yield 79.5: 20.5 e.r. **B:** 80% yield 57:43 e.r.	(*S*)-**2.74** **A:** 34% yield 85.5:14.5 e.r. **B:** >95**% yield** **89:11 e.r.**	–	–	–

Scheme 2.17: Effect of urea *N*-alkylation on the enantioselective fluorination of *rac*-**2.76** with CsF. Yield determined by ^{19}F NMR using 4-fluoroanisole as internal standard. e. r. determined by HPLC using a chiral non-racemic stationary phase.

Optimisation of the fluorination of *rac*-**2.76** catalysed by (*S*)-**2.74** allowed to enhance the enantiomeric ratio to a maximum of 94:6 e.r. for the reactions performed in $CHCl_3$ at -15 °C and in 1,2,3-trifluorobenzene at –10 °C, while maintaining synthetically useful yields (89%

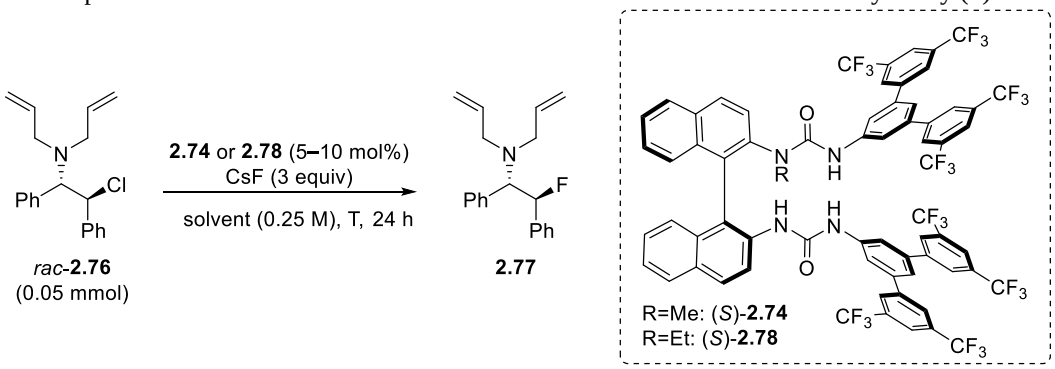
and 81%, respectively, see Chapter 5 Tables 5.1–5.3 for the full screening tables). The enantiocontrol was not significantly improved at lower temperature, while yields dropped considerably ($CHCl_3$, –30 °C: 35%; 1,2,3-trifluorobenzene, –15 °C: 49%). For this reason, we focused our efforts on the synthesis of catalysts analogous to (*S*)-**2.74** with bulkier *N*-alkyl groups. This strategy had proved fruitful in the past for the enantioselective fluorination of β-bromosulfides.[8] Attempts to synthesise bis-urea (*S*)-**2.78**, featuring *N*-ethylation and the polyfluorinated terphenyl motif, afforded the desired product in less than 10% yield when the previously optimised protocol was employed (Scheme 2.18A; see also Chapter 3). Deprotonation of *N*-Et BINAM followed by reaction with the preformed isocyanate was equally unsuccessful. Finally, Dr. Gabriele Pupo succeeded in synthesising the catalyst reacting bis-urea (*S*)-**2.49** with an excess of ethyl iodide (51% yield, Scheme 2.18B).



Scheme 2.18: Synthesis of catalyst (*S*)-**2.78**. A) Attempts to obtaining (*S*)-**2.78** according to the previously optimised procedure failed. B) Successful synthesis, involving urea alkylation following the urea coupling. Optimisation of the alkylation and the final synthesis were performed by Dr. G. Pupo.

Catalyst (*S*)-**2.78** was tested in the fluorination of *rac*-**2.76** with CsF in $CHCl_3$, affording **2.77** in similar yield and slightly improved enantiocontrol than *N*-methylated (*S*)-**2.74** (90.5:9.5 e.r., entry 2 *versus* 89:11 e.r., entry 1, Table 2.6). Anhydrous $CHCl_3$ from an Acroseal™ bottle was used in these experiments to ensure reproducibility of the results, and the solvent was filtered on basic alumina prior to the reaction to remove traces of HCl. No precautions were taken to exclude moisture and the CsF was used as provided by the supplier (fine powder). A control experiment employing CsF dried *in vacuo* at 200 °C for 48 h and using Schlenk techniques furnished the same results (>95% yield, 90.5:9.5 e.r., entry 3). The enantiomeric ratio could be improved to 95:5 e.r. running the reaction at -15 °C (75% yield, entry 4), while further decreasing the temperature caused a drop in yield (38% yield at –30 °C, entry 5). 1,2,3-trifluorobenzene was also tested at –15 °C, giving worse enantiocontrol than $CHCl_3$ at the same temperature (94:6 e.r., entry 6).

Table 2.6: Optimisation of the enantioselective fluorination of *rac*-**2.76** with CsF catalysed by (*S*)-**2.78**

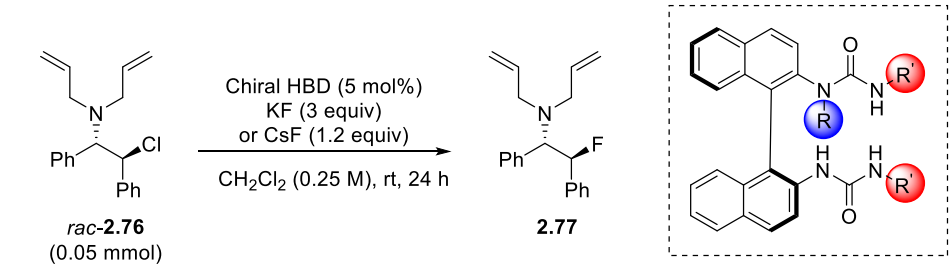


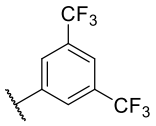
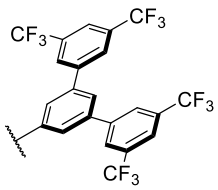
Entry	*Catalyst*	*Solvent*	*Temperature (° C)*	*Yield* [a]	*e.r.* [b]
1[c]	(*S*)-**2.74**	$CHCl_3$	22	>95%	89:11
2[c]	(*S*)-**2.78**	$CHCl_3$	22	>95%	90.5:9.5
3[c] [d]	(*S*)-**2.78**	$CHCl_3$	22	>95%	90.5:9.5
4	(*S*)-**2.78**	$CHCl_3$	–15	75%	95:5
5[e]	(*S*)-**2.78**	$CHCl_3$	–30	38%	95:5
6	(*S*)-**2.78**	1,2,3-trifluorobenzene	–15	85%	94:6

Reaction conditions: *rac*-**2.76** (0.05 mmol), 3 equiv of CsF, 10 mol% of catalyst, 0.25 M, stirring at 900 rpm, 24 h. [a] Yield determined by ^{19}F NMR using 4-fluoroanisole as internal standard. [b] e. r. determined by HPLC using a chiral non-racemic stationary phase. [c] 5 mol% of catalyst; [d] Reaction performed using Schlenk techniques and CsF dried *in vacuo* at 200 °C for 48 h. [e] 48 h.

2.5 Optimisation of the Enantioselective Fluorination with KF

Having optimised the reaction with CsF, we turned our attention to the fluorination with KF. Preliminary results with achiral Schreiner's urea showed that fluorination with KF was feasible, but the yield of **2.15** obtained using KF as a fluorine source was lower than with CsF when 1.2 equivalents of MF were used (15% versus 61%, Table 2.4). We thus selected the β-chloroamine *rac*-**2.76**, which was more reactive than β-chloroamine *rac*-**2.14**, for evaluating the performance of a small library of catalysts (5 mol% loading) in the asymmetric fluorination with KF (Scheme 2.19). The fluorination conducted with 3 equivalents of KF afforded **2.77** in the same yield as the reaction run with 1.2 equivalents of CsF. Importantly, stirring efficiency had a stronger influence on yield when KF was used compared to CsF. The enantioselectivity in the presence of the same catalyst was independent of the fluoride source employed.

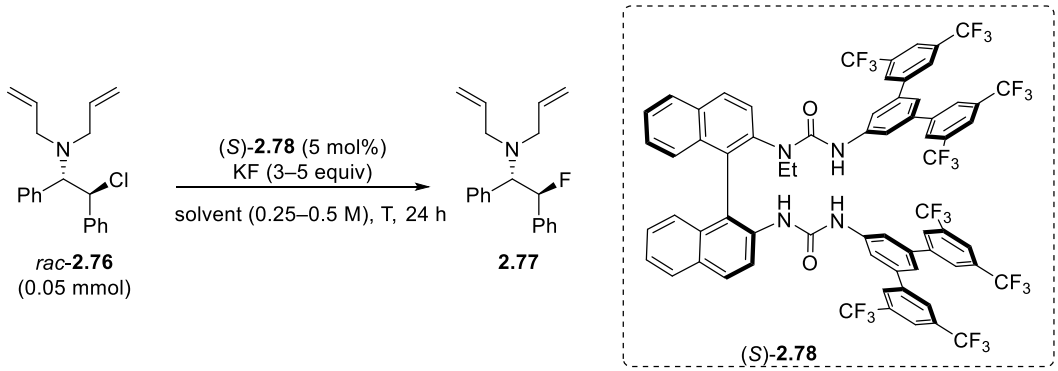


R'=	R= H	R= Me	R= Et	R= ^{i}Pr
	(*S*)-**2.4** **KF:** >95% yield 55:45 e.r. **CsF:** >95% yield 60:40 e.r.	(*S*)-**2.8** **KF:** >95% yield 85:15 e.r. **CsF:** >95% yield 85:15 e.r.	(*S*)-**2.71** **KF:** >95% yield 86:14 e.r. **CsF:** >95% yield 86:14 e.r.	(*S*)-**2.3** **KF:** 83% yield 86:14 e.r. **CsF:** >95% yield 86:14 e.r.
	(*S*)-**2.49** **KF:** 77% yield 55:45 e.r. **CsF:** 80% yield 57:43 e.r.	(*S*)-**2.74** **KF:** 72% yield 88:12 e.r. **CsF:** >95% yield 89:11 e.r.	(*S*)-**2.78** **KF:** 80% yield 90.5:9.5 e.r. **CsF:** >95% yield 90.5:9.5 e.r.	–

Scheme 2.19: Catalyst screening for the enantioselective fluorination of *rac*-**2.76** with KF. Results of the fluorination with CsF are reported for comparison. Yield determined by ^{19}F NMR using 4-fluoroanisole as internal standard. e. r. determined by HPLC using a chiral non-racemic stationary phase.

Further optimisations revealed that 5 equivalents of KF and increased concentration (0.5 M) enhanced the yield (see Chapter 5, Table 5.4). 1,2-Difluorobenzene (1,2-DFB, entry 2, Table 2.7), which already showed improved results for the enantioselective desymmetrisation of *meso*-episulfonium ions,[8] and α,α,α-trifluorotoluene ($PhCF_3$, entry 3) gave the best results at room temperature both in terms of yield (≥95%) and enantioselectivity (93:7 e.r.). Chlorinated solvents afforded **2.77** in good yields at room temperature (80%, entries 4 and 6) and at 0 °C (CH_2Cl_2: 80% yield, entry 11; $CHCl_3$: >95% yield, entry 12). The selectivity was comparable to that of other solvents screened and could be improved by reducing the temperature to –15 °C (71% isolated yield, 95:5 e.r., entry 14). The importance of removing traces of HCl from the $CHCl_3$ prior to the reaction is evident from the comparison of entry 6 (80% yield, 90.5:9.5 e.r.), where the solvent was filtered on basic alumina, and entry 7 (52% yield, 85:15 e.r.), where the solvent was used directly from the bottle. In the second case both yield and enantioselectivity were severely diminished. Optimal conditions for the enantioselective fluorination of *rac*-**2.76** with KF thus employed 5 equivalents of the salt, 10 mol% of catalyst (*S*)-**2.78** and dry $CHCl_3$ (0.5 M), which was filtered on basic alumina immediately before performing the reaction. The rection was run at –15 °C for 72 h.

Table 2.7: Solvent and temperature screening for the enantioselective fluorination of *rac*-**2.76** with KF catalysed by (*S*)-**2.78**



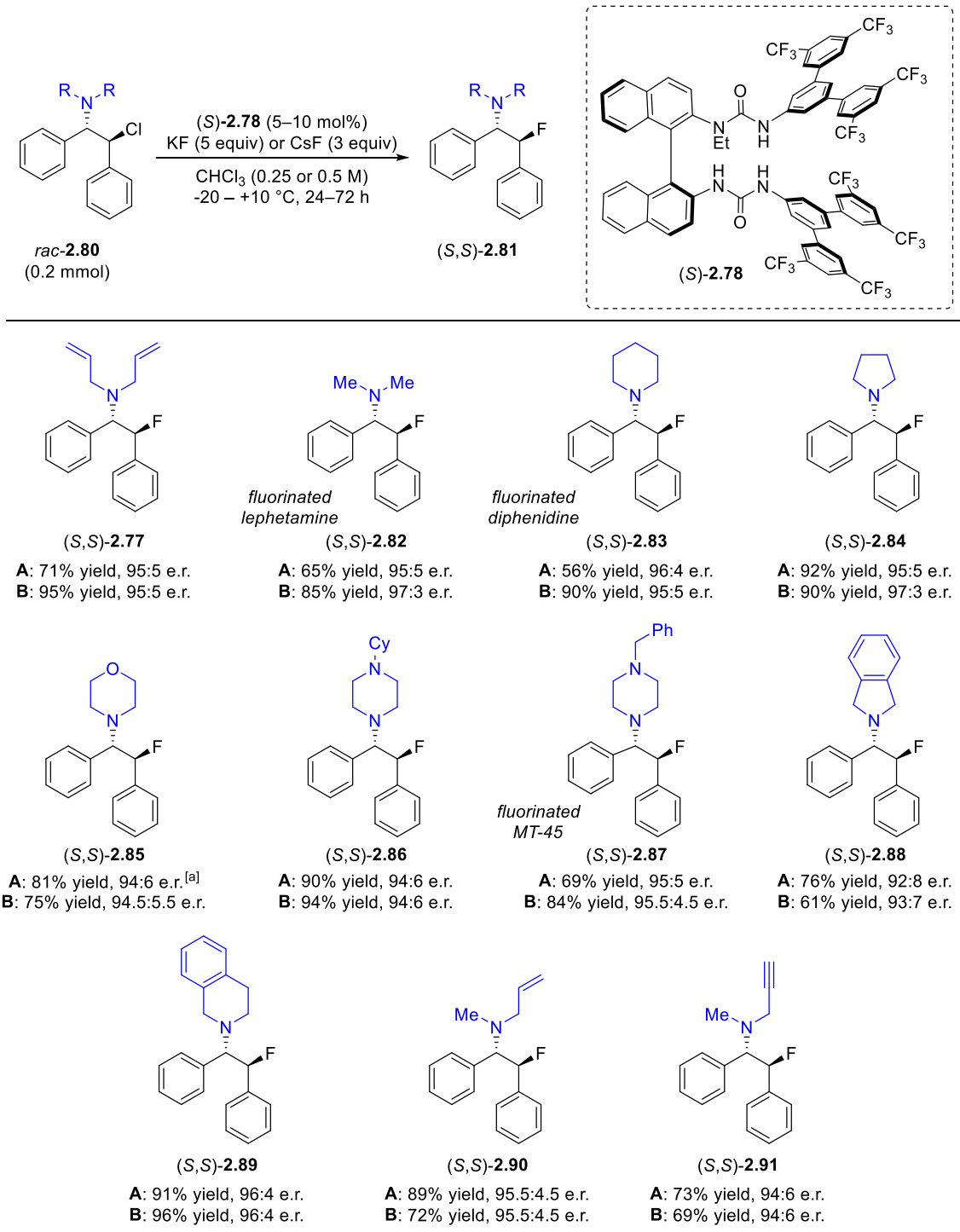
Entry	*Solvent (Concentration/M)*	*KF (equiv)*	*Temperature (° C)*	*Yield* [a]	*e.r.* [b]
1	CH_3CN (0.25)	3	22	9%	–
2	1,2-DFB (0.25)	3	22	95%	93:7
3	$PhCF_3$ (0.25)	3	22	>95%	93:7
4	CH_2Cl_2 (0.25)	3	22	80%	90.5:9.5
5	PhCl (0.25)	3	22	17%	93:7
6[c]	$CHCl_3$ (0.25)	3	22	80%	90.5:9.5
7	$CHCl_3$ (0.25)	3	22	52%	85:15
8	$PhCH_3$ (0.25)	3	22	36%	93:7
9	1,2-DFB (0.5)	5	0	58%	94:6
10	$PhCF_3$ (0.5)	5	0	77%	94:6
11	CH_2Cl_2 (0.5)	5	0	80%	93:7
12[c]	$CHCl_3$ (0.5)	5	0	>95%	93.5:6.5
13[c],[d]	$CHCl_3$ (0.5)	5	–10	72%	94.5:5.5
14[c],[d]	$CHCl_3$ (0.5)	5	–15	71%[e]	95:5

Reaction conditions: 0.05 mmol of *rac*-**2.76**, KF (3–5 equiv), (*S*)-**2.78** (5 mol%), stirring at 900 rpm for 24 h. [a] Determined by ^{19}F NMR using 4-fluoroanisole as internal standard; [b] e.r.= enantiomeric ratio, determined by HPLC using a chiral non-racemic stationary phase; [c] Dry $CHCl_3$, filtered on basic alumina to remove residual HCl; [d] 10 mol% of (*S*)-**2.78** were used; [e] isolated yield after 72 h. 1,2-DFB = 1,2-difluorobenzene.

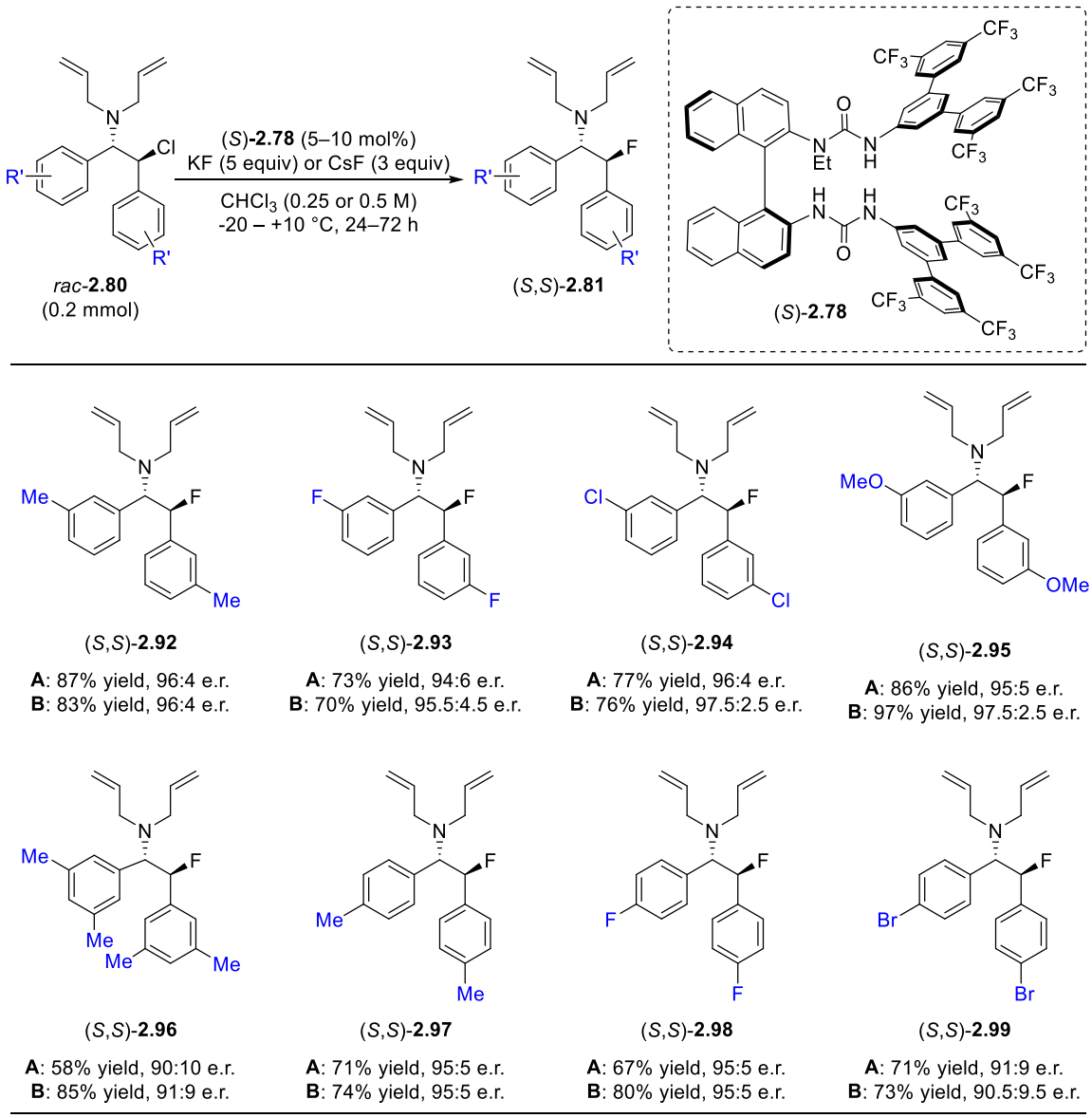
2.6 Enantioselective Fluorination of Stilbene-Derived β-Chloroamines

2.6.1 Substrate Scope

Having optimised the asymmetric fluorination both with CsF and KF, we next moved to study the scope of this reaction (Schemes 2.20–2.21). The same enantioselectivity was obtained with the two fluorine sources for reactions run at the same temperature. Yields were comparable using the conditions optimised for each salt (3 equiv of CsF, 0.25 M in $CHCl_3$ and 5 equiv of KF, 0.5 M in $CHCl_3$). The reaction tolerated a broad range of substituted amines (Scheme 2.20), including dimethylamine **2.82** (65% yield, 95:5 e.r.) and heterocycles frequently encountered in FDA approved drugs, such as piperidine, piperazine, pyrrolidine and morpholine (up to 92% yield and 96:4 e.r.).[25] A series of fluorinated analogues of 1,2-diphenylethylamines,[26,27] which have antagonist activity towards the NMDA receptors and have been investigated as analgesics, could be accessed in enantioenriched form *via* HB-PTC with KF. These include the analogues of lephetamine (NMe_2: 65% yield, 95:5 e.r.),[28] diphenidine (Piperidine: 56% yield, 96:4 e.r.),[29] and MT-45 (*N*-cyclohexyl piperazine: 90% yield, 94:6 e.r.).[30] Substrates with different *N*-substituents, which can form two diastereomeric *meso*-aziridinium ions, were also fluorinated in high yield and selectivity (**2.89**: 91% yield, 96:4 e.r.; **2.90**: 89% yield, 95.5:4.5 e.r.; **2.91**: 73% yield, 94:6 e.r.). The effect of substituents on the phenyl rings was also evaluated (Scheme 2.21). Meta- and para-substitution was well-tolerated, regardless of the electronic properties of the substituents. Accordingly, β-fluoroamines **2.92–2.99** were obtained in 58–87% yield and enantiomeric ratio between 90:10 and 96:4 e.r..



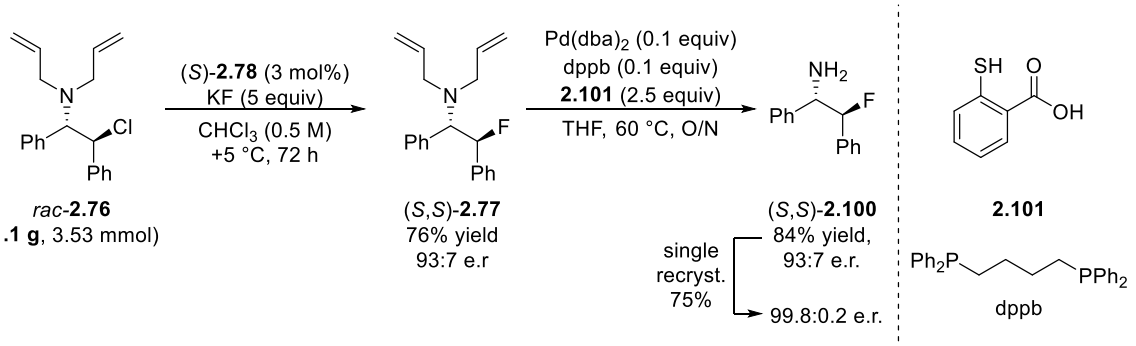
Scheme 2.20: Enantioselective desymmetrisation of *meso*-aziridinium ions with KF and CsF under HB-PTC: effect of substrates *N*-substitution. **Conditions A**: *rac*-**2.80** (0.2 mmol), KF (5 equiv), (*S*)-**2.78** (5–10 mol%), dry $CHCl_3$ passed on basic alumina to remove residual HCl (0.5 M). **Conditions B**: *rac*-**2.80** (0.2 mmol), CsF (3 equiv), (*S*)-**2.78** (5–10 mol%), dry $CHCl_3$ passed on basic alumina to remove residual HCl (0.25 M). Isolated yields. e.r. determined by HPLC using a chiral non-racemic stationary phase. [a] 15 mol% of (*S*)-**2.78** used.



Scheme 2.21: Enantioselective desymmetrisation of *meso*-aziridinium ions with KF and CsF under HB-PTC: effect of substrates aryl substitution. Conditions A: *rac*-**2.80** (0.2 mmol), KF (5 equiv), (*S*)-**2.78** (5–10 mol%), dry $CHCl_3$ passed on basic alumina to remove residual HCl (0.5 M). Conditions B: *rac*-**2.80** (0.2 mmol), CsF (3 equiv), (*S*)-**2.78** (5–10 mol%), dry $CHCl_3$ passed on basic alumina to remove residual HCl (0.25 M). Isolated yields. e.r. determined by HPLC using a chiral non-racemic stationary phase.

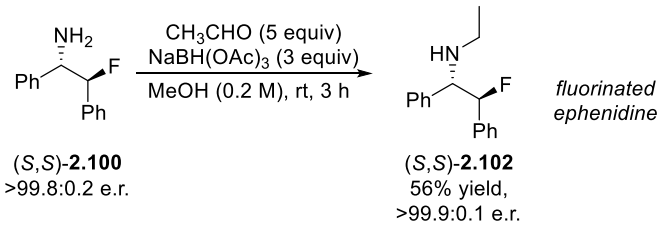
2.6.2 Derivatisation of Enantioenriched β-Fluoroamines

The versatility of the methodology was demonstrated with the gram-scale synthesis of β-fluoro *N*-diallylamine **2.77** and its conversion to the primary amine **2.100** (Scheme 2.22). The fluorination was conducted on 1.1 g of the corresponding chloride using 5 equivalents of KF with a reduced catalyst loading (3 mol% of (*S*)-**2.78**) at 5 °C, and afforded **2.77** in 76% yield and 93:7 e.r.. Deprotection was achieved under Pd(0) catalysis using 2.5 equivalents of thiosalicylic acid as nucleophile, according to a literature procedure.[24] The primary amine **2.100** was obtained in 84% yield and no erosion of enantiomeric ratio (93:7 e.r.) following aqueous work-up. Single recrystallisation from hot hexane and $CHCl_3$ (one drop) afforded **2.100** in high enantiopurity (99.8:0.2 e.r., 75% crystallisation yield).



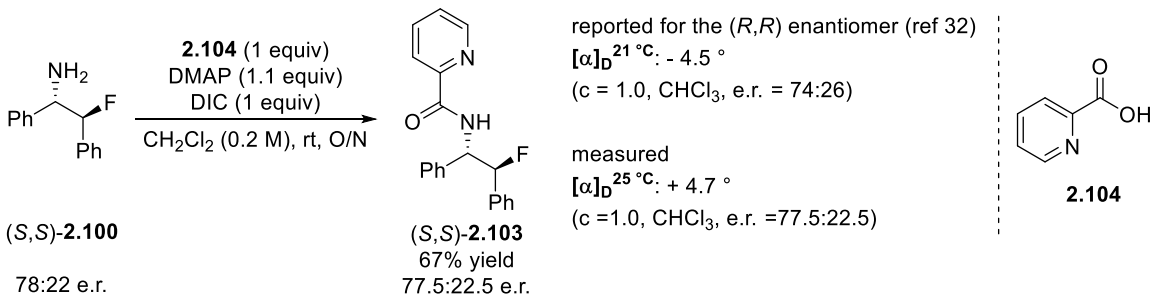
Scheme 2.22: Gram scale fluorination of *rac*-**2.76** and deprotection. O/N = overnight.

The crystalised product was converted into the secondary amine **2.102** *via* reductive amination with acetaldehyde (56% yield, Scheme 2.23). Fluorinated ephenidine **2.102**,[31] another member of the 1,2-diphenylethylamine family with antagonist activity towards the NMDA receptor, could be accessed as a single enantiomer according to this three-step protocol. We were unable to obtain the same product directly *via* asymmetric HB-PTC, due to the difficulties in synthesising the chloride precursor: the optimised conditions involving reaction of the corresponding alcohol with MsCl and Et_3N gave a complex mixture that could not be purified.



Scheme 2.23: Derivatisation of primary β-fluoroamine **2.100** *via* reductive amination to access secondary β-fluoroamines, exemplified by the synthesis of the fluorinated analogue of ephenidine.

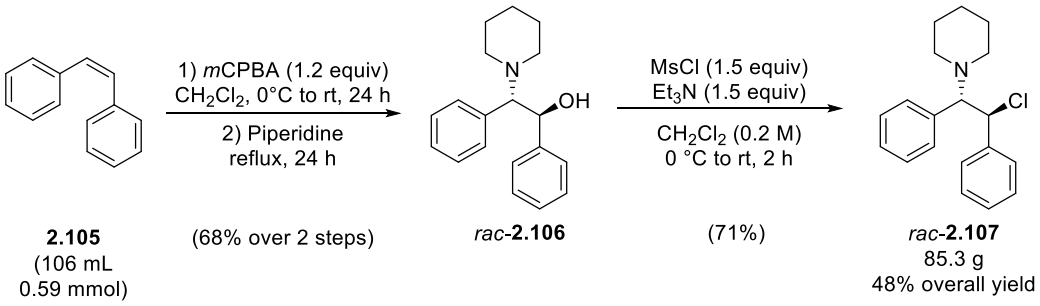
The absolute configuration of **2.77** was assigned by derivatisation to the corresponding picolinic amide **2.103** whose optical rotation is reported (Scheme 2.24).[32] After deprotection, amide coupling was performed on the primary amine recovered from the mother liquor of the crystallisation of **2.100**, which had an e.r. of 78:22. No erosion of the e.r. was observed under the coupling conditions employed (picolinic acid, 1 equiv, DMAP = 4-(dimethylamino)pyridine, 1.1 equiv and DIC = *N,N′*-diisopropylcarbodiimide 1.1 equiv), as confirmed by HPLC analysis on a chiral non-racemic stationary phase of **2.103** (77.5:22.5 e.r.). The reported optical rotation of (*R*,*R*)-**2.103** in $CHCl_3$ had negative sign ($[\alpha]_D^{21\ °C} = -4.5\ °$).[32] The optical rotation of **2.103** synthesised by us had positive sign in $CHCl_3$ ($[\alpha]_D^{25\ °C} = +4.7\ °$). This allowed us to assign (*S*,*S*) as the absolute configuration of β-fluoro *N*-diallylamine **2.77** and, by analogy, of the other stilbene-derived products. This was later confirmed by single crystal X-ray diffraction of **2.83** (section 2.7).



Scheme 2.24: Derivatisation of **2.100** to the corresponding picolinamide to determine the absolute configuration of **2.77** by comparison with literature values of optical rotation. O/N = overnight.

2.7 Enantioselective Fluorination with KF on 50 g Scale

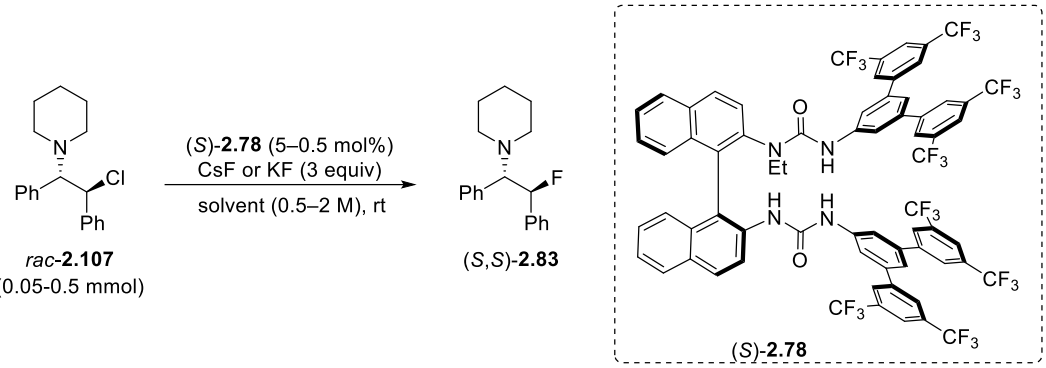
The enantioselective fluorination with KF could be scaled-up to 50 g of precursor: this was demonstrated with the synthesis of the fluorinated analogue of diphenidine **2.83** performed by Dr. Gabriele Pupo. No special precautions to exclude air or moisture were required and, as long as it was supplied as a powder, KF did not need any pre-treatment. A glass round-bottom flask was employed as reaction vessel. Dr. Gabriele Pupo synthesised β-chloroamine *rac*-**2.107** from *cis*-stilbene oxide (105 mL, 59 mmol) with only minor modifications from the procedure I had previously developed, which were introduced to avoid chromatographic purification of the intermediates (Scheme 2.25).



Scheme 2.25: Synthesis of *rac*-**2.107**, starting material for the multigram-scale fluorination with KF under HB-PTC. The synthesis was performed by Dr. G. Pupo.

Optimisation of the reaction conditions aiming at reducing the catalyst loading were initially conducted by myself in $CHCl_3$ using the more reactive CsF (Table 2.8, entries 1–4). While the yield remained excellent (≥95%) even at reduced catalyst loading, the enantiomeric ratio decreased significatively from 93:7 e.r. in the presence of 5 mol% of (*S*)-**2.78** to 88:12 e.r. at 0.5 mol% loading. In contrast, the reaction in CH_2Cl_2 with 1 mol% of (*S*)-**2.78** afforded **2.83** in >95% yield and 92:8 e.r. (entry 5). This solvent was thus selected for screening the fluorination with KF (entries 6–12). Decreasing the amount of catalyst from 5 mol% to 0.5 mol% had little impact on selectivity with this fluoride source, but longer reaction times were required to obtain yields ≥95% (entries 6–9). Yields could be improved increasing the concentration to 2 M (entries 10–12).

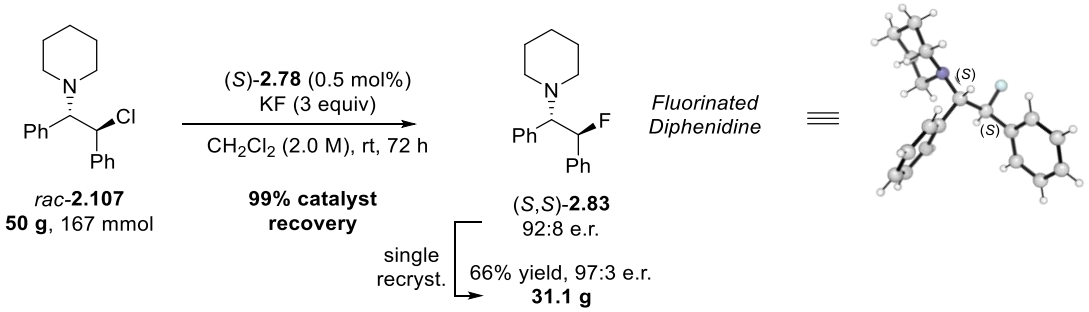
Table 2.8: Optimisation of the reaction conditions for the multi-decagram scale fluorination of *rac*-**2.107** under HB-PTC



Entry	*Scale (mmol)*	*MF*	*Solvent (concentration/M)*	*(S)-2.78 (mol%)*	*Time (h)*	*Yield* [a]	*e.r.* [b]
1	0.05	CsF	$CHCl_3$ (0.25)	5	24	>95%	93:7
2	0.05	CsF	$CHCl_3$ (0.25)	2	24	>95%	92:8
3	0.05	CsF	$CHCl_3$ (0.25)	1	24	>95%	90.5:9.5
4	0.05	CsF	$CHCl_3$ (0.25)	0.5	24	95%	88:12
5	0.05	CsF	CH_2Cl_2 (0.25)	1	24	>95%	92:8
6	0.05	KF	CH_2Cl_2 (0.25)	5	48	>95%	92.5:7.5
7	0.05	KF	CH_2Cl_2 (0.25)	2	48	>95%	92:8
8	0.05	KF	CH_2Cl_2 (0.25)	1	48	>95%	92:8
9	0.05	KF	CH_2Cl_2 (0.25)	0.5	72	95%	91:9
10	0.50	KF	CH_2Cl_2 (0.5)	0.5	13	23%	91.5:8.5
11	0.50	KF	CH_2Cl_2 (1)	0.5	13	64%	92.5:7.5
12	0.50	KF	CH_2Cl_2 (2)	0.5	13	85%	92:8

Reaction conditions: *rac*-**2.107**, CsF or KF (3 equiv), (*S*)-**2.78**, in $CHCl_3$ or CH_2Cl_2 stirring at 900 rpm at rt. [a] Determined by ^{19}F NMR using 4-fluoroanisole as internal standard; [b] e.r.= enantiomeric ratio, determined by HPLC using a chiral non-racemic stationary phase.

Based on these results, Dr. Gabriele Pupo performed the fluorination on 50 g of *rac*-**2.107** in CH_2Cl_2 (2 M) using 3 equivalents of KF and 0.5 mol% of (*S*)-**2.78** at rt (Scheme 2.26). Fluorinated diphenidine **2.83** was obtained in the same enantiomeric ratio as the small-scale trials (92:8). The product was separated from the catalyst by acid/base work-up and crystalised in hot MeOH to afford **2.83** in 97:3 e.r. (66% yield). Quantitative recovery of the catalyst (99%) was achieved by flash column chromatography over silica gel. Crystals of **2.83**, both as free-base and HCl salt, suitable for X-ray diffraction were obtained, confirming the (*S*,*S*) absolute configuration for stilbene-derived β-fluoroamines.[1]



Scheme 2.26: 50 g scale asymmetric fluorination with KF to access fluorinated diphenidine **2.83**, and its crystal structure, which confirmed the (*S*,*S*) absolute configuration for stilbene-derived β-fluoroamines. Reaction and crystallisation performed by Dr. G. Pupo.

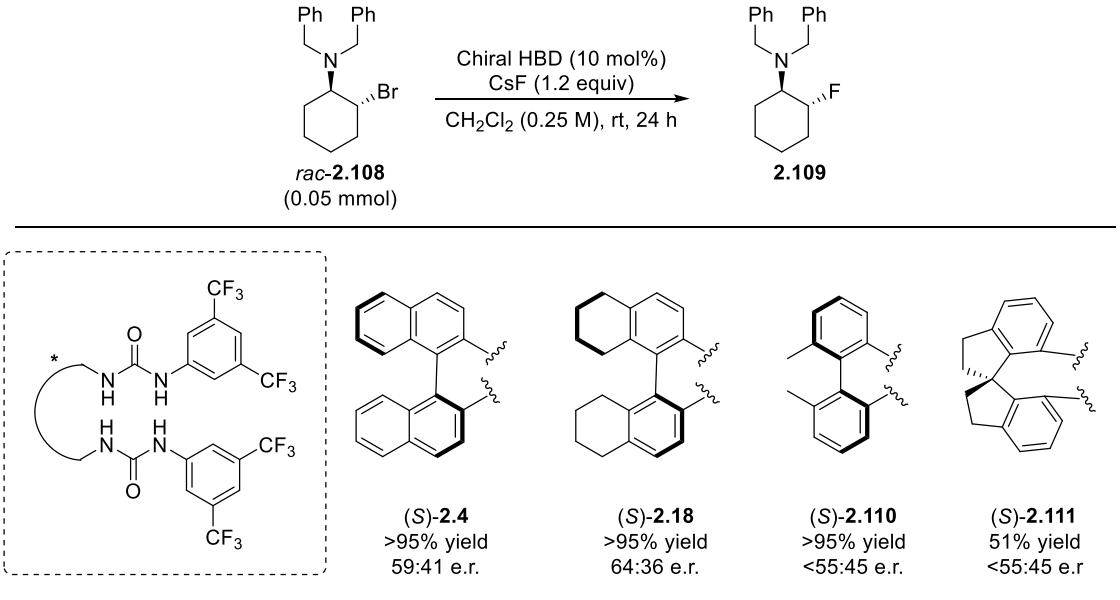
2.8 Enantioselective Fluorination of Aliphatic β-Haloamines

2.8.1 Reaction Optimisation

We sought to expand the scope of the fluorination under HB-PTC to aliphatic substrates, and we selected *trans*-*N*,*N*-dibenzyl-2-bromocyclohexan-1-amine *rac*-**2.108** for preliminary investigations. Deprotection of the corresponding fluorinated product affords valuable *trans*-2-fluorocyclohexan-1-amine, which is incorporated in compounds investigated for the treatment of Alzheimer's (sections 1.2.2.1 and 4.4.1).[33,34] Synthesis of the starting material was performed according to literature procedures, involving epoxide ring opening with dibenzyl amine,[35] and bromination of the intermediate alcohol.[36] The bromination proceeds through an aziridinium ion to afford the *trans* product. A crystal structure of *trans*-*N*,*N*-dibenzyl-2-bromocyclohexan-1-amine *rac*-**2.108** has been previously reported, confirming the *trans* relationship of the bromo and amino substituents.[36]

This substrate was tested in the asymmetric fluorination with CsF (1.2 equiv) in the presence of a series of C_2-symmetric bis-ureas with different chiral scaffolds (Scheme 2.27). All of these were competent phase-transfer catalysts, but only the BINAM-

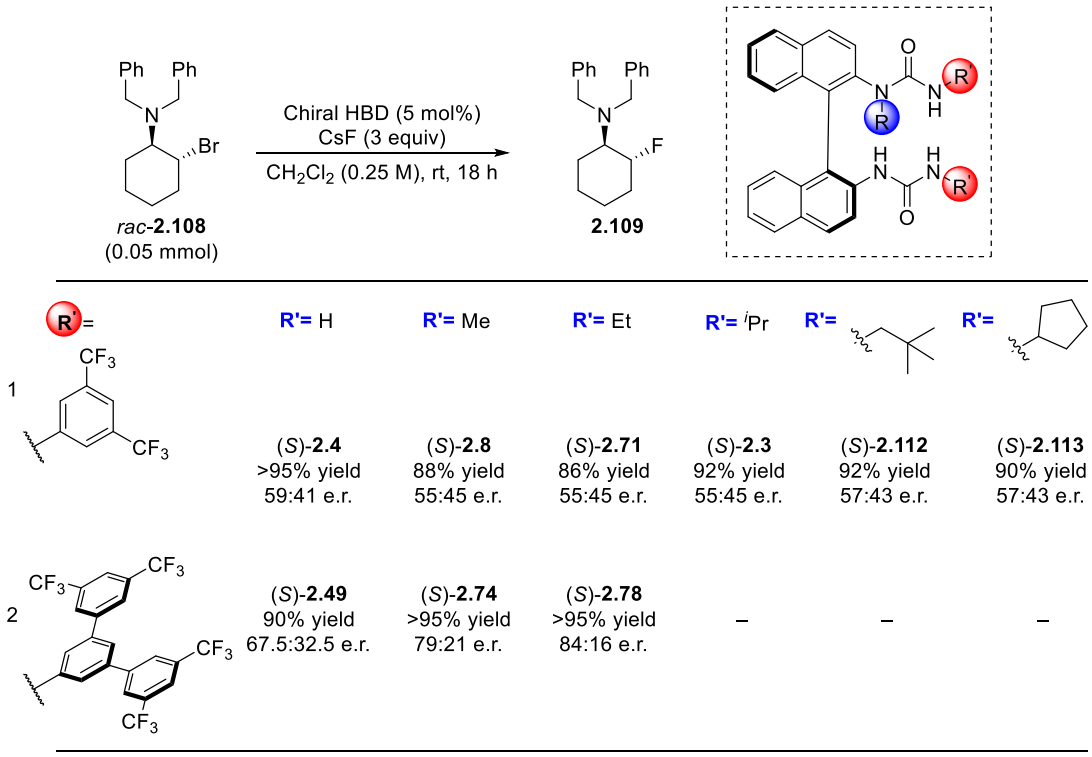
derivatives (*S*)-**2.4** and (*S*)-**2.18** afforded **2.109** in non-racemic form (59:41 e.r. and 64:36 e.r., respectively).



Scheme 2.27: Preliminary evaluation of bis-ureas with different C_2-symmetric chiral scaffolds for the enantioselective fluorination of aliphatic *rac*-**2.108** with CsF under HB-PTC. Yield determined by ^{19}F NMR using 4-fluoroanisole as internal standard. e. r. determined by HPLC using a chiral non-racemic stationary phase.

Introduction of 3,3'-substituents on the BINAM scaffold resulted in complete loss of enantioselectivity (see Chapter 5, Scheme 5.2), and urea *N*-alkylation did not improve the enantiocontrol in the series bearing the 3,5-bis(trifluoromethyl)phenyl rings (Scheme 2.28, entry 1). Extension of the π-system of the achiral side of the urea was the single most beneficial modification for enantioselectivity ((*S*)-**2.49**: 67.5:32.5 e.r., entry 2 *versus* (*S*)-**2.4**: 59:41 e.r., entry 1). Methylation of (*S*)-**2.49** furnished a further gain in selectivity ((*S*)-**2.74**: 79:21 e.r.) and even a better result was obtained extending the *N*-alkyl chain from methyl to ethyl ((*S*)-**2.78**: 84:16 e.r.). While it would have been interesting to evaluate the effect of a bulkier group, such as the ^{i}Pr, within this series, this catalyst could not be accessed at the time. In fact, urea formation under the optimised conditions was unsuccessful with R substituents bulkier than a methyl group (section 2.4.3), and the best-performing catalyst (*S*)-**2.78** (R=Et) was synthesised *via* S_N2 substitution of bis-urea **2.49**

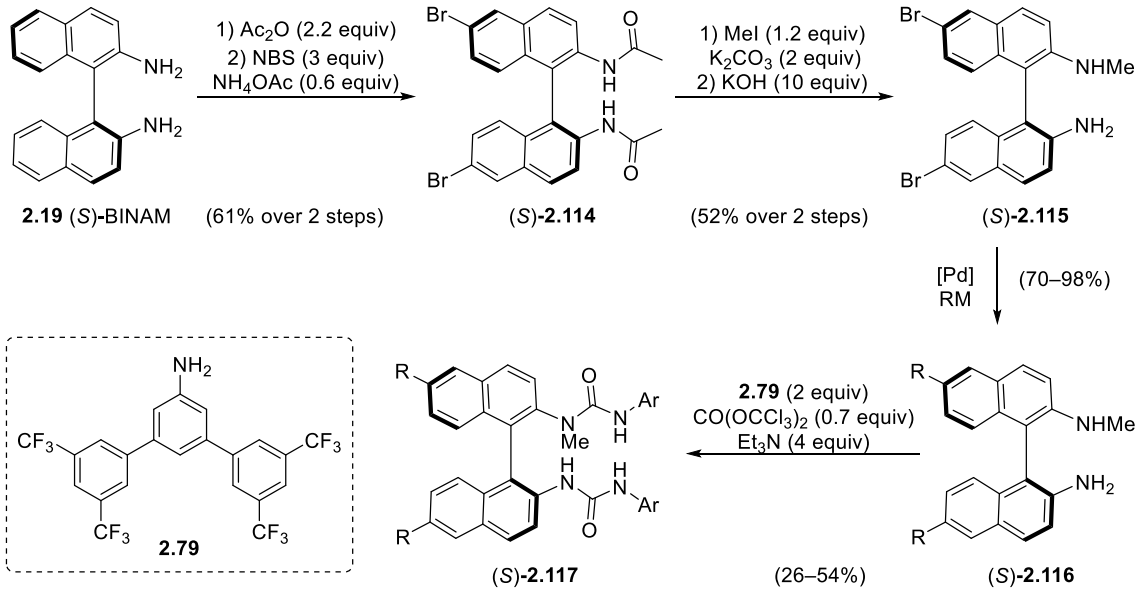
with EtI. An alternative method to access catalysts with bulkier R groups is reported in Chapter 3.



Scheme 2.28: Effect of bis-urea *N*-alkylation on the outcome of the enantioselective fluorination of *rac*-**2.108** with CsF. Yield determined by ^{19}F NMR using 4-fluoroanisole as internal standard. e. r. determined by HPLC using a chiral non-racemic stationary phase.

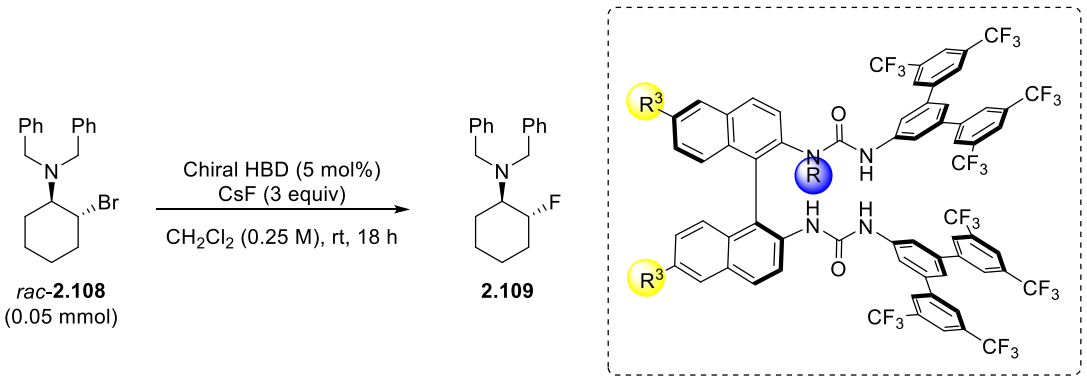
Next, we evaluated the effect of BINAM 6,6'-substitution in combination with the terphenyl system derived from aniline **2.79**, because the latter feature was important to achieve high levels of enantiocontrol. The catalysts evaluated include both non-alkylated and *N*-methyl bis-ureas. *N*-methyl (*S*)-**2.117** was synthesised combining the procedures reported in section 2.4.1 for 6,6' bromination and aniline alkylation (Scheme 2.29). (*S*)-BINAM **2.19** was protected as the acetamide, rather than as trifluoroacetamide, because the latter did not afford the desired brominated product. Methylation of intermediate (*S*)-**2.114** was sluggish and required four days at 60 °C to afford synthetically useful yields of the monoalkylated product. Attempts to form the ureas on the bis-bromo derivatives

(*S*)-**2.27** and (*S*)-**2.115** failed, thus Pd-catalysed cross coupling to install the desired substituents was performed on the free aniline before urea coupling.



Scheme 2.29: Synthesis of 6,6'-disubstituted *N*-methyl bis-urea organocatalysts.

The performance of 6,6'-substituted catalysts was comparable to that of unsubstituted (*S*)-**2.49** and (*S*)-**2.74** but they did not offer any improvement compared to (*S*)-**2.78** (Scheme 2.30).



R^3	H	CH_3	
R=H	(*S*)-**2.49** 90% yield 67.5:32.5 e.r.	(*S*)-**2.118** >95% yield 70:30 e.r.	-
R=Me	(*S*)-**2.74** >95% yield 79:21 e.r.	(*S*)-**2.119** >95% yield 80:20 e.r.	(*S*)-**2.120** >95% yield 78.5:21.5 e.r.

Scheme 2.30: Effect of 6,6' substitution of the bis-urea scaffold on the outcome of the enantioselective fluorination of *rac*-**2.108** with CsF. Yield determined by ^{19}F NMR using 4-fluoroanisole as internal standard. e. r. determined by HPLC using a chiral non-racemic stationary phase.

Figure 2.6 summarises how structural modifications of the catalyst scaffold affect enantioselectivity in the fluorination of aliphatic *rac*-**2.108**. Introduction of the polytrifluoromethylated terphenyl π-system and urea *N*-alkylation are required for good selectivity. A positive trend between the chain length and enantioselectivity was observed, with catalyst (*S*)-**2.78** (R=Et) performing best. 3,3'-Substitution of the BINAM scaffold affords β-fluoroamine **2.109** in racemic form, while introduction of substituents in the 6 and 6' positions has no effect on the enantiomeric ratio or only marginally improves it.

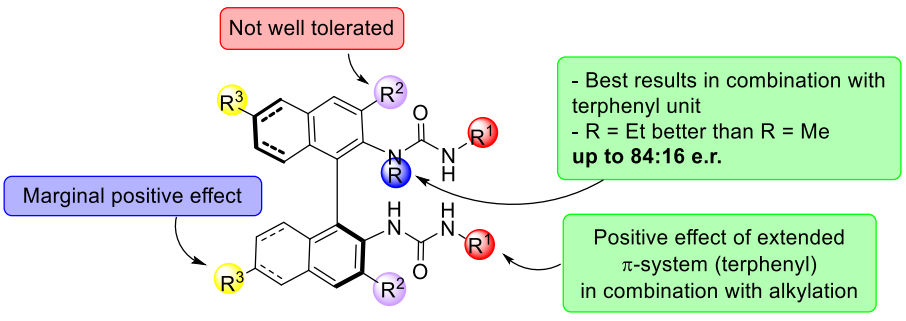
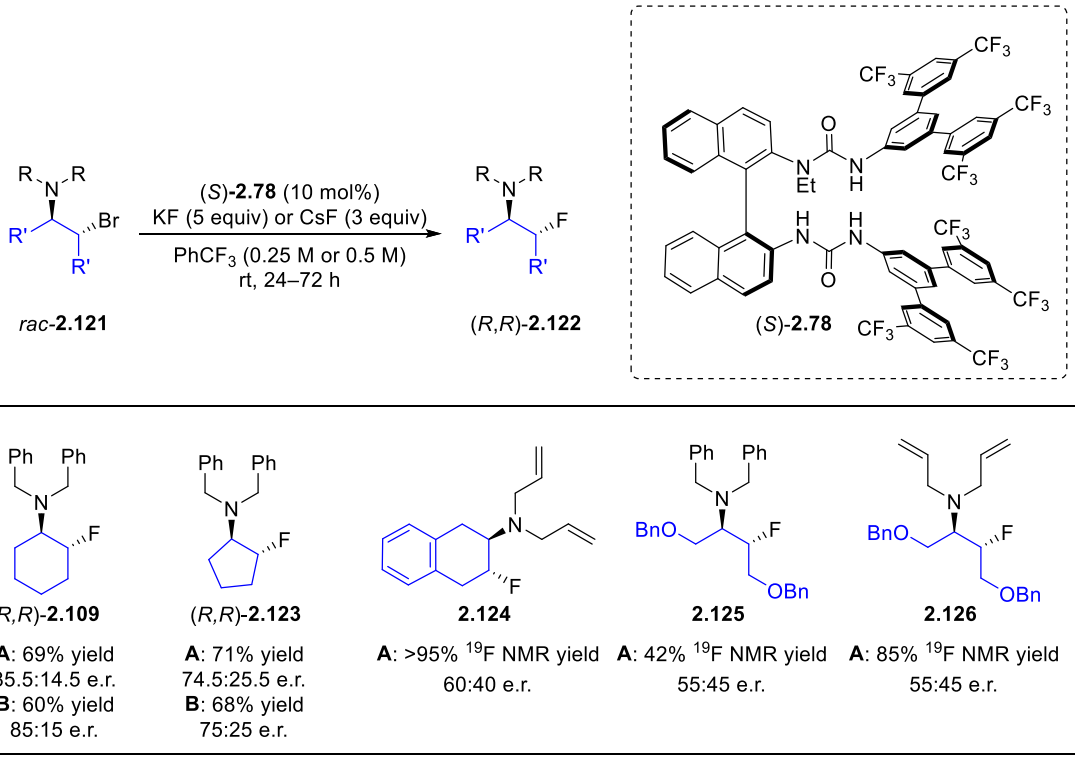


Figure 2.6: Summary of the effect of bis-urea structural modifications on the enantioselectivity of the fluorination of aliphatic β-bromoamine *rac*-**2.108**.

Catalyst (*S*)-**2.78** was selected for further optimisation. Among the solvents screened (see Chapter 5, Table 5.5), $PhCF_3$ gave the best enantiomeric ratio (85.5:15.5 e.r. *versus* 84:16 e.r. in CH_2Cl_2), and improved yields when KF was used as fluorine source (47% *versus* 25% in CH_2Cl_2). Thus, optimal conditions for aliphatic substrates consisted in reacting the β-bromoamine precursors in $PhCF_3$ (0.5 M) at room temperature with 5 equivalents of KF in the presence of 5 mol% of (*S*)-**2.78**.

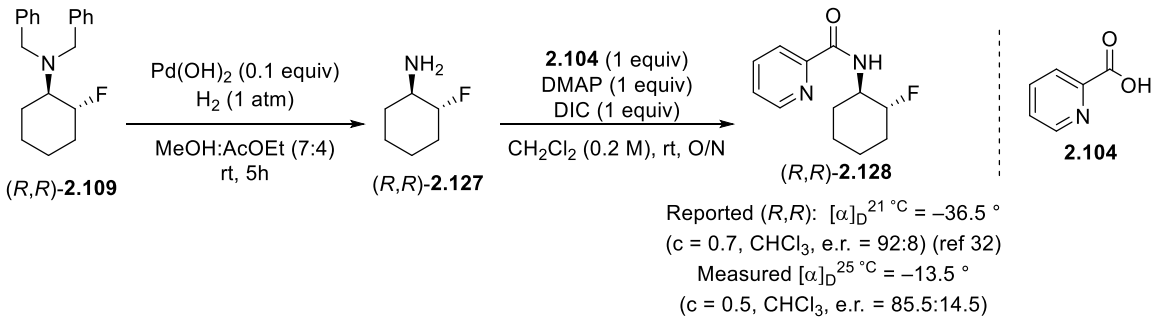
2.8.2 Substrate Scope

Next, we evaluated other aliphatic substrates in the asymmetric fluorination with KF in the presence of catalyst (*S*)-**2.78** (Conditions A, Scheme 2.31). Six- and five-membered rings afforded the corresponding fluorinated products in good isolated yields and moderate enantioselectivity, which was substantially different between the two cyclic compounds (**2.109**: 85.5:14.5 e.r.; **2.123**: 74.5:24.5 e.r.). Similar results were obtained using CsF (conditions B). While reactivity was retained for the tetrahydro naphthyl derivative **2.124** and the linear β-fluoroamines **2.125** and **2.126**, the enantioselectivity for these substrates was very poor regardless of *N*-substitution. The latter had a marked effect on yield, with *N*-allylamine **2.126** being obtained in 85% yield compared to 42% yield for the corresponding *N*-benzylamine **2.125**. The same dependence of yield on *N*-substitution was noted for stilbene derived β-fluoroamine **2.77** *versus* **2.15**.



Scheme 2.31: Scope of the enantioselective fluorination of aliphatic β-haloamines with KF and CsF under HB-PTC. **Conditions A:** *rac*-**2.121** (0.2 mmol), KF (5 equiv), (*S*)-**2.78** (5–10 mol%), $PhCF_3$ (0.5 M). **Conditions B:** *rac*-**2.121** (0.2 mmol), CsF (3 equiv), (*S*)-**2.78** (5–10 mol%), $PhCF_3$ (0.25 M). Isolated yields unless stated otherwise. e.r. determined by HPLC using a chiral non-racemic stationary phase.

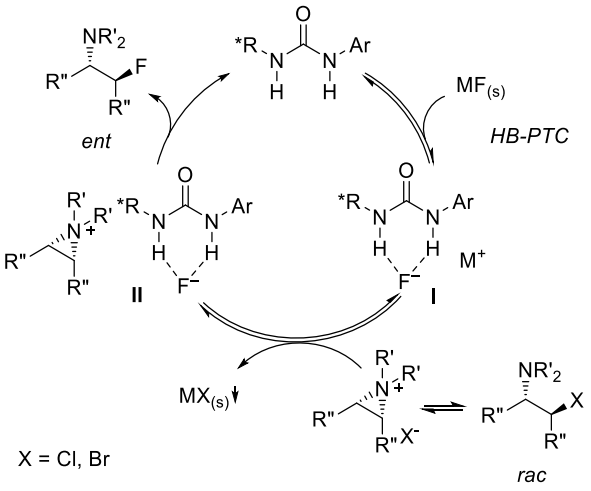
Cyclic aliphatic substrates are structurally different from the stilbene-derived ones previously synthesised, and since the stilbene rings played a major role in determining the observed enantioselectivity, it was not appropriate to assign the absolute configuration of the aliphatic products by analogy (see also section 2.9.2). Instead, the benzylic groups of **2.109** were removed with catalytic hydrogenation and the primary amine **2.127** was coupled with picolinic acid in the presence of di-isopropylcarbodiimide (DIC) and 4-dimethylaminopirydine (DMAP) to afford picolinamide **2.128** (Scheme 2.32). **2.128** has been previously synthesised in enantioenriched form (92:8 e.r.) by the Doyle group, which assigned the absolute configuration of the product as (*R*,*R*) based on literature data and X-ray crystallography.[32] The reported optical rotation in $CHCl_3$ was $[\alpha]_D^{21\ °C} = -36.5\ °$ (92:8 e.r.), and our measured value was $[\alpha]_D^{25\ °C} = -13.5\ °$ (85.5:14.5 e.r.). This allowed us to assign (*R*,*R*) as the absolute configuration of **2.109**. By analogy we assigned (*R*,*R*) configuration to the cyclic **2.123**.



Scheme 2.32: Derivatisation of **2.109** as picolinamide **2.128** to determine the absolute configuration. Comparison of the optical rotation with literature values allowed to assign (*R*,*R*) configuration to cyclic aliphatic β-fluoroamines.[32]

2.9 Experimental and Computational Insights into the Reaction Mechanism

The enantioselective desymmetrisation of *meso*-aziridinium ions with alkali metal fluorides is proposed to proceed according to the general HB-PTC mechanism (section 2.1). The urea acts as a phase-transfer catalyst towards the alkali metal fluoride, leading to formation of a chiral hydrogen bonded-fluoride complex (**I**, Scheme 2.33). Following ion pairing with the *meso*-aziridinium ion generated *in situ*, the reactive intermediate **II** is formed. This undergoes irreversible fluorination to afford the enantioenriched product and regenerate the catalyst.



Scheme 2.33: Proposed catalytic cycle for the enantioselective desymmetrisation of *meso*-aziridinium ions with MF under HB-PTC conditions.

2.9.1 Experimental Evidence for the Phase-Transfer Role of (*S*)-2.78

Experimental evidence of the ability of (*S*)-**2.78** to act as phase-transfer catalyst towards CsF have been obtained by Dr. Francesco Ibba in a series of NMR experiments (Figures 2.7–2.9).[1] (*S*)-**2.78** (20 mg, 0.014 mmol) and CsF (114 mg, 0.75 mmol) were stirred in CD_2Cl_2 (0.6 mL) for 2 h. After this time, the solid was removed by filtration through a syringe filter (0.45 µm PTFE membrane), and the filtrate was analysed by NMR. Compared to the ^{1}H NMR spectrum of the free catalyst (Figure 2.7, bottom), the spectrum of this sample showed significative line broadening which, together with the downfield shifting of NHs protons, suggested that the ureas were interacting with the fluoride anion (Figure 2.7, top). The fluoride resonance was not visible in the ^{19}F NMR spectrum and it was hypothesised that this was due to excessive line broadening.

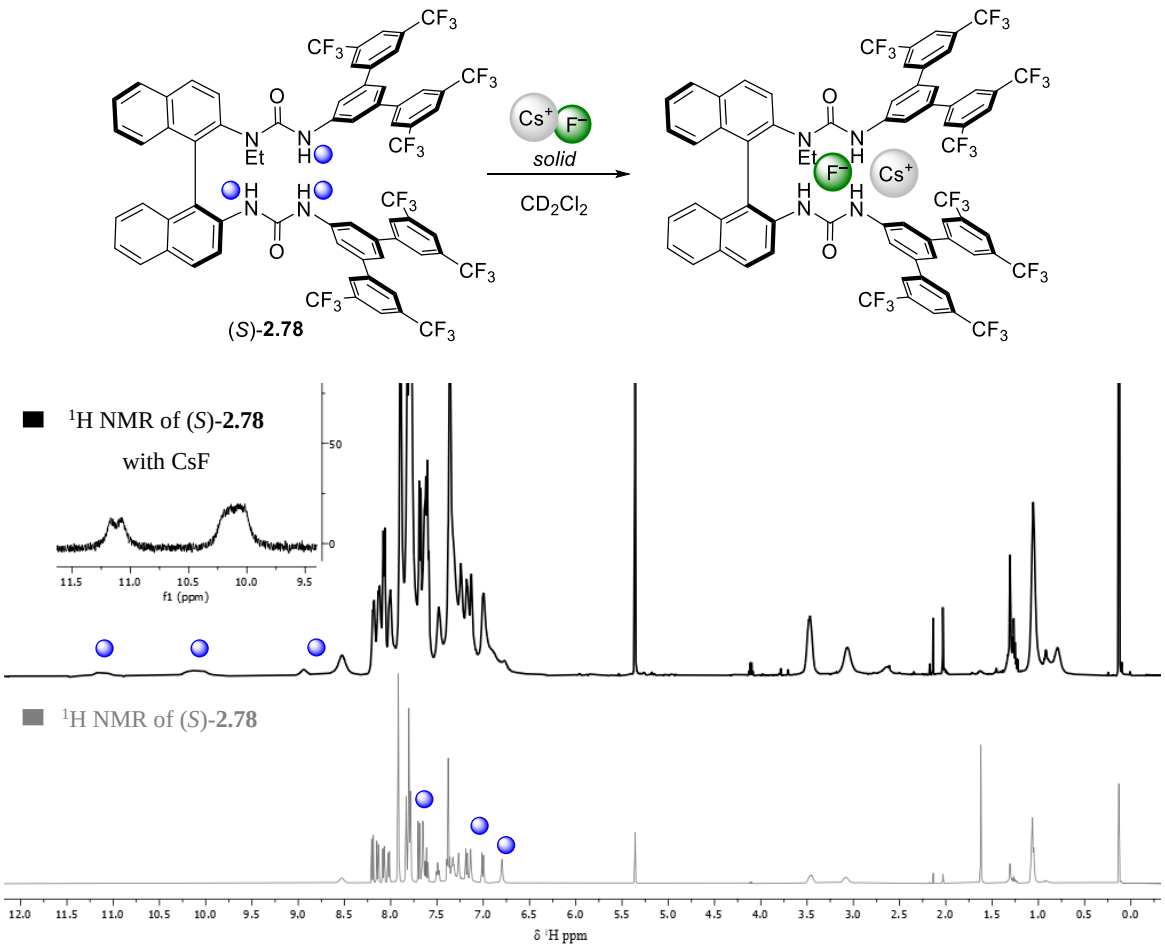


Figure 2.7: ^{1}H NMR spectrum of (*S*)-**2.78** after stirring the catalyst with CsF in CD_2Cl_2 for 2 h (top) and ^{1}H NMR spectrum of (*S*)-**2.78** in absence of fluoride (CD_2Cl_2). Experiment performed by Dr. F. Ibba.

The same experiment described above, in which solid CsF and (*S*)-**2.78** were stirred in CD_2Cl_2, was repeated. After filtration of the solid, the sample was evaporated to dryness and the residue dissolved in 1 mL of CD_3OD, to weaken the complexation of fluoride by the bis-urea. Signals at –150 ppm and –38 ppm were observed in the ^{19}F and ^{133}Cs NMR spectra respectively, proving the presence of CsF in solution.[i] As a control experiment, CsF was stirred in CD_2Cl_2 alone for two hours, the solid was filtered and the filtrate concentrated to dryness and redissolved in CD_3OD. No signals were detected in this case either in the ^{19}F or ^{133}Cs NMR spectra.

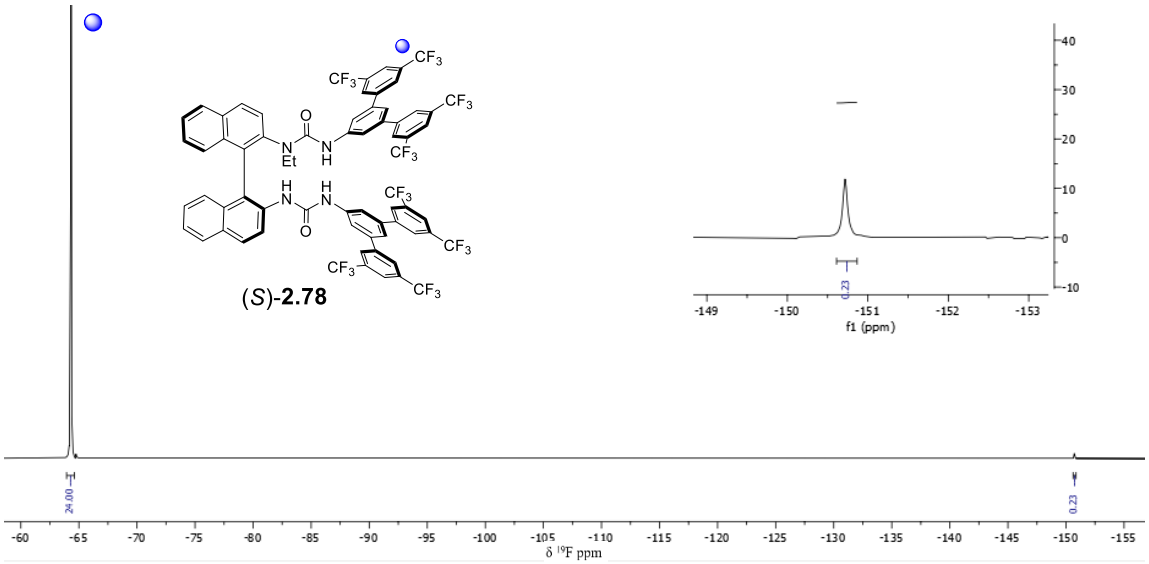


Figure 2.8: ^{19}F NMR spectrum in CD_3OD of the filtrate from a mixture of (*S*)-**2.78** and CsF stirred in CD_2Cl_2 for 2 h. Experiment performed by Dr. F. Ibba.

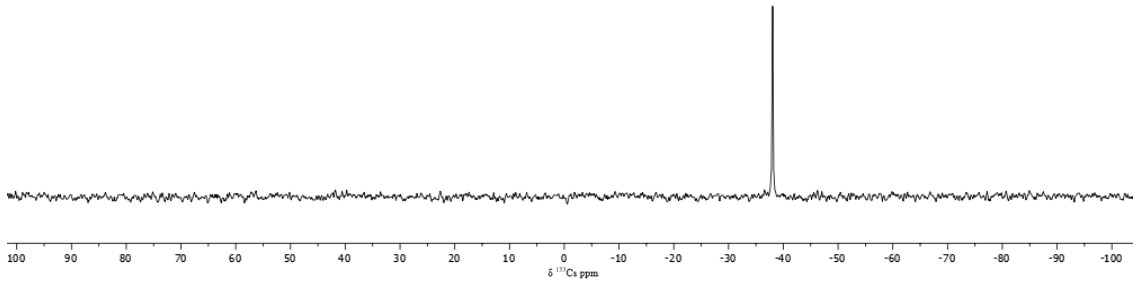


Figure 2.9: ^{133}Cs NMR spectrum in CD_3OD of the filtrate from a mixture of (*S*)-**2.78** and CsF stirred in CD_2Cl_2 for 2 h. Experiment performed by Dr. F. Ibba.

[i] The signals of CsF in CD_3OD are at –150 ppm for the fluoride ion (^{19}F NMR spectrum) and –38 ppm for the Cs^+ cation (^{133}Cs NMR spectrum). This was determined by dissolving CsF in CD_3OD and recording the ^{19}F and ^{133}Cs NMR spectra.

2.9.2 Computational Investigations

Molecular dynamics simulations (MD) and density functional theory (DFT) calculations were performed by Dr. David Ascough to gain further insight into the catalyst-fluoride binding mode and the observed enantioselectivity. This analysis revealed that, similarly to the *N*-alkyl catalysts previously disclosed ((*S*)-**2.3**), (*S*)-**2.78** binds fluoride with three hydrogen bonds and the urea bearing the alkyl chain adopts an *anti-syn* conformation (Figure 2.10). A stable and persistent complex in $CHCl_3$ at 373 K is thus formed.

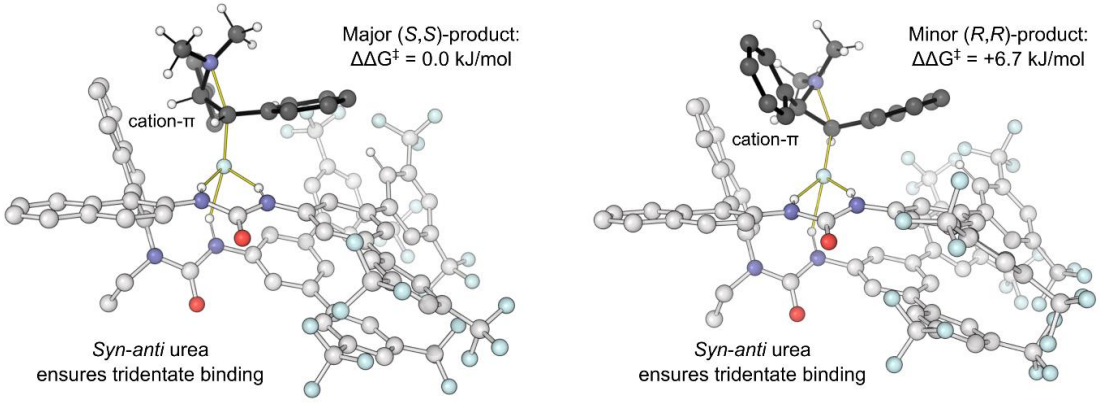


Figure 2.10: Computed lowest TSs to the major and minor product at the ωB97X-D3/(ma)-def2-TZVPP/COSMO($CHCl_3$)//M06-2X/def2-SVP(TZVPPD)/CPCM($CHCl_3$) level of theory. Computations performed by Dr. D. Ascough. Figure adapted from reference 1.

In agreement with the crystal structure obtained for **2.83**, calculations predict that the (*S*) catalyst favours the formation of the (*S*,*S*) enantiomer for stilbene-derived **2.82** (NMe_2), with a predicted enantiomeric ratio of 95:5 at 273.15 K, which is in line with the experimental results. In both the lowest energy transitions states leading to the major (TS_{major}) and minor (TS_{minor}) enantiomers the catalyst adopts the same conformation (Figure 2.11): intramolecular π-π stacking between the terphenyl units contributes to rigidify the catalyst structure, reducing the number of accessible conformations.

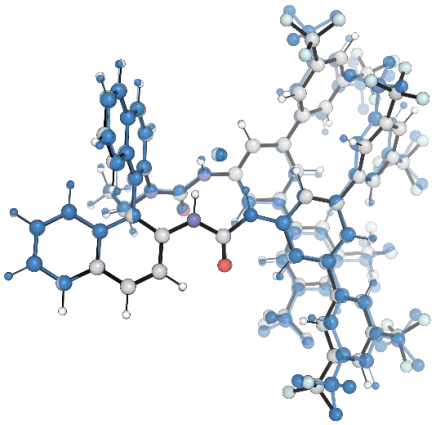


Figure 2.11: Superposition of the TS_{major} (conventional colouring) and TS_{minor} (blue) to underline the similarity of the conformation adopted by the catalyst in the two TSs. The aziridinium ion has been removed for clarity. Computations performed by Dr. D. Ascough. Figure adapted from reference 1.

The substrate interacts with the catalyst with the nitrogen substituents pointing towards the solvent, which explains the broad tolerance of *N*-substitution observed experimentally, and the high enantioselectivity observed for substrates that might give rise to diastereomeric aziridinium ions (Figure 2.12, i). In both TSs, there is a cation-π interaction between the positively charged aziridinium and the catalyst binaphthyl backbone, but this interaction is stronger in the TS_{major} (Figure 2.12, ii). Additionally, geometrical distortions are present in the TS_{minor} due to increased steric crowding compared to TS_{major} (Figure 2.12, iii). Finally, for stilbene-derived aziridinium ions, substrate conformation plays a key role in differentiating the two TSs (Figure 2.12, iv). In the TS_{major}, the phenyl ring adjacent to the carbon undergoing substitution is free to rotate to ensure optimal conjugation with the forming and breaking bonds, thus favouring nucleophilic substitution. In the TS_{minor}, this rotation is restricted, and this contributes to half of the computed energy difference between the TSs. The same substrate conformation preference was observed for stilbene-derived episulfonium ions and explains why lower level of enantioselectivity are obtained with aliphatic substrates which lack this differentiating element. In this latter case, the main cation-π interaction between the aziridinium ion and the catalyst is retained, orienting the *N*-substituents outside the catalytic pocket, but minor changes in the docking of the

substrate can take place to minimise steric clashes. This explains the observed reversed selectivity, with preferential formation of the (*R*,*R*) enantiomer for cyclic aliphatic β-fluoroamines.

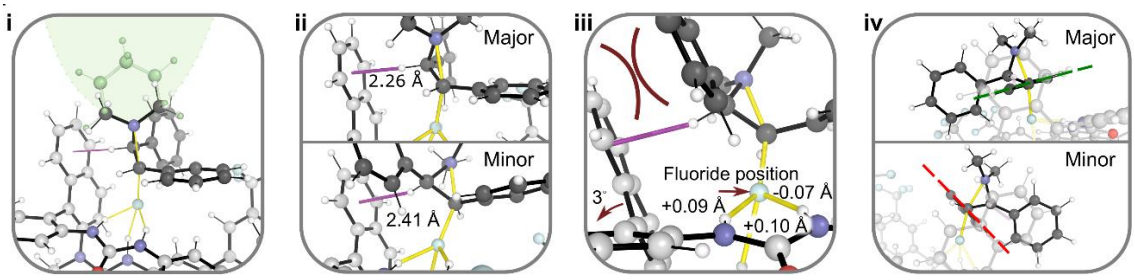


Figure 2.12: Highlights of the key features of the TSs. i) In both TSs, the *N*-substituents point outside the catalytic pocket, explaining the broad tolerance. ii) Shorter substrate-catalyst cation-π interaction in the TS_{major}. iii) Steric crowding in the TS_{minor} (illustrated). Distortions are relative to TS_{major}. iv) Substrate conformation: TS_{major} allows for better conjugation of the Ph ring with the breaking C–N and forming C–F bond. Computations and graphical design by Dr. D. Ascough. Figure adapted from reference 1.

2.10 Conclusions

Hydrogen bonding phase-transfer catalysis (HB-PTC) was successfully applied to the activation of economical, abundant and easy-to-handle KF for the synthesis of highly valuable enantioenriched β-fluoroamines. Stilbene-derived substrates afforded the corresponding products in up to 92% yield and 96:4 e.r. Within this class, a broad range of *N*-substituents were tolerated. *Para*- and *meta*-substituted stilbene-derivatives were also fluorinated in high enantioselectivity, while the enantiomeric ratio obtained with non-benzylic substrates was moderate (up to 84:16 e.r. for the cyclohexyl derivative **2.109**). For both classes, the best-performing catalyst was *N*-ethylated bis-urea (*S*)-**2.78**, bearing an extended polyfluorinated terphenyl unit. Further structural modifications of the catalyst scaffold are required to increase the enantiocontrol for the fluorination of aliphatic substrates. Analogues with bulkier *N*-substituents were not accessible using the current synthetic route, but from the data collected, it is expected that they might improve the

enantioselectivity for the model cyclohexyl derivative **2.109**. An alternative synthetic route is therefore needed, and various options are explored in Chapter 3.

The fluorination with KF can be scaled-up to 50 g in round-bottom flasks using 0.5 mol% of bis-urea (*S*)-**2.78**. This was demonstrated with the synthesis of the fluorinated analogue of diphenidine (*S*,*S*)-**2.83** (66% yield and 97:3 e.r. after single crystallisation). The catalyst could be quantitatively recovered by chromatographic purification (99% recovery). Pd(0)-catalysed deprotection of β-fluoro-*N*-diallylamine (*S*,*S*)-**2.77** afforded stilbene-derived primary amine (*S*,*S*)-**2.100**, which could be converted into the corresponding secondary amine (*S*,*S*)-**2.102** (fluorinated ephenidine) and picolinamide (*S*,*S*)-**2.103** with no erosion of the enantiomeric ratio. Overall, fluorination under HB-PTC is operationally simple and can be performed in standard glassware without any precautions to exclude air or moisture and no need to pre-treat the metal fluoride salt. The only requirements, being a phase-transfer process, are that the MF is used as a fine powder and efficient mixing is achieved. Mixing in round-bottom flasks with magnetic stirring bars and in industrial reactors with mechanical impellers produces substantially different flow patterns. Therefore, further investigations of this aspect are required prior to the industrialisation of this protocol. This is explored in Chapter 4.

2.11 References

(1) Pupo, G.; Vicini, A. C.; Ascough, D. M. H.; Ibba, F.; Christensen, K. E.; Thompson, A. L.; Brown, J. M.; Paton, R. S.; Gouverneur, V. "Hydrogen Bonding Phase-Transfer Catalysis with Potassium Fluoride: Enantioselective Synthesis of β-Fluoroamines." *J. Am. Chem. Soc.* **2019**, *141*, 2878–2883.

(2) Liotta, C. L.; Harris, H. P. "The Chemistry of 'Naked' Anions. I. Reactions of the 18-Crown-6 Complex of Potassium Fluoride with Organic Substrates in Aprotic Organic Solvents." *J. Am. Chem. Soc.* **1974**, *96*, 2250–2252.

(3) Ooi, T.; Doda, K.; Maruoka, K. "Distinct Advantage of the *in Situ* Generation of Quaternary Ammonium Fluorides under Phase-Transfer Conditions toward Catalytic Asymmetric Synthesis." *Org. Lett.* **2001**, *3*, 1273–1276.

(4) Yan, H.; Jang, H. Bin; Lee, J. W.; Kim, H. K.; Lee, S. W.; Yang, J. W.; Song, C. E. “A Chiral-Anion Generator: Application to Catalytic Desilylative Kinetic Resolution of Silyl-Protected Secondary Alcohols.” *Angew. Chemie - Int. Ed.* **2010**, *49*, 8915–8917.

(5) Pfeifer, L.; Engle, K. M.; Pidgeon, G. W.; Sparkes, H. A.; Thompson, A. L.; Brown, J. M.; Gouverneur, V. “Hydrogen-Bonded Homoleptic Fluoride–Diarylurea Complexes: Structure, Reactivity and Coordinating Power.” *J. Am. Chem. Soc.* **2016**, *138*, 13314–13325.

(6) Ford, D. D.; Lehnherr, D.; Kennedy, C. R.; Jacobsen, E. N. “Anion-Abstraction Catalysis: The Cooperative Mechanism of α-Chloroether Activation by Dual Hydrogen-Bond Donors.” *ACS Catal.* **2016**, *6*, 4616–4620.

(7) Brak, K.; Jacobsen, E. N. “Asymmetric Ion-Pairing Catalysis.” *Angew. Chemie - Int. Ed.* **2013**, *52*, 534–561.

(8) Pupo, G.; Ibba, F.; Ascough, D. M. H.; Vicini, A. C.; Ricci, P.; Christensen, K. E.; Pfeifer, L.; Morphy, J. R.; Brown, J. M.; Paton, R. S.; Gouverneur, V. “Asymmetric Nucleophilic Fluorination under Hydrogen Bonding Phase-Transfer Catalysis.” *Science* **2018**, *360*, 638–642.

(9) Ibba F.; Pupo, G.; Thompson, A. L.; Brown, J. M.; Claridge, T. D. W.; Gouverneur, V. “Impact of Multiple Hydrogen Bonds with Fluoride on Catalysis: Insight from NMR Spectroscopy”, *J. Am. Chem. Soc.* **2020**, *142*, 19731–19744.

(10) O’Hagan, D.; Schaffrath, C.; Cobb, S. L.; Hamilton, J. T. G.; Murphy, C. D. “Biosynthesis of an Organofluorine Molecule.” *Nature* **2002**, *416*, 279–279.

(11) Senn, H. M.; O’Hagan, D.; Thiel, W. “Insight into Enzymatic C–F Bond Formation from QM and QM/MM Calculations.” *J. Am. Chem. Soc.* **2005**, *127*, 13643–13655.

(12) *CRC Handbook of Chemistry and Physics*, 85th ed.; Lide, D. R., Ed.; CRC Press: Boca Raton, FL, 2004.

(13) Anderson, S. R.; Ayers, J. T.; DeVries, K. M.; Ito, F.; Mendenhall, D.; Vanderplas, B. C. “The Preparation of β-Substituted Amines from Mixtures of Epoxide Opening Products via a Common Aziridinium Ion Intermediate.” *Tetrahedron Asymmetry* **1999**, *10*, 2655–2663.

(14) Carter, C.; Fletcher, S.; Nelson, A. “Towards Phase-Transfer Catalysts with a Chiral Anion: Inducing Asymmetry in the Reactions of Cations.” *Tetrahedron Asymmetry* **2003**, *14*, 1995–2004.

(15) Fleming, E. M.; McCabe, T.; Connon, S. J. “Novel Axially Chiral Bis-Arylthiourea-Based Organocatalysts for Asymmetric Friedel-Crafts Type Reactions.” *Tetrahedron Lett.* **2006**, *47*, 7037–7042.

(16) Liu, X. G.; Jiang, J. J.; Shi, M. “Development of Axially Chiral Bis(Arylthiourea)-Based Organocatalysts and Their Application in the Enantioselective Henry Reaction.” *Tetrahedron Asymmetry* **2007**, *18*, 2773–2781.

(17) Chan, A. S.-C.; Fu-Yao Zhang. “Chiral Aminophosphines.” US005919981A, 1999.

(18) Kano, T.; Tanaka, Y.; Osawa, K.; Yurino, T.; Maruoka, K. “Facile Synthesis of Structurally Diverse 3,3′-Disubstituted 1,1′-Binaphthyl-2,2′-Diamines in Optically Pure Forms.” *J. Org. Chem.* **2008**, *73*, 7387–7389.

(19) Hartmann, E.; Denmark, S. E. “Structural, Mechanistic, Spectroscopic, and Preparative Studies on the Lewis Base Catalyzed, Enantioselective Sulfenofunctionalization of Alkenes.” *Helv. Chim. Acta* **2017**, *100*, e1700158.

(20) Jakab, G.; Tancon, C.; Zhang, Z.; Lippert, K. M.; Schreiner, P. R. “(Thio)Urea Organocatalyst Equilibrium Acidities in DMSO.” *Org. Lett.* **2012**, *14*, 1724–1727.

(21) Lippert, K. M.; Hof, K.; Gerbig, D.; Ley, D.; Hausmann, H.; Guenther, S.; Schreiner, P. R. “Hydrogen-Bonding Thiourea Organocatalysts: The Privileged 3,5-Bis(Trifluoromethyl)Phenyl Group.” *European J. Org. Chem.* **2012**, 5919–5927.

(22) Etter, M. C.; Zia-Ebrahimi, M.; Urbañczyk-Lipkowska, Z.; Panunto, T. W. “Hydrogen Bond Directed Cocrystallization and Molecular Recognition Properties of Diarylureas.” *J. Am. Chem. Soc.* **1990**,

112, 8415–8426.

(23) Etter, M. C. “Encoding and Decoding Hydrogen-Bond Patterns of Organic Compounds.” *Acc. Chem. Res.* **1990**, *23*, 120–126.

(24) Duthion, B.; Pardo, D. G.; Cossy, J. “Enantioselective Synthesis of β-Fluoroamines from β-Amino Alcohols: Application to the Synthesis of LY503430.” *Org. Lett.* **2010**, *12*, 4620–4623.

(25) Vitaku, E.; Smith, D. T.; Njardarson, J. T. “Analysis of the Structural Diversity, Substitution Patterns, and Frequency of Nitrogen Heterocycles among U.S. FDA Approved Pharmaceuticals.” *J. Med. Chem.* **2014**, *57*, 10257–10274.

(26) Sahai, M. A.; Davidson, C.; Dutta, N.; Opacka-Juffry, J. “Mechanistic Insights into the Stimulant Properties of Novel Psychoactive Substances (Nps) and Their Discrimination by the Dopamine Transporter—in Silico and in Vitro Exploration of Dissociative Diarylethylamines.” *Brain Sci.* **2018**, *8*, 63–82.

(27) Berger, M. L.; Schweifer, A.; Rebernik, P.; Hammerschmidt, F. “NMDA Receptor Affinities of 1,2-Diphenylethylamine and 1-(1,2-Diphenylethyl)Piperidine Enantiomers and of Related Compounds.” *Bioorganic Med. Chem.* **2009**, *17*, 3456–3462.

(28) Janiri, L.; Persico, M. L.; Tempesta, E. “Dual Effects of Lephetamine on Spontaneous and Evoked Firing in the Cortex.” *Neuropharmacology* **1989**, *28*, 1405–1410.

(29) Luethi, D.; Hoener, M. C.; Liechti, M. E. “Effects of the New Psychoactive Substances Diclofensine, Diphenidine, and Methoxphenidine on Monoaminergic Systems.” *Eur. J. Pharmacol.* **2018**, *819*, 242–247.

(30) Natsuka, K.; Nakamura, H.; Negoro, T.; Uno, H.; Nishimura, H. “Studies on 1-Substituted 4-(1,2-Diphenylethyl)Piperazine Derivatives and Their Analgesic Activities. 2. Structure-Activity Relationships of l-Cycloalkyl-4-(l,2-Diphenylethyl)Piperazines.” *J. Med. Chem.* **1978**, *21*, 1265–1269.

(31) Kang, H.; Park, P.; Bortolotto, Z. A.; Brandt, S. D.; Colestock, T.; Wallach, J.; Collingridge, G. L.; Lodge, D. “Ephenidine: A New Psychoactive Agent with Ketamine-like NMDA Receptor Antagonist Properties.” *Neuropharmacology* **2017**, *112*, 144–149.

(32) Kalow, J. A.; Doyle, A. G. “Enantioselective Fluoride Ring Opening of Aziridines Enabled by Cooperative Lewis Acid Catalysis.” *Tetrahedron* **2013**, *69*, 5702–5709.

(33) Coburn, C. A.; Egbertson, M. S.; Graham, S. L.; McGaughey, G. B.; Stauffer, S. R.; Yang, W.; Lu, W.; Fahr, B. “Spiropiperidine Beta-Secretase Inhibitors for the Treatment of Alzheimer’s Disease.” WO 011810, 2007.

(34) Sakamoto, H.; Sugimoto, T. “Preparation of Heterocyclic Compounds as Cholinergic Muscarinic M1 Receptor Positive Allosteric Modulators”. WO 129622, 2013.

(35) Meguro, M.; Asao, N.; Yamamoto, Y. “Ytterbium Triflate and High Pressure-Mediated Ring Opening of Epoxides with Amines.” *J. Chem. Soc. Perkin Trans. 1* **1994**, 2597–2601.

(36) Chong, H.-S.; Sun, X.; Chen, Y.; Wang, M. “Synthesis, Characterization, and Nucleophilic Ring Opening Reactions of Cyclohexyl-Substituted β-Haloamines and Aziridinium Ions.” *Tetrahedron Lett.* **2015**, *56*, 946–948.

Intentionally left blank

Chapter 3:

Scale-up of the Synthesis of Mono-*N*-Alkyl Bis-Ureas for HB-PTC

3.1 Project Aim

Recently, Gouverneur and co-workers introduced Hydrogen Bonding Phase-Transfer Catalysis (HB-PTC),[1] a new concept in asymmetric catalysis for the activation of inorganic fluoride salts as nucleophiles. Application of HB-PTC to the activation of KF and CsF for the enantioselective synthesis of β-fluoroamines was discussed in Chapter 2.[2] *N*-alkyl bis-urea (S)-**2.78** (Figure 3.1A) gave the highest enantiomeric ratios (e.r.) in the desymmetrisation of both stilbene-derived (up to 96:4 e.r.) and cyclic aliphatic (up to 85.5:14.5 e.r.) *meso*-aziridinium ions. Parallel research within the group revealed that the related *N*-alkyl bis-urea (*S*)-**2.3** (Figure 3.1B) provided the highest levels of enantiocontrol in the desymmetrisation of *meso*-episulfonium[1] and azetidinium ions.[3]

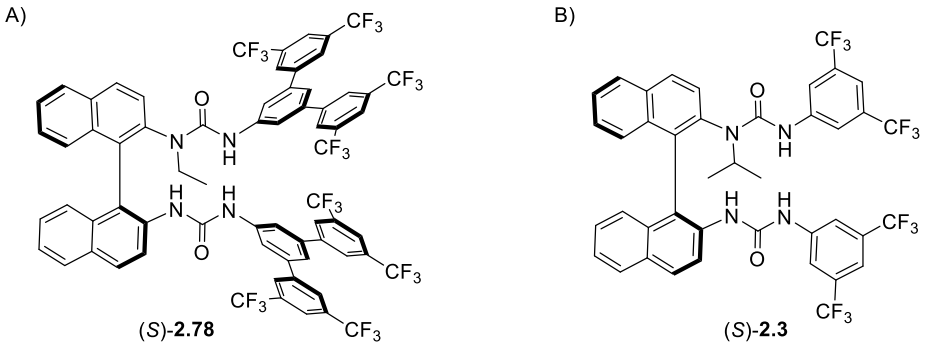
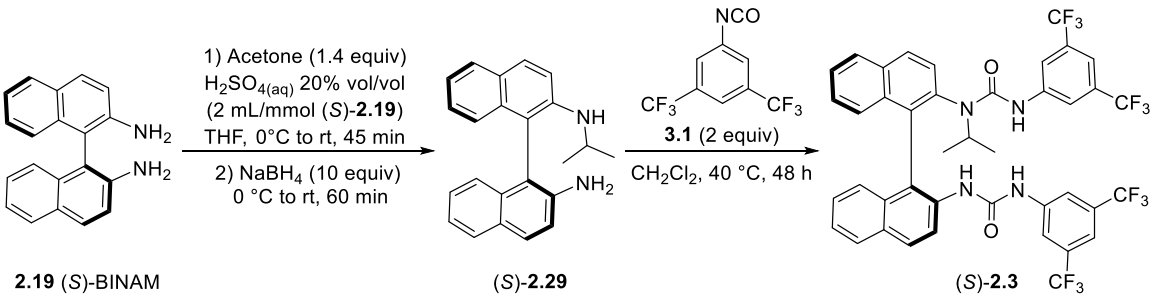


Figure 3.1: Organocatalysts for HB-PTC successfully applied to the enantioselective desymmetrisation of *meso*-aziridinium ions with KF and CsF (A)[2] and *meso*-episulfonium and azetidinium ions with CsF (B).[1,3]

We required multigram quantities (>10 g) of catalyst (*S*)-**2.78** for the scale-up studies of asymmetric HB-PTC described in Chapter 4. Moreover, chemical suppliers have shown interest in the commercialisation of this novel class of organocatalysts. For these reasons, we aimed to develop a robust and efficient synthesis to access both (*S*)-**2.3** and (*S*)-**2.78** on >10 g scale. The original route to (*S*)-**2.3** could be easily scaled up with only minor modifications (section 3.2), while a novel strategy was required to access (*S*)-**2.78** on scale (section 3.3).

3.2 Scale-up of the Synthesis of Catalyst (*S*)-2.3

The original synthetic route to catalyst (*S*)-**2.3** involved a two-step synthesis from commercially available (*S*)-BINAM ([1,1'-binaphthalene]-2,2'-diamine) **2.19** (Scheme 3.1A).[1] Reductive amination of (*S*)-**2.19** (1.5 g) with acetone, sulfuric acid and sodium borohydride was performed according to a reported procedure,[4] affording (*S*)-*N*^{2}-isopropyl-[1,1'-binaphthalene]-2,2'-diamine ((*S*)-*N*-^{i}Pr-BINAM) **2.29** in 57% yield after silica gel column chromatography.[1] Coupling with the commercially available 3,5-bis(trifluoromethyl)phenyl isocyanate **3.1** in refluxing CH_2Cl_2 yielded 2.45 g of bis-urea (*S*)-**2.3** (91% yield).



Scheme 3.1: Synthesis of catalyst (*S*)-**2.3**. Step 1: Acetone and aqueous H_2SO_4 (20% vol/vol) were stirred together for 45 min at 0 °C prior to the addition of (*S*)-BINAM at rt, followed by portion-wise addition of $NaBH_4$ at 0 °C. Step 2: Isocyanate **3.1** was added at rt to a solution of (*S*)-**2.29** in CH_2Cl_2, then the reaction was stirred at reflux for 48 h. A) Small scale (1.5 g) synthesis. B) Large scale (10 g) synthesis.

The scale-up of this synthesis starting from 10 g of (*S*)-BINAM **2.19** followed the same protocol with minor modifications (Scheme 3.1B). In the first step, the portion-wise addition of sodium borohydride to the acidic reaction mixture was carried out over 45 minutes to avoid excessive gas evolution. The reaction was performed under nitrogen flow to minimise the fire hazard related to hydrogen gas evolution, and the reaction temperature was maintained at 0 °C to control the exotherm. Following chromatographic purification on silica gel, (*S*)-*N*-^{i}Pr-BINAM **2.29** was obtained in 60% yield (6.8 g) which compares favourably with the 1.5 g scale reaction (57% yield).

In the urea formation step, slow addition of isocyanate **3.1** was required to maintain consistent stirring, due to formation of a precipitate upon isocyanate addition. The precipitate slowly dissolved if the addition was interrupted. The yield of catalyst (*S*)-**2.3** after chromatographic purification (silica gel) followed by crystallisation—achieved by layering hexane (6 mL/g) on a solution of (*S*)-**2.3** in Et_2O (1.2 mL/g)—was 80% (14 g). This is slightly lower than the yield of the small scale (91% yield), but in that case the catalyst was only purified by column chromatography on silica gel.

On a large scale, the main impurity observed in the urea formation step was intermediate mono-urea **3.2**, which had been previously characterised (Figure 3.2).[5] Achiral Schreiner's urea **2.16** (Figure 3.2) can be formed in the presence of adventitious water, and it is an undesired side-product because it is catalytically active in the fluorination with metal alkali fluorides, leading to formation of racemic product.[1] Its removal by chromatographic purification on silica gel is complicated by its scarce solubility, which results in extended retention time. To avoid formation of **2.16** during work-up, MeOH was added at the end of the reaction to quench unreacted isocyanate. This afforded carbamate **3.3** (Figure 3.2), which is more easily separable from the desired product by column chromatography.

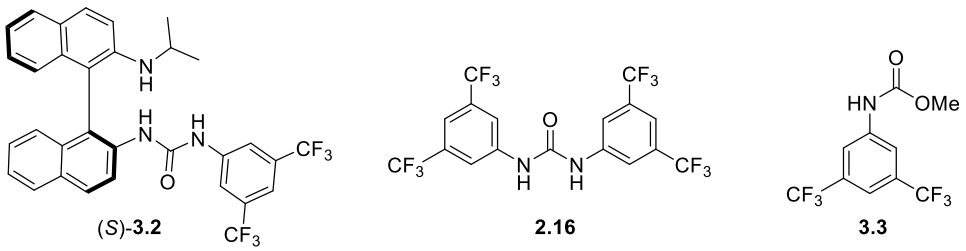


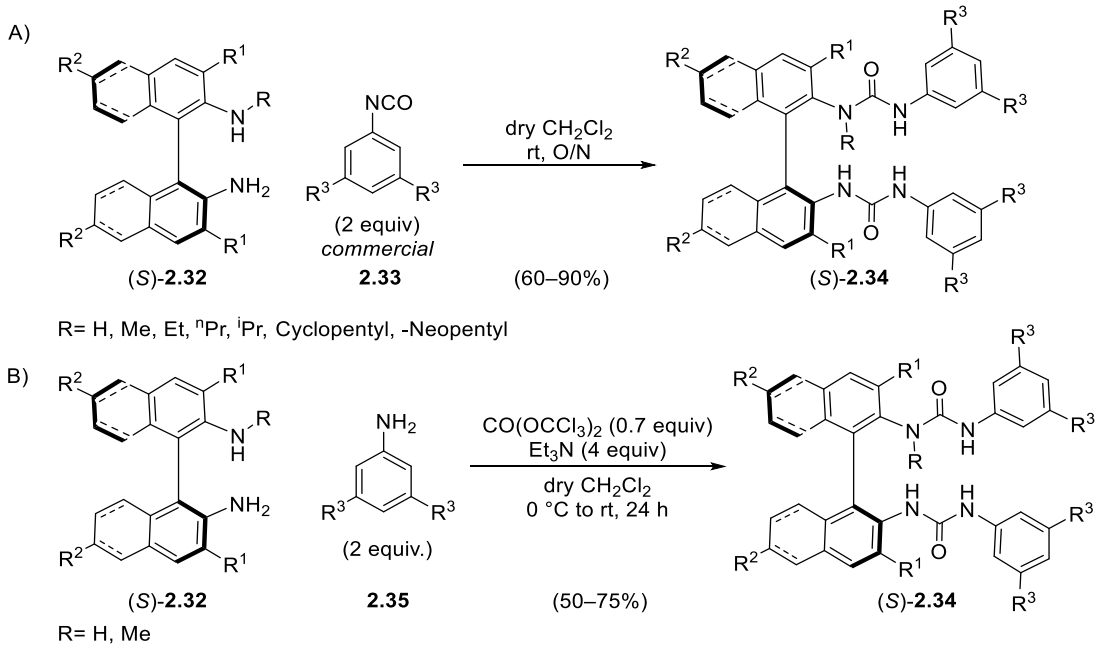
Figure 3.2: Side-products formed in the synthesis of (*S*)-**2.3**.

Overall, synthesis of (*S*)-**2.3** was successfully scaled up ten-fold maintaining the good yield previously achieved on the small scale (48% overall yield from 10 g of (*S*)-BINAM *versus* 52% from 1.5 g). Further optimisations should focus on increasing the yield of the reductive amination and removing the need of chromatographic purification for both steps.

3.3 Scale-up of the Synthesis of Catalyst (*S*)-2.78

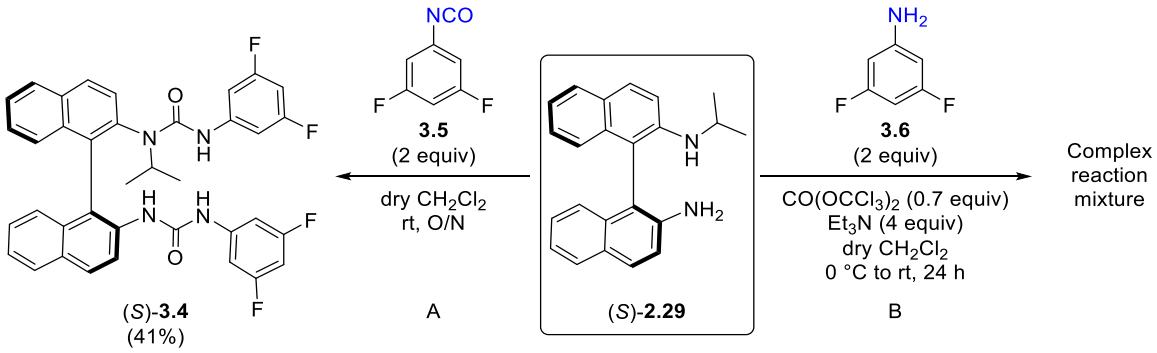
3.3.1 Urea Synthesis *via in situ* Formation of the Isocyanate: Limitations

The synthesis of catalyst (*S*)-**2.3** reported in section 3.2 represents the general approach to BINAM-derived bis-ureas described in Chapter 2 (section 2.4.1). According to this strategy, chiral BINAM-derived anilines (*S*)-**2.32** were coupled with the achiral isocyanate in the last synthetic step. The reaction afforded the desired bis-ureas in good to high yields when commercial isocyanates were employed (Scheme 3.2A), and it was used to generate the first library of *N*-alkyl bis-urea organocatalysts.[1] A broad range of linear and branched *N*-alkyl chains were tolerated.[5] This strategy was then extended to non-commercial isocyanates, which were generated *in situ* from the corresponding achiral aniline **2.35** and bis(trichloromethyl) carbonate (*i.e.* triphosgene), prior to the addition of chiral (*S*)-**2.32** in a one-pot-two-step protocol (Scheme 3.2B). This gave access to bis-ureas **2.47–2.49** and **2.69–2.70** (R=H) described in Chapter 2 in moderate to good yields (50–75%). Yields were generally lower compared to the reactions with pre-formed and purified isocyanates.



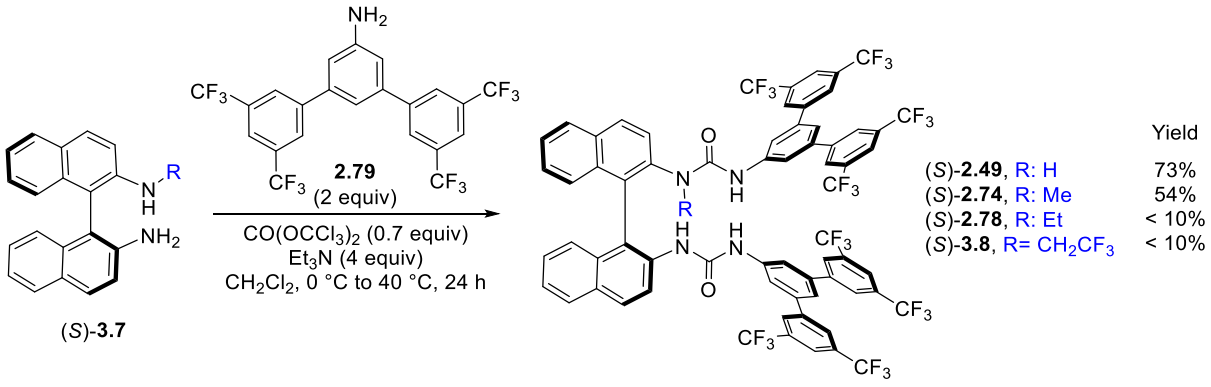
Scheme 3.2: Urea formation between chiral (*S*)-BINAM-derived anilines and achiral isocyanates to access bis-urea catalysts. A) Use of commercial isocyanates; B) formation of the isocyanate *in situ* with triphosgene in a one-pot-two-step protocol.

The one-pot-two-step protocol showed its limitations when it was extended to (*S*)-*N*-alkyl BINAM derivatives. For instance, the reaction between (*S*)-*N*-^{i}Pr-BINAM **2.29** and 3,5-difluorophenyl isocyanate afforded the desired bis-urea (*S*)-**3.4** in 41% yield when pre-formed isocyanate **3.5** was employed (Scheme 3.3A), but a complex reaction mixture was obtained using 3,5-difluoroaniline **3.6** as the isocyanate precursor (Scheme 3.3B).[5]



Scheme 3.3: Comparison of the outcome of the urea formation reaction of (*S*)-**2.29** with: A) pre-formed and purified isocyanate **3.5**; B) the same isocyanate generated *in situ* from aniline **3.6**.

While the reaction of unsubstituted (*S*)-BINAM and achiral aniline **2.79** afforded the desired bis-urea (*S*)-**2.49** in good yield (73%, Scheme 3.4), the yield of *N*-methyl bis-urea (*S*)-**2.74** was less satisfactory (54%) and only traces of bis-urea (*S*)-**2.78** were obtained with the bulkier (*S*)-*N*-Et-BINAM. Similarly, no product was formed when chiral (*S*)-BINAM bore a 2,2,2-trifluoroethyl group. The poor yield was due to formation of side-products, whose assignment is reported in the next section.



Scheme 3.4: Effect of R on the yield of urea formation of *N*-alkyl BINAM-derived anilines (*S*)-**3.7** with achiral aniline **2.79** according to the one-pot-two-step protocol involving *in situ* formation of the isocyanate.

3.3.1.1 Side-Products Assignment

The products obtained in the reaction between the BINAM-derived chiral aniline and achiral aniline **2.79** according to the one-pot-two-step protocol with *in situ* formation of the isocyanate were isolated and characterised. Mono-ureas (*S*)-**3.9** (R = Et) and (*S*)-**3.10** (R = CH_2CF_3, Figure 3.3A) derived from incomplete reaction of the chiral *N*-alkyl BINAM-derived bis-aniline with the isocyanate, which was generated in a stoichiometric amount. They might further react to afford the desired product (bis-ureas (*S*)-**2.78**, R= Et, and (*S*)-**3.8**, R= CH_2CF_3 p. 112). Alternatively, they might give rise to the side-products described below (**3.14** R= Et, and **3.15**, R= CH_2CF_3, pp. 114–117). Mono-ureas (*S*)-**3.11** (R=Et) and (*S*)-**3.12** (R = CH_2CF_3, Figure 3.3B) deriving from addition of the secondary aniline to the isocyanate were not detected.

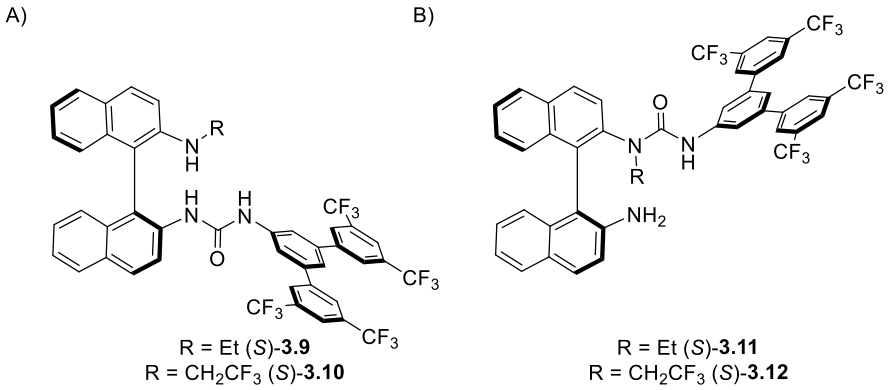


Figure 3.3: Potential mono-ureas formed in the coupling of (*S*)-BINAM-derived anilines with one equivalent of isocyanate. A) Formation of the urea on the primary aniline; observed. B) Formation of the urea on the secondary aniline; not observed.

Mono-urea (*S*)-**3.9** (Figure 3.3A) was fully characterised and its assignment was based on the combination of HRMS[i] and NMR experiments. Confirmation that the primary aniline of the *N*-alkyl BINAM-derivative had reacted with the isocyanate was obtained by a ^{1}H-^{13}C HSQC experiment, which showed the presence of two urea protons at 6.74 ppm and 6.55 ppm (Figure 3.4). The aniline proton was detected at 3.61 ppm.

[i] *m/z* calculated for $C_{45}H_{30}F_{12}ON_3$ $[M+H]^+$ 856.2192; found 856.2180

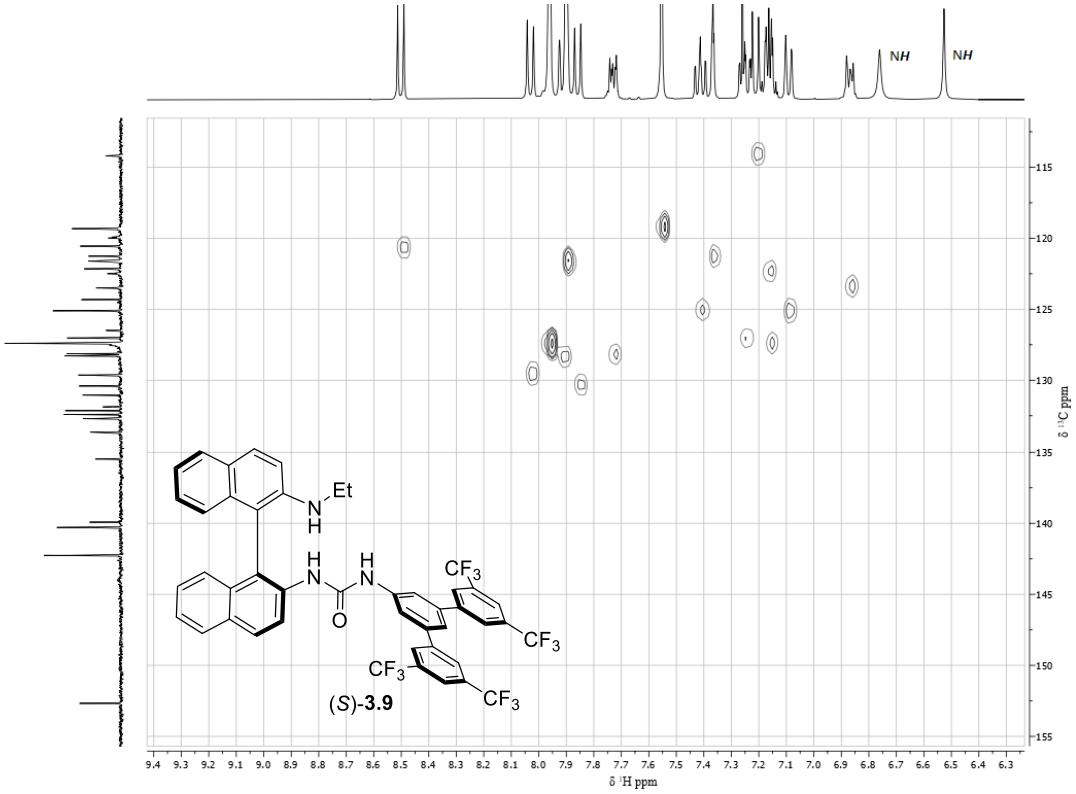
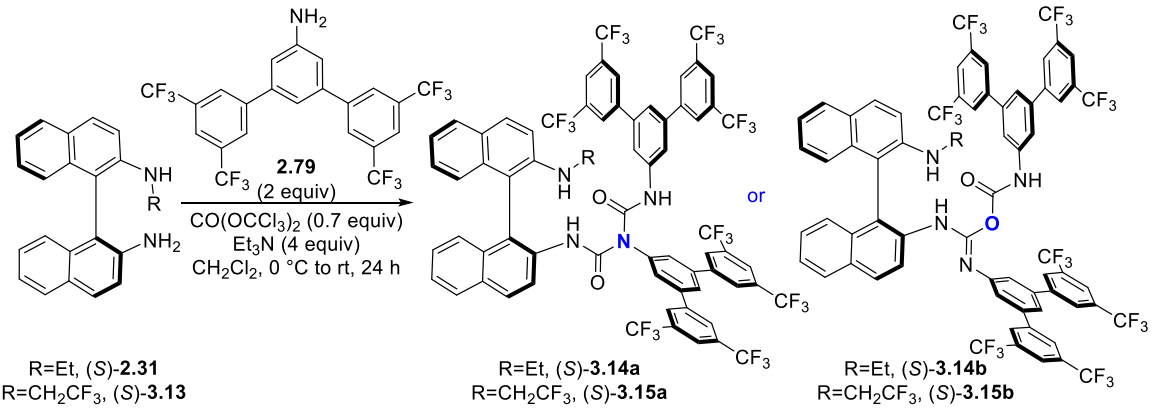


Figure 3.4: ^{1}H-^{13}C HSQC in $CDCl_3$ of (*S*)-**3.9**, detail of the aromatic region. The number of visible correlations (16) is consistent with formation of a mono-urea. The presence of two proton signals in the aromatic region not correlating with any carbon signal suggests that reaction took place on the primary aniline.

The main product obtained in the reaction of chiral anilines (*S*)-**2.31** and (*S*)-**3.13** with achiral urea **2.79** according to the one-pot-two-steps protocol involving *in situ* formation of the isocyanate were (*S*)-**3.14** and (*S*)-**3.15** respectively (Scheme 3.5).



Scheme 3.5: Main products isolated in the urea formation between *N*-alkyl BINAM-derived anilines (R= Et, CH_2CF_3) and achiral aniline **2.79** according to the one-pot-two-step protocol with *in situ* formation of the isocyanate.

Assignment of (*S*)-**3.15** (R = CH_2CF_3) was achieved using a combination of 1D and 2D NMR experiments in $CDCl_3$. The presence of two carbonyl groups was inferred by analysis of the ^{13}C NMR spectrum (resonances at 154.4 ppm and 152.2 ppm), while ^{1}H-^{15}N HSQC allowed to identify the NH protons (11.87, 6.38 ppm and 3.68 ppm). ^{1}H-^{13}C and ^{1}H-^{15}N HMBC were used to confirm that the isocyanate had reacted with the primary aniline (Figure 3.5. See also Figure 3.6A for the key ^{1}H-^{13}C HMBC correlation) and not on the secondary aniline, and to determine connectivity. To confirm that no substitution had taken place on the naphthyl rings, the analysis was repeated in THF-d_8, which allowed us to unambiguously determine the signals multiplicity (Figure 3.6B). Finally, the corresponding mono-urea (*S*)-**3.10** was obtained by hydrolysis of (*S*)-**3.15**, further sustaining the identity of the proposed side-product. Two structures are compatible with the spectroscopic data collected: carbamoyl urea (*S*)-**3.15a**, and (*S*)-**3.15b** (Figure 3.5). Formation of carbamoyl ureas similar to (*S*)-**3.15a** by reaction of arylureas and isocyanates has been reported.[6,7] The lack of reports of structures similar to (*S*)-**3.15b** might imply that this alternative could be unstable, undergoing 1,3(*O*-*N*) acyl transfer to (*S*)-**3.15a**.[8–10]

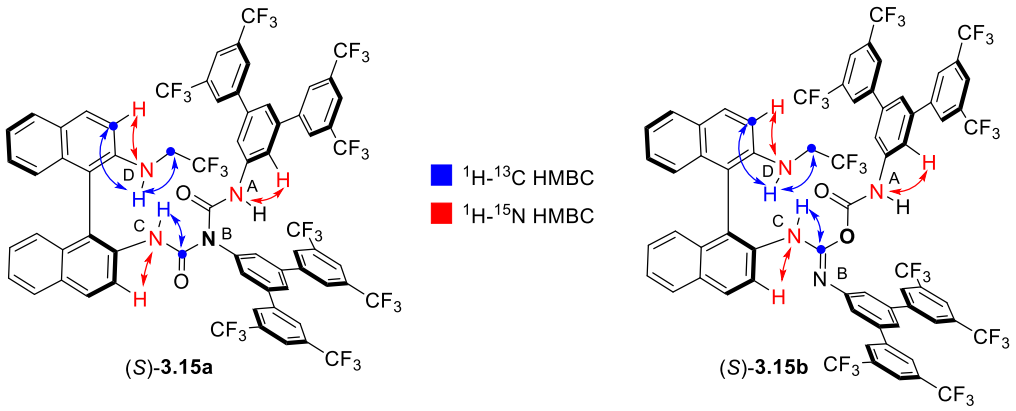


Figure 3.5: Key ^{1}H-^{13}C (blue) and ^{1}H-^{15}N HMBC (red) correlations used to assign the structure of (*S*)-**3.15**.

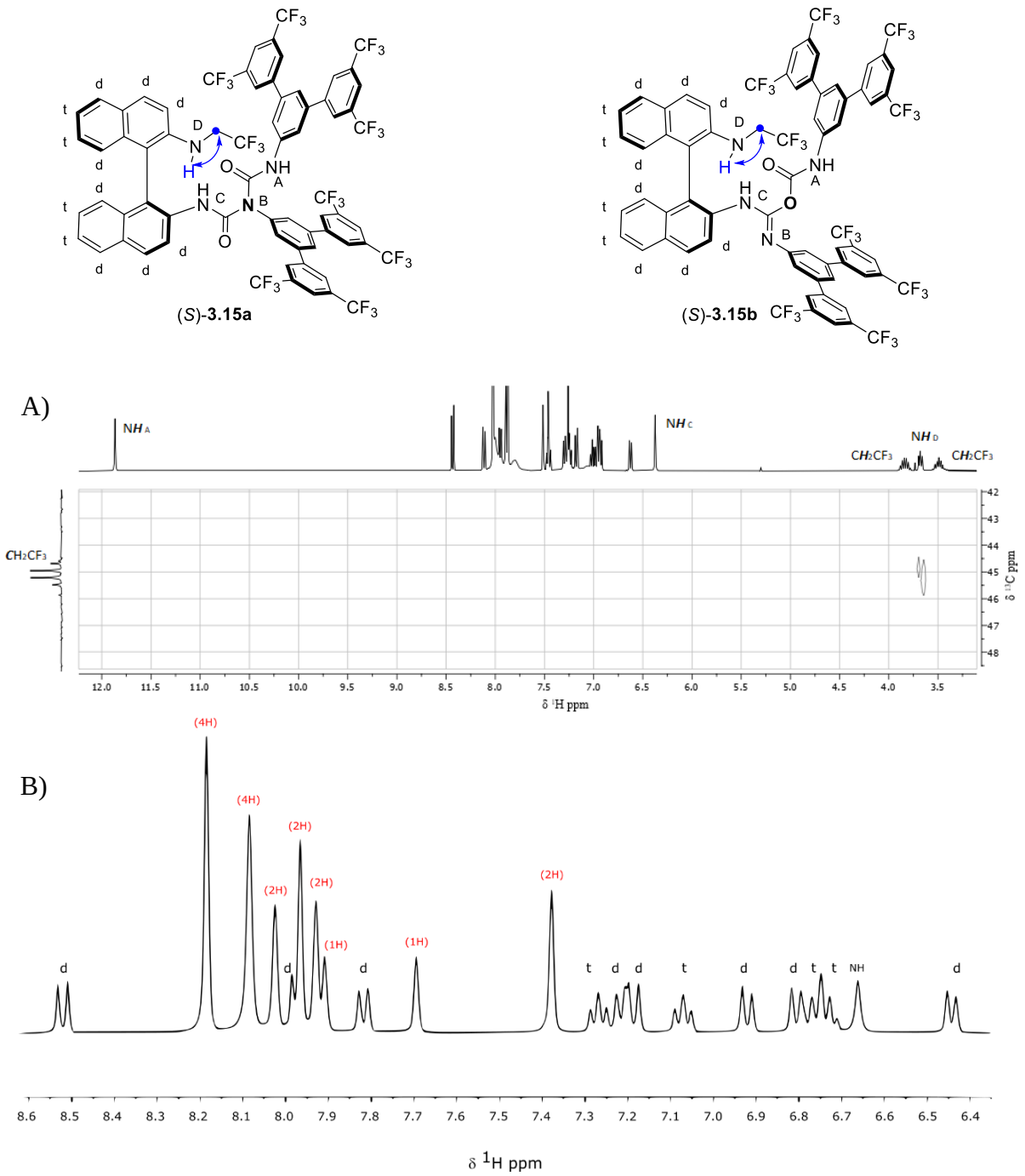


Figure 3.6: Proposed structures for the main side-product obtained in the urea formation reaction according to the one-pot-two-step protocol with *in situ* generation of the isocyanate. A) Detail of the ^{1}H-^{13}C HMBC spectrum in $CDCl_3$ showing the presence of an aniline functional group. The correlation is indicated with a blue arrow on the structure. B) Detail of the aromatic region of the ^{1}H NMR spectrum in THF-d_8 with reported multiplicity for the binaphthyl signals (black), matching the proposed structures (*S*)-**3.15a** and (*S*)-**3.15b**. The signals of the terphenyl units are reported in red together with the integration values.

The most characteristic feature of the ^{1}H NMR spectrum of (*S*)-**3.15**, was the strongly deshielded N_A–H proton (11.87 ppm in $CDCl_3$), which might be due to an intramolecular hydrogen bonding with formation of a six-membered ring (Figure 3.7).[11]

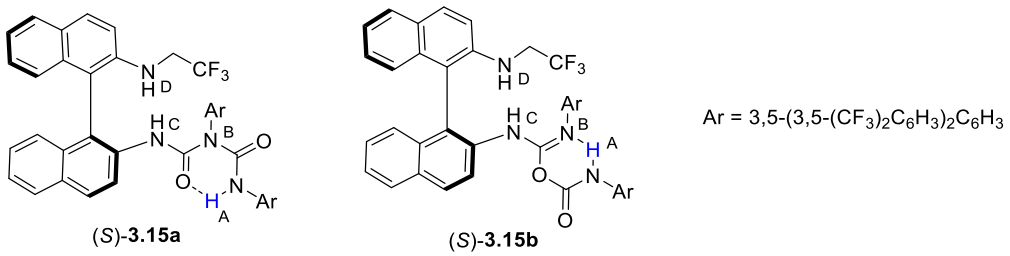
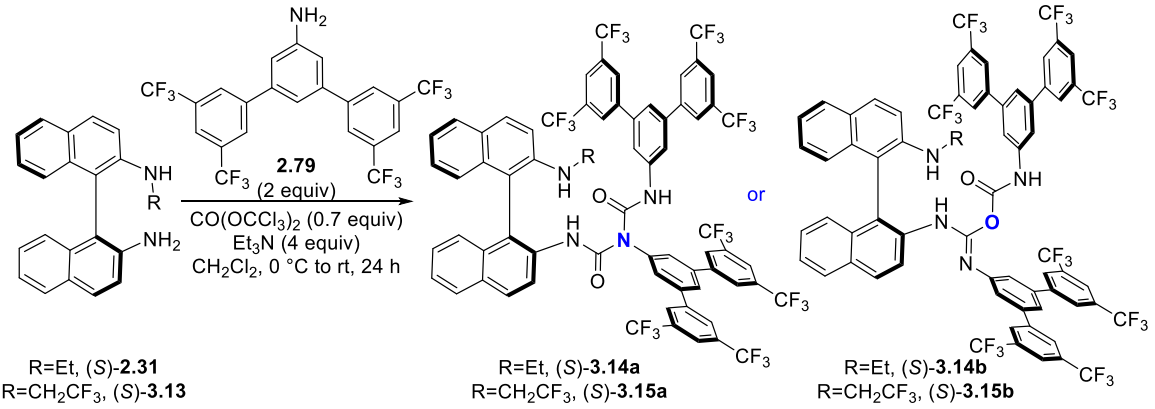


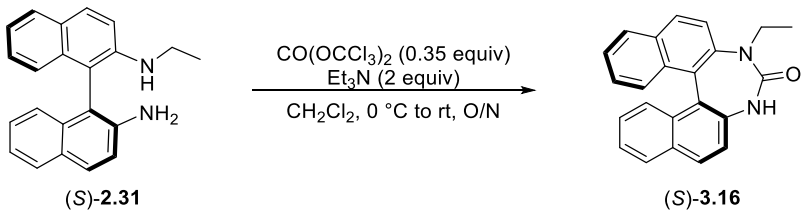
Figure 3.7 Proposed intramolecular hydrogen bonding to rationalise the unusually deshielded NH proton resonating at 11.87 ppm in $CDCl_3$.

An equally deshielded signal (11.93 ppm) was found in the ^{1}H NMR spectrum of the main product obtained in the reaction of (*S*)-*N*-Et-BINAM **2.31** with aniline **2.79** in the presence of triphosgene and Et_3N. For this reason, the product was assigned to either (*S*)-**3.14a** or (*S*)-**3.14b** by analogy (Scheme 3.6).



Scheme 3.6: Main products isolated in the urea formation between *N*-alkyl BINAM-derived anilines (R= Et, CH_2CF_3) and achiral aniline **2.79** according to the one-pot-two-step protocol for the *in situ* formation of the isocyanate.

Additionally, the cyclic urea (*S*)-**3.16** was formed if residual triphosgene was present in the reaction mixture when chiral (*S*)-**2.31** was added to the isocyanate generated *in situ*. To confirm its identity, (*S*)-**3.16** was prepared independently by stirring (*S*)-*N*-Et-BINAM **2.31** and triphosgene in CH_2Cl_2 (0.05 M) overnight (Scheme 3.7).



Scheme 3.7: Formation of cyclic urea (*S*)-**3.16** by reaction of (*S*)-*N*-Et-BINAM **2.31** with triphosgene.

A key correlation between the urea carbonyl and both the methylene of the ethyl chain and the urea proton (NH) confirmed the presence of the bridging urea (Figure 3.8). Moreover, a peak corresponding to the protonated adduct was found by high-resolution mass spectrometry (*m/z* calculated for $C_{23}H_{19}ON_2$ $[M+H]^+$ 339.1492, found 339.1493).

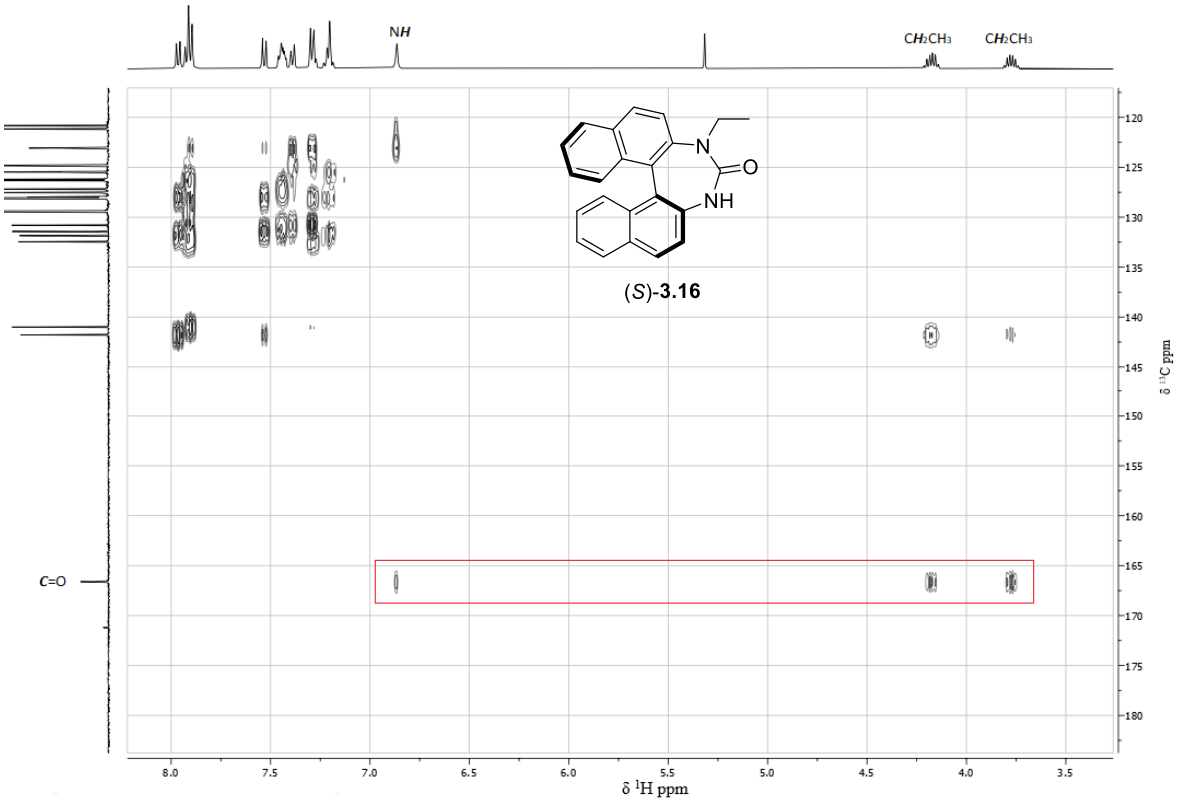
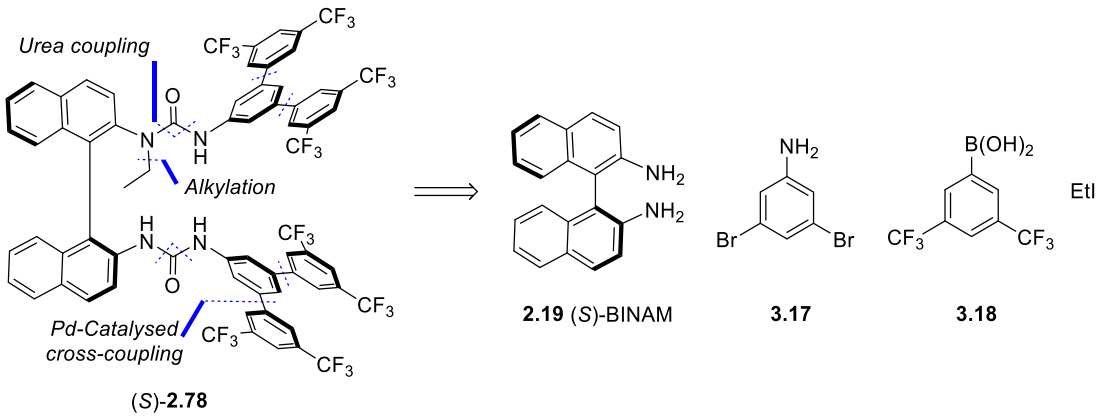


Figure 3.8: ^1H-^{13}C HMBC in $CDCl_3$ of (*S*)-**3.16**, showing the correlation between the C=O and both the urea NH proton and the methylene protons.

3.3.2 Overview of Alternative Synthesis of Catalyst (*S*)-2.78

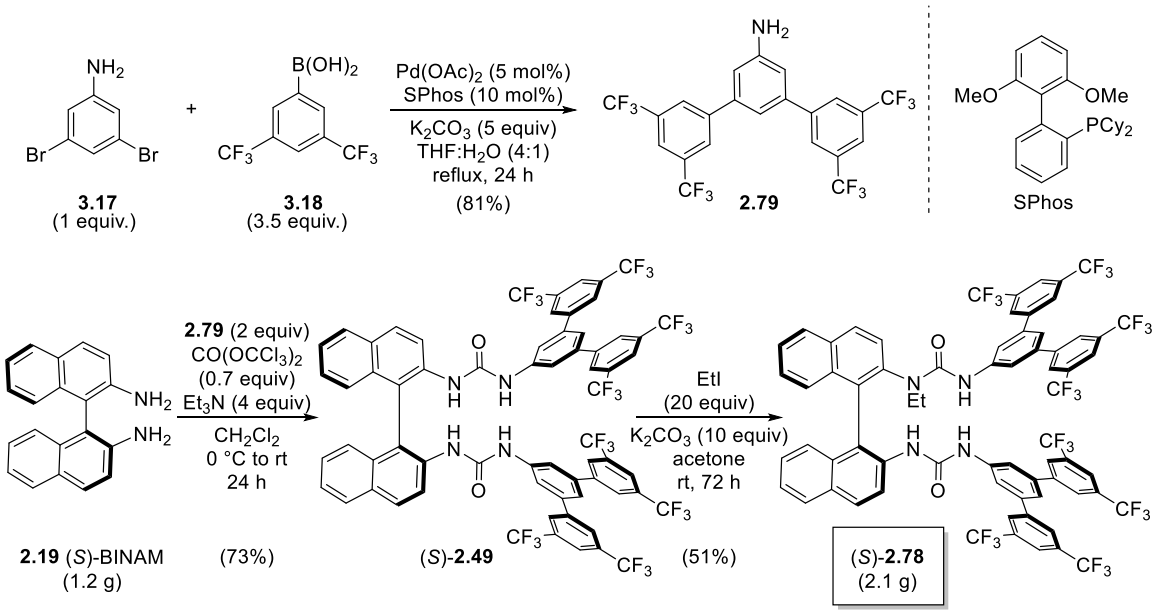
Since we were unable to access (*S*)-**2.78** according to the one-pot-two-step protocol reported in section 3.3.1, three alternative routes were proposed. These were based on the same key disconnections and commercial precursors (Scheme 3.8) but differed in the reaction order. *Route 1* involved urea formation between (*S*)-BINAM and an achiral aniline bearing the polyfluorinated terphenyl unit, followed by alkylation (section 3.3.3). The achiral aniline was synthesised by Suzuki-Miyaura cross-coupling of 3,5-dibromoaniline **3.17** and (3,5-bis(trifluoromethyl)phenyl)boronic acid **3.18** prior to urea formation. In *route 2* the order was reversed: alkylation of (*S*)-BINAM was performed first, followed by urea formation and finally by a quadruple Suzuki-Miyaura cross-coupling (section 3.3.4). *Route 3* relied on urea formation in the last synthetic step in which (*S*)-*N*-Et-BINAM was coupled with a pre-formed and purified isocyanate (section 3.3.5). The latter was obtained from the same aniline employed in *route 1*.



Scheme 3.8: Retrosynthetic analysis of (*S*)-**2.78** showing the key disconnections and the commercial precursors employed in all the proposed forward synthesis. Bottom: reactions order of the three routes explored. CC = Cross-coupling.

3.3.3 Route 1: Published Procedure

The first route explored is the published procedure described in the previous chapter (section 2.4.3).[2] It consisted of a three-step linear synthesis involving Suzuki-Miyaura cross-coupling to afford achiral aniline **2.79**, urea formation according to the one-pot-two-step protocol based on the *in situ* formation of the isocyanate, and alkylation of bis-urea (*S*)-**2.49** with ethyl iodide (Scheme 3.9). It afforded 2.10 g of (*S*)-**2.78** starting from 1.2 g of (*S*)-BINAM (37% overall yield). The main advantage of the synthesis is that it does not require protection of the chiral bis-aniline, because the alkylation is performed on bis-urea (*S*)-**2.49**, making it the shortest route evaluated (3 steps in the longest linear sequence = LLS, or 2 steps from (*S*)-BINAM). The main disadvantage of this strategy is the complex chromatographic purification required in the final step to remove the side-products formed in the alkylation, which makes it unsuitable for further scale-up. Moreover, the route lacks modularity: any modification of the terphenyl units requires a *de novo* synthesis of the desired analogue, and *N*-alkylation is limited to primary unbranched alkyl chains that can be introduced *via* S_N2 substitution.

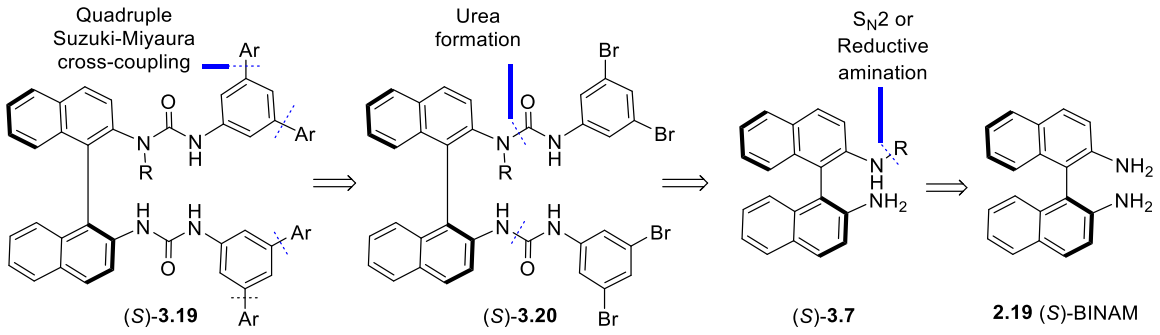


Scheme 3.9: Published route to access (*S*)-**2.78**, involving urea formation followed by alkylation (2 steps from (*S*)-BINAM, 37% overall yield). The synthesis is highly efficient for obtaining (*S*)-**2.78**, but it is not easily scalable.

3.3.4 Route 2: The Quadruple Suzuki-Miyaura Cross-Coupling Route

The second route was devised to allow rapid generation of a library of catalysts of general structure (*S*)-**3.19** (Scheme 3.10), bearing different functionalities on the terphenyl unit. Introduction of this structural element improved the enantiocontrol in the fluorination of both stilbene-derived (up to 96:4 e.r) and aliphatic aziridinium ions (up to 85.5:14.5 e.r., Chapter 2). For this reason, we were interested in evaluating the effect of structural modifications of the π-system.

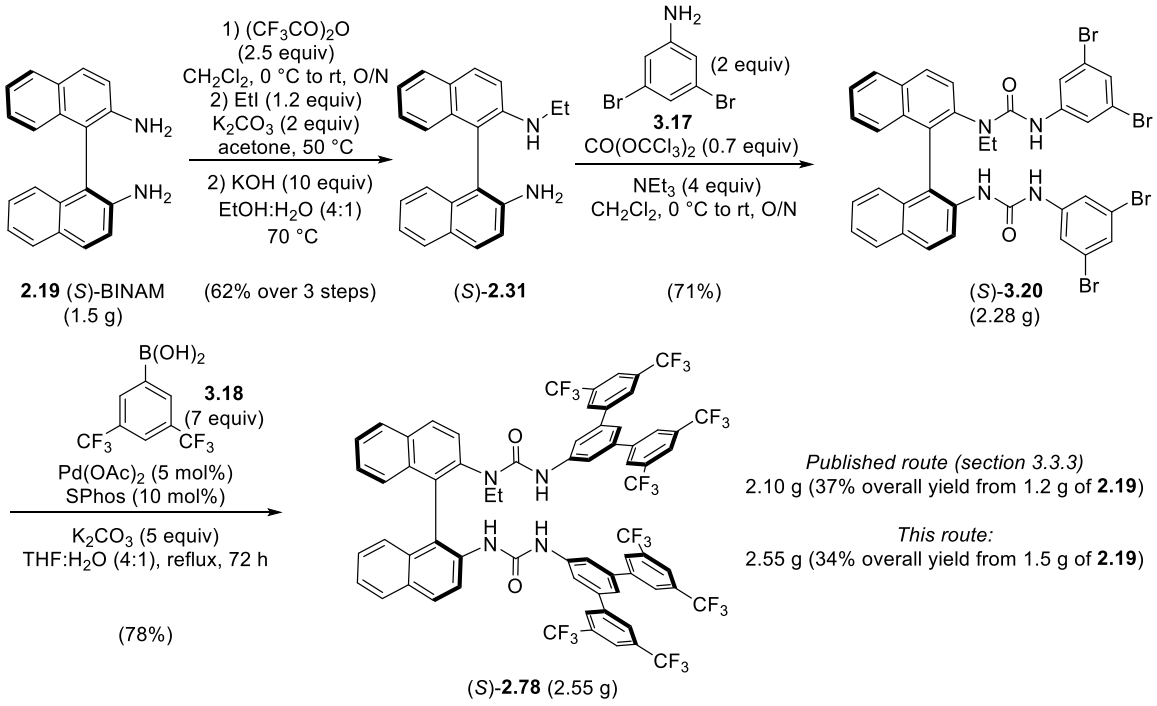
The "quadruple Suzuki-Miyaura cross-coupling route" relies on this reaction to install the desired functionalities on the common precursor bis-urea (*S*)-**3.20** in the last step of the synthesis (Scheme 3.10). The key intermediate bis-urea (*S*)-**3.20** could be obtained coupling chiral *N*-alkyl BINAM-derivative (*S*)-**3.7** with 3,5-dibromoaniline, according to the one-pot-two-step protocol involving *in situ* formation of the isocyanate. Either S_N2 substitution with the appropriate alkyl iodide or reductive amination could be used to access the desired chiral *N*-alkyl bis-aniline (*S*)-**3.7**.



Scheme 3.10: Retrosynthetic analysis of the "quadruple Suzuki-Miyaura cross-coupling route" to access a library of *N*-alkyl BINAM-derived bis-ureas characterised by different substitution of the terphenyl units.

3.3.4.1 Route Validation

The feasibility of this route was validated with the synthesis of known (*S*)-**2.78** starting from 1.5 g of (*S*)-BINAM (Scheme 3.11). A three-step protection-alkylation-deprotection sequence previously reported afforded (*S*)-*N*-Et-BINAM **2.31** in 62% overall yield.[1] Urea formation with *in situ* generated 3,5-dibromophenyl isocyanate proceeded smoothly, affording (*S*)-**3.20** in 71% yield (2.28 g) when the previously optimised conditions were employed (3,5-bromoaniline: 2 equiv, triphosgene: 0.7 equiv, Et_3N: 4 equiv). The Pd-catalysed cross-coupling between bis-urea (*S*)-**3.20** and boronic acid **3.18** proceeded fully to the desired product, whose NMR spectra matched those of bis-urea (*S*)-**2.78** synthesised according to route 1. The Suzuki-Miyaura reaction was conducted on two batches of 1 g each of (*S*)-**3.20,** obtaining 1.30 g (81% yield) and 1.25 g (78% yield) of catalyst (*S*)-**2.78** after chromatographic purification on silica gel.



Scheme 3.11: Synthesis of catalyst (*S*)-**2.78** *via* the "quadruple Suzuki-Miyaura cross-coupling route".

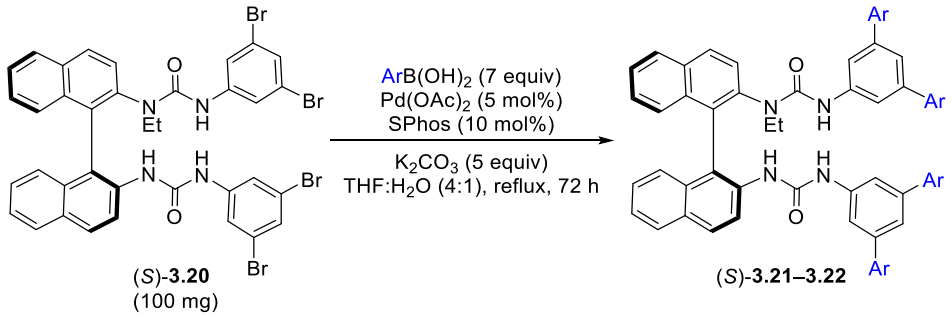
In spite of the increased number of synthetic steps (5 *versus* 3), this route afforded (*S*)-**2.78** in similar yield to the published route (34% overall yield *versus* 37% from (*S*)-BINAM).[2]

Moreover, the final Suzuki-Miyaura cross-coupling furnished bis-urea (*S*)-**2.78** as the sole product, greatly simplifying its purification.

3.3.4.2 Library Generation

Next, the same route was employed for the synthesis of bis-ureas (*S*)-**3.21**–**3.22**. (*S*)-**3.21**, with methoxy substituents in place of the trifluoromethyl groups, was obtained in 56% yield (entry 2, Table 3.1). The analogue (*S*)-**3.22**, characterised by a single meta ester functionality (3-COOMe) was afforded in 65% yield (entry 3). These yields compare favourably with that of model (*S*)-**2.78** (63%, entry 1) when the synthesis was performed on the same scale (100 mg).

Table 3.1: Synthesis of bis-ureas characterised by different terphenyl substituents



(*S*)-**3.20** (100 mg)

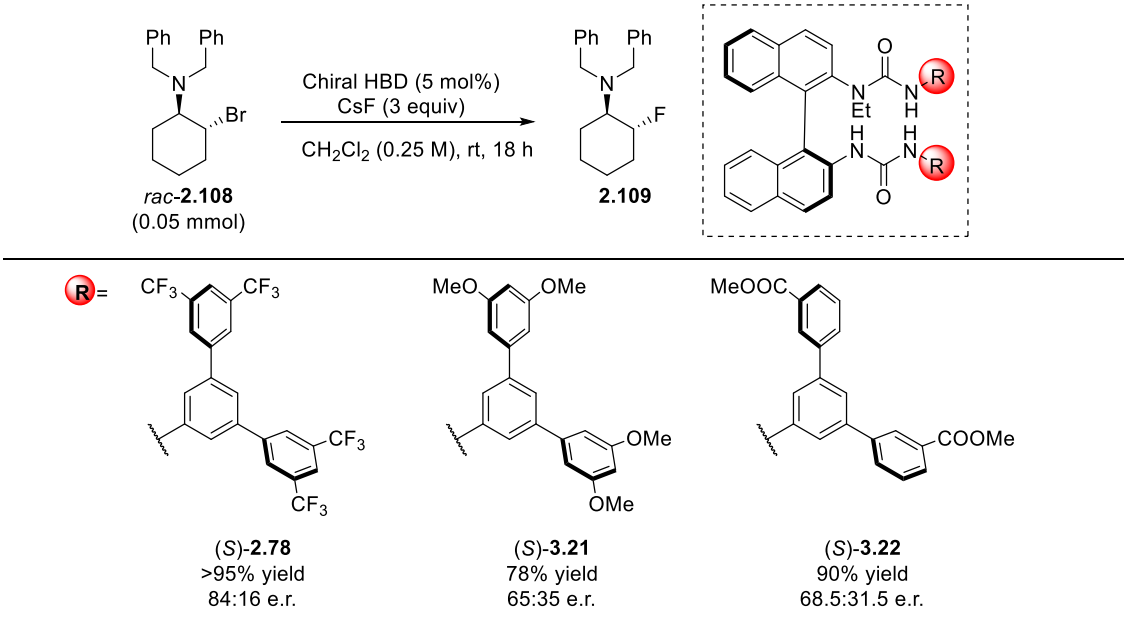
(*S*)-**3.21–3.22**

Entry	*Bis-urea*	*Ar*	*Isolated yield of bis-urea*
1	(*S*)-**2.78**	3,5-$(CF_3)_2C_6H_3$	63%
2	(*S*)-**3.21**	3,5-$(OMe)_2C_6H_3$	56%
3	(*S*)-**3.22**	3-$(COOMe)_2C_6H_3$	65%

Reaction conditions: (*S*)-**3.20** (100 mg, 1 equiv), $ArB(OH)_2$ (7 equiv), $Pd(OAc)_2$ (5 mol%), SPhos (10 mol%), K_2CO_3 (5 equiv), degassed THF: degassed H_2O (4:1), reflux, 24–72 h. SPhos = 2-Dicyclohexylphosphino-2′,6′-dimethoxybiphenyl.

Bis-ureas (*S*)-**3.21–3.22** were tested in the enantioselective fluorination of *rac*-**2.108** and their performance compared with that of (*S*)-**2.78** (Scheme 3.12). (*S*)-**3.21** and (*S*)-**3.22** afforded **2.109** in slightly reduced yield compared to (*S*)-**2.78** (**3.21**: 78% yield, **3.22**: 90% yield *versus* **2.78**: > 95%). In contrast, both catalysts showed poorer enantiocontrol than

(*S*)-**2.78** affording **2.109** in similar e.r. (**3.21**: 65:35 e.r.; **3.22**: 68.5:31.5 e.r. *versus* **2.78**: 84:16 e.r.).



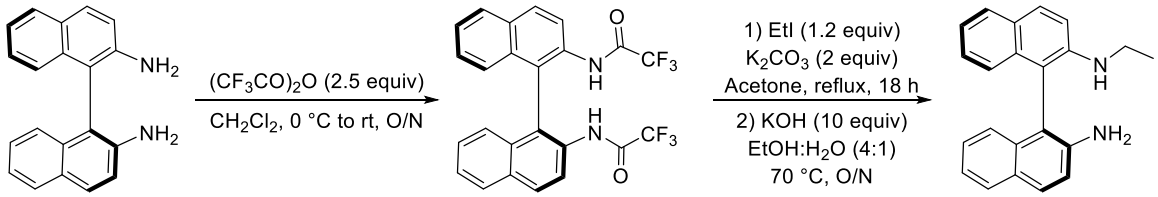
Scheme 3.12: Effect of structural modification of the terphenyl unit in the enantioselective fluorination of *rac*-**2.108** with CsF.

3.3.4.3 Scale-up

The quadruple Suzuki-Miyaura cross-coupling route was also evaluated for the scale-up of (*S*)-**2.78**, due to the cleaner reaction profile of its final step compared to that of the published procedure (Route 1, section 3.3.3).[2] In fact, the late-stage alkylation of bis-urea (*S*)-**2.49** with EtI required a minimum of two chromatographic purifications (silica gel) to maximise purity and yield of the final catalyst, which was not ideal on a large scale (>20 g).

The alkylation of (*S*)-BINAM **2.19** did not require extensive optimisation and could be successfully performed on 40 g of starting material. The reaction afforded 26.6 g of (*S*)-*N*-Et-BINAM **2.31** in comparable yield to the first trial on 2.4 g (60% yield, *versus* 62% yield on 40 g and 2.4 g scale respectively, Table 3.2). 10 g of unreacted (*S*)-BINAM (25%) were recovered, making the recycling of starting material an attractive strategy to increase the efficiency of this protocol.

Table 3.2: Scale-up of (*S*)-BINAM alkylation with EtI



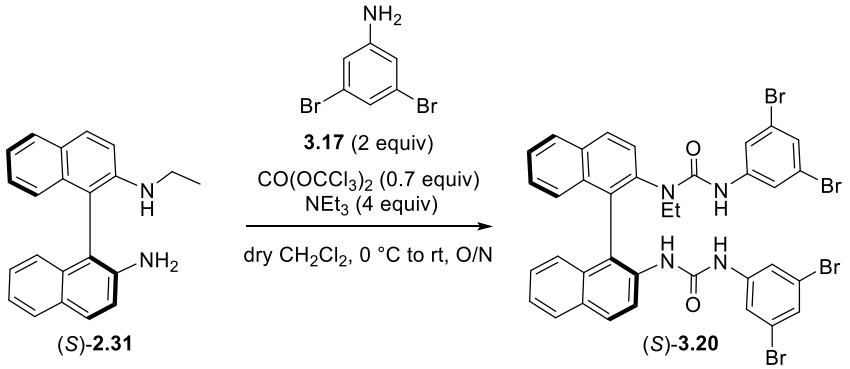
2.19 (*S*)-BINAM (*S*)-**3.23** (*S*)-**2.31**

Entry	*Scale*	*Yield of isolated (S)-**2.31** (over 3 steps)*	*Comments*
1	1.5 g (5.3 mmol)	62% (1.02 g)	–
2	15 g (53 mmol)	65% (10.7 g)	–
3	40 g (140 mmol)	60% (26.3 g)	(SM recovered: 10 g, 25%) → 80% yield BRSM

Reaction conditions: *Step 1*: (*S*)-**2.19 (**1 equiv), dry CH_2Cl_2 (0.5 M), dropwise addition of trifluoracetic anhydride (2.5 equiv) at 0 °C, 0 °C to rt, O/N. Crude used in the next step. *Step 2:* **3.23** (1 equiv), EtI (1.2 equiv), K_2CO_3 (2 equiv), acetone (0.25 M), reflux, 18 h. Crude used in the next step. *Step 3:* crude reaction mixture from step 2, grinded KOH (10 equiv), EtOH:H_2O = 4:1 (0.25 M), 70 °C, O/N. O/N = overnight. BRSM: Based on recovered stating material.

Urea formation proved problematic on a scale >10 g, affording the desired product in 45% yield, which is significantly lower than the 71% yield obtained for the 1 g scale reaction (Table 3.3). This was probably due to less efficient mixing on a larger scale, due to precipitation of a white thick solid caused by addition of Et_3N.

Table 3.3: Scale-up of the urea formation according to the one-pot-two-step protocol with *in situ* formation of the isocyanate from achiral aniline **3.17**.

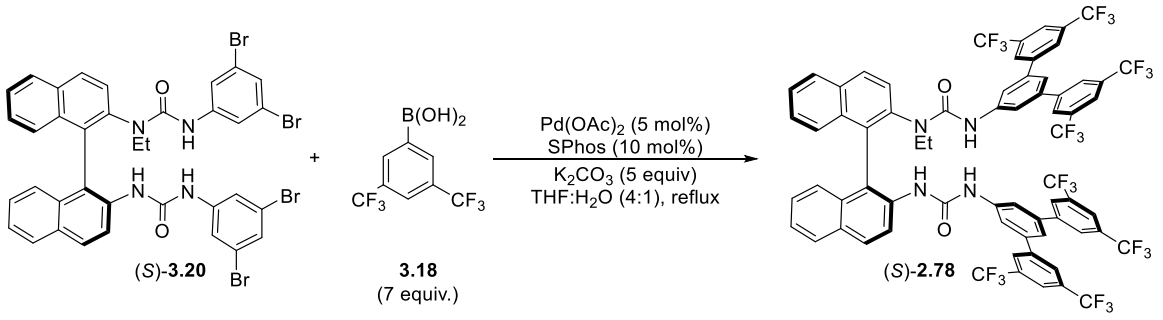


Entry	*Scale*	*Yield of isolated (S)-**3.20***
1	1.0 g (3.2 mmol)	71% (1.97 g)
2	10.6 g (34 mmol)	45% (13.3 g)

Reaction conditions: (i) triphosgene (0.7 equiv) in dry CH_2Cl_2 (0.1 M), dropwise addition of **3.17** (2 equiv), dropwise addition of dry Et_3N (4 equiv) at 0 °C in dry CH_2Cl_2 (0.1 M), 0 °C to rt, 2 h. (ii) (*S*)-**2.31** (1 equiv), rt, O/N. O/N = overnight

Finally, the quadruple palladium catalysed cross-coupling proceeded smoothly and was completed in 24 h (Table 3.4). The catalyst obtained after chromatographic purification on silica gel (14.6 g, 74% yield) was further purified by crystallisation achieved by layering heptane (17 mL/g) on a solution of (*S*)-**2.78** in $CHCl_3$ (8 mL/g) at rt, affording 10.1 g of pure (*S*)-**2.78** (69% recrystallisation yield). Due to the problematic urea formation step, this route was judged not suitable for scale-up.

Table 3.4: Scale-up of the quadruple Suzuki-Miyaura cross-coupling.

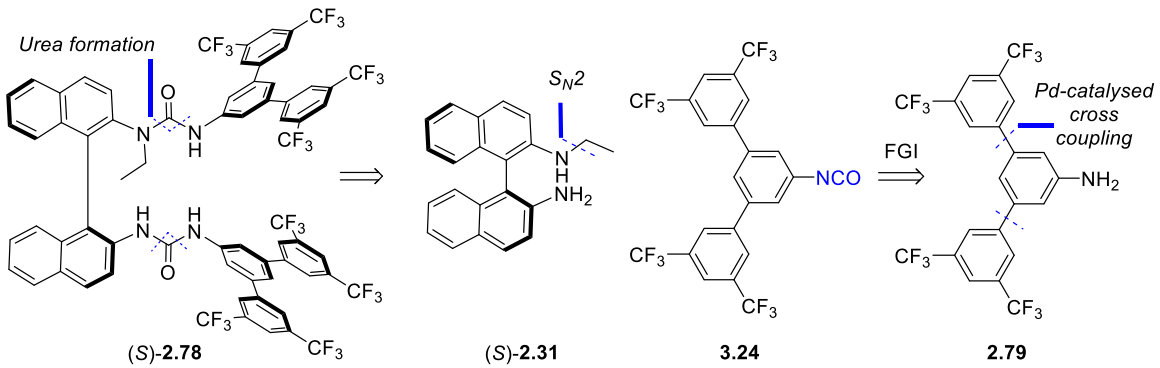


Entry	*Scale*	*Time*	*Yield of isolated (S)-**2.78***	*Comments*
1	100 mg (0.15 mmol)	72 h	63% (132 mg)	–
2	1 g (1.15 mmol)	48 h	81% (1.30 g)	–
2	1 g (1.15 mmol)	48 h	78% (1.25 g)	–
3	12.2 g (14.1 mmol)	24 h	51% (10.1 g)	Yield after recrystallisation. (**2.78** was isolated in ~75% yield)

Reaction conditions: (*S*)-**3.20** (1 equiv), **3.18** (7 equiv), $Pd(OAc)_2$ (5 mol%), SPhos (10 mol%), K_2CO_3 (5 equiv), degassed THF: degassed H_2O (4:1), reflux, 24–72 h. SPhos = 2-Dicyclohexylphosphino-2′,6′-dimethoxybiphenyl; FCC = Flash Column Chromatography.

3.3.5 Route 3: The Isocyanate Route

The third route proposed relies on the isolation of isocyanate **3.24**, to avoid formation of the side-products obtained when the isocyanate was generated *in situ* (section 3.3.1). The proposed route involves coupling of **3.24** with (*S*)-*N*-Et-BINAM **2.31** (Scheme 3.13), for which we already demonstrated the scalability starting from up to 40 g of (*S*)-BINAM (Table 3.2, section 3.3.4.3). Isocyanate **3.24** can be obtained from the corresponding aniline **2.79**, which can be synthesised from a commercial precursor *via* Pd-catalysed cross-coupling.

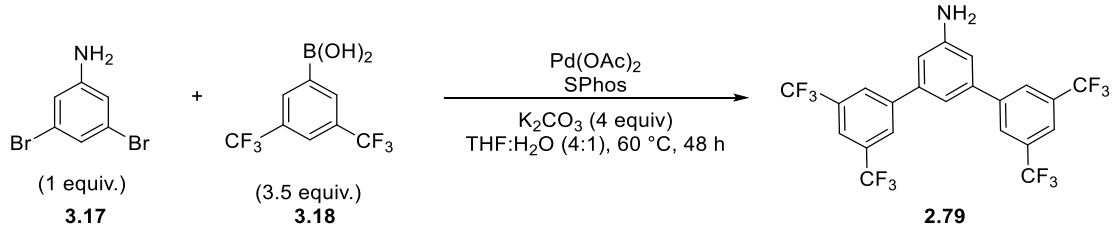


Scheme 3.13: Retrosynthetic analysis of the "isocyanate route" to access catalyst (*S*)-**2.78**.

3.3.5.1 Scale-up

First, we evaluated the possibility of reducing the catalyst loading in the Suzuki-Miyaura cross-coupling to access aniline **2.79** (Table 3.5, entries 1–3). The yield was unaffected despite a 10-fold reduction of transition metal (entry 3), thus these conditions (0.5 mol% of $Pd(OAc)_2$ and 1 mol% of 2-dicyclohexylphosphino-2′,6′-dimethoxybiphenyl, SPhos) were selected for the scale up of the coupling on 30 g of 3,5-bromoaniline (entry 5). At lower catalyst loadings, a short silica plug was sufficient to remove the metal and ligands from the product and **2.79** was used in the subsequent step without any further purifications.

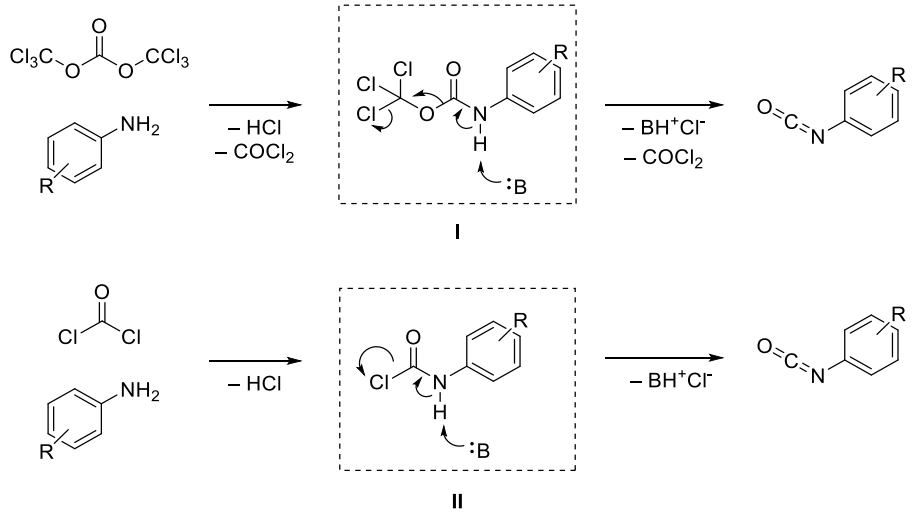
Table 3.5: Effect of catalyst loading in the Suzuki-Miyaura cross-coupling to access aniline **2.79**



Entry	*Mass of **3.17***	*$Pd(OAc)_2$ (mol%)*	*SPhos (mol %)*	*Yield of isolated **2.79***
1	1 g (3.98 mmol)	5	10	81% (1.67 g)
2	1 g (3.98 mmol)	1	2	91% (1.88 g)
3	1 g (3.98 mmol)	0.5	1	81% (1.66 g)
4	5 g (19.9 mmol)	0.5	1	90% (10.0 g)
5	30 g (119.6 mmol)	0.5	1	86% (53.1 g)

Reaction conditions: **3.17** (1 equiv), **3.18** (3.5 equiv), $Pd(OAc)_2$, SPhos, K_2CO_3 (4 equiv), degassed THF: degassed H_2O (4:1), reflux, 48 h. SPhos= 2-dicyclohexylphosphino-2′,6′-dimethoxybiphenyl.

Synthesis of the isocyanate was achieved reacting the corresponding aniline with triphosgene in the presence of a base. Triphosgene owes is name to the fact that it is synthetically equivalent to three molecules of phosgene (Scheme 3.14) and is a popular alternative to phosgene on scales up to pilot plant because it is an easy-to-handle solid.[12] Nevertheless, it is highly toxic, and the same precautions adopted when manipulating phosgene must be followed.[12,13]



Scheme 3.14: Synthesis of isocyanates using triphosgene. A first equivalent of phosgene is generated upon addition of the aniline to the carbonate with formation of intermediate **I**. Loss of HCl from **I** releases a second equivalent of phosgene and generates the desired isocyanate, consuming the third equivalent of phosgene.

To avoid excessive manipulation of isocyanate **3.24**, its synthesis was conducted reacting aniline **2.79** with triphosgene under Schotten-Baumann conditions (Figure 3.9, top). These involve the use of a biphasic system consisting of an organic solvent and an aqueous basic solution to neutralise the HCl formed in the reaction. Phase separation at the end of the reaction allows for easy recovery of the product. The procedure was first tested on 250 mg of aniline **2.79**, monitoring the reaction progression *via* ^{1}H NMR (Figure 3.9, bottom). After 30 min, the ^{1}H NMR spectrum revealed the presence of a single species whose signals differs from those of the starting aniline. Its identity as the desired isocyanate was confirmed by IR (intense band at 2298 cm^{-1}, characteristic of the C=O stretching vibration of an isocyanate), ^{13}C NMR (quaternary carbon at 125.5 ppm in $CDCl_3$) and HRMS (APCI$^-$ *m/z* calculated for $C_{23}H_8ONF_{12}$ $(M–H)^-$ 542.0420, found 542.0207).

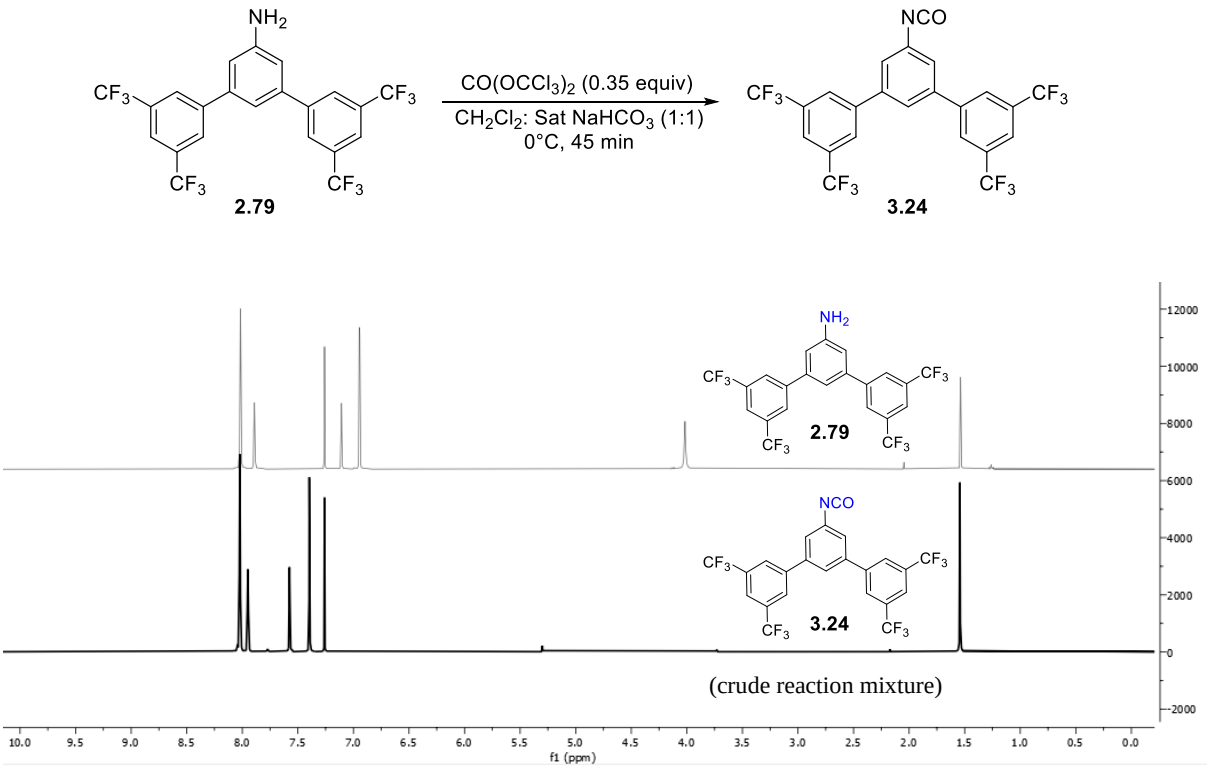
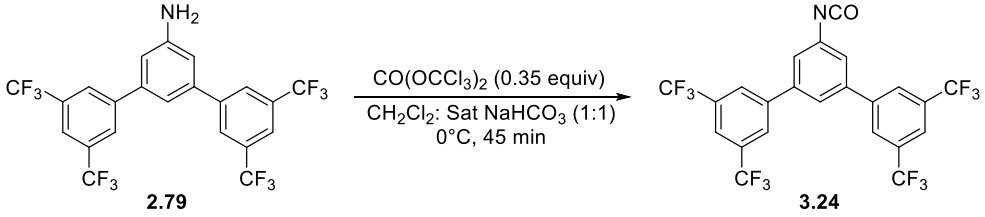


Figure 3.9: Top: Synthesis of isocyanate **3.24**. Bottom: Reaction monitoring *via* ^{1}H NMR. The spectrum of the starting material (aniline **2.79**) is showed in grey, the spectrum of the crude reaction mixture at the end of the reaction is showed in black.

The reaction was scaled up to 2.5 g, 25 g and 54 g, consistently obtaining >80% yield of crude product (Table 3.6). Direct use of the crude isocyanate in the urea formation gave rise to reproducibility issues, which were solved by recrystallising the reagent from hot hexane (20 mL/g) and THF (0.75 mL/g), (67% recrystallisation yield). The yield could be increased recrystallising the mother liquor a second time from the same solvent mixture (hexane 20 mL/g, THF 0.5 mL/g, 52% recrystallisation yield).

Table 3.6: Optimisation of the Isocyanate synthesis



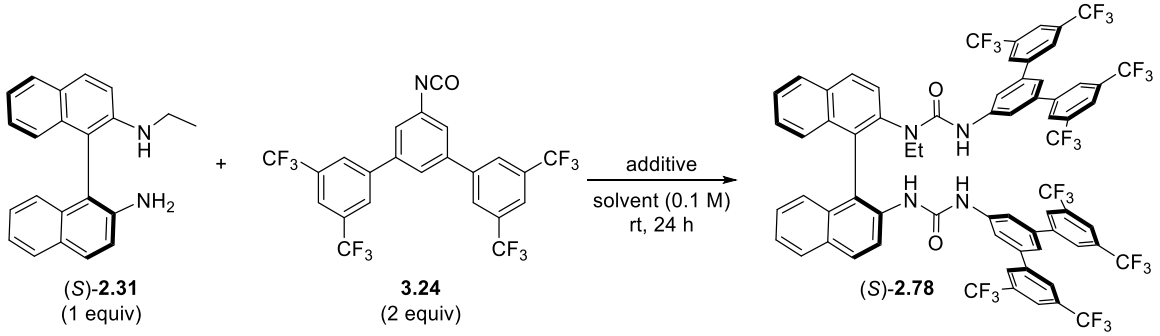
Entry	*Scale*	*Yield (crude)*[a]
1	250 mg (0.48 mmol)	60% (156 mg)
2	2.5 g (4.83 mmol)	80% (2.1 g)
3	25 g (48.3 mmol)	87% (22.8 g)
4	25 g (48.3 mmol)	88% (23.1 g)
5	54 g (104.4 mmol)	84% (47.6 g)

Reaction conditions: 2.79 (1 equiv), triphosgene (0.45 equiv), CH_2Cl_2/Sat $NaHCO_{3\,(aq)}$ (1:1), 0 °C, 45 min. [a] Batches from entries 3–5 were combined and recrystallised together (67% recrystallisation yield. The yield of the recrystallisation could be enhanced to 84% if the product remaining in the mother liquor was recrystallised a second time).

Finally, we evaluated the optimal coupling conditions for urea formation. Using the conditions previously employed with commercial isocyanates (2 equiv of recrystallised isocyanate **3.24**, 1 equiv of (*S*)-*N*-Et-BINAM **2.31**, 0.1 M in anhydrous CH_2Cl_2 at rt), the target compound (*S*)-**2.78** was obtained in 75% ^{19}F NMR yield with no formation of side product **3.14** (entry 1, Table 3.7). Addition of powdered 3 Å molecular sieves further improved the yield (83%, entry 2). Interestingly, the reaction conducted in the presence of 2 equiv of Et_3N (entry 3) was low yielding (17%) and showed a significant (~20%) presence of undesired **3.14** (judged by the signal at 11.93 ppm in the ^1H NMR spectrum and estimated by quantitative ^{19}F NMR). This was the only case among those screened in which

3.14 was detected, suggesting that Et_3N, which is also used in the one-pot-two-step protocol for the *in situ* formation of the isocyanates, might be involved in its formation. Addition of 0.5 equiv of DMAP was also detrimental, affording the target bis-urea in 56% yield (entry 4) due to side-reactions. A complex mixture of products was obtained, none of which was **3.14**. On the contrary, pyridine had no adverse effect on the reaction in CH_2Cl_2 (82%, entry 5) and greatly improved the yield of the reaction in THF (83% *versus* 50%, entries 6–7).

Table 3.7: Optimisation of the urea formation reaction between aniline (*S*)-**2.31** and isocyanate **3.24**



Entry	*(S)-**2.31***	*Solvent*	*Additive*	*Yield*[a]
1	100 mg	CH_2Cl_2	–	75%
2	100 mg	CH_2Cl_2	3 Å MS (powdered)	83%
3	100 mg	CH_2Cl_2	2 equiv Et_3N	17%
4	100 mg	CH_2Cl_2	0.5 equiv DMAP/ 3 Å MS (powdered)	56%
5	100 mg	CH_2Cl_2/pyridine 5:1	3 Å MS (powdered)	82%
6	100 mg	THF	3 Å MS (powdered)	50%
7	100 mg	THF/pyridine 5:1	3 Å MS (powdered)	83%
8	1g	CH_2Cl_2	3 Å MS (powdered)	84% (75%)
9	1g	THF/pyridine 5:1	3 Å MS (powdered)	82% (80%)

[a] Yields determined by ^{19}F NMR using hexafluorobenzene as internal standard, isolated yields in parenthesis.

The two highest yielding reactions (CH_2Cl_2, entry 2, Table 3.7; THF/pyridine =5:1, entry 5) were scaled up to 1 g, obtaining comparable yields (84%, entry 8 *versus* 82%, entry 9). Nevertheless, the reaction in THF/pyridine was judged cleaner by HPLC and ^{19}F NMR analysis of the crude mixture (Figure 3.10) which in turn resulted in more facile purification *via* column chromatography (in case of entry 8 some mixed fractions were discarded).

Moreover, the solid obtained after the work up was more crystalline, which led to the selection of these conditions for the scale up, for which we wanted to avoid chromatographic purification. The scale-up was conducted on 13 g of (*S*)-*N*-Et-BINAM **2.31** and afforded 57.9 g of crude (*S*)-**2.78** as an off-white solid (94% purity based on quantitative ^{19}F NMR).

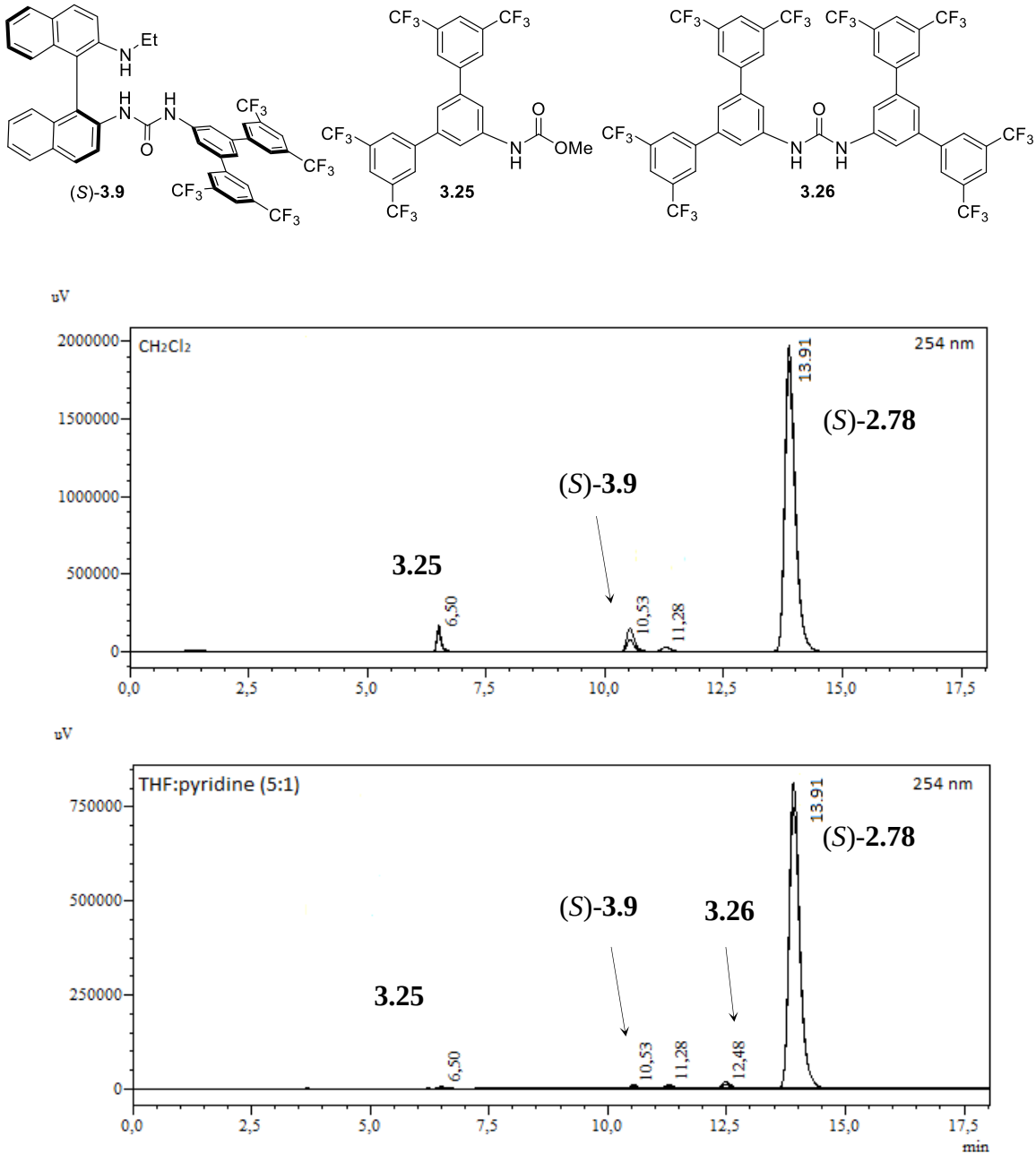
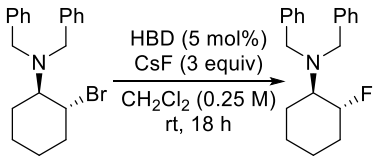


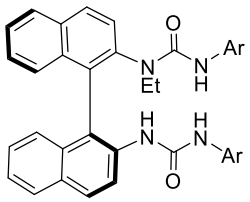
Figure 3.10: HPLC of the crude urea formation step in CH_2Cl_2 (top) and THF/piridine (bottom). **HPLC conditions:** Luna C-18, H_2O:Acetonitrile = 15:85 to 2:98 over 3 min, then hold at 2:98 for 15 min.

The main impurities formed in the reaction were intermediate mono-urea **3.9** (Figure 3.10), and carbamate **3.25** obtained by quenching unreacted isocyanate with methanol at the end of the reaction. Additionally, if the reaction is not conducted in strictly anhydrous conditions, achiral urea **3.26** could be formed. Impurities **3.9**, **3.25**–**3.26** were tested in the fluorination with CsF of *rac*-**2.108**, the model substrate selected for the scale-up of HB-PTC with alkali metal fluorides reported in Chapter 4. The same conditions employed in the screening reactions with chiral catalysts were evaluated (HBD loading: 5 mol%, CsF: 3 equiv, CH_2Cl_2: 0.25 M, rt, 18 h), to allow direct comparison between the impurities and the chiral bis-urea (*S*)-**2.78** (Table 3.8). All impurities were active as phase-transfer catalysts, affording β-fluoroamine **2.109** in 20–58% yield. As they might result in competitive fluorination affording **2.109** in low e.r., their removal was deemed necessary.

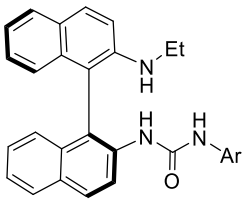
Table 3.8: Reactivity in the fluorination of *rac*-**2.108** of the impurities generated in the final step of the synthesis of bis-urea (*S*)-**2.78** compared to the chiral bis-urea.



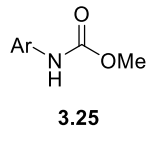
rac-**2.108** (0.05 mmol) **2.109**



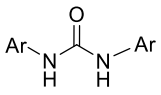
(*S*)-**2.78**



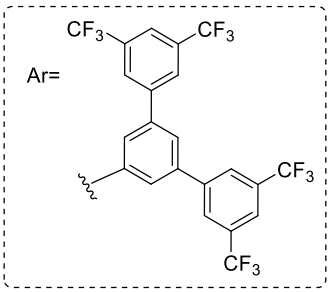
(*S*)-**3.9**



3.25



3.26

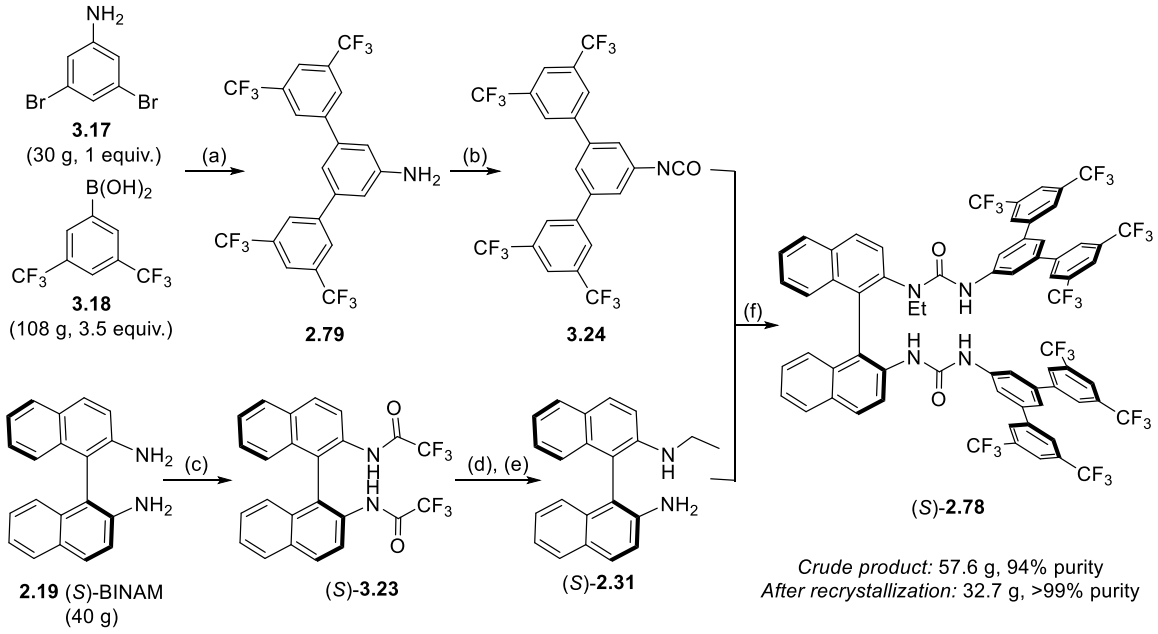


Entry	*HBD*	*Yield*[a]	*e.r.*[b]
1	–	No reaction	–
2	(*S*)-**2.78**	>95%	84:16
3	(*S*)-**3.9**	58%	55:45
4	**3.25**	20%	–
5	**3.26**	33%	–

Reaction conditions: *rac*-**2.108** (0.05 mmol), HBD (5 mol%), CH_2Cl_2 (0.25 M) rt, stirring at 900 rpm for 18 h. [a]Yield determined by ^{19}F NMR using 4-fluoroanisole as internal standard. [b] e.r. determined by HPLC using a chiral non-racemic stationary phase.

Various solvents were considered for recrystallisation (see Chapter 5, Tables 5.6) which ultimately led to the selection of a mixture of heptane and EtOH. 42.02 g of (*S*)-**2.78** (98% pure from quantitative ^{19}F NMR) were obtained recrystallising the crude product from hot heptane (5 mL/g) and EtOH (6 mL/g). Further 9.93 g of comparable purity were recovered from the mother liquor through a second recrystallisation (hot heptane 5 mL/g, EtOH 15 mL/g). The two fractions were combined and recrystallised a second time from hot heptane (5 mL/g) and EtOH (1 mL/g) to further improve the purity (32.7 g, 56% yield, >99% purity, assessed by quantitative ^{19}F NMR).

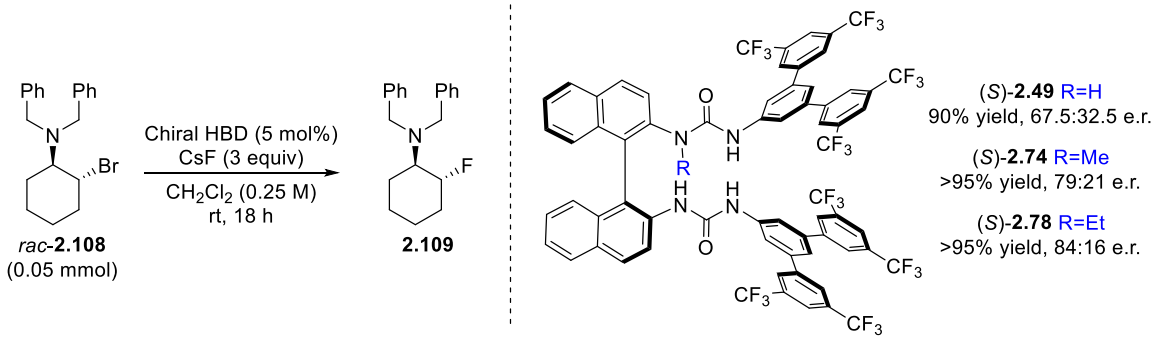
Scheme 3.15 reports an overview of the convergent route employed in the scale-up of catalyst (*S*)-**2.78**. This started with a Suzuki-Miyaura cross-coupling of commercially available 3,5-dibromoaniline **3.17** and 3,5-bis(trifluoromethyl)phenyl boronic acid **3.18** to afford aniline **2.79** in 86% yield. The aniline was subsequently converted into the corresponding isocyanate **3.24** under Schotten-Baumann conditions (71% yield, after recrystallisation). Coupling of isocyanate **3.24** with (*S*)-*N*-Et-BINAM **2.31**, obtained in a three-step protection-alkylation-deprotection sequence (60% over three steps), afforded the desired bis-urea organocatalyst in 56% yield and >99% purity after two crystallisations. The low yield of the final urea-coupling step (56% *versus* 80% for the 1 g reaction) is due to losses in the crystallisation, and the yield might be increased purifying the catalyst remained in the mother liquor by column chromatography over silica gel. The "isocyanate route" thus represent a convenient synthesis to access (*S*)-**2.78** both on small (50% overall yield from 0.91 g of (*S*)-BINAM) and large scale (34% overall yield from 40 g of (*S*)-BINAM).



Scheme 3.15: Synthesis of (*S*)-**2.78**. Reaction conditions: (a) $Pd(OAc)_2$ (0.5 mol%), SPhos (1 mol%), K_2CO_3 (4 equiv), degassed THF: H_2O (4:1, 0.2 M), 60 °C, 48 h. 86% yield; (b) triphosgene (0.35 equiv), CH_2Cl_2: aqueous $NaHCO_{3\ (sat)}$ (1:1), 0 °C, 45 min. 71% yield; (c) trifluoroacetic anhydride (2.5 equiv), anhydrous CH_2Cl_2 (0.5 M), 0 °C to rt, overnight; (d) EtI (1.2 equiv), K_2CO_3 (2 equiv), acetone (0.25 M), reflux, 18 h; (e) aqueous KOH (65% wt/v): EtOH (1:4, 0.25 M), 70 °C, overnight. 60% yield over three steps; (f) powdered 3 Å MS, anhydrous THF:pyridine (5:1, 0.12 M), rt, 36 h. 56% yield.

3.3.5.2 Library Generation

We had previously noted (section 2.8.1) that increasing the size of the *N*-alkyl chain of bis-ureas bearing the terphenyl unit improved the enantiocontrol in the fluorination of *rac*-**2.108** (Scheme 3.16). For this reason, we were interested in evaluating the effect of bulkier *N*-substituents.



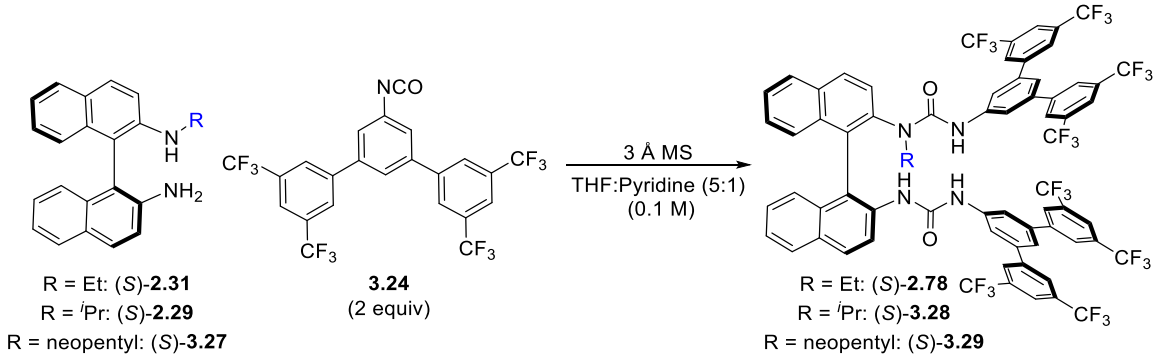
Scheme 3.16: Effect of *N*-substitution in the enantioselective fluorination of *rac*-**2.108** with CsF. Scheme from Chapter 2, section 2.8.1.

Catalyst with *N*-substituents bulkier than R=Me were not accessible using the one-pot-two-step protocol involving *in situ* generation of the isocyanate, due to formation of side-

products (section 3.3.1). Moreover, the first route developed to access (*S*)-**2.78** (section 3.3.3) was inadequate for their synthesis, because the *N*-alkyl substituent was introduced on the urea by S_N2 substitution, limiting R to primary, unbranched alkyl chains. On the contrary, in principle any *N*-alkyl BINAM-derived bis-aniline was a suitable partner for the urea formation according to the "isocyanate route". This opened the possibility to install branched alkyl chains *via* reductive amination prior to the urea formation step.

We subjected anilines (*S*)-**2.29** (R = ^{i}Pr) and (*S*)-**3.27** (R = neopentyl), obtained by reductive amination, to the optimised urea formation conditions (isocyanate **3.24**: 2 equiv, powdered 3 Å MS, anhydrous THF:pyridine (5:1)). Increasing the steric bulk of the R substituent led to diminished yields of the desired bis-urea (Table 3.9). In the case of aniline (*S*)-**2.29**, bearing an isopropyl chain, synthetically useful yields of bis-urea (*S*)-**3.28** could be obtained by prolonged reaction time (72 h, 45% yield, entry 2), while neopentyl-substituted (*S*)-**3.27** did not afford the desired product (*S*)-**3.30**, even at high temperature (up to 70 °C). Analysis of the crude reaction mixture by ^{1}H NMR and TLC showed the presence only of unreacted starting material and intermediate mono-urea.

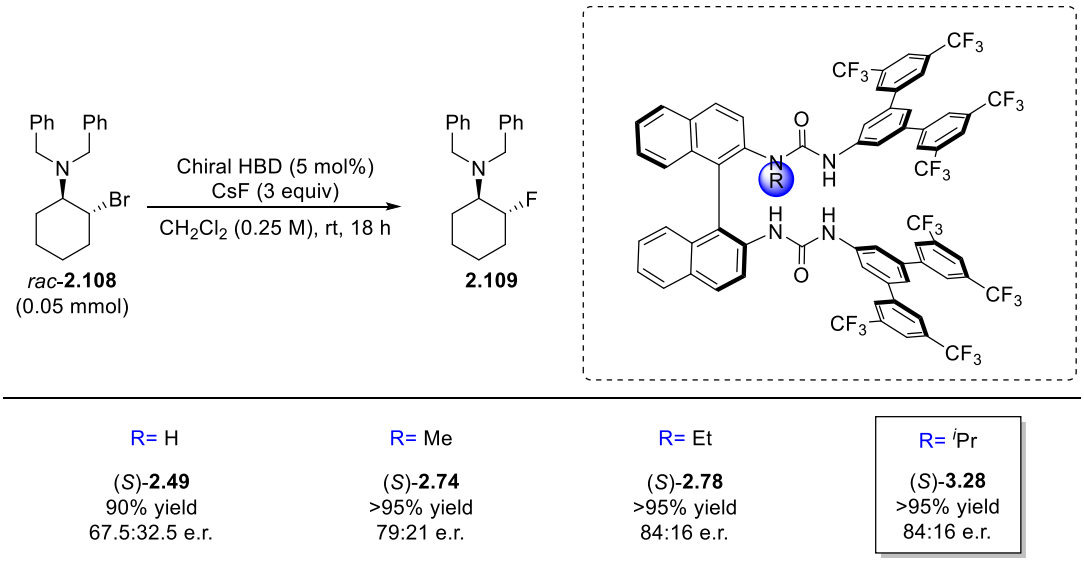
Table 3.9: The isocyanate route applied to the synthesis of *N*-alkyl bis-urea with various R substituents



Entry	*R*	*Temperature*	*Time (h)*	*Isolated yield of bis-urea*
1[a]	Et	rt	24	80%
2	^{i}Pr	rt	72	45%
3	neopentyl	rt to 70 °C	72	Not formed

Reaction conditions: Chiral aniline (100 mg, 1 equiv), **3.24** (2 equiv), powdered 3 Å MS, anhydrous THF:pyridine = 5:1 (0.1 M). Yields are isolated yields. [a] reaction on 1 g.

N-isopropyl bis-urea (*S*)-**3.28** was tested in the enantioselective fluorination of *rac*-**2.108** (Scheme 3.17) and compared with the performance of the catalysts previously synthesised bearing the polyfluorinated terphenyl units. All catalysts have similar reactivity (>90% yield) but differ in term of selectivity. Methylation ((*S*)-**2.74**) furnished a substantially more enantioselective catalyst compared to the non-alkylated analogue (*S*)-**2.49** (79:21 *versus* 67.5:32.5 e.r.). The trend was retained increasing the chain length to an ethyl group ((*S*)-**2.78**, 84:16 e.r), however no further gain in enantioselectivity was obtained introducing the more sterically demanding isopropyl ((*S*)-**3.28** 84:16 e.r).



Scheme 3.17: Effect of bis-urea *N*-alkylation in combination with the polyfluorinated terphenyl units on the enantioselective fluorination of *rac*-**2.108** with CsF.

3.4 Conclusions

The scale-up of the synthesis of *N*-alkyl bis-ureas (*S*)-**2.3** and (*S*)-**2.78** to >10 g was reported in this chapter. The published route to bis-urea (*S*)-**2.3** required only minor adaptations, affording 14.0 g of catalyst in 48% overall yield from (*S*)-BINAM (Figure 3.11A). On the contrary, several routes were explored for the synthesis of (*S*)-**2.78**, leading to the selection of a synthesis based on isolation of the isocyanate. This route afforded 32.7 g of (*S*)-**2.78** in 34% overall yield from 40 g of (*S*)-BINAM (Figure 3.11B). This catalyst was used in the scale-up studies described in Chapter 4.

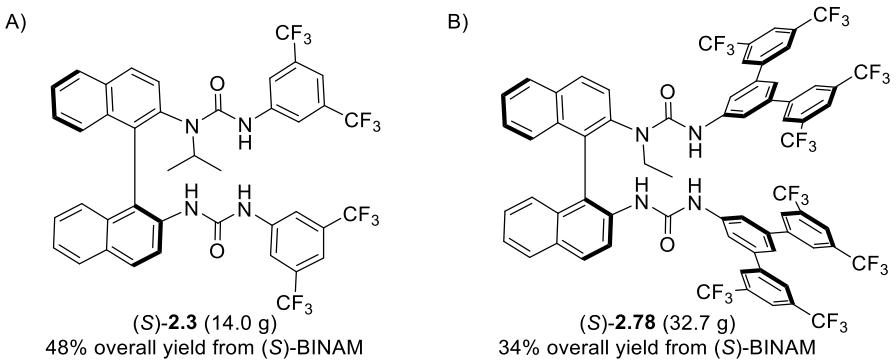
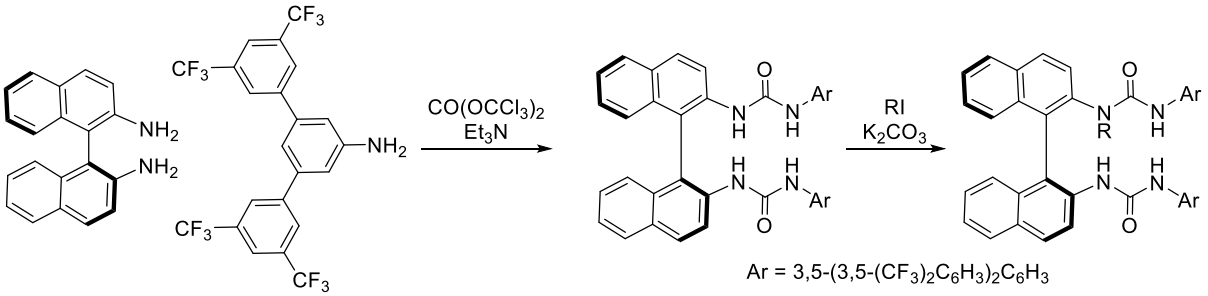


Figure 3.11: Scale-up of catalyst (*S*)-**2.3** and (*S*)-**2.78**.

A comparison of the routes investigated for the synthesis of (*S*)-**2.78** is reported in Scheme 3.18. *Route 1* (Scheme 3.18A) was based on urea formation followed by alkylation and afforded (*S*)-**2.78** in 37% overall yield from 1.2 g of (*S*)-BINAM.[2] This route is the shortest (3 steps LLS, or 2 step from (*S*)-BINAM) and does not require any protection. Its main disadvantage is the difficult purification of the final catalyst, which makes it unsuitable for scale-up. Moreover, the synthesis is not well-suited for the rapid generation of analogues with different substituents on the terphenyl rings and does not give access to bis-ureas bearing branched *N*-alkyl chains.

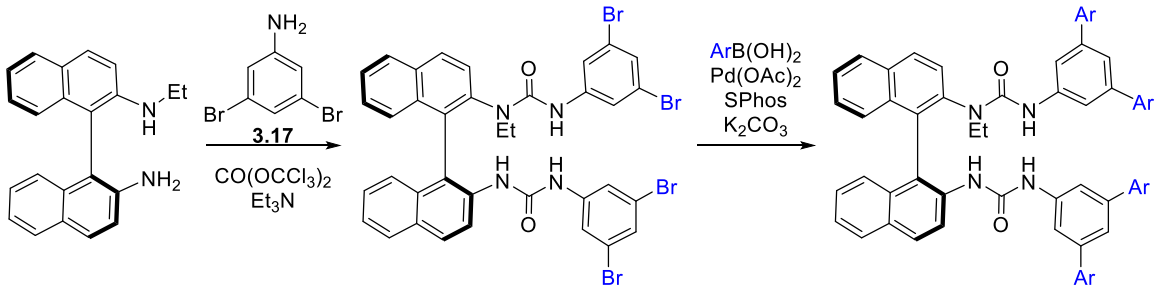
A) Route 1 (*published route, ref. 2*)



2.19 (*S*)-BINAM (1.2 g) | **2.79** (2 equiv) | (*S*)-**2.49** (73%) | (*S*)-**2.78** R=Et (2.1 g, 51%)

- √ 2 steps from (*S*)-BINAM, linear
- √ 37% overall yield from (*S*)-BINAM
- X Not scalable
- X Limited to *N*-alkyl chain introduced by S_N2 substitution with RI
- √ No protection required
- X Lack of modularity in the terphenyl synthesis

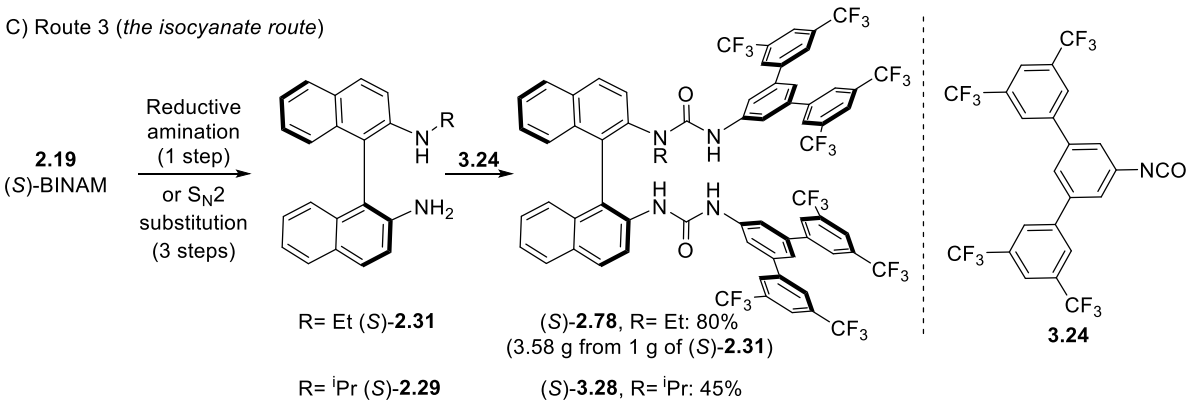
B) Route 2 (*the quadruple Suzuki-Miyaura cross-coupling route*)



(*S*)-**2.31** 62% over 3 steps from (*S*)-BINAM | (*S*)-**3.20** (71%) | (*S*)-**2.78** Ar = 3,5-$(CF_3)_2C_6H_3$ 78% (1.25 g from 1 g of (*S*)-**3.20**)

- X 5 steps from (*S*)-BINAM, linear
- √ 34% overall yield from (*S*)-BINAM
- X Not scalable
- √ Potentially applicable to *N*-alkyl chains installed by reductive aminatio
- X Requires BINAM protection
- √ Modular for the terphenyl synthesis

C) Route 3 (*the isocyanate route*)



R= Et (*S*)-**2.31** | (*S*)-**2.78**, R= Et: 80% (3.58 g from 1 g of (*S*)-**2.31**) | **3.24**

R= ^{i}Pr (*S*)-**2.29** | (*S*)-**3.28**, R= ^{i}Pr: 45%

- √ 4 steps from (*S*)-BINAM, **convergent**
- √ 50% overall yield from 0.91 g of (*S*)-BINAM
  34% overall yield from 40 g of (*S*)-BINAM
- √ **Scalable** (up to >30 g of (*S*)-**2.78**)
- √ Applicable to *N*-alkyl chains installed by S_N2 or reductive amination
- X Requires BINAM protection for R=Me, Et
- X Lack of modularity

Scheme 3.18: Alternative synthetic routes to bis-urea (*S*)-**2.78** comparing their advantages and disadvantages.

Route 2, the "quadruple Suzuki-Miyaura cross-coupling route" (Scheme 3.18B), is based on a linear synthesis involving (*S*)-BINAM alkylation, urea formation and a quadruple Pd-catalysed cross coupling (5 steps). Despite the increased length, including two extra-steps for protection/deprotection of the aniline functionalities, it afforded (*S*)-**2.78** in similar yield than *route 1* (34% overall yield from (*S*)-BINAM *versus* 37%). This route is the most indicated for library generation, allowing to differentiate the terphenyl unit in the last synthetic step. This synthesis is not reliable on scale, thus is not indicated for scale-up.

Route 3, the "isocyanate route" (Scheme 3.18C), is a convergent route in which (*S*)-*N*-alkyl BINAM and purified isocyanate, synthesised from the corresponding aniline, are coupled together in the final step of the synthesis. The desired bis-urea (*S*)-**2.78** is the only product of the final step, which greatly simplify its purification. The protocol can be readily scaled up affording 32.7 g of (*S*)-**2.78** (34% overall yield). Importantly, recrystalised isocyanate must be used in the urea formation reaction, which might make this synthesis unpractical on a small scale. This route allows to access *N*-alkyl bis-urea bearing substituents that can be installed *via* reductive amination, although yields are reduced in the presence of bulkier substituents. Catalyst (*S*)-**3.28** (R= ^{i}Pr), previously inaccessible, was obtained in 45% yield according to this route.

Routes 2 and *3* enabled the preparation of new catalysts, which were tested in the enantioselective fluorination of *rac*-**2.108**, the model substrate used in the scale-up studies reported in Chapter 4. None of them gave better enantioselectivities that (*S*)-**2.78**. The enantiomeric ratio of 85.5:14.5 for β-fluoroamine **2.109** obtained in the presence of (*S*)-**2.78** in $PhCF_3$ thus remains the highest level of enantioselectivity achieved in the fluorination of aliphatic aziridinium ions.

3.5 References

(1) Pupo, G.; Ibba, F.; Ascough, D. M. H.; Vicini, A. C.; Ricci, P.; Christensen, K. E.; Pfeifer, L.; Morphy, J. R.; Brown, J. M.; Paton, R. S.; Gouverneur, V. "Asymmetric Nucleophilic Fluorination under Hydrogen Bonding Phase-Transfer Catalysis." *Science* **2018**, *360*, 638–642.

(2) Pupo, G.; Vicini, A. C.; Ascough, D. M. H.; Ibba, F.; Christensen, K. E.; Thompson, A. L.; Brown, J. M.; Paton, R. S.; Gouverneur, V. "Hydrogen Bonding Phase-Transfer Catalysis with Potassium Fluoride: Enantioselective Synthesis of β-Fluoroamines." *J. Am. Chem. Soc.* **2019**, *141*, 2878–2883.

(3) Roagna, G.; Ascough, D. M. H.; Ibba, F.; Vicini, A. C.; Christensen, K. E.; Peschiulli, A.; Oehlrich, D.; Misale, A.; Trabanco, A. A.; Paton, R. S.; Pupo, G.; Gouverneur, V. "Hydrogen Bonding Phase-Transfer Catalysis with Ionic Reactants : Enantioselective Synthesis of γ-Fluoroamines." *J. Am. Chem. Soc.* **2020**, *142*, 14045–14051.

(4) Kim, K. H.; Lee, D.; Lee, Y.; Ko, D.; Ha, D. "Enantioselective Oxidative Coupling of Methyl 3-Hydroxy-2-Naphthoate Using Mono-*N*-Alkylated Octahydrobinaphthyl-2,2'-Diamine Ligand." *Tetrahedron* **2004**, *60*, 9037–9042.

(5) Ibba F.; Pupo, G.; Thompson, A. L.; .; Brown, J. M.; Claridge, T. D. W.; Gouverneur, V. "Impact of Multiple Hydrogen Bonds with Fluoride on Catalysis: Insight from NMR Spectroscopy", *J. Am. Chem. Soc*. **2020**, *142*, 19731–19744.

(6) Habib, N. S.; Rieker, A. "A Convenient Method for the Synthesis of Sterically Hindered Aryl Isocyanates." *Zeitschrift fur Naturforsch. - Sect. B J. Chem. Sci.* **1984**, *39*, 1593–1597.

(7) Wagner, K. "Niedermolekulare Polyisocyanate Mit Biuret-Struktur." *Angew. Chemie* **1962**, *74*, 799–801.

(8) Mumm, O. "Umsetzung von Säureimidchloriden Mit Salzen Organischer Säuren Und Mit Cyankalium." *Ber. Dtsch. Chem.Ges.* **1910**, *43*, 886–893.

(9) Curtin, D. Y.; Miller L. L. "The isolation and rearrangement of simple isoimides (iminoanhydrides)" *Tetrahedron Letters*, **1965**, *6*, 1869–1876.

(10) Schwarz, J. S. P. "Preparation of acyclic isoimides and their rearrangement rates to imides" *J. Org. Chem.* **1972**, *37*, 2906–2908.

(11) Claridge, T. D. W. *High-Resolution NMR Techniques in Organic Chemistry*, 3rd ed.; Elsevier Ltd., 2016.

(12) Cotarca, L.; Geller, T.; Répási, J. "Bis(Trichloromethyl)Carbonate (BTC, Triphosgene): A Safer Alternative to Phosgene?" *Org. Process Res. Dev.* **2017**, *21*, 1439–1436.

(13) Publich Health England. "Phosgene." *Compend. Chem. Hazard* **2019**.

Intentionally left blank

Chapter 4:

Scale-up of Enantioselective Fluorination under HB-PTC in a Mechanically Stirred 1 L Glass Reactor

4.1 Mixing in Industrial Reactors

Reactions on a laboratory scale are generally performed in round bottom flasks (RBF) equipped with a magnetic stirring bar, which provides the required mixing by spinning under the influence of a rotating magnetic field. In heterogeneous systems where a solid is present, rotation of the stirring bar on the bottom of the flask might contribute to grinding the solid particles. A vortex might occasionally be formed at high stirring speeds. This flow pattern does not provide good radial and vertical mixing, but due to the small volumes involved ($\leq$ 1 L) mass and heat transfer are rarely a major issue at this scale.[1]

The industrial equivalent of RBFs are batch reactors, closed systems in which all reagents are charged at the beginning of the reaction and the product(s) removed at the end, and semi-batch reactors, in which some reagents are added during the course of the reaction to the stirred reaction mass. The reaction vessel are cylindrical tanks and mixing is achieved by mechanical stirring. The lower surface area to volume ratio reduces heat transfer compared to RBFs, thus detailed studies must be undertaken to evaluate the thermal safety of a process prior to scale-up to more than 5 L (section 4.2). The flow pattern is also significantly different, and this might affect the outcome of the reaction. Models have been developed to predict the effect of mixing in a stirred tank upon scale-up based on dimensional analysis and the principle of geometrical similarity.[2] Due to the challenges involved and the importance of mixing operations in many industrial sectors, development of reliable models is still an area of intense research.

The Reynolds number (*Re*) provides a mean to predict the flow regime within a moving fluid. The Reynolds number is a dimensionless quantity defined as the ratio of inertial to viscous forces within a moving fluid characterised by different internal velocities.[3] At low Reynolds number, viscous forces prevail and the fluid moves in parallel layers each characterised by its own velocity (laminar flow). In these conditions mixing between

different layers is limited. At high Reynolds number, the fluid moves in a chaotic manner, with frequent changes of pressure and direction which favour mixing (turbulent flow). Swirling of the fluid with formation of eddies —a circular movement of the fluid— moving in the opposite direction to the overall flow dissipates the kinetic energy transferred to the fluid by the agitator rotation. Highly turbulent regimes are thus characterised by high dissipation energy rates. Generally, as the scale of the vessel increases, the fluid regime becomes more turbulent.[4]

Mixing problems can arise at different scales (macro, meso, or micromixing).[5] Macromixing is mixing of the bulk reaction mass, which can be quantified by evaluating the time necessary for a small volume of fluid to complete a full cycle of the reactor. The mixing time increases with the scale of the vessel and might become the limiting step for very fast reactions. Typical macromixing problems are related to homogenisation of the reaction mixture. Mesomixing refers to the turbulent dispersion of added regents in a semi-batch process. Poor mixing at the meso scale will result in reagents accumulation, which might give rise to side reactions. Solutions to this problem include reducing the feed rate, moving the feed point closer to the impeller region, varying the diameter of the feed pipe, or using multiple feed points. Micromixing is turbulent mixing at the molecular level.

The density, particle size distribution, and shape of a solid reagent/catalyst are important parameters to consider when optimising the mixing of a heterogeneous system.[6] To achieve stable suspension, both a strong circulation (macromixing) and an adequate level of turbulence (micromixing) are required. Full suspension is necessary to maximise mass transfer because it ensures that the whole surface area of the particles is available. Usually it is not necessary, and sometimes not possible, to reach homogeneous conditions of suspension. The agitator rotational speed (N) at which no particle resides on the bottom of the tank for more than 1 s is defined as the “speed of just suspension” (N_{js}).[7] This ensures

the optimal combination of mass transfer and power required by the agitator. Further increasing N results in only minimal improvement of the mass transfer, due to increased turbulence, but the power required to rotate the impeller increases with the cube of N.[4] On the micro scale, increase in turbulence causes the reduction of the thickness of the film of fluid surrounding the solid particles, thus enhancing mass transfer.[6]

The choice of the impeller is extremely important to achieve the desired circulation patterns and turbulence.[4] Impellers can be divided into radial and axial types according to the flow pattern that they create inside the reaction vessel. An example of a radial impeller is the Rushton turbine (Figure 4.1A). The vertical blades of the Rushton turbine pump the fluid in a radial direction towards the reactor walls, thus creating two separate circulating loops above and below the impeller. These types of impellers are commonly used for gas-liquid reactions where they provide high levels of dispersion of the gas. Axial impellers usually have pitched blades and depending on the direction of rotation can pump the fluid downwards (down-pumping) or upwards (up-pumping). The first configuration is the most common and results in the creation of a single loop (Figure 4.1B). The hydrofoil is a typical example of axial impeller. The 45° down-pumping pitched blade turbine (PTB, Figure 4.1C) produces a pattern in between the axial and radial, and it is defined as a mixed impeller. Together with the hydrofoil it is a common choice for the suspension of solids.

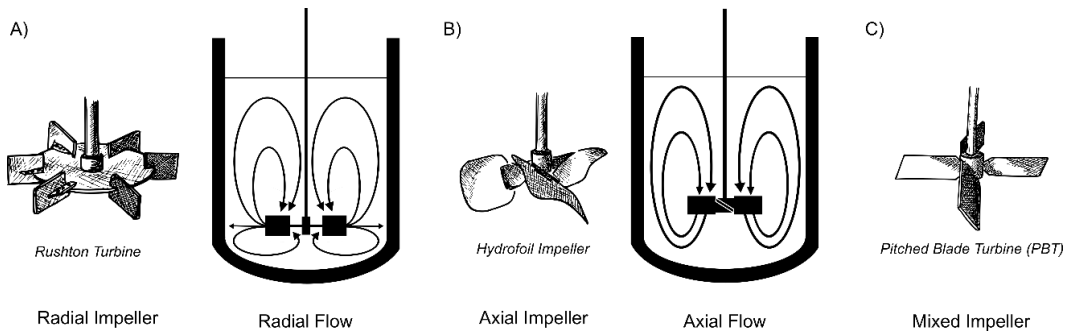


Figure 4.1: Typical impellers used in industrial reactors, classified by type of flow pattern induced in the vessel. A) An example of a radial impeller and its associated flow. B) An example of an axial impeller and its associated flow. C) Pitched blade turbine, a mixed impeller.

Impellers are characterised by the power number (P_0), a dimensionless number that quantifies the power that a specific impeller can transmit to the fluid. The power number is a function of the impeller type and location in the vessel, as well as the Reynolds number. In the laminar regime the power number and Reynolds number are inversely proportional, while the power number is constant in the turbulent regime for fully baffled tanks.[5]

Industrial reactors are normally equipped with one or more baffles to prevent the fluid from swirling. This would cause the liquid to rotate as a solid body producing little or no mixing. Moreover, creation of a vortex might result in formation of an emulsion due to air incorporation. Including baffles in the reactor set up breaks the vortex, restoring the impeller flow pattern. Finally, the relative dimension of the impeller (D) and tank (T) diameters, the off-bottom clearance (C) and the liquid height (H) have an impact on the flow pattern and influence the overall mixing. Ratio of $D/T \leq 0.4$ and $D/T \sim 0.6$ have been suggested for axial and radial impellers respectively, where D is the impeller diameter and T is the tank diameter (Figure 4.2).

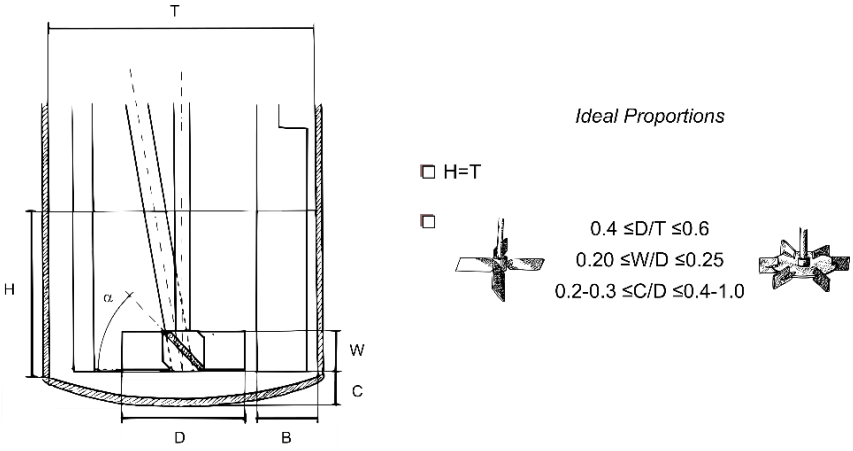


Figure 4.2: Typical geometrical parameters for mechanically stirred vessels.

4.2 Calorimetry in Process Safety

4.2.1 Differential Scanning Calorimetry (DSC)

Differential scanning calorimetry (DSC) is a technique widely used in industry to measure the thermal properties of a material. In process safety it is a routine preliminary test to evaluate the thermal stability of pure compounds and mixtures, while in material science it is used to determine the presence of phase transitions. It is based on the comparison of the heat required to increase the temperature of the analysed sample and that of a reference material, when both are heated under the same conditions. Practically, the experiment can be conducted monitoring the temperature of both samples while the heat flow is kept constant (heat-flow calorimetry), or measuring the electrical power required to maintain the two samples at the same temperature for the whole experiment (power compensation calorimetry).[8] If the analysed sample undergoes a physical or chemical transformation, this will be detected by the difference in the two responses.

The heat flow is plotted against the temperature to obtain a DSC curve. Endothermic events, such as melting of a solid, will appear as negative peaks, while exothermic ones, such as decomposition, will give rise to positive peaks. The enthalpy associated with a specific transformation can be obtained by integration of the corresponding peaks in the DSC curve, which also provides information on the onset of decomposition.

Due to its fast response, ease of the test, and the limited amount of material required, DSC is the first test conducted in process safety to assess the thermal stability of both pure materials and reaction mixtures.[9] The sample (a few mg) is weighed in an appropriate container, which is subsequently sealed. Gold-plated crucibles are often used for this purpose because they are chemically inert and capable of withstanding pressure build up. In reporting the upper temperature limit at which the material can be safely handled, it is

best practice to subtract 100 °C from the recorded onset of decomposition, as this might be affected by the scanning rate.

4.2.2 Reaction Calorimetry (RC)

Reaction calorimetry (RC) is the measurement of the heat released or absorbed during a chemical reaction.[10] The rate of energy exchange provides information on the reaction kinetics, while thermodynamic data are obtained by integration of the graph reporting the energy exchanged as a function of time. The reaction of interest is performed in a calorimeter, an adiabatic jacketed reaction vessel which allows precise monitoring of the energy exchanged by the reacting system, as well as precise control of the reaction temperature. Calorimeters used in industry are normally equipped with systems that allow the continuous feed of reagents, to simulate semi-batch conditions typically encountered at large scale (Figure 4.3).

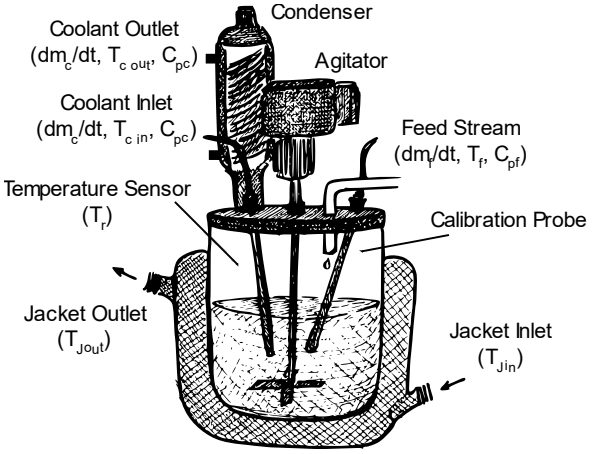


Figure 4.3: An example of heat flow reaction calorimeter. The relevant physical quantities involved in the energy balance are indicated in parenthesis.

Various techniques can be used to monitor the energy exchange, which in turn result in different set-up and operational modes. Heat flow calorimeters are one of the most common. They measure the difference between the temperature of the reaction mass and

the temperature of the jacket and use this data to calculate the heat exchanged by the reaction according to equation 4.1.[10]

$$Q_r = U * A(T_r - T_j) + mC_p \frac{dT_r}{dt} + \frac{dm_f}{dt} C_{pf}(T_r - T_f) + \frac{dm_c}{dt} C_{pc}(T_{c\,out} - T_{c\,in}) + K_{loss}(T_r - T_{amb})$$ (eq. 4.1)

Q_r is the heat flow due to the reaction. The first term on the right side [$UA(T_r-T_j)$] refers to the heat exchanged through the wall of the reactor between the reaction mass at temperature T_r and the jacket fluid at temperature T_j. It depends on the temperature difference between the two sides of the wall (T_r-T_j), the wetted heat transfer area (A), and the overall heat transfer coefficient (U). The product U*A is not constant during the reaction and it is unknown. The second term ($m*C_p*dT_r/dt$) quantifies the heat accumulation of the reaction mass. This is dependent on the reaction mass (m) and its specific heat (C_p), which might vary during the reaction and needs to be determined for each RC experiment. If the feed does not have the same temperature of the reaction mass ($T_r \neq T_f$), this will contribute to the energy balance as expressed in the third term, where m_f is the mass of the feed stream, and C_{pf} its specific heat. In case of multiple feeds, each one will contribute to the total mass balance in a similar way, and more terms should be included in the equation. Evaporation of the solvent removes heat from the reaction mass, and this contribution is most conveniently calculated by applying an energy balance on the coolant of the condenser (fourth term on the right) considering the mass of fluid at the condenser involved in the exchange (m_c), its specific heat (C_{pc}) and the temperature difference between the coolant inlet and outlet ($T_{c\,out}-T_{c\,in}$). Finally, as no real system is perfectly adiabatic, loss towards the external ambient are inevitable, especially when the temperature difference between the reaction and the environment (T_r-T_{amb}) is high, thus the fifth term should be included for completeness. This final term is dependent on how well insulated the calorimeter is (K_{loss}), and it is usually approximated to zero for heat flow calorimeters.

A calibration heater of known power is used to determine the unknown parameters (the product U*A and C_p) at the beginning and end of the reaction, and thus one of the disadvantages of this method is that it cannot provide real time data. Each calibration involves two distinct parts (Figure 4.4).

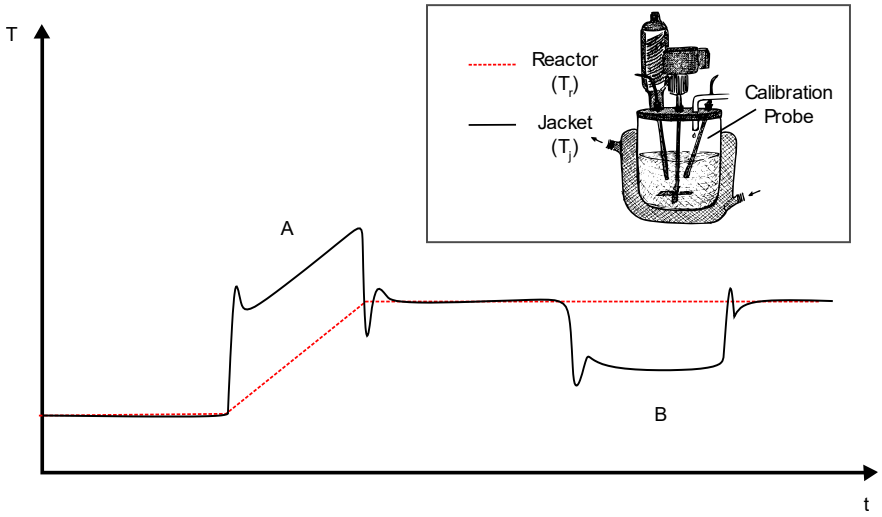


Figure 4.4: Typical reactor (red) and jacket (black) temperature profile during a calibration experiment. Data from (A) are used to calculate C_p, and data from (B) to obtain U*A.[10]

First, the temperature of the jacket is increased linearly in adiabatic conditions (Qr = 0, Figure 4.4A). This causes an increase in the temperature of the reaction mass and can be expressed mathematically with eq. 4.2.

$$0 = U * A(T_r - T_j) + mC_p \frac{dT_r}{dt} \qquad \text{(eq. 4.2)}$$

After the temperature of the reactor has reached equilibrium with the temperature of the jacket, the calibration heater is turned on, while the calorimeter maintains the desired isothermal temperature inside the reactor regulating the temperature of the jacket (figure 4.4B). This situation corresponds to eq. 4.3, where the heat flow can be determined from the heater power.

$$Q_r = UA(T_r - T_j) \qquad \text{(eq. 4.3)}$$

Solving simultaneously eq. 4.2 and 4.3 furnishes the value of U*A and C_p.

Heat flow calorimetry is routinely applied in process safety to determine whether a given reaction would lead to thermal runaway in certain conditions. Thermal runaway is caused by the lack of control of the reaction temperature, whose build up above a certain threshold results in undesired side-reactions, usually strongly exothermic, and/or pressure increase which ultimately can lead to vessel failure, possibly explosively, and release of its content. In a typical RC experiment, the heat released by the reaction is accurately measured. This allows, upon integration, to determine the reaction enthalpy (eq. 4.4) and subsequently calculate the adiabatic increase in temperature (ΔT_{ad}, eq. 4.5).

$$\Delta H = \int_{t_1}^{t_2} Q_r dt \qquad \text{(eq. 4.4)}$$

$$\Delta T_{ad} = \frac{\Delta H}{m C_p} \qquad \text{(eq. 4.5)}$$

To assess the thermal safety of a chemical process, a systematic approach has been developed based on the runaway scenario and its classification into five critical classes.[11] In a runaway scenario, failure of the cooling system is evaluated at the point of maximum reagents accumulation, which is the worse-case scenario because it leads to the maximum release of heat. The reaction temperature, originally at $T_{process}$, is increased by the value $\Delta T_{ad\ (1)}$. The new temperature reached is defined as the "maximum temperature of the synthesis reaction" (MTSR). If this is above the temperature at which secondary exothermic reactions are triggered, this might cause a further increase of temperature (Figure 4.5A).[12] The kinetics of the secondary reactions is another important parameter, which led to the definition of the "time to maximum rate under adiabatic conditions" (TMR_{ad}). The time required to the secondary interactions to reach their maximum rate depends on the temperature at which they are initially triggered. For this reason, the temperature at which TMR_{ad} = 24 h (T_{D24}) is of particular importance for risk assessment, because this would allow enough time to take the appropriate countermeasures. Finally, technical reasons might prevent the reaction to reach any of the above temperatures, for instance because

they are above the boiling point of the solvent, whose evaporation will contribute to removing heat from the reaction mass. The maximum temperature reachable for technical reasons is defined as MTT (maximum technical temperature). The relative value of T_p, MTSR, T_{D24} and MTT can be used to define five classes (Figure 4.5B), which are useful for risk assessment and for choosing the appropriate safety systems to mitigate the risk.[13]

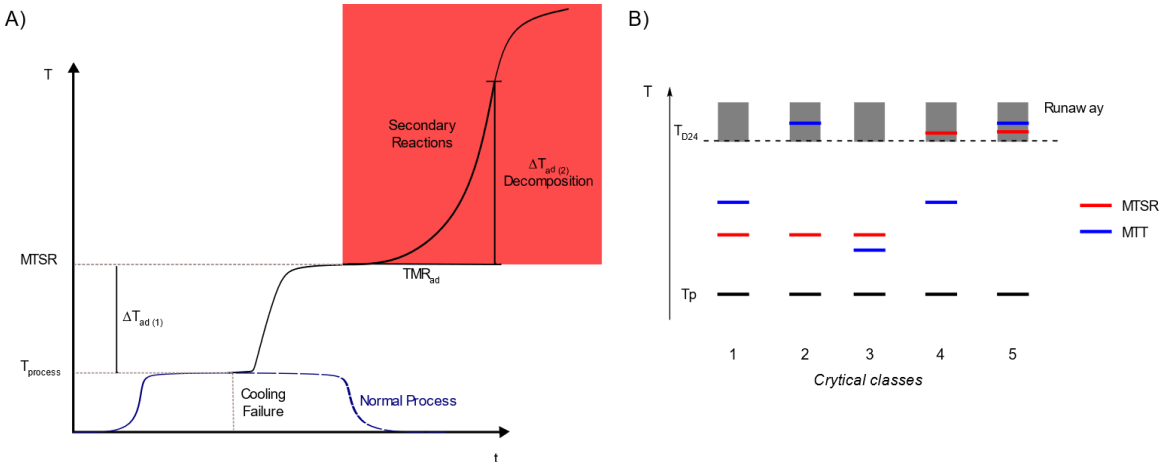


Figure 4.5: Risk assesment of the thermal safety of a reaction. A) Graphical representation of the data required for a complete assesment. B) Stoessel's critical classes.[11]

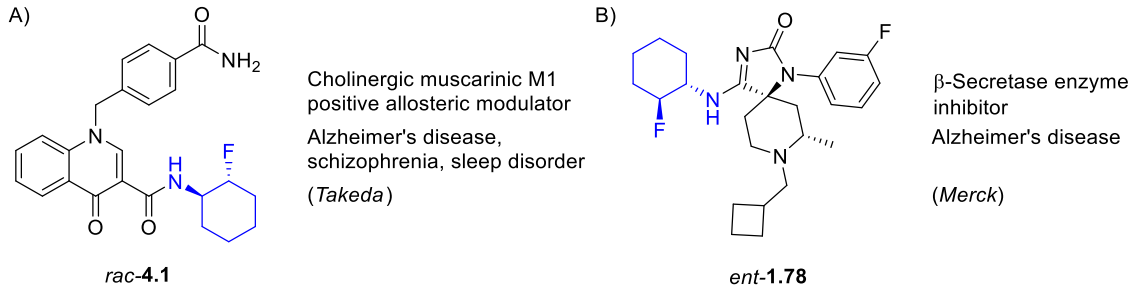
4.3 Project Aim

In Chapter 2, the scalability of enantioselective HB-PTC fluorination was demonstrated with the synthesis of the fluorinated analogue of Diphenidine **2.83**, starting from 50 g of *rac*-(2-chloro-1,2-diphenylethyl)piperidine **2.107** (section 2.7).[14] This result gave us confidence that HB-PTC could be applied to multigram scale, but since the scale-up was performed in a round-bottom flask, it was unclear whether the transformation could be translated to mechanically stirred vessels as used in industrial settings. In fact, due to the heterogeneous nature of the reaction, we anticipated that mixing would have a strong influence on HB-PTC. To investigate this, we collaborated with SANOFI to scale up the HB-PTC protocol to 200 g of β-haloamine precursor in a 1 L mechanically stirred vessel.

4.4 *Trans*-2-fluorocyclohexan-1-amine

β-Fluoroamines have an important role in medicinal chemistry (section 1.2.2.1), where the introduction of fluorine has been exploited as an NMR probe for binding studies,[15] and for the fine-tuning of physicochemical properties.[16] In this context, the availability of enantiopure building blocks featuring this motif is of great importance to assess at an early stage the behaviour of different stereoisomers in a biological system.

Trans-2-fluorocyclohexan-1-amine has been incorporated into compounds investigated for the treatment of Alzheimer's disease and other CNS pathologies (Figure 4.6). Racemic 4-quinolone **4.1** is part of a SAR study of positive allosteric modulators of the cholinergic muscarinic M1 receptor conducted by Takeda.[17] This receptor is involved in learning and memory as well as sleep and neuropathic pain, and the use of positive allosteric modulators, which enhance the ability of acetylcholine to bind to M1, has been suggested for the treatment of schizophrenia and neurodegenerative disorders.[18,19] Spiropiperidines such as **1.78** have been developed by Merck as inhibitors of the β-secretase enzyme (BACE), which is involved in the formation of the β-amyloid plaques found in patients affected by Alzheimer's disease.[20]

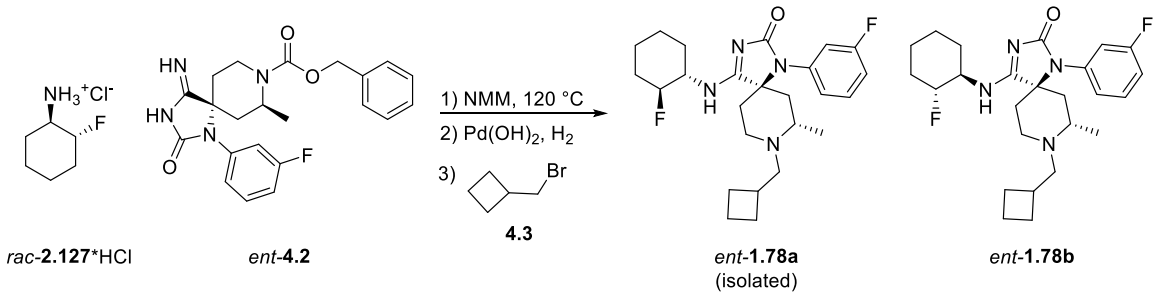


rac-**4.1** *ent*-**1.78**

Figure 4.6: A) An example of a 4-quinolone incorporating the *trans*-2-fluorocyclohexan-1-amine motif studied for the treatment of NCS pathologies.[17] B) An example of a spiropiperidine incorporating the *trans*-2-fluorocyclohexan-1-amine motif studied for the treatment of Alzheimer's disease.[20]

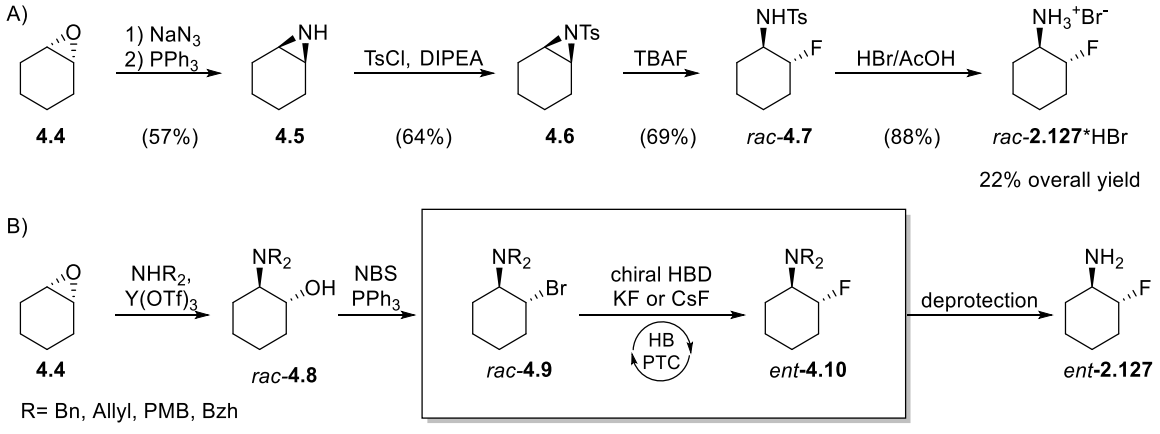
In both examples the patented route relies on racemic *trans*-2-fluorocyclohexan-1-amine **2.127** and either the racemate was tested in the biological essay (*rac*-**4.1**) or the

diastereoisomers obtained by reaction with enantiopure **4.2** were separated by preparative HPLC at the end of the synthesis (Scheme 4.1).



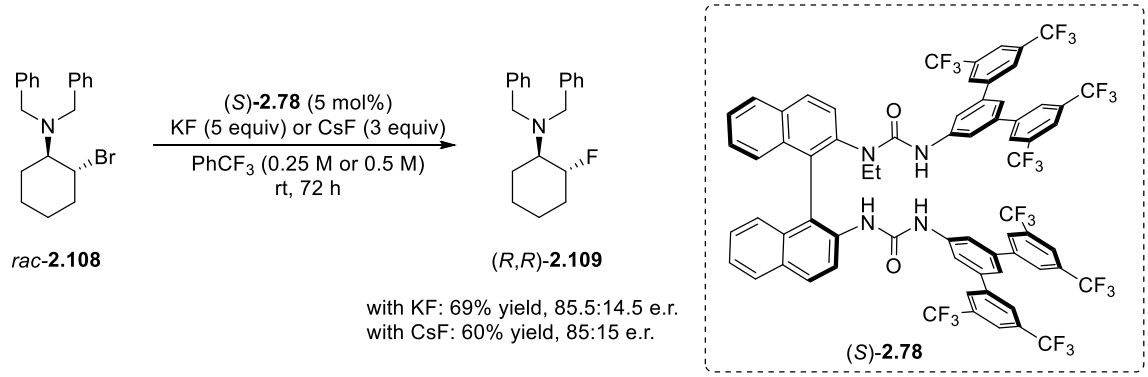
Scheme 4.1: Merck's synthesis of **1.78** from racemic *trans*-2-fluorocyclohexan-1-amine*HCl salt.[20] NMM= *N*-Methylmorpholine.

The reported procedure to racemic *trans*-2-fluorocyclohexan-1-amine **2.127** involves fluoride ring opening of the corresponding activated aziridine **4.6,** followed by deprotection under acidic conditions to afford the HBr salt of **2.127** in 22% overall yield from commercial cyclohexene oxide (Scheme 4.2A).[20] The procedure is lengthy and low yielding, which is reflected in the high price of this building block (Fluorochem; £ 553/g). While classical resolution of the two enantiomers might be feasible taking advantage of the amino functionality, this would result in the loss of half of the material, further reducing the yield.



Scheme 4.2: A) Reported synthesis to racemic **2.127***HBr salt.[20] B) Proposed enantioselective synthesis of **2.127** *via* asymmetric HB-PTC. DIPEA= *N*,*N*-diisopropylethylamine; PMB= *p*-methoxybenzyl; Bzh= benzhydryl.

We envisioned that asymmetric HB-PTC could provide access to this building block in enantiopure form (Scheme 4.2B). Previously, we have reported that a protected analogue of **2.127**, the *N*-dibenzylamine **2.109**, can be obtained from the corresponding bromide **2.108** upon enantioselective fluorination under HB-PTC (Chapter 2, section 2.8).[14] Using KF (5 equiv) as fluorine source, (*R*,*R*)-**2.109** was obtained in 69% isolated yield (40.7 mg) and 85.5:14.5 e.r., while fluorination with CsF (3 equiv) afforded (*R*,*R*)-**2.109** in 60% isolated yield (35.5 mg) and 85:15 e.r. (Scheme 4.3).



Scheme 4.3: Synthesis of β-fluoroamine (*R*,*R*)-**2.109**, a protected analogue of *trans*-2-fluorocyclohexan-1-amine **2.127**, *via* enantioselective HB-PTC fluorination with alkali metal fluorides.

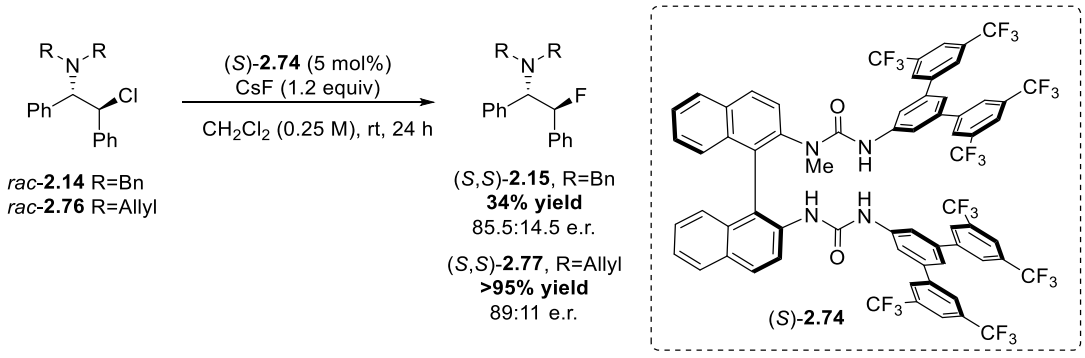
In both cases, the reaction took 72 h and required 10 mol% of catalyst (*S*)-**2.78**, conditions which are far from ideal for industrial applications. Specifically, a 10 mol% catalyst loading on 1 kg scale of substrate *rac*-**2.108** would require ~390 g of bis-urea (*S*)-**2.78**. This chapter reports the development of an efficient synthesis of more than 100 g of (*R*,*R*)-**2.109** and improved enantiomeric ratio using a catalyst loading of <1 mol%. The scale-up was conducted in a mechanically stirred vessel, demonstrating the scalability of HB-PTC in conditions relevant for industrial processes. Scale-up of the synthesis of bis-urea (*S*)-**2.78** used in this study was reported in Chapter 3.

4.5 Optimisation of the Reaction Conditions

4.5.1 Substrate Selection

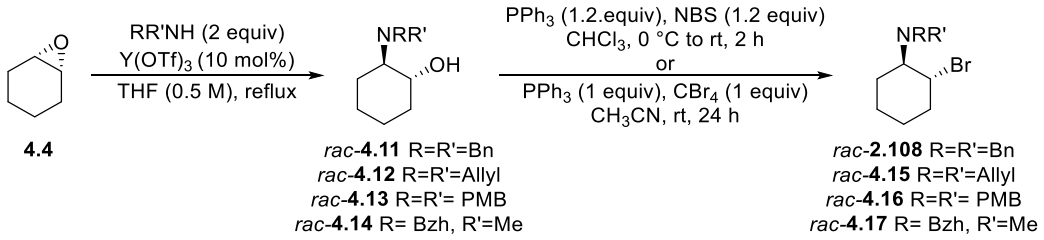
4.5.1.1 Protecting Group

From previous studies (Chapter 2, section 2.4.3), we were aware that the choice of protecting group had a marked influence on the yield of the fluorination of stilbene-derived β-chloroamines *rac*-**2.14** (NBn_2) and *rac*-**2.76** ($NAllyl_2$, Scheme 4.4). On the other hand, nitrogen substitution had little effect on enantioselectivity, and this was rationalised by the fact that the nitrogen substituents point outside the catalytic pocket in the TSs (section 2.9.2).



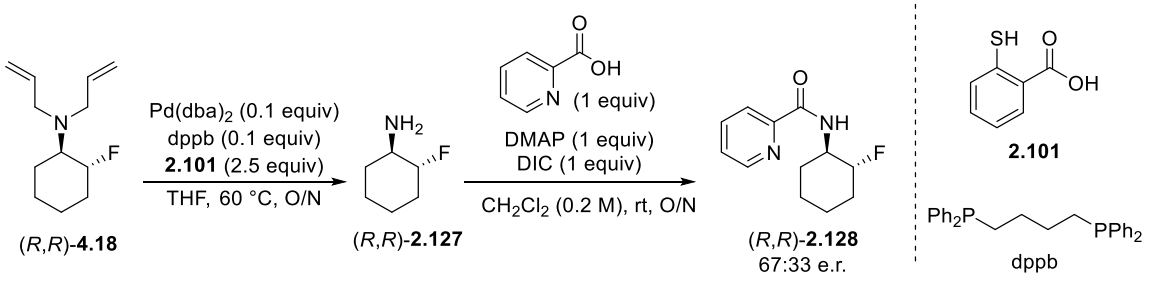
Scheme 4.4: Enantioselective fluorination under HB-PTC of *rac*-**2.14** (NBn_2) and *rac*-**2.76** ($NAllyl_2$), which affords very different yields of the corresponding β-fluoroamines in the presence of the same catalyst (*S*)-**2.74**.

Aiming at reducing the catalyst loading, we began our study towards the scale-up of HB-PTC fluorination evaluating different alkyl protecting groups for the cyclohexyl derivative. Synthesis of the starting β-bromoamines involves ring opening of cyclohexene oxide with the appropriate secondary amine,[21] followed by bromination with either PPh_3/NBS or PPh_3/CBr_4 (Scheme 4.5).[22] The synthesis is stereospecific, and only the *trans* β-bromoamine was obtained in all cases. This was confirmed by the large value of the vicinal coupling constant ($^3J_{H(ax)\text{-}H(ax)} \sim 11$ Hz) observed in the ^{1}H NMR spectra, which is indication of the presence of *trans* axial hydrogens on the carbons bearing the heteroatoms.[23]



Scheme 4.5: Synthesis of cyclic β-bromoamines bearing different protecting groups. PMB= *p*-methoxybenzyl; Bzh= benzhydryl.

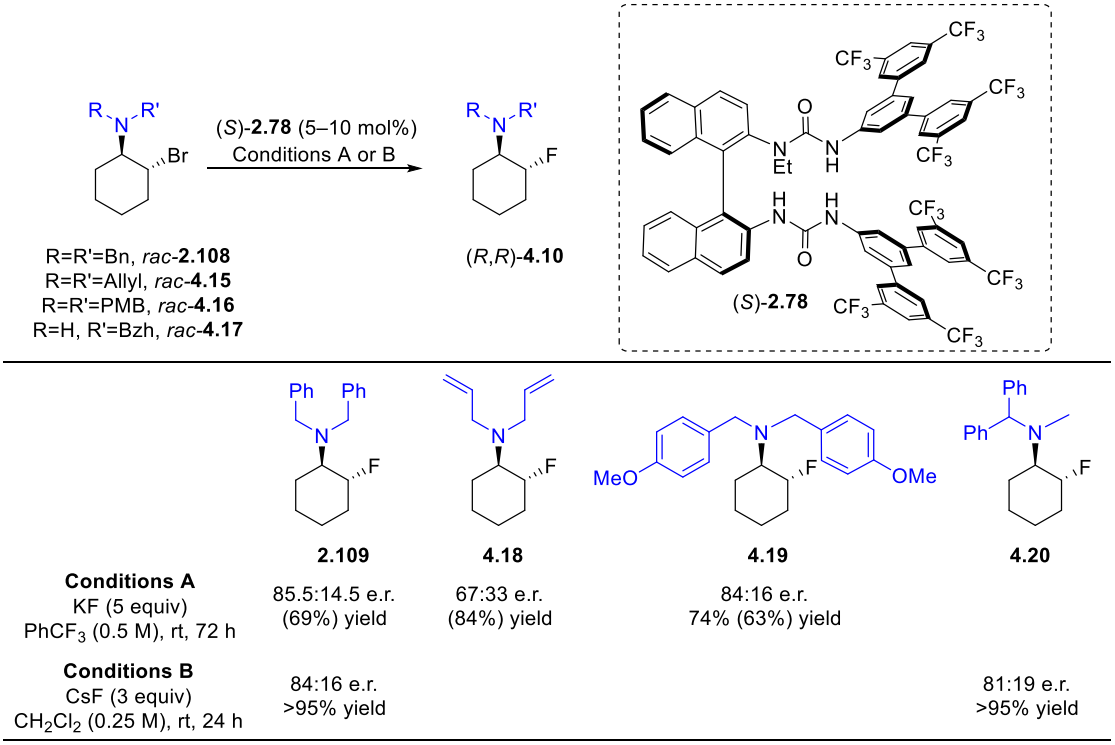
β-Bromoamines **4.15–4.17** were fluorinated with either KF or CsF in the presence of catalyst (*S*)-**2.78**. The e.r. of the corresponding β-fluoroamines was determined by HPLC using a chiral non-racemic stationary phase equipped with a photodiode array detector. The absence of a chromophore in *N*,*N*-diallyl β-fluoroamine **4.18** required derivatisation for e.r determination. The allylic group was removed under Pd-catalysis and the primary amine coupled with picolinic acid in the presence of *N,N′*-diisopropylcarbodiimide (DIC) and 4-dimethylaminopyridine (DMAP) to afford picolinamide **2.128** (Scheme 4.6).[24] Picolinic acid was chosen as derivatisation reagent because **2.128** has been previously synthesised in enantioenriched form (92:8 e.r.) by the Doyle group,[24] which allowed us to assign the absolute configuration of cyclic aliphatic β-fluoroamines by comparison with literature data (see also Chapter 2, section 2.8.2).



Scheme 4.6: Derivatisation of (*R,R*)-**4.18** to the corresponding picolinamide to determine the e.r. *via* HPLC using a chiral non-racemic stationary phase. O/N = overnight

The results of the fluorination, using either KF (conditions A) or CsF (conditions B) are reported in Scheme 4.7. Conditions A are the optimised conditions for the fluorination of aliphatic substrates with KF reported in Chapter 2 and the yields are for the isolated

products. Conditions B were used at the beginning of the PhD project and the corresponding tests were not repeated under optimised conditions with KF.



Scheme 4.7: Effect of the *N*-protection in the enantioselective fluorination under HB-PTC of β-bromoamines derived from cyclohexene. PMB= *p*-Methoxybenzyl, Bzh: Benzhydryl. Yield determined by ^{19}F NMR using 4-fluoroanisole as internal standard. Isolated yields in parenthesis. e. r. determined by HPLC using a chiral non-racemic stationary phase.

A marked dependence of enantioselectivity on the nature of nitrogen substituents was found, which is in stark contrast to the stilbene-derived substrates. β-Bromoamines bearing benzyl (**2.108**), *p*-methoxy benzyl (*rac*-**4.16**), and benzhydryl groups (*rac*-**4.17**) afforded the fluorinated products in similar and moderate enantioselectivity (81:19–85.5:14.5 e.r., Scheme 4.7), while allylic substitution (*rac*-**4.15**) caused a drastic drop in enantiocontrol (67:33 e.r.). Computations performed by Dr. David Ascough with an NMe_2 aliphatic substrate revealed it docks into the catalytic pocket in a similar manner to the stilbene derivatives, retaining the main cation-π stacking interaction. The nitrogen substituents are still pointing towards the solvent, but the catalytic pocket is broad and open, allowing the aziridinium ion to adjust its position. For stilbene-derived substrates the aromatic rings

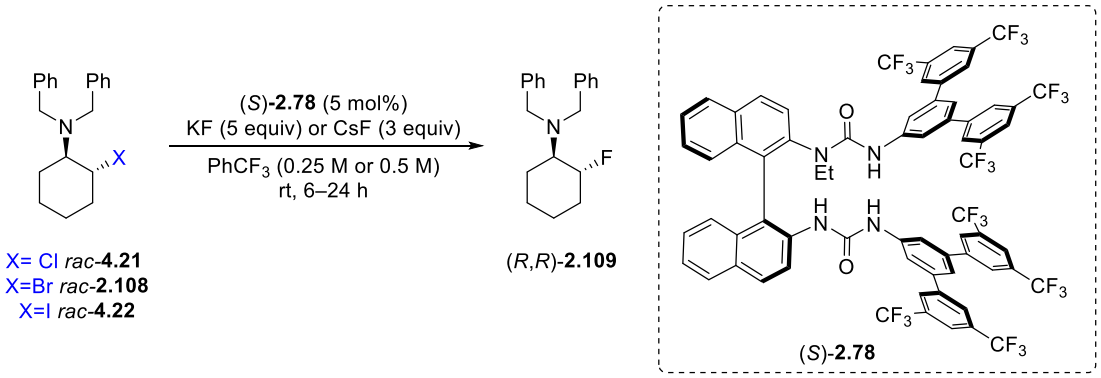
dominate the docking pose, since the substrate adopts a conformation that maximises conjugation of the ring with the breaking and forming bonds at the benzylic position. In the absence of the stilbene rings, the position and angle of the cation-π interaction can vary. In these conditions we cannot rule out a possible additional π-π stacking interaction between the catalyst and the *N*-benzyl substituents of β-bromoamines *rac*-**2.108,** *rac*-**4.16** and *rac*-**4.17**, which might contribute to the enhanced e.r. observed experimentally.

As previously observed in the case of the stilbene derived substrates, β-haloamines bearing *N*-allyl groups were the most reactive. The higher conversion resulted in easier chromatographic purification and an enhanced yield (84% isolated yield of (*R*,*R*)-**4.18** *versus* 69% of (*R*,*R*)-**2.109** and 63% of (*R*,*R*)-**4.19**). Nevertheless, full conversion could be obtained for *rac*-**2.108** using CsF in CH_2Cl_2 (conditions B) instead of KF in $PhCF_3$ (conditions A) with only a slightly diminished enantioselectivity (84:16 *versus* 85.5:14.5 e.r.). We had already demonstrated that removal of both *N*-benzyl groups could be easily achieved with no erosion of enantiopurity (Chapter 2, section 2.8.2). In addition, the required dibenzylamine starting material is commercially available in large amounts. For these reasons, the *N*,*N*-dibenzylated substrate was selected for scale-up experimentations.

4.5.1.2 Leaving Group

Next, the effect of different leaving groups was evaluated with both KF and CsF. *Trans*-β-chloroamine *rac*-**4.21** and *trans*-β-iodoamine *rac*-**4.22** were synthesised from the corresponding alcohol according to literature procedures, and the analytical data were in agreement with those previously reported.[22] The results of the fluorination with 5 mol% of (*S*)-**2.78** in $PhCF_3$ are reported in Table 4.1.

Table 4.1: Effect of the leaving group in the enantioselective fluorination under HB-PTC of β-haloamines derived from cyclohexene

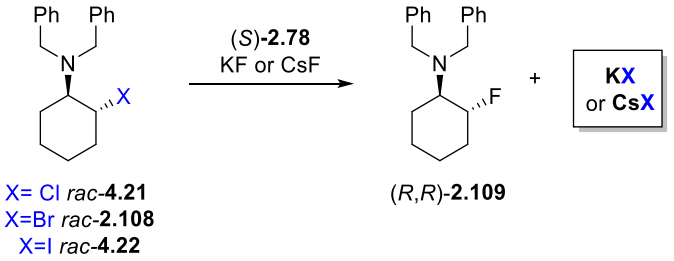


Entry	*MF*	*X*	*Time (h)*	*Yield* [a]	*e.r.* [b]
1	KF	Cl	24	No reaction	–
2	KF	Br	24	46%	85:15
3	KF	I	24	No reaction	–
4	CsF	Cl	6	traces	–
5	CsF	Br	6	22%	85:15
6	CsF	I	6	71%	85:15

Fluorination with KF: β-haloamine (0.1 mmol), KF (5 equiv), (*S*)-**2.78** (5 mol%), $PhCF_3$ (0.5 M) rt, stirring at 900 rpm for 24 h. **Fluorination with CsF:** β-haloamine (0.05 mmol), CsF (3 equiv), (*S*)- **2.78** (5 mol%), $PhCF_3$ (0.25 M), rt, stirring at 900 rpm for 6 h. [a] Yield determined by ^{19}F NMR using 4-fluoroanisole as internal standard. [b] e.r. determined by HPLC using a chiral non-racemic stationary phase.

When KF was used as fluorine source, only bromide *rac*-**2.108** afforded the desired product (entry 2, Table 4.1), while no reaction was observed in the presence of chloride *rac*-**4.21** (entry 1) or iodide *rac*-**4.22** (entry 3). Chloride *rac*-**4.21** was unreactive also in the presence of CsF (entry 4), while bromide *rac*-**2.108** and iodide *rac*-**4.22** afforded the fluorinated product in 22% and 71% ^{19}F NMR yield respectively after 6 h (entries 5–6). The enantiomeric excess was identical for both the bromide and iodide starting material (85:15), consistent with the proposed mechanism in which the urea coordinates the nucleophile but not the leaving group in the enantiodetermining step (see Chapter 2).

The observed trend in reactivity can be rationalised by considering the complete chemical equation, including the inorganic salts that are co-products of the fluorination (Scheme 4.8).



Scheme 4.8: Complete chemical equation for the enantioselective fluorination under HB-PTC of β-haloamines derived from cyclohexene, showing the co-products formed.

Overall the reaction involves the cleavage of a relatively "weak" carbon-halogen bond C–X (Table 4.2) and of the "strong" ionic interaction within the metal fluoride salt (KF or CsF) to form a "stronger" C–F bond (458 kJ/mol)[25] and a "weaker" ionic salt (KX or CsX Table 4.3). The heavier the halogen leaving group, the larger the difference between the energies of the C–F and C–X bonds (Table 4.2), thus making the reaction increasingly more favourable moving from chloride to iodide from the perspective of the organic molecule. On the other hand, the lattice energy of the alkali metal halides decreases with increasing radius of the halogen (Table 4.3), making the reaction increasingly less favourable down the halogen group. The balance of these opposite trends ultimately determines which leaving group is optimal with each alkali metal fluoride.

Table 4.2: Average carbon-halides bond energies, and their difference with the average C–F bond energy

Entry	*X*	*Average Bond Energy C–X (kJ/mol)*[25]	*Δ (E_{C-F} - E_{C-X}) (kJ/mol)*
1	F	458	–
2	Cl	327	158
3	Br	285	200
4	I	213	272

Table 4.3: Lattice energy of potassium and cesium halides and their difference with KF and CsF lattice energies

Entry	*KX*	*Lattice Energy (kJ/mol)* [26]	*Δ (E_{KX}–E_{KF}) (kJ/mol)*	*CsX*	*Lattice Energy (kJ/mol)* [26]	*Δ (E_{CsX}–E_{CsF}) (kJ/mol)*
1	KF	–829	–	CsF	–759	–
2	KCl	–720	109	CsCl	–670	89
3	KBr	–691	138	CsBr	–647	112
4	KI	–650	179	CsI	–613	146

In view of the experimental results described above (Table 4.1) β-bromoamine *rac*-**2.108** was selected as model substrate for the scale-up, because it could be fluorinated by both KF and CsF. In fact, the fluoride source had not been selected at this stage. The synthesis of 1 kg of the precursor *rac*-**2.108** was outsourced to WuXi AppTec and was based on our published procedure involving epoxide opening followed by bromination with NBS and PPh_3.[14]

4.5.2 Fluoride Source

Having selected **2.108** as model substrate, we then focused on the fluoride source (KF or CsF) for the optimisation of the reaction conditions. KF is ten times cheaper than CsF per mole (bulk prices for 100 kg: KF £ 22.5/kg, £ 1.3/mol; CsF: £ 90/kg, £ 13.7/mol),[i] and both fluoride sources are more economical than TBAF (Bulk prices for 100 kg of TBAF solution 1 M in THF: £ 54/kg of solution, £ 58.6/mol).[i] Economical considerations are extremely important on industrial scale, but less relevant for batches <1 kg as in the case of this project, so we conducted our preliminary investigations using both salts. A different behaviour of the two fluorine sources could be anticipated, due to their different physicochemical properties. On one hand, activation of CsF is more facile because of the smaller lattice energy (KF: 829 kJ/mol *versus* CsF: 759 kJ/mol, see also Chapter 2 section 2.2). On the other hand, KF is less dense (KF: 2.48 g/cm^3 *versus* CsF: 4.12 g/cm^3), and thus easier to suspend in a mechanically stirred vessel (section 4.1).

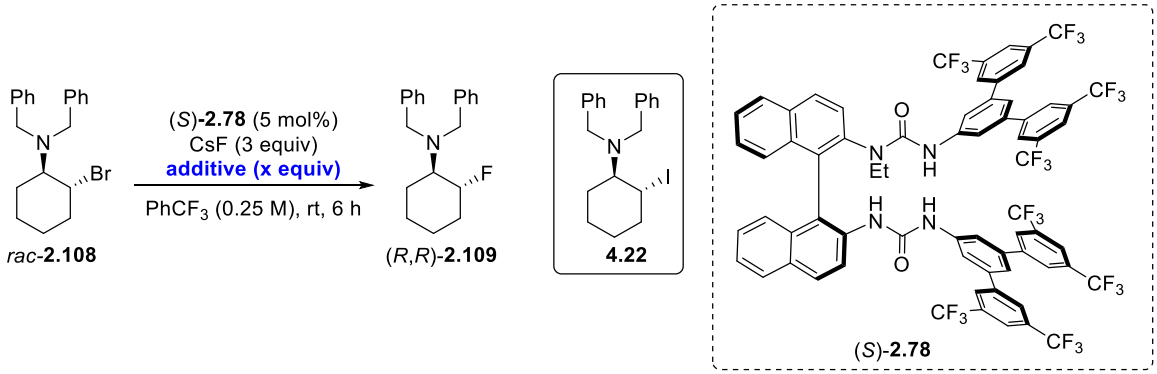
All the screening reactions described in this section were conducted in so-called "batch" conditions: the solid reagents were added first to a glass vial followed by the solvent.

[i] October 2019, quote requested by SANOFI to their suppliers.

4.5.2.1 Enantioselective Fluorination with CsF: Effect of Additives

The previously optimised conditions consisted of stirring *rac*-**2.108** with 3 equivalents of CsF and 10 mol% of bis-urea (*S*)-**2.78** in $PhCF_3$ (0.25 M) at rt for 72 h.[14] The product was obtained in 60% isolated yield and 85:15 e.r.. The moderate yield was due to incomplete conversion, and difficulties in separating the product (*R,R*)-**2.109** from unreacted starting material *rac*-**2.108** by silica gel column chromatography. To improve the yield, various additives were screened employing initially 5 mol% of (*S*)-**2.78** (Table 4.4).

Table 4.4:Effect of additives on the enantioselective fluorination of *rac*-**2.108** with CsF under HB-PTC.



Entry	*Additive (equiv)*	*Yield of (R,R)-**2.109**[a]*	*e.r. [b]*	*Yield of **4.22**[c]*
1	–	22%	85:15	–
2	CsOMs (1)	77%	85:15	–
3	CsOMs (0.5)	79%	85:15	–
4	CsOMs (0.2)	74%	85:15	–
5	KOTf (0.5)	73%	85:15	–
6[d]	NaBARF (0.5)	67%	77:23	–
7	KI (0.5)	75%	85:15	traces
8	CsI (0.5)	71%	85:15	traces
9	TBAI (0.5)	0%	–	15%
10[e]	TBAI (0.025)	10%	–	traces
11	TBABr (0.5)	0%	–	–

Conditions: *rac*-**2.108** (0.05 mmol), CsF (3 equiv), (*S*)-**2.78** (5 mol%), $PhCF_3$ (0.25 M), rt, stirring at 900 rpm for 6 h. [a] Yield determined by ^{19}F NMR using 4-fluoroanisole as internal standard. [b] e.r. determined by HPLC using a chiral non-racemic stationary phase. [c] Yield determined by ^{1}H NMR using 4-fluoroanisole as internal standard. [d] Side-products were detected in the ^{1}H NMR spectrum. [e] 10% of catalyst loading, TBAI/ (*S*)-**2.78** =1/ 2.

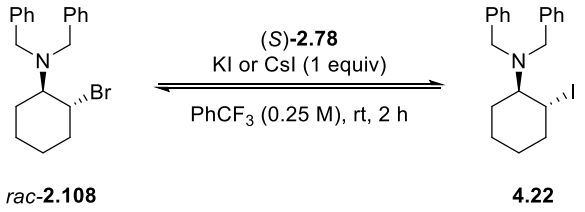
Addition of 1 equiv of CsOMs enhanced the yield of (*R*,*R*)-**2.109** from 22% (entry 1, Table 4.4) to 77% (entry 2). Substochiometric amounts of CsOMs (0.2–0.5 equiv) were equally effective in promoting formation of the desired product (74–79% yield, entries 3–4), suggesting a catalytic role of the additive. In all these cases no other products were detected in the ^{1}H NMR of the crude reaction mixture, and the e.r. of fluoride (*R*,*R*)-**2.109** was unaffected (85:15 e.r.). Increased yield and unmodified enantioselectivity were observed also in the presence of salts such as KOTf, KI and CsI (71–75% yield, 85:15 e.r., entries 5, 7–8). We hypothesised that the beneficial effect of the additives was due to formation of a looser ion pair between the aziridinium and the anion of the salts compared to the aziridinium bromide ion pair. To test this hypothesis, we evaluated NaBARF (BARF= Tetrakis(3,5-bis(trifluoromethyl) phenyl)borate) as additive for the fluorination. (*R*,*R*)-**2.109** was obtained in superior yield compared to the reaction in its absence (67% entry 6, *versus* 22%), but the yield was slightly lower compared to other additives. Moreover, the enantiomeric ratio of (*R*,*R*)-**2.109** obtained in the fluorination in the presence of NaBARF was lower compared to the other test reactions (77:23 e.r. *versus* 85:15 e.r.), suggesting that a more complex mechanism might be operative, at least in this case.

Importantly, only insoluble additives had a beneficial effect on the yield of (*R*,*R*)-**2.109**. Addition of soluble TBAI (0.5 equiv, entry 9) completely suppressed the fluorination, affording instead the corresponding *trans*-β-iodoamine **4.22** in low yield (15%). Traces of **4.22** were formed also in the presence of insoluble KI or CsI. The fluorination was also suppressed when 0.5 equivalents of TBABr were added to the reaction (entry 11). We speculated that the detrimental effect of soluble additives could be due to saturation of the urea receptor by the large excess of the anion in solution (ratio TBAX/(*S*)-**2.78** = 10:1). This hypothesis is consistent with the observation that reactivity is partially restored (10%

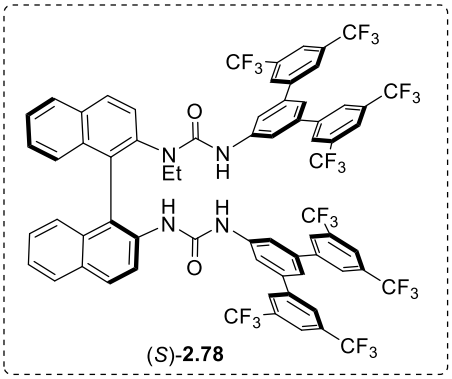
yield of (*R*,*R*)-**2.109,** entry 10) when the catalyst is used in excess compared to TBAI (ratio TBAI: (*S*)-**2.78** = 1:2).

When insoluble salts such as CsI and KI are employed, it is likely that (*S*)-**2.78** acts as phase transfer catalyst both towards CsF and the additive. Control experiments were performed stirring β-bromoamine **2.108** in $PhCF_3$ with 1 equivalent of either KI or CsI with or without organocatalyst (*S*)-**2.78** (Table 4.5). After 2 h the reaction mixture was filtered through celite and the crude analysed by quantitative ^1H NMR. Formation of *trans*-β-iodoamine **4.22** was detected only when the catalyst was present (entries 2 and 4), which supports the phase-transfer mechanism towards the additive. The e.r. of **4.22** was not determined.

Table 4.5: Iodination of *rac*-**2.108** with KI or CsI under HB-PTC conditions.



rac-**2.108** **4.22**



(*S*)-**2.78**

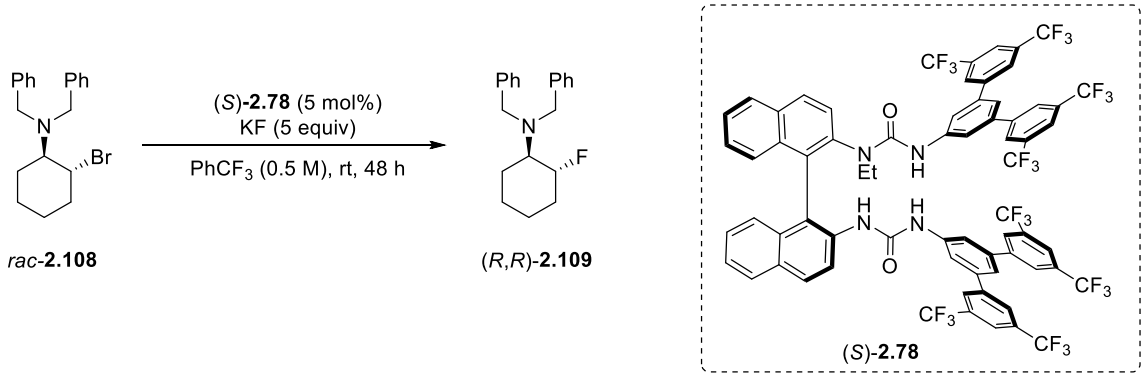
Entry	*Reagent*	*(S)-2.78*	***2.108***	***4.22***
1	KI	–	100%	–
2	KI	5 mol%	66%	34%
3	CsI	–	100%	–
4	CsI	5 mol%	76%	24%

Conditions: *rac*-**2.108** (0.05 mmol), $PhCF_3$ (0.25 M), rt, stirring at 900 rpm for 2 h. After filtration through celite the mixture was analysed by ^1H NMR and conversions are reported.

4.5.2.2 Enantioselective Fluorination with KF: Effect of Additives

The published conditions for the fluorination of *rac*-**2.108** in the presence of KF employed 10 mol% of bis-urea (*S*)-**2.78** and required 72 h to reach a satisfactory conversion, affording β-fluoroamine (*R*,*R*)-**2.109** in 68% isolated yield and 85.5:14.5 e.r.[14] The catalyst loading could be reduced to 5 mol% without negatively affecting the yield (65% ^{19}F NMR yield after 48 h, entry 2, Table 4.6), but further reduction to 2 mol% or lower was detrimental.

Table 4.6: Effect of catalyst loading on the enantioselective fluorination with KF of *rac*-**2.108** under HB-PTC.



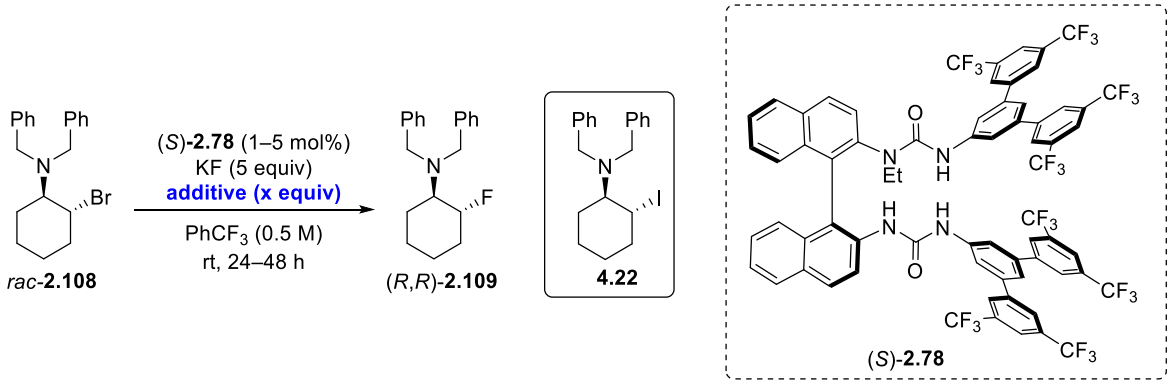
Entry	*Catalyst Loading (mol%)*	*Yield* [a]	*e.r.* [b]
1	10	68%[c]	85.5:14.5
2	5	65%	84.5:15.5
3	2	21%	83:17
4	1	9%	–

Conditions: *rac*-**2.108** (0.25 mmol), KF (5 equiv), (*S*)-**2.78,** $PhCF_3$ (0.5 M), rt, stirring at 900 rpm for 48 h. [a] Yield determined by ^{19}F NMR using 4-fluoroanisole as internal standard. [b] e.r. determined by HPLC using a chiral non-racemic stationary phase. [c] Isolated yield after 72 h.

Given the improved yield observed in the fluorination of *rac*-**2.108** with CsF in the presence of insoluble salts as additives, the same screening was conducted for the fluorination with KF at both 5 mol% and 1 mol% of catalyst loading (Table 4.7). The screening reactions in the presence of 5 mol% of (*S*)-**2.78** could be directly compared to the fluorination with CsF (section 4.5.2.1) and some important differences were immediately apparent. First, addition of KOTf, KOMs and CsOMs was beneficial only when at least 0.5 equivalents of additive were used (Table 4.7, entries 5–7 *versus* 1–4), and the effect was less marked than observed with CsF. Secondly, addition of either KI or CsI (entries 8–10) was detrimental because it

resulted in the competitive formation of *trans*-β-iodoamine **4.22**. While the latter is a competent substrate for the fluorination with CsF, it is unreactive with KF (section 4.5.1.2). Addition of NaBARF (entry 11) afforded (*R*,*R*)-**2.109** in comparable yield to the other salts screened, but in slightly diminished enantioselectivity (82:18 e.r.). Finally, addition of either 18-crown-6 (entry 12), which enhances the solubility of potassium salts, or soluble TBABr (entry 13) completely supressed the reaction. We speculated that in both cases this might be due to the presence of excess bromide in solution. When the catalyst loading was reduced to 1 mol%, none of the previously screened additives in any stoichiometry proved beneficial (entries 14–17).

Table 4.7: Effect of additives on the enantioselective fluorination with KF of *rac*-**2.108** under HB-PTC.



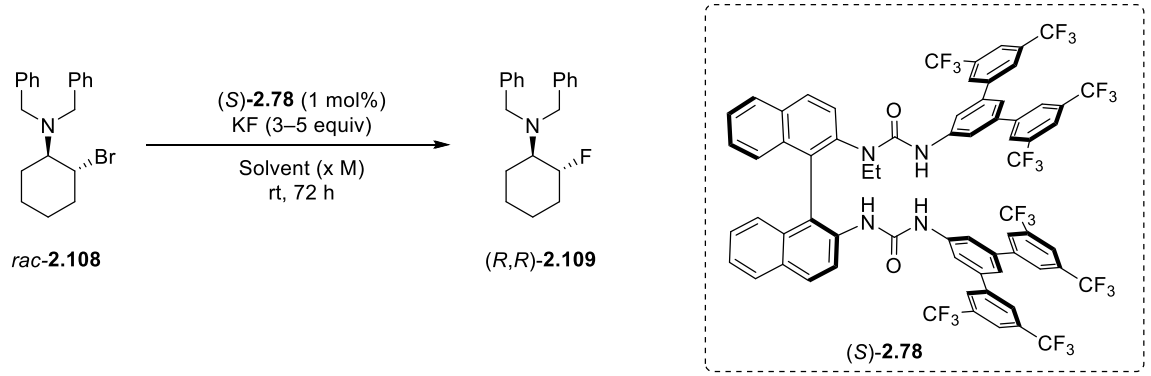
Entry	*(S)-**2.78***	*Additive (equiv)*	*Yield of (R,R)-**2.109**[a]*	*e.r.* [b]	*Yield of **4.22**[c]*
1	5 mol%	–	31%	85:15	–
2	5 mol%	KOTf (0.2)	33%	84.5:15.5	–
3	5 mol%	KOMs (0.2)	35%	85:15	–
4	5 mol%	CsOMs (0.2)	28%	85:15	–
5	5 mol%	KOTf (0.5)	50%	85:15	–
6	5 mol%	KOMs (0.5)	43%	85:15	–
7	5 mol%	CsOMs (1)	66%	85.5:15.5	–
8	5 mol%	KI (0.2)	23%	84:16	22%
9	5 mol%	KI (0.5)	21%	84:16	61%
10	5 mol%	CsI (0.5)	30%	84:16	42%
11	5 mol%	NaBARF (0.5)	37%	82:18	–
12	5 mol%	18-crown-6 (0.5)	No reaction	–	–
13	5 mol%	TBABr (0.5)	No reaction	–	–
14	1 mol%	–	9%	–	–
15	1 mol%	KOTf (0.1)	10%	–	–
16	1 mol%	KOTf (0.5)	traces	–	–
17	1 mol%	KOTf (1)	traces	–	–

Conditions: *rac*-**2.108** (0.25 mmol), KF (5 equiv), (*S*)-**2.78** (1–5 mol%), $PhCF_3$ (0.5 M), rt, stirring at 900 rpm. [a] Yield determined by ^{19}F NMR using 4-fluoroanisole as internal standard. [b] e.r. determined by HPLC using a chiral non-racemic stationary phase. [c] Yield determined by ^{1}H NMR using 4-fluoroanisole as internal standard.

4.5.2.3 Enantioselective Fluorination with KF: Solvent and Concentration Screening

In the fluorination with KF, additives afforded no improvement in the yield of (*R*,*R*)-**2.109** when 1 mol% of catalyst loading was used. Therefore, we focused on the solvent, reaction concentration, and KF equivalents (Table 4.8). The best results in terms of reactivity were obtained using chlorinated solvents (CH_2Cl_2: 45%, entry 8 or anhydrous $CHCl_3$: 59%, entry 9) with slight erosion of the enantiomeric ratio (81:19 e.r. *versus* 85:15 e.r.). The conversion being less than satisfactory, KF was not investigated further as fluorinating reagent.

Table 4.8: Enantioselective fluorination of *rac*-**2.108** with KF: solvent and concentration optimisation



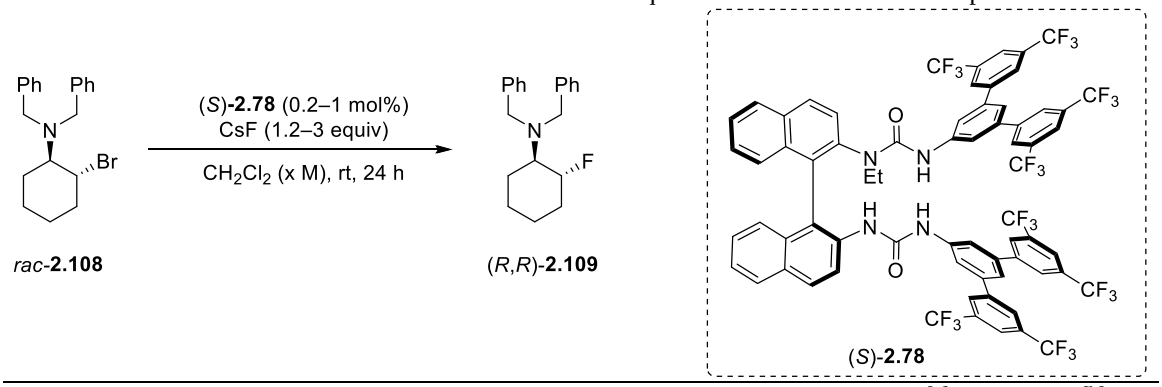
Entry	*Solvent*	*Concentration (M)*	*KF (equiv)*	*Yield* [a]	*e.r.* [b]
1	$PhCF_3$	1	5	15%	85:15
2	1,2-DFB	1	5	23%	81:19
3	CH_2Cl_2	1	5	27%	81.5:18.5
4	$PhCF_3$	2	5	24%	85:15
5	CH_2Cl_2	2	5	47%	81:19
6	$PhCF_3$	2	3	27%	85:15
7	1,2-DFB	2	3	25%	81:19
8	CH_2Cl_2	2	3	45%	81:19
9	$CHCl_3$[c]	2	3	59%	81.5:18.5

Conditions: *rac*-**2.108** (0.5 mmol), KF (5 equiv), (*S*)-**2.78** (1 mol%), rt, stirring at 900 rpm for 72 h. [a] Yield determined by ^{19}F NMR using 4-fluoroanisole as internal standard. [b] e.r. determined by HPLC using a chiral non-racemic stationary phase. [c] Anhydrous, filtered on basic alumina. 1,2-DFB = 1,2-difluorobenzene.

4.5.2.4 Enantioselective Fluorination with CsF: Solvent and Concentration Screening

A similar optimisation of solvent, concentration and equivalents of fluorinating reagent was conducted with CsF (Tables 4.9–4.10). It was immediately apparent that this fluorinating reagent was more reactive: while fluorination of *rac*-**2.108** with 5 equiv of KF in CH_2Cl_2 (1 M) in the presence of 1 mol% of (*S*)-**2.78** afforded (*R*,*R*)-**2.109** in 27% yield after 72 h (entry 3, Table 4.8), the reaction with 3 equiv of CsF using the same catalyst loading was completed in only 24 h (>95% yield, entry 2, Table 4.9). The catalyst loading could be reduced to 0.5 mol% with no erosion of enantioselectivity while maintaining good reactivity (88% yield, 81:19 e.r., entry 3). Further reduction to 0.2 mol% resulted in a lower yield and reduced enantioselectivity (33% yield, 79:21 e.r., entry 4). As observed in the fluorination with KF, increasing the concentration improved the yield, which allowed reduction of the equivalents of CsF required to reach full conversion from 3 to 1.2 (entries 3, 5–6).

Table 4.9: Enantioselective fluorination of *rac*-**2.108**: CsF equivalents and concentration optimisation

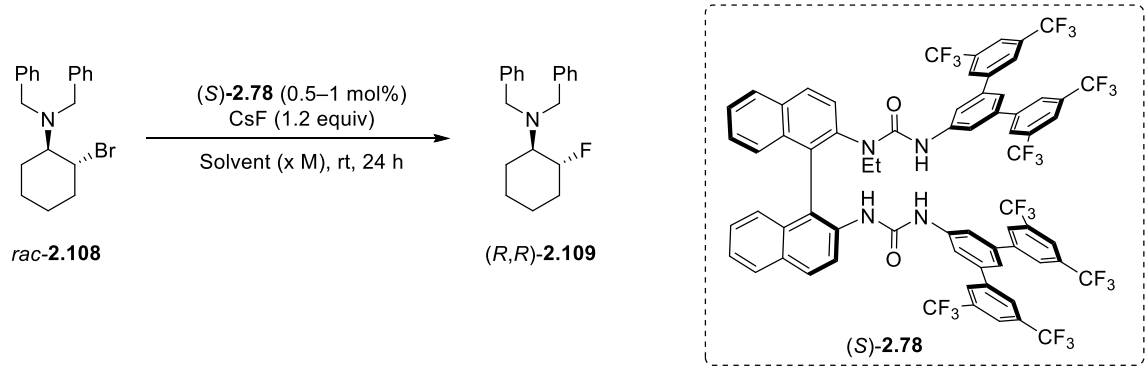


Entry	*(Conc./M)*	*(S)-**2.78** (mol%)*	*CsF (equiv)*	*Yield* [a]	*e.r.* [b]
1	0.5	1	3	91%	81:19
2	1	1	3	>95%	82:18
3	1	0.5	3	88%	81:19
4	1	0.2	3	33%	79:21
5	1	0.5	1.2	42%	81.5:18.5
6	2	0.5	1.2	87%	82:18

Conditions: *rac*-**2.108** (0.25 mmol), CsF, (*S*)-**2.78**, CH_2Cl_2, rt, stirring at 900 rpm for 24 h. [a] Yield determined by ^{19}F NMR using 4-fluoroanisole as internal standard. [b] e.r. determined by HPLC using a chiral non-racemic stationary phase.

In an effort to develop more sustainable processes, pharmaceutical companies are replacing traditional solvents with more environmentally friendly alternatives.[27,28] CH_2Cl_2 is an undesired solvent due to its toxicity and the rising concern of its ozone-depleting action, which might lead to its ban in the future.[29] Thus a screening of alternative solvents was conducted, but no efficient alternatives were found (Table 4.10). Moderate yields were obtained in $PhCF_3$ (65%, entry 2) and 1,2-difluorobenzene (1,2-DFB, 66%, entry 4) with 1 mol% of (*S*)-**2.78**, but yields in these solvents were poor at reduced catalyst loading ($PhCF_3$: traces, 1,2-DFB: 30%, entries 10–11). On the contrary, the reaction in CH_2Cl_2 in the presence of 0.5 mol% of (*S*)-**2.78** afforded (*R*,*R*)-**2.109** in 87% yield (entry 9).

Table 4.10: Enantioselective fluorination of *rac*-**2.108** with CsF: solvent and concentration optimisation



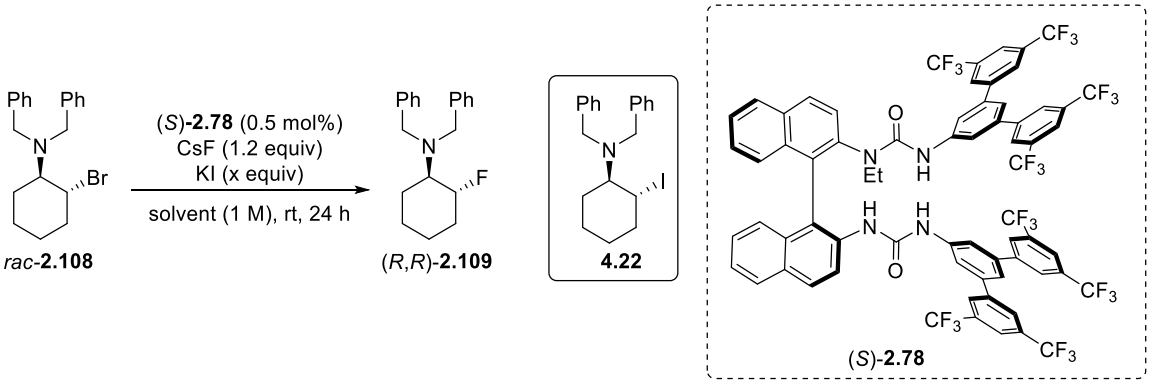
rac-**2.108** (*R*,*R*)-**2.109** (*S*)-**2.78**

Entry	*Solvent (Conc./M)*	*(S)-**2.78** (mol%)*	*Yield* [a]	*e.r.* [b]
1	CH_2Cl_2 (1)	1	90%	82:18
2	$PhCF_3$ (1)	1	65%	85:15
3	$PhCH_3$ (1)	1	21%	84.5:15.5
4	1,2-DFB (1)	1	66%	81.5:18.5
5	BuCN (1)	1	10%	–
6	MeTHF (1)	1	traces	–
7	Anisole (1)	1	35%	84:16
8	EtOAc (1)	1	traces	–
9	**CH_2Cl_2 (2)**	**0.5**	**87%**	**82:18**
10	$PhCF_3$ (2)	0.5	traces	–
11	1,2-DFB (2)	0.5	30%	82:18

Conditions: *rac*-**2.108** (0.25 mmol), CsF (1.2 equiv), (*S*)-**2.78**, rt, stirring at 900 rpm for 24 h. [a] Yield determined by ^{19}F NMR using 4-fluoroanisole as internal standard. [b] e.r. determined by HPLC using a chiral non-racemic stationary phase. 1,2-DFB: 1,2-difluorobenzene

We next evaluated the effect of additives in the solvents that gave the highest yields (CH_2Cl_2, 1,2-DFB and $PhCF_3$, Table 4.11), but as previously observed for the enantioselective fluorination with KF (section 4.5.2.2), addition of KI had no effect or was detrimental at reduced catalyst loading (0.5 mol% *versus* 5 mol% used in section 4.5.2.1).

Table 4.11: Effect of additives on the enantioselective fluorination of *rac*-**2.108** with CsF in the presence of 0.5 mol% of (*S*)-**2.78**



Entry	*Solvent*	*KI equiv*	*Yield of (R,R)-**2.109**[a]*	*e.r. [b]*	*Yield of **4.22**[c]*
1	$PhCF_3$	–	34%	84:16	–
2	$PhCF_3$	0.1	29%	83.5:16.5	traces
3	$PhCF_3$	0.5	24%	84:16	traces
4	1,2-DFB	–	39%	81:19	–
5	1,2-DFB	0.1	31%	81.5:18.5	traces
6	1,2-DFB	0.5	17%	81.5:18.5	34%
7	CH_2Cl_2	–	42%	81.5:18.5	–
8	CH_2Cl_2	0.1	43%	82:18	traces
9	CH_2Cl_2	0.5	40%	81.5:18.5	17%

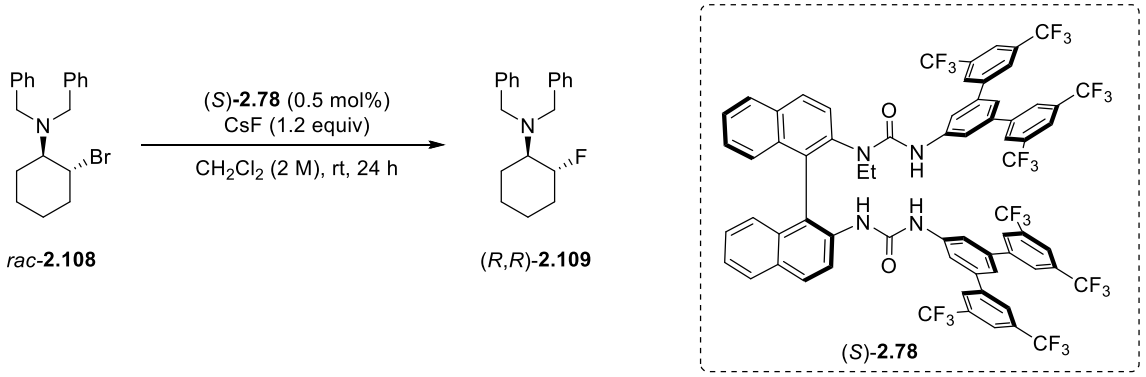
Conditions: *rac*-**2.108** (0.3 mmol), CsF (1.2 equiv), (*S*)-**2.78** (0.5 mol%), solvent (1 M), rt, stirring at 900 rpm for 24 h. [a] Yield determined by ^{19}F NMR using 4-fluoroanisole as internal standard. [b] e.r. determined by HPLC using a chiral non-racemic stationary phase. [c] Yield determined by ^{1}H NMR using 4-fluoroanisole as internal standard.

4.5.2.5 Enantioselective Fluorination with CsF: Granulometry and Water Content

In preparation to scale-up, we performed additional experiments to assess the impact of CsF purity and granulometry (Table 4.12). Purity had no effect on the reaction outcome (entries 2–3), while the fluorination was higher yielding when CsF was used in powder form (particle distribution: 2–300 µm, 87% yield, entry 2) compared to millimetric particles

(1–2 mm, 25% yield, entry 1), as expected for a phase-transfer mechanism. Water content had an impact on yield but did not affect enantioselectivity. CsF as provided by the supplier[ii] afforded (*R*,*R*)-**2.109** in 86% yield and 81:19 e.r. (entry 3), compared to 74% yield and 81.5:18.5 e.r using CsF dried at 200 °C *in vacuo* for 48 h (entry 4). Finally, addition of water to the reaction with dry CsF was highly detrimental for reactivity: 10 mol% (0.46% mass of H_2O/mass CsF) of added water reduced the yield of (*R*,*R*)-**2.109** to 65% (entry 5), and 50 mol% (4.8% mass of H_2O/mass CsF) completely suppressed the fluorination (entry 6). Control of CsF granulometry and water content are thus important parameters to ensure reproducibility between different batches.

Table 4.12: Effect of CsF purity, granulometry and water content on the enantioselective fluorination of *rac*-**2.108** under HB-PTC.



Entry	*CsF (purity)*	*H_2O/ CsF (w/w %)*	*Yield* [a]	*e.r.* [b]
1	Particle[c] (99.9%)	–	25%	81.5:18.5
2	Powder[d] (99.9%)	–	87%	81.5:18.5
3	Powder[d] (99%)[e]	–	86%	81:19
4	Powder[d], dry[f] (99%)	–	74%	81.5:18.5
5	Powder[d], dry[f] (99%)	H_2O (0.96)	65%	82:18
6	Powder[d], dry[f] (99%)	H_2O (4.8)	traces	–

Conditions: *rac*-**2.108** (1.40 mmol), CsF (1.2 equiv), (*S*)-**2.78** (0.5 mol%), CH_2Cl_2 (2 M), rt, stirring at 900 rpm for 24 h. [a] Yield determined by ^{19}F NMR using 4-fluoroanisole as internal standard. [b] e.r. determined by HPLC using a chiral non-racemic stationary phase. [c] Particle distribution: 1–2 mm. [d] Particle distribution: 2–300 μm. [e] Water content: 0.98% w/w. [f] Dried *in vacuo* at 200 °C for 48 h and reaction performed using Schlenk technique.

[ii] Fluorochem, 0.98% w/w H_2O/CsF (determined by Karl-Fisher titration by the supplier).

CsF 99% supplied by Fluorochem was selected for the scale-up, due to its availability in powder form and lower price (£ 214.00/ kg) compared to the CsF 99.9% trace metal basis from Sigma Aldrich that we used in previous studies (£ 271.20/ kg, supplied as particles of variable size). The batch of CsF used in the scale-up was analysed by optical microscopy. The CsF particles consisted of plates and irregular prisms with a particle size distribution between 2 and 300 μm (Figure 4.7).

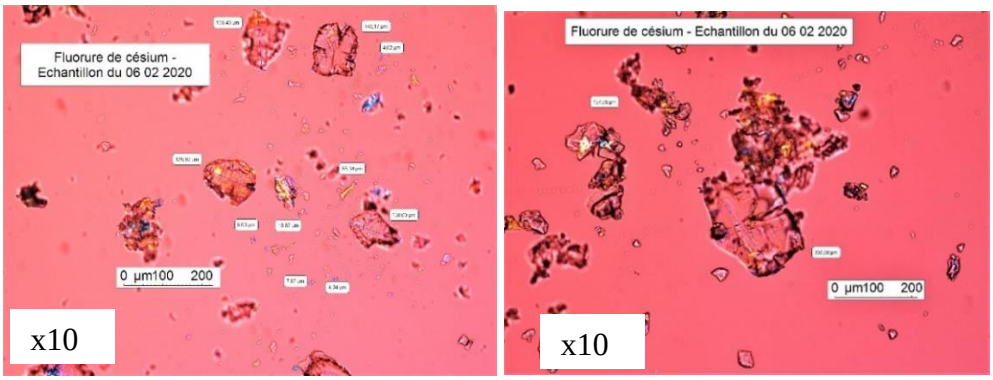


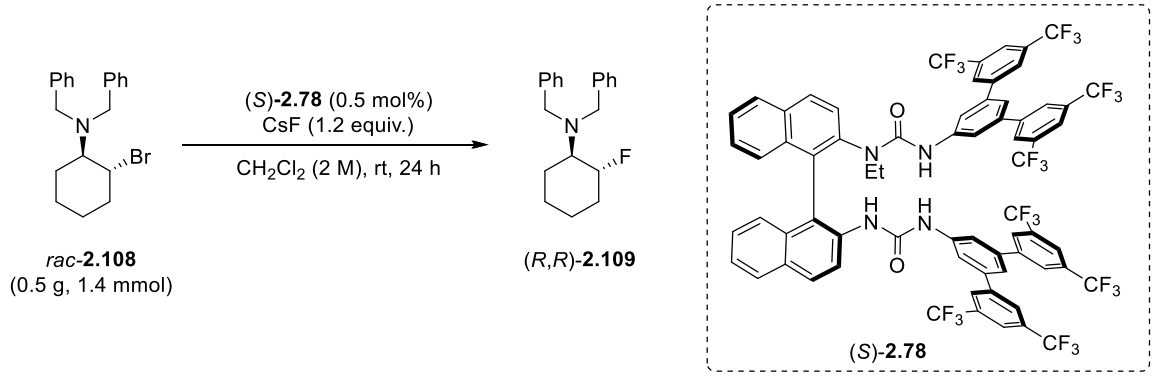
Figure 4.7: Analysis by optical microscopy of the batch of CsF used in the scale-up (batch FCB077873, catalogue code: 001648, Fluorochem). Analysis conducted by Dr. Robert Benoit (SANOFI).

4.6 Scale-up in Round-bottom Flasks

Next, we assessed whether the order of addition of the reagents to the reaction vessel was important. The batch conditions used in the previous screening reactions, where all the solid reagents were charged first followed by addition of the solvent, are rarely used on industrial scale due to the potential safety hazard posed by reagent accumulation. Starting from 0.5 g of *rac*-**2.108** and using batch conditions, (*R*,*R*)-**2.109** was obtained in 88% ^{19}F NMR yield and 81.5:15.5 e.r. after 24 h (entry 1, Table 4.13). When the catalyst and CsF were pre-stirred for 45 min before addition of the substrate as a solid, the outcome of the fluorination was unchanged (83% ^{19}F NMR yield after 24 h, 82:18 e.r., entry 2). The same outcome (82% ^{19}F NMR yield in 24 h, 82:18 e.r., entry 3) was obtained if the starting material *rac*-**2.108** and the catalyst were stirred alone for 45 min before addition of solid CsF.

Addition order is thus inconsequential, and we selected this last procedure for the reaction in a mechanically stirred reactor on 200 g of β-bromoamine *rac*-**2.108** (Section 4.9).

Table 4.13: Effect of the order of additions of reagents on the enantioselective fluorination of *rac*-**2.108** with CsF



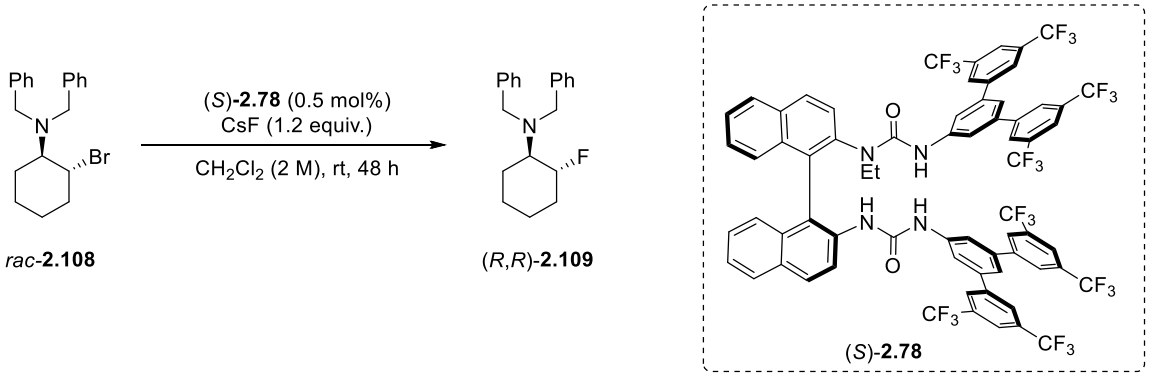
Entry		*Conditions*	*Yield* [a]	*e.r.* [b]
1	**Batch**	Solid reagents added to the vial before addition of CH_2Cl_2.	88%	81.5:18.5
2	**Semi-batch**	(*S*)-**2.78** and CsF were stirred in CH_2Cl_2 for 45 min before addition of *rac*-**2.108** as a solid.	83%	82:18
3	**Semi-batch**	(*S*)-**2.78** and *rac*-**2.108** were stirred in CH_2Cl_2 for 45 min before addition of solid CsF.	82%	82:18

Reaction conditions: *rac*-**2.108** (0.5 g), CsF (1.2 equiv) and (*S*)-**2.78** (0.5 mol%), CH_2Cl_2 (2 M) stirring at rt, 900 rpm in a vial for 24. [a] Yield determined by ^{19}F NMR using 4-fluoroanisole as internal standard; isolated yields in parenthesis. [b] e.r. determined by HPLC using a chiral non-racemic stationary phase.

Prior to performing the fluorination in the mechanically stirred reactor, we evaluated the scalability of the reaction in round-bottom flasks (RBFs, Table 4.14). The yields given are both ^{19}F NMR yield determined on the crude prior to purification and isolated yields after aqueous work-up (in parenthesis). More details on the isolation and purification of the desired β-fluoroamine (*R*,*R*)-**2.109** are given in sections 4.7 and 4.8, respectively. Two parallel reactions on 5 g each were run first in two different laboratories (University of Oxford and SANOFI) using different reagents and catalyst batches to evaluate reproducibility (entries 1–2, Table 4.14, information on the reagents are reported in the caption). The reactions gave the same outcome; thus, we further scaled the fluorination up

to 10 g and 50 g, always reaching full conversion within 48 h. After aqueous work-up (section 4.7) the product was isolated in 84–90% yield and 81.5:18.5–82:18 e.r.

Table 4.14: Scale-up of the enantioselective fluorination of *rac*-**2.108** with CsF in RBFs



Entry	*Scale*	*Conversion*[a]	*Isolated Yield*	*e.r.* [b]
1[c]	5 g (14 mmol)	>95%	84 %	81.5:18.5
2[d]	5 g (14 mmol)	>95%	91%	81.5:18.5
3	10 g (28 mmol)	>95%	93%	82:18
4	50 g (140 mmol)	>95%	90%	81.5:18.5

Reaction conditions: Batch conditions, *rac*-**2.108**, CsF (1.2 equiv) and (*S*)-**2.78** (0.5 mol%), CH_2Cl_2 (2 M) stirring at rt, 900 rpm in a vial or RBF for 24–48 h. [a] Estimated by analysis of the ^{1}H-NMR spectrum of the crude reaction mixture; [b] e.r. determined by HPLC using a chiral non-racemic stationary phase. [c] *rac*-**2.108** was synthetised in Oxford, CsF 99% was purchased from Fluorochem, (*S*)-**2.78** was synthesised *via* the "quadruple Suzuki-Miyaura cross coupling route" (section 3.3.4), the CH_2Cl_2 was purchased from Sigma-Aldrich (stabilised with amylene). Unoptimised isolation conditions. [d] *rac*-**2.108** was outsourced to WuXi AppTec, CsF 99% was purchased from Fluorochem (batch FCB077873), (*S*)-**2.78** was synthesised by "the isocyanate route" (section 3.3.5), the CH_2Cl_2 was purchased from Carlo Erba Reagents (stabilised with amylene). These reagents were used in section 4.9 as well.

4.7 Optimisation of the Isolation and Work-up Conditions

In parallel with the optimisation of the reaction, we optimised the isolation conditions to maximise product recovery. At the end of the fluorination, the crude reaction mixture was filtered through a short plug of silica gel to remove the inorganic salts and any residual fluoride present in solution. The plug was then washed with a 1:1 mixture of CH_2Cl_2:Et_2O. This protocol has been used in the screening reactions reported in the previous sections (section 4.5–4.6), and it was retained in the scale-up with substitution of Et_2O with the less volatile and less flammable $^iPr_2O$ (boiling point: 69 °C, flash point: –28 °C, closed cup).

The use of Et_2O is discouraged in industrial settings due to its low boiling point (34.6 °C), flash point (–40 °C, closed cup) and autoignition temperature (180 °C) as well as its tendency to form peroxides.[27,28]

On a small scale (≤ 100 mg) product isolation and purification were done by means of silica gel chromatography. To avoid chromatographic purification, we sought to exploit the higher basicity of the product (an amine) compared to the catalyst (a bis-urea) using an acidic aqueous extraction for their separation. This involved a first extraction with HCl, to protonate the product and bring it into the aqueous phase, followed by neutralisation with NaOH and a second extraction with CH_2Cl_2 to recover the free base. The catalyst was retained in the organic phase of the first extraction, and its purification is reported in section 4.10. Various solvents were tested for the first extraction with the aim to maximise purity and recovery of (*R*,*R*)-**2.109**: this led to the selection of $^{i}Pr_2O$ for the organic phase. Et_2O performed equally well, but it was disregarded for safety concerns. CH_2Cl_2 was able to solubilise the hydrochloric salt of the product, which was identified in the ^{1}H NMR of the organic phase by the presence of a broad signal at 12.42 ppm, alongside the cyclohexyl and benzylic protons. Accordingly, product recovery was poor (13%). Finally, product recovery using EtOAc (84%) was slightly less than for ethers (quantitative).

It is worth noting at this point that the solubility of the product (*R*,*R*)-**2.109** in ether (Et_2O and $^{i}Pr_2O$) is superior to that of the starting material *rac*-**2.108**. In case of poor conversion in the fluorination, EtOAc is a better solvent to dissolve the crude reaction mixture. The same protocol described above, involving a first extraction with HCl, neutralisation with NaOH and a second extraction with CH_2Cl_2, but using EtOAc as the organic phase for the first extraction, can be used to recover unreacted starting material. At very low conversion (<20%), trituration in $^{i}Pr_2O$ is an effective means to purify the starting material *rac*-**2.108** from the product (*R*,*R*)-**2.109**.

4.8 Optimisation of the Recrystallisation

The product of fluorination under HB-PTC had only a moderate e.r. (81.5:18.5 e.r.). Different solvents were evaluated for the recrystallisation of the free amine (*R*,*R*)-**2.109** with the aim to obtain it enantiopure, but no enhancement was observed in any case (see Chapter 5, Table 5.7). In most cases e.r erosion (73:27–79.5:20.5 e.r.) was found instead.

The difficulties experienced in recrystalising the free amine were expected considering its low melting point (69–71 °C), and it prompted us to perform the recrystallisation of the corresponding salt. Since the anion might have an impact, different salts were synthesised (Table 4.15). Strong inorganic acid (HCl, HBr, entries 1–2, Table 4.15), trifluoroacetic acid (TFA, entry 4) and sulfonic acids (entries 6–7) afforded the desired salts, while triflic acid caused product decomposition (entry 8). Weak carboxylic acids, such as acetic (pKa=12.3, DMSO entry 3)[30] or benzoic acid (pKa=11.1, DMSO entry 5)[30] were unable to protonate (*R*,*R*)-**2.109**. This is in line with the expected lower basicity of the amine caused by the presence of the neighbouring fluorine.[iii]

Table 4.15: Acids evaluated in the formation of the HX salt of (*R*,*R*)-**2.109**

Entry	*Acid*	*Acid pKa (DMSO)* [30]	*Note*
1	HCl	1.8	6 M in ^{i}PrOH
2	HBr	0.9	Generated *in situ* from AcBr/MeOH[31]
3	AcOH	12.3	Free amine recovered
4	CF_3COOH (TFA)	3.45	–
5	BzOH	11.3	Free amine recovered
6	MsOH	1.6	–
7	TsOH	8.45[a]	–
8	TfOH	0.3	Degradation

[a] measured in CH_3CN.[32]

[iii] Typical values for tertiary, non-fluorinated amines: pK_a Et_3NH^+ = 9.0, DMSO;[38] pK_a $BnMe_2NH^+$ = 7.6, DMSO;[39]
ΔpK_a for monofluorination in the β position is ΔpK_a =1,7[16], section 1.2.1.2.

Next, the HCl, HBr, CF_3COOH, MsOH and TsOH salt of (*R,R*)-**2.109** were tested in the recrystallisation employing a variety of solvents and solvent mixtures. The tests were performed on 0.5 g of salt, adding 500 μL (corresponding to 1vol=1 mL/g) of solvent and warming up the mixture to the boiling point. If no dissolution was obtained, the procedure was repeated with addition of further 500 μL of solvent until a maximum of 10 vol (5 mL). When solubilisation was attained, the system was left at rt for 24 h, after which the recrystallisation yield was determined by weighing the solid obtained. In the absence of precipitation, the system was first transferred in the fridge (+ 4 °C) for further 24 h, and then in the freezer (–20 °C). In all cases, after having determined the yield, the recrystallised salt was neutralised with NaOH 5 M and the e.r. was determined on the free base by chiral phase HPLC analysis. Selected results of the trials are reported in Table 4.16 (see Chapter 5, Tables 5.8–5.12 for the full screening results). Only recrystallisation of the TFA salt afforded (*R,R*)-**2.109***HX in more than 95:5 e.r. when EtOAc was used as solvent (96:4 e.r., 47% yield entry 5, Table 4.16). A slightly worse e.r. but better recovery was obtained for the recrystallisation of the same salt from ^{i}PrOH (94:6 e.r. and 64% yield, entry 4). Recrystallisation of the TsOH salt in toluene (entry 9) caused precipitation of the racemate (32%, 58:42 e.r.) and enantioenrichment of the mother liquor (97:3 e.r.).

Table 4.16: Selected recrystallisation results of (*R,R*)-**2.109***HX

Entry	*Salt*	*Solvent (mL/g)*	*Recrystallisation yield*	*e.r.*
1	**2.109***HCl	^{i}PrOH (2)	91%	82.5:17.5
2	**2.109***HBr	^{i}PrOH (1)	56%	80.5:19.5
3	**2.109***TFA	EtOH (1)	50%	74:26
4	**2.109*TFA**	**^{i}PrOH (1)**	**64%**	**94:6**
5	**2.109*TFA**	**EtOAc (1)**	**47%**	**96:4**
6	**2.109***MsOH	EtOH (2)	48%	83:16
7	**2.109***MsOH	^{i}PrOH (2)	83%	84.5:15.5
8	**2.109***TsOH	EtOAc (1)	45%	61.5:38.5
9	**2.109***TsOH	Toluene (2)	32%	58:42 (ML: 97:3)

The starting e.r. of (*R,R*)-**2.109** was 81.5:18.5 e.r. ML = Mother liquor.

As recrystallisation of (*R*,*R*)-**2.109***TFA gave the highest enhancement of e.r., we scaled the process up to 5 g of salt (entries 1–3, Table 4.17) to determine the optimal aging time and temperature to maximise both recovery and enantioselectivity. To achieve this, after dissolution of the salt, the solution was slowly cooled to the desired temperature, which was maintained constant with a thermostatic bath. The recrystallisation was performed while stirring to maintain homogeneous conditions of temperature and oversaturation. Recrystallisation in ^{i}PrOH furnished a higher recovery compared to EtOAc (57% *versus* 41%, entries 1 and 3) with a similar level of enantioenrichment (97:3 *versus* 97.5:2.5). When the recrystallisation was further scaled up to 40 g (entries 4–7) it became apparent that strict control of the temperature and of the recrystallisation time were necessary to obtain the desired level of enrichment.

Table 4.17: Scale-up of the recrystallisation of (*R*,*R*)-**2.109***TFA

Entry	**2.109***TFA (g)	Solvent (mL/g)	Cooling to (°C)	Aging for (h)	Recrystallisation yield	e.r.
1	5	^{i}PrOH (1)	25	3	57%	97:3
2	5	^{i}PrOH (1)	35	18	50%	97:3
3	5	EtOAc (0.6)	25	3	41%	97.5:2.5
4	40	^{i}PrOH (1)	25	18	77%	82:18
5	40	^{i}PrOH (1)	30	4	79%	85:15
6	**40**	**^{i}PrOH (1)**	**35**	**5**	**50%**	**97.5:2.5**
7	40	^{i}PrOH (1)	35	18	67%	85:15

The starting e.r. of (*R*,*R*)-**2.109** was 81.5:18.5 e.r.

4.9 Scale-up in a Mechanically Stirred 1 L Reactor

4.9.1 Fluorination on 200 g of *rac*-2.108

Having demonstrated the scalability of the reaction in magnetically stirred RBFs up to 50 g (section 4.6) and having developed a reliable method to isolate (section 4.7) and purify the product (section 4.8), we were ready for the scale-up on 200 g of *rac*-**2.108** in a mechanically stirred reactor. For this experiment, we used the 1 L heat-flow calorimeter OptiMax™ from Mettler Toledo, which enabled us to collect calorimetric data during the reaction (section 4.9.3). Full details of the set-up are reported in Figure 4.8. The mixing was provided by a 45° down-pumping four-blade pitched blade turbine (PBT) positioned at 10 mm from the reactor bottom. Additionally, the reactor was equipped with a flat glass baffle, a calibration probe, and a temperature probe, also having an off-bottom clearance of 10 mm. While the last two inserts were required for the RC study, they also acted as additional baffles contributing to disruption of the vortex generated by the impeller rotation.

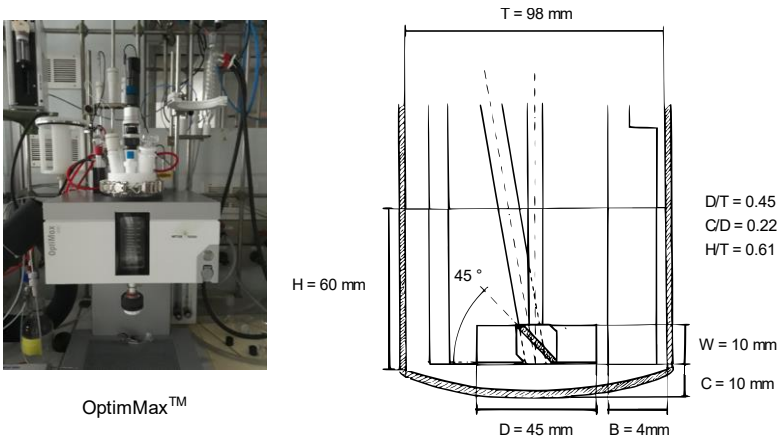


Figure 4.8: Set-up of the OptiMax™ HFCal Mettler Toledo reactor for the fluorination on 200 g of *rac*-**2.108**.

The reactor was charged with 250 mL of CH_2Cl_2 and 200 g of *rac*-**2.108**. The jacket temperature was set at 22 °C and the stirring speed at 1100 rpm. When the substrate was fully solubilised (determined by visual inspection) and the temperature was stable at 22 °C, the catalyst was added as a solid, followed by the solid CsF in a single charge. The reaction was monitored by quantitative ^{19}F NMR and compared with a 10 g scale reaction run in a

magnetically stirred RBF (Figure 4.9). The profiles of the two graphs are in good agreement. Though the yield of the 200 g scale reaction was slightly lower after the first 24 h (75% *versus* 88%), both reactions reached completion within 48 h.

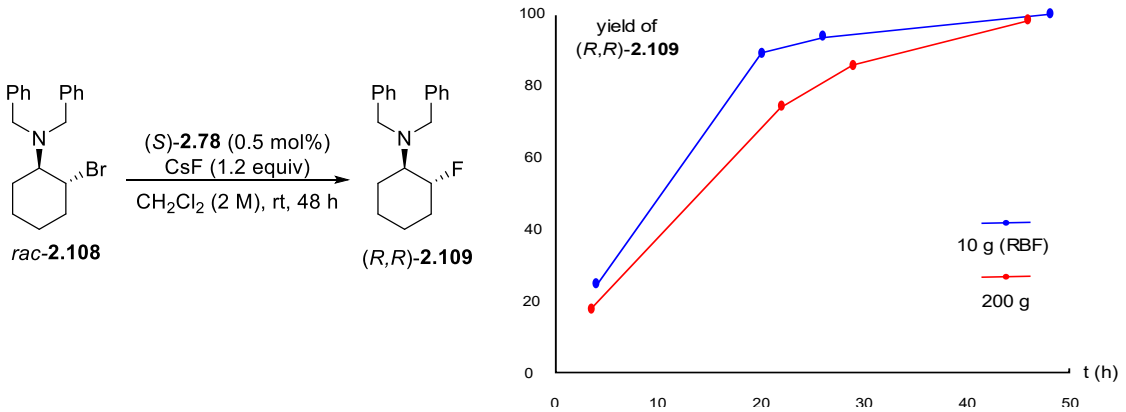
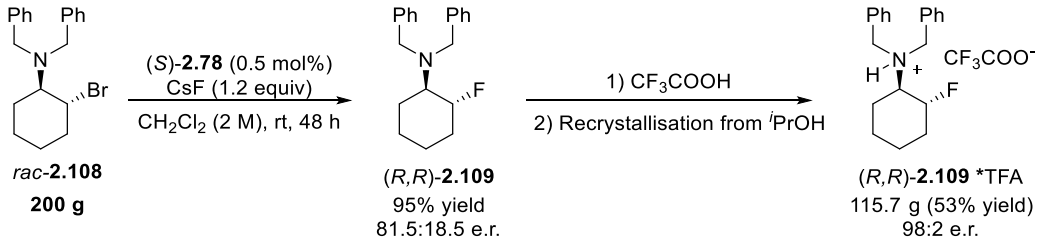


Figure 4.9: Fluorination under magnetic stirring (10 g scale, reaction in RBF, blue line) and under mechanical stirring (200 g scale, reaction in the OptiMax^{TM}, red line).

After filtration, the product was separated from the catalyst according to the acid-base extraction described in section 4.7. This afforded 157.39 g of (*R*,*R*)-**2.109** (95% yield and 81.5:18.5 e.r.). After formation of the trifluoroacetic acid (TFA) salt, the recrystallisation was performed in ^{i}PrOH, cooling the solution to 35 °C over 2 h and then maintaining this temperature for a further 4 h. After this time, the solid was filtered and washed twice with cold (+4 °C) ^{i}PrOH to afford 115.7 g of TFA*(*R*,*R*)-**2.109** in 98:2 e.r. (53% recrystallisation yield). The e.r. of recrystallised TFA*(*R*,*R*)-**2.109** was determined on 5 samples taken randomly and neutralised with $NaOH_{(aq)}$ 5 M. The free base was then analysed by HPLC using a chiral non-racemic stationary phase. All the samples had the same e.r. (98:2 e.r.).



Scheme 4.9: HB-PTC enantioselective fluorination with CsF on 200 g of *rac*-**2.108** and recrystallisation of (*R*,*R*)-**2.109***TFA.

4.9.2 Preliminary Results on Mixing Parameters

The OptiMax™ was able to achieve a high level of energy dissipation, providing the best conditions for a heterogeneous reaction involving a solid suspension. To collect further data, we repeated the fluorination on the same scale (200 g) in a 1 L Radley reactor. The impeller was the same as the OptiMax™, a PTFE 45 ° down-pumping PBT, but the maximum motor speed achievable was 678 rpm (*versus* 1100 rpm for the OptiMax™). The reactor was equipped with four equally spaced flat baffles. The order of additions of the reagents was the same as for the reaction described in section 4.9.1. Samples were taken regularly and analysed by quantitative ^{19}F NMR revealing that the reaction stalled at 11% conversion after 24 h. No further conversion was recorded in the subsequent 48 h. To verify whether this was due to poor mixing, we collected two samples from the stirred reaction at 24 h and 48 h and transferred them in vials equipped with magnetic stirring bars. Care was taken in sampling also the suspended solid, but due to the non-homogeneous suspension, the amount of CsF in the two samples might have been different. The samples were stirred in the vials for a further 48 h after which they were passed through a silica plug, and the conversion estimated by ^{1}H NMR. While in the meanwhile the conversion in the main reactor was still at 11%, the magnetically stirred samples reached 58% and 77% conversion. No further catalyst nor CsF were added to the samples: the only difference compared to the Radley reactor was the type of mixing.

Previously, we had observed dependence of the reaction conversion on mixing when we conducted the fluorination in an unbaffled 500 mL Mettler Toledo RC1AP01™ calorimeter equipped with a glass 45 ° down-pumping PBT. In that case, the calibration and temperature probes were insufficient to provide adequate baffling and a vortex was formed. The fluorination was conducted on 100 g of *rac*-**2.108**, following the same protocol as

reported in section 4.9.1. The yield after 28 h was 50% (determined by quantitative ^{19}F NMR) and it did not improve after a further 24 h (56%).

As described in section 4.1, the phase transfer is influenced by the ability of the reactor to fully suspend the solid particles and by the level of energy dissipation achieved, which has also an impact on precipitation of CsBr. CsF and CsBr are dense solids (4.12 g/cm^3 and 4.44 g/cm^3 respectively) difficult to suspend. We considered the two reactions described above, which did not proceed to full conversion (11% and 56% yield), and two that reached completion, namely the 200 g scale fluorination performed in the OptiMax™ (>95% yield) and a 3 g scale performed in a TOP45 autoclave reactor of 22 mL capacity, fully baffled, stirred by a four-bladed turbine (95% yield). We performed preliminary calculations using Dynochem® to investigate the mixing parameters of these trials.[33] Dynochem® is a software widely used by process chemists and engineers in the pharmaceutical and agrochemical industries to evaluate the impact of scale-up on mixing and heat transfer. The toolbox is based on engineering correlations and calculation approaches generally accepted within the community and has been developed by experts in fluid mixing.

The most relevant parameters at the scale of the tests (< 1 L) are the maximum energy dissipation rate at the impeller region (ε_{max}) and the impeller average turbulent shear rate (γ_{imp}). The energy dissipation rate ε is the most important parameter for mixing because it represents the rate at which the impeller kinetic energy is dissipated in the fluid, through the formation of eddies. It varies greatly within a stirred tank, with the region near the impeller blades having the highest value and the liquid surface the lowest. The local maximum energy dissipation rate at the impeller region (ε_{max}) has been calculated according to eq. 4.6, which is based on the flow of the trailing vortex produced by a turbine.[34] χ is a parameter that quantifies the relative size of the trailing vortex and the impeller blade width. Reported values are between 12 and 17, so the calculation is based

on χ=15. P_0 is the power number of the impeller, N is the impeller speed in s^{-1} and D the impeller diameter in m.

$$\varepsilon_{max} = 0.104\,\chi P_0^{3/4} N^3 D^2 \quad \text{(eq. 4.6)}$$

The shear rate γ is the rate at which fluid layers move past each other and it is associated with the spatial velocity gradient within the fluid. In a stirred tank both turbulent and laminar shear rates exist. The impeller average turbulent shear rate (γ_{imp}) has been calculated according to eq.4.7.[35,36]

$$\gamma_{imp} = \left(\frac{0.3P}{V_{imp}\mu}\right)^{1/2} \quad \text{(eq. 4.7)}$$

P is the power input and 0.3P is used in the calculation because it has been demonstrated that 30% of the power is dissipated in the impeller region.[35] μ is the liquid viscosity and V_{imp} is the bottom impeller zone volume calculated according to eq. 4.8.

$$V_{imp} = \frac{D^4}{4\pi^{D/4}} \quad \text{(eq. 4.8)}$$

A clear cut-off at ε_{max} ~ 300 W/Kg and γ_{imp} ~ 10 000 s^{-1} was found between the reactions that reached full conversion and those that stalled at around 50% conversion or less (Table 4.18).

Table 4.18: Maximum energy dissipation rate ε_{max} and impeller average share rate γ_{imp} for different reactor set-ups.

Entry	*Reactor volume*	*Conversion[a] (48 h)*	*ε_{max} (W/Kg)*	*γ_{imp} (s^{-1})*
1	22 mL	95%	330	12 000
2	1 L	97%	310	10 000
3	1 L	11%	80	5 000
4	0.5 L	56%	20	2 000

Conditions: *Entry 1:* TOP45 autoclave reactor (tank: 725-4), 22 cm^3, 100% baffled, four-bladed turbine, 2050 rpm, on 3 g of *rac*-**2.108**. *Entry 2:* OptiMax™ HFCal Mettler Toledo, 1 L, 98% baffled, 45° down-pumping four-blade PBT, 1100 rpm, on 200 g of *rac*-**2.108** *Entry 3:* Radley reactor, 1 L, 100% baffled, 45° down-pumping four-blade PBT, 678 rpm, on 200 g of *rac*-**2.108**. *Entry 4:* RC1AP01™ calorimeter Mettler Toledo, 0.5 L, 31% baffled (temperature and calibration probes), 45° down-pumping four-blade PBT, 600 rpm, on 100 g of *rac*-**2.108**; [a] Determined by ^{1}H NMR. Calculations performed by Diké-Michel Alozie (SANOFI).

High shear rates might contribute to increased corrosion and result in low CsBr particle size distribution. This can potentially be problematic on an industrial scale, due to increased wall deposit and, depending on the agglomeration mechanism, reduced filterability of the crude reaction mixture. Analysis by optical (Figure 4.10) and scanning electron microscopy (SEM, Figure 4.11) of solid CsBr formed in the 200 g scale fluorination run in the OptiMax™ was performed to collect preliminary data. The solid consisted of agglomerates (about 100 µm) of spherical particles with narrow particle size distribution (5–10 µm).

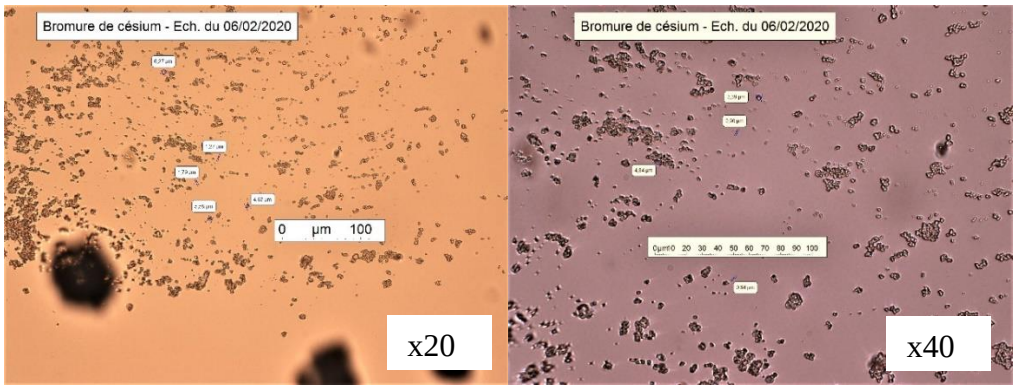


Figure 4.10: Optical microscopy analysis of a sample of CsBr obtained in the fluorination on 200 g of *rac*-**2.108** at different magnification. Analysis conducted by Dr. Robert Benoit (SANOFI).

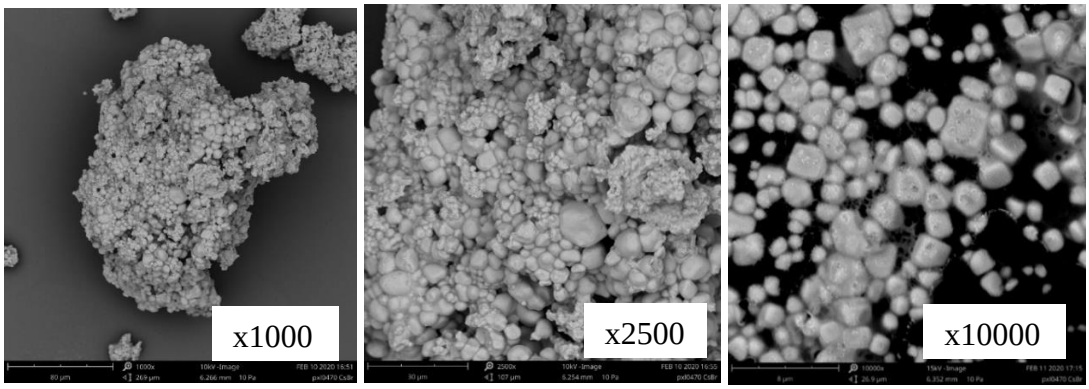


Figure 4.11: SEM analysis of a sample of CsBr obtained in the fluorination on 200 g of *rac*-**2.108** at different magnification. The CsBr consisted of both conglomerates (left, centre) and small particles (1–2 µm, right). Analysis conducted by Dr. Robert Benoit (SANOFI).

4.9.3 Calorimetric Experiments

4.9.3.1 Differential Scanning Calorimetry (DSC) Tests

Prior to scale-up, preliminary DSC tests were run on samples of pure starting material *rac*-**2.108**, catalyst (*S*)-**2.78** and product (*R*,*R*)-**2.109**, as well as on the reaction mixture sampled immediately after addition of CsF and after 48 h. The samples were weighed in gold-plated crucibles of 40 µL capacity without taking any precaution to exclude oxygen (air atmosphere). The analysis was conducted in the 0 °C to 400 °C range applying a heating rate of 5 °C/min using a Mettler Toledo instrument. The results of the tests are reported in Figures 4.12–4.14. The DSC curves of the initial reaction mixture, sampled immediately after addition of CsF, and of the starting material are overlaid to emphasise their similarity (Figure 4.12). The same is done for the DSC curves of the final reaction mixture, sampled after 48 h, and of the product (Figure 4.13).

In all cases, major decomposition events (*i.e*. releasing more than 100 J/g) do not take place below 150 °C. The substrate *rac*-**2.108** is stable up to 150 °C, when it decomposes with a highly exothermic peak (159 J/g), characterised by a slow onset of decomposition. The product (*R*,*R*)-**2.109** melts at 77 °C with a low specific latent heat of fusion (L_f = 67 J/g). This event is followed by a small exothermic peak (20 J/g) at 95 °C, probably due to air oxidation, and by a significantly exothermic decomposition (274 J/g) starting at 215 °C. The catalyst (*S*)-**2.78** starts melting at 210 °C (MP: 228 °C) followed immediately by decomposition with release of 64.5 J/g (Figure 4.14). Dilution in CH_2Cl_2 (2 M) reduces the amount of heat exchanged by the starting material and product, but qualitatively the curves of the reaction mixture follow those of pure **2.108** (Figure 4.12) and **2.109** (Figure 4.13).

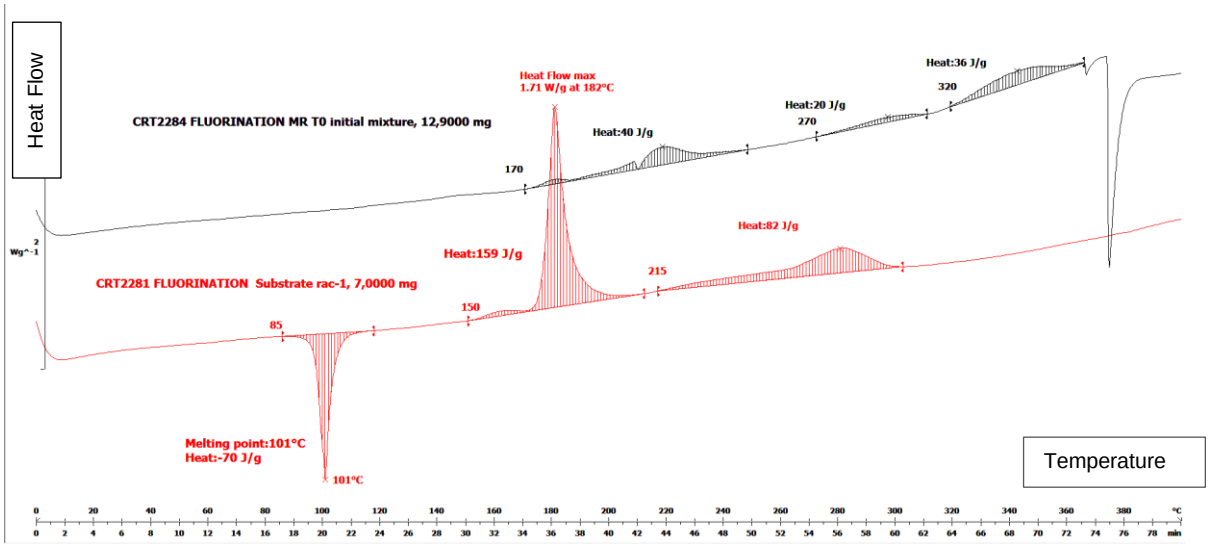


Figure 4.12: DSC curve of the starting material *rac*-**2.108** (red) overlaid with the DSC curve of the reaction mixture sampled immediately after addition of CsF (black). Analysis performed by Philippe Courtes (SANOFI).

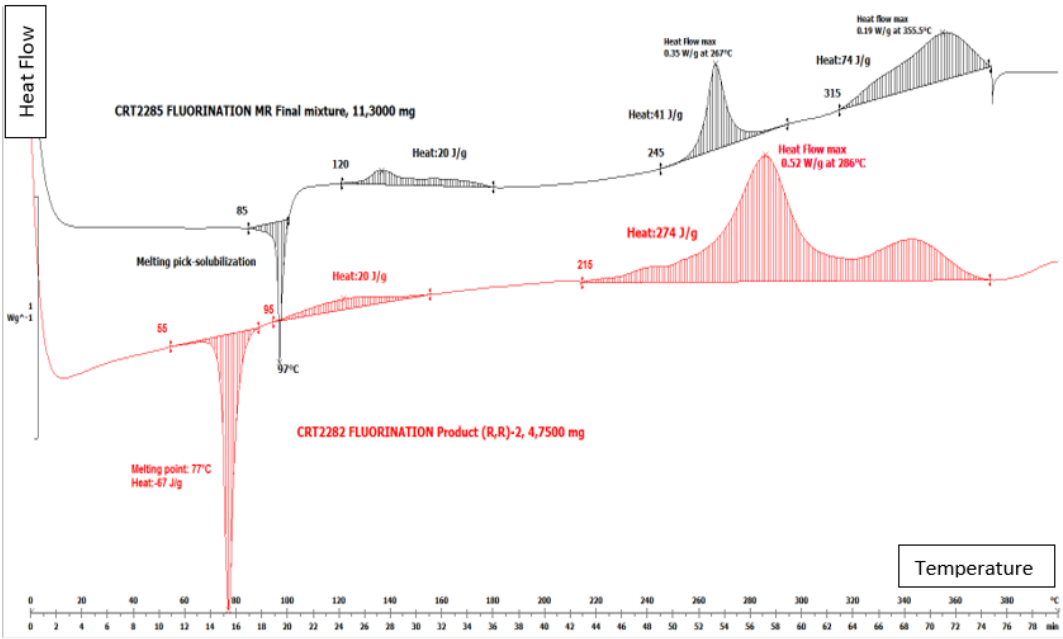


Figure 4.13: DSC curve of the product (*R*,*R*)-**2.109** (red) overlaid with the DSC curve of the reaction mixture sampled after 48 h from the beginning of the reaction (black). Analysis performed by Philippe Courtes (SANOFI).

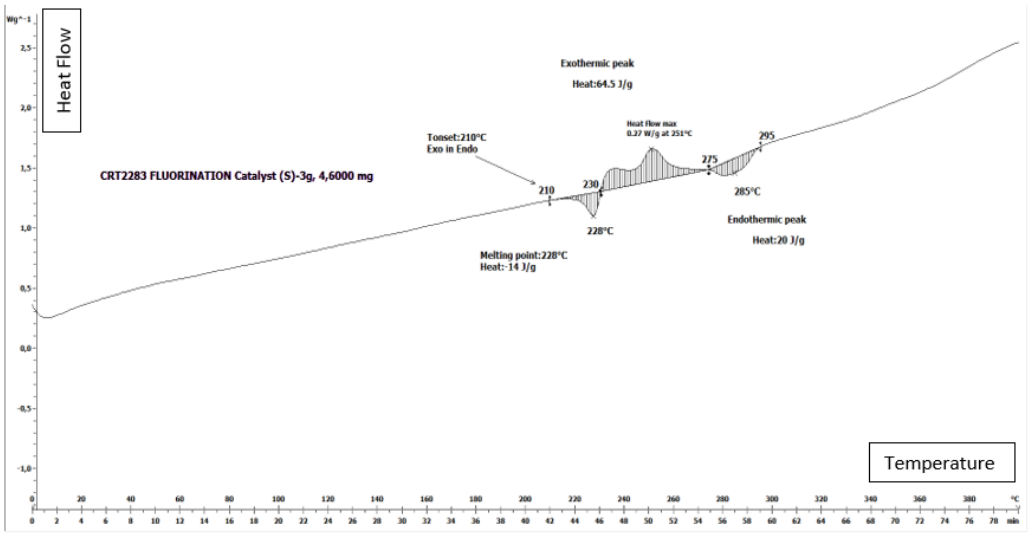


Figure 4.14: DSC curve of the pure catalyst (*S*)-**2.78**. Analysis performed by Philippe Courtes (SANOFI).

4.9.3.2 Reaction Calorimetry (RC) Experiment

The reaction reported in section 4.9.1 was performed in a heat flow calorimetric reactor (OptiMax^{TM}). A calibration was performed on the solution of *rac*-**2.108** in CH_2Cl_2, prior to the addition of the catalyst and CsF, and at the end of the reaction. This furnished the initial value of U = 102 $WK^{-1}m^{-2}$ and C_p = 1.1 $Jg^{-1}K^{-1}$ and a final value of U = 99 $WK^{-1}m^{-2}$ and C_p = 1.0 $Jg^{-1}K^{-1}$ which were used in subsequent calculations. The charging protocol was described in section 4.9.1 and, since the addition order of the reagents had no effect on the reaction outcome (section 4.6) it was chosen to separate the contribution of substrate dissolution (endothermic ΔH = + 28 kJ/mol) from the heat released by the reaction (ΔH = – 30 kJ/mol of *rac*-**2.108**).

The graph of the heat flow as function of time (orange) is shown in Figure 4.15, alongside the temperature of the reaction mass (red). The heat flow measured immediately after addition of CsF reached its maximum value and then it declined steadily. Samples for

reaction monitoring *via* ^{19}F NMR were taken after 3.5 h, 22 h, 29 h and 46 h. These perturbations are clearly visible in Figure 4.15.

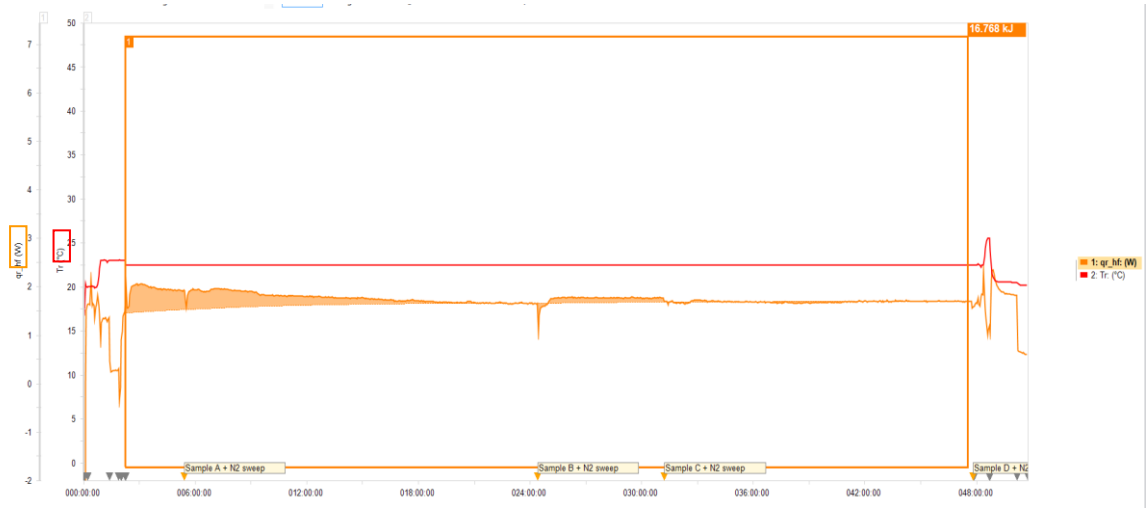


Figure 4.15: Thermogram of the enantioselective fluorination of *rac*-**2.108** with CsF under HB-PTC. Red: Temperature inside the reactor; orange: heat flow due to the reaction.

The Mettler Toledo software calculated the heat exchanged by the reaction (Q_R = 17 kJ) by integration of the curve of the heat flow as function of time. Accurate measurement of Q_R is not possible because the signal is weak and recorded over a long period of time (48 h). The molar enthalpy (ΔH) was calculated by dividing Q_r by the moles of **2.108** (0.558 mol, eq. 4.9).

$$\Delta H = \frac{Q_r}{n_{2.108}} \qquad \text{(eq.4.9)}$$

$$\Delta T_{ad} = \frac{\Delta H}{mC_p} \qquad \text{(eq. 4.5)}$$

ΔT_{ad} was calculated according to eq. 4.5 (section 4.2.2) and found to be 28 °C. If this value is added to the temperature of the reaction (Tp = 22 °C), this would reach 50 °C (=MTSR), which exceeds the boiling point of CH_2Cl_2 (40 °C = MTT). Decomposition of both the starting material and the product does not start below 150 °C resulting in the order T_p <MTT < MTSR <<T_{onset} which corresponds to the critical class 3 according to Stoessel classification (Figure 4.5B, section 4.2.2).[11] Provided that the amount of solvent is

sufficient, its evaporation would limit the maximum reaction temperature to 40 °C, where no decomposition is taking place. The thermal risk might thus be controlled employing a condenser of the appropriate size. Moreover, reagent accumulation is not an issue, because since the reaction takes 48 h to reach completion the reaction heat is released over a long period of time.

Table 4.19: Process parameters for the definition of the critical class.

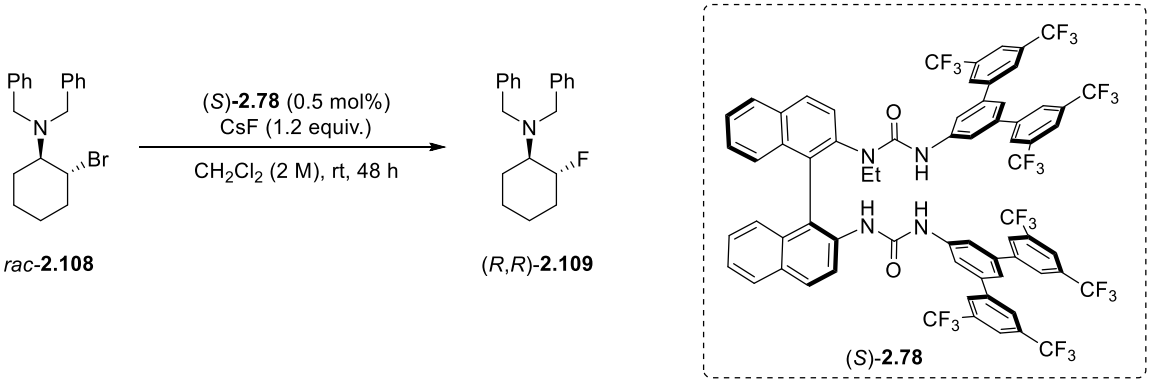
Parameter	*Value*	*Comment*
Tp	22 °C	Process Temperature
MTT	40 °C	CH_2Cl_2 BP
ΔT_{ad}	28 °C	From RC
MTSR	50 °C	From RC
T_{onset}	170 °C	From DSC on the initial reaction mixture
T_{ex}	70 °C	T_{onset} –100 °C

MTT = Maximum Technical Temperature; in an open system, this corresponds to the solvent boiling point. MTSR = Maximum Temperature of the Synthesis Reaction; the maximum temperature reached by the reaction mass in adiabatic conditions due to the heat released by the main reaction.

4.10 Catalyst Recovery and Degradation

The catalyst from the 200 g scale fluorination was separated from the product by aqueous work-up (section 4.7) and purified by recrystallisation (heptane 5 mL/g and EtOH 1 mL/g), recovering 2.02 g of (*S*)-**2.78** (52%). Alternatively, catalyst purification can be achieved by silica gel chromatography (heptane: EtOAc = 100% to 90:10, gradient, ~63% recovery). This second method was used to purify the catalyst in the small scale (1–50 g) test reactions. Both (*S*)-**2.78** recovered by recrystallisation (entry 2, Table 4.20) and by chromatography (entry 3) were tested in the fluorination of 5 g of *rac*-**2.108** affording (*R,R*)-**2.109** in comparable yield and enantioselectivity to newly synthesised (*S*)-**2.78** (entry 1). The catalyst used in entries 2 and 3 was separated from the product by aqueous work-up, purified by chromatography on silica gel with an automated CombiFlash® (59% and 67% recovery, respectively), combined and used again in the fluorination obtaining comparable results to the previous reactions (entry 4).

Table 4.20: Performance of recovered (*S*)-**2.78** in the enantioselective fluorination of *rac*-**2.108** with CsF.



Entry	*Rac-**2.108***	*Cycle*	*Yield [a]*	*e.r. [b]*	*(S)-**2.78** Recovery [c]*
1	5 g	0	91%	81:18	65%
2[d]	5 g	1	88%	82:18	59%
3[e]	5 g	1	89%	81:19	67%
4[f]	4.5 g	2	81%	81.5:18.5	–

Reaction conditions: *Rac*-**2.108**, CsF (1.2 equiv), (*S*)-**2.78** (0.5 mol%), rt, stirring at 900 rpm for 48 h. [a] Isolated yields. [b] e.r. determined by HPLC using a chiral non-racemic stationary phase. [c] The catalyst was recovered by flash column chromatography (FCC) using a CombiFlash®. [d] (*S*)-**2.78** used in the fluorination was recovered by recrystallisation from the reaction on 200 g of *rac*-**2.108**. [e] (*S*)-**2.78** used in the fluorination was recovered by FCC with a CombiFlash® from the reaction on 50 g of *rac*-**2.108**. [f] (*S*)-**2.78** used in the fluorination was recovered by FCC with a CombiFlash® from entries 2 and 3.

The fluorination performed with doubly recovered catalyst was monitored by quantitative ^{19}F NMR and compared with a 10 g scale reaction employing newly synthesised catalyst (Figure 4.16). The reactions were comparable, and both reached completion within 48 h. The lower isolated yield for the fluorination performed in the presence of doubly recycled catalyst (81% *versus* 88–90%) was probably due to the loss of product during sampling from the very concentrated (2 M) reaction mixture, since the final ^{19}F NMR yield was the same as for the previous reactions (>95% yield) and purification was performed according to the optimised protocol.

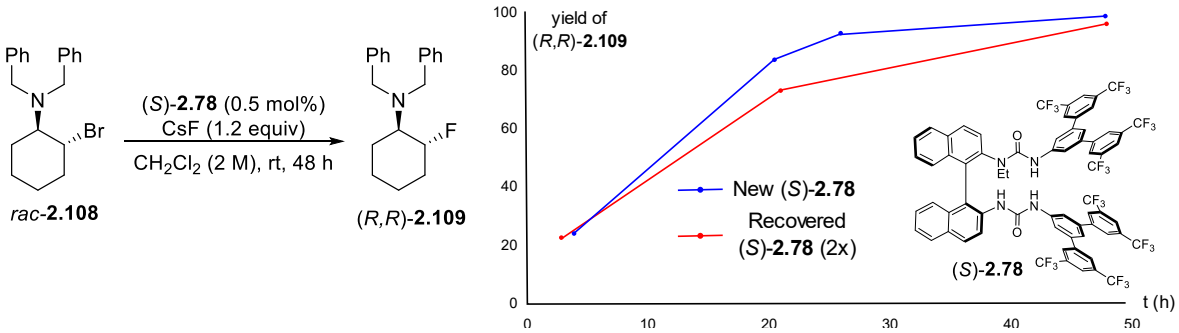


Figure 4.16: Comparison of the enantioselective fluorination of *rac*-**2.108** with newly synthetised catalyst (*S*)-**2.78** (blue) and (*S*)-**2.78** recycled two times (red). Yields are determined by ^{19}F NMR using 4-fluoroanisole as internal standard.

The low catalyst recovery observed was not due to losses during the filtration through silica or in the aqueous work-up. This was determined by accurately weighing the crude product after each recovery step for a reaction performed on 10 g of β-fluroamine *rac*-**2.108**. The crude catalyst from this experiment was purified by manual column chromatography, resulting in 37% recovery (73 mg). The total mass of the fractions collected corresponded to the mass of the crude charged on the column. The main impurity isolated (70 mg, 30%) was assigned to the product of nucleophilic substitution between (*S*)-**2.78** and *rac*-**2.108** (**4.23**, Figure 4.17). The other fractions isolated by column chromatography contained the product (*R*,*R*)-**2.109** and a complex mixture which was not assigned.

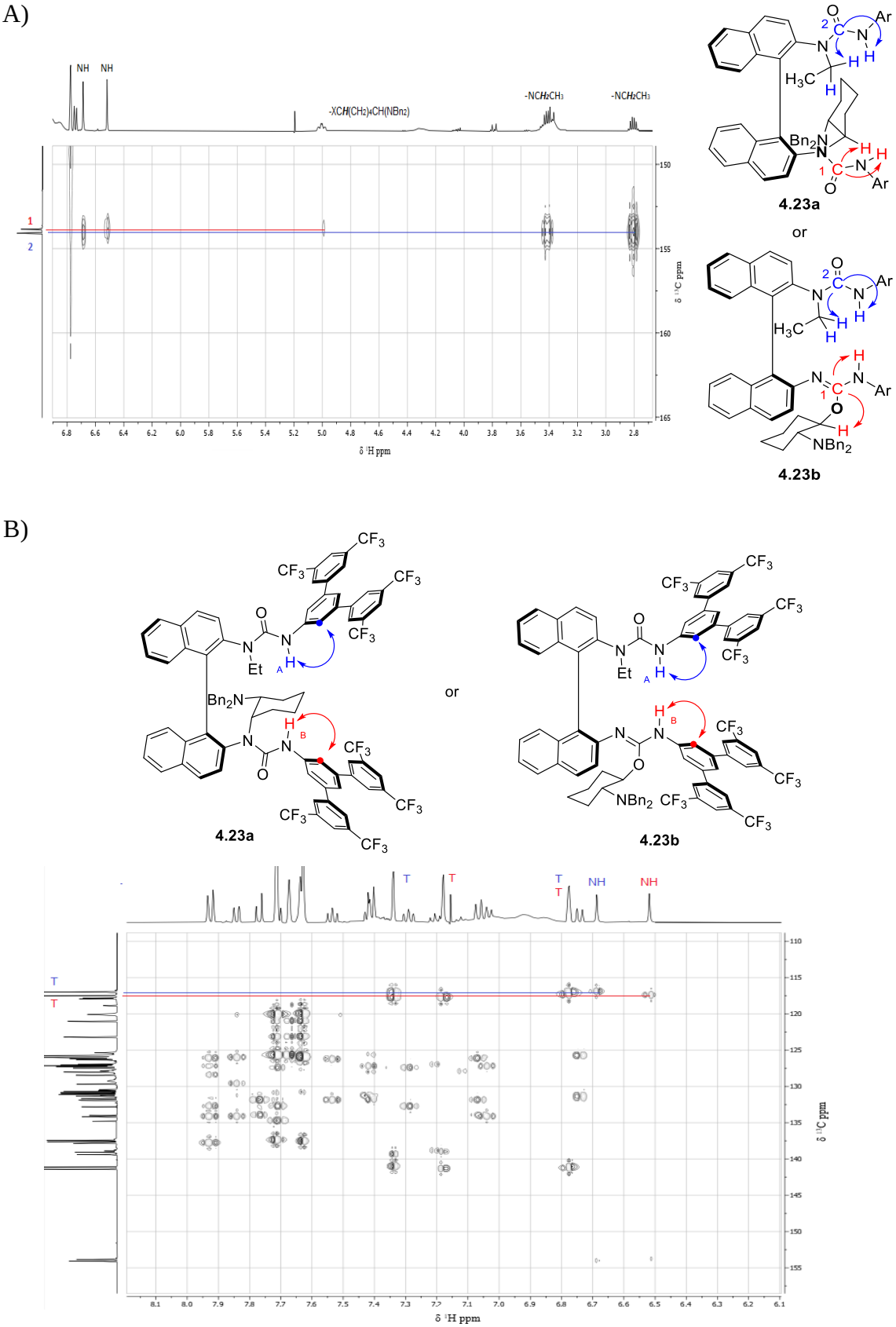
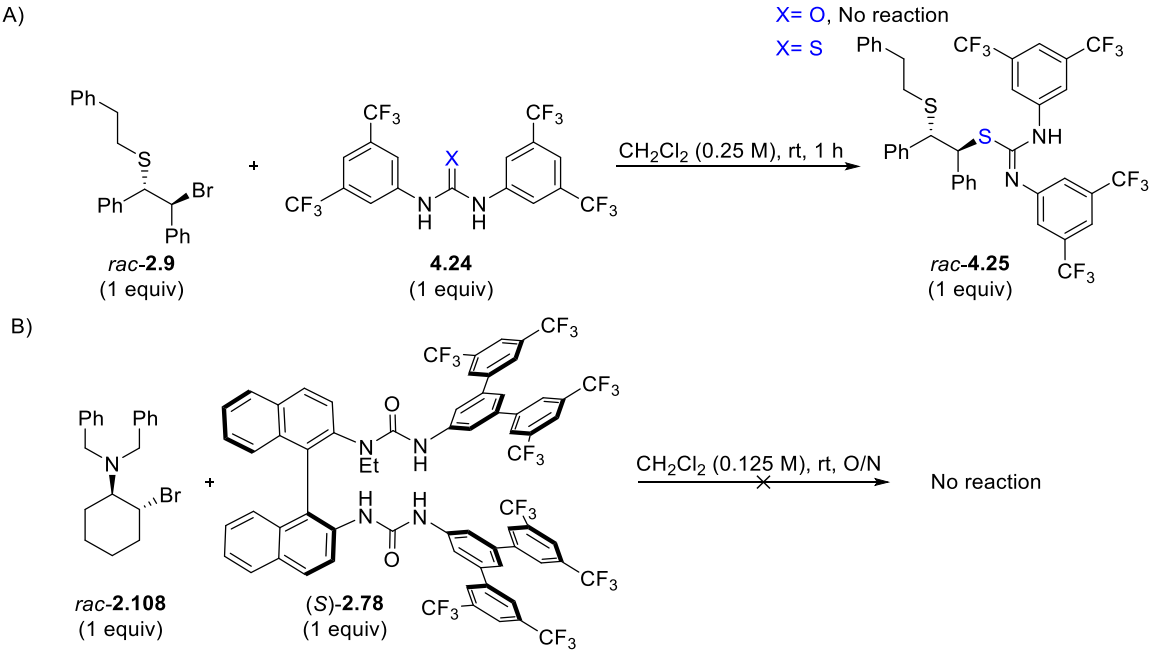


Figure 4.17: A) Detail of the ^{1}H-^{13}C HMBC showing correlation of the two C=O with two different NH and with the methylene of the ethyl chain and the methine of the cyclohexyl, respectively. X=N or O. B) Detail of the ^{1}H-^{13}C HMBC showing correlation between the NH protons and the carbons of the terphenyl system in the ortho position. T= terphenyl.

Assignment of **4.23** was based on HRMS and a combination of NMR experiments. The ^{1}H NMR had signals consistent with the presence of both the cyclohexyl ring and the catalyst backbone, with the overall number of protons matching the proposed structure. In addition, a peak corresponding to the proposed $[M+H]^+$ was found by high resolution mass spectrometry (ESI^+, calculated 1676.4515, found 1676.4432). Key correlations in the ^{1}H-^{13}C HSQC allowed assignment of the signals of the two NHs, as well as those of the diastereotopic protons of the ethyl chain and of the methines of the cyclohexyl ring. Finally, ^{1}H-^{13}C HMBC was used to determine the regiochemistry of the substitution (Figure 4.17). Both carbons of the carbonyls correlated with an NH, excluding the possibility that the alkylated urea has acted as nucleophile. This was confirmed by the presence of a correlation between C^1=O and the CH on the cyclohexyl ring, and C^2=O and the methylene from the ethyl chain (Figure 4.17A). A further correlation between NH_B and the carbon in the ortho position of the terphenyl ring was visible, excluding alkylation of the external nitrogen (Figure 4.17B). The information collected were not sufficient to discriminate between *N*-(**4.23a**) or *O*-alkylation (**4.23b**). The urea can attack either carbon of the aziridinium, giving rise to two diastereoisomers, but we have been unable to isolate both. Attempts to grow crystals of **4.23** suitable for X-ray analysis to determine which of the two diastereoisomers was formed were unsuccessful.

A similar product to **4.23** was isolated by stirring an achiral thiourea organocatalyst with an episulfonium precursor in CH_2Cl_2, while when the same experiment was performed using the corresponding urea, the catalyst was recovered intact (scheme 4.10A).[37] Similarly, **4.23** was not formed if bis-urea (*S*)-**2.78** (80 mg, 1 equiv) and *rac*-**2.108** (20 mg, 1 equiv) were stirred together in the absence of CsF (scheme 4.10B).



Scheme 4.10: Precedented example showing degradation of a thiourea catalyst due to nucleophilic substitution on the episulfonium (A).[37] Degradation is not observed for ureas in the absence of CsF (A and B).

No degradation was observed in the fluorination reaction using KF (Figure 4.18, top). When CsF was used instead, additional peaks were visible in the CF_3 region (around –63 ppm) in the ^{19}F NMR spectra of the crude reaction mixture (Figure 4.18, bottom).

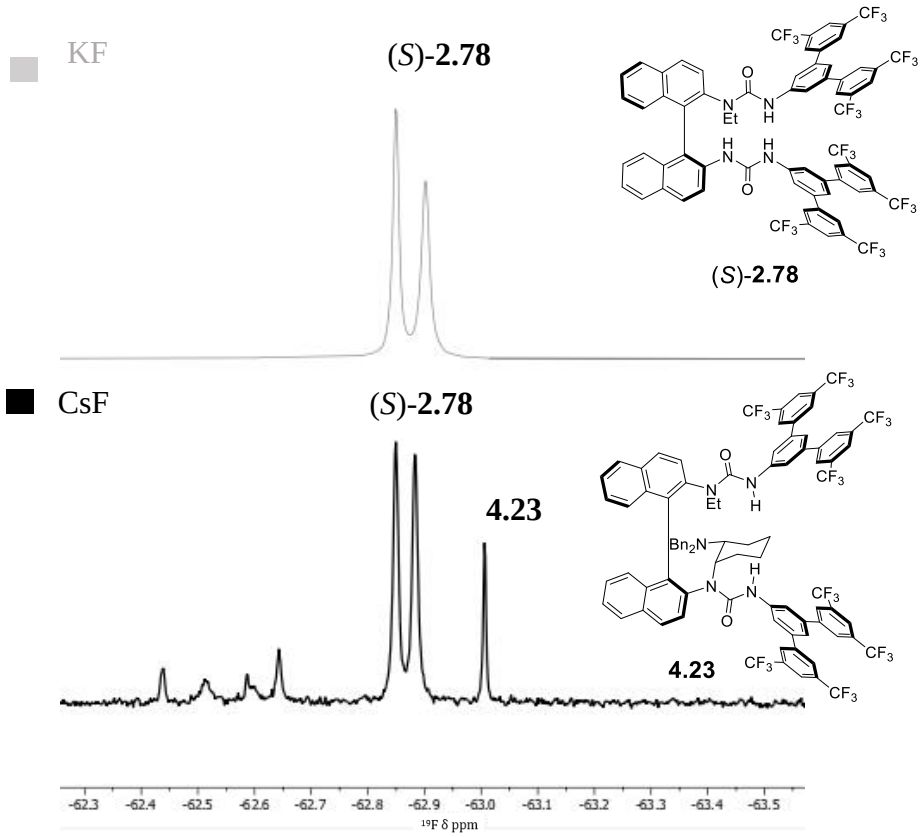
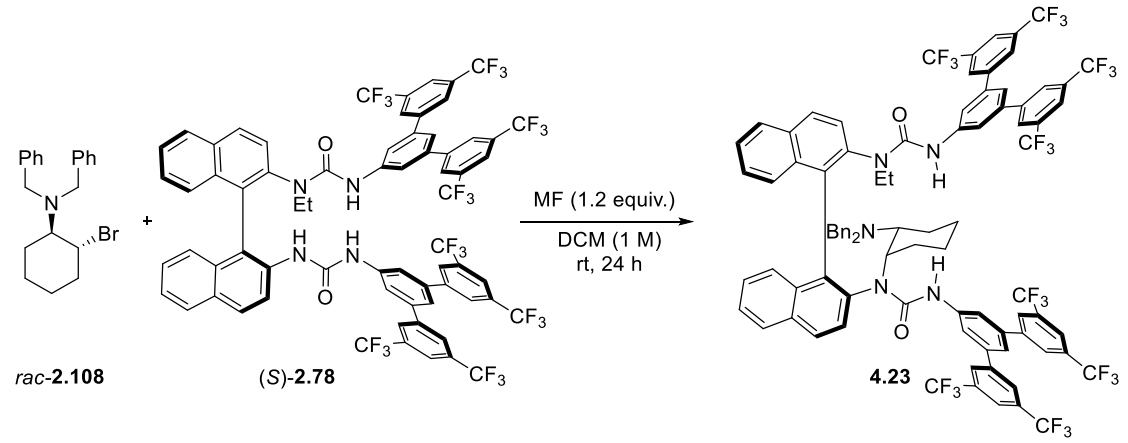


Figure 4.18: ^{19}F NMR of the crude reaction mixture showing the detail of the CF_3 region. Top (grey): no degradation of (*S*)-**2.78** is observed in the fluorination or *rac*-**2.108** with KF (1 mol% of (*S*)-**2.78**). Bottom (black): degradation of (*S*)-**2.78** in the fluorination of *rac*-**2.108** with CsF (1 mol% of (*S*)-**2.78**).

The extent of degradation was dependent on the catalyst loading, but not on CsF batches nor on the water content (Table 5.21). Fluoride might be acting as a base in the formation of **4.23**, and this hypothesis is supported by the observation that the same degradation product was formed stirring (*S*)-**2.78** and *rac*-**2.108** with Cs_2CO_3. In this case, the main product of the reaction was the carbonate derived from *rac*-**2.108**.

Table 4.21: Dependence of (*S*)-**2.78** on catalyst loading and MF



Entry	*Catalyst loading*	*Reagent*	*Recovery of (S)-**2.78** [a]*	*Yield of **4.23**[a]*
1	5 mol%	KF	93%	No degradation
2	5 mol%	CsF 99.9%	81%	1%
3	5 mol%	CsF 99%	77%	1%
4	5 mol%	CsF dry [b]	83%	1%
5	0.5 mol%	CsF 99.9%	31%	16%
6	0.5 mol%	CsF 99%	40%	16%
7	0.5 mol%	CsF dry [b]	35%	19%

Note: In all reactions, the main product obtained is β-fluoroamine **2.109**. [a] Determined by ^{19}F NMR using 4-fluoroanisole as internal standard. [b] Dried *in vacuo* at 200 °C for 48 h. The reaction was performed using Schlenk technique.

Overall, even though recovered (*S*)-**2.78** performs as well as the newly synthesised catalyst, the extent of degradation observed at low catalyst loading (<5 mol%) in the fluorination with CsF would probably make catalyst recovery not economically advantageous.

4.11 Conclusions

Asymmetric HB-PTC was applied to the multigram synthesis of (*R*,*R*)-*N*,*N*-dibenzyl-2-fluorocyclohexan-1-amine **2.109**, which is an *N*-protected precursor of a valuable fluorinated building block in medicinal chemistry (*trans*-2-fluorocyclohexan-1-amine). *N*-Benzyl protection was selected due to the higher level of enantiocontrol induced with catalyst (*S*)-**2.78** compared to *N*-allyl protection. Both bromide (as in *rac*-**2.108**) and iodide (as in *rac*-**4.22**) can be used as leaving groups in the fluorination with CsF, while no reaction is observed with *rac*-**4.22** using KF as fluorine source. Chloride (as in *rac*-**4.21**) is not a suitable leaving group in either fluorination.

Both KF and CsF were evaluated for the scale-up, and the reaction conditions were optimised to reduce the catalyst loading from 10 mol% to 0.5 mol% and the reaction time from 72 h to 48 h. Insoluble salts such as MI, MOTf, MOMs and MOTs (M= K, Cs), which enhanced the yield of (*R*,*R*)-**2.109** in the fluorination with CsF using 5 mol% of bis-urea (*S*)-**2.78**, were ineffective or detrimental at low catalyst loading (≤ 1mol%), and only marginally improved the fluorination with KF. For both fluoride salts, the highest yields were obtained in CH_2Cl_2. CsF was ultimately selected for the scale-up due to the better yields obtained at reduced catalyst loading (≤ 1mol%). Particle size distribution and water content of CsF were found to have an impact on conversion but not on enantioselectivity, while CsF of 99.9% and 99% purity were equally effective.

The fluorination can be performed in standard RBFs with magnetic stirring at up to 50 g scale, affording (*R*,*R*)-**2.109** consistently in ~90% isolated yield (>95% ^{19}F NMR yield) and 81.5:18.5 e.r. A single recrystallisation of the trifluoroacetate salt of (*R*,*R*)-**2.109** from ^{i}PrOH enhanced the e.r. up to 98:2. Scale-up to fluorination of 200 g of precursor was achieved in a mechanically stirred 1 L reactor equipped with a 45° down-pumping PTB and flat glass baffles to ensure full suspension of solid CsF. Comparable results with the

reactions run in RBFs were obtained (95% yield, 81.5:18.5 e.r.). Preliminary calculations revealed that the local energy dissipation (ε_{max}) and the local turbulent shear rates (γ_{imp}) in the impeller region are important parameters at this scale, with the best conversions obtained above ε_{max} = 300 W/kg and γ_{imp} = 10000 s^{-1}. Further studies toward the industrialisation of the process should focus on the investigation of long-term corrosion effects and on the filterability of the crude reaction mixture, as both might be problematic on scale due to the high shear rates required in the reaction.

As part of the scale-up, the thermal safety of the reaction was evaluated by DSC and RC. The fluorination is exothermic ($\Delta H = -30$ kJ/mol) and can be assigned to Stoessel's critical class 3. This is characterised by MTT (CH_2Cl_2 boiling point = 40 °C) being lower than MTSR (80 °C). A condenser of appropriate size is thus a viable means to maintain control of the reaction mass temperature, especially because the heat is released over a long time (48 h).

Recyclability of the catalyst was evaluated. While purified bis-urea (S)-**2.78** gave the same results as newly synthesised catalyst, its recovery was moderate, due to extensive degradation. The main degradation product (**4.23)** was characterised as the product of alkylation of the non-alkylated urea on the substrate. **4.23** is not formed in the absence of CsF nor in the fluorination with KF, and the extent of degradation is dependent on catalyst loading.

In conclusion, this study represents the proof of principle of the scalability of HB-PTC to industrial vessels, demonstrating that heterogeneous enantioselective fluorination with alkali metal fluorides can be successfully scaled-up in mechanically stirred reactors. This offers a convenient method to access highly sought after enantioenriched building blocks from safe, abundant, and economical alkali metal fluorides.

4.12 References

(1) Magnetic Drivers for Mixers. In *Advances in industrial mixing a companion to the handbook of industrial mixing*; Kresta, S. M.; Etchells, A. W. I.; Dickey, D. S.; Atiemo-Obeng, V. A. Eds.; John Wiley & Sons, Inc.: Hoboken, NJ, 2016; pp 559–566.

(2) Zlokarnik, M. *Scale-up in Chemical Engineering*; Wiley-VCH: Weinheim, Germany, 2002.

(3) Rapp, B. E. Fluids. In *Microfluidics: Modelling, Mechanics and Mathematics*; Elsevier, 2017; pp 243–264.

(4) Flow Patterns and Mixing. In *Advances in industrial mixing a companion to the handbook of industrial mixing*; Kresta, S. M., Etchells, A. W. I., Dikey, D. S., Atiemo-Obeng, V. A., Eds.; John Wiley & Sons, Inc.: Hoboken, NJ, 2016; pp 153–188.

(5) *Advances in Industrial Mixing*; Kresta, S. M., Etchells, A. W. I., Dickey, D. S., Atiemo-Obeng, V. A., Eds.; John Wiley & Sons, Inc.: Hoboken, NJ, 2016.

(6) Solid-Liquid Mixing. In *Advances in industrial mixing a companion to the handbook of industrial mixing*; Kresta, S. M., Etchells, A. W. I., Dickey, D. S., Atiemo-Obeng, V. A., Eds.; John Wiley & Sons, Inc.: Hoboken, NJ, 2016; pp. 357–450.

(7) Zwietering, T. N. "Suspending of Solid Particles in Liquid by Agitators." *Chem. Eng. Sci.* **1968**, *9*, 244–253.

(8) Fortunato, A. DSC: History, Instruments and Devices. In *Drug-Biomembrane Interaction Studies The Application of Calorimetric Techniques*; Pignatello, R., Ed.; Woodhead Publishing, 2013; pp 169–212.

(9) Frurip, D. J.; Elwell, T. "Effective Use of Differential Scanning Calorimetry in Reactive Chemicals Hazard Evaluation." *Process Saf. Prog.* **2007**, *26*, 51–58.

(10) Landau, R. N. "Expanding the Role of Reaction Calorimetry." *Thermochim. Acta* **1996**, *289*, 101–126.

(11) Stoessel, F. "Planning Protection Measures against Runaway Reactions Using Criticality Classes." *Process Saf. Environ. Prot.* **2009**, *87*, 105–112.

(12) Gygax, R. "Chemical Reaction Engineering for Safety." *Chem. Eng. Sci.* **1988**, *43*, 1759–1771.

(13) Stoessel, F. *Thermal Safety of Chemical Processes: Risk Assessment and Process Design*; Wiley-VCH: Weinheim,Germany, 2008.

(14) Pupo, G.; Vicini, A. C.; Ascough, D. M. H.; Ibba, F.; Christensen, K. E.; Thompson, A. L.; Brown, J. M.; Paton, R. S.; Gouverneur, V. "Hydrogen Bonding Phase-Transfer Catalysis with Potassium Fluoride: Enantioselective Synthesis of β-Fluoroamines." *J. Am. Chem. Soc.* **2019**, *141*, 2878–2883.

(15) Dalvit, C.; Fagerness, P. E.; Hadden, D. T. A.; Sarver, R. W.; Stockman, B. J. "Fluorine-NMR Experiments for High-Throughput Screening: Theoretical Aspects, Practical Considerations, and Range of Applicability." *J. Am. Chem. Soc.* **2003**, *125*, 7696–7703.

(16) Morgenthaler, M.; Schweizer, E.; Hoffmann-Röder, A.; Fischer, H.; Bendels, S.; Zimmerli, D.; Schneider, J. "Predicting and Tuning Physicochemical Properties in Lead Optimization: Amine Basicities." *ChemMedChem* **2007**, *2*, 1100–1115.

(17) Sakamoto, H.; Sugimoto, T. "Preparation of Heterocyclic Compounds as Cholinergic Muscarinic M1 Receptor Positive Allosteric Modulators." WO 129622, 2013.

(18) Melancon, B. J.; Tarr, J. C.; Panarese, J. D.; Wood, M. R.; Lindsley, C. W. "Allosteric Modulation of the M1 Muscarinic Acetylcholine Receptor: Improving Cognition and a Potential Treatment for Schizophrenia and Alzheimer's Disease." *Drug Discov. Today* **2013**, *18*, 1185–1199.

(19) Felder, C. C.; Goldsmith, P. J.; Jackson, K.; Sanger, H. E.; Evans, D. A.; Mogg, A. J.; Broad, L. M. "Current Status of Muscarinic M1 and M4 Receptors as Drug Targets for Neurodegenerative Diseases." *Neuropharmacology* **2018**, *136*, 449–458.

(20) Coburn, C. A.; Egbertson, M. S.; Graham, S. L.; McGaughey, G. B.; Stauffer, S. R.; Rajapakse, H. A.; Nantermet, P. G.; Stachel, S. R.; Yang, W.; Lu, W.; Fahr, B. "Spiropiperidine Beta-Secretase Inhibitors for the Treatment of Alzheimer's Disease." WO 011833, 2007.

(21) Meguro, M.; Asao, N.; Yamamoto, Y. "Ytterbium Triflate and High Pressure-Mediated Ring Opening of Epoxides with Amines." *J. Chem. Soc. Perkin Trans. 1* **1994**, 2597–2601.

(22) Chong, H.-S.; Sun, X.; Chen, Y.; Wang, M. "Synthesis, Characterization, and Nucleophilic Ring Opening Reactions of Cyclohexyl-Substituted β-Haloamines and Aziridinium Ions." *Tetrahedron Lett.* **2015**, *56*, 946–948.

(23) Karplus, M. "Vicinal Proton Coupling in Nuclear Magnetic Resonance." *J. Am. Chem. Soc.* **1963**, *85*, 2870–2871.

(24) Kalow, J. A.; Doyle, A. G. "Enantioselective Fluoride Ring Opening of Aziridines Enabled by Cooperative Lewis Acid Catalysis." *Tetrahedron* **2013**, *69*, 5702–5709.

(25) Clayden, J.; Greeves, N.; Warren, S. *Organic Chemistry*, 2nd ed.; Oxford University Press, 2012.

(26) *CRC Handbook of Chemistry and Physics*, 85th ed.; Lide, D. R., Ed.; CRC Press: Boca Raton, FL, 2004.

(27) Prat, D.; Hayler, J.; Wells, A. "A Survey of Solvent Selection Guides." *Green Chem.* **2014**, *16*, 4546–4551.

(28) Prat, D.; Pardigon, O.; Flemming, H. W.; Letestu, S.; Ducandas, V.; Isnard, P.; Guntrum, E.; Senac, T.; Ruisseau, S.; Cruciani, P.; Hosek, P. "Sanofi's Solvent Selection Guide: A Step Toward More Sustainable Processes." *Org. Process Res. Dev.* **2013**, *17*, 1517–1525.

(29) Hossaini, R.; Chipperfield, M. P.; Montzka, S. A.; Leeson, A. A.; Dhomse, S. S.; Pyle, J. A. "The Increasing Threat to Stratospheric Ozone from Dichloromethane." *Nat. Commun.* **2017**, *8*, 1–9.

(30) Bordwell, F. G. "Equilibrium Acidities in Dimethyl Sulfoxide Solution." *Acc. Chem. Res.* **1988**, *21*, 456–463.

(31) Lesk, A.; Nudelman, A. "Acetyl Bromide-Alcohols as Convenient Reaction Systems for: A) Removal of *N*-Tert-Boc, *N*-Cbz and *N*-Ac Protective Groups, b) Esterifications and Transesterifications, c) Debenzylation of Aryl-*O*-Benzyl Ethers." *Synth. Commun.* **1999**, *29*, 1405–1408.

(32) Eckert, F.; Leito, I.; Kaljurand, I.; Kutt, A.; Klamt, A.; Diedenhofen, M. "Prediction of Acidity in Acetonitrile Solution with COSMO-RS." *J. Comput. Chem.* **2009**, *30*, 799–810.

(33) "Dynochem 5, Scale-up Systems Limited, Dublin, Ireland (2019)" www.scale-up.com (accessed May 11, 2020).

(34) Grenville, r. k.; Brown, D. A. R. A "Method for Comparing Impellers' Generation of Flow and Turbulence." In *MIXING XXIII*; Mayan Riviera Mexico.

(35) Mishra, V. P.; Joshi, J. B. LDA Measurements of Flow in Stirred Gas-Liquid Reactors, Fluid Mechanics of Mixing. In *Fluid mechanics of mixing. Fluid mechanics and its applications*; King, R., Ed.; Springer: Dordrecht, 1992; pp 217–224.

(36) Sánchez Pérez, J. A.; Rodríguez Porcel, E. M.; Casas López, J. L.; Fernández Sevilla, J. M.; Chisti, Y. "Shear Rate in Stirred Tank and Bubble Column Bioreactors." *Chem. Eng. J.* **2006**, *124*, 1–5.

(37) Pupo, G.; Ibba, F.; Ascough, D. M. H.; Vicini, A. C.; Ricci, P.; Christensen, K. E.; Pfeifer, L.; Morphy, J. R.; Brown, J. M.; Paton, R. S.; Gouverneur, V. "Asymmetric Nucleophilic Fluorination under Hydrogen Bonding Phase-Transfer Catalysis." *Science* **2018**, *360*, 638–642.

(38) Crampton, M. R.; Robotham, I. A. "Acidities of Some Substituted Ammonium Ions in Dimethyl Sulfoxide." *J. Chem. Res. - Part S* **1997**, 22–23.

(39) Kreevoy, M. M.; Wang, Y. "Kinetic and Equilibrium Acid-Base Behavior of Tertiary Amines in Anhydrous and Moist Dimethyl Sulfoxide." *J. Phys. Chem.* **1977**, *81*, 1924–1928.

Intentionally left blank

Chapter 5:
Experimental

5.1 General Experimental

Unless otherwise stated, all reagents were purchased from commercial suppliers (Acros, Alfa Aesar, Apollo Scientific, Fisher, Fluorochem and Sigma-Aldrich/Merck) and used without further purification. Unless otherwise stated, solvents were used without prior drying/degassing. Dry solvents were purchased from commercial suppliers. Reactions requiring anhydrous conditions are clearly stated and were conducted after flame-drying of the appropriate reaction vessel (round-bottom two-neck flasks or Schlenk) and under an inert atmosphere of nitrogen. KF (99.9% trace metal basis from Alfa Aesar) was used as provided by the supplier (fine powder) and used without pre-drying. CsF (99.9% trace metal basis from Sigma-Aldrich) for reaction development, Chapter 2, was ground prior to the reaction and used without pre-drying. CsF (99% from Flurochem) for the scale-up, Chapter 4, was used as provided by the supplier (fine powder) and used without pre-drying. The dry chloroform employed in the fluorination described in Chapter 2 was purchased from Acros and passed on a column of basic alumina prior to use (to ensure absence of HCl impurities). The CH_2Cl_2 used in the scale-up (Chapter 4) was purchased by Carlo-Erba Reagents and used as provided by the supplier. Reactions were monitored by thin layer chromatography (TLC) on silica gel pre-coated aluminium sheets (Merck Kieselgel 60 F_{254} plates). Visualisation was accomplished by irradiation with UV light at 254 nm, and/or phosphomolybdic acid (PMA) stain, and/or cerium ammonium molybdate (CAM) stain, and/or permanganate stain. Flash column chromatography (FCC) was performed on Merck silica gel (60, particle size 0.040-0.063 mm).

Optical rotations were measured on an Autopol L 2000 (Schmidt-Haensh) at 589 nm, 25 °C. Data are reported as: $[\alpha]_D^T$, concentration (c in g/100 mL), and solvent. The absolute configuration of the stilbene-derived β-fluoroamines was determined by X-ray analysis of compound **2.83** and further confirmed by comparing the optical rotation values of

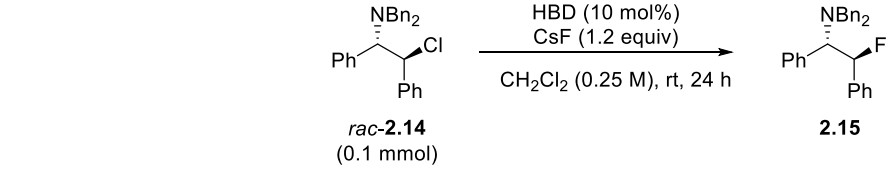
compound **2.103** (derived from β-fluoroamine **2.77**) to literature values. The configuration of the other stilbene-derived β-fluoroamines **2.82-2.99** was assigned by analogy. The absolute configuration of aliphatic cyclic **2.109** was determine comparing the optical rotation values of the corresponding β-fluoropicolinamide derivative **2.128** to literature values. The configuration of the other aliphatic cyclic products (**2.123**, **4.18**, **4.19** and **4.20**) was assigned by analogy to **2.109**.

All NMR spectra were recorded on Bruker AVIIIHD 400, AVIIIHD 500 or VII 500. ^{1}H and ^{13}C NMR spectral data are reported as chemical shifts (δ) in parts per million (ppm) relative to the solvent peak using the Bruker internal referencing procedure (edlock). ^{19}F NMR spectra are referenced relative to $CFCl_3$. Data are reported as follows: chemical shift, multiplicity (s = singlet, d = doublet, t = triplet, q = quartet, pent = pentet, sept = septet, br = broad, m = multiplet), coupling constants (Hz) and integration. NMR spectra were processed with MestReNova 11.0. High resolution mass spectra (HRMS, *m/z*) were recorded on a Thermo Exactive mass spectrometer equipped with Waters Acquity liquid chromatography system using either the heated electrospray (HESI-II) probe for positive electrospray ionisation (ESI^+) or the atmospheric pressure chemical ionisation (APCI) probe. Infrared spectra were recorded as the neat compound or in solution using a Bruker tensor 27 FT-IR spectrometer. Absorptions are reported in wavenumber (cm^{-1}). Melting points of solids were measured on a Griffin apparatus and are uncorrected. The enantiomeric ratios were determined on spectroscopically pure compounds (after purification) by HPLC analysis on a Shimadzu *i*-Prominence LC-2030 (PDA detector) employing a chiral non/racemic stationary phase column specified in the individual experiment by comparing the samples with the appropriate racemic mixtures.

5.2 Additional Data from Chapter 2

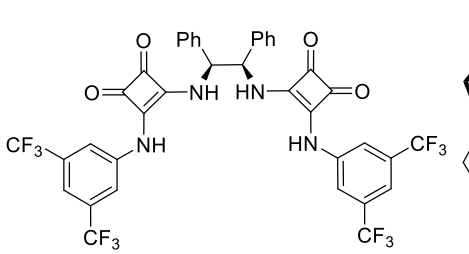
5.2.1 Additional Screening Reactions from Chapter 2

5.2.1.1 Stilbene-Derived Substrates: Enantioselective fluorination with CsF

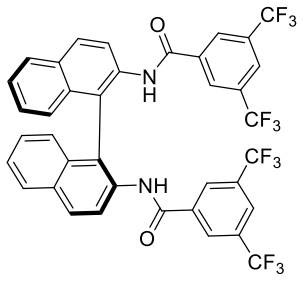


rac-**2.14**
(0.1 mmol)

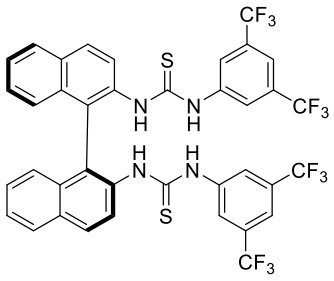
2.15



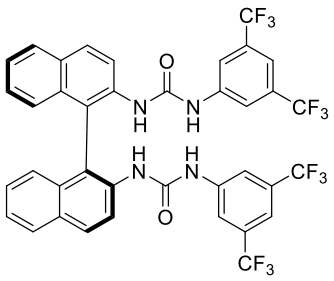
(*S,R*)-**5.1**
No reaction



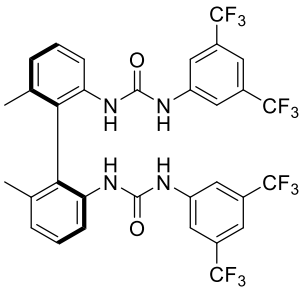
(*S*)-**5.2**
No reaction



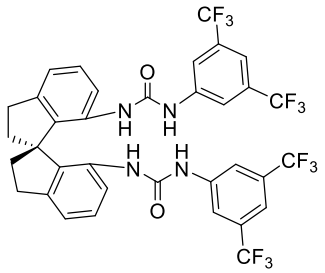
(*S*)-**5.3**
No reaction



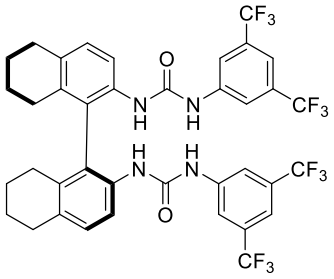
(*S*)-**2.4**
89% yield
65:35 e.r.



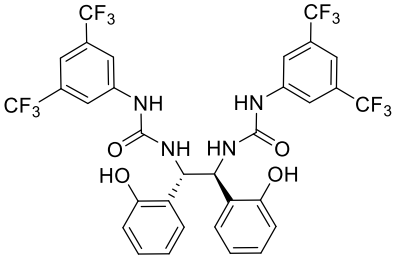
(*S*)-**2.110**
97% yield
67.5:32.5 e.r.



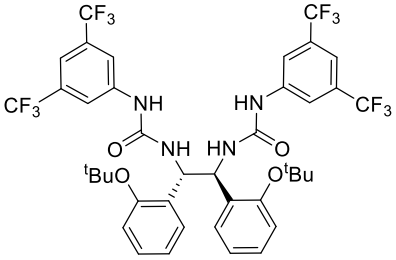
(*S*)-**2.111** (5 mol%)
35% yield
< 55:45



(*S*)-**2.18**
93% yield
76:24 e.r.



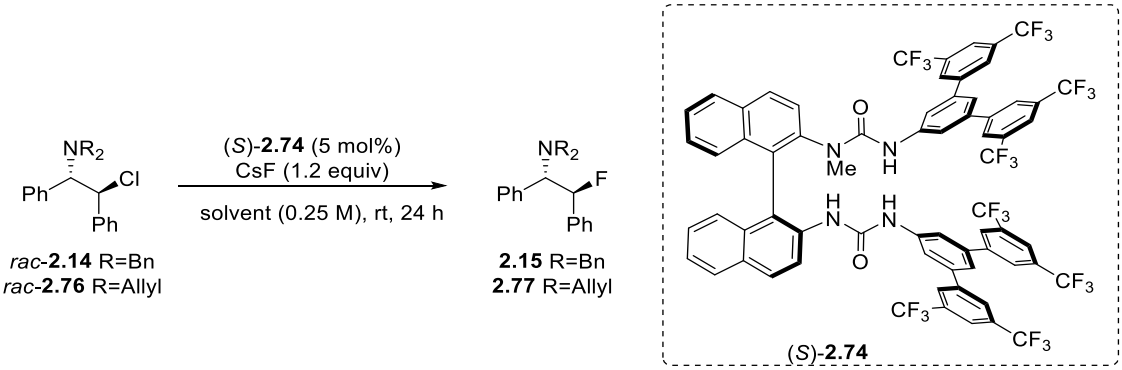
(*S,S*)-**5.4**
29% yield
64:36 e.r.



(*S,S*)-**5.5**
67% yield
55:45 e.r.

Scheme 5.1: Preliminary screening of hydrogen bond donors (HBD) for the enantioselective fluorination of *rac*-**2.14** with CsF. **Reaction conditions:** *rac*-**2.14** (0.1 mmol), 1.2 equiv of CsF, 10 mol% of HBD, 0.25 M in CH_2Cl_2, rt, stirring at 1200 rpm, 24 h. Yield determined by ^{19}F NMR using 4-Fluoranisole as internal standard; e.r. determined by HPLC using a chiral non-racemic stationary phase.

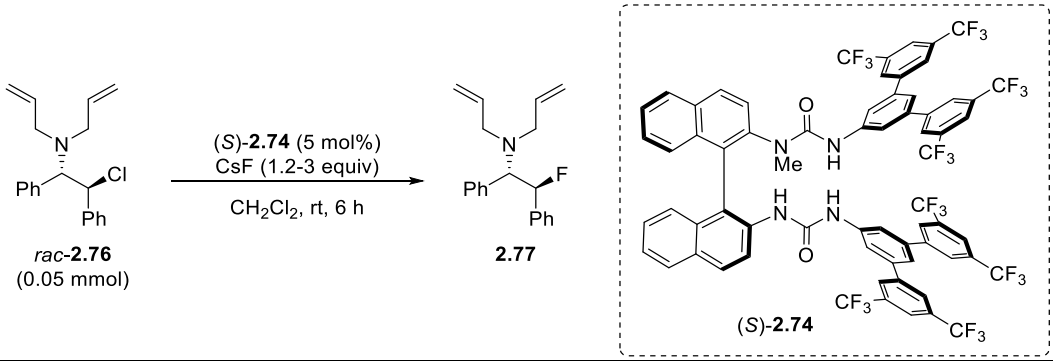
Table 5.1: Solvent screening for the enantioselective fluorination of *rac*-**2.14** and *rac*-**2.76** with CsF catalysed by (*S*)-**2.74**



Entry	*Substrate*	*Solvent*	*Yield* [a]	*e.r.* [b]
1	**2.14**	CH_3CN	Traces	–
2	**2.14**	CH_2Cl_2	43%	85.5:14.5
3	**2.14**	DCE	22%	87:13
4	**2.14**	CH_2Br_2	35%	86.5:13.5
5	**2.14**	$CHCl_3$ (filtered on basic alumina)	41%	83:17
6	**2.14**	Chlorobenzene	13%	89:11
7	**2.14**	1,2-Dichlorobenzene	14%	89.5:10.5
8	**2.14**	Fluorobenzene	Traces	–
9	**2.14**	1,2-Difluororobenzene	16%	88.5:11.5
10	**2.14**	1,3-Difluororobenzene	16%	87.5:12.5
11	**2.14**	1,4-Difluorobenzene	Traces	–
12	**2.14**	1,2,3-trifluorobenzene	22%	87.5:12.5
13	**2.14**	$PhCF_3$	34%	91:9
14[c]	**2.14**	"	94%	90.5:8.5
15	**2.14**	1,3-bis(trifluoromethyl)benzene	9%	–
16[c]	**2.14**	"	51%	93:7 (>99.9:0.1)[d]
17	**2.76**	CH_2Cl_2	>95%	89:11
18	**2.76**	DCE	>95%	90:10
19	**2.76**	CH_2Br_2	78%	90.5:9.5
20[e]	**2.76**	$CHCl_3$ (filtered on basic alumina)	>95%	89:11
21	**2.76**	Chlorobenzene	54%	93.5:6.5
22	**2.76**	1,2-Dichlorobenzene	36%	93.5:6.5
23	**2.76**	Fluorobenzene	70%	92:8
24	**2.76**	1,2-Difluororobenzene	95%	91:9
25	**2.76**	1,3-Difluororobenzene	>95%	91:9
26	**2.76**	1,2,3-trifluorobenzene	80%	92:8
27	**2.76**	$PhCF_3$	45%	92.5:7.5
28	**2.76**	1,3-bis(trifluoromethyl)benzene	76%	91:9

Reaction conditions: *rac*-**2.14** or *rac*-**2.76** (0.05 mmol), 1.2 equiv of CsF, 5 mol% of catalyst (*S*)-**2.74**, solvent 0.25 M, rt., stirring at 900 rpm, 24 h. [a] Yield determined by ^{19}F NMR using 4-fluoroanisole as internal standard. [b] e. r. determined by HPLC using a chiral non-racemic stationary phase. [c] Catalyst loading: 10 mol%, 3 days. [d] After single recrystallisation. [e] 3 equiv of CsF, 6 h. Dry $CHCl_3$ was filtered on basic alumina before the reaction to remove traces of HCl.

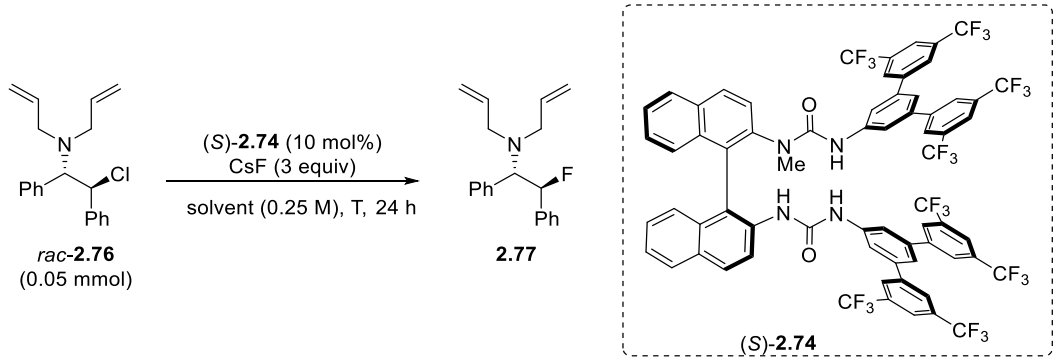
Table 5.2: Effect of concentration and CsF equivalents on the enantioselective fluorination of *rac*-**2.76** with CsF catalysed by (*S*)-**2.74**



Entry	*Concentration*	*CsF equiv*	*Yield* [a]	*e.r.* [b]
1	0.1 M	1.2	65%	89:11
2	0.25 M	1.2	77%	89:11
3	0.5 M	1.2	80%	89:11
4	0.25 M	3	95%	89:11

Reaction conditions: *rac*-**2.76** (0.05 mmol), 1.2–3 equiv of CsF, 5 mol% of catalyst (*S*)-**2.74**, 0.1–0.5 M, rt., stirring at 900 rpm, 6 h. [a] Yield determined by ^{19}F NMR using 4-fluoroanisole as internal standard. [b] e. r. determined by HPLC using a chiral non-racemic stationary phase.

Table 5.3: Temperature and solvent screening for the enantioselective fluorination of *rac*-**2.76** with CsF catalysed by (*S*)-**2.74**

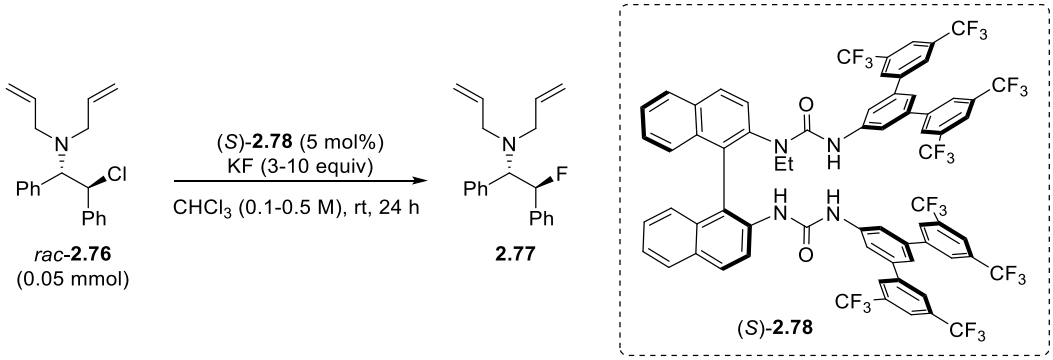


Entry	*Solvent*	*Temperature (° C)*	*Yield* [a]	*e.r.* [b]
1[c], [d]	CH_2Cl_2	0	>95%	93:7
2[c], [d]	CH_2Cl_2	–20	54%	91:9
3 [d]	DCE	–5	67%	94:6
4	$CHCl_3$	–5	95%	93:7
5	$CHCl_3$	–10	95%	93:7
6	$CHCl_3$	–15	89%	94:6
7	$CHCl_3$	–30	35%	95.5:5.5
8	CH_2Br_2	–5	66%	93.5:6.5
9 [d]	Fluorobenzene	–5	55%	94:6
10	1,2-difluorobenzene	–5	64%	93:7
11	1,3-difluorobenzene	–5	70%	93:7
12	1,2,3-trifluorobenzene	–5	88%	93:7
13	1,2,3-trifluorobenzene	–10	81%	94:6
14	1,2,3-trifluorobenzene	–15	49%	94:6
15	$PhCF_3$	–5	15%	93:7
16	1,3-bis(trifluoromethyl)benzene	–5	8%	93.5:6.5
17[d]	1,2-dichlorobenzene	–5	No reaction	–
18	Chlorobenzene	–5	12%	95:5
19	Chlorobenzene/ CH_2Cl_2 = 1:1	–5	72%	93.5:6.5
20	Chlorobenzene/ CH_2Cl_2 = 3:1	–5	20%	94:6
21	Chlorobenzene/$CHCl_3$ 3:1	–20	7%	93:7
22	Chlorobenzene/$CHCl_3$ 1:1	–20	13%	93.5:6.5
23	Chlorobenzene/$CHCl_3$ 1:3	–20	52%	94.5:5.5

Reaction conditions: *rac*-**2.76** (0.05 mmol), 3 equiv of CsF, 10 mol% of catalyst (*S*)-**2.74**, 0.25 M, stirring at 900 rpm, 24 h. [a] Yield determined by ^{19}F NMR using 4-fluoroanisole as internal standard. [b] e. r. determined by HPLC using a chiral non-racemic stationary phase. [c] 1.2 equiv of CsF; [d] 72 h.

5.2.1.2 Stilbene-Derived Substrates: Enantioselective Fluorination with KF

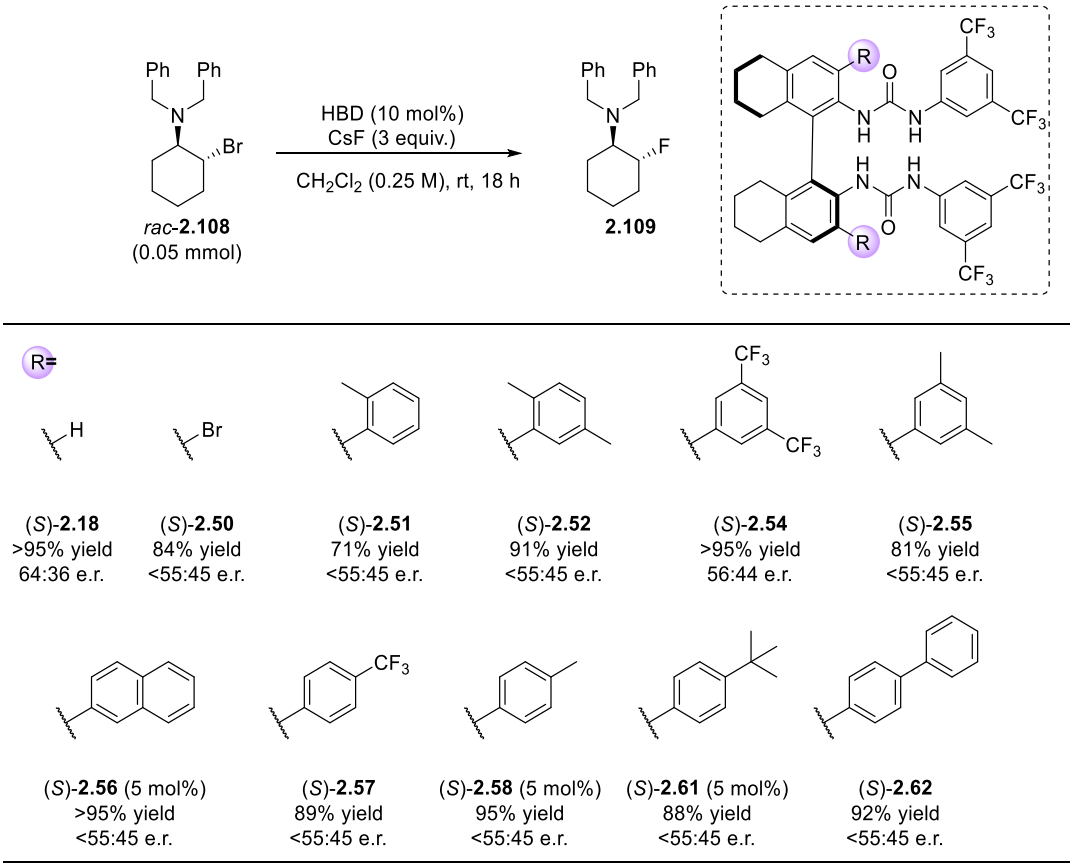
Table 5.4: Effect of concentration and KF equivalents on the enantioselective fluorination of *rac*-**2.76** with KF catalysed by (*S*)-**2.78**



Entry	*KF (equiv)*	*Concentration (M)*	*Time (h)*	*Yield*[a]	*e.r.*[b]
1	3	0.25	5	14%	89.5:10.5
2	5	0.25	5	18%	90.5:9.5
3	10	0.25	5	55%	90.5:9.5
4	3	0.1	24	20%	90:10
5	3	0.5	5	59%	90:10
6	5	0.5	5	87%	90.5:9.5
7	5	0.5	24	>95%	90.5:9.5

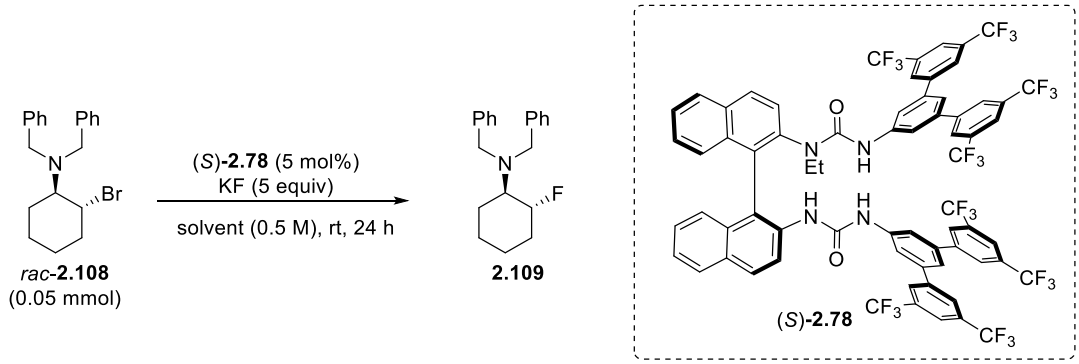
Reaction conditions: 0.05 mmol of *rac*-**2.76**, KF, (*S*)-**2.78** (5 mol%) in dry $CHCl_3$ (filtered on basic alumina to remove residual HCl), stirring at 900 rpm at rt for the indicated time. [a] Determined by ^{19}F NMR using 4-fluoroanisole as internal standard; [b] e.r.= enantiomeric ratio, determined by HPLC using a chiral non-racemic stationary phase.

5.2.1.3 Enantioselective Fluorination of Aliphatic Substrates



Scheme 5.2: Effect of 3,3' substitution of the bis-urea scaffold on the outcome of the enantioselective fluorination of *rac*-**2.108** with CsF. Yield determined by ^{19}F NMR using 4-fluoroanisole as internal standard; e.r. (= enantiomeric ratio) determined by HPLC using a chiral non-racemic stationary phase.

Table 5.5: Solvent screening for the enantioselective fluorination of *rac*-**2.108** with KF catalysed by (*S*)-**2.78**



Entry	*Solvent*	*Yield* [a]	*e.r.*[b]
1	CH_2Cl_2	25%	84:16
2	DCE	25%	81:19
3	$CHCl_3$ [c]	20%	83.5:16.5
4	CH_2Br_2	traces	–
5	Fluorobenzene	14%	–
6	1,2-difluorobenzene	28%	83.5:16.5
7	$PhCF_3$	47%	85.5:15.5
8	1,3-bis(trifluoromethyl)benzene	9%	–
9	Chlorobenzene	12%	–
10	$PhCH_3$	traces	–

Conditions: *rac*-**2.108** (0.05 mmol), KF (5 equiv), (*S*)-**2.78** (5 mol%), solvent (0.5 M) rt, stirring at 900 rpm for 24 h. [a] Yield determined by ^{19}F NMR using 4-fluoroanisole as internal standard. [b] e.r. determined by HPLC using a chiral non-racemic stationary phase. [c] Dry $CHCl_3$, filtered on basic alumina to remove residual HCl.

5.2.2 Experimental Procedures and Characterisation of Compounds in Chapter 2

5.2.2.1 Catalyst Synthesis and Characterisation

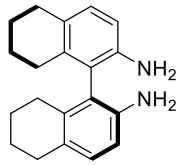
Catalysts **2.3**,[1] **2.4–2.8**,[1] **2.16**,[1] **2.18**,[2] **2.39–2.46**,[2,3] **2.50–2.58, 2.61, 2.64–2.65, 2.67–2.72, 2.110–2.113**[2], **2.118** were already available in the laboratory or were synthesised by others. The catalyst reported in this section were made entirely by myself, or in collaboration with Dr. Gabriele Pupo. His contribution is clearly stated.

General Procedure A: Suzuki-Miyaura Cross Coupling

A two-necks round bottom flask, equipped with a stirring bar and a condenser was charged with the aryl halide (1 equiv), the boronic acid/ester (3.5 equiv), SPhos (0.1 equiv) and K_2CO_3 (5 equiv). The flask was capped with a rubber septum and then evacuated and backfilled with N_2 (this sequence was repeated 3 times). Degassed THF and degassed H_2O (in a 5:1 ratio, 0.08 M as total concentration of aryl halide) were added *via* a syringe and the reaction mixture was stirred until complete solubilisation of the solids before addition of $Pd(OAc)_2$ (0.05 equiv). The septum was then replaced by a glass cap and the reaction mixture was stirred at reflux for the indicated time (usually overnight). The reaction mixture was then cooled to rt, diluted with water and extracted three times with CH_2Cl_2. The combined organic layers were washed with brine, dried over $MgSO_4$ and evaporated *in vacuo*. The crude product was purified by FCC on silica gel.

Chiral Anilines

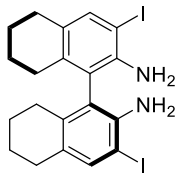
(*S*)-5,5',6,6',7,7',8,8'-octahydro-[1,1'-binaphthalene]-2,2'-diamine (2.20)



(*S*)-**2.20**

A two-necks round bottom flask was evacuated and backfilled with nitrogen (three times) prior of charging it with (*S*)-[1,1'-binaphthalene]-2,2'-diamine ((*S*)-BINAM, 3.5 g, 13.3 mmol, 1 equiv) and PtO_2 (340 mg, 1.23 mmol, 0.1 equiv) followed by AcOH and H_2O (120 mL in total, 10:1). The flask was very carefully evacuated and backfilled with hydrogen (this sequence was repeated 4 times). The reaction mixture was then stirred at 50 °C for 60 h, then cooled to rt and filtered through a celite pad rinsing with EtOAc. The solvents were removed *in vacuo* and the crude product was purified by FCC on silica gel (*n*-hexane: EtOAc = 90:10 to 80:20, gradient) to afford (*S*)-**2.20** as a pale brown solid (2.68 g, 69% yield). **^{1}H NMR** (400 MHz, $CDCl_3$) δ 6.92 (d, J = 8.1 Hz, 2H), 6.62 (d, J = 8.1 Hz, 2H), 3.31 (br s, 4H), 2.81 – 2.63 (m, 4H), 2.28 (dt, J = 17.3, 6.3 Hz, 2H), 2.17 (dt, J = 17.3, 6.3 Hz, 2H), 1.76 – 1.62 (m, 8H). **^{13}C NMR** (101 MHz, $CDCl_3$) δ 141.7, 136.4, 129.4, 127.8, 122.1, 113.2, 29.5, 27.1, 23.6, 23.4. **MS** (ESI^+) *m/z* calculated for $C_{20}H_{25}N_2^+$ $[M+H]^+$ 292.2, found 292.2. Analytical data were in agreement with those previously published.[4]

(*S*)-3,3'-diiodo-5,5',6,6',7,7',8,8'-octahydro-[1,1'-binaphthalene]-2,2'-diamine (2.21)

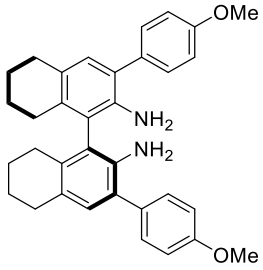


(*S*)-**2.21**

Bis-aniline (*S*)-**2.21** was synthesised according to a reported literature procedure.[5] To a stirred solution of (*S*)-**2.20** (1.67 g, 5.7 mmol, 1equiv) and $CaCO_3$ (914 mg, 17.1 mmol, 3 equiv) in CH_2Cl_2 (40 mL) and MeOH (16 mL) was added benzyltrimethylammonium dichloroiodate (3.98 g, 11.4 mmol, 2 equiv) at 0°C. The reaction mixture was warmed to rt and stirred for 2 h. The mixture was then quenched with saturated $NaHCO_3$ and saturated Na_2SO_3 at 0°C and extracted with CH_2Cl_2. The combined organic layers were washed with brine, dried over

Na_2SO_4 and concentrated. The residue was purified by FCC on silica gel (*n*-hexane: EtOAc = 98:2) to afford (*S*)-**2.21** a pale brown solid (2.39 g, 77% yield). **^{1}H NMR** (400 MHz, $CDCl_3$) δ 7.44 (s, 2H), 3.72 (br s, 4H), 2.68 (t, J = 6.0 Hz, 4H), 2.26 – 2.03 (m, 4H), 1.74–159 (m, 8H). **^{13}C NMR** (101 MHz, $CDCl_3$) δ 141.8, 138.9, 136.8, 130.0, 122.0, 81.7, 29.04, 26.9, 23.3, 23.1. **MS** (ESI^+) *m/z* calculated for $C_{20}H_{23}I_2N_2^+$ $[M+H]^+$ 545.0, found 545.0. Analytical data were in agreement with those previously published.[5]

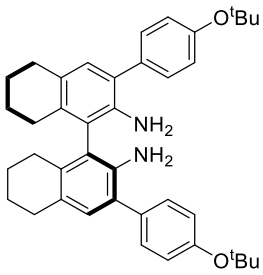
(*S*)-3,3'-bis(4-methoxyphenyl)-5,5',6,6',7,7',8,8'-octahydro-[1,1'-binaphthalene]-2,2'-diamine (5.6)



(*S*)-**5.6**

The title compound was prepared from (*S*)-**2.21** (150 mg) and (4-methoxyphenyl)boronic acid (149 mg) following the *general procedure A*. Purification by FCC on silica gel (I column: *n*-hexane: EtOAc = 90:10, II column: *n*-hexane: EtOAc = 80:20 to 0:100, gradient) afforded (*S*)-**5.6** as a pale pink solid (119 mg, 84% yield). **^{1}H NMR** (400 MHz, $CDCl_3$) δ 7.47 – 7.42 (m, 4H), 7.01 – 6.96 (m, 4H), 6.92 (s, 2H), 3.86 (s, 6H), 3.54 (br s, 4H), 2.81 – 2.73 (m, 4H), 2.40 (dt, J = 17.1, 6.0 Hz, 2H), 2.28 (dt, J = 17.2, 6.2 Hz, 2H), 1.83 – 1.69 (m, 8H); **^{13}C NMR** (101 MHz, $CDCl_3$) δ 158.6, 139.0, 135.3, 132.5, 130.4, 130.4, 127.4, 125.4, 122.4, 114.2, 55.4, 29.4, 27.2, 23.7, 23.5; **IR** (thin layer film): ν (cm^{-1}) 3458, 3362, 2924, 2853, 2834, 1606, 1511, 1458, 1288, 1243, 1176, 1035, 843; **HRMS** (ESI^+) *m/z* calculated for $C_{34}H_{37}O_2N_2^+$ $[M+H]^+$ 505.2850, found 505.2845; **$[\alpha]_D^{25\ °C}$** = +44.8° (c = 0.4, $CHCl_3$).

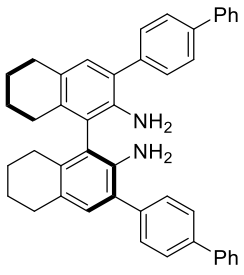
(*S*)-3,3'-bis(4-(tert-butoxy)phenyl)-5,5',6,6',7,7',8,8'-octahydro-[1,1'-binaphthalene]-2,2'-diamine (5.7)



(*S*)-**5.7**

The title compound was prepared from (*S*)-**2.21** (150 mg) and 4-tert-butoxybenzeneboronic acid, pinacol ester (271 mg) following the *general procedure A*. Purification by FCC on silica gel (*n*-hexane: EtOAc = 95:5) afforded (*S*)-**5.7** as a white solid (94 mg, 57% yield). **^{1}H NMR** (400 MHz, $CDCl_3$) δ 7.39 (d, *J* = 8.8 Hz, 4H), 7.05 (d, *J* = 8.7 Hz, 4H), 6.93 (s, 2H), 3.54 (br s, 4H), 2.83–2.69 (m, 4H), 2.38 (dt, *J* = 17.2, 6.0 Hz, 2H), 2.27 (dt, *J* = 17.1, 6.1 Hz, 2H), 1.83 – 1.65 (m, 8H); **^{13}C NMR** (101 MHz, $CDCl_3$) δ 154.4, 138.9, 135.4, 135.1, 130.4, 129.7, 127.4, 125.5, 124.4, 122.4, 78.6, 29.4, 29.0, 27.2, 23.7, 23.5. **IR** (thin layer film): ν (cm^{-1}) 3459, 3364, 2975, 2927, 2927, 2855, 1603, 1506, 1457, 1389, 1236, 1160, 924, 897; **MP** 189−191 °C. **HRMS** (ESI^+) *m/z* calculated for $C_{40}H_{49}N_2O_2^+$ $[M+H]^+$ 589.37886, found 589.37817.

(*S*)-3,3'-di([1,1'-biphenyl]-4-yl)-5,5',6,6',7,7',8,8'-octahydro-[1,1'-binaphthalene]-2,2'-diamine (5.8)

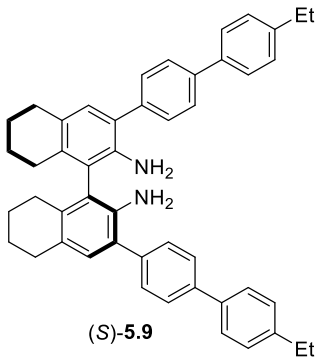


(*S*)-**5.8**

The title compound was prepared from (*S*)-**2.21** (500 mg) and 4-biphenylboronic acid (637 mg) following the *general procedure A*. Purification by FCC on silica gel (*n*-hexane: EtOAc = 95: 5) afforded (*S*)-**5.8** as a white solid (467 mg, 85% yield). **^{1}H NMR** (400 MHz, $CDCl_3$) *δ* 7.69 – 7.62 (m, 8H), 7.62 – 7.57 (m, 4H), 7.49 – 7.43 (m, 4H), 7.39 – 7.33 (m, 2H), 6.97 (s, 2H), 3.60 (br s, 4H), 2.84 – 2.71 (m, 4H), 2.46 – 2.22 (m, 4H), 1.83 – 1.67 (m, 8H). **^{13}C NMR** (101 MHz, $CDCl_3$) *δ* 140.9, 139.8, 139.2, 139.0, 135.8, 130.4, 129.7, 128.9, 127.6, 127.5, 127.4, 127.2, 125.3, 122.5, 29.5, 27.2, 23.7, 23.5. **IR** (thin layer film): ν (cm^{-1}) 3464, 3379, 3027, 2926, 2854, 1063, 1487, 1457, 843, 770,

734, 696; **MP** 144 – 151 °C; **HRMS** (ESI^+) *m/z* calculated for $C_{44}H_{41}N_2^+$ $[M+H]^+$ 597.32643, found 597.32581; **$[\alpha]_D^{25\,°C}$** = +54.2 ° (c = 0.5, $CHCl_3$).

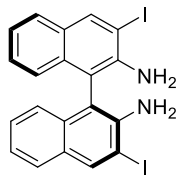
(*S*)-3,3'-bis(4'-ethyl-[1,1'-biphenyl]-4-yl)-5,5',6,6',7,7',8,8'-octahydro-[1,1'-binaphthalene]-2,2'-diamine (5.9)



(*S*)-**5.9**

The title compound was prepared from (*S*)-**2.21** (150 mg) and (4'-ethyl-[1,1'-biphenyl]-4-yl)boronic acid (221 mg) following the *general procedure A*. Purification by FCC on silica gel (*n*-hexane: EtOAc =98:2 to 97:3, gradient) afforded (*S*)-**5.9** as a pale yellow solid (136 mg, 74% yield). **^{1}H NMR** (400 MHz, $CDCl_3$) δ 7.76 – 7.70 (m, 4H), 7.68 – 7.61 (m, 8H), 7.39 – 7.33 (m, 4H), 7.06 (s, 2H), 3.68 (br s, 4H), 2.90 – 2.93 (m, 4H), 2.78 (q, *J* = 7.6 Hz, 4H), 2.56 – 2.32 (m, 4H), 1.90 – 1.75 (m, 8H), 1.36 (t, *J* = 7.6 Hz, 6H); **^{13}C NMR** (101 MHz, $CDCl_3$) δ 143.5, 139.7, 139.0, 138.9, 138.3, 135.7, 130.4, 129.6, 128.4, 127.5, 127.3, 127.0, 125.4, 122.5, 29.5, 28.6, 27.2, 23.7, 23.5, 15.7; **IR** (thin layer film): ν (cm^{-1}) 3463, 3371, 3023, 2962, 2927, 2855, 1604, 1498, 1456, 1117, 1006, 822; **MP** 167– 168 °C; **HRMS** (ESI^+) *m/z* calculated for $C_{48}H_{49}N_2^+$ $[M+H]^+$ 653.3890, found 653.3884; **$[\alpha]_D^{25\,°C}$** = +188.3 (c = 0.4, $CHCl_3$).

(*S*)-3,3'-diiodo-[1,1'-binaphthalene]-2,2'-diamine (2.24)

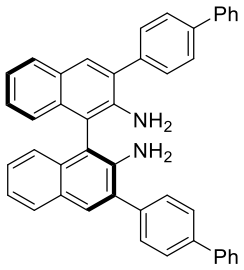


(*S*)-**2.24**

Bis-aniline (*S*)-**2.24** was synthesised according to a reported literature procedure.[5] To a stirred solution of (*S*)-**2.21** (700 mg, 1.28 mmol, 1 equiv) in anhydrous benzene (25 mL) was added DDQ (2,3-dichloro-5,6-dicyano-1,4-benzoquinone, 1.20 g, 5.3 mmol, 5 equiv) at rt. The flask was transferred in a preheated bath (80 °C) and the mixture was refluxed for 5 min. Upon consumption of the starting material, the reaction mixture was directly purified by FCC on silica gel (*n*-hexane: EtOAc = 98: 2 to 95: 5, gradient) to afford (*S*)-**2.24** as a white solid

(220 mg, 32% yield). **^{1}H NMR** (400 MHz, $CDCl_3$) δ 8.43 (s, 2H), 7.71 – 7.67 (m, 2H), 7.26 – 7.18 (m, 4H), 7.00 – 6.92 (m, 2H), 4.11 (br s, 4H). **^{13}C NMR** (101 MHz, $CDCl_3$) δ 142.1, 139.7, 133.2, 129.6, 127.8, 127.8, 124.0, 123.3, 112.8, 88.2. **MS** (ESI^+) *m/z* calculated for $C_{20}H_{15}I_2N_2^+$ $[M+H]^+$ 537.0, found 537.0. Analytical data were in agreement with those previously published.[5]

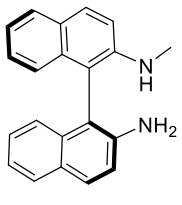
(*S*)-3,3'-di([1,1'-biphenyl]-4-yl)-[1,1'-binaphthalene]-2,2'-diamine (2.25)



(*S*)-**2.25**

The title compound was prepared from (*S*)-**2.24** (200 mg) and 4-biphenylboronic acid (257 mg) following the *general procedure A*. Purification by FCC on silica gel (*n*-hexane: CH_2Cl_2 = 80:20 to 60:40) afforded (*S*)-**2.25** as a white solid (197 mg, 90% yield). **^{1}H NMR** (400 MHz, $CDCl_3$) δ 7.91 – 7.85 (m, 4H), 7.78 – 7.67 (m, 12H), 7.52 (t, *J* = 7.6 Hz, 4H), 7.47 – 7.38 (m, 2H), 7.35 – 7.21 (m, 6H), 3.97 (br s, 4H). **^{13}C NMR** (101 MHz, $CDCl_3$) δ 140.9, 140.6, 140.6, 138.3, 133.2, 130.4, 129.9, 129.9, 129.0, 128.4, 128.3, 127.6, 127.6, 127.2, 127.0, 124.0, 122.8, 113.2; **IR** (thin layer film): ν (cm^{-1}) 3479, 3379, 3056, 2918, 2360, 1620, 1601, 1488, 1433, 1399, 1117, 844, 767, 737, 697. **HRMS** (ESI^+) *m/z* calculated for $C_{44}H_{33}N_2^+$ $[M+H]^+$ 589.26383, found 589.26355. **$[\alpha]_D^{25\ °C}$** = +326.8 ° (c = 0.6, $CHCl_3$).

(*S*)-*N*^{2}-methyl-[1,1'-binaphthalene]-2,2'-diamine (2.30)

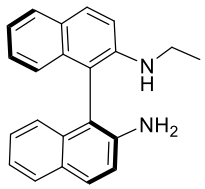


(*S*)-**2.30**

A round-bottom flask was charged with (*S*)-*N*,*N*'-([1,1'-binaphthalene]-2,2'-diyl)bis(2,2,2-trifluoroacetamide)[1] (2.0 g, 4.20 mmol, 1 equiv), K_2CO_3 (1.16 g, 8.4 mmol, 2 equiv.) and methyl iodide (274 µL, 4.41 mmol, 1.05 equiv) in acetone (17 ml, 0.25 M). The reaction mixture was stirred at reflux for 18 h, after which it was cooled to rt and the solvent was removed *in vacuo*. The residue was redissolved in EtOH:H_2O (4:1, 0.25 M) and 2.36 g (42 mmol, 10 equiv.) of

grinded KOH were added. The reaction mixture was stirred at 70 °C for overnight, then it was cooled to rt and diluted with EtOAc and H_2O. Phases were separated and the organic layer was extracted twice with EtOAc. The combined organic layers were washed with brine, dried over $MgSO_4$ and evaporated *in vacuo*. The crude product was purified by FCC on silica gel (*n*-hexane: EtOAc = 98:2 to 90:10, gradient) affording (*S*)-**2.30** as a white solid (1.0 g, 80% yield). **^{1}H NMR** (400 MHz, $CDCl_3$) δ 7.84 (d, J = 8.9 Hz, 1H), 7.77– 7.70 (m, 3H), 7.22–7.04 (m, 6H), 6.99–6.91 (m, 2H), 3.65 (s, 2H), 2.77 (s, 3H), 1.48 (s br, 1H); **^{13}C NMR** (126 MHz, $CDCl_3$) δ 144.9, 142.8, 133.9, 133.4, 129.8, 129.6, 128.5, 128.2, 128.1, 127.8, 126.9, 126.8, 124.0, 123.7, 122.5, 122.1, 118.4, 113.6, 112.5, 112.3, 31.4; **IR** (thin layer film): ν (cm^{-1}) 3349, 2813, 1616, 1594, 1508, 1494, 1470, 1420, 1381, 1337, 1300, 1280, 1247, 1212, 1168, 1153, 1022, 951, 912, 811, 773, 748; **MP** 177–178 °C; **HRMS** (ESI^+) *m/z* calculated for $C_{21}H_{19}N_2$ $(M+H)^+$ 299.1542, found 299.1538; **$[\alpha]_D^{25\ °C}$** = -144.8 ° (c = 1.0, $CHCl_3$).

(*S*)-*N*^{2}-ethyl-[1,1'-binaphthalene]-2,2'-diamine (2.31)

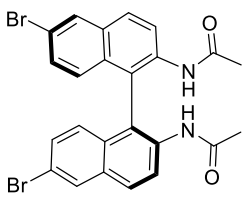


(*S*)-**2.31**

A round-bottom flask was charged with (*S*)-*N*,*N*'-([1,1'-binaphthalene]-2,2'-diyl)bis(2,2,2-trifluoroacetamide)[1] (2.5 g, 5.3 mmol, 1 equiv), K_2CO_3 (1.46 g, 10.6 mmol, 2 equiv.) and ethyl iodide (510 μL, 6.4 mmol, 1.2 equiv) in acetone (20 ml, 0.25 M). The reaction mixture was stirred at reflux for 18 h, after which it was cooled to rt and the solvent was removed *in vacuo*. The residue was redissolved in EtOH:H_2O (4:1, 0.25 M) and 2.97 g (53 mmol, 10 equiv.) of grinded KOH were added. The reaction mixture was stirred at 70 °C for overnight, then it was cooled to rt and diluted with EtOAc and H_2O. Phases were separated and the organic layer was extracted twice with EtOAc. The combined organic layers were washed with brine, dried over $MgSO_4$ and evaporated *in vacuo*. The crude product was purified by FCC on silica gel (*n*-hexane: EtOAc = 98:2 to 90:10, gradient) affording (*S*)-**2.31** as a white solid

(1.02 g, 62% yield). **^{1}H NMR** (400 MHz, $CDCl_3$) δ 7.79 (d, J = 9.1 Hz, 1H), 7.67–7.74 (m, 3H), 7.20–7.03 (m, 6H), 6.98–6.94 (m, 1H), 6.93–6.80 (m, 1H), 6.56 (s br,3H), 3.16 (q, J = 7.1 Hz, 2H), 0.95 (t, J = 7.1 Hz, 3H); **^{13}C NMR** (126 MHz, $CDCl_3$) δ 144.4, 143.0, 134.0, 133.6, 129.6, 129.5, 128.5, 128.2, 128.1, 127.7, 126.8, 126.7, 124.0, 123.8, 122.4, 121.9, 118.3, 114.3, 112.5, 112.4, 38.7, 15.2; **IR** (thin layer film): ν (cm^{-1}) 3435, 3370, 3348, 2964, 1614, 1596, 1567, 1508, 1494, 1470, 1427, 1378, 1349, 1334, 1304, 1280, 1259, 1246, 1213, 1166, 1144, 1066, 1023, 964, 928, 860, 821, 810, 773, 755, 748, 683; **MP** 159–160 °C; **HRMS** (ESI^+) *m/z* calculated for $C_{22}H_{21}N_2$ $(M+H)^+$ 313.1699, found 313.1699; **$[\alpha]_D^{25}$ $^{\circ}C$** = –170.4 ° (c = 1.0, $CHCl_3$).

(*S*)-*N*,*N*'-(6,6'-dibromo-[1,1'-binaphthalene]-2,2'-diyl)diacetamide (2.114)

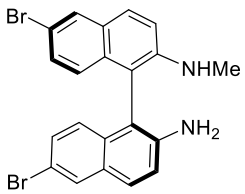


(*S*)-**2.114**

In a flame-dried round-bottom flask (*S*)-[1,1'-binaphthalene]-2,2'-diamine ((*S*)-BINAM, 5 g, 18 mmol, 1 equiv) was dissolved in anhydrous CH_2Cl_2 and the solution cooled to 0 °C. At 0 °C acetic anhydride (3.65 mL, 38.7 mmol, 2.2 equiv) was added dropwise. The reaction mixture was warmed to rt and stirred for overnight, after which the solution was washed with water and brine. Volatiles were removed *in vacuo* to afford 7.1 g of (*S*)-*N*,*N*'-([1,1'-binaphthalene]-2,2'-diyl)diacetamide as a greyish solid. The solid was dissolved in CH_3CN and NH_4OAc (830 mg, 11 mmol, 0.6 equiv) was added. The solution was cooled to 0 °C and at this temperature NBS (9.6 g, 54 mmol, 3 equiv) was added portion-wise. The reaction was warmed to rt and stirred for 3 h. After disappearance of (*S*)-*N*,*N*'-([1,1'-binaphthalene]-2,2'-diyl)diacetamide (monitored by TLC, eluent: EtOAc: CH_2Cl_2=50:50), the reaction was cooled to 0 °C and quenched with a saturated aqueous solution of Na_2SO_3. The reaction mixture was diluted with EtOAc and washed with NaOH (1 M) and brine. The organic layer was dried over $MgSO_4$ and concentrated *in vacuo*. The crude product was purified by FCC on silica gel (CH_2Cl_2: EtOAc= 90:10 to 85:15, gradient)

to obtain (*S*)-**2.114** as a pale orange solid (5.74 g, 61% yield over two steps). **^{1}H NMR** (400 MHz, $CDCl_3$) δ 8.33 (d, *J* = 8.9 Hz, 2H), 8.11 (d, *J* = 2.0 Hz, 2H), 7.96 (d, *J* = 9.1 Hz, 2H), 7.34 (dd, *J* = 9.0, 2.0 Hz, 2H), 6.92 (s, 2H), 6.85 (dt, *J* = 9.0, 0.7 Hz, 2H), 1.86 (s, 6H); **^{13}C NMR** (101 MHz, $CDCl_3$) δ 169.5, 135.2, 132.5, 130.9, 130.7, 130.4, 129.0, 126.9, 124.1, 122.1, 120.0, 24.0. Analytical data were in agreement with those previously published.[6]

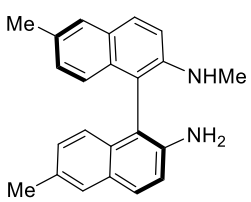
(*S*)-6,6'-dibromo-N^2-methyl-[1,1'-binaphthalene]-2,2'-diamine (2.115)



(*S*)-**2.115**

In a pressure tube, bis-acetamide (*S*)-**2.114** (4 g, 7.6 mmol, 1 equiv), MeI (810 μL, 12.9 mmol, 1.7 equiv) and K_2CO_3 (2.1 g, 15.2 mmol, 2 equiv) were stirred in acetone (0.25 M) at 60 °C for 4 days. After this time, volatiles were evaporated and the crude re-dissolved in a mixture of EtOH and H_2O (4:1, 0.1 M as total concentration of bis-acetamide). Grinded KOH (4.3 g, 76 mmol, 10 equiv) was added and the reaction was stirred at 70 °C for 48 h. The mixture was then cooled to rt and EtOAc was added. Phases were separated and the aqueous phase was extracted three times with EtOAc. The combined organic phases were washed with brine, dried over $MgSO_4$ and evaporated *in vacuo*. Purification by FCC on silica gel (pentane: EtOAc = 100:0 to 90:10, gradient) afforded (*S*)-**2.115** as a pale brown solid. (1.8 g, 52% yield over two steps). **^{1}H NMR** (500 MHz, $CDCl_3$) δ 7.96 (d, *J* = 2.1 Hz, 2H), 7.84 (d, *J* = 8.9 Hz, 1H), 7.74 (d, *J* = 8.8 Hz, 1H), 7.32 – 7.23 (m, 3H), 7.17 (d, *J* = 8.8 Hz, 1H), 6.87 (dd, *J* = 12.3, 9.0 Hz, 2H), 3.71 (br s, 3H), 2.87 (s, 3H); **^{13}C NMR** (126 MHz, $CDCl_3$) δ 145.7, 143.4, 132.5, 132.0, 130.3, 130.3, 130.3, 130.2, 129.8, 129.2, 129.0, 128.7, 125.8, 125.4, 119.4, 116.2, 115.3, 114.4, 111.8, 111.2, 31.0; **IR** (thin layer film) ν (cm^{-1}) = 3381, 1614, 1590, 1498, 1338, 772; **MP** 183–184 °C; **HRMS** (ESI^+) *m/z* calculated for $C_{21}H_{17}N_2Br_2$ $[M+H]^+$ 454.9753, found 454.9753; **$[\alpha]_D^{25\,°C}$** = –37.8 ° (c = 0.5, $CHCl_3$).

(*S*)-*N*^{2},6,6'-trimethyl-[1,1'-binaphthalene]-2,2'-diamine (5.10)

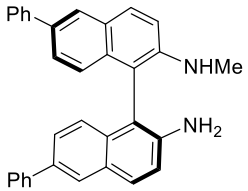


(*S*)-**5.10**

Following the procedure reported by Tan,[7] in a flame-dried Schlenk tube under inert atmosphere, (*S*)-**2.115** (200 mg, 0.44 mmol, 1 equiv) and [1,1'-Bis(diphenylphosphino)-ferrocene]-dichloropalladium(II) (32 mg, 10 mol%) were dissolved in dry and degassed THF. Methyl magnesium chloride (1.2 mL, 3.5 mmol, 8 equiv, 3 M in THF) was then added dropwise through a rubber septum. The septum was then replaced with a cooling finger. The reaction was stirred at 80 °C for 18 h and then cooled to 0 °C prior of carefully quenching it with water. The reaction mixture was extracted three times with EtOAc. The organic layer was washed with brine, dried over $MgSO_4$ and evaporated *in vacuo*. Purification by FCC on silica gel (*n*-hexane: EtOAc = 100:0 to 94:6, gradient) afforded (*S*)-**5.10** as a pale yellow solid (141 mg, 98% yield). **^{1}H NMR** (400 MHz, $CDCl_3$) δ 7.84 (d, J = 8.9 Hz, 1H), 7.73 (d, J = 8.7 Hz, 1H), 7.58 (s, 2H), 7.27 – 7.21 (m, 1H), 7.12 (d, J = 8.7 Hz, 1H), 7.06–7.01 (m, 2H), 6.98–6.91 (m, 2H), 3.60 (s, 3H), 2.83 (br s, 3H), 2.44 (s, 3H), 2.43 (s, 3H); **^{13}C NMR** (101 MHz, $CDCl_3$) δ 144.9, 142.3, 132.2, 132.0, 131.8, 131.2, 129.1, 129.1, 129.0, 128.9, 128.9, 127.9, 127.4, 127.3, 124.1, 123.8, 118.6, 113.7, 112.9, 112.3, 31.4, 21.4, 21.4; **IR** (thin layer film) ν (cm^{-1}) = 3420, 3377, 2916, 1600, 1501, 1342, 819; MP 98–100 °C; **HRMS** (ESI) *m/z* calculated for $C_{23}H_{23}N_2^+$ $[M+H]^+$ 327.1856, found 327.1854; **$[\alpha]_D^{25\ °C}$** = –72.2 ° (c = 0.5, $CHCl_3$).

(*S*)-*N*^{2}-methyl-6,6'-diphenyl-[1,1'-binaphthalene]-2,2'-diamine (5.11)

The title compound was prepared from (*S*)-**2.115** (150 mg) and phenylboronic acid pinacol ester (236 mg) following the *general procedure A*. Purification by FCC on silica gel (I column: pentane:EtOAc = 98:2 to 90:10, gradient; II column: toluene: Et_2O= 100:0 to

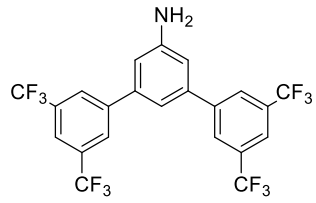


(*S*)-**5.11**

99:1, gradient) afforded (*S*)-**5.11** as a pale yellow solid (105 mg, 70% yield). **^{1}H NMR** (400 MHz, $CDCl_3$) δ 8.03 (t, J = 2.1 Hz, 2H), 8.00 (d, J = 8.9 Hz, 1H), 7.89 (dd, J = 8.9, 0.7 Hz, 1H), 7.67 (dt, J = 8.2, 1.3 Hz, 4H), 7.53 – 7.41 (m, 6H), 7.36 – 7.28 (m, 3H), 7.22 – 7.10 (m, 3H), 3.75 (s, 3H), 2.89 (s, 3H); **^{13}C NMR** (101 MHz, $CDCl_3$) δ [overlapping signals] 145.7, 143.3, 141.5, 141.4, 135.4, 134.6, 133.3, 132.9, 130.3, 130.1, 128.9, 128.9, 127.9, 127.2, 127.2, 127.0, 126.9, 126.7, 126.6, 126.3, 126.3, 124.7, 124.3, 118.9, 114.0, 112.4, 111.7, 31.2; **IR** (thin layer film) ν (cm^{-1}) = 3380, 3016, 1619, 1596, 1494, 1304, 909, 779, 697; **MP** 142-144 °C; **HRMS** (ESI^+) *m/z* calculated for $C_{33}H_{27}N_2$ $[M+H]^+$ 451.2169, found 451.2165; **$[\alpha]_D^{25\,°C}$** = + 85.3 ° (c = 0.4, $CHCl_3$).

Achiral anilines

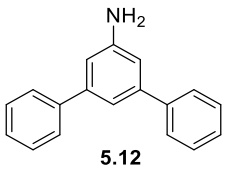
3,3'',5,5''-tetrakis(trifluoromethyl)-[1,1':3',1''-terphenyl]-5'-amine (2.79)



2.79

Aniline **2.79** was prepared from 3,5-dibromoaniline (2.79 g) and (3,5-bis(trifluoromethyl)phenyl)boronic acid (10.00 g) following the *general procedure A*. Purification by FCC on silica gel (pentane: CH_2Cl_2 = 70:30) afforded **2.79** as a white solid (4.63 g, 81% yield). **^{1}H NMR** (400 MHz, $CDCl_3$) δ 8.03 (s, 4H), 7.90 (s, 2H), 7.12 (br t, J = 1.7 Hz, 1H), 6.96 (d, J = 1.6 Hz, 2H), 4.03 (br s, 2H); **^{19}F NMR** (377 MHz, $CDCl_3$) δ –62.82 (s, 12F); **^{13}C NMR** (101 MHz, $CDCl_3$) δ 148.1, 143.2, 140.9, 132.3 (q, $J_{C–F}$ = 33.3 Hz), 127.5, 123.5 (q, $J_{C–F}$ = 273.0), 121.5, 116.5, 114.1; **IR** (thin layer film) ν (cm^{-1}) = 3407, 1624, 1602, 1400, 1309, 1170, 1124, 899, 842, 753, 705; **MP** 123 – 124 °C; **HRMS** (ESI^+) *m/z* calculated for $C_{22}H_{12}F_{12}N^+$ $[M+H]^+$ 518.07726, found 518.07727.

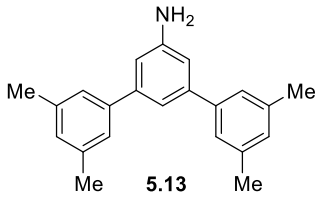
3,5-diphenylaniline (5.12)



5.12

Aniline **5.12** was prepared from 3,5-dibromoaniline (2.00 g) and phenylboronic acid (3.41 g) following the *general procedure A*. Purification by FCC on silica gel (*n*-hexane: EtOAc = 95:5 to 80:20, gradient) afforded **5.12** as a white solid (1.83 g, 93% yield). **^{1}H NMR** (400 MHz, $CDCl_3$) δ 7.65 – 7.59 (m, 4H), 7.47–7.41 (m, 4H), 7.39 – 7.32 (m, 2H), 7.22 (t, *J* = 1.6 Hz, 1H), 6.90 (d, *J* = 1.5 Hz, 2H), 3.83 (s, 2H); **^{13}C NMR** (101 MHz, $CDCl_3$) δ 147.2, 143.1, 141.5, 128.8, 127.5, 127.3, 117.2, 113.1; **IR** (thin layer film): ν (cm^{-1}) 3372, 3030, 2927, 1615, 1595, 1576, 1498, 1415, 857, 758, 698; **MP** 106–109 °C; **HRMS** (ESI^+) *m/z* calculated for $C_{18}H_{16}N^+$ $[M+H]^+$ 246.12773, found 246.12787.

3,3'',5,5''-tetramethyl-[1,1':3',1''-terphenyl]-5'-amine (5.13)



5.13

Aniline **5.13** was prepared from 3,5-dibromoaniline (500 mg) and 3,5-dimethylphenylboronic acid (1.05 g) following the *general procedure A*. Purification by FCC on silica gel (*n*-hexane: EtOAc = 90:10) afforded **5.13** as a white solid (428 mg, 71% yield). **^{1}H NMR** (400 MHz, $CDCl_3$) δ 7.29 (s, 4H), 7.23 (s, 1H), 7.05 (s, 2H), 6.91 (s, 2H), 3.79 (s, 2H), 2.43 (s, 12H); **^{13}C NMR** (101 MHz, $CDCl_3$) δ 147.0, 143.1, 141.6, 138.2, 129.0, 125.2, 117.1, 113.0, 21.5; **IR** (thin layer film) ν (cm^{-1}) = 3375, 3025, 2918, 2857,1593, 1457, 840, 697; **MP** 174 – 175 °C; **HRMS** (ESI^+) *m/z* calculated for $C_{22}H_{24}N^+$ $[M+H]^+$ 302.1903, found 302.1901.

Bis-ureas Organocatalysts

Catalysts (*S*)-**2.38**, (*S*)-**2.59 (***S*)-**2.60,** (*S*)-**2.62** (*S*)-**2.63** (*S*)-**2.66,** (*S*)-**2.73** were synthesised according to the *general procedure B*, catalyst (*S*)-**2.49,** (*S*)-**2.74** (*S*)-**2.119,** (*S*)-**5.14** according to the *general procedure C*.

General procedure B: urea-coupling with pre-formed isocyanates

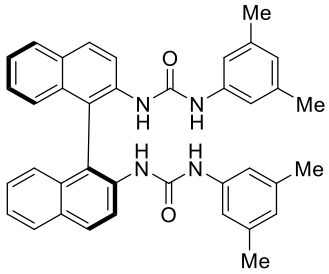
A flame dried Schlenk tube capped with a rubber septum was charged with the (*S*)-BINAM-derived bis-aniline (1 equiv) and then evacuated and backfilled with N_2 (three times). Anhydrous CH_2Cl_2 (0.1 M) was added *via* a syringe followed by dropwise addition of the isocyanate (2 equiv). The reaction mixture was then stirred at rt until disappearance of the aniline starting material (checked by TLC, eluent: pentane/EtOAc), and then MeOH was added and stirred for further 5 min. Volatiles were removed *in vacuo* and the crude product was purified by FCC on silica gel.

General procedure C: urea coupling with in situ generated isocyanates

In a flame-dried Schlenk tube under inert atmosphere, triphosgene (0.7 equiv) was dissolved in CH_2Cl_2 (0.1 M with respect to the chiral BINAM-derived aniline). The solution was cooled to 0 °C and the achiral aniline (2 equiv) was added at this temperature. Then NEt_3 (4 equiv) was added dropwise at 0 °C and the reaction mixture was stirred at rt for 2 h under a flow of nitrogen. After disappearance of the achiral aniline (monitored by TLC from a sample of the reaction mixture quenched with a drop of MeOH; eluent: pentane/EtOAc), the (*S*)-BINAM-derived aniline (1 equiv) was added as a solid and the reaction stirred at rt for 24 h (until TLC showed no further conversion). An excess of MeOH was added and the reaction mixture stirred for further 5 min. Water was then added and the

layers were separated. The aqueous one was extracted twice with CH_2Cl_2. The combined organic layers were washed with brine, dried over $MgSO_4$ and evaporated *in vacuo*. The crude mixture was then purified by FCC on silica gel.

(*S*)-1,1'-([1,1'-binaphthalene]-2,2'-diyl)bis(3-(3,5-dimethylphenyl)urea) (2.38)

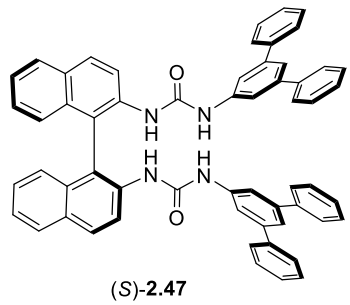


(*S*)-**2.38**

Bis-urea (*S*)-**2.38** was prepared from (*S*)-(−)-1,1′-Binaphthyl-2,2′-diamine ((*S*)-BINAM, 150 mg) and 3,5-dimethylphenyl isocyanate (148 μL) following the *general procedure B.* Additionally, 13 mg (0.2 equiv) of DMAP were added to favour the coupling. Purification by FCC on silica gel (CH_2Cl_2: EtOAc = 99:1 to 95:5, gradient) afforded (*S*)-**2.38** as a white solid (214 mg, 70% yield). **^{1}H NMR** (500 MHz, $CDCl_3$) δ 8.28 (d, J = 9.1 Hz, 2H), 7.92 (d, J = 9.0 Hz, 2H), 7.85 (d, J = 8.5 Hz, 2H), 7.36 (ddd, J = 8.1, 6.8, 1.1 Hz, 2H), 7.15 (ddd, J = 8.3, 6.7, 1.3 Hz, 2H), 6.93 (d, J = 8.5, 2H), 6.68 (br s, 2H), 6.62 (br s, 2H), 6.57 (s, 6H), 2.07 (s, 12H). **^{13}C NMR** (126 MHz, $CDCl_3$) δ 154.1, 138.9, 137.2, 135.7, 132.9, 130.9, 129.7, 128.3, 127.1, 126.3, 125.3, 125.2, 122.2, 120.9, 119.2, 21.3. **IR** (thin layer film): ν (cm^{-1}) 3351, 2921, 2857, 1659, 1617, 1599, 1565, 1502, 1427, 1273, 1217, 837, 746, 687; **MP** 190 – 191 °C; **HRMS** ($APCI^+$) *m/z* calculated for $C_{38}H_{35}N_4O_2^+$ $[M+H]^+$ 579.27545; found 579.27448; **$[\alpha]_D^{25\,°C}$** = –46.6 (c = 0.6, $CHCl_3$).

1,1'-([1,1'-binaphthalene]-2,2'-diyl)bis(3-([1,1':3',1''-terphenyl]-5'-yl)urea) (2.47)

Synthesised by Dr. Gabriele Pupo

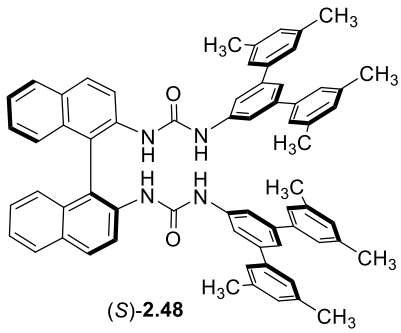


(*S*)-**2.47**

In a flame-dried Schlenk tube, achiral aniline **5.12** (127 mg, 0.52 mmol, 2 equiv), CDI (1,1'-carbonyldiimidazole, 93 mg, 0.57 mmol, 2.2 equiv) and DMAP (4-(dimethylamino)pyridine, 5 mg, 0.04 mmol, 0.2 equiv.) were dissolved in anhydrous DMSO (2.6 ml, 0.1 M) and stirred overnight at rt. After this time, (*S*)-BINAM (75 mg, 0.26 mmol, 1 equiv.) was added as a solid and the reaction mixture was stirred for further 24 h at 78 °C. Then, the reaction mixture was diluted with CH_2Cl_2 and washed with LiCl (three times). The organic layer was dried over $MgSO_4$, evaporated *in vacuo* and the crude product was purified by FCC on silica gel (I column: pentane: EtOAc = 90:10 to 70:30, gradient; II column: *n*-hexane:CH_2Cl_2 = 75:25). White solid (96 mg, 48% yield). **^{1}H NMR** (500 MHz, $CDCl_3$) δ 8.27 (d, *J* = 9.0 Hz, 2H), 7.91 (d, *J* = 9.0 Hz, 2H), 7.80 (d, *J* = 8.1 Hz, 2H), 7.58 – 7.47 (m, 4H), 7.40 – 7.24 (m, 24H), 7.17 (ddd, *J* = 8.3, 6.8, 1.3 Hz, 2H), 7.13 (br s, 2H), 7.00 (d, *J* = 8.2 Hz, 2H), 6.72 (s, 2H); **^{13}C NMR** (126 MHz, $CDCl_3$) [overlapping signals] δ 153.9, 142.3, 140.6, 138.6, 135.4, 132.9, 130.8, 129.6, 128.6, 128.2, 127.4, 127.2, 127.1, 125.2, 122.4, 121.6, 120.9, 118.0; **IR** (thin layer film) ν (cm^{-1}) = 3367, 3054, 1686, 1597, 1567, 1498, 1427,1266, 1221, 757; **HRMS** (APCI$^+$) *m/z* calculated for $C_{58}H_{43}O_2N_4$ $[M+H]^+$ 827.3380, found 827.3375; **$[\alpha]_D^{25\,°C}$** = –61.4 ° (c = 0.5, $CHCl_3$).

(*S*)-1,1'-([1,1'-binaphthalene]-2,2'-diyl)bis(3-(3,3'',5,5''-tetramethyl-[1,1':3',1''-terphenyl]-5'-yl)urea) (2.48)

Synthesised by Dr. Gabriele Pupo

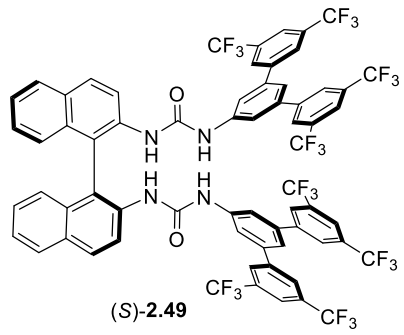


(*S*)-**2.48**

In a flame-dried Schlenk tube, achiral aniline **5.13** (210 mg, 0.70 mmol, 2 equiv), CDI (1,1'-carbonyldiimidazole, 124 mg, 0.77 mmol, 2.2 equiv) and DMAP (4-(dimethylamino)pyridine, 8.5 mg, 0.07 mmol, 0.2 equiv.) were dissolved in anhydrous DMSO (3.5 ml, 0.1 M) and stirred overnight at rt. After this time, (*S*)-BINAM (100 mg, 0.35 mmol, 1 equiv.) was added as a solid and the reaction mixture was stirred for further 24 h at 78 °C. Then, the reaction mixture was diluted with CH_2Cl_2 and washed with LiCl (three times). The organic layer was dried over $MgSO_4$, evaporated *in vacuo* and the crude product was purified by FCC on silica gel (CH_2Cl_2: *n*-hexane= 80:20 to CH_2Cl_2: Et_2O =98:2, gradient; II column: *n*-hexane:CH_2Cl_2 = 75:25). White solid (110 mg, 34% yield). **^{1}H NMR** (400 MHz, $CDCl_3$) δ 8.18 – 8.11 (m, 2H), 7.70 (br s, 2H), 7.63 (d, *J* = 8.1 Hz, 2H), 7.26 – 7.13 (m, 10H), 7.05 (t, *J* = 7.8 Hz, 2H), 6.95 (s, 8H), 6.89 (d, *J* = 8.5 Hz, 2H), 6.85 (s, 4H), 6.55 (s, 2H), 2.21 (s, 24H); **^{13}C NMR** (101 MHz, $CDCl_3$) δ 154.1, 142.7, 140.6, 138.1, 135.4, 132.7, 130.7, 129.7, 129.1, 128.2, 127.1, 125.1, 125.1, 125.0, 122.2, 122.0, 120.7, 118.7, 118.5, 21.4; **IR** (thin layer film) ν (cm^{-1}) = 3334, 3027, 2917, 1668, 1596, 1563, 1504, 1427, 1272, 12717, 844, 747, 697; **MP** 199–200 °C; **HRMS** ($APCI^+$) *m/z* calculated for $C_{66}H_{59}O_2N_4$ $[M+H]^+$ 939.4632, found 939.4605; $\mathbf{[\alpha]_D^{25\,°C}}$ = –41.6 ° (c = 0.6, $CHCl_3$).

(*S*)-1,1'-([1,1'-binaphthalene]-2,2'-diyl)bis(3-(3,3'',5,5''-tetrakis(trifluoromethyl)-[1,1':3',1''-terphenyl]-5'-yl)urea) (2.49)

Synthesised by Dr. Gabriele Pupo

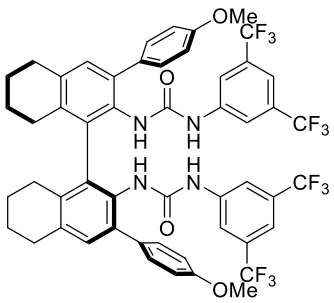


(*S*)-**2.49**

Bis-urea (*S*)-**2.49** was prepared from (*S*)-BINAM (1.476 g) and achiral aniline **2.79** (1.28 g) following the *general procedure C*. Aniline **2.79** was added as a solution in CH_2Cl_2 (37 mL). Purification by FCC on silica gel (pentane: CH_2Cl_2 = 80:20 to 0:100) afforded (*S*)-**2.49** as a white solid (4.23 g, 73% yield). **^{1}H NMR** (400 MHz, DMSO-d_6) δ 9.33 (br s, 2H), 8.43 (d, J = 9.1 Hz, 2H), 8.14 (d, J = 9.1 Hz, 2H), 8.10 (s, 8H), 8.04 (d, J = 8.3 Hz, 2H), 7.99 (s, 4H), 7.64 (s, 4H), 7.61 (s, 2H), 7.52 (s, 2H), 7.44 (t, J = 7.4 Hz, 2H), 7.28 (t, J = 8.0 Hz, 2H), 6.84 (d, J = 8.6 Hz, 2H); **^{19}F NMR** (376 MHz, DMSO-d_6) δ –61.4 (s, 24F); **^{13}C NMR** (101 MHz, DMSO-d_6) δ 153.0, 142.2, 141.0, 138.2, 136.2, 132.9, 130.8 (q, $J_{C–F}$ = 33.0 Hz), 130.3, 128.9, 128.2, 127.3, 126.7, 124.8, 124.6, 123.1 (q, $J_{C–F}$ = 272.8 Hz), 122.8, 121.1, 119.6, 119.4, 117.2; **IR** (thin layer film) ν (cm^{-1}) = 3361, 1691, 1599, 1569, 1505, 1428, 1396, 1367, 1278, 1220, 1177, 1131, 1107, 900, 866, 844, 824, 747, 705, 682, 638; **MP** not determined (decomposition at T >200 °C); **HRMS** ($APCI^+$) *m/z* calculated for $C_{66}H_{35}O_2N_4F_{24}$ $[M+H]^+$ 1371.2371, found 1371.2368; **$[\alpha]_D^{25\ °C}$ =** –96.7 ° (c = 0.5, $CHCl_3$).

(*S*)-1,1'-(3,3'-bis(4-methoxyphenyl)-5,5',6,6',7,7',8,8'-octahydro-[1,1'-binaphthalene]-2,2'-diyl)bis(3-(3,5-bis(trifluoromethyl)phenyl)urea) (2.59)

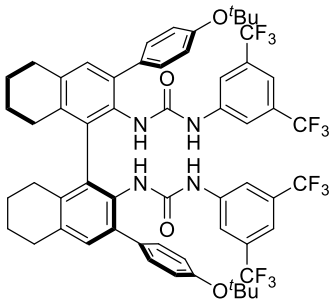
Synthesised by Dr. Gabriele Pupo



(*S*)-**2.59**

Bis-urea (*S*)-**2.59** was prepared from (*S*)-**5.6** (50 mg) and 3,5-bis(trifluoromethyl)phenyl isocyanate (35 μL) following the *general procedure B*. Purification by FCC on silica gel (CH_2Cl_2: *n*-hexane = 70:30 to CH_2Cl_2: EtOAc = 70:30, gradient) afforded (*S*)-**2.59** as a white solid (72 mg, 61% yield). **^{1}H NMR** (400 MHz, $CDCl_3$) δ 7.33 (dd, J = 8.9, 2.4 Hz, 10H), 7.18 (s, 2H), 6.88 – 6.78 (m, 4H), 6.54 (s, 2H), 6.25 (s, 2H), 3.70 (s, 6H), 2.87 (t, J = 6.3 Hz, 4H), 2.36 – 2.11 (m, 4H), 1.85 – 1.69 (m, 8H); **^{19}F NMR** (377 MHz, $CDCl_3$) δ –63.18; **IR** (thin layer film): ν (cm^{-1}) 3343, 2979, 2934, 1606, 1509, 1473, 1386, 1277, 1177, 1135, 734; **HRMS** ($APCI^+$) *m/z* calculated for $C_{52}H_{43}F_{12}N_4O_4^+$ $[M+H]^+$ 1015.3087; found 1015.3068; **$[\alpha]_D^{25\,°C}$** = +289.7 (c = 0.3, $CHCl_3$).

(*S*)-1,1'-(3,3'-bis(4-(tert-butoxy)phenyl)-5,5',6,6',7,7',8,8'-octahydro-[1,1'-binaphthalene]-2,2'-diyl)bis(3-(3,5-bis(trifluoromethyl)phenyl)urea) (2.60)



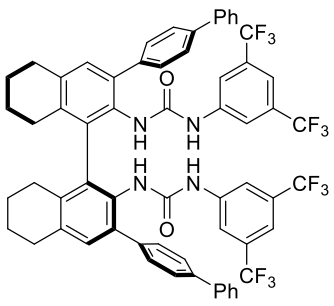
(*S*)-**2.60**

Bis-urea (*S*)-**2.60** was prepared from (*S*)-**5.7** (86 mg) and 3,5-bis(trifluoromethyl)phenyl isocyanate (54 μL) following the *general procedure B*. Purification by FCC on silica gel (CH_2Cl_2 100% to CH_2Cl_2: EtOAc = 98:2, gradient) afforded *S*)-**2.60** as a pale yellow solid (120 mg, 73% yield). **^{1}H NMR** (500 MHz, DMSO-d_6, 90 °C) δ 8.89 (br s, 2H), 7.86 (s, 4H), 7.46 (s, 2H), 7.41 (s, 2H), 7.31 (d, J = 8.2 Hz, 4H), 7.06 (s, 2H), 6.87 (d, J = 8.2 Hz, 4H), 2.88 – 2.71 (m, 4H), 2.49 – 2.41 (m, 2H), 2.17 – 2.07 (m, 2H), 1.77 – 1.59 (m, 8H), 1.21

(s, 18H); **^{19}F NMR** (470 MHz, DMSO-d_6, 90 °C) δ –61.90; **^{13}C NMR** (126 MHz, DMSO-d_6, 90 °C) δ 154.6, 154.0, 142.6, 137.8, 137.7, 136.5, 135.3, 135.1, 131.2 (q, $J_{C–F}$ = 32.8 Hz) 130.6, 130.1, 129.5, 123.7 (q, $J_{C–F}$ = 273.3 Hz), 123.1, 118.3, 114.1, 78.2, 29.6, 28.9, 27.2, 23.0, 22.8; **IR** (thin layer film): ν (cm^{-1}) 3343, 2979, 2934, 1606, 1509, 1473, 1386, 1277, 1177, 1135, 734; **MP** 167 – 170°C; **HRMS** (APCI$^+$) *m/z* calculated for $C_{58}H_{55}F_{12}N_4O_4^+$ $[M+H]^+$ 1099.40372; found 1099.39954. ; **$[\alpha]_D^{25\ °C}$** = +198.3 (c = 0.55, $CHCl_3$).

(*S*)-1,1'-(3,3'-di([1,1'-biphenyl]-4-yl)-5,5',6,6',7,7',8,8'-octahydro-[1,1'-binaphthalene]-2,2'-diyl)bis(3-(3,5-bis(trifluoromethyl)phenyl)urea) (2.62)

Synthesised by Dr. Gabriele Pupo

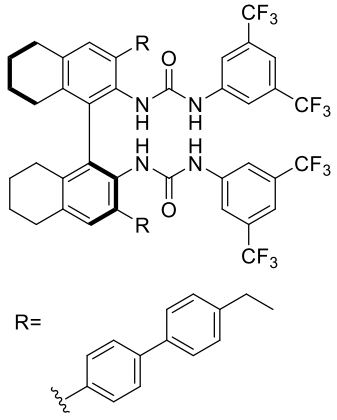


(*S*)-**2.62**

Bis-urea (*S*)-**2.63** was prepared from (*S*)-**5.8** (78 mg) and 3,5-bis(trifluoromethyl)phenyl isocyanate (66 μL) following the *general procedure B*. Purification by FCC on silica gel (*n*-hexane: CH_2Cl_2 = 80:20 to 50:50, gradient) afforded (*S*)-**2.62** as a white solid (80 mg, 55% yield). **^{1}H NMR** (400 MHz, $CDCl_3$) δ 7.52 – 7.13 (m, 26H), 6.36 (s, 2H), 6.35 (br s, 2H), 2.82 (t, *J* = 6.2 Hz, 4H), 2.21 (qt, *J* = 17.0, 6.1 Hz, 4H), 1.70 (dq, *J* = 20.8, 5.1, 4.6 Hz, 8H); **^{19}F NMR** (376 MHz, $CDCl_3$) δ –63.16; **^{13}C NMR** (101 MHz, $CDCl_3$) δ 153.2, 140.4, 140.2, 139.4, 138.2, 137.9, 136.9, 136.4, 135.8, 131.8 (q, $J_{C–F}$ = 34.1 Hz), 131.5, 128.9, 128.8, 128.7, 127.4, 127.3, 126.9, 123.0 (q, $J_{C–F}$ = 272.4 Hz), 118.9, 116.4, 29.7, 27.7, 23.0, 22.7. **HRMS** (APCI$^+$) *m/z* calculated for $C_{62}H_{47}F_{12}N_4O_2^+$ $[M+H]^+$ 1107.3502; found 1107.3481.

(S)-1,1'-(3,3'-bis(4'-ethyl-[1,1'-biphenyl]-4-yl)-5,5',6,6',7,7',8,8'-octahydro-[1,1'-binaphthalene]-2,2'-diyl)bis(3-(3,5-bis(trifluoromethyl)phenyl)urea) (2.63)

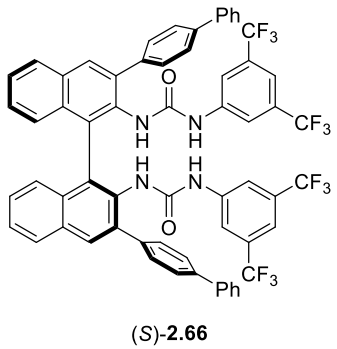
Synthesised by Dr. Gabriele Pupo



(*S*)-**2.63**

Bis-urea (*S*)-**2.63** was prepared from (*S*)-**5.9** (50 mg) and 3,5-bis(trifluoromethyl)phenyl isocyanate (39 μL) following the *general procedure B*. Purification by FCC on silica gel (*n*-hexane: CH_2Cl_2 = 50:50) afforded (*S*)-**2.63** as a white solid (62 mg, 70% yield). **^{1}H NMR** (400 MHz, $CDCl_3$) δ 7.50 – 7.28 (m, 16H), 7.23 (s, 2H), 7.15 (dd, J = 19.0, 8.5 Hz, 6H), 6.46 (br s, 4H), 2.87 – 2.74 (m, 4H), 2.58 (q, J = 7.6 Hz, 4H), 2.31 – 2.07 (m, 4H), 1.81 – 1.61 (m, 8H), 1.17 (t, J = 7.6 Hz, 6H); **^{19}F NMR** (377 MHz, $CDCl_3$) δ –63.13; **HRMS** (APCI$^+$) *m/z* calculated for $C_{66}H_{55}F_{12}N_4O_2^+$ $[M+H]^+$ 1163.4128; found 1163.4105.

(*S*)-1,1'-(3,3'-di([1,1'-biphenyl]-4-yl)-[1,1'-binaphthalene]-2,2'-diyl)bis(3-(3,5-bis(trifluoromethyl)phenyl)urea) (2.66)

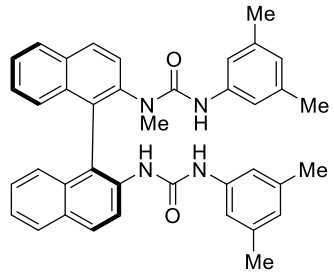


(*S*)-**2.66**

Bis-urea (*S*)-**2.66** was prepared from (*S*)-**2.25** (90 mg) and 3,5-bis(trifluoromethyl)phenyl isocyanate (54 μL) following the *general procedure B*. Purification by FCC on silica gel (*n*-hexane: CH_2Cl_2 = 60:40 to CH_2Cl_2 100%, gradient) afforded (*S*)-**2.66** as a white solid (150 mg, 91% yield). **^{1}H NMR** (500 MHz, DMSO-d_6, 90 °C) δ 8.95 (br s, 2H), 8.11 (s, 2H), 8.05 (d, J = 8.4, 2H), 7.84 (s, 2H), 7.76 – 7.59 (m, 16H), 7.53 – 7.42 (m, 6H), 7.41 – 7.34 (m, 4H), 7.33 – 7.26 (m, 4H); **^{19}F NMR** (470 MHz, DMSO-d_6, 90 °C) δ –61.89; **^{13}C NMR** (126 MHz, DMSO-d_6, 90 °C) δ 153.9, 142.2, 140.4, 139.5, 139.2, 138.9, 133.9,

132.7, 132.4, 131.6, 130.9, 129.9, 129.9, 129.3, 128.6, 127.8, 126.9, 126.8, 126.6, 126.1, 123.7 (q, $J_{C–F}$ = 272.6 Hz), 118.4, 114.4, 103.2; **IR** (thin layer film): ν (cm^{-1}) 2867, 1683, 1576, 1474, 1384, 1277, 1179, 1133, 670, 681, 628; **MP** 185 – 187 °C; **HRMS** ($APCI^+$) *m/z* calculated for $C_{62}H_{39}F_{12}N_4O_2^+$ $[M+H]^+$ 1099.28759; found 1099.28711. **$[\alpha]_D^{25\ °C}$** = +240.8 (c = 0.6, $CHCl_3$).

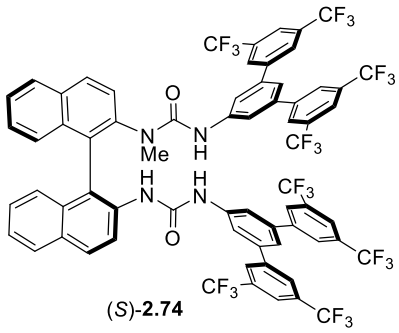
(*S*)-3-(3,5-bis(trifluoromethyl)phenyl)-1-(2'-(3-(3,5-bis(trifluoromethyl)phenyl)ureido)-[1,1'-binaphthalen]-2-yl)-1-methylurea (2.73)



(*S*)-**2.73**

Bis-urea (*S*)-**2.73** was prepared from (*S*)-**2.30** and 3,5-bis(trifluoromethyl)phenyl isocyanate (84 μL) following the *general procedure B*. Additionally, 7.2 mg (0.2 equiv) of DMAP were added to favour the coupling. Purification by FCC on silica gel (*n*-hexane: CH_2Cl_2 = 30:70 to CH_2Cl_2:EtOAc = 98:2, gradient) afforded (*S*)-**2.73** as a white solid (109 mg, 60% yield). **^{1}H NMR** (500 MHz, $CDCl_3$) δ 8.76 (d, *J* = 9.1 Hz, 1H), 8.09 (d, *J* = 8.8 Hz, 1H), 7.98 (d, *J* = 9.4 Hz, 1H), 7.97 (d, *J* = 8.1, 1Hz), 7.91 (d, *J* = 8.1 Hz, 1H), 7.62 – 7.47 (m, 3H), 7.36 (t, *J* = 7.5 Hz, 1H), 7.29 (7, *J* = 7.90 Hz, 1H), 7.26 – 7.09 (m, 3H), 6.96 (s, 2H), 6.92 (d, *J* = 8.5 Hz, 1H), 6.78 (s, 2H), 6.72 (s, 1H), 6.58 (s, 1H), 6.44 (s, 1H), 2.83 (s, 3H), 2.18 (s, 12H); **^{13}C NMR** (126 MHz, $CDCl_3$) δ 156.9, 152.5, 140.8, 138.8, 138.4, 138.1, 137.2, 136.8, 133.6, 133.2, 133.2, 131.2, 130.5, 129.6, 129.4, 128.4, 128.1, 127.2, 127.0, 126.9, 126.8, 126.7, 126.3, 124.9, 124.3, 123.8, 119.2, 119.1, 117.6, 116.8, 36.2, 21.3, 21.2; **IR** (thin layer film): ν (cm^{-1}) 3334, 2972, 1614, 1550, 1504, 1470, 1427, 1283, 1205, 1190, 1116, 823, 750, 688; **MP** 172–173 °C; **HRMS** ($APCI^+$) *m/z* calculated for $C_{39}H_{37}N_4O_2^+$ $[M+H]^+$ 593.2922; found 529.2913; **$[\alpha]_D^{25\ °C}$** = –59.0 (c = 0.5, $CHCl_3$).

(*S*)-1-methyl-3-(3,3'',5,5''-tetrakis(trifluoromethyl)-[1,1':3',1''-terphenyl]-5'-yl)-1-(2'-(3-(3,3'',5,5''-tetrakis(trifluoromethyl)-[1,1':3',1''-terphenyl]-5'-yl)ureido)-[1,1'-binaphthalen]-2-yl)urea (2.74)

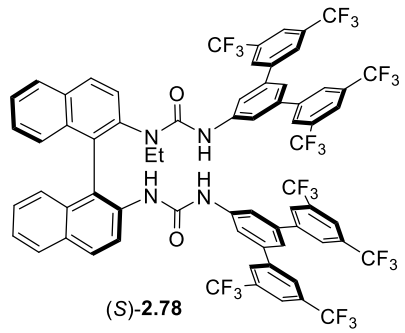


(*S*)-**2.74**

Bis-urea (*S*)-**2.74** was prepared from (*S*)-**2.30** (363.8 mg) and achiral aniline **2.79** (1.28 g) following the *general procedure C*. Aniline **2.79** was added as a solution in CH_2Cl_2 (9 mL). Purification by FCC on silica gel (pentane: Et_2O = 80:20) afforded (*S*)-**2.74** as a white solid (929.6 mg, 54% yield). **^{1}H NMR** (500 MHz, DMSO-d_6) δ 8.77 (br s, 1H), 8.73 (d, J = 7.9 Hz, 1H), 8.43 (d, J = 8.4 Hz, 1H), 8.26 (d, J = 8.4 Hz, 1H), 8.11 (d, J = 8.8 Hz, 1H), 8.00 (s, 5H), 7.90 – 7.71 (m, 10H), 7.69 (d, J = 7.4 Hz, 1H), 7.58 (s, 1H), 7.51 – 7.44 (m, 3H), 7.38 (br t, J = 6.5 Hz, 1H), 7.33 – 7.18 (m, 5H), 7.12 (d, J = 8.4 Hz, 1H), 6.69 (br d, J = 7.4 Hz, 1H), 2.60 (s, 3H); **^{19}F NMR** (470 MHz, DMSO-d_6) δ –61.5 (two overlapped singlets, 24F); **^{13}C NMR** (126 MHz, DMSO-d_6) [overlapping signals] δ 154.0, 152.3, 142.2, 141.8, 140.6, 140.0, 138.0, 137.4, 136.1, 133.7, 133.0, 132.7, 131.9, 131.4 130.6 (q, $J_{C–F}$ = 32.9 Hz), 130.5 (q, $J_{C–F}$ = 32.9 Hz), 129.5, 128.9, 128.2, 127.7, 127.4, 127.1, 126.9, 126.7, 125.8, 124.8, 124.3, 123.1 (q, $J_{C–F}$ = 273.2 Hz), 123.0 (q, $J_{C–F}$ = 272.9 Hz), 120.9 (m), 120.7, 120.5, 119.8 (overlapped), 119.3, 118.6, 116.4, 36.2; **IR** (thin layer film) ν (cm^{-1}) = 3330, 1599, 1551, 1507, 1468, 1428, 1397, 1367, 1279, 1180, 1132, 900, 865, 844, 825, 751, 705, 683, 639; **MP** not determined (decomposition at T >200 °C); **HRMS** (APCI$^+$) *m/z* calculated for $C_{67}H_{37}O_2N_4F_{24}$ $[M+H]^+$ 1385.2578, found 1385.2525; **$[\alpha]_D^{25\,°C}$** = –106.9 ° (c = 0.5, $CHCl_3$).

1-ethyl-3-(3,3'',5,5''-tetrakis(trifluoromethyl)-[1,1':3',1''-terphenyl]-5'-yl)-1-(2'-(3-(3,3'',5,5''-tetrakis(trifluoromethyl)-[1,1':3',1''-terphenyl]-5'-yl)ureido)-[1,1'-binaphthalen]-2-yl)urea (2.78)

Synthesised by Dr. Gabriele Pupo



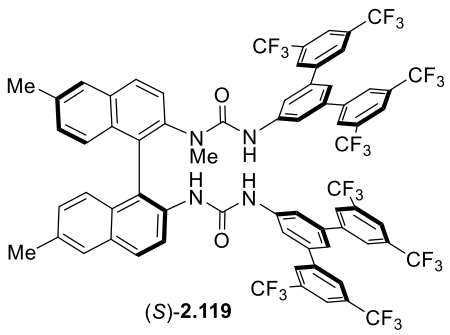
(*S*)-**2.78**

To a solution of (*S*)-**2.49** (4.05 g, 2.95 mmol, 1 equiv) in acetone (0.1 M, 29 mL) were added iodoethane (4.74 mL, 59 mmol, 20 equiv.) and K_2CO_3 (4.076 g, 29.5 mmol, 10 equiv.). The reaction mixture was stirred at rt for 72 h. After filtration on celite, the solvent was evaporated *in vacuo*. To the crude mixture were added CH_2Cl_2 and H_2O. The aqueous phase was then extracted with CH_2Cl_2 three times. The combined organic layers were washed with brine, dried over $MgSO_4$ and evaporated *in vacuo.* The crude mixture was purified by FCC (Pentane:EtOAc = 100:0 to 80:20, gradient) to afford a white solid (2.10 g, 51% yield). **^{1}H NMR** (500 MHz, $CDCl_3$) δ 8.49 (br s, 1H), 8.15 (d, J = 8.9 Hz, 1H), 8.08 (d, J = 9.3 Hz, 1H), 8.01 (d, J = 8.4 Hz, 1H), 7.96 (d, J = 7.9 Hz, 1H), 7.84 (s, 4H), 7.77 (s, 2H), 7.74 (s, 2H), 7.72 (s, 4H), 7.64 (d, J = 8.7 Hz, 1H), 7.59 (s, 2H), 7.56 (t, J = 7.5 Hz, 1H), 7.44 (t, J = 7.1 Hz, 1H), 7.33 (t, J = 7.1 Hz, 1H), 7.30 (s, 3H), 7.21 (s, 3H), 7.15 (d, J = 8.4 Hz, 1H), 7.05 (s, 1H), 6.96 (d, J = 8.4 Hz, 1H), 6.72 (s, 1H), 3.44 – 3.33 (m, 1H), 3.07 (br s, 1H), 1.05 (t, J = 7.0 Hz, 3H); **^{19}F NMR** (470 MHz, $CDCl_3$) δ –62.9 (s, 12F), –63.0 (s, 12F); **^{13}C NMR** (126 MHz, $CDCl_3$) [overlapping signals] δ 156.1, 152.7, 142.2, 141.6, 140.1, 139.9, 139.8, 139.7, 138.6, 135.3, 133.9, 133.4, 133.3, 132.3 (q, $J_{C–F}$ = 33.0 Hz), 132.0 (q, $J_{C–F}$ = 33.0 Hz), 131.9, 130.8, 130.3, 128.7, 128.5, 128.1, 127.8, 127.4, 127.1, 127.0, 126.7, 125.3, 123.2 (q, $J_{C–F}$ = 273.0 Hz), 123.1 (q, $J_{C–F}$ = 272.9 Hz), 121.6 (m), 121.5 (m), 121.3, 120.7, 120.3, 120.0 119.9, 118.2, 44.4, 13.6; **IR** (thin layer film) ν (cm^{-1}) = 3323, 2929, 1600, 1756, 1507, 1469, 1367, 1279, 1179, 1132, 901, 845, 706, 683; **MP** not

determined (decomposition at T >200 °C); **HRMS** (APCI$^+$) *m/z* calculated for $C_{68}H_{39}O_2N_4F_{24}$ $[M+H]^+$ 1399.2684, found 1399.2690; **$[\alpha]_D^{25\,°C}$** = –116.1 ° (c = 0.5, $CHCl_3$).

N. B. When the *general procedure C* was used to prepare (*S*)-**2.78**, only very poor yields were obtained (<10% yield).

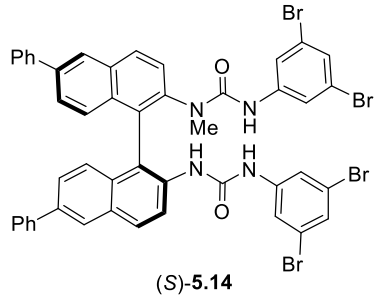
1-(6,6'-dimethyl-2'-(3-(3,3'',5,5''-tetrakis(trifluoromethyl)-[1,1':3',1''-terphenyl]-5'-yl)ureido)-[1,1'-binaphthalen]-2-yl)-1-methyl-3-(3,3'',5,5''-tetrakis(trifluoromethyl)-[1,1':3',1''-terphenyl]-5'-yl)urea (2.119)



(*S*)-**2.119**

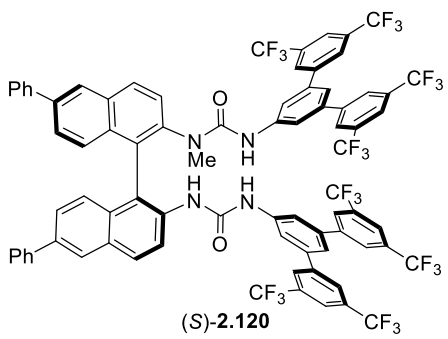
Bis-urea (*S*)-**2.119** was prepared from (*S*)-**5.10** (50 mg) and achiral aniline **2.79** (158 mg) following *the general procedure C*. Purification by FCC on silica gel (pentane: Et_2O = 80:20) afforded (*S*)-**2.119** as a white solid (55 mg, 26% yield). **^{1}H NMR** (500 MHz, $CDCl_3$) δ 8.37 (br s, 1H), 8.05 (d, J = 8.7 Hz, 1H), 7.98 (d, J = 9.0 Hz, 1H), 7.83 (s, 4H), 7.79–7.70 (m, 10H), 7.63 (d, J = 8.7 Hz, 1H), 7.58 (s, 2H), 7.32 (s, 2H), 7.22 – 7.00 (m, 7H), 6.90 (d, J = 8.6 Hz, 1H), 6.67 (s, 1H), 2.90 (s, 3H), 2.49 (s, 6H); **^{19}F NMR** (470 MHz, $CDCl_3$) δ –62.96, –63.01; **^{13}C NMR** (126 MHz, $CDCl_3$) [overlapping signals] δ 156.3 (br), 152.8, 142.2, 141.7, 140.2, 139.9, 139.8, 139.7, 138.9 (br), 137.5, 135.0 (br), 133.5, 132.3 (q, $J_{C\text{-}F}$ = 33.4 Hz), 132.2 (q, $J_{C\text{-}F}$ = 33.3 Hz), 132.0, 131.6, 130.1 (br), 130.4, 130.2, 129.7 (2 signals), 127.70, 127.6, 127.1 (m), 127.0 (m), 126.7, 126.3, 125.5, 123.2 (q, $J_{C\text{-}F}$ = 272.7 Hz), 123.1 (q, $J_{C\text{-}F}$ = 272.7 Hz), 121.7 (m), 121.5 (m), 121.7 (br), 120.6 (br), 120.2, 118.3, 37.3, 21.7, 21.6: **IR** (thin layer film) ν (cm^{-1}) = 3305, 1601, 1366, 1276, 1174, 1128, 901, 866, 705, 683; **MP** 250 – 251 °C; **HRMS** (ESI$^-$) *m/z* calculated for $C_{69}H_{39}O_2N_4F2_4$ $[M–H]^-$ 1411.2695, found 1411.1749; **$[\alpha]_D^{25\,°C}$** = –107.4 ° (c = 0.47, $CHCl_3$).

(*S*)-3-(3,5-dibromophenyl)-1-(2'-(3-(3,5-dibromophenyl)ureido)-6,6'-diphenyl-[1,1'-binaphthalen]-2-yl)-1-methylurea (5.14)


(*S*)-**5.14**

Bis-urea (*S*)-**5.14** was prepared from (*S*)-**5.11** (80 mg) and 3,5-dibromoaniline (89 mg) following the *general procedure C*. Purification by FCC on silica gel (*n*-hexane: Et_2O = 98:2 to 80:20, gradient) afforded (*S*)-**5.14** as a white solid (148.8 mg, 82% yield). **^{1}H NMR** (400 MHz, $CDCl_3$) δ 8.59 (d, J = 9.1 Hz, 1H), 8.21 – 8.09 (m, 3H), 8.04 (d, J = 9.2 Hz, 1H), 7.70–7.63 (m, 4H), 7.61 – 7.29 (m, 15H), 7.25 – 7.12 (m, 3H), 7.02 (d, J = 8.8 Hz, 1H), 6.58 (s, 1H), 2.86 (s, 3H); **^{13}C NMR** (101 MHz, $CDCl_3$) δ 156.0 (br), 151.6, 140.7, 140.5, 140.2, 140.1 (br), 140.0, 139.6, 137.1, 135.9 (br), 133.6, 132.7, 132.2, 131.1, 130.7, 130.3, 130.0, 129.8, 129.0, 129.0 (br), 128.1, 127.8, 127.5, 127.4, 127.2, 127.2, 127.1, 126.7, 126.3, 126.0, 125.6, 123.0, 122.8, 122.3, 120.2, 119.8 (br), 37.0; **IR** (thin layer film) ν (cm^{-1}) =3353, 1643, 1579, 1526, 1491, 1441, 1256, 757; **MP** 220–222 °C; **HRMS** (ESI^+) *m/z* calculated for $C_{47}H_{33}O_2N_4Br_4$ $[M+H]^+$ 1000.9342, found 1000.9318; **$[\alpha]_D^{25\ °C}$** = –52.7 ° (c = 0.5, $CHCl_3$).

1-(6,6'-diphenyl-2'-(3-(3,3'',5,5''-tetrakis(trifluoromethyl)-[1,1':3',1''-terphenyl]-5'-yl)ureido)-[1,1'-binaphthalen]-2-yl)-1-methyl-3-(3,3'',5,5''-tetrakis(trifluoromethyl)-[1,1':3',1''-terphenyl]-5'-yl)urea (2.120)


(*S*)-**2.120**

A Schlenk tube, equipped with a stirring bar and a condenser was charged with (*S*)-**5.14** (78 mg, 0.10 mmol, 1 equiv), 3,5-bis(trifluoromethyl)benzyl boronic acid (180 mg, 0.70 mmol, 7 equiv), SPhos (8.2 mg, 0.02 mmol, 0.2 equiv) and K_2CO_3 (94 mg,

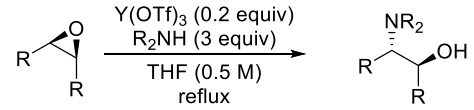
0.50 mmol, 5 equiv). The flask was then evacuated and backfilled with N_2 (this sequence was repeated 3 times). Degassed THF (1 mL) and degassed H_2O (250 μL) (in a 4: 1 ratio, 0.08 M as total concentration) were added at rt. The reaction mixture was warmed up to 60 °C prior of the addition of $Pd(OAc)_2$ (2.3 mg, 0.1 mmol 0.1 equiv). The reaction mixture was stirred at reflux for 24 h, then it was cooled to rt, diluted with H_2O and extracted three times with CH_2Cl_2. The combined organic layers were washed with brine, dried over $MgSO_4$ and evaporated *in vacuo*. The crude product was purified by FCC (pentane: CH_2Cl_2 = 60:40 to 10:90 gradient). White solid, 79 mg, 67% yield. **^{1}H NMR** (400 MHz, $CDCl_3$) δ 8.58 (br s, 1H), 8.27 – 8.12 (m, 4H), 7.85 (s, 4H), 7.81 – 7.55 (m, 17H), 7.52 – 7.43 (m, 4H), 7.42 – 7.36 (m, 2H), 7.35 – 7.27 (m, 3H), 7.25 –7.17 (m, 2H), 7.11 (d, J = 8.8 Hz, 1H), 7.07 (s, 1H), 6.72 (br s, 1H), 2.99 (s, 3H); **^{19}F NMR** (377 MHz, $CDCl_3$) δ -62.93, -62.99; **^{13}C NMR** (126 MHz, $CDCl_3$) [overlapping singals] δ 156.4, 152.5, 142.1, 141.5, 140.3, 140.1, 140.1, 139.9, 139.6, 139.6, 137.6 (br), 135.9 (br), 133.6, 132.8, 132.4, 132.2 (q, $J_{C–F}$= 33), 132.1 (q, $J_{C–F}$= 33), 131.3, 131.1, 130.5, 129.0, 127.9, 127.6, 127.4, 127.3, 127.1, 127.0, 126.9, 126.9, 126.29, 126.1, 125.9, 123.2(q, $J_{C–F}$= 273.1), 123.1 (q, $J_{C–F}$= 273.8), 121.6 (m), 121.4 (m), 120.8 (br), 120.2, 118.0, 38.8. **IR** (thin layer film) ν (cm^{-1}) = 3658, 2981, 2889, 1462, 1382, 1252, 1150, 1073, 954, 818; **MP** not determined (decomposition at T >200 °C); **HRMS** (ESI^+) *m/z* calculated for $C_{79}H_{45}O_2N_4F_{24}$ $[M+H]^+$ 1537.3154, found 1537.3141; **$[\alpha]_D^{25\ °C}$** = – 63.5 ° (c = 0.41, $CHCl_3$).

5.2.2.2 Substrates Synthesis and Characterisation

β-Aminoalcohols

β-Aminoalcohols *rac*-**2.13,** *rac*-**2.106** and *rac*-**5.15–5.33, 4.11–4.14** were prepared by heating the corresponding *meso*-epoxides[8] in the presence of the appropriate secondary amine either with a Lewis acid (*rac*-**2.13,** *rac*-**5.15** *rac*-**5.25–5.33, 4.11–4.14**, *General procedure D*) or neat (*rac*-**2.106**, *rac*-**5.16–5.24**, *General procedure E*). For the synthesis of *rac*-**5.16** and *rac*-**5.21**, the hydrochloride salt of the amine was used and details for the release of the free amine are given in the specific experiment.

General Procedure D: Synthesis of β-Aminoalcohols via Lewis Acid Catalysed Epoxide Ring Opening

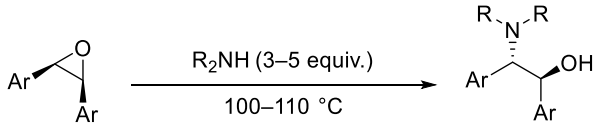


R= Bn, Allyl

rac-**2.13, 5.15 5.25–5.33, 4.11–4.14**

Following a slightly modified procedure from the one reported by Yamamoto,[9] in a flame-dried two-neck round bottom flask, the *cis*-epoxide (1 equiv), the secondary amine (3 equiv) and $Y(OTf)_3$ (0.2 equiv) were refluxed in anhydrous THF (0.5 M) under inert atmosphere until complete conversion of the epoxide (14–72 h, monitored by TLC). The reaction mixture was then cooled to rt and the solvent evaporated *in vacuo*. The residue was re-dissolved in EtOAc washed with a saturated solution of $NaHCO_3$. The layers were separated, and the aqueous phase was extracted twice with EtOAc. The combined organic layers were dried over $MgSO_4$, filtered and concentrated under reduced pressure. The crude product was purified by FCC over silica gel.

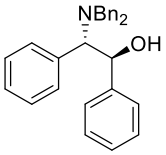
General Procedure E: Synthesis of β-Aminoalcohols under Neat Conditions



rac-**2.106**
5.16–5.24

In a pressure tube, the *cis*-epoxide was dissolved in 3–5 equivalents of the amine and stirred at 100–110 °C until complete conversion of the starting material (14–48 h, monitored by TLC). The excess amine was then removed by evaporation under reduced pressure and the crude product was directly purified by FCC over silica gel.

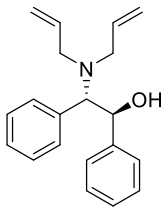
***Rac*-2-(dibenzylamino)-1,2-diphenylethan-1-ol (2.13)**



rac-**2.13**

Alcohol *rac*-**2.13** was prepared according to the *general procedure D* (24 h) from *cis*-stilbene oxide (2.94 g, 15 mmol) and dibenzylamine (5.6 mL, 30 mmol). Purification by FCC on silica gel (pentane: EtOAc = 98:2 to 9:1, gradient) afforded *rac*-**2.13** as a white solid (4.62 g, 79% yield). **^{1}H NMR** (400 MHz, $CDCl_3$) δ 7.45 – 7.28 (m, 13H), 7.21 – 7.14 (m, 2H), 7.11 – 6.99 (m, 5H), 5.26 (s, 1H), 5.23 (d, J = 10.3 Hz, 1H), 4.11 (d, J = 13.2 Hz, 2H), 3.80 (d, J = 10.3 Hz, 1H), 3.13 (d, J = 13.2 Hz, 2H); **^{13}C NMR** (101 MHz, $CDCl_3$) δ 141.6, 138.6, 133.2, 130.4, 129.2, 128.8, 128.2, 128.0, 127.9, 127.6, 127.4, 127.4, 71.1, 69.3, 53.8; **IR** (thin layer film): ν (cm^{-1}) 3373, 3061, 3028, 2845, 1494, 1453, 1401, 1189, 1074, 1054, 1026, 882, 748, 697; **MP** 134 −135 °C; **HRMS** (ESI^+) *m/z* calculated for $C_{28}H_{28}NO^+$ $[M+H]^+$ 394.21654, found 394.21627.

***rac*-2-(diallylamino)-1,2-diphenylethan-1-ol (5.15)**

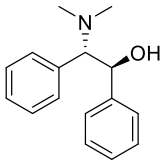


rac-**5.15**

Alcohol *rac*-**5.15** was prepared following the *general procedure D* (48 h), from *cis*-stilbene oxide (3.5 g, 17.8 mmol, 1 equiv) and diallylamine (6.6 mL, 53.5 mmol, 3 equiv). Purification by FCC (pentane:Et_2O = 98:2) afforded *rac*-**5.15** as a pale yellow solid (3.26 g, 63% yield). **^{1}H NMR** (400 MHz, $CDCl_3$)

δ 7.36 – 7.06 (m, 10H), 5.92 (tdd, *J* = 14.0, 8.6, 4.1 Hz, 2H), 5.25 (d, *J* = 13.7 Hz, 4H), 5.09 – 5.04 (m, 2H), 3.92 (d, *J* = 10.3 Hz, 1H), 3.54 (ddt, *J* = 13.9, 4.1, 2.0 Hz, 2H), 2.68 (dd, *J* = 14.0, 8.6 Hz, 2H); **^{13}C NMR** (101 MHz, $CDCl_3$) δ 141.6, 136.3, 133.6, 130.2, 128.1, 128.0, 127.8, 127.5, 127.5, 118.3, 71.1, 69.8, 52.8; **IR** (thin layer film) ν (cm^{-1}) = 3356, 3064, 3030, 2824, 1642, 1493, 1451, 1400, 1335, 1081, 1053, 972, 757, 698, 607; **MP** 44 – 46 °C; **HRMS** (ESI^+) *m/z* calculated for $C_{20}H_{24}NO^+$ $[M+H]^+$ 294.18524, found 294.18507.

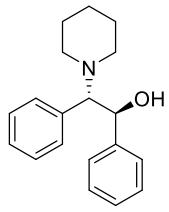
***rac*-2-(dimethylamino)-1,2-diphenylethan-1-ol (5.16)**



rac-**5.16**

In a pressure tube, dimethylamine hydrochloride (2.45 g, 30 mmol, 5 equiv) and sodium hydroxide (2.4 g, 60 mmol, 10 equiv) were dissolved in 30 mL of MeOH/Water (1:1) and stirred at 0 °C for 10 min before addition of *cis*-stilbene oxide (1.2 g, 6.0 mmol, 1 equiv). The pressure tube was sealed, and the reaction stirred at 65 °C overnight. The reaction mixture was then allowed to cool to rt and extracted with EtOAc. The combined organic layers were washed with brine, dried over $MgSO_4$ and evaporated to dryness. Purification by FCC (pentane:EtOAc = 90:10 to 80:20, gradient) afforded *rac*-**5.16** as a white solid (1.20 g, 83% yield). **^{1}H NMR** (400 MHz, $CDCl_3$) δ 7.23 – 7.10 (m, 5H), 7.10 – 6.90 (m, 5H), 4.91 (d, *J* = 10.3 Hz, 1H), 3.47 (d, *J* = 10.3 Hz, 1H), 2.16 (s, 6H); **^{13}C NMR** (101 MHz, $CDCl_3$) δ 141.5, 132.4, 130.2, 128.0, 127.8, 127.8, 127.4, 127.4, 75.9, 71.1, 40.9; **IR** (thin layer film) ν (cm^{-1}) = 3291, 3030, 2941, 2903, 2869, 2835, 2789, 1602, 1493, 1474, 1079, 1051, 1036, 877, 700; **MP** 88 – 91 °C; **HRMS** (ESI^+) *m/z* calculated for $C_{16}H_{20}NO^+$ $[M+H]^+$ 242.15394, found 242.15385.

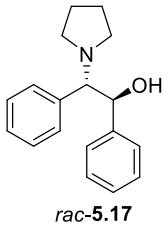
***rac*-1,2-diphenyl-2-(piperidin-1-yl)ethan-1-ol (2.106)**



rac-**2.106**

Alcohol *rac*-**2.106** was prepared following the *general procedure E* (14 h), from *cis*-stilbene oxide (2.32 g, 11.8 mmol, 1 equiv) and piperidine (6.0 mL, 59 mmol, 5 equiv). Purification by FCC (pentane:Et_2O = 100:0 to 90:10, gradient with 4% of NEt_3) *rac*-**2.106** as a white solid (2.22 g, 67% yield). **For the multi-decagram scale reaction** *(synthesis performed by Dr. Gabriele Pupo): cis*-stilbene (91.7 g, 0.47 mol, 1 equiv) was dissolved in piperidine (184 mL, 1.4 mol, 4 equiv) and refluxed for 24 h. The reaction was then cooled to rt and the excess amine was removed under vacuum. *n*-hexane was added and after stirring for 15 min, the solution was filtered and the solid was washed with cold *n*-hexane (this was done to remove unreacted *cis*-stilbene from the previous epoxidation step). The brown solid was then dried overnight under vacuum and directly used for the successive step without any further purification (111.7 g, 0.40 mol, 85% yield). **^{1}H NMR** (500 MHz, $CDCl_3$) δ 7.32 – 7.22 (m, 5H), 7.20 – 7.09 (m, 5H), 5.36 (br s, 1H), 5.06 (d, J = 10.3 Hz, 1H), 3.56 (d, J = 10.3 Hz, 1H), 2.67 (br s, 2H), 2.31 (br s, 2H), 1.81 – 1.58 (m, 4H), 1.48 – 1.25 (m, 2H); **^{13}C NMR** (126 MHz, $CDCl_3$) δ 141.8, 133.5, 130.1, 128.0, 127.9, 127.7, 127.4, 127.4, 77.2, 70.5, 50.4, 26.7, 24.4; **IR** (thin layer film) ν (cm^{-1}) = 3320, 3030, 2933, 2852, 1452, 1407, 1217, 1195, 1156, 1088, 1052, 1025, 984, 875, 758, 745, 700; **MP** 96 – 97 °C; **HRMS** (ESI^+) *m/z* calculated for $C_{19}H_{24}NO^+$ $[M+H]^+$ 282.18524, found 282.18495.

***rac*-1,2-diphenyl-2-(pyrrolidin-1-yl)ethan-1-ol (5.17)**

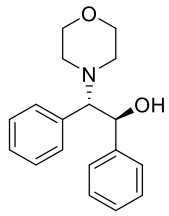


rac-**5.17**

Alcohol *rac*-**5.17** was prepared following the *general procedure E* (14 h), from *cis*-stilbene oxide (2.0 g, 10.2 mmol, 1 equiv) and pyrrolidine (4.0 mL, 51 mmol, 5 equiv). Purification by FCC (CH_2Cl_2:MeOH = 98:2) afforded *rac*-**5.17** as a white solid (2.27 g, 83% yield). **^{1}H NMR** (400 MHz, $CDCl_3$) δ 7.40 – 7.24

(m, 5H), 7.22 – 7.10 (m, 5H), 5.29 (br s, 1H), 5.02 (d, *J* = 9.9 Hz, 1H), 3.85 (d, *J* = 10.0 Hz, 1H), 2.72 – 2.62 (m, 2H), 2.57 – 2.44 (m, 2H), 1.79 – 1.64 (m, 4H); **^{13}C NMR** (101 MHz, $CDCl_3$) δ 141.9, 133.5, 130.4, 128.0, 127.9, 127.7, 127.4, 127.3, 72.1, 71.8, 48.1, 22.8; **IR** (thin layer film) ν (cm^{-1}) = 3370, 3027, 2954, 2925, 1620, 1452, 1261, 1081, 1056, 701; **MP** 80 – 81 °C; **HRMS** (ESI^+) *m/z* calculated for $C_{18}H_{22}NO^+$ $[M+H]^+$ 268.16959, found 268.16949. Spectroscopic data were in agreement with the ones previously reported in literature.[10]

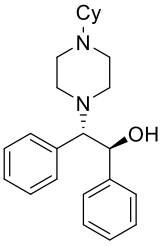
***rac*-2-morpholino-1,2-diphenylethan-1-ol (5.18)**



rac-**5.18**

Alcohol *rac*-**5.18** was prepared following the *general procedure E* (24 h), from *cis*-stilbene oxide (1.00 g, 5.0 mmol, 1 equiv) and morpholine (2.2 mL, 25 mmol, 5 equiv). Purification by FCC (*n*-hexane:EtOAc = 100:0 to 60:40, gradient) afforded *rac*-**5.18** as a white solid (1.22 g, 86% yield). **^{1}H NMR** (500 MHz, $CDCl_3$) δ 7.35 – 7.23 (m, 5H), 7.23 – 7.15 (m, 3H), 7.14 – 7.09 (m, 2H), 5.13 (br s, 1 H), 5.11 (d, *J* = 10.3 Hz, 1H), 3.84 (ddd, *J* = 9.8, 6.4, 3.0 Hz, 2H), 3.79 (ddd, *J* = 11.0, 6.4, 2.9 Hz, 2H), 3.61 (d, *J* = 10.3 Hz, 1H), 2.81 – 2.65 (m, 2H), 2.49 – 2.39 (m, 2H); **^{13}C NMR** (126 MHz, $CDCl_3$) [overlapped signals] δ 141.2, 132.7, 130.0, 128.0 (overlapped), 127.6, 127.4, 76.9, 70.4, 67.4, 49.3 (br); **IR** (thin layer film) ν (cm^{-1}) = 3352, 3030, 2912, 2851, 1452, 1402, 1115, 1028, 994, 912, 873, 700; **HRMS** (ESI^+) *m/z* calculated for $C_{18}H_{22}NO_2^+$ $[M+H]^+$ 284.16451, found 284.16437. Spectroscopic data were in agreement with the ones previously reported in literature.[11]

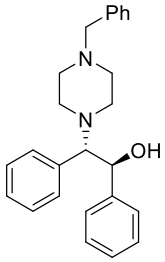
***rac*-2-(4-cyclohexylpiperazin-1-yl)-1,2-diphenylethan-1-ol (5.19)**



rac-**5.19**

Alcohol *rac*-**5.19** was prepared following the *general procedure E* (14 h), dissolving *cis*-stilbene oxide (1.00 g, 5.0 mmol, 1 equiv) and 1-cyclohexylpiperazine (2.50 g, 15 mmol, 3 equiv) in 5 mL of EtOH. Purification by FCC (pentane:EtOAc = 80:20 with 3% Et_3N) afforded *rac*-**5.19** as a white solid (1.57 g, 86% yield). **^{1}H NMR** (500 MHz, DMSO-d_6, 70 °C) δ 7.48 – 7.27 (m, 10H), 5.29 (d, J = 9.9 Hz, 1H), 5.08 (br s, 1H), 3.87 (d, J = 9.9 Hz, 1H), 2.85 – 2.69 (m, 6H), 2.57 – 2.50 (m, 2H), 2.40 – 2.33 (m, 1H), 2.00 – 1.86 (m, 4H), 1.77 (dt, J = 12.8, 2.9 Hz, 1H), 1.48 – 1.23 (m, 5H); **^{13}C NMR** (126 MHz, DMSO-d_6, 70 °C) δ 142.0, 133.7, 129.5, 127.2, 127.2, 127.0, 126.8, 126.5, 74.7, 69.6, 62.1, 48.8, 48.6, 28.2, 25.6, 24.8; **IR** (thin layer film) ν (cm^{-1}) = 3335, 2922, 2851, 1405, 1187, 1148, 1000, 977, 703; **MP** 153 – 157 °C; **HRMS** (ESI^+) *m/z* calculated for $C_{24}H_{33}N_2O^+$ $[M+H]^+$ 365.25984, found 365.25830.

***rac*-2-(4-benzylpiperazin-1-yl)-1,2-diphenylethan-1-ol (5.20)**

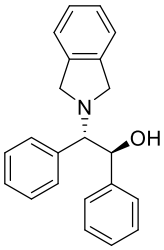


rac-**5.20**

Alcohol *rac*-**5.20** was prepared following the *general procedure E* (14 h), from *cis*-stilbene oxide (1.00 g, 5.0 mmol, 1 equiv) and 1-benzylpiperazine (2.6 mL, 15 mmol, 3 equiv). Purification by FCC (pentane:EtOAc = 95:5 to 90:10, gradient) afforded *rac*-**5.20** as a pale yellow solid (1.40 g, 75% yield). **^{1}H NMR** (500 MHz, $CDCl_3$) δ 7.37 – 7.23 (m, 10H), 7.22 – 7.14 (m, 3H), 7.13 – 7.08 (m, 2H), 5.24 (br s, 1H), 5.09 (d, J = 10.3 Hz, 1H), 3.63 (d, J = 10.3 Hz, 1H), 3.57– 3.50 (m, 2H), 2.90 – 2.31 (m, 8H); **^{13}C NMR** (126 MHz, $CDCl_3$) δ 141.5, 138.0, 133.1, 130.0, 129.3, 128.3, 128.0, 128.0, 127.9, 127.5, 127.4, 127.2, 76.4, 70.5, 63.2, 53.6, 49.6 (br); **IR** (thin layer film) ν (cm^{-1}) = 3327, 3030, 2934, 2853, 1725, 1452, 1408, 1271,

1091, 1052, 1025, 700; **MP** 135 – 137 °C; **HRMS** (ESI$^+$) *m/z* calculated for $C_{25}H_{29}N_2O^+$ $[M+H]^+$ 373.22744, found 373.22736.

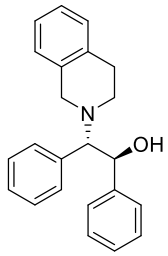
***rac*-2-(isoindolin-2-yl)-1,2-diphenylethan-1-ol (5.21)**



rac-**5.21**

In an extraction funnel, isoindoline hydrochloride (2.1 g, 13.5 mmol, 3 equiv) was dissolved in Et_2O and washed with NaOH (1 M). Phases were separated and the aqueous phase was extracted twice with Et_2O. The combined organic phases where dried over $MgSO_4$, filtered and concentrated *in vacuo*. The residue was dissolved in 3 mL of EtOH and transferred into a pressure tube. *Cis*-stilbene oxide (785 mg, 4.0 mmol, 1 equiv) was added and the pressure tube sealed. The reaction mixture was stirred at 100 °C overnight. Volatiles were evaporated *in vacuo* and the crude product was purified by FCC (pentane:Et_2O = 100:0 to 90:10, gradient) to afford *rac*-**5.21** as a brown solid (1.18 g, 94% yield). **^{1}H NMR** (400 MHz, $CDCl_3$) δ 7.25 – 7.14 (m, 4H), 7.14 – 7.03 (m, 10H), 5.05 (d, J = 9.5 Hz, 1H), 4.03 – 3.90 (m, 5H); **^{13}C NMR** (101 MHz, $CDCl_3$) δ 141.5, 139.2, 134.3, 130.2, 128.2, 128.0, 127.8, 127.4, 127.3, 126.8, 122.4, 72.4, 72.1, 54.0; **IR** (thin layer film) ν (cm^{-1}) = 3366, 3029, 2894, 2803, 1493, 1453, 1398, 1188, 1112, 1075, 909, 741, 700; **MP** 131 – 132 °C; **HRMS** (ESI$^+$) *m/z* calculated for $C_{22}H_{22}NO^+$ $[M+H]^+$ 316.16959, found 316.16907.

***rac*-2-(3,4-dihydroisoquinolin-2(1H)-yl)-1,2-diphenylethan-1-ol (5.22)**

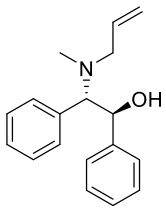


rac-**5.22**

Alcohol *rac*-**5.22** was prepared following the *general procedure E* (14 h), from *cis*-stilbene oxide (1.0 g, 5.0 mmol, 1 equiv) and tetrahydroisoquinoline (3.2 mL, 25 mmol, 5 equiv). Purification by FCC (pentane:EtOAc = 100:0 to 97:3, gradient) afforded *rac*-**5.22** as an ivory solid (1.55 g, 94% yield). **^{1}H NMR** (400 MHz, $CDCl_3$); δ 7.35 – 7.12 (m,

13H), 7.07 (dd, *J* = 6.4, 2.5 Hz, 1H), 5.24 (d, *J* = 10.3 Hz, 1H), 5.18 (br s, 1H), 4.00 – 3.80 (m, 2H), 3.70 (d, *J* = 14.5 Hz, 1H), 3.19 – 3.09 (m, 1H), 3.10 – 2.96 (m, 2H), 2.59 (ddd, *J* = 11.8, 7.3, 5.1 Hz, 1H); **^{13}C NMR** (101 MHz, $CDCl_3$) [overlapping signals] δ 141.4, 134.7, 134.1, 133.0, 130.1, 128.8, 128.1, 128.0, 127.5 (overlapped), 126.7, 126.3, 125.8, 76.3, 70.9, 52.1, 46.6, 29.9; **IR** (thin layer film) ν (cm^{-1}) = 3350, 3028, 2916, 2832, 1495, 1453, 1403, 1193, 1127, 1086, 1048, 909, 760, 739, 700; **MP** 117 – 121 °C; **HRMS** (ESI^+) *m/z* calculated for $C_{23}H_{24}NO^+$ $[M+H]^+$ 330.18634, found 330.18497 .

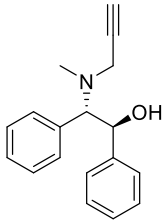
***rac*-2-(allyl(methyl)amino)-1,2-diphenylethan-1-ol (5.23)**



rac-**5.23**

Alcohol *rac*-**5.23** was prepared following the *general procedure E* (48 h), from *cis*-stilbene oxide (1.0 g, 5.0 mmol, 1 equiv) and *N*-Allylmethylamine (2.4 mL, 25 mmol, 5 equiv). Purification by FCC (pentane:EtOAc = 98:2 to 90:10, gradient) afforded *rac*-**5.23** as a white solid (1.16 g, 87% yield). **^{1}H NMR** (500 MHz, $CDCl_3$) δ 7.31 – 7.22 (m, 5H), 7.20 – 7.10 (m, 5H), 6.00 – 5.87 (m, 1H), 5.25 – 5.23 (m, 1H), 5.22 – 5.20 (m, 1H), 5.06 (d, *J* = 10.4 Hz, 1H), 3.75 (d, *J* = 10.4 Hz, 1H), 3.18 (dd, *J* = 13.5, 5.6, Hz, 1H), 2.95 (dd, *J* = 13.5, 7.3 Hz, 1H), 2.26 (s, 3H); **^{13}C NMR** (126 MHz, $CDCl_3$) δ 141.6, 136.1, 133.0, 130.2, 128.0, 128.0, 127.8, 127.5, 127.5, 118.1, 73.8, 71.0, 57.5, 37.0; **IR** (thin layer film) ν (cm^{-1}) = 3329, 3030, 2881, 1643, 1493, 1452, 1399, 1335, 1274, 1185, 1127, 1081, 1034, 1013, 921, 757, 699. **MP** 63 – 64 °C; **HRMS** (ESI^+) *m/z* calculated for $C_{18}H_{22}NO^+$ $[M+H]^+$ 268.16959, found 268.16915.

***rac*-2-(methyl(prop-2-yn-1-yl)amino)-1,2-diphenylethan-1-ol (5.24)**

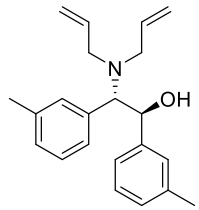


rac-**5.24**

Alcohol *rac*-**5.24** was prepared following the *general procedure E* (48 h), from *cis*-stilbene oxide (750 mg, 3.8 mmol, 1 equiv) and *N*-Methylpropargylamine (1.3 mL, 15 mmol, 4 equiv). Purification by FCC (pentane:EtOAc = 98:2 to 90:10, gradient) afforded *rac*-**5.24** as a white solid

(500 mg, 49% yield). **^{1}H NMR** (500 MHz, $CDCl_3$) δ 7.31 – 7.23 (m, 5H), 7.21 – 7.12 (m, 5H), 5.08 (d, *J* = 10.2 Hz, 1H), 4.88 (br s, 1H), 3.98 (d, *J* = 10.2 Hz, 1H), 3.34 (dd, *J* = 16.2, 2.5 Hz, 1H), 3.13 (dd, *J* = 16.2, 2.5 Hz, 1H), 2.35 (s, 3H), 2.32 (t, *J* = 2.4 Hz, 1H); **^{13}C NMR** (126 MHz, $CDCl_3$) δ 141.4, 132.4, 130.2, 128.1 (overlapped), 128.0, 127.6, 127.5, 80.2, 73.1, 73.0, 71.2, 44.0, 34.0; **IR** (thin layer film) ν (cm^{-1}) = 3364, 3291, 3031, 2879,2803, 1423, 1357, 1302, 1186, 1016, 759, 670; **MP** 58 – 60 °C; **HRMS** (ESI^+) *m/z* calculated for $C_{18}H_{20}NO^+$ $[M+H]^+$ 266.15394, found 266.15396.

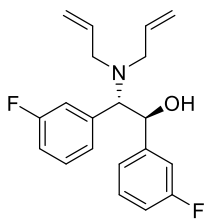
***rac*-2-(diallylamino)-1,2-di-*m*-tolylethan-1-ol (5.25)**



rac-**5.25**

Alcohol *rac*-**5.25** was prepared following the *general procedure D* (48 h), from *cis*-2,3-di-*m*-tolyloxirane (1.10 g, 4.5 mmol, 1 equiv) and diallylamine (1.7 mL, 14 mmol 3 equiv). Purification by FCC (*n*-hexane: Et_2O = 100:0 to 98:2, gradient) afforded *rac*-**5.25** as a colourless oil (1.00 g, 70% yield). **^{1}H NMR** (500 MHz, $CDCl_3$); *δ* 7.15 (t, *J* = 7.5 Hz, 1H), 7.07 (s, 1H), 7.04 – 7.00 (m, 2H), 6.95 – 6.91 (m, 3H), 6.89 (s, 1H), 5.94 – 5.86 (m, 2H), 5.23 (d, *J* = 13.3 Hz, 4H), 5.07 (br s, 1H), 5.02 (d, *J* = 10.3 Hz, 1H), 3.87 (d, *J* = 10.3 Hz, 1H), 3.51 (d, *J* = 14.0 Hz, 2H), 2.67 (dd, *J* = 8.3, 14.0 Hz, 2H), 2.3 (s, 3H), 2.2 (s, 3H); **^{13}C NMR** (126 MHz, $CDCl_3$) *δ* 141.5, 137.5, 137.4, 136.4, 133.5, 131.0, 128.5, 128.2, 128.1, 127.9, 127.8, 127.1, 124.7, 118.2, 70.9, 69.4, 52.8, 21.7, 21.5; **IR** (thin layer film) ν (cm^{-1}) = 3356, 3025, 2977, 2921, 2826, 1642, 1607, 1489, 1448, 1398, 1318, 1245, 1153, 1093, 1055, 994, 972, 920, 885, 848, 782, 703; **HRMS** (ESI^+) *m/z* calculated for $C_{22}H_{28}NO^+$ $[M+H]^+$ 322.2165, found 322.2164.

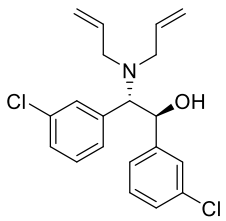
***rac*-2-(diallylamino)-1,2-bis(3-fluorophenyl)ethan-1-ol (5.26)**



rac-**5.26**

Alcohol *rac*-**5.26** was prepared following the *general procedure D* (24 h), from *cis*-2,3-bis(3-fluorophenyl)oxirane (800 mg, 3.4 mmol, 1 equiv) and diallylamine (1.2 mL, 10.3 mmol, 3 equiv). Purification by FCC (*n*-hexane:Et_2O = 100:0 to 95:5 gradient) afforded *rac*-**5.26** as a white solid (1.00 g, 88% yield). **^{1}H NMR** (500 MHz, $CDCl_3$); δ 7.28 – 7.19 (m, 1H), 7.01 – 7.03 (m, 1H), 6.99 – 6.90 (m, 2H), 6.90 – 6.80 (m, 2H), 6.80 – 6.75 (m, 2H), 5.90 – 5.79 (m, 2H), 5.29 – 5.18 (m, 4H), 4.96 (d, J = 10.6 Hz, 1H), 4.95 (br s, 1H), 3.82 (d, J = 10.6 Hz, 1H), 3.49 (d, J = 14 Hz, 2H), 2.63 (dd, J = 9.3, 14 Hz, 2H); **^{19}F NMR** (470 MHz, $CDCl_3$); –112.6 (m, 1F), –113.4 (m, 1F); **^{13}C NMR** (126 MHz, $CDCl_3$); 162.78 (d, $J_{C–F}$ = 245 Hz), 162.6 (d, J_{C-F} = 245 Hz), 144.05 (d, $J_{C–F}$ = 8 Hz), 136.02 (d, $J_{C–F}$ = 8.0 Hz), 135.84, 129.75 (d, $J_{C–F}$ = 8.5 Hz), 129.54 (d, J_{C-F} = 8.5 Hz), 125.78 (d, $J_{C–F}$ = 2.8 Hz), 123.23 (d, $J_{C–F}$ = 2.8 Hz), 118.73, 116.81 (d, $J_{C–F}$ = 21.3 Hz), 115.04 (d, $J_{C–F}$ = 21.3 Hz), 114.6 (d, $J_{C–F}$ = 21.3 Hz), 114.11 (d, $J_{C–F}$ = 21.3 Hz), 70.60, 69.35, 52.84; **IR** (thin layer film) ν (cm^{-1}) = 3366, 3080, 2826, 1643, 1614, 1589, 1488, 1447, 1398, 1314, 1247, 1137, 1079, 1054, 995, 958, 923, 878, 782, 759, 705, 696; **MP** 60 – 63 °C; **HRMS** (ESI^+) *m/z* calculated for $C_{20}H_{22}F_2NO^+$ $[M+H]^+$ 330.1664, found 330.1663.

***rac*-1,2-bis(3-chlorophenyl)-2-(diallylamino)ethan-1-ol (5.27)**

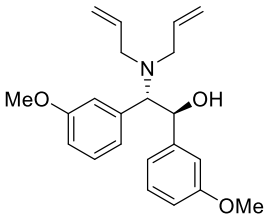


rac-**5.27**

Alcohol *rac*-**5.27** was prepared following the *general procedure D* (*24* h), from *cis*-2,3-bis(3-chlorophenyl)oxirane (1.00 g, 3.7 mmol, 1 equiv) and diallylamine (1.3 mL, 11 mmol, 3 equiv). Purification by FCC (*n*-hexane:Et_2O = 100:0 to 90:10 gradient) afforded *rac*-**5.27** as colourless oil (0.98 g, 70% yield). **^{1}H NMR** (500 MHz, $CDCl_3$); δ 7.27 – 7.18 (m, 3H), 7.13 – 7.03 (m, 3H), 7.00 – 6.93 (m, 2H), 5.90 – 5.80 (m, 2H), 5.28 – 5.21 (m, 4H), 4.95

(d, *J* = 10.5 Hz, 1H), 3.80 (d, *J* = 10.5 Hz, 1H), 3.49 (d, *J* = 14 Hz, 2H), 2.64 (dd, *J* = 8.7, 14 Hz, 2H); **^{13}C NMR** (126 MHz, $CDCl_3$) δ 143.4, 135.8, 135.4, 134.3, 134.2, 130.0, 129.5, 129.4, 128.3, 128.6, 127.9, 127.4, 125.8, 118.8, 70.5, 69.4, 52.8; **IR** (thin layer film) ν (cm^{-1}) = 3358, 3077, 2825, 1643, 1596, 1572, 1477, 1431, 1127, 1394, 1311, 1259, 1191, 1096, 1081, 1058, 996, 973, 922, 885, 836, 785, 733; **HRMS** (ESI^+) *m/z* calculated for $C_{20}H_{22}NOCl_2^+$ $[M+H]^+$ 362.1073, found 362.1071.

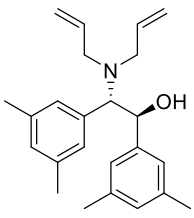
***rac*-2-(diallylamino)-1,2-bis(3-methoxyphenyl)ethan-1-ol (5.28)**



rac-**5.28**

Alcohol *rac*-**5.28** was prepared following the *general procedure D* (24 h), from *cis*-2,3-bis(3-methoxyphenyl)oxirane (800 mg, 3.12 mmol, 1 equiv) and diallylamine (1.16 mL, 9.37 mmol, 3 equiv). Purification by FCC (*n*-hexane:Et_2O = 90:10 to 80:20, gradient) afforded *rac*-**5.28** as a pale yellow oil (788 mg, 71% yield). **^{1}H NMR** (500 MHz, $CDCl_3$) δ 7.19 (t, *J* = 8.0 Hz, 1H), 7.05 (t, *J* = 7.9 Hz, 1H), 6.81 – 6.75 (m, 3H), 6.73 (d, *J* = 7.7 Hz, 1H), 6.66 (d, *J* = 8.2 Hz, 1H), 6.63 (s, 1H), 5.95 – 5.83 (m, 2H), 5.27 – 5.18 (m, 4H), 5.04 (br s, 1H), 5.00 (d, *J* = 10.4 Hz, 1H), 3.85 (d, *J* = 10.4 Hz, 1H), 3.75 (s, 3H), 3.68 (s, 3H), 3.54 – 3.48 (m, 2H), 2.68 (dd, *J* = 14.1, 8.6 Hz, 2H); **^{13}C NMR** (126 MHz, $CDCl_3$) δ 159.3 (overlapped), 143.3, 136.3, 135.2, 129.0, 129.0, 122.5, 120.0, 118.3, 116.6, 113.1, 112.9, 112.6, 70.9, 69.1, 55.3, 55.2, 52.9. **IR** (thin layer film) ν (cm^{-1}) = 3350, 2936, 2835, 1600, 1585, 1490, 1260, 1154, 1046, 877. **HRMS** could not be recorded as the compound did not ionize and/or decomposed under any standard technique.

***rac*-2-(diallylamino)-1,2-bis(3,5-dimethylphenyl)ethan-1-ol (5.29)**

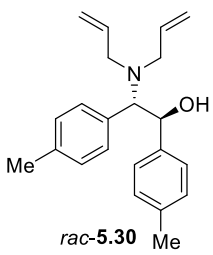


rac-**5.29**

Alcohol *rac*-**5.29** was prepared following the *general procedure D* (24 h), *cis*-2,3-bis(3,5-dimethylphenyl)oxirane (1.00 g, 4 mmol, 1 equiv) and diallylamine (1.5 mL, 12 mmol, 3 equiv). Purification by FCC

(*n*-hexane:Et_2O = 100:0 to 98:2 gradient) afforded *rac*-**5.29** as a white solid (550 mg, 40% yield). **^{1}H NMR** (500 MHz, $CDCl_3$); δ 6.84 (s, 1H), 6.81 (s, 2H), 6.74 (s, 1H), 6.70 (s , 2H), 5.93 – 5.85 (m, 2H), 5.22 (d, *J* = 13.8 Hz, 4H), 4.95 (d, *J* = 10.3 Hz, 1H), 3.84 (d, *J* = 10.3 Hz, 1H), 3.50 – 3.43 (m, 2H), 2.65 (dd, *J* = 8.7, 14 Hz, 2H), 2.26 (s, 6H), 2.17 (s, 6H); **^{13}C NMR** (126 MHz, $CDCl_3$) δ 141.5, 137.3, 137.2, 136.6, 133.5, 129.3, 129.2, 128.0, 125.5, 118.1, 70.8, 69.0, 52.8, 21.6, 21.4; **IR** (thin layer film) ν (cm^{-1}) = 3363, 3078, 3008, 2976, 2918, 1642, 1605, 1448, 1416, 1399, 1377, 1311, 1291, 1158, 1114, 1064, 994, 974, 919, 860, 849, 748, 704; **MP** 99 – 102 °C; **HRMS** (ESI^+) *m/z* calculated for $C_{24}H_{32}NO^+$ $[M+H]^+$ 350.2478, found 350.2479.

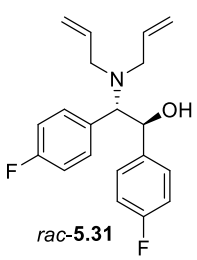
***rac*-2-(diallylamino)-1,2-di-*p*-tolylethan-1-ol (5.30)**



rac-**5.30**

cis-2,3-di-p-tolyloxirane (900 mg, 4.02 mmol, 1 equiv), diallylamine (1.48 mL, 12.0 mmol, 3 equiv) and $ZnCl_2$ (1.1 g, 8.04 mmol, 2 equiv) were stirred in DMF (8 mL, 0.5 M) at 70 °C for 24 h. The reaction mixture was then cooled to rt, diluted with water and extracted three times with CH_2Cl_2. The combined organic layers were washed twice with LiCl (10% w/v solution), dried on $MgSO_4$ and evaporated *in vacuo*. Purification by FCC (*n*-hexane:Et_2O = 100:0 to 95:5, gradient) afforded *rac*-**5.30** as a yellow oil (410 mg, 31% yield). **^{1}H NMR** (500 MHz, $CDCl_3$) δ 7.11 – 7.08 (m, 2H), 7.06 (d, *J* = 7.8 Hz, 2H), 7.02 – 6.97 (m, 2H), 6.96 (d, *J* = 7.9 Hz, 2H), 5.89 (dddd, *J* = 18.1, 9.8, 8.6, 4.1 Hz, 2H), 5.28 – 5.23 (m, 2H), 5.22– 5.20 (m, 2H), 5.07 (br s, 1H), 5.00 (d, *J* = 10.4 Hz, 1H), 3.87 (d, *J* = 10.3 Hz, 1H), 3.53 – 3.47 (m, 2H), 2.63 (dd, *J* = 14.0, 8.6 Hz, 2H), 2.29 (s, 3H), 2.22 (s, 3H); **^{13}C NMR** (126 MHz, $CDCl_3$) [overlapped signals] δ 138.6, 137.3, 136.9, 136.5, 130.5, 130.0, 128.8, 128.8, 127.4, 118.2, 70.8, 69.2, 52.8, 21.2. **IR** (thin layer film) ν (cm^{-1}) = 3364, 3008, 2978, 2922, 1643, 1448, 1396, 1327, 1057, 920, 814; **HRMS** (ESI^+) *m/z* calculated for $C_{22}H_{28}NO^+$ $[M+H]^+$ 322.21654, found 322.21658.

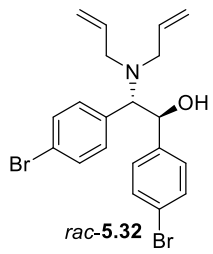
***rac*-2-(diallylamino)-1,2-bis(4-fluorophenyl)ethan-1-ol (5.31)**



rac-**5.31**

Alcohol *rac*-**5.31** was prepared following the *general procedure D* (72 h), from *cis*-2,3-bis(4-fluorophenyl)oxirane (1.03 g, 4.44 mmol, 1equiv) and diallylamine (13 mL, 13.3 mmol, 3 equiv). Purification by FCC (pentane:EtOAc = 100:0 to 90:10) afforded *rac*-**5.31** as a colourless oil (1.053 g, 73% yield). **^{1}H NMR** (500 MHz, $CDCl_3$) δ 7.16 – 7.11 (m, 2H), 7.07 – 7.02 (m, 2H), 6.99 – 6.93 (m, 2H), 6.87 – 6.81 (m, 2H), 5.88 (dddd, J = 16.9, 10.4, 8.6, 4.1 Hz, 2H), 5.28 – 5.18 (m, 4H), 4.99 (br s, 1H), 4.97 (d, J = 10.4 Hz, 1H), 3.83 (d, J = 10.3 Hz, 1H), 3.53 – 3.48 (m, 2H), 2.63 (dd, J = 13.9, 8.7 Hz, 2H); **^{19}F NMR** (470 MHz, $CDCl_3$) δ –114.00 – –114.09 (m, 1F), –115.02 – –115.16 (m,1F); **^{13}C NMR** (126 MHz, $CDCl_3$) δ 162.4 (d, $J_{C–F}$ = 246.0 Hz), 162.2 (d, $J_{C–F}$ = 245.8 Hz), 137.1 (d, $J_{C–F}$ = 3.4 Hz), 136.1, 131.5 (d, $J_{C–F}$ = 7.9 Hz), 129.3 (d, $J_{C–F}$ = 3.6 Hz), 129.0 (d, $J_{C–F}$ = 8.1 Hz), 118.5, 115.2 (d, $J_{C–F}$ = 21.1 Hz), 115.0 (d, $J_{C–F}$ = 21.4 Hz), 70.8, 69.3, 52.8.

***rac*-1,2-bis(4-bromophenyl)-2-(diallylamino)ethan-1-ol (5.32)**

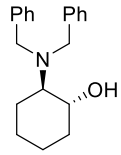


rac-**5.32**

Alcohol *rac*-**5.32** was prepared following the *general procedure D* (24 h), from *cis*-2,3-bis(4-bromophenyl)oxirane (540 mg, 1.5 mmol, 1 equiv) and diallylamine (0.55 mL, 4.5 mmol, 3 equiv). Purification by FCC (*n*-hexane:Et_2O = 100:0 to 80:20, gradient) afforded *rac*-**5.32** as a white solid (450 mg, 67% yield). **^{1}H NMR** (500 MHz, $CDCl_3$); δ 7.40 (d, J = 8.3, 2H), 7.26 (d, J = 8.3, 2H), 7.02 (d, J = 8.3 Hz, 2H), 6.93 (d, J = 8.3 Hz, 2H), 5.92 – 5.78 (m, 2H), 5.29 – 5.49 (m, 4H), 4.92 (d, J = 10.3 Hz, 1H), 3.76 (d, J = 10.3 Hz, 1H), 3.47 (d, J = 14.0 Hz, 2H), 2.59 (dd, J = 8.7, 14.0 Hz, 2H); **^{13}C NMR** (126 MHz, $CDCl_3$) δ 140.5, 136.0, 132.4, 131.7, 131.6, 131.4, 129.2, 122.3, 121.6, 118.8, 70.6, 69.4, 52.9; **IR** (thin layer film) ν (cm^{-1}) = 3372, 3068, 3015, 2973, 2916, 2830, 2810, 1486, 1446, 1389, 1353,

1340, 1324, 1286, 1103, 1008, 998, 974, 87, 799, 727; **MP** 119 – 120 °C; **HRMS** (ESI^+) *m/z* calculated for $C_{20}H_{22}NOBr_2^+$ $[M+H]^+$ 450.00736, found 450.00641.

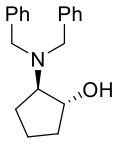
***Trans*-2-(dibenzylamino)cyclohexan-1-ol (4.11)**



rac-**4.11**

Trans-2-(dibenzylamino)cyclohexan-1-ol *rac*-**4.11** was prepared following the *general procedure D* (24 h) from cyclohexene oxide (5 mL, 50 mmol) and dibenzylamine (18.5 mL, 100 mmol), using 0.1 equiv of $Y(OTf)_3$. Purification by FCC (pentane: EtOAc = 95 : 5 to 10 : 1, gradient) afforded *rac*-**4.11** as a white solid (11.32 g, 78% yield). **^{1}H NMR** (400 MHz, $CDCl_3$) δ 7.36 – 7.20 (m, 10H), 3.85 (d, *J* = 13.3 Hz, 1H), 3.77 (brs, 1H), 3.51 (td, *J* = 10.0, 4.4 Hz, 1H), 3.37 (d, *J* = 13.3 Hz, 1H), 2.36 (ddd, *J* = 11.9, 9.7, 3.4 Hz, 1H), 2.12 – 2.02 (m, 1H), 2.02 – 1.92 (m, 1H), 1.82 – 1.74 (m, 1H), 1.72 – 1.61 (m, 1H), 1.32 – 1.03 (m, 4H); **^{13}C NMR** (101 MHz, $CDCl_3$) δ 139.51, 129.01, 128.54, 127.23, 69.05, 64.16, 53.62, 33.25, 25.54, 24.17, 22.14; **MS** (ESI^+) *m/z* calculated for $C_{20}H_{26}NO^+$ $[M+H]^+$ 296.2, found 296.2. **HRMS** (ESI^+) *m/z* calculated for $C_{20}H_{26}NO^+$ $[M+H]^+$ 296.20089, found 296.20081. Spectroscopic data were in agreement with the ones previously reported in literature.[12]

***rac*-2-(dibenzylamino)cyclopentan-1-ol (5.33)**



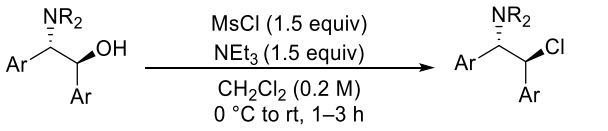
rac-**5.33**

Alcohol *rac*-**5.33** was prepared following the *general procedure D* (overnight) from cyclopentene oxide (872 µl, 10 mmol, 1 equiv) and dibenzylamine (3.8 mL, 20 mmol, 2 equiv). Purification by FCC (pentane: EtOAc = 95:5 to 80:20, gradient) afforded *rac*-**5.33** as a white solid (2.51 g, 90% yield). **^{1}H NMR** (400 MHz, $CDCl_3$) *δ* 7.43 – 7.36 (m, 4H), 7.36 – 7.29 (m, 4H), 7.29 – 7.21 (m, 2H), 4.09 (q, *J* = 7.4 Hz, 1H), 3.79 (d, *J* = 13.8 Hz, 2H), 3.52 (d, *J* = 13.8 Hz, 2H), 2.99 – 2.92 (m, 1H), 1.98 (br s, 1H), 1.94-184 (m, 1H), 1.83 – 1.74 (m, 1H), 1.70 – 1.55 (m, 3H), 1.49 –1.39 (m, 1H); **^{13}C NMR** (101 MHz, $CDCl_3$) *δ* 140.2, 128.7, 128.4, 127.0, 73.8, 68.8, 55.1, 31.7, 22.1,

20.1; **IR** (thin layer film) ν (cm^{-1}) = 3391, 3061, 3027, 2954, 2872, 1493, 1453, 1362, 1248, 1105, 978, 737, 697; MP 47 – 50 °C; HRMS (ESI^+) *m/z* calculated for $C_{19}H_{24}NO^+$ $[M+H]^+$ 282.18524 found 282.18514.

β-Haloamines

General Procedure F: Synthesis of β-Chloroamines



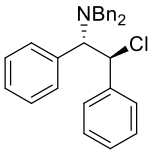
rac-**2.13, 2.106**
5.15–5.32

rac-**2.13, 2.75, 2.107**
5.35–5.50

Following the procedure reported by Nelson,[10] the appropriate aminoalcohol (1 equiv) was dissolved in anhydrous CH_2Cl_2 (0.2 M) and the solution was cooled to 0 °C. NEt_3 (1.5 equiv) was added at once, followed by dropwise addition of MsCl (1.5 equiv) at 0 °C. The reaction mixture was warmed to rt and stirred for 1–3 h. After disappearance of both the starting material and the mesylate intermediate (monitored by ^1H NMR), the reaction mixture was washed with $NaHCO_3$ (sat.) and brine. The organic layers were dried over $MgSO_4$, filtered, and evaporated *in vacuo*. The crude product was then purified with a short silica plug.

N.B. No degradation was observed when silica plugs were employed for purification, however extended contact with silica led to hydrolysis of these compounds.

rac-N, N-dibenzyl-2-chloro-1,2-diphenylethan-1-amine (2.14)

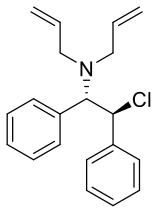


rac-**2.14**

Chloride *rac*-**2.14** was prepared according to the *general procedure F* from *rac*-**2.13** (4.6 g, 11.8 mmol) followed by purification through a silica pad using CH_2Cl_2 as eluent. White solid (4.42 g, 90% yield). **^{1}H NMR** (400 MHz,

$CDCl_3$) δ 7.60 (d, J = 7.7, 4H), 7.37 (t, J = 7.7, 4H), 7.31 – 7.13 (m, 5H), 7.10 – 7.02 (m, 5H), 6.98 – 6.92 (m, 2H), 5.57 (d, J = 11.4 Hz, 1H), 4.27 (d, J = 11.4 Hz, 1H), 4.09 (d, J = 13.6 Hz, 2H), 3.11 (d, J = 13.7 Hz, 2H); **^{13}C NMR** (101 MHz, $CDCl_3$) δ 140.1, 139.6, 134.3, 129.4, 129.2, 128.4, 128.3, 128.1, 128.1, 128.0, 127.5, 127.1, 67.9, 63.3, 53.8; **IR** (thin layer film): ν (cm^{-1}) 3028, 2926, 2360, 1602, 1493, 1453, 1374, 1124, 743, 719, 696; **MP** 151 −153 °C. **HRMS** ($APCI^+$) *m/z* calculated for $C_{28}H_{27}ClN^+$ $[M+H]^+$ 412.18265, found 412.18188.

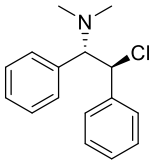
***Rac*-*N*, *N*-diallyl-2-chloro-1,2-diphenylethan-1-amine (2.76)**



rac-**2.76**

Chloride *rac*-**2.76** was prepared according to the *general procedure F* from *rac*-**5.12** (2.50 g, 8.5 mmol) followed by purification through a silica pad using toluene as eluent. White solid (2.40 g, 90% yield). **^{1}H NMR** (400 MHz, $CDCl_3$) δ 7.24 – 7.06 (m, 8H), 7.01 – 6.96 (m, 2H), 5.97 (dddd, J = 17.3, 10.2, 8.1, 4.2 Hz, 2H), 5.41 (d, J = 11.0 Hz, 1H), 5.32 – 5.25 (m, 2H), 5.24 – 5.17 (m, 2H), 4.37 (d, J = 11.0 Hz, 1H), 3.56 – 3.48 (m, 2H), 2.73 (dd, J = 14.2, 8.1 Hz, 2H); **^{13}C NMR** (101 MHz, $CDCl_3$) δ 140.2, 137.3, 135.2, 129.3, 128.4, 128.2, 128.0, 128.0, 127.3, 117.2, 68.8, 63.8, 53.1. **IR** (thin layer film) ν (cm^{-1}) = 3065, 3030, 2813, 1641, 1494, 1453, 1417, 1211, 1030, 920, 720, 696; **MP** 47 – 49 °C; **HRMS** ($APCI^+$) *m/z* calculated for $C_{20}H_{23}ClN^+$ $[M+H]^+$ 312.15135, found 312.15100.

***Rac*-1(-2-chloro-*N*,*N*-dimethyl-1,2-diphenylethan-1-amine (5.34)**

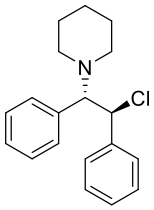


rac-**5.34**

Chloride *rac*-**5.34** was prepared according to the *general procedure F* from *rac*-**5.16** (1.00 g, 4.0 mmol) followed by purification through a silica pad using CH_2Cl_2:EtOAc 1:1 as eluent. Ivory solid (710 mg, 68% yield). **^{1}H NMR** (400 MHz, $CDCl_3$) δ 7.27 – 7.09 (m, 8H), 7.02 – 6.97 (m, 2H), 5.39 (d, J = 10.8 Hz, 1H), 4.13 (d, J = 10.8 Hz, 1H), 2.35 (s, 6H); **^{13}C NMR** (101 MHz, $CDCl_3$) δ 139.8,

133.6, 129.5, 128.4, 128.2, 128.1, 127.8, 127.5, 74.8, 63.2, 41.1. **IR** (thin layer film) ν (cm^{-1}) = 3030, 2968, 2936, 2826, 2783, 1493, 1452, 1267, 1174, 1047, 784, 717, 704; **MP** 51 – 55 °C; **HRMS** (ESI^+) *m/z* calculated for $C_{16}H_{19}ClN^+$ $[M+H]^+$ 260.12005, found 260.12015. Spectroscopic data were in agreement with the ones previously reported in literature.[13]

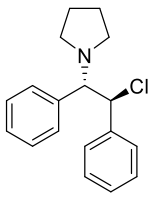
***Rac*-1-(2-chloro-1,2-diphenylethyl)piperidine (2.107)**



rac-**2.107**

Chloride *rac*-**2.107** was prepared according to the *general procedure F* from *rac*-**2.106** (2.22 g, 7.9 mmol) followed by purification through a silica pad using pentane:EtOAc = 90:10 as eluent. White solid (1.45 g, 61% yield). **For the multi-decagram scale reaction** *(performed by Dr. Gabriele Pupo):* The alcohol *rac*-**2.106** (111.7 g, 0.4 mol, 1 equiv) was dissolved in CH_2Cl_2 (0.5 M, 800 mL) and the solution was cooled to 0 °C. MsCl (46 mL, 0.6 mol, 1.5 equiv) followed by dry NEt_3 (83 mL, 0.6 mol, 1.5 equiv) were slowly added (dropping funnel) at 0 °C. The reaction mixture was then stirred at rt for 2 h. After quenching at 0 °C by addition of $NaHCO_3$ (sat.), the aqueous phase was extracted three times with Et_2O and the combined organic phases were washed with brine, dried over $MgSO_4$ and evaporated *in vacuo*. The crude product was quickly passed through a silica plug (pentane:EtOAc = 70:30). Finally, the light brown solid was washed with small amounts of Et_2O to afford a white solid (85.3 g, 71% yield). **^{1}H NMR** (400 MHz, $CDCl_3$) δ 7.24 – 7.19 (m, 2H), 7.19 – 7.06 (m, 6H), 6.98 – 6.93 (m, 2H), 5.39 (d, *J* = 10.8 Hz, 1H), 4.04 (d, *J* = 10.8 Hz, 1H), 2.57 – 2.48 (m, 2H), 2.41 – 2.33 (m, 2H), 1.73 – 1.54 (m, 4H), 1.40 – 1.30 (m, 2H); **^{13}C NMR (**101 MHz, $CDCl_3$) δ 140.0, 134.9, 129.2, 128.2, 128.1, 127.9, 127.6, 127.2, 75.4, 62.8, 50.4, 26.4, 24.6; **IR** (thin layer film) ν (cm^{-1}) = 3030, 2932, 2851, 2802, 1493, 1452, 1306, 1200, 1161, 1102, 990, 869, 718, 696, 658; **MP** 93 – 95 °C; **HRMS** (ESI^+) *m/z* calculated for $C_{29}H_{23}ClN^+$ $[M+H]^+$ 300.15135, found 300.15118.

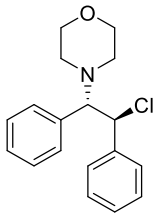
***Rac*-1(-2-chloro-1,2-diphenylethyl)pyrrolidine (5.35)**



rac-**5.35**

Chloride *rac*-**5.35** was prepared according to the *general procedure F* from *rac*-**5.17** (2.27 g, 8.5 mmol) followed by purification through a silica pad using *n*-hexane:Et_2O (96:4 to 80:20, gradient) as eluent. Ivory solid (1.73 g, 71% yield). **^{1}H NMR** (400 MHz, $CDCl_3$) δ 7.21 – 7.03 (m, 8H), 7.05 – 6.93 (m, 2H), 5.44 (d, *J* = 7.5 Hz, 1H), 4.08 (d, *J* = 7.4 Hz, 1H), 2.79 – 2.65 (m, 2H), 2.64 – 2.50 (m, 2H), 1.84 – 1.67 (m, 4H); **^{13}C NMR** (101 MHz, $CDCl_3$) δ 139.1, 136.4, 130.0, 128.5, 127.9, 127.9, 127.5, 127.4, 74.5, 64.4, 50.9, 23.4. **IR** (thin layer film) ν (cm^{-1}) = 3061, 2956, 2798, 1994, 1452, 1358, 1312, 1127, 1075, 1031, 702; **MP** 42 – 43 °C; **HRMS** (ESI^+) *m/z* calculated for $C_{18}H_{21}ClN^+$ $[M+H]^+$ 286.13570, found 286.13539. Spectroscopic data were in agreement with the ones previously reported in literature.[10]

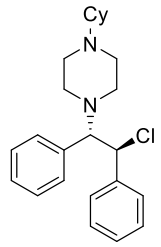
***Rac*-4-(2-chloro-1,2-diphenylethyl)morpholine (5.36)**



rac-**5.36**

Chloride *rac*-**5.36** was prepared according to the *general procedure F* from *rac*-**5.18** (600 mg, 2.12 mmol) followed by purification through a silica pad using *n*-hexane:EtOAc (100:0 to 90:10, gradient) as eluent. Pale pink solid (562.6 mg, 88% yield). **^{1}H NMR** (400 MHz, $CDCl_3$) δ 7.27 – 7.11 (m, 8H), 7.02 – 6.96 (m, 2H), 5.42 (d, *J* = 10.4 Hz, 1H), 4.09 (d, *J* = 10.4 Hz, 1H), 3.83 (ddd, *J* = 11.0, 6.3, 3.1 Hz, 2H), 3.76 (ddd, *J* = 11.0, 6.1, 3.1 Hz, 2H), 2.62 (ddd, *J* = 9.9, 6.4, 3.0 Hz, 2H), 2.52 (ddd, *J* = 10.7, 6.3, 3.0 Hz, 2H); **^{13}C NMR** (101 MHz, $CDCl_3$) δ 139.6, 134.4, 129.3, 128.4, 128.2, 128.1, 128.0, 127.7, 75.3, 67.4, 62.4, 49.7; **IR** (thin layer film) ν (cm^{-1}) = 3030, 2957, 2855, 2818, 1494, 1451, 1114, 697; **MP** 142 – 145 °C; **HRMS** ($APCI^+$) *m/z* calculated for $C_{28}H_{21}ClNO^+$ $[M+H]^+$ 3012.13062, found 3012.13062.

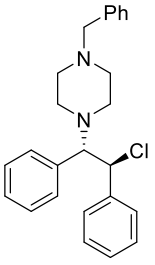
***Rac*-1-(2-chloro-1,2-diphenylethyl)-4-cyclohexylpiperazine (5.37)**



rac-**5.37**

Chloride *rac*-**5.37** was prepared according to the *general procedure F* from *rac*-**5.19** (750 mg, 2.00 mmol) followed by purification through a silica pad using CH_2Cl_2:EtOAc (100:0 to 80:20, gradient) as eluent. White solid (541 mg, 71% yield). **^{1}H NMR** (500 MHz, DMSO-d_6) δ 7.36 (d, J = 7.6 Hz, 2H), 7.16 – 7.04 (m, 8H), 5.88 (d, J = 11.3 Hz, 1H), 4.23 (d, J = 11.4 Hz, 1H), 2.65 – 2.06 (m, 9H), 1.73 – 1.61 (m, 4H), 1.57 – 1.47 (m, 1H), 1.23 – 0.94 (m, 5H); **^{13}C NMR** (126 MHz, DMSO-d_6) δ 140.3, 133.9, 129.3, 128.2, 128.1, 127.7, 127.3, 126.9, 72.5, 62.6, 62.0, 48.7, 48.3, 28.2, 25.9, 25.2; **IR** (thin layer film) ν (cm^{-1}) = 2928, 2853, 2817, 1494, 1452, 1376, 1287, 1145, 1005, 703; **MP** 103 – 105 °C; **HRMS** ($APCI^+$) *m/z* calculated for $C_{24}H_{32}ClN_2^+$ $[M+H]^+$ 383.22485, found 383.22513.

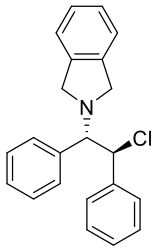
***Rac*-1-benzyl-4-(-2-chloro-1,2-diphenylethyl)piperazine (5.38)**



rac-**5.38**

Chloride *rac*-**5.38** was prepared according to the *general procedure F* from *rac*-**5.20** (660 mg, 1.77 mmol) followed by purification through a silica pad using *n*-hexane:Et_2O (100:0 to 85:15, gradient) as eluent. White solid (458 mg, 66% yield). **^{1}H NMR** (400 MHz, $CDCl_3$) δ 7.30 – 7.18 (m, 7H), 7.16 – 7.06 (m, 6H), 6.96 – 6.91 (m, 2H), 5.37 (d, J = 10.6 Hz, 1H), 4.07 (d, J = 10.6 Hz, 1H), 3.48 (s, 2H), 2.64–2.42 (m, 8H); **^{13}C NMR** (101 MHz, $CDCl_3$) δ 139.9, 138.3, 134.6, 129.4, 129.3, 128.3, 128.3, 128.2, 128.0, 127.9, 127.5, 127.1, 74.8, 63.3, 62.7, 53.6, 49.1 (br); **IR** (thin layer film) ν (cm^{-1}) = 3062, 2934, 2813, 1494, 1453, 1137, 1007, 733, 698; **MP** 112 – 114 °C; **HRMS** (ESI^+) *m/z* calculated for $C_{25}H_{28}ClN_2^+$ $[M+H]^+$ 391.19355, found 391.19302.

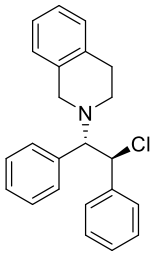
***Rac*-2-(-2-chloro-1,2-diphenylethyl)isoindoline (5.39)**



rac-**5.39**

Chloride *rac*-**5.39** was prepared according to *the general procedure F* from *rac*-**5.21** (530 mg, 1.68 mmol) followed by purification by FCC using pentane:Et_2O (100:0 to 98:2, gradient) as eluent. Due to the limited stability of the compound, the solvent was evaporated under a flow of nitrogen without evaporation *in vacuo* (thus avoiding warm water baths). White solid (200 mg, 34% yield). **^{1}H NMR** (500 MHz, $CDCl_3$) δ 7.21 – 7.14 (m, 12H), 7.10 – 7.02 (m, 2H), 5.53 (d, *J* = 6.7 Hz, 1H), 4.36 (d, *J* = 6.8 Hz, 1H), 4.20 (d, *J* = 11.9 Hz, 2H), 4.09 (d, *J* = 11.9 Hz, 2H); **^{13}C NMR** (126 MHz, $CDCl_3$) [overlapping signals] δ 139.4, 138.5, 136.5, 130.1, 128.5, 128.1, 127.9, 127.8, 126.9, 122.4, 74.9, 64.3, 57.1; **IR** (thin layer film) ν (cm^{-1}) = 3030, 2939, 2892, 2793, 1493, 1464, 1363, 1314, 1133, 1077, 909, 742, 702; **MP** 84 – 86 °C; **HRMS** (ESI^+) *m/z* calculated for $C_{22}H_{21}ClN^+$ $[M+H]^+$ 334.13570, found 334.13528.

***Rac*-2-(2-chloro-1,2-diphenylethyl)-1,2,3,4-tetrahydroisoquinoline (5.40)**

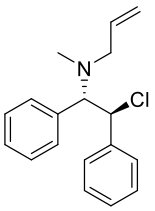


rac-**5.40**

Chloride *rac*-**5.40** was prepared according to the *general procedure F* from *rac*-**5.22** (750 mg, 2.3 mmol) followed by purification through a silica pad using pentane:Et_2O (100:0 to 95:5, gradient) as eluent. White solid (628 mg, 78% yield). **^{1}H NMR** (400 MHz, $CDCl_3$) δ 7.33 – 7.28 (m, 2H), 7.27 – 7.08 (m, 11H), 7.07 – 7.02 (m, 1H), 5.58 (d, *J* = 10.5 Hz, 1H), 4.34 (d, *J* = 10.5 Hz, 1H), 3.83 (d, *J* = 14.5 Hz, 1H), 3.73 (d, *J* = 14.6 Hz, 1H), 3.22 – 3.03 (m, 2H), 2.96 (dt, J = 16.0, 4.5 Hz, 1H), 2.68 (ddd, *J* = 10.4, 8.2, 4.3 Hz, 1H); **^{13}C NMR** (101 MHz, $CDCl_3$) δ 139.8, 135.2, 134.8, 134.7, 129.3, 128.8, 128.4, 128.2, 128.1, 128.0, 127.6, 126.6, 126.0, 125.6, 74.7, 62.9, 52.7, 46.1, 30.0; **IR** (thin layer film) ν (cm^{-1}) = 3028, 2916, 2805, 1495, 1454, 1134, 1099, 1001, 936, 730, 697. **MP** 85 – 87 °C; **HRMS** ($APCI^+$) *m/z* calculated for

$C_{23}H_{23}ClN^+$ $[M+H]^+$ 348.15135, found 348.15155. Spectroscopic data were in agreement with the ones previously reported in literature.[13]

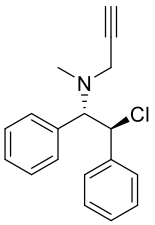
***Rac*-*N*-(2-chloro-1,2-diphenylethyl)-*N*-methylprop-2-en-1-amine (5.41)**



rac-**5.41**

Chloride *rac*-**5.41** was prepared according to the *general procedure F* from *rac*-**5.23** (700 mg, 2.6 mmol) followed by purification through a silica pad using pentane:Et_2O (100:0 to 90:10, gradient) as eluent. White solid (581 mg, 83% yield). **^{1}H NMR** (400 MHz, $CDCl_3$) δ 7.24 – 7.06 (m, 8H), 6.99 – 6.94 (m, 2H), 5.99 (dddd, J = 17.5, 10.2, 7.6, 5.1 Hz, 1H), 5.40 (d, J = 11.0 Hz, 1H), 5.28 – 5.18 (m, 2H), 4.24 (d, J = 10.9 Hz, 1H), 3.24 (ddt, J = 13.7, 5.2, 1.8 Hz, 1H), 2.89 (dd, J = 13.7, 7.6 Hz, 1H), 2.30 (s, 3H); **^{13}C NMR** (101 MHz, $CDCl_3$) δ 140.0, 136.8, 134.3, 129.4, 128.4, 128.2, 128.1, 127.9, 127.4, 117.5, 72.2, 63.4, 57.3, 37.6; **IR** (thin layer film) ν (cm^{-1}) = 3063, 3030, 2974, 2853, 2793, 1642, 1493, 1451, 1205, 1156, 1020, 998, 921, 758, 720, 697. **MP** 60 – 61 °C; **HRMS** (ESI^+) *m/z* calculated for $C_{18}H_{21}ClN^+$ $[M+H]^+$ 286.13570, found 286.13580.

***Rac*-*N*-(2-chloro-1,2-diphenylethyl)-*N*-methylprop-2-yn-1-amine (5.42)**

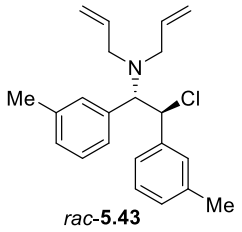


rac-**5.42**

Chloride *rac*-**5.42** was prepared according to the *general procedure F* from *rac*-**5.24** (500 mg, 1.88 mmol) followed by purification through a silica pad using pentane:Et_2O (100:0 to 90:10, gradient) as eluent. White solid (420 mg, 79% yield).**^{1}H NMR** (500 MHz, $CDCl_3$) δ 7.27 – 7.23 (m, 2H), 7.23 – 7.13 (m, 6H), 7.08 – 7.03 (m, 2H), 5.45 (d, J = 9.8 Hz, 1H), 4.46 (d, J = 9.8 Hz, 1H), 3.44 (dd, J = 16.5, 2.5 Hz, 1H), 3.16 (dd, J = 16.6, 2.4 Hz, 1H), 2.44 (s, 3H), 2.32 (t, J = 2.5 Hz, 1H); **^{13}C NMR** (126 MHz, $CDCl_3$) δ 139.5, 134.0, 129.7, 128.2 (overlapped), 128.1, 127.9, 127.8, 80.0, 73.2, 71.9, 62.9, 44.2, 37.8; **IR** (thin layer film) ν (cm^{-1}) = 3293, 3030, 2796,

1493, 1452, 1208, 1122, 1076, 1059, 1022, 757, 696; **MP** 45–46 °C; **HRMS** (ESI^+) *m/z* calculated for $C_{18}H_{19}ClN^+$ $[M+H]^+$ 284.12005, found 284.11990.

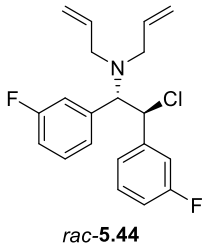
***Rac*-*N*-allyl-*N*-(-2-chloro-1,2-di-m-tolylethyl)prop-2-en-1-amine (5.43)**



rac-**5.43**

Chloride *rac*-**5.43** was prepared according to the *general procedure F* from *rac*-**5.25** (480 mg, 2.8 mmol) followed by purification through a silica pad using toluene as eluent. White solid (280 mg, 55% yield). **^{1}H NMR** (400 MHz, $CDCl_3$) δ 7.10 – 6.95 (m, 4H), 6.95 – 6.86 (m, 2H), 6.86 – 6.83 (m, 2H), 6.06 – 5.88 (m, 2H), 5.37 (d, *J* = 11.0 Hz, 1H), 5.27 (d, *J* = 17.0 Hz, 2H), 5.19 (d, *J* = 10.4 Hz, 2H), 4.30 (d, J = 11, 1H), 3.48 (d, *J* = 14.5, 2H), 2.71 (dd, *J* = 8.0, 14.5 Hz, 2H), 2.24 (s, 3H), 2.22 (s, 3H); **^{13}C NMR** (101 MHz, $CDCl_3$) δ 140.2, 137.9, 137.4, 137.3, 135.1, 130.1, 128.9, 128.8, 128.2, 128.0, 127.7, 126.3, 125.2, 117.1, 68.4, 64.0, 53.2, 21.6, 21.4; **IR** (thin layer film) ν (cm^{-1}) = 3022, 2920, 2813, 1641, 1605, 1489, 1445, 1417, 1378, 1344, 1262, 1155, 1123, 1093, 1042, 997, 973, 918, 883, 791, 775, 708; **MP** 54 – 56 °C **HRMS** ($APCI^+$) *m/z* calculated for $C_{22}H_{27}ClN^+$ $[M+H]^+$ 340.1826, found 340.1826.

***Rac*-*N*-allyl-*N*-2-chloro-1,2-bis(3-fluorophenyl)ethyl)prop-2-en-1-amine (5.44)**

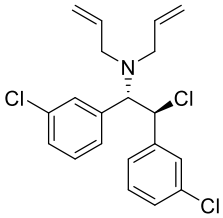


rac-**5.44**

Chloride *rac*-**5.44** was prepared according to the *general procedure F* from *rac*-**5.26** (500 mg, 1.5 mmol) followed by purification through a silica pad using toluene as eluent. White solid (350 mg, 65% yield). **^{1}H NMR** (500 MHz, $CDCl_3$) δ 7.19 – 7.07 (m, 2H), 7.00 – 6.90 (m, 2H), 6.88 – 6.78 (m, 2H), 6.75 (d, J = 8.0 Hz, 1H), 6.68 (d, *J* = 9.5 Hz, 1H) 5.99 – 5.87 (m, 2H), 5.35 – 5.17 (m, 5H), 4.28 (d, *J* = 10.7 Hz, 1H), 3.49 (d, *J* = 14.6 Hz, 2H), 2.70 (dd, *J* = 14.2, 8.0 Hz, 2H); **^{19}F NMR** (470 MHz, $CDCl_3$) δ –112.6 (m, 1F), –112.7 (m, 1F); **^{13}C NMR** (126 MHz, $CDCl_3$) δ 162.6 (d, J_{C-F} = 246.6 Hz), 162.5 (d, J_{C-F} = 246.6 Hz), 141.3 (d,

$J_{C–F}$ = 8 Hz), 139.6 (d, $J_{C–F}$ = 8 Hz), 136.8, 130.0 (d, $J_{C–F}$ = 8.5 Hz), 129.6 (d, $J_{C–F}$ = 8.5 Hz), 124.9 (d, $J_{C–F}$ = 2.8 Hz), 123.9 (d, $J_{C–F}$ = 2.8 Hz), 178.6, 115.9 (d, $J_{C–F}$ = 20.7 Hz), 115.3 (d, $J_{C–F}$ = 20.7 Hz), 115.1 (d, $J_{C–F}$ = 22.3 Hz), 114.5 (d, $J_{C–F}$ = 21.3 Hz), 68.3, 62.4, 53.1; **IR** (thin layer film) ν (cm^{-1}) = 3078, 2926, 2814, 1641, 1612, 1590, 1488, 1446, 1418, 1344, 1258, 1140, 1077, 998, 976, 922, 878, 782, 767, 734, 703; **MP** 65 – 66 °C; **HRMS** ($APCI^+$) *m/z* calculated for $C_{20}H_{21}ClF_2N^+$ $[M+H]^+$ 348.1325, found 348.1323.

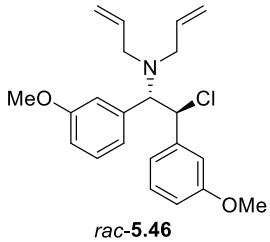
***Rac*-*N*-allyl-*N*-2-chloro-1,2-bis(3-chlorophenyl)ethyl)prop-2-en-1-amine (5.45)**



rac-**5.45**

Chloride *rac*-**5.45** was prepared according to the *general procedure F* from *rac*-**5.27** (540 mg, 1.5 mmol) followed by purification through a silica pad using toluene as eluent. White solid (540 mg, 90% yield). **^{1}H NMR** (500 MHz, $CDCl_3$) δ 7.21 (s, 1H), 7.18 – 7.02 (m, 5H), 6.96 (s, 1H), 6.86 – 6.82 (s, 1H), 5.92 (dddd, *J* = 17.9, 10.1, 8.0, 4.3 Hz, 2H), 5.35 – 5.16 (m, 5H), 4.26 (d, *J* = 10.8 Hz, 1H), 3.53 – 3.42 (m, 2H), 2.71 (dd, *J* = 8.0, 14.6, 5.0 Hz, 2H); **^{13}C NMR** (126 MHz, $CDCl_3$) δ 141.8, 137.0, 136.7, 134.3, 134.2, 129.8, 129.4, 129.1, 128.5, 128.3, 127.8, 127.3, 126.4, 117.7, 68.4, 62.3, 53.1; **IR** (thin layer film) ν (cm^{-1}) = 3076, 3008, 2977, 2925, 2814, 1641, 1593, 1573, 1476, 1430, 1344, 1265, 1210, 1195, 1155, 1124, 1096, 1080, 1049, 998, 975, 922, 883, 845; **MP** 67 – 68 °C; **HRMS** ($APCI^+$) *m/z* calculated for $C_{20}H_{21}Cl_3N^+$ $[M+H]^+$ 382.0705, found 382.0702.

***Rac*-*N*-allyl-*N*-(2-chloro-1,2-bis(3-methoxyphenyl)ethyl)prop-2-en-1-amine (5.46)**

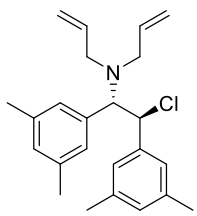


rac-**5.46**

Chloride *rac*-**5.46** was prepared according to the *general procedure F* from *rac*-**5.28** (750 mg, 2.12 mmol) followed by purification through a silica pad using *n*-hexane:Et_2O 80:20 as eluent. White solid (592 mg, 79% yield). **^{1}H NMR** (400 MHz, $CDCl_3$) δ 7.14 – 7.02 (m, 2H), 6.84 – 6.79 (m, 1H), 6.77 (t, *J* = 2.6 Hz, 1H), 6.69 – 6.63

(m, 2H), 6.60 (dt, *J* = 7.6, 1.2 Hz, 1H), 6.53 – 6.50 (m, 1H), 5.95 (dddd, *J* = 17.2, 10.1, 8.1, 4.2 Hz, 2H), 5.35 (d, *J* = 10.9 Hz, 1H), 5.31 – 5.24 (m, 2H), 5.21 – 5.17 (m, 2H), 4.31 (d, *J* = 10.9 Hz, 1H), 3.71 (s, 3H), 3.70 (s, 3H), 3.50 (ddt, *J* = 14.3, 4.2, 2.0 Hz, 2H), 2.74 (ddt, *J* = 14.2, 8.1, 1.0 Hz, 2H); **^{13}C NMR** (101 MHz, $CDCl_3$) δ 159.4, 159.2, 141.7, 137.3, 136.8, 129.4, 128.9, 121.6, 120.6, 117.2, 115.5, 114.1, 113.4, 112.3, 68.5, 63.6, 55.3, 55.2, 53.2. **IR** (thin layer film) ν (cm^{-1}) = 3076, 3004, 2936, 2834, 1600, 1585, 1491, 1436, 1261, 1154, 1046, 921, 730; **MP** 69 – 70 °C; **HRMS** (ESI^+) *m/z* calculated for $C_{22}H_{27}ClNO_2^+$ $[M+H]^+$ 372.17248, found 372.17236.

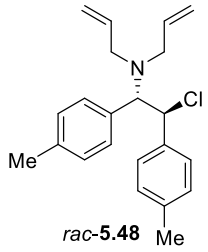
***Rac*-*N*-allyl-*N*-2-chloro-1,2-bis(3,5-dimethylphenyl)ethyl)prop-2-en-1-amine (5.47)**



rac-**5.47**

Chloride *rac*-**5.47** was prepared according to the *general procedure F* from *rac*-**5.29** (450 mg, 1.3 mmol) followed by purification through a silica pad using toluene as eluent. White solid (300 mg, 61% yield). **^{1}H NMR** (400 MHz, $CDCl_3$); δ 6.82 (s, 2H), 6.74 (d, *J* = 8.7 Hz, 2H), 6.59 (s, 2H), 6.03 – 5.90 (m, 2H), 5.35 (d, *J* = 10.6 Hz, 1H), 5.27 (d, *J* = 17.3 Hz, 2H), 5.19 (d, *J* = 10 Hz, 2H), 4.27 (d, *J* = 10.6 Hz, 1H), 3.50 – 3.42 (m, 2H), 2.70 (dd, *J* = 8.7, 1.4 Hz, 2H), 2.21 (s, 6H), 2.18 (s, 6H); **^{13}C NMR** (101 MHz, $CDCl_3$) δ 140.1, 137.7, 137.6, 137.0, 134.9, 129.8, 128.8, 127.2, 126.0, 117.2, 68.1, 64.1, 53.2, 21.5, 21.3; **IR** (thin layer film) ν (cm^{-1}) = 3075, 3010, 2918, 2812, 1640, 1604, 1446, 1416, 1376, 1344, 1288, 1265, 1206, 1123, 1038, 997, 975, 916, 850, 774, 727, 698, 689, 660; **MP** 109 – 110 °C; **HRMS** (ESI^+) *m/z* calculated for $C_{24}H_{31}ClN^+$ $[M+H]^+$ 368.2139, found 368.2141.

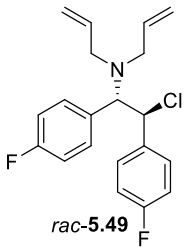
***Rac*-*N*-allyl-*N*-(2-chloro-1,2-di-p-tolylethyl)prop-2-en-1-amine (5.48)**



rac-**5.48**

Chloride *rac*-**5.48** was prepared according to the *general procedure F* from *rac*-**5.30** (380 mg, 1.18 mmol) followed by purification by FCC using pentane:Et_2O (95:5 to 90:10, gradient) as eluent. White solid (346 mg, 86% yield). **^{1}H NMR** (500 MHz, $CDCl_3$) δ 7.10 (d, J = 7.6 Hz, 2H), 6.98 (d, J = 7.5 Hz, 2H), 6.95 (d, J = 7.8 Hz, 2H), 6.87 (d, J = 7.5 Hz, 2H), 6.02 – 5.90 (m, 2H), 5.39 (d, J = 11.0 Hz, 1H), 5.27 (d, J = 17.3 Hz, 2H), 5.19 (d, J = 10.1 Hz, 2H), 4.33 (d, J = 11.0 Hz, 1H), 3.48 (ddd, J = 14.3, 4.3, 2.1 Hz, 2H), 2.68 (dd, J = 14.3, 8.1 Hz, 2H), 2.23 (s, 3H), 2.21 (s, 3H); **^{13}C NMR** (126 MHz, $CDCl_3$) δ 137.7, 137.5, 137.4, 136.8, 132.0, 129.2, 129.1, 128.7, 128.0, 117.1, 68.1, 63.8, 53.1, 21.2, 21.1; **IR** (thin layer film) ν (cm^{-1}) = 3008, 2977, 2922, 2812, 1641, 1513, 1344, 1263, 1042, 919, 811, 739; **MP** 55 – 56 °C; **HRMS** (ESI^+) *m/z* calculated for $C_{22}H_{27}ClN^+$ $[M+H]^+$ 340.18265, found 340.18288.

***Rac*-*N*-allyl-*N*-(2-chloro-1,2-bis(4-fluorophenyl)ethyl)prop-2-en-1-amine (5.49)**

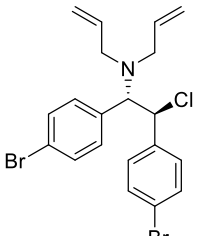


rac-**5.49**

Chloride *rac*-**5.49** was prepared according to the *general procedure F* from *rac*-**5.31** (900 mg, 2.73 mmol) followed by purification by FCC using pentane:Et_2O (100:0 to 98:2, gradient) as eluent. White solid (776 mg, 82% yield). **^{1}H NMR** (500 MHz, $CDCl_3$) δ 7.17 – 7.12 (m, 2H), 6.95 – 6.81 (m, 6H), 5.94 (dddd, J = 17.2, 10.2, 8.0, 4.2 Hz, 2H), 5.33 (d, J = 10.9 Hz, 1H), 5.26 (dtd, J = 17.3, 2.0, 1.0 Hz, 2H), 5.20 (dtd, J = 10.2, 1.9, 0.8 Hz, 2H), 4.29 (d, J = 10.9 Hz, 1H), 3.49 (ddt, J = 14.2, 4.1, 2.0 Hz, 2H), 2.77 – 2.63 (m, 2H); **^{19}F NMR** (377 MHz, $CDCl_3$) δ –113.41– –113.49 (m, 1F), –114.52 – –114.62 (m, 1F); **^{13}C NMR** (126 MHz, $CDCl_3$) δ 162.1 (d, $J_{C–F}$ = 247.6 Hz), 162.0 (d, $J_{C–F}$ = 245.6 Hz), 137.0, 136.0 (d, $J_{C–F}$ = 3.3 Hz), 131.0 (d, $J_{C–F}$ = 3.4 Hz), 130.7 (d, $J_{C–F}$ = 7.8 Hz), 129.8 (d, $J_{C–F}$ = 8.2 Hz), 117.5, 115.4 (d, $J_{C–F}$ = 21.6 Hz), 115.1 (d, $J_{C–F}$ = 21.1 Hz), 68.4, 62.8, 53.1; **IR** (thin layer film) ν (cm^{-1}) = 307,

278, 2814, 1604, 1509, 1230, 1159, 922, 833, 750; **MP** 81 – 83 °C; **HRMS** (ESI^+) *m/z* calculated for $C_{20}H_{21}F_2ClN^+$ $[M+H]^+$ 348.13251, found 348.13226.

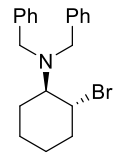
***Rac*-*N*-allyl-*N* -2-chloro-1,2-bis(4-bromophenyl)ethyl)prop-2-en-1-amine (5.50)**



rac-**5.50**

Chloride *rac*-**5.50** was prepared according to the *general procedure F* from *rac*-**5.32** (450 mg, 1.0 mmol) followed by purification through a silica pad using toluene as eluent. White solid (320 mg, 68% yield). **^{1}H NMR** (400 MHz, $CDCl_3$); δ 7.37 – 7.24 (m, 4H), 7.10 – 7.02 (m, 2H), 6.86 –6.79 (m, 2H), 6.01 – 5.84 (m, 2H), 5.34 – 5.16 (m, 5H) 4.26 (d, *J* = 10.9 Hz, 1H), 3.52 – 3.40 (m, 2H), 2.67 (dd, *J* = 8, 14.8 Hz, 2H); **^{13}C NMR** (101 MHz, $CDCl_3$) δ 139.0, 136.8, 133.9, 131.7, 131.4, 130.7, 129.8, 122.2, 121.6, 117.6, 68.2, 62.4, 53.1; **IR** (thin layer film) ν (cm^{-1}) = 3077, 3007, 2976, 2924, 2814, 1641, 1590, 1521, 1488, 1447, 1416, 1405, 1183, 1125, 1106, 1074, 1010, 975, 921, 881, 834, 752, 726, 704; **MP** 83 – 86 °C; **HRMS** (ESI^+) *m/z* calculated for $C_{20}H_{21}ClNBr_2^+$ $[M+H]^+$ 467.9724, found 467.9728.

***Rac*-*N*,*N*-dibenzyl-2-bromocyclohexan-1-amine (2.108)**

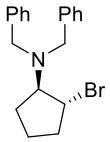


rac-**2.108**

Following the procedure reported by Chong,[14] in a flame-dried round-bottom-flask, alcohol *rac*-**4.11** (3.49 g, 12 mmol, 1 equiv) and PPh_3 (3.78 g, 14.4 mmol, 1.2 equiv) were dissolved in anhydrous $CHCl_3$ (60.0 mL, 0.2 M). The reaction mixture was cooled to 0 °C and *N*-bromosuccinimide (NBS, 2.56 g, 14.4 mmol, 1.2 equiv) was added portion-wise. The reaction was stirred at rt until disappearance of the starting material (monitored by TLC). The solvent was removed *in vacuo* and the crude product was purified by FCC on silica gel (Pentane:EtOAc = 100:0 to 95:5, gradient). White solid (1.96 g, 45%). **^{1}H NMR** (400 MHz, CDCl3) δ 7.52 (d, *J* = 7.3 Hz, 4H), 7.36 – 7.28 (m, 4H), 7.27 – 7.20 (m, 2H), 4.16 (td, *J* = 11.4, 4.3 Hz, 1H), 3.88 (d, *J* = 13.7 Hz, 2H), 3.47

(d, *J* = 13.7 Hz, 2H), 2.67 (td, *J* = 11.3, 3.7 Hz, 1H), 2.47 – 2.36 (m, 1H), 2.17 – 2.06 (m, 1H), 1.86 – 1.71 (m, 2H), 1.69 – 1.61 (m, 1H), 1.39 – 1.06 (m, 3H); **^{13}C NMR** (101 MHz, CDCl3) *δ* 140.0, 129.2, 128.2, 126.9, 63.3, 55.8, 53.7, 38.9, 27.7, 26.3, 25.3; **IR** (thin layer film): ν (cm^{-1}) = 3061, 3026, 2933, 2856, 2802, 1494, 1452, 1141, 745, 697; **MP** 93 – 95 °C; **HRMS** (ESI^+) *m/z* calculated for $C_{20}H_{25}BrN^+$ $[M+H]^+$ 358.11649, found 358.11694. Spectroscopic data were in agreement with the ones previously reported in literature.[14]

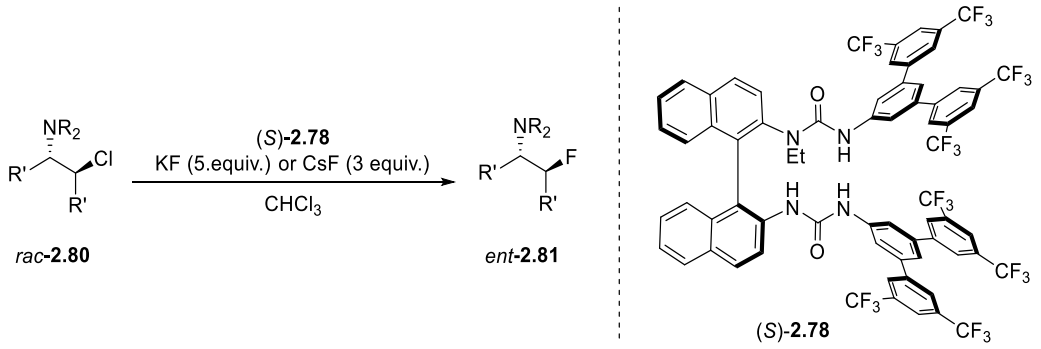
***Rac*-*N*,*N*-dibenzyl-2-bromocyclopentan-1-amine (5.51)**



rac-**5.51**

Alcohol *rac*-**5.33** (750 mg, 2.66 mmol, 1 equiv) was dissolved in anhydrous CH_2Cl_2 (6.7 mL, 0.2 M) and the solution was cooled to 0 °C. NEt_3 (403 μL, 3.99 mmol, 1.5 equiv) was added at once, followed by dropwise addition of MsBr (634 μL, 3.99 mmol, 1.5 equiv) at 0 °C. The reaction mixture was warmed to rt and stirred for 6 h. After disappearance of both the starting material and the mesylate intermediate (monitored by ^{1}H NMR), the reaction mixture was washed with $NaHCO_3$ (sat.). The organic layer was dried over $MgSO_4$, filtered and evaporated *in vacuo*. The crude product was then purified with a short silica plug (Pentane:Et_2O = 98:2) to afford *rac*-**5.51** as a pale yellow solid (647 mg, 71% yield). **^{1}H NMR** (500 MHz, CDCl3) *δ* 7.44 – 7.39 (m, 4H), 7.33 – 7.28 (m, 4H), 7.25 – 7.20 (m, 2H), 4.33 (q, *J* = 6.9 Hz, 1H), 3.75 (d, *J* = 14.0, 2H), 3.60 (d, *J* = 14.0, 2H), 3.56 – 3.50 (m, 1H), 2.22 – 2.15 (m, 1H), 1.99 – 1.90 (m, 1H), 1.88 – 1.80 (m, 1H), 1.78 – 1.56 (m, 3H); **^{13}C NMR** (126 MHz, CDCl3) *δ* 138.9, 128.8, 128.3, 127.1, 69.6, 54.7, 51.5, 36.6, 25.4, 22.6; **IR** (thin layer film): ν (cm-1) = 3027, 2961, 2801, 1493, 1453, 1363, 1028, 743, 698; **MP** 40 – 42 °C; **HRMS** (ESI^+) *m/z* calculated for $C_{19}H_{23}BrN^+$ $[M+H]^+$ 344.10084, found 344.10092.

5.2.2.3 Asymmetric Fluorination under HB-PTC



Asymmetric fluorination with KF

In a vial equipped with a magnetic stirring bar were sequentially added the β-haloamine (1 equiv), the catalyst, KF (5 equiv) and dry $CHCl_3$ (0.5 M, pre-cooled at the same temperature as the reaction). The vial was sealed, and the reaction mixture was stirred at 900 rpm at the appropriate temperature for the indicated time. The crude mixture was then filtered through a small plug of silica (and eluted with cold CH_2Cl_2/EtOAc = 1:1), evaporated to dryness under reduced pressure and directly purified by FCC.

For reaction optimisation the crude mixture was analysed by ^{1}H and ^{19}F NMR (4-fluoroanisole as internal standard) to determine the yield; an aliquot of the reaction mixture was purified by preparative TLC and analysed by HPLC (chiral stationary phase) to determine the e.r.

Asymmetric fluorination with CsF

In a vial equipped with a magnetic stirring bar were sequentially added the β-haloamine (1 equiv), the catalyst, CsF (3 equiv) and dry $CHCl_3$ (0.25 M, pre-cooled at the same temperature as the reaction). The vial was sealed and the reaction mixture was stirred at 900 rpm at the appropriate temperature for the indicated time. The crude mixture was then

filtered through a small plug of silica (and eluted with cold CH_2Cl_2/EtOAc = 1:1), evaporated to dryness under reduced pressure and directly purified by FCC.

For reaction optimisation the crude mixture was analysed by ^{1}H and ^{19}F NMR (4-fluoroanisole as internal standard) to determine the yield; an aliquot of the reaction mixture was purified by preparative TLC and analysed by HPLC (chiral stationary phase) to determine the e.r.

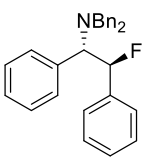
Note: KF (99.9% trace metal basis from Alfa Aesar) was used as provided (fine powder) by the supplier and used without pre-drying. CsF (99.9% trace metal basis from Sigma-Aldrich) was ground prior to the reaction and used without pre-drying. The dry $CHCl_3$ was passed on a column of basic alumina prior to use to ensure absence of HCl impurities.

Racemate synthesis:

The racemic reference products for HPLC analysis were obtained using the same procedure as above (KF or CsF, 3 equiv) and Schreiner's urea catalyst **2.16** (rt). Alternatively, the corresponding chloride was reacted with AgF (1.2 equiv) in CH_3CN at 60 °C for 2 h.

5.2.2.4 Product Characterisation

(1*S*,2*S*)-*N*,*N*-dibenzyl-2-fluoro-1,2-diphenylethan-1-amine (2.15)

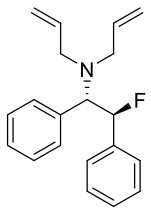


rac-**2.15**

Fluoride **2.15** was not isolated in enantioenriched form. The analytical data refers to the racemic product. See the main text (Chapter 2) for the results in the screening reactions. White solid. **^{1}H NMR** (400 MHz, $CDCl_3$) δ 7.38 –

7.13 (m, 20H), 6.01 (dd, *J* = 47.5, 7.5 Hz, 1H), 4.20 – 4.09 (m, 3H), 3.33 (d, *J* = 13.8 Hz, 2H). **^{19}F NMR** (377 MHz, $CDCl_3$) δ –181.42 (dd, *J* = 47.8, 18.5 Hz). **^{13}C NMR** (101 MHz, $CDCl_3$) δ 139.89, 138.57 (d, *J* = 19.9 Hz), 135.43 (d, *J* = 4.2 Hz), 129.89, 128.87, 128.33, 128.19, 128.16, 127.62, 126.93, 126.81, 126.74, 94.96 (d, *J* = 179.7 Hz), 66.16 (d, *J* = 20.5 Hz), 54.69 (d, *J* = 2.3 Hz); **IR** (thin layer film): ν (cm^{-1}) 3061, 3028, 2930, 2803, 2366, 1602,1494, 1453, 1356, 1133, 1074, 1028, 973, 759, 745, 698. **MP** 112 −114 °C; **HRMS** ($APCI^+$) *m/z* calculated for $C_{28}H_{27}FN^+$ $[M+H]^+$ 396.21220, found 396.21152. **HPLC separation:** DAICEL CHIRALPAK® IB-3, Heptane: ^{i}PrOH = 99:1, 1 mL/min; t_1 = 3.28 min, t_2 = 3.83 min.

(1*S*,2*S*)-*N*-allyl-*N*-((1*S*,2*S*)-2-fluoro-1,2-diphenylethyl)prop-2-en-1-amine (2.77)



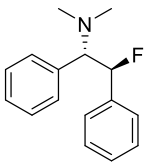
(*S*,*S*)-**2.77**

Fluoride (*S*,*S*)-**2.77** was prepared from *rac*-**2.76** (62.4 mg, 0.2 mmol) according to the general procedure. **Fluorination with KF**: 10 mol% of catalyst (*S*)-**2.78**. The reaction was stirred at –15 °C for 72 h. *Purification:* FCC, eluent = *n*-hexane:Et_2O (100:0 to 99.6:0.4, gradient). Colourless oil, 42.0 mg, 71% yield, e.r. = 95:5. **Fluorination with CsF**: 10 mol% of catalyst (*S*)-**2.78**. The reaction was stirred at –15 °C for 72 h. *Purification:* FCC, eluent = *n*-hexane:Et_2O (100:0 to 99.6:0.4, gradient). Colourless oil, 56.3 mg, 95% yield, e.r. = 95:5. **Gram scale reaction**: In a round bottom flask, *rac*-**2.76** (1.1 g, 3.53 mmol, 1 equiv), catalyst (*S*)-**2.78** (148 mg, 0.105 mmol, 3 mol%) and KF (1.025 g, 17.6 mmol, 5 equiv) were stirred at +5 °C in dry $CHCl_3$ at 900 rpm. After 96 h the reaction mixture was filtered through a silica plug eluting with CH_2Cl_2/EtOAc = 1:1. *Purification:* FCC, eluent = *n*-hexane:Et_2O (100:0 to 99.6:0.4, gradient) to elute the pure product (colourless oil, 794 mg, 76% yield, e.r. = 93:7); then *n*-hexane:EtOAc (95:5 to 80:20, gradient) to recover the catalyst (140 mg, 94% catalyst recovery). **^{1}H NMR** (400 MHz, $CDCl_3$) *δ* 7.19 – 7.06 (m, 10H), 5.82 (dd, *J* = 47.2, 7.2 Hz, 1H), 5.69 (dddd, *J* = 17.5, 10.1, 7.6, 4.9 Hz, 2H), 5.11 – 4.99 (m, 4H), 4.15 (dd, *J* = 18.2,

7.2 Hz, 1H), 3.47 – 3.40 (m, 2H), 2.83 (dd, J = 14.3, 7.6 Hz, 2H); **^{19}F NMR** (377 MHz, $CDCl_3$) δ –179.25 (dd, J = 47.2, 18.2 Hz, 1F); **^{13}C NMR** (101 MHz, $CDCl_3$) δ 138.7 (d, J_{C-F} = 20.3 Hz), 137.1, 136.6 (d, J_{C-F} = 4.5 Hz), 129.7 (d, J_{C-F} = 1.2 Hz), 128.2 (d, J_{C-F} = 2.0 Hz), 128.1, 128.0, 127.4, 127.0 (d, J_{C-F} = 6.7 Hz), 117.1, 95.3 (d, J_{C-F} = 178.6 Hz), 67.3 (d, J_{C-F} = 20.9 Hz), 54.0 (d, J_{C-F} = 2.1 Hz); **IR** (thin layer film) ν (cm^{-1}) = 3066, 3031, 2923, 2814, 1641, 1495, 1453, 1418, 1205, 1124, 1080, 1031, 918, 759, 698, 607; **HRMS** ($APCI^+$) *m/z* calculated for $C_{20}H_{23}FN^+$ $[M+H]^+$ 296.18090, found 296.18069; **$[\alpha]_D^{25\ °C}$** = +27.5 ° (c = 0.5, $CHCl_3$, e.r. = 95:5); **HPLC separation:** DAICEL CHIRALPAK® IA-3, Heptane:^{i}PrOH = 99.75:0.25, 1 mL/min; t_1 = 3.37 min (minor), t_2 = 3.61 min (major).

The absolute configuration was assigned by derivatising (*S*,*S*)-**2.77** to its corresponding β-fluoropicolinamide **2.103** (p.291).[15] This assignment was further confirmed by single crystal x-ray diffraction analysis of **2.83**. The configuration of the other stilbene-derived β-fluoroamines (**2.82**, **2.84-2.99**) was assigned by analogy.

(1*S*,2*S*)-2-fluoro-*N*,*N*-dimethyl-1,2-diphenylethan-1-amine (2.82)

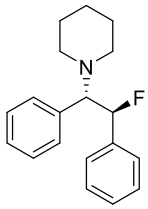


(*S*,*S*)-**2.82**

Fluoride (*S*,*S*)-**2.82** was prepared from *rac*-**5.34** (52.0 mg, 0.2 mmol) according to the general procedure. **Fluorination with KF**: 10 mol% of catalyst (*S*)-**2.78**. The reaction was stirred at +5 °C for 72 h. *Purification:* FCC, eluent = Toluene:Et_2O (100:0 to 95:5, gradient +2% NEt_3). Colourless oil, 34.2 mg, 65% yield, e.r. = 95:5. **Fluorination with CsF**: 10 mol% of catalyst (*S*)-**2.78**. The reaction was stirred at 0 °C for 72 h. *Purification:* FCC eluent = Toluene:Et_2O (100:0 to 95:5, gradient +2% NEt_3). Colourless oil, 41.3 mg, 85% yield, e.r. = 97:3. **^{1}H NMR** (400 MHz, $CDCl_3$) δ 7.14 – 7.02 (m, 8H), 6.95 (dd, J = 7.6, 2.0 Hz, 2H), 5.76 (dd, J = 47.5, 8.8 Hz, 1H), 3.80 (dd, J = 12.3, 8.8 Hz, 1H), 2.29 (s, 6H); **^{19}F NMR** (376 MHz, $CDCl_3$) δ –172.86 (dd, J = 47.6, 12.3 Hz, 1F); **^{13}C NMR** (101 MHz, $CDCl_3$) δ 138.1 (d, J_{C-F} = 20.1

Hz), 135.2 (d, $J_{C\text{-}F}$ = 6.8 Hz), 129.6, 128.3 (d, $J_{C\text{-}F}$ = 2.3 Hz), 128.1, 128.0, 127.6, 127.1 (d, $J_{C\text{-}F}$ = 6.2 Hz), 94.2 (d, $J_{C\text{-}F}$ = 177.3 Hz), 74.3 (d, $J_{C\text{-}F}$ = 22.1 Hz), 42.7 (d, $J_{C\text{-}F}$ = 1.8 Hz); **IR** (thin layer film) ν (cm^{-1}) = 3032, 2967, 2825, 2781, 1603, 1494, 1309, 992, 758, 697; **HRMS** (ESI^+) *m/z* calculated for $C_{16}H_{19}FN^+$ $[M+H]^+$ 244.14960, found 244.14951. $[\alpha]_D^{25\,°C}$ = –22.7 ° (c = 0.9, $CHCl_3$, e.r. = 97:3); **HPLC separation:** DAICEL CHIRALPAK® ID-3, Heptane: ^{i}PrOH = 99.6:0.4 + 0.1% diethyl amine, 1 mL/min; t_1 = 4.05 min (major), t_2 = 4.44 min (minor).

1-((1*S*,2*S*)-2-fluoro-1,2-diphenylethyl)piperidine (2.83)

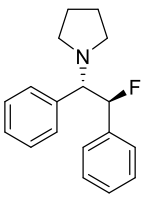


(*S*,*S*)-**2.83**

Fluoride (*S*,*S*)-**2.83** was prepared from *rac*-**2.107** (60.0 mg, 0.2 mmol) according to the general procedure. **Fluorination with KF**: 10 mol% of catalyst (*S*)-**2.78**. The reaction was stirred at –10 °C for 72 h. *Purification:* FCC, eluent = pentane:Et_2O (100:0 to 97:3, gradient). White solid, 36.3 mg, 56% yield, e.r. = 96:4. **Fluorination with CsF**: 10 mol% of catalyst (*S*)-**2.78**. The reaction was stirred at –10 °C for 24 h. *Purification:* FCC eluent = pentane:Et_2O (100:0 to 94:6, gradient). White solid, 51.0 mg, 90% yield, e.r. = 95:5. **Multi-Decagram scale reaction** *(Performed by Dr. Gabriele Pupo):* A 250 mL round-bottom flask was charged with chloride *rac*-**2.107** (50.0 g, 300 mmol, 1 equiv), catalyst (*S*)-**2.78** (1.169 g, 0.836 mmol, 0.5 mol%) and KF (29.10 g, 501.7 mmol, 3 equiv). CH_2Cl_2 was added (84 mL, 2 M) and the mixture was stirred at rt for 72 h. After filtration on a celite pad (eluted with Et_2O), the solvent was removed *in vacuo* and the crude mixture was re-dissolved in Et_2O. A 1 M solution of HCl was added and the product was extracted from the organic phase into the aqueous phase three times (as the HCl salt). The organic phase (containing the catalyst) was evaporated *in vacuo* and after purification by FCC (Pent:EtOAc 100:0 to 80:20, gradient), 1.157 g of catalyst (*S*)-**2.78** were recovered (99% recovery). The pH of the combined aqueous phases was then raised to 8–9 with a 3 M NaOH solution. EtOAc was

added and the aqueous phase was extracted with EtOAc three times. The combined organic layers were washed with brine, dried over $MgSO_4$ and evaporated *in vacuo.* The crude product (45.1 g, e.r.= 92:8) was purified by recrystallisation from warm MeOH (45.1 mL, reflux to rt) to afford (*S,S*)-**2.83** as a white solid (31.1 g, 66% yield, e.r.= 97:3). **^{1}H NMR** (400 MHz, $CDCl_3$) δ 7.19 – 7.15 (m, 8H), 7.08 – 7.03 (m, 2H), 5.88 (dd, J = 47.4, 8.5 Hz, 1H), 3.93 (dd, J = 13.4, 8.5 Hz, 1H), 2.61 (ddd, J = 11.1, 7.0, 3.7 Hz, 2H), 2.50 (ddd, J = 11.0, 7.0, 3.6 Hz, 2H), 1.72 – 1.53 (m, 4H), 1.42–1.34 (m, 2H); **^{19}F NMR** (377 MHz, $CDCl_3$) δ –174.27 (dd, J = 47.3, 13.6 Hz, 1F); **^{13}C NMR** (101 MHz, $CDCl_3$) δ 138.4 (d, $J_{C\text{-}F}$ = 20.2 Hz), 135.8 (d, $J_{C\text{-}F}$ = 6.4 Hz), 129.6, 128.1 (d, $J_{C\text{-}F}$ = 2.2 Hz), 127.9, 127.7, 127.3, 127.0 (d, $J_{C\text{-}F}$ = 6.4 Hz), 93.7 (d, $J_{C\text{-}F}$ = 177.9 Hz), 74.6 (d, $J_{C\text{-}F}$ = 21.8 Hz), 51.5, 26.2, 24.6; **IR** (thin layer film) ν (cm^{-1}) = 3031, 2932, 2802, 1494, 1452, 1160, 988, 758, 698; **MP** 63 – 65 °C; **HRMS** ($APCI^+$) *m/z* calculated for $C_{19}H_{23}FN^+$ $[M+H]^+$ 284.18090, found 284.18103. **$[\alpha]_D^{25\ °C}$** = –33.8 ° (c = 0.5, $CHCl_3$, e.r. = 95:5); **HPLC separation:** DAICEL CHIRALPAK® IC-3 Heptane:EtOH:*n*$BuNH_2$ = 99.5:0.1:0.4, 1 mL/min: t_1 = 3.40 min (major), t_2 = 4.01 min (minor).

(1*S*,2*S*)-(2-fluoro-1,2-diphenylethyl)pyrrolidine (2.84)

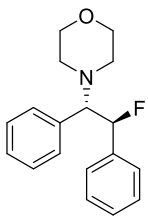


(*S,S*)-**2.84**

Fluoride (*S,S*)-**2.84** was prepared from *rac*-**5.35** (57.2 mg, 0.2 mmol) according to the general procedure. **Fluorination with KF**: 10 mol% of catalyst (*S*)-**2.78**. The reaction was stirred at 0 °C for 72 h. *Purification:* FCC, eluent = pentane:Et_2O (98:2 to 95:5, gradient). White solid, 49.5 mg, 92% yield, e.r. = 94.5:5.5. **Fluorination with CsF**: 10 mol% of catalyst (*S*)-**2.78**. The reaction was stirred at –20 °C for 36 h. *Purification:* FCC, eluent = *n*-hexane:Et_2O (98:2 to 96:4, gradient). White solid, 48.5 mg, 90% yield, e.r. = 97:3. **^{1}H NMR** (500 MHz, $CDCl_3$) δ 7.16 – 7.09 (m, 6H), 7.04–6.98 (m, 4H), 5.75 (dd, J = 46.8, 7.6 Hz, 1H), 3.70 (dd, J = 13.2, 7.6 Hz, 1H), 2.80 – 2.68 (m, 2H), 2.62 – 2.53 (m, 2H), 1.83 – 1.72 (m, 4H); **^{19}F NMR**

(471 MHz, $CDCl_3$) δ –170.81 (dd, J = 47.3, 13.4 Hz, 1F); **^{13}C NMR** (126 MHz, $CDCl_3$) δ 138.5 (d, $J_{C\text{-}F}$ = 7.5 Hz), 138.1 (d, $J_{C\text{-}F}$ = 20.7 Hz), 129.3, 128.0 (d, $J_{C\text{-}F}$ = 2.0 Hz), 127.9, 127.8, 127.4, 126.8 (d, $J_{C\text{-}F}$ = 6.6 Hz), 97.3 (d, $J_{C\text{-}F}$ = 177.6 Hz), 74.9 (d, $J_{C\text{-}F}$ = 23.0 Hz), 53.4 (d, $J_{C\text{-}F}$ = 3.4 Hz), 23.4; **IR** (thin layer film) ν (cm^{-1}) = 3032, 2966, 2793, 1493, 1454, 1131, 996, 763, 698; **MP** 58 – 60 °C; **HRMS** (ESI^+) *m/z* calculated for $C_{18}H_{21}FN^+$ $[M+H]^+$ 270.16525, found 270.16513; **$[\alpha]_D^{25\ °C}$** = –25.5 ° (c = 0.5, $CHCl_3$, e.r. = 97:3); **HPLC separation**: DAICEL CHIRALPAK® IC-3, Heptane:EtOH = 99.75:0.25 + 0.2% *n*$BuNH_2$, 1 mL/min; t_1 = 3.30 min (minor), t_2 = 3.49 min (major).

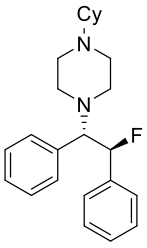
4-((1*S*,2*S*)-2-fluoro-1,2-diphenylethyl)morpholine (2.85)


(*S*,*S*)-**2.85**

Fluoride (*S*,*S*)-**2.85** was prepared from *rac*-**5.36** (60.4 mg, 0.2 mmol) according to the general procedure. **Fluorination with KF**: 15 mol% of catalyst (*S*)-**2.78**. The reaction was stirred at +10 °C for 72 h. *Purification:* FCC, eluent = CH_2Cl_2: pentane = 95:5 to CH_2Cl_2:EtOAc = 97:3, gradient. White solid, 46.6 mg, 81% yield, e.r. = 94:6. **Fluorination with CsF**: 10 mol% of catalyst (*S*)-**2.78**. The reaction was stirred at +5 °C for 72 h. Purification: FCC eluent = CH_2Cl_2:pentane = 95:5 to CH_2Cl_2:EtOAc = 97:3, gradient. White solid, 43.0 mg, 75% yield, e.r. = 94.5:5.5. **^{1}H NMR** (400 MHz, $CDCl_3$) δ 7.19 – 7.13 (m, 6H), 7.13 – 7.09 (m, 2H), 7.07 – 7.03 (m, 2H), 5.83 (dd, J = 47.1, 7.9 Hz, 1H), 3.83 (dd, J = 14.9, 7.9 Hz, 1H), 3.73 (dd, J = 5.5, 3.9 Hz, 4H), 2.64 (dd, J = 6.0, 3.5 Hz, 4H); **^{19}F NMR** (377 MHz, $CDCl_3$) δ –171.87 (dd, J = 47.2, 15.0 Hz, 1F); **^{13}C NMR** (101 MHz, $CDCl_3$) δ 138.0 (d, $J_{C\text{-}F}$ = 20.6 Hz), 136.2 (d, $J_{C\text{-}F}$ = 6.9 Hz), 129.4, 128.2 (d, $J_{C\text{-}F}$ = 2.1 Hz), 128.0, 127.9, 127.6, 126.8 (d, $J_{C\text{-}F}$ = 6.4 Hz), 95.0 (d, $J_{C\text{-}F}$ = 178.1 Hz), 74.6 (d, $J_{C\text{-}F}$ = 21.9 Hz), 67.3, 51.6 (d, $J_{C\text{-}F}$ = 2.9 Hz); **IR** (thin layer film) ν (cm^{-1}) = 3032, 2957, 2852, 2815, 1494, 1452, 1117, 993, 881, 760, 699; **MP** 59 – 62 °C; **HRMS** ($APCI^+$) *m/z* calculated for $C_{18}H_{21}FNO^+$ $[M+H]^+$ 286.16017, found 286.16010; **$[\alpha]_D^{25\ °C}$** = –29.4 ° (c = 0.5, $CHCl_3$, e.r. = 94.5:5.5); **HPLC**

separation: DAICEL CHIRALPAK® IC-3, Heptane:^{i}PrOH:*n*BuNH$_2$ = 99.0: 0.9: 0.1, 1 mL/min; t_1 = 9.89 min (major), t_2 = 10.97 min (minor).

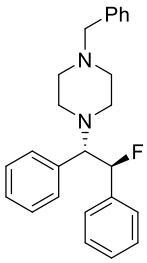
1-cyclohexyl-4-((1*S*,2*S*)-2-fluoro-1,2-diphenylethyl)piperazine (2.86)



(*S*,*S*)-**2.86**

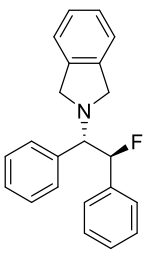
Fluoride (*S*,*S*)-**2.86** was prepared from *rac*-**5.37** (76.6 mg, 0.2 mmol) according to the general procedure. **Fluorination with KF**: 10 mol% of catalyst (*S*)-**2.78**. The reaction was stirred at +5 °C for 72 h. *Purification:* FCC, eluent = CH_2Cl_2: pentane = 95:5 to CH_2Cl_2:MeOH = 98:2, gradient. White solid, 66.6 mg, 90% yield, e.r. = 94:6. **Fluorination with CsF**: 10 mol% of catalyst (*S*)-**2.78**. The reaction was stirred at 0 °C for 72 h. *Purification:* FCC eluent = CH_2Cl_2: pentane = 95:5 to CH_2Cl_2:MeOH = 98:2, gradient. White solid, 67.4 mg, 94% yield, e.r. = 96:4. **^{1}H NMR** (500 MHz, $CDCl_3$) δ 7.18 – 7.08 (m, 8H), 7.04 – 7.00 (m, 2H), 5.82 (dd, *J* = 47.3, 8.2 Hz, 1H), 3.89 (dd, *J* = 13.7, 8.2 Hz, 1H), 2.84 – 2.61 (m, 7H), 2.33 (br s, 1H), 1.95 (br s, 2H), 1.85 – 1.74 (m, 2H), 1.66 – 1.58 (m, 1H), 1.28 – 1.17 (m, 5H), 1.15 – 1.05 (m, 1H); **^{19}F NMR** (377 MHz, $CDCl_3$) δ –172.48 (d, *J* = 49.1 Hz, 1F); **^{13}C NMR** (126 MHz, $CDCl_3$) δ 138.0 (d, $J_{C\text{-}F}$ = 20.4 Hz), 135.8 (d, $J_{C\text{-}F}$ = 6.7 Hz), 129.4, 128.2 (d, $J_{C\text{-}F}$ = 2.1 Hz), 128.0, 127.9, 127.5, 126.9 (d, $J_{C\text{-}F}$ = 6.3 Hz), 94.6 (d, $J_{C\text{-}F}$ = 178.0 Hz), 74.0 (d, $J_{C\text{-}F}$ = 21.8 Hz), 63.9, 50.3, 49.2, 28.6, 26.1, 25.7; **IR** (thin layer film) ν (cm^{-1}) = 3062, 3031, 2918, 2853, 2814, 1494, 1452, 1282, 1153, 994, 759, 699; **MP** 92 – 95 °C; **HRMS** (ESI$^+$) *m/z* calculated for $C_{24}H_{32}FN_2^+$ $[M+H]^+$ 367.25440, found 367.25519; **$[\alpha]_D^{25\,°C}$** = –21.1 ° (c = 0.5, $CHCl_3$, e.r. = 94:6); **HPLC separation:** DAICEL CHIRALPAK® IA-3, Heptane:EtOH = 99:1 +0.2% *n*BuNH$_2$, 1 mL/min; t_1 = 6.29 min (minor), t_2 = 7.19 min (major).

1-benzyl-4-((1*S*,2*S*)-2-fluoro-1,2-diphenylethyl)piperazine (2.87)


(*S*,*S*)-**2.87**

Fluoride (*S*,*S*)-**2.87** was prepared from *rac*-**5.38** (78.0 mg, 0.2 mmol) according to the general procedure. **Fluorination with KF**: 10 mol% of catalyst (*S*)-**2.78**. The reaction was stirred at 0 °C for 72 h. *Purification:* FCC, eluent = CH_2Cl_2:EtOAc (100:0 to 50:50, gradient). White solid, 51.8 mg, 69% yield, e.r. = 95:5. **Fluorination with CsF**: 10 mol% of catalyst (*S*)-**2.78**. The reaction was stirred at 0 °C for 48 h. *Purification:* FCC eluent = CH_2Cl_2:EtOAc (100:0 to 50:50, gradient), white solid, 63.0 mg, 84% yield, e.r. = 95.5:4.5. **^{1}H NMR** (400 MHz, $CDCl_3$) δ 7.32 – 7.20 (m, 5H), 7.19 – 7.11 (m, 8H), 7.06 – 7.02 (m, 2H), 5.84 (dd, J = 47.2, 8.2 Hz, 1H), 3.89 (dd, J = 14.1, 8.2 Hz, 1H), 3.50 (s, 2H), 2.76 – 2.60 (m, 4H), 2.57–2.45 (m, 4H); **^{19}F NMR** (377 MHz, $CDCl_3$) δ –173.21 (dd, J = 47.3, 14.1 Hz, 1F); **^{13}C NMR** (101 MHz, $CDCl_3$) δ 138.2 (d, $J_{C\text{-}F}$ = 18.3 Hz), 138.1, 135.8 (d, $J_{C\text{-}F}$ = 6.3 Hz), 129.5, 129.3, 128.1, 128.1 (d, $J_{C\text{-}F}$ = 1.9 Hz), 127.9 (overlapped), 127.4, 127.0, 126.9 (d, $J_{C\text{-}F}$ = 6.5 Hz), 94.3 (d, $J_{C\text{-}F}$ = 178.1 Hz), 74.1 (d, $J_{C\text{-}F}$ = 21.8 Hz), 63.1, 53.5, 50.5. **IR** (thin layer film) ν (cm^{-1}) = 3030, 2932, 2811, 1494, 1454, 1289, 1137, 1006, 759, 698; MP 56 – 58 °C; **HRMS** (ESI^+) *m/z* calculated for $C_{25}H_{28}FN_2^+$ $[M+H]^+$ 375.22310, found 375.22314. **[α]$_D^{25\ °C}$** = –22.7 ° (c = 0.5, $CHCl_3$, e.r. = 95.5:4.5); **HPLC separation:** DAICEL CHIRALPAK® IA-3, Heptane:EtOH = 99.5:0.5 +0.2% diethyl amine, 1 mL/min; t_1 = 6.40 min (major), t_2 = 8.55 min (minor).

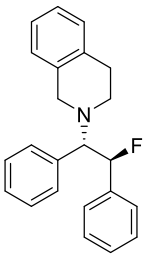
2-((1*S*,2*S*)-2-fluoro-1,2-diphenylethyl)isoindoline (2.88)


(*S*,*S*)-**2.88**

Fluoride (*S*,*S*)-**2.88** was prepared from *rac*-**5.39** (68.0 mg, 0.2 mmol) according to the general procedure. **Fluorination with KF**: 10 mol% of catalyst (*S*)-**2.78**. The reaction was stirred at 0 °C for 72 h. *Purification:* FCC, eluent = pentane:Et_2O (100:0 to 97:3, gradient). White solid, 48.0 mg, 76%

yield, e.r. = 92:8. **Fluorination with CsF**: 10 mol% of catalyst (*S*)-**2.78**. The reaction was stirred at –10 °C for 72 h. *Purification:* FCC, eluent = pentane:Et_2O (100:0 to 97.5:2.5, gradient). White solid, 39.0 mg, 61% yield, e.r. = 93:7. **^{1}H NMR** (500 MHz, $CDCl_3$) δ 7.21 – 7.13 (m, 10H), 7.12 – 7.08 (m, 2H), 7.05 – 7.01 (m, 2H), 5.79 (dd, J = 47.0, 7.6 Hz, 1H), 4.17 – 4.11 (m, 2H), 4.10 – 4.00 (m, 3H); **^{19}F NMR** (470 MHz, $CDCl_3$) δ –170.50 (dd, J = 47.1, 13.2 Hz, 1F); **^{13}C NMR** (126 MHz, $CDCl_3$) δ 139.9, 138.2 (d, $J_{C\text{-}F}$ = 7.8 Hz), 137.8 (d, $J_{C\text{-}F}$ = 20.8 Hz), 129.4, 128.3, 128.2 (d, $J_{C\text{-}F}$ = 2.1 Hz), 127.9, 127.7, 126.9, 126.8, 122.3, 98.1 (d, $J_{C\text{-}F}$ = 178.0 Hz), 74.6 (d, $J_{C\text{-}F}$ = 22.7 Hz), 59.0 (d, $J_{C\text{-}F}$ = 3.9 Hz); **IR** (thin layer film) ν (cm^{-1}) = 3031, 2940, 2790, 1490, 1454, 1337, 1264, 1137, 1075, 992, 764, 745, 700; **MP** 79 – 80 °C; **HRMS** (ESI^+) *m/z* calculated for $C_{22}H_{21}FN^+$ $[M+H]^+$ 318.16525, found 318.16501. **$[\alpha]_D^{25\,°C}$** = –16.8 ° (c = 0.5, $CHCl_3$, e.r. = 92:8); **HPLC separation**: DAICEL CHIRALPAK® IA-3, Heptane:^{i}PrOH = 99:1, 1 mL/min; t_1 = 4.52 min (minor), t_2 = 5.54 min (major).

2-((1*S*,2*S*)-2-fluoro-1,2-diphenylethyl)-1,2,3,4-tetrahydroisoquinoline (2.89)

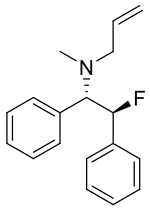


(*S*,*S*)-**2.89**

Fluoride (*S*,*S*)-**2.89** was prepared from *rac*-**5.40** (66.0 mg, 0.2 mmol) according to the general procedure. **Fluorination with KF**: 10 mol% of catalyst (*S*)-**2.78**. The reaction was stirred at 0 °C for 72 h. *Purification:* FCC eluent = pentane:Et_2O (100:0 to 98:2, gradient). Colourless oil, 60.5 mg, 91% yield, e.r. = 96:4. **Fluorination with CsF**: 5 mol% of catalyst (*S*)-**2.78**. The reaction was stirred at 0 °C for 72 h. *Purification:* FCC, eluent = pentane:Et_2O (100:0 to 98:2, gradient). Colourless oil, 63.6 mg, 96% yield, e.r. = 96:4. **^{1}H NMR** (500 MHz, $CDCl_3$) δ 7.22 – 7.08 (m, 13H), 7.03 – 6.99 (m, 1H), 5.97 (dd, J = 47.1, 8.0 Hz, 1H), 4.10 (dd, J = 14.3, 8.0 Hz, 1H), 3.93 (d, J = 14.8 Hz, 1H), 3.84 (d, J = 14.8 Hz, 1H), 3.09 (dt, J = 10.8, 5.2 Hz, 1H), 2.97 (ddd, J = 16.2, 8.0, 5.0 Hz, 1H), 2.92 – 2.76 (m, 2H); **^{19}F NMR** (471 MHz, $CDCl_3$) δ –172.35 (dd, J = 47.4, 14.3 Hz, 1F); **^{13}C NMR** (126 MHz, $CDCl_3$) δ 138.3 (d, $J_{C\text{-}F}$ = 20.5

Hz), 136.4 (d, $J_{C\text{-}F}$ = 6.5 Hz), 135.3, 134.7, 129.6, 128.8, 128.3 (d, $J_{C\text{-}F}$ = 2.1 Hz), 128.1, 128.1 , 127. 7, 127.0 (d, $J_{C\text{-}F}$ = 6.4 Hz), 126.8, 126.1, 125.6, 95.0 (d, $J_{C\text{-}F}$ = 178.1 Hz), 73.9 (d, $J_{C\text{-}F}$ = 22.0 Hz), 53. 9 (d, $J_{C\text{-}F}$ = 3.2 Hz), 48.2 (d, $J_{C\text{-}F}$ = 2.2 Hz), 29.7; **IR** (thin layer film) ν (cm^{-1}) = 3030, 2919, 2803, 1586, 1496, 1454, 1133, 1087, 995, 935, 742, 698; **HRMS** (ESI^+) *m/z* calculated for $C_{23}H_{23}FN^+$ $[M+H]^+$ 332.18090, found 332.18057. **$[\alpha]_D^{25\,°C}$** = –45.6 ° (c = 0.5, $CHCl_3$, e.r. = 96:4); **HPLC separation**: DAICEL CHIRALPAK® IF-3, Heptane:^{i}PrOH = 99:1, 1 mL/min; t_1 = 4.77 min (major), t_2 = 5.83 min (minor).

***N*-((1*S*,2*S*)-2-fluoro-1,2-diphenylethyl)-*N*-methylprop-2-en-1-amine (2.90)**

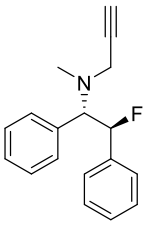


(*S*-*S*)-**2.90**

Fluoride (*S*,*S*)-**2.90** was prepared from *rac*-**5.41** (53.9 mg, 0.2 mmol) according to the general procedure. **Fluorination with KF**: 10 mol% of catalyst (*S*)-**2.78**. The reaction was stirred at –10 °C for 72 h. *Purification:* FCC, eluent = pentane:Et_2O (100:0 to 95:5, gradient). Colourless oil, 48 mg, 89% yield, e.r. = 95.5:4.5. **Fluorination with CsF**: 10 mol% of catalyst (*S*)-**2.78**. The reaction was stirred at –15 °C for 72 h. FCC, eluent = pentane:Et_2O (100:0 to 95:5, gradient). Colourless oil, 38.5 mg, 72% yield, e.r. = 95.5:4.5. **^{1}H NMR** (500 MHz, $CDCl_3$) *δ* 7.23 – 7.14 (m, 8H), 7.10 – 7.06 (m, 2H), 5.97 – 5.81 (m, 1H), 5.88 (dd, *J* = 47.5, 8.5 Hz, 1H), 5.23 – 5.09 (m, 2H), 4.10 (dd, *J* = 13.8, 8.5 Hz, 1H), 3.26 (dd, *J* = 13.7, 5.2 Hz, 1H), 2.99 (dd, *J* = 13.7, 7.3 Hz, 1H), 2.38 (s, 3H); **^{19}F NMR** (471 MHz, $CDCl_3$) *δ* –174.62 (dd, *J* = 47.5, 13.8 Hz, 1F); **^{13}C NMR** (126 MHz, $CDCl_3$) δ= 138.3 (d, $J_{C\text{-}F}$ = 20.1 Hz), 136.6, 135.5 (d, $J_{C\text{-}F}$ = 6.2 Hz), 129.7, 128.3 (d, $J_{C\text{-}F}$ = 2.3 Hz), 128.1 128.0, 127.6, 127.1 (d, $J_{C\text{-}F}$ = 6.5 Hz), 117.5, 94.4 (d, $J_{C\text{-}F}$ = 177.5 Hz), 71.4 (d, $J_{C\text{-}F}$ = 21.8 Hz), 58.4, 38.7 (d, $J_{C\text{-}F}$ = 2.1 Hz); **IR** (thin layer film) ν (cm^{-1}) = 3065, 3032, 2928, 2794, 1494, 1453, 1207, 996, 919, 759, 698; **HRMS** (ESI^+) *m/z* calculated for $C_{18}H_{21}NF^+$ $[M+H]^+$ 270.16525, found 270.16501. **$[\alpha]_D^{25\,°C}$** = –5.0° (c = 0.5, $CHCl_3$, e.r. = 95.5:4.5); **HPLC separation**: DAICEL

CHIRALPAK® IA, Heptane:^{i}PrOH:*n*BuNH$_2$ = 99.5:0.4:0.1, 1 mL/min; t_1 = 5.47 min (minor), t_2 = 6.00 min (major).

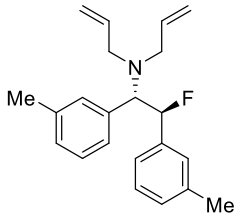
***N*-((1S,2S)-2-fluoro-1,2-diphenylethyl)-*N*-methylprop-2-yn-1-amine (2.91)**



(*S*-*S*)-**2.91**

Fluoride (*S*,*S*)-**2.91** was prepared from *rac*-**5.42** (56.8 mg, 0.2 mmol) according to the general procedure. **Fluorination with KF**: 10 mol% of catalyst (*S*)-**2.78**. The reaction was stirred at 0 °C for 72 h. *Purification:* FCC, eluent = pentane:Et$_2$O (100:0 to 95:5, gradient). Colourless oil, 39.3 mg, 73% yield, e.r. = 94:6. **Fluorination with CsF**: 10 mol% of catalyst (*S*)-**2.78**. The reaction was stirred at 0 °C for 72 h. *Purification:* FCC eluent = pentane:Et$_2$O (100:0 to 95:5, gradient). Colourless oil, 36.9 mg, 69% yield, e.r. = 96:4. **^{1}H NMR** (500 MHz, $CDCl_3$) δ δ 7.17–7.13 (m, 6H), 7.11 – 7.05 (m, 4H), 5.81 (dd, *J* = 47.0, 7.9 Hz, 1H), 4.14 (dd, *J* = 14.1, 7.9 Hz, 1H), 3.52 (dd, *J* = 17.0, 2.4 Hz, 1H), 3.28 (dd, *J* = 17.0, 2.3 Hz, 1H), 2.53 (d, *J* = 1.9 Hz, 3H), 2.27 (t, *J* = 2.4 Hz, 1H); **^{19}F NMR** (471 MHz, $CDCl_3$) δ –170.82 (dd, *J* = 47.2, 14.2 Hz, 1F); **^{13}C NMR** (126 MHz, $CDCl_3$) δ 138.11 (d, $J_{C\text{-}F}$ = 20.6 Hz), 136.67 (d, $J_{C\text{-}F}$ = 7.0 Hz), 129.54, 128.22 (d, $J_{C\text{-}F}$ = 2.2 Hz), 128.13, 127.96, 127.71, 126.95 (d, $J_{C\text{-}F}$ = 6.4 Hz), 95.77 (d, $J_{C\text{-}F}$ = 177.7 Hz), 79.42, 73.33, 71.26 (d, $J_{C\text{-}F}$ = 22.7 Hz), 45.16 (d, $J_{C\text{-}F}$ = 3.1 Hz), 40.23 (d, $J_{C\text{-}F}$ = 4.0 Hz); **IR** (thin layer film) ν (cm^{-1}) = 3296, 2924, 1454, 1019, 759, 699, 625; **HRMS** (ESI$^+$) *m/z* calculated for $C_{18}H_{19}FN^+$ $[M+H]^+$ 268.14960, found 268.14926. **$[\alpha]_D^{25\ °C}$** = +48.5 ° (c = 0.5, $CHCl_3$, e.r. = 94:6); **HPLC separation:** DAICEL CHIRALPAK® IC-3, Heptane:^{i}PrOH = 99:1, 1 mL/min; t_1 = 4.15 min (major), t_2 = 4.63 min (minor).

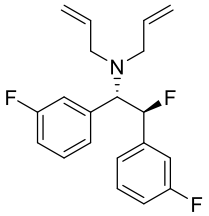
***N*-allyl-*N*-((1*S*,2*S*)-2-fluoro-1,2-di-m-tolylethyl)prop-2-en-1-amine (2.92)**



(*S*,*S*)-**2.92**

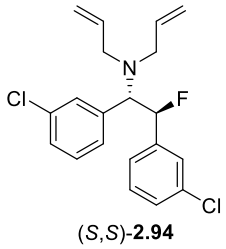
Fluoride (*S*,*S*)-**2.92** was prepared from *rac*-**5.43** (68.0 mg, 0.2 mmol) according to the general procedure. **Fluorination with KF**: 5 mol% of catalyst (*S*)-**2.78**. The reaction was stirred at 0 °C for 72 h. *Purification:* FCC, eluent = pentane:Et_2O (100:0 to 99:1, gradient). Colourless oil, 56.3 mg, 87% yield, e.r. = 96:4. **Fluorination with CsF**: 5 mol% of catalyst (*S*)-**2.78**. The reaction was stirred at 0 °C for 24 h. *Purification:* FCC eluent = *n*-hexane:Et_2O (100:0 to 98.7:1.3, gradient). Colourless oil, 53.5 mg, 83% yield, e.r. = 96:4. **^{1}H NMR** (400 MHz, $CDCl_3$) δ 7.16 – 7.10 (m, 2H), 7.07 – 6.96 (m, 6H), 5.86 (dd, J = 47.2, 7.1 Hz, 1H), 5.83–5.72 (m, 2H), 5.22 – 5.06 (m, 4H), 4.18 (dd, J = 18.5, 7.1 Hz, 1H), 3.50 (ddt, J = 14.3, 5.0, 1.8 Hz, 2H), 2.91 (dd, J = 14.3, 7.5 Hz, 2H), 2.30 (s, 3H), 2.29 (s, 3H); **^{19}F NMR** (377 MHz, $CDCl_3$) δ –179.33 (dd, J = 47.3, 18.6 Hz, 1F); **^{13}C NMR** (101 MHz, $CDCl_3$) δ 138.7 (d, $J_{C\text{-}F}$ = 20.1 Hz), 137.6, 137.3, 136.6 (d, $J_{C\text{-}F}$ = 4.4 Hz), 130.5, 128.9, (d, $J_{C\text{-}F}$ = 2.0 Hz), 128.1, 127.9, 127.9, 127.7 (d, $J_{C\text{-}F}$ = 6.6 Hz), 126.7, 124.1, 124.0, 117.0, 95.5 (d, $J_{C\text{-}F}$ = 178.3 Hz), 67.1 (d, $J_{C\text{-}F}$ = 20.7 Hz), 54.1 (d, $J_{C\text{-}F}$ = 2.1 Hz), 21.7, 21.5; **IR** (thin layer film) ν (cm^{-1}) = 3009, 2921, 2813, 1641, 1607, 1489, 1447, 1417, 1159, 997, 917, 787, 703; **HRMS** (ESI^+) *m/z* calculated for $C_{22}H_{27}FN^+$ $[M+H]^+$ 324.21220, found 324.21282. **$[\alpha]_D^{25\ °C}$** = +24.0 ° (c = 0.5, $CHCl_3$, e.r. = 96:4); **HPLC separation**: DAICEL CHIRALPAK® IA-3, Heptane:^{i}PrOH = 99:1, 1 mL/min; t_1 = 2.51 min (minor), t_2 = 2.88 min (major).

***N*-allyl-*N*-((1S,2S)-2-fluoro-1,2-bis(3-fluorophenyl)ethyl)prop-2-en-1-amine (2.93)**


(*S*,*S*)-**2.93**

Fluoride (*S*,*S*)-**2.93** was prepared from *rac*-**5.44** (69.6 mg, 0.2 mmol) according to the general procedure. **Fluorination with KF**: 10 mol% of catalyst (*S*)-**2.78**. The reaction was stirred at +10 °C for 72 h. *Purification:* FCC, eluent = pentane:Et_2O (100:0 to 99.6:0.4, gradient). Colourless oil, 48.2 mg, 73% yield, e.r. = 94:6. **Fluorination with CsF**: 10 mol% of catalyst (*S*)-**2.78**. The reaction was stirred at 0 °C for 72 h. *Purification:* FCC eluent = pentane:Et_2O (100:0 to 99.5:0.5, gradient). Colourless oil, 46.5 mg, 70% yield, e.r. = 95.5:4.5. **^{1}H NMR** (400 MHz, $CDCl_3$) δ 7.27 – 7.18 (m, 2H), 7.02 – 6.90 (m, 6H), 5.85 (dd, J = 46.8, 6.4 Hz, 1H), 5.71 (dddd, J = 17.5, 10.1, 7.6, 4.8 Hz, 2H), 5.19 – 5.06 (m, 4H), 4.16 (dd, J = 20.5, 6.5 Hz, 1H), 3.48 (ddt, J = 14.2, 4.8, 1.8 Hz, 2H), 2.96 – 2.85 (m, 2H); **^{19}F NMR** (377 MHz, $CDCl_3$) δ –112.83 (td, J = 9.3, 6.0 Hz, 1F), –113.12 (td, J = 9.0, 5.6 Hz, 1F), –181.74 (dd, J = 46.8, 20.5 Hz, 1F); **^{13}C NMR** (101 MHz, $CDCl_3$) δ 162.8 (d, $J_{C\text{-}F}$ = 247.6 Hz), 162.7 (d, $J_{C\text{-}F}$ = 246.4 Hz), 140.1 (dd, $J_{C\text{-}F}$ = 21.0, 7.2 Hz), 139.1 (dd, $J_{C\text{-}F}$ = 6.4, 3.8 Hz), 136.6, 129.7 (dd, $J_{C\text{-}F}$ = 8.2, 2.7 Hz), 125.2 (dd, $J_{C\text{-}F}$ = 2.8, 1.3 Hz), 122.4 (dd, $J_{C\text{-}F}$ = 7.1, 2.9 Hz), 117.4, 116.4 (dd, $J_{C\text{-}F}$ = 21.5, 1.7 Hz), 115.2 (dd, $J_{C\text{-}F}$ = 21.1, 1.7 Hz), 114.6 (d, $J_{C\text{-}F}$ = 21.0 Hz), 113.9 (d, $J_{C\text{-}F}$ = 7.6 Hz), 113.7 (d, $J_{C\text{-}F}$ = 7.5 Hz), 94.7 (dd, $J_{C\text{-}F}$ = 180.8, 1.9 Hz), 66.6 (dd, $J_{C\text{-}F}$ = 20.7, 1.6 Hz), 54.1 (d, $J_{C\text{-}F}$ = 2.4 Hz); **IR** (thin layer film) ν (cm^{-1}) = 3077, 2816, 1642, 1591, 1489, 1449, 1251, 1243, 923, 788, 767, 700; **HRMS** ($APCI^+$) *m/z* calculated for $C_{20}H_{21}F_3N^+$ $[M+H]^+$ 332.16206, found 332.16168. **$[\alpha]_D^{25\,°C}$** = +23.8 ° (c = 0.5, $CHCl_3$, e.r. = 95.5:4.5); **HPLC separation:** DAICEL CHIRALPAK® IB-3, Heptane:^{i}PrOH = 99.5:0.5, 1 mL/min; t_1 = 3.23 min (minor), t_2 = 3.90 min (major).

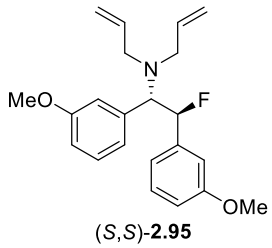
***N*-allyl-*N*-((1*S*,2*S*)-1,2-bis(3-chlorophenyl)-2-fluoroethyl)prop-2-en-1-amine (2.94)**



(*S*,*S*)-**2.94**

Fluoride (*S*,*S*)-**2.94** was prepared from *rac*-**5.45** (76.0 mg, 0.2 mmol) according to the general procedure. **Fluorination with KF**: 10 mol% of catalyst (*S*)-**2.78**. The reaction was stirred at +10 °C for 72 h. *Purification:* FCC, eluent = pentane:Et_2O (100:0 to 99.68:0.32, gradient). Colourless oil, 55.8 mg, 77% yield, e.r. = 94:6. **Fluorination with CsF**: 10 mol% of catalyst (*S*)-**2.78**. The reaction was stirred at 0 °C for 72 h. *Purification:* FCC eluent = pentane:Et_2O (100:0 to 99.5:0.5, gradient). Colourless oil, 55.0 mg, 76% yield, e.r. = 97.5:2.5. **^{1}H NMR** (400 MHz, $CDCl_3$) δ 7.29 – 7.18 (m, 6H), 7.08 (dt, J = 6.5, 1.8 Hz, 2H), 5.82 (dd, J = 46.7, 6.1 Hz, 1H), 5.68 (dddd, J = 17.6, 10.2, 7.6, 4.9 Hz, 2H), 5.18 – 5.08 (m, 4H), 4.12 (dd, J = 21.5, 6.1 Hz, 1H), 3.47 (ddt, J = 14.4, 4.9, 1.8 Hz, 2H), 2.87 (dd, J = 14.4, 7.6 Hz, 2H); **^{19}F NMR** (377 MHz, $CDCl_3$) δ –182.86 (dd, J = 46.8, 21.5 Hz, 1F); **^{13}C NMR** (101 MHz, $CDCl_3$) δ 140.4 (d, $J_{C\text{-}F}$ = 21.0 Hz), 138.6 (d, $J_{C\text{-}F}$ = 3.4 Hz), 136.5, 134.3, 134.1, 129.6 (d, $J_{C\text{-}F}$ = 1.8 Hz), 129.5, 129.4, 128.5 (d, $J_{C\text{-}F}$ = 1.7 Hz), 127.9, 127.7 (d, $J_{C\text{-}F}$ = 1.5 Hz), 126.9 (d, $J_{C\text{-}F}$ = 7.6 Hz), 124.8 (d, $J_{C\text{-}F}$ = 7.1 Hz), 117.5, 94.9 (d, $J_{C\text{-}F}$ = 181.1 Hz), 66.5 (d, $J_{C\text{-}F}$ = 20.6 Hz), 54.1 (d, $J_{C\text{-}F}$ = 2.4 Hz); **IR** (thin layer film) ν (cm^{-1}) = 3076, 2925, 2817, 1596, 1572, 1477, 1431, 1205, 1082, 999, 922, 787, 706; **HRMS** ($APCI^+$) *m/z* calculated for $C_{20}H_{21}Cl_2FN^+$ $[M+H]^+$ 364.10296, found 364.10324. **$[\alpha]_D^{25\,°C}$** = +15.8 ° (c = 0.5, $CHCl_3$, e.r. = 97.5:2.5); **HPLC separation:** DAICEL CHIRALPAK® IA-3, Heptane:^{i}PrOH = 99.5:0.5, 1 mL/min; t_1 = 3.04 min (minor), t_2 = 3.32 min (major).

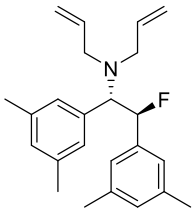
***N*-allyl-*N*-((1*S*,2*S*)-2-fluoro-1,2-bis(3-methoxyphenyl)ethyl)prop-2-en-1-amine (2.95)**



(*S*,*S*)-**2.95**

Fluoride (*S*,*S*)-**2.95** was prepared from *rac*-**5.46** (74.4 mg, 0.2 mmol) according to the general procedure. **Fluorination with KF**: 10 mol% of catalyst (*S*)-**2.78**. The reaction was stirred at +10 °C for 36 h. *Purification:* FCC, eluent = *n*-hexane:Et_2O (96:4). Colourless oil, 61.3 mg, 86% yield, e.r. = 95.5. **Fluorination with CsF**: 5 mol% of catalyst (*S*)-**2.78**. The reaction was stirred at 0 °C for 36 h. *Purification:* FCC eluent = pentane:Et_2O (96:4). Colourless oil, 69.0 mg, 97% yield, e.r. = 97.5:2.5. **^{1}H NMR** (400 MHz, $CDCl_3$) δ 7.21 – 7.11 (m, 2H), 6.87 – 6.67 (m, 6H), 5.96 – 5.73 (m, 3H), 5.22 – 5.05 (m, 4H), 4.19 (dd, J = 18.3, 7.1 Hz, 1H), 3.75 (s, 3H), 3.74 (s, 3H), 3.51 (ddt, J = 14.2, 4.8, 1.8 Hz, 2H), 2.93 (dd, J = 14.3, 7.6 Hz, 2H); **^{19}F NMR** (377 MHz, $CDCl_3$) δ –179.64 (dd, J = 47.2, 18.3 Hz, 1F); **^{13}C NMR** (101 MHz, $CDCl_3$) δ 159.2, 159.2, 140.1 (d, $J_{C\text{-}F}$ = 20.3 Hz), 138.0 (d, $J_{C\text{-}F}$ = 4.4 Hz), 137.0, 129.0, 128.9, 121.9, 119.2 (d, $J_{C\text{-}F}$ = 6.8 Hz), 117.0, 115.5 (d, $J_{C\text{-}F}$ = 1.3 Hz), 113.8 (d, $J_{C\text{-}F}$ = 1.9 Hz), 112.5, 112.3 (d, $J_{C\text{-}F}$ = 7.2 Hz), 95.0 (d, $J_{C\text{-}F}$ = 179.3 Hz), 67.0 (d, $J_{C\text{-}F}$ = 20.7 Hz), 55.2, 55.1, 53.9 (d, $J_{C\text{-}F}$ = 2.1 Hz); **IR** (thin layer film) ν (cm^{-1}) = 3076, 3004, 2936, 2835, 1601, 1491, 1455, 1264, 1158, 1047, 997, 920, 788, 700; **HRMS** ($APCI^+$) *m/z* calculated for $C_{22}H_{27}FNO_2^+$ $[M+H]^+$ 356.20203, found 356.20133. **$[\alpha]_D^{25\,°C}$** = +13.0 ° (c = 0.5, $CHCl_3$, e.r. = 97.5:2.5); **HPLC separation:** DAICEL CHIRALPAK® IA-3, Heptane: ^{i}PrOH: diethyl amine = 99.2:0.7:0.1, 1 mL/min; t_1 = 3.74 min (minor), t_2 = 4.49 min (major).

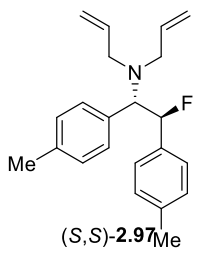
***N*-allyl-*N*-((1*S*,2*S*)-1,2-bis(3,5-dimethylphenyl)-2-fluoroethyl)prop-2-en-1-amine (2.96)**



(*S*,*S*)-**2.96**

Fluoride (*S*,*S*)-**2.96** was prepared from *rac*-**5.47** (73.6 mg, 0.2 mmol) according to the general procedure. **Fluorination with KF**: 10 mol% of catalyst (*S*)-**2.78**. The reaction was stirred at –15 °C for 72 h. *Purification:* FCC, eluent = pentane:Et_2O (100:0 to 99.55:0.45, gradient). Colourless oil, 40.9 mg, 58% yield, e.r. = 90:10. **Fluorination with CsF**: 10 mol% of catalyst (*S*)-**2.78**. The reaction was stirred at –20 °C for 72 h. *Purification:* FCC eluent = pentane:Et_2O (100:0 to 99.55:0.45, gradient). Colourless oil, 59.6 mg, 85% yield, e.r. = 91:9. **^{1}H NMR** (500 MHz, $CDCl_3$) δ 6.87 (s, 4H), 6.82 (s, 2H), 5.91 – 5.71 (m, 3H), 5.16 (d, J = 17.3 Hz, 2H), 5.11 (d, J = 10.1 Hz, 2H), 4.14 (dd, J = 19.3, 6.9 Hz, 1H), 3.50 (ddd, J = 14.4, 4.8, 1.9 Hz, 2H), 2.92 (dd, J = 14.4, 7.5 Hz, 2H), 2.28 (s, 6H), 2.27 (s, 6H); **^{19}F NMR** (471 MHz, $CDCl_3$) δ –179.64 (dd, J = 47.6, 19.3 Hz, 1F); **^{13}C NMR** (126 MHz, $CDCl_3$): δ 138.7 (d, $J_{C\text{-}F}$ = 19.8 Hz), 137.5, 137.3, 137.3, 136.5 (d, $J_{C\text{-}F}$ = 4.0 Hz), 129.7 (d, $J_{C\text{-}F}$ = 2.1 Hz), 128.9, 127.6, 124.8 (d, $J_{C\text{-}F}$ = 6.7 Hz), 116.8, 95.7 (d, $J_{C\text{-}F}$ = 178.0 Hz), 66.8 (d, $J_{C\text{-}F}$ = 20.4 Hz), 54.1 (d, $J_{C\text{-}F}$ = 2.2 Hz), 21.6, 21.4; **IR** (thin layer film) ν (cm^{-1}) = 3076, 3009, 2919, 2813, 1641, 1607, 1448, 1417, 1163, 1125, 1037, 917, 851, 710; **HRMS** (ESI^+) *m/z* calculated for $C_{24}H_{31}FN^+$ $[M+H]^+$ 352.24350, found 352.24319. $[\alpha]_D^{25\ °C}$ = +16.5 ° (c = 0.5, $CHCl_3$, e.r. = 90:10); **HPLC separation**: DAICEL CHIRALPAK® IA-3 Heptane: ^{i}PrOH = 99:1, 1 mL/min; t_1 = 2.30 min (minor), t_2 = 2.69 min (major).

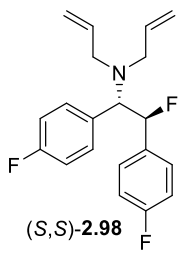
***N*-allyl-*N*-((1*S*,2*S*)-2-fluoro-1,2-di-p-tolylethyl)prop-2-en-1-amine (2.97)**



(*S*,*S*)-**2.97**

Fluoride (*S*,*S*)-**2.97** was prepared from *rac*-**5.48** (68.0 mg, 0.2 mmol) according to the general procedure. **Fluorination with KF**: 10 mol% of catalyst (*S*)-**2.78**. The reaction was stirred at –10 °C for 60 h. *Purification:* FCC, eluent = *n*-hexane:Et_2O (100:0 to 99.4:0.6, gradient). Colourless oil, 50 mg, 71% yield, e.r. = 95:5. **Fluorination with CsF**: 10 mol% of catalyst (*S*)-**2.78**. The reaction was stirred at –10 °C for 24 h. *Purification:* FCC eluent = *n*-hexane:Et_2O (100:0 to 99.2:0.8, gradient). Colourless oil, 48.1 mg, 74% yield, e.r. = 95:5. **^{1}H NMR** (400 MHz, $CDCl_3$) δ 7.13 (d, J = 8.0, Hz, 2H), 7.06–7.03 (m, 6H), 5.96 – 5.73 (m, 3H), 5.22 – 5.07 (m, 4H), 4.22 (dd, J = 16.6, 7.8 Hz, 1H), 3.51 (ddt, J = 14.3, 5.0, 1.8 Hz, 2H), 2.95 – 2.81 (m, 2H), 2.29 (s, 3H), 2.28 (s, 3H); **^{19}F NMR** (377 MHz, $CDCl_3$) δ –176.66 (dd, J = 47.3, 16.5 Hz); **^{13}C NMR** (101 MHz, $CDCl_3$) δ 137.9 (d, $J_{C\text{-}F}$ = 2.3 Hz), 137.4, 136.9, 135.7 (d, $J_{C\text{-}F}$ = 20.3 Hz), 133.2 (d, $J_{C\text{-}F}$ = 4.9 Hz), 129.5, 128.8, 127.1 (overlapped), 116.9, 95.0 (d, $J_{C\text{-}F}$ = 177.5 Hz), 66.8 (d, $J_{C\text{-}F}$ = 21.1 Hz), 54.0 (d, $J_{C\text{-}F}$ = 2.0 Hz), 21.3, 21.2; **IR** (thin layer film) ν (cm^{-1}) = 3076, 3008, 2923, 2813, 1641, 1515, 1447, 1417, 1115, 997, 918, 814; **HRMS** (APCI$^+$) *m/z* calculated for $C_{22}H_{27}FN^+$ $[M+H]^+$ 324.21220, found 324.21213; **$[\alpha]_D^{25\,°C}$** = +21.0 ° (c = 0.5, $CHCl_3$, e.r. = 95:5); **HPLC separation**: DAICEL CHIRALPAK® OJ-H Heptane: ^{i}PrOH = 99.2:0.8, 1 mL/min; t_1 = 5.30 min (minor), t_2 = 6.12 min (major).

***N*-allyl-*N*-((1*S*,2*S*)-2-fluoro-1,2-bis(4-fluorophenyl)ethyl)prop-2-en-1-amine (2.98)**

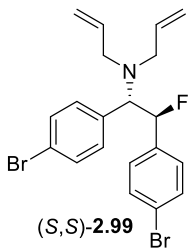


(*S*,*S*)-**2.98**

Fluoride (*S*,*S*)-**2.98** was prepared from *rac*-**5.49** (69.6 mg, 0.2 mmol) according to the general procedure. **Fluorination with KF**: 10 mol% of catalyst (*S*)-**2.78**. The reaction was stirred at –5 °C for 72 h. *Purification:* FCC eluent = pentane:Et_2O (100:0 to 99.69:0.31, gradient). Colourless oil,

44.7 mg, 67% yield, e.r. = 95:5. **Fluorination with CsF**: 10 mol% of catalyst (*S*)-**2.78**. The reaction was stirred at –10 °C for 72 h. *Purification:* FCC, eluent = pentane:Et_2O (100:0 to 99.65:0.35, gradient). Colourless oil, 52.8 mg, 80% yield, e.r. = 95:5. **^{1}H NMR** (400 MHz, $CDCl_3$) δ 7.21 – 7.16 (m, 2H), 7.15 – 7.09 (m, 2H), 6.98 – 6.90 (m, 4H), 5.93 – 5.68 (m, 3H), 5.21 – 5.08 (m, 4H), 4.17 (dd, *J* = 18.5, 7.0 Hz, 1H), 3.49 (ddt, *J* = 14.3, 4.9, 1.8 Hz, 2H), 2.89 (dd, *J* = 14.3, 7.6 Hz, 2H); **^{19}F NMR** (376 MHz, $CDCl_3$) δ –113.54 – –113.66 (m, 1F), –114.59 – –114.72 (m, 1F), –177.78 (dd, *J* = 46.6, 18.5 Hz, 1F); **^{13}C NMR** (101 MHz, $CDCl_3$) δ 162.6 (d, $J_{C\text{-}F}$ =247.5 Hz), 162.1 (d, $J_{C\text{-}F}$ = 246.4 Hz) 136.7, 134.4 (dd, $J_{C\text{-}F}$ = 21.0, 3.3 Hz), 132.3 (t, $J_{C\text{-}F}$ = 4.0 Hz), 131.1 (dd, $J_{C\text{-}F}$ =7.9, 1.3 Hz), 128.7 (dd, $J_{C\text{-}F}$ = 8.3, 6.5 Hz), 117.4, 115.1 (d, $J_{C\text{-}F}$ = 20.9 Hz), 115.0 (d, $J_{C\text{-}F}$ =21.2 Hz), 94.8 (d, $J_{C\text{-}F}$ = 179.1 Hz), 66.7 (d, $J_{C\text{-}F}$ = 21.4 Hz), 53.9 (d, $J_{C\text{-}F}$ = 2.2 Hz); **IR** (thin layer film) ν (cm^{-1}) = 3078, 2926, 2814, 1606, 1511, 1227, 1159, 921, 834; **HRMS** (ESI^+) *m/z* calculated for $C_{20}H_{21}F_3N^+$ $[M+H]^+$ 332.16206, found 332.16180. **$[\alpha]_D^{25\,°C}$** = +23.7 ° (c = 0.5, $CHCl_3$, e.r. = 95:5); **HPLC separation**: DAICEL CHIRALPAK® OJ-H Heptane:^{i}PrOH = 99:1, 1 mL/min; t_1 = 6.16 min (minor), t_2 = 7.66 min (major).

***N*-allyl-*N*-((1*S*,2*S*)-1,2-bis(4-bromophenyl)-2-fluoroethyl)prop-2-en-1-amine (2.99)**

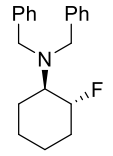


(*S*,*S*)-**2.99**

Fluoride (*S*,*S*)-**2.99** was prepared from *rac*-**5.50** (93.9 mg, 0.2 mmol) according to the general procedure. **Fluorination with KF**: 10 mol% of catalyst (*S*)-**2.78**. The reaction was stirred at +5 °C for 72 h. *Purification:* FCC eluent = pentane:Et_2O (100:0 to 99:1, gradient). Colourless oil, 64 mg, 71% yield, e.r. = 91:9. **Fluorination with CsF**: 10 mol% of catalyst (*S*)-**2.78**. The reaction was stirred at –5 °C for 72 h. *Purification:* FCC, eluent = pentane:Et_2O (100:0 to 99:1, gradient). Colourless oil, 68.0 mg, 73% yield, e.r. = 90.5:9.5. **^{1}H NMR** (500 MHz, $CDCl_3$) δ 7.41– 7.37 (m, 4H), 7.08 (d, *J* = 8.2 Hz, 2H), 7.04 (d, *J* = 8.3 Hz, 2H), 5.80 (dd, *J* = 47.0, 6.8 Hz, 1H) 5.88 – 5.65 (m, 2H), 5.18 – 5.08 (m, 4H), 4.12 (dd, *J* = 19.4, 6.8 Hz,

1H), 3.46 (ddd, *J* = 14.3, 4.6, 2.2 Hz, 2H), 2.85 (dd, *J* = 14.3, 7.6 Hz, 2H); **^{19}F NMR** (471 MHz, $CDCl_3$) δ –180.69 (dd, *J* = 47.0, 19.6 Hz, 1F); **^{13}C NMR** (126 MHz, $CDCl_3$) δ 137.3 (d, $J_{C\text{-}F}$ = 20.9 Hz), 136.5, 135.2 (d, $J_{C\text{-}F}$ = 4.0 Hz), 131.3, 131.2, 131.1 (d, $J_{C\text{-}F}$ = 1.3 Hz), 128.4 (d, $J_{C\text{-}F}$ = 6.8 Hz), 122.7 (d, $J_{C\text{-}F}$ = 2.3 Hz), 121.6, 117.4, 94.5 (d, $J_{C\text{-}F}$ = 179.9 Hz), 66.4 (d, $J_{C\text{-}F}$ = 21.1 Hz), 53.8 (d, $J_{C\text{-}F}$ = 2.2 Hz); **IR** (thin layer film) ν (cm^{-1}) = 3077, 2977, 2924, 2814, 1164, 1594, 1488, 1405, 1073, 1010, 920, 819, 804; **HRMS** (ESI^+) *m/z* calculated for $C_{20}H_{21}Br_2FN^+$ $[M+H]^+$ 452.00193, found 452.00165; **$[\alpha]_D^{25\,°C}$** = –8.4 ° (c = 0.9, $CHCl_3$, e.r. = 90.5:9.5); **HPLC separation**: DAICEL CHIRALPAK® OJ-H, Heptane:EtOH:diethyl amine = 98.9:1.0:0.1, 1 mL/min; t_1 = 6.23 min (minor), t_2 = 10.97 min (major).

(1*R*,2*R*)-*N*,*N*-dibenzyl-2-fluorocyclohexan-1-amine (2.109)



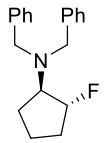
(R,R)-**2.109**

Fluoride (*R*,*R*)-**2.109** was prepared from *rac*-**2.108** (72 mg, 0.2 mmol) according to the general procedure using CF_3Ph as solvent. **Fluorination with KF**: 10 mol% of catalyst (*S*)-**2.78**. The reaction was stirred at rt for 72 h. *Purification:* FCC on silica gel, eluent = *n*-hexane:Et_2O (100:0 to 99.6:0.4, gradient). White solid, 40.7 mg, 69% yield, e.r. = 85.5:14.5. **Fluorination with CsF**: 10 mol% of catalyst (*S*)-**2.78**. The reaction was stirred at rt for 72 h. *Purification*: FCC, eluent = *n*-hexane:Et_2O (100:0 to 99.6:0.4, gradient). White solid, 35.5 mg, 60% yield, e.r. = 85:15. **^{1}H NMR** (400 MHz, CDCl3) δ 7.42 – 7.07 (m, 10H), 4.55 (dddd, *J* = 50.7, 10.4, 10.4, 4.8 Hz, 1H), 3.75 (d, *J* = 13.9 Hz, 2H), 3.67 (d, *J* = 14.0 Hz, 2H), 2.68 – 2.54 (m, 1H), 2.12 – 1.97 (m, 1H), 1.91 – 1.76 (m, 1H), 1.67 – 1.52 (m, 2H), 1.35 – 1.17 (m, 2H), 1.15 – 0.93 (m, 2H); **^{19}F NMR** (376 MHz, CDCl3) δ –174.71 (d, *J* = 50.6 Hz); **^{13}C NMR** (101 MHz, CDCl3) δ 140.7, 128.6, 128.1, 126.6, 93.3 (d, $J_{C–F}$ = 177.9 Hz), 61.2 (d, $J_{C–F}$ = 14.8 Hz), 54.4, 32.6 (d, $J_{C–F}$ = 17.5 Hz), 27.7 (d, $J_{C–F}$ = 8.8 Hz), 24.9 (d, $J_{C–F}$ = 2.2 Hz), 24.0 (d, $J_{C–F}$ = 11.4 Hz). **IR** (thin layer film) ν (cm^{-1}) = 3026, 2937, 2860, 1602, 1494, 1453, 1030, 989, 773, 746,

698; **MP** 69 – 71 °C; **HRMS** (ESI$^+$) *m/z* calculated for $C_{20}H_{25}FN^+$ $[M+H]^+$ 298.19655, found 298.19650; **[α]$_D^{25\,°C}$** = –9.0 ° (c = 0.2, $CHCl_3$, e.r. = 85.5:14.5); **HPLC separation:** DAICEL CHIRALPAK® IB-3, Heptane:^{i}PrOH = 99:1, 1 mL/min; t_1 = 3.02 min (minor), t_2 = 3.66 min (major). Spectroscopic data were in agreement with the ones previously reported in literature.[14]

The absolute configuration was assigned by derivatising (*R*,*R*)-**2.109** to its corresponding β-fluoropicolinamide **2.128** (p.292).[15] The configuration of the other aliphatic cyclic products (**2.123**, **4.18**–**4.20**) was assigned by analogy.

(1*R*,2*R*)-*N*,*N*-dibenzyl-2-fluorocyclopentan-1-amine (**2.123**)



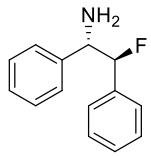
(R,R)-**2.123**

Fluoride (*R*,*R*)-**2.123** was prepared from *rac*-**5.51** (68.8 mg, 0.2 mmol) according to the general procedure using CF_3Ph as solvent. **Fluorination with KF**: 10 mol% of catalyst (*S*)-**2.78**. The reaction was stirred at rt for 24 h. *Purification*: FCC, eluent = pentane: Et_2O (100:0 to 99.4:06, gradient). Colourless oil, 40.0 mg, 70% yield, e.r. = 74.5:25.5. **Fluorination with CsF**: 10 mol% of catalyst (*S*)-**2.78**. The reaction was stirred at rt for 24 h. *Purification*: FCC, eluent = pentane: Et_2O (100:0 to 99.4:06, gradient). Colourless oil, 38.7 mg, 68% yield, e.r. = 75:25; **^{1}H NMR** (400 MHz, $CDCl_3$) δ 7.41 – 7.36 (m, 4H), 7.34 – 7.28 (m, 4H), 7.27 – 7.19 (m, 2H), 5.15 (ddt, *J* = 54.0, 6.9, 3.6 Hz, 1H), 3.70 (d, *J* = 14.1 Hz, 2H), 3.63 (d, *J* = 14.1 Hz, 2H), 3.37 (dtd, *J* = 28.5, 8.5, 3.9 Hz, 1H), 2.01 – 1.72 (m, 3H), 1.72 – 1.48 (m, 3H); **^{19}F NMR** (376 MHz, $CDCl_3$) δ –172.99 (dtd, *J* = 53.5, 28.3, 23.5 Hz, 1F); **^{13}C NMR** (101 MHz, $CDCl_3$) δ 139.9, 128.8, 128.3, 127.0, 97.1 (d, J_{C-F} = 176.9 Hz), 68.1 (d, J_{C-F} = 22.3 Hz), 55.5, 32.8 (d, J_{C-F} = 22.8 Hz), 27.4 (d, J_{C-F} = 5.8 Hz), 22.0 (d, J_{C-F} = 2.1 Hz); **IR** (thin layer film) ν (cm^{-1}) = 3062, 3028, 2959, 2875, 1603, 1494, 1454, 1363, 1110, 1075, 1028, 956745, 698; **HRMS** (ESI$^+$) *m/z* calculated for $C_{19}H_{23}FN^+$ $[M+H]^+$ 284.18090, found 284.18088; **[α]$_D^{25\,°C}$** = –10.0 °

(c = 0.5, $CHCl_3$, e.r. = 74.5:25.5); **HPLC separation:** DAICEL CHIRALPAK® IF-3, Heptane:MTBE = 99:1, 1 mL/min; t_1 = 5.15 min (major), t_2 = 5.66 min (minor).

5.2.2.5Deprotection and Further Modification

(1*S*,2*S*)-2-fluoro-1,2-diphenylethan-1-amine (2.100)

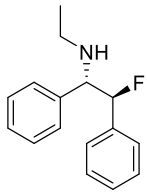


(*S*,*S*)-**2.100**

Fluoride (*S*,*S*)-**2.100** was synthesized *via* a slightly modified version of the deprotection protocol previously reported by Cossy *et al*..[16] In a flame-dried two-neck round bottom flask, $Pd(dba)_2$ (154 mg, 0.27 mmol, 0.1 equiv) and 1,4-bis(diphenylphosphino)butane (dppb, 115 mg, 0.27 mmol, 0.1 equiv) were stirred at rt in degassed THF (20 mL) for 15 min. Then (*S*,*S*)-**2.77** (794 mg, 2.7 mmol, 1 equiv; e.r. = 93:7) was added as a solution in THF (6 mL) followed by thiosalicylic acid (1.036 g, 6.75 mmol, 2.5 equiv). The reaction mixture was stirred at 60 °C overnight, then it was diluted with Et_2O and acidified with HCl 1 M (checked with pH paper). The layers were separated and the aqueous one was washed 3 times with Et_2O prior of being neutralized with NaOH 2.5 M (checked with pH paper). The aqueous layer was extracted three times with EtOAc, dried on $MgSO_4$ and evaporated *in vacuo*. The crude product was purified by FCC (CH_2Cl_2:EtOAc = 100:0 to 80:20, gradient) to afford (*S*,*S*)-**2.100** as a white solid (489.2 mg, 84% yield, e.r. = 93:7). Recrystallisation of 450 mg of the obtained compound from warm *n*-hexane (1 drop of $CHCl_3$) afforded (*S*,*S*)-**2.100** in > 99.8:0.2 e.r. (370.0 mg, 72% recrystallisation yield). **^{1}H NMR** (400 MHz, $CDCl_3$) δ 7.24 – 6.97 (m, 10H), 5.36 (dd, J = 47.3, 7.0 Hz, 1H), 4.21 (dd, J = 14.5, 7.0 Hz, 1H), 1.70 (s, 2H); **^{19}F NMR** (376 MHz, $CDCl_3$) δ –182.68 (dd, J = 47.4, 14.6 Hz, 1F); **^{13}C NMR** (101 MHz, $CDCl_3$) δ 140.3 (d, $J_{C\text{-}F}$ = 6.1 Hz), 137.4 (d, $J_{C\text{-}F}$ = 20.3 Hz), 128.5 (d, $J_{C\text{-}F}$ = 1.7 Hz), 128.4, 128.2, 127.9, 127.8, 126.5 (d, $J_{C\text{-}F}$ = 7.0 Hz), 98.7 (d, $J_{C\text{-}F}$ = 177.6 Hz), 61.6 (d, $J_{C\text{-}F}$ = 23.1 Hz). **IR** (thin layer film) ν (cm^{-1}) = 3388, 3064, 3032, 2918, 2849, 1604, 1495, 1454, 1074, 1027, 1018, 834,

764, 698; MP 47 – 50 °C; **HRMS** (ESI$^+$) *m/z* calculated for $C_{14}H_{15}FN^+$ $[M+H]^+$ 216.11830, found 216.11813. **$[\alpha]_D^{25\,°C}$** = –96.2 ° (c = 0.5, $CHCl_3$, e.r. > 99.8:0.2); **HPLC separation:** DAICEL CHIRALPAK® IB-3, Heptane:^{i}PrOH:EtOH = 97:2:1 + 0.1% ethanol amine, 1 mL/min; t_1 = 5.28 min (major), t_2 = 6.94 min (minor). Spectroscopic data were in agreement with the ones previously reported in literature.[17]

(1*S*,2*S*)-*N*-ethyl-2-fluoro-1,2-diphenylethan-1-amine (2.102)

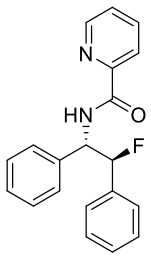


(*S*,*S*)-**2.102**

In a round bottom flask, CH_3CHO (294 µL, 5 mmol, 5 equiv) was dissolved in MeOH (5 mL, 0.2 M). (*S*,*S*)-**2.100** (1 equiv, 1 mmol, 215 mg; e.r. > 99.8:0.2) and $NaBH(OAc)_3$ (635mg, 3 mmol, 3 equiv) were subsequently added as solids. The reaction was stirred at rt for 3 h then quenched with $NaHCO_3$ (sat.) and extracted three times with EtOAc. The combined organic layers were washed with brine, dried over $MgSO_4$ and evaporated *in vacuo.* The crude brown oil was purified by FCC (pentane:Et_2O 100:0 to 90:10, gradient) to afford a pale yellow oil (137.1 mg, 56% yield, e.r. > 99.9:0.1). **^{1}H NMR** (400 MHz, $CDCl_3$) δ 7.25 – 7.14 (m, 6H), 7.13 – 7.05 (m, 2H), 7.05 – 6.96 (m, 2H), 5.40 (dd, *J* = 47.7, 8.2 Hz, 1H), 4.04 (dd, *J* = 10.6, 8.2 Hz, 1H), 2.59 – 2.40 (m, 2H), 1.91 (s br, 1H), 1.10 (t, *J* = 7.1 Hz, 3H); **^{19}F NMR** (376 MHz, $CDCl_3$) δ –177.82 (dd, *J* = 47.7, 10.7 Hz)**; ^{13}C NMR** (101 MHz, $CDCl_3$) δ 138.5 (d, $J_{C\text{-}F}$ = 6.7 Hz), 137.2 (d, $J_{C\text{-}F}$ = 19.9 Hz), 128.7, 128.5 (d, $J_{C\text{-}F}$ = 1.9 Hz), 128.2, 128.0, 127.7, 126.8 (d, $J_{C\text{-}F}$ = 6.7 Hz), 98.2 (d, $J_{C\text{-}F}$ = 177.9 Hz), 69.0 (d, $J_{C\text{-}F}$ = 22.6 Hz), 41.8, 15.5; **IR** (thin layer film) ν (cm^{-1}) = 3032, 2967, 2818, 1454, 1340, 1208, 1151, 1062, 1032, 758, 698; **HRMS** (ESI$^+$) *m/z* calculated for $C_{16}H_{19}FN^+$ $[M+H]^+$ 244.14960, found 244.14954. **$[\alpha]_D^{25\,°C}$** = –68.3 ° (c = 0.4, $CHCl_3$, e.r. > 99.9:0.1); **HPLC separation**: DAICEL CHIRALPAK® OJ-H Hept:EtOH = 96:4, 1 mL/min; t_1 = 5.09 min (major), t_2 = 6.22 min (minor).

N.B. Attempts to access this compound *via* asymmetric fluorination from the corresponding chloride were unsuccessful as the synthesis of the chloride precursor proved to be very challenging (mixture of products, poor yields).

***N*-((1S,2S)-2-fluoro-1,2-diphenylethyl)picolinamide (2.103)**



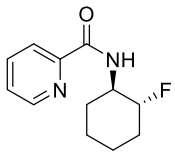
(*S*,*S*)-**2.103**

β-Fluoroamide (*S*,*S*)-**2.103** was synthesized according to the procedure reported by Doyle.[15] In a flame-dried Schlenk tube, β-fluoroamine (*S*,*S*)-**2.100** (80.0 mg, 0.37 mmol, 1 equiv, 78:22 e.r.) was dissolved in anhydrous CH_2Cl_2. Picolinic acid (45.8 mg, 0.37 mmol, 1 equiv), DMAP (50.0 mg, 0.41 mmol, 1.1 equiv) and *N*, *N'*-diisopropylcarbodiimide (63.5 mg, 0.41 mmol, 1 equiv) were added and the reaction stirred overnight at rt. After disappearance of the starting material (monitored by TLC), *n*-hexane was added and the solid removed by filtration. The filtrate was evaporated *in vacuo* and the crude product purified by FCC (pentane:EtOAc = 90:10 to 70:30, gradient). White solid (80 mg, 67% yield). **^{1}H NMR** (400 MHz, $CDCl_3$) δ 8.84 (d, *J* = 9.1 Hz, 1H), 8.56 (d, *J* = 4.9 Hz, 1H), 8.07 (d, *J* = 7.8 Hz, 1H), 7.78 (td, *J* = 7.7, 1.7 Hz, 1H), 7.40 (dd, *J* = 7.6, 4.8, 1.3 Hz, 1H), 7.36 – 7.20 (m, 10H), 5.81 (dd, *J* = 46.0, 4.4 Hz, 1H), 5.59 (ddd, *J* = 21.4, 9.1, 4.4 Hz, 1H); **^{19}F NMR** (376 MHz, $CDCl_3$) δ –188.34 (dd, *J* = 45.9, 21.4 Hz); **^{13}C NMR** (101 MHz, $CDCl_3$) *δ* 163.9, 149.6, 148.3, 138.4 (d, $J_{C\text{-}F}$ = 2.0 Hz), 137.4, 136.8 (d, $J_{C\text{-}F}$ = 20.7 Hz), 128.7 (overlapped), 128.4, 128.0, 127.6, 126.4, 126.1 (d, $J_{C\text{-}F}$ = 7.3 Hz), 122.5, 95.6 (d, $J_{C\text{-}F}$ = 180.9 Hz), 57.7 (d, $J_{C\text{-}F}$ = 21.6 Hz). Spectroscopic data were in agreement with the ones previously reported in literature.[15]

The reported value for the (*R*,*R*)-enantiomer was $[\alpha]_D^{21\ °C}$ = –4.5 ° (c = 1.0, $CHCl_3$, e.r. = 74:26).[15] Our measured value was $[\alpha]_D^{25\ °C}$ = +4.7 ° (c = 1.0, $CHCl_3$, e.r. = 77.5:22.5) indicating (*S*,*S*) configuration for **2.103** (and consequently for its precursors **2.100** and

2.77). The configuration of the other stilbene-derived β-fluoroamines (**2.82-2.99**) was assigned by analogy. Finally, this assignment was further confirmed by single crystal x-ray diffraction analysis of **2.83**.

***N*-((1R,2R)-2-fluorocyclohexyl)picolinamide (2.128)**



(R,R)-**2.128**

A Schlenk tube under inert atmosphere was charged with fluoride (*R,R*)-**2.109** (40 mg, 0.135 mmol, 1 equiv) and Pearlman's catalyst ($Pd(OH)_2$ 20 wt% on carbon, 10 mg, 0.1 equiv). MeOH (700 μL) and EtOAc (400 μL) were added *via* a syringe. The flask was evacuated and backfilled with H_2 (balloon) three times. The reaction mixture was stirred at rt, for 5 h, then it was filtered through a silica pad (CH_2Cl_2/MeOH) and the solvent removed *in vacuo*. The crude product (15 mg) was dissolved in CH_2Cl_2 (675 μL, 0.2 M) and picolinic acid (16.6 mg, 0.135 mmol, 1 equiv), DMAP (18.1 mg, 0.149 mmol, 1.1 equiv) and di-isopropyl carbodiimide (DIC, 18.7 mg, 0.149 mmol, 1.1 equiv) were added. The reaction mixture was stirred at rt for overnight. After this time, *n*-hexane was added to precipitate the urea co-product. The solid was filtered and the filtrate concentrate to dryness. The crude product was purified by FCC over silica gel (*n*-hexane:EtOAc= 95:5 to 80:20 gradient). **^{1}H NMR** (400 MHz, $CDCl_3$) δ 8.55 (d, J = 4.2 Hz, 1H), 8.21 (d, J = 7.8 Hz, 1H), 8.11 (d, J = 6.9 Hz, 1H), 7.85 (ddd, J = 7.7, 7.7, 1.6 Hz, 1H), 7.43 (ddd, J = 7.5, 4.7, 1.1 Hz, 1H), 4.44 (dddd, J = 50.1, 9.8, 9.7, 4.5 Hz, 1H), 4.21−4.09 (m, 1H), 2.22−2.13 (m, 2H), 1.86−1.80 (m, 1H), 1.75−1.58 (m, 2H), 1.47−1.29 (m, 3H); **^{19}F NMR** (376 MHz, $CDCl_3$) δ −178.5 (d, J = 50.2 Hz); **^{13}C NMR** (101 MHz, $CDCl_3$) δ 164.3, 150.0, 148.2, 137.6, 126.4, 122.6, 93.5 (d, J_{C-F} = 179.5 Hz), 52.6 (d, J_{C-F} = 18.1 Hz), 31.4 (d, J_{C-F} = 17.9 Hz), 31.0 (d, J_{C-F} = 5.4 Hz), 24.1, 23.5 (d, J_{C-F} = 10.3 Hz). Analytical data were in agreement with those previously published.[15] **$[\alpha]_D^{25\,°C}$** = –13.5 ° (c = 0.5, $CHCl_3$, e.r. = 85.5:14.5). **HPLC separation:** DAICEL

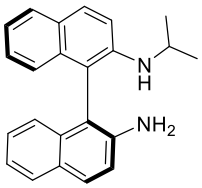
CHIRALPAK® AS-H, *n*-hexane:^{i}PrOH = 90:10, 1 mL/min; t_1 = 15.5 min (major), t_2 = 17.7 min (minor).

The reported value for the (*R*,*R*)-enantiomer was $[\alpha]_D^{21\ °C}$ = –36.5 ° (c = 0.7, $CHCl_3$, e.r. = 92:8).[15] Our measured value was $[\alpha]_D^{25\ °C}$ = –13.5 ° (c = 0.5, $CHCl_3$, e.r. = 85.5:14.5) indicating (*R*,*R*) configuration for **2.128** (and consequently for its precursors **2.109**). The configuration of the other aliphatic cyclic products (**2.123**, **4.18–4.20** was assigned by analogy.

5.3 Additional Data from Chapter 3

5.3.1 Procedures for the Multigram Synthesis of Catalyst (*S*)-2.3 and (*S*)-2.78

(*S*)-*N*^{2}-isopropyl-[1,1'-binaphthalene]-2,2'-diamine (2.29)

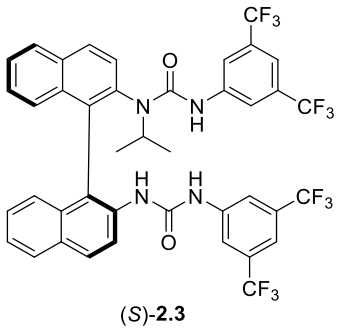


(*S*)-**2.29**

THF (140 mL) and acetone (3.6 mL) were transferred in a three-neck round bottom flask equipped with a thermometer and a stirring bar and connected to the nitrogen line. The solution was cooled to 0 °C and an aqueous solution of H_2SO_4 20% vol/vol (70 mL, 2 mL/mol (*S*)-BINAM) was slowly added while stirring. The ice bath was removed, and the solution stirred for further 45 min at rt. After this time, (*S*)-BINAM (10 g, 35 mmol, 1 equiv) was added as a solid at rt. A brown solution was obtained. The solution was cooled to 0 °C and stirred for 10 min before addition of $NaBH_4$ under a nitrogen flow. Solid $NaBH_4$ (13 g, 350 mmol, 10 equiv) was added portion-wise over 45 min. ***Careful!*** This causes precipitation of a solid and vigorous evolution of hydrogen. After completion of the addition, the reaction mixture was stirred for further 60 min at rt. Then, the solution was cooled to 0 °C and 250 mL of aqueous KOH (1 M) were slowly added to rise the pH of the reaction mixture to 8 (monitored by pH paper). The reaction mixture was transferred into a separating funnel and

EtOAc (210 mL) was added. The layers were separated and the aqueous one was extracted twice with EtOAc (2x 100 mL). The organic phases were combined, washed with brine (300 mL), dried over $MgSO_4$ and concentrated *in vacuo*. The crude reaction mixture was purified by FCC on silica gel (dry loading, eluent: pentane: EtOAc = 97:3 to 90:10, gradient) to afford 6.8 g (60% yield) of (*S*)-**2.29** as a white solid. Analytical data were in agreement with those previously published.[1] R_f = 0.26; pentane:EtOAc = 95:5, visualisation: UV light, λ= 254 nm.

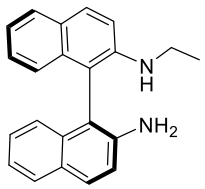
(*S*)-3-(3,5-bis(trifluoromethyl)phenyl)-1-(2'-(3-(3,5-bis(trifluoromethyl)phenyl)ureido)-[1,1'-binaphthalen]-2-yl)-1-isopropylurea (2.3)


(*S*)-**2.3**

In a flame-dried two-neck round bottom flask, equipped with a stirring bar and a condenser, (*S*)-**2.29** (6.8 g, 21 mmol, 1 equiv) was dissolved in anhydrous CH_2Cl_2 (50 mL). The solution was cooled to 0 °C and 3,5-Bis(trifluoromethyl)phenyl isocyanate (7.8 mL, 42 mmol, 2 equiv) was added dropwise over 15 min while stirring. A precipitate is formed upon addition of the isocyanate, making stirring difficult: slow addition is required to avoid blockage of the stirring bar. The reaction mixture was then heated to reflux for 48 h under a nitrogen flux. After ~30 min from the end of isocyanate addition, the precipitate is completely dissolved, and the reaction mixture is a yellow solution. After disappearance of the starting material (monitored by TLC, eluent: pentane:EtOAc = 90:10; detection: UV light, λ= 254 nm. R_f product: 0.10, R_f starting material: 0.56), 1 mL of MeOH was added to quench any residual isocyanate, and the reaction mixture stirred for further 15 min. The solvent was evaporated under reduced pressure and the crude product was purified by FCC on silica gel (dry loading, I column eluent: pentane: EtOAc = 95:5 to 80:20 gradient; II column eluent: pentane:acetone = 95:5 to 85:15, gradient), to afford 14.9 g of product. The product (10.45 g) was dissolved in Et_2O (12 mL, 1.2 mL/g) at rt and recrystallised by

layering *n*-hexane (66 mL, 6 mL/g) on the Et_2O solution at rt for 24 h. The crystals were collected on a filter and washed with cold *n*-hexane to afford 9.74 g of pure catalyst as a white solid (93% recrystallisation yield). Analytical data were in agreement with those previously published.[1] R_f = 0.49; pentane:EtOAc = 80:20, visualisation: UV light, λ= 254 nm.

(*S*)-*N*^{2}-Ethyl-[1,1'-binaphthalene]-2,2'-diamine (2.31)



(*S*)-**2.31**

a) Protection:

A flame-dried, 500 mL, 3-neck round bottom flask, equipped with a magnetic stirring bar and a dropping funnel, was charged with (*S*)-BINAM (40 g, 0.14 mol, 1 equiv) under nitrogen flow. Anhydrous CH_2Cl_2 (280 ml, 0.5 M) was added and the suspension cooled to 0 °C. Trifluoroacetic anhydride (49 mL, 0.35 mol, 2.5 equiv) was then added dropwise over a period of 30 min at 0 °C. After completion of the addition, the reaction was warmed to rt and stirred for 18 h. As the reaction proceeds, the suspended solid completely dissolves and at the end of the reaction a solution is obtained. Volatiles were evaporated *in vacuo* (***Careful!*** Trifluoroacetic acid is a co-product of the reaction) to afford 65.8 g of (*S*)-*N*-*N*'-([1,1′-binaphthalene]-2,2′-diyl)bis(2,2,2-trifluoroacetamide) as a brown solid (99% yield). The crude product was use in the next step without any further purification. Analytical data were in agreement with those previously published.[1] R_f = 0.13; pentane:EtOAc = 90:10, visualisation: UV light, λ= 254 nm.

b) Alkylation:

A 2 L, 2-neck round bottom flask, equipped with a magnetic stirring bar and a condenser, was charged with (*S*)-*N*-*N*'-([1,1′-binaphthalene]-2,2′-diyl)bis(2,2,2-trifluoroacetamide) (65.8 g, 0.14 mmol, 1 equiv) under nitrogen flow. Acetone was added at once (560 mL, 0.25 M) and the solution was cooled to 0 °C. K_2CO_3 (110 g, 0.28 mol, 2 equiv) was added

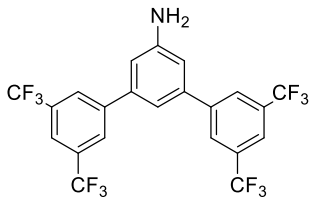
portion-wise while stirring, followed by addition of EtI (13.5 mL, 0.168 mol, 1.2 equiv) *via* a syringe. The reaction mixture was stirred at reflux for 18 h under a nitrogen blanket. After this time, it cooled to rt and the solid was filtered off. Volatiles were evaporated *in vacuo* and the residue was carried on in the subsequent step.

c) Deprotection:

The residue was dissolved in EtOH (450 mL) and a basic solution of KOH (78 g, 1.4 mol, 10 equiv) in water (110 mL) was carefully added while stirring at 0 °C. When the addition was completed, the reaction mixture was stirred at 70 °C for 18 h (monitored by TLC, pentane:Et_2O = 80:20) under a nitrogen blanket. As the reaction proceeds, a precipitate is formed. After disappearance of the starting material (monitored by TLC, eluent: pentane:Et_2O = 80:20; detection: UV light, λ= 254 nm. Starting materials have characteristic brownish spot at this wavelength, while the products are characterised by bright blue spots), the mixture was cooled to rt and then diluted with EtOAc (200 mL). The layers were separated and the aqueous one was extracted three times with EtOAc (3x100 mL). The organic layers were combined, washed with brine (200 mL) and dried over $MgSO_4$. The crude product was purified by FCC on silica gel (Eluent: pentane:EtOAc = 97:3 to 95:5, gradient) to afford (*S*)-*N*^{2}-ethyll-[1,1'-binaphthalene]-2,2'-diamine **2.31** as a pale yellow solid (26.3 g, 60% yield). (*Note:* the bis-alkylated product tends to tail in this eluent system, contaminating the initial fractions of product. Nevertheless, as the bis-alkylated urea is not a competent catalyst in HB-PTC, this impurity can be carried on in the next step). Increasing the eluent polarity to pentane:EtOAc = 80:20, 10 g of (*S*)-(–)-1,1′-binaphthyl-2,2′-diamine were recovered (25%, 93% purity from ^{1}H NMR analysis). Analytical data were in agreement with those previously published (see section 5.2.2.1).[1]

R_f = 0.31; pentane:EtOAc = 90:10, visualisation: UV light, λ= 254 nm.

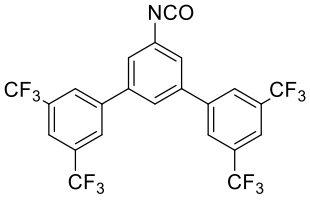
3,3'',5,5''-tetrakis(trifluoromethyl)-[1,1':3',1''-terphenyl]-5'-amine (2.79)



2.79

A 1 L, two-necks, round bottom flask, equipped with a stirring bar and a condenser was charged with 3,5-dibromoaniline (30 g, 0.12 mol, 1 equiv), (3,5-bis(trifluoromethyl)phenyl)boronic acid (108 g, 0.42 mol, 3.5 equiv) and SPhos (2-Dicyclohexylphosphino-2′,6′-dimethoxybiphenyl; 490 mg, 0.012 mol, 1 mol%). The flask was then evacuated and backfilled with nitrogen three times, prior of the addition of degassed THF (480 mL) and degassed water (120 mL). The reaction mixture was cooled to 0 °C, and nitrogen was bubbled into it for further 20 min while stirring. After 20 min, K_2CO_3 (90 g, 0.48 mol, 4 equiv) was added to the stirred mixture portion-wise at 0 °C. After the completion of the addition, the temperature was raised to 60 °C and $Pd(OAc)_2$ (134 mg, 0.006 mol, 0.5 mol%) was added while stirring. The reaction mixture was stirred at reflux over weekend under a nitrogen flow. After disappearance of the starting material (monitored by TLC, pentane: EtOAc = 90:10, UV light, λ= 254 nm), the reaction mixture was cooled to rt and diluted with CH_2Cl_2 (500 mL). Phases were separated and the aqueous one was extracted twice with CH_2Cl_2 (100 mL). The combined organic layers were washed with brine (500 mL), dried over $MgSO_4$ and concentrated *in vacuo*. The crude product was purified on a short silica plug (pentane: CH_2Cl_2 = 95:5 to 70:30, gradient) to afford **2.79** as a white solid (53 g, 86% yield). Analytical data were in agreement with those previously published (see section 5.2.2.1).[18] R_f = 0.22; pentane: EtOAc = 90:10, visualisation: UV light, λ= 254 nm.

5'-isocyanato-3,3'',5,5''-tetrakis(trifluoromethyl)-1,1':3',1''-terphenyl (3.24)

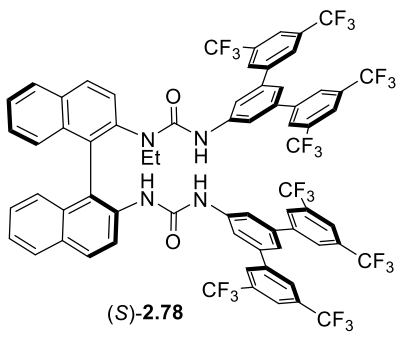


3.24

The reaction was performed under a nitrogen flow and with mechanical stirring in a 3 L three-necks round-bottom flask, equipped with a dropping funnel and an outlet leading to a $NaHCO_3$ trap (to quench the phosgene that might escape the reaction vessel). The reaction vessel was charged with triphosgene (11.438 g, 0.39 mol, 0.37 equiv) followed by CH_2Cl_2 (600 mL). The resulting solution was cooled to 0 °C and a solution of aniline **2.79** (54 g, 0.10 mol, 1 equiv) in CH_2Cl_2 (300 mL) was added *via* the dropping funnel over 15 min. The dropping funnel was then washed with 100 mL of CH_2Cl_2 to quantitatively transfer the aniline into the reaction vessel. Next, a saturated aqueous solution of $NaHCO_3$ (1 L) was added slowly *via* the dropping funnel. The addition causes the precipitation of a solid. Initial slow addition is necessary to ensure homogeneous stirring and thus reproducible results. At the end of the addition the reaction mixture was stirred at 0 °C for further 45 min. At this point, the layers were separated and the organic phase was passed through a plug of $MgSO_4$, and the solvent was removed *in vacuo* to afford 47.6 g of **3.24** as a white solid. The crude product was recrystallised from refluxing *n*-hexane (20 mL/g) and THF (0.75 mL/g), cooling from reflux to rt over 5 h, to afford 31.9 g of pure **3.24** (67% yield of recrystallisation). The mother liquor was recrystallised a second time from refluxing *n*-hexane (20 mL/g) and THF (0.5 mL/g), cooling from reflux to rt over 5 h, to obtain further 11.4 g of **3.24** in comparable purity to the first recrystallisation (52% II recrystallisation yield). White crystalline solid (40 g, 71% yield) **^{1}H NMR** (400 MHz, $CDCl_3$) δ 8.02 (br s, 4H), 7.95(br s, 2H), 7.58 (t, J = 1.6 Hz, 1H), 7.40 (d, J = 1.6 Hz, 2H); **^{19}F NMR** (376 MHz, $CDCl_3$) δ –62.81; **^{13}C NMR** (101 MHz, $CDCl_3$) δ 141.7, 141.3, 135.8, 132.8 (q, J = 33.5 Hz), 127.7 – 127.5 (m), 125.5, 124.1, 123.3 (q, J = 273.6 Hz), 123.8, 122.41 – 122.07 (m); **IR** (thin layer film) ν (cm^{-1}) = 2298, 1831, 1601, 1372, 1279, 1176,

1133, 1114, 1077, 943, 907, 872, 845, 819, 735, 705, 683; **MP**: 145–147 °C; **HRMS** (APCI$^-$) *m/z* calculated for $C_{23}H_8ONF_{12}(M–H)^-$ 542.0420, found 542.0207.

(*S*)-1-ethyl-3-(3,3'',5,5''-tetrakis(trifluoromethyl)-[1,1':3',1''-terphenyl]-5'-yl)-1-(2'-(3-(3,3'',5,5''-tetrakis(trifluoromethyl)-[1,1':3',1''-terphenyl]-5'-yl)ureido)-[1,1'-binaphthalen]-2-yl)urea (2.78)



(*S*)-**2.78**

A flame dried 2-neck round bottom flask equipped with a magnetic stirrer and a dropping funnel, was loaded with activated 3 Å powdered molecular sieves (2.3 g) and 5'-isocyanato-3,3",5,5"-tetrakis(trifluoromethyl)-1,1':3',1"-terphenyl **3.24** (45.22 g, 83.2 mmol, 2 equiv) under inert atmosphere. Anhydrous THF was added (280 mL) and the suspension was cooled to 0 °C. At 0 °C anhydrous pyridine (60 mL) was added *via* a syringe, followed by dropwise addition *via* the dropping funnel of a solution of (*S*)-**2.31** (13 g, 41.6 mmol, 1 equiv) in THF (40 mL) over 20 min. The reaction mixture was warmed to rt and stirred for 36 h. After this time, MeOH (50 mL) was added to quench any residual isocyanate and the reaction mixture was stirred for further 15 min, filtered and the solvent removed *in vacuo*. The residue was re-dissolved in CH_2Cl_2 (300 mL), washed with HCl 1 M (2x 200 mL), brine (150 mL), dried over $MgSO_4$ and concentrated to dryness to yield 57.9 g of crude product as an ivory solid. The crude product was dissolved in refluxing heptane (5 mL/g) and EtOH (6 mL/g). The suspension was filtered when hot and cooled slowly to –20 °C to yield 42.02 g of (*S*)-**2.78** as a white solid. The mother liquor was recrystallised from refluxing *n*-heptane (5 mL/g) and EtOH (15 mL/g) at –20 °C to obtain further 9.93 g of (*S*)-**2.78** of comparable purity. The crystallised were combined and a second recrystallisation was performed (refluxing *n*-heptane 5 mL/g and EtOH 1 mL/g, cooling to -20 °C) to afford (*S*)-**2.78** in 56% yield (white solid, 32.7 g). Analytical data were in

agreement with those previously published (see also section 5.2.2.1).[18] R_f = 0.74; pentane:EtOAc = 80:20, visualisation: UV light, λ= 254 nm.

5.3.2 Optimisation of the Recrystallisation of Catalyst (*S*)-2.78

The tests were performed on 100 mg of crude (*S*)-**2.78**, adding 100 μL (corresponding to 1 vol=1 mL/g) of solvent and warming up the mixture to the boiling point. If no dissolution was obtained, the procedure was repeated with addition of further 100 μL of solvent. Additions were stopped when 2 mL (20 mL/g) had been added, and if solubilisation was not attained, the solvent was discarded. When a binary mixture was used, 100 mg of (*S*)-**2.78** were suspended in 0.5 ml (5 mL/g) of Heptane or Cyclohexane and the second solvent added in aliquots of 100 μL (1 mL/g). In those cases where solubilisation was attained, the system was left at rt for 2 h. In absence of precipitation, the system was transferred into an ice bath (0 °C) for further 2 h and subsequently, if still no precipitation had occurred, in the freezer (–20 °C) for overnight. In case of precipitation, the solvent was removed with a syringe, and the crystals washed once with 100 μL of cold heptane (0 °C).

Both the combination of heptane (5 m/g) and $CHCl_3$ (4 mL/g, entry 6, Table 5.6) and heptane (5 mL/g) and EtOH (6 mL/g, entry 8) were suitable for the recrystallisation. The first combination (heptane/$CHCl_3$) had previously been used in the recrystallisation of (*S*)-**2.78** synthesised *via* the quadruple Suzuki-Miyaura cross coupling (Route 3, section 3.3.4), but the product precipitated as a very fine powder, which was difficult to retain during the filtration. Plus, EtOH is a greener solvent compared to $CHCl_3$.[19,20] These considerations led to the selection of a mixture of heptane/EtOH for the crystallisation of catalyst (*S*)-**2.78** (Chapter 3, section 3.3.5).

Table 5.6: Recrystallisation conditons tested

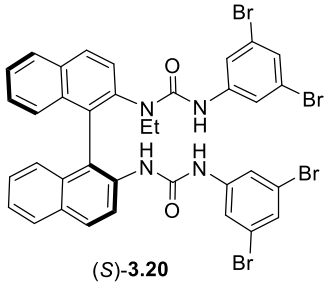
Entry	*Solvent 1 (mL/g)*	*Solvent 2 (mL/g)*	*Dissolves?*	*Does it crystallise? (T)*
1	Toluene (5)	–	Yes	Yes (rt)
				not filterable
2	Toluene (10)	–	Yes	Yes (rt)
				not filterable
3	Toluene (15)	–	Yes	Yes (0 °C)
				not filterable
4	Heptane (20)	–	No	–
5	EtOH (10)[a]	–	Yes	Yes (–20 °C)
				poor yield
6	**Heptane (5)**	**$CHCl_3$ (4)**	**Yes**	**Yes (0 °C)**
7	Heptane (5)	EtOAc (0.5)	No	–
			oil formed	
8	**Heptane (5)**	**EtOH (6)**	**Yes**	**Yes (0 °C)**
9	Heptane (5)	^{i}PrOH (0.7)	Yes	No
10	Heptane (5)	THF (0.3)	Yes	No
11	Heptane (5)	1,4-dioxane (0.4)	Yes	No
12	Cyclohexane (5)	THF (0.1)	Yes	No
13	Cyclohexane (5)	1,4-dioxane (0.15)	Yes	No
14	Cyclohexane (5)	EtOH (0.5)	Yes	No

[a] 2 mL/g were sufficient for dissolving most of the crude. Further addition did not improve the solubilisation and the mixture was filtered through cotton when hot.

5.3.3 Experimental Procedures and Characterisation of Compounds from Chapter 3

5.3.3.1 Bis-urea Organocatalysts

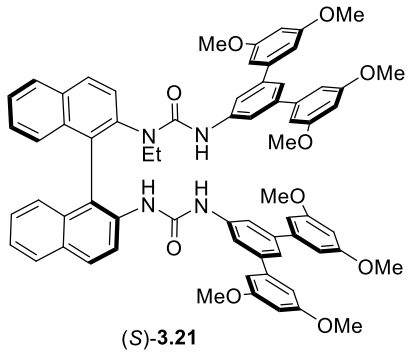
(*S*)-3-(3,5-dibromophenyl)-1-(2'-(3-(3,5-dibromophenyl)ureido)-[1,1'-binaphthalen]-2-yl)-1-ethylurea (3.20)



(*S*)-**3.20**

In a flame-dried two-neck round-bottom flask under inert atmosphere, triphosgene (665 mg, 2.24 mmol, 0.7 equiv) was dissolved in CH_2Cl_2 (32 mL) and cooled to 0 °C. 3,5-Dibromoaniline (1.6 g, 6.4 mmol, 2 equiv) was added as a solid at 0 °C. Then NEt_3 (1.8 mL, 12.8 mmol, 4 equiv) was added dropwise at 0 °C and the reaction mixture was stirred at rt for 2 h under a flow of nitrogen. (*S*)-**2.31** (1 g, 3.2 mmol, 1 equiv) was then added as a solid and the reaction stirred at rt for 24 h (until TLC showed no further conversion). After this time, the reaction was quenched by addition of methanol followed by water and the aqueous phase was extracted with CH_2Cl_2 three times. The combined organic layers were washed with brine, dried over $MgSO_4$ and evaporated *in vacuo*. The crude mixture was then purified by FCC over silica gel (pentane: CH_2Cl_2 = 80:20 to 20:80, gradient) to afford a white solid (2.3 g, 80% yield). **^{1}H NMR** (500 MHz, $CDCl_3$) δ 8.58 (br d, J = 9.1 Hz, 1H), 8.09 (d, J = 8.7 Hz, 1H), 7.99–7.95 (m, 2H), 7.90 (d, J = 8.1 Hz, 1H), 7.57 – 7.42 (m, 4H), 7.41 – 7.30 (m, 4H), 7.30 – 7.17 (m, 4H), 7.11 (s, 1H), 7.07 (d, J = 8.5 Hz, 1H), 6.91 – 6.82 (m, 1H), 6.59 (br s, 1H), 3.17 (dq, J = 14.5, 7.1 Hz, 1H), 3.07 (br s, 1H), 0.96 (t, J = 7.2 Hz, 3H); **^{13}C NMR** (126 MHz, $CDCl_3$) [overlapping signals] δ 156.0, 151.8, 140.8, 139.8, 139.0, 136.1, 133.8, 133.3, 133.2, 131.4, 130.7, 130.0, 129.9, 129.8, 128.7, 128.3, 128.2, 128.0, 127.6, 127.4, 127.2, 126.8, 124.9, 124.5, 123.2, 123.0, 122.4, 120.2, 119.3, 44.4, 13.4; **IR** (thin layer film) ν (cm^{-1}) = 3334, 1635, 1579, 1529, 1507, 1428, 1257, 747; **MP** 196–198 °C; **HRMS** (ESI^+) *m/z* calculated for $C_{36}H_{27}O_2N_4Br_4$ $[M+H]^+$ 862.8873, found 862.8864; **$[\alpha]_D^{25\,°C}$** = –82.4 ° (c = 0.5, $CHCl_3$).

1-ethyl-3-(3,3'',5,5''-tetramethoxy-[1,1':3',1''-terphenyl]-5'-yl)-1-(2'-(3-(3,3'',5,5''-tetramethoxy-[1,1':3',1''-terphenyl]-5'-yl)ureido)-[1,1'-binaphthalen]-2-yl)urea (3.21)

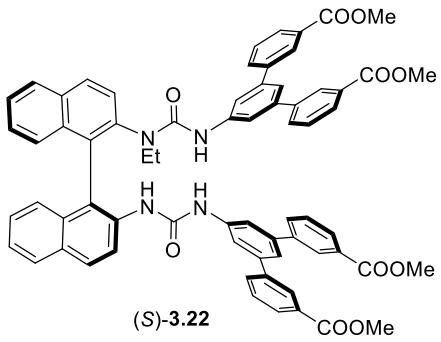


(*S*)-**3.21**

A Schlenk tube equipped with a stirring bar was charged with bis-urea (*S*)-**3.20** (150 mg, 0.17 mmol, 1 equiv), 3,5-bis(OMe)benzylboronic acid (221 mg, 1.21 mmol, 7 equiv), SPhos (14 mg, 0.034 mmol, 0.2 equiv) and K_2CO_3 (160 mg, 0.85 mmol, 5 equiv). The Schlenk was capped with a rubber septum and then evacuated and backfilled with N_2 (this sequence was repeated three times). Degassed THF (1.7 mL) and degassed H_2O (420 μL) (in a 4: 1 ratio, 0.08 M as total concentration of **3.20**) were added *via* a syringe and the reaction mixture was stirred until complete solubilisation of the solids before addition of $Pd(OAc)_2$ (3.8 mg, 0.17 mmol 0.1 equiv). The septum was then replaced by a cooling finger and the reaction mixture was stirred at reflux for 24 h. The reaction mixture was then cooled to rt, diluted with water, and extracted three times with CH_2Cl_2. The combined organic layers were washed with brine, dried over $MgSO_4$ and evaporated *in vacuo*. The crude product was purified by FCC over silica gel (Ist column: pentane:EtOAc = 90:10 to 65:35 gradient; II column: CH_2Cl_2:Et_2O 100% to 95:5, gradient). White solid, 104 mg, 56% yield. **^{1}H NMR** (500 MHz, $CDCl_3$) δ 8.74 (s, 1H), 8.13 (d, *J* = 8.6 Hz, 1H), 8.04 (d, *J* = 9.1 Hz, 1H), 7.99 (d, *J* = 8.1 Hz, 1H), 7.93 (d, *J* = 8.2 Hz, 1H), 7.75 – 7.43 (m, 5H), 7.43 – 7.15 (m, 8H), 6.91 (d, *J* = 8.5 Hz, 1H), 6.59 (d, *J* = 2.3 Hz, 5H), 6.51 (d, *J* = 2.3 Hz, 5H), 6.35 (dt, *J* = 10.9, 2.3 Hz, 4H), 3.77 (s, 12H), 3.74 (s, 12H), 3.31 (br s, 1H), 3.11 (br s, 1H), 1.08 (t, *J* = 7.1 Hz, 3H); **^{13}C NMR** (126 MHz, $CDCl_3$) [overlapping signals] δ 160.8, 160.7, 156.6, 152.5, 143.2, 142.6, 142.3, 142.0, 139.3, 138.9, 137.9, 136.7, 133.8, 133.3, 133.2, 131.7, 130.4, 129.9, 129.6, 128.5, 128.2, 128.1, 127.3, 127.0, 126.9, 124.9, 124.1, 122.8, 120.7, 120.2,

119.7, 117.01 105.4, 105.2, 99.6, 99.3, 55.3, 55.3, 42.6, 12.6. **IR** (thin layer film) ν (cm^{-1}) = 3334, 2969, 2838, 1588, 1548, 1505, 1414, 1269, 1203, 1152, 1063, 828, 750, 694; **MP** 178–179 °C; **HRMS** (ESI^+) *m/z* calculated for $C_{68}H_{63}O_{10}N_4$ $[M+H]^+$ 1095.4539, found 1095.4528; $[\alpha]_D^{25\,°C}$ = –57.6 ° (c = 0.49, $CHCl_3$).

Dimethyl (*S*)-5'-(3-(2'-(3-(3,3''-bis(methoxycarbonyl)-[1,1':3',1''-terphenyl]-5'-yl)-1-ethylureido)-[1,1'-binaphthalen]-2-yl)ureido)-[1,1':3',1''-terphenyl]-3,3''-dicarboxylate (3.22)

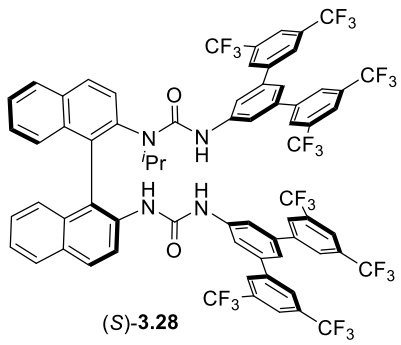


(*S*)-**3.22**

A Schlenk tube, equipped with a stirring bar was charged with bis-urea (*S*)-**3.20** (150 mg, 0.17 mmol, 1 equiv), (3-(methoxycarbonyl)phenyl)boronic acid (218 mg, 1.21 mmol, 7 equiv), SPhos (14 mg, 0.034 mmol, 0.2 equiv) and K_2CO_3 (160 mg, 0.85 mmol, 5 equiv). The Schlenk was capped with a rubber septum and then evacuated and backfilled with N_2 (this sequence was repeated three times). Degassed THF (1.7 mL) and degassed H_2O (420 μL) (in a 4: 1 ratio, 0.08 M as total concentration of **3.20**) were added *via* a syringe and the reaction mixture was stirred until complete solubilisation of the solids before addition of $Pd(OAc)_2$ (3.8 mg, 0.17 mmol 0.1 equiv). The septum was then replaced by a cooling finger and the reaction mixture was stirred at reflux for 24 h. The reaction mixture was then cooled to rt, diluted with water, and extracted three times with CH_2Cl_2. The combined organic layers were washed with brine, dried over $MgSO_4$ and evaporated *in vacuo*. The crude product was purified by FCC over silica gel (Ist column: pentane:EtOAc = 90:10 to 60:40 gradient; II column: CH_2Cl_2:Et_2O 100% to 98:2, gradient). White solid, 120 mg, 65% yield. **^{1}H NMR** (500 MHz, $CDCl_3$) δ 8.81 (br d, *J* = 9.2 Hz, 1H), 8.18 – 8.11 (br d, *J* = 9.2 Hz, 1H), 8.10 – 7.81 (m, 11H), 7.65 (d, *J* = 8.7 Hz, 1H), 7.59 – 7.36 (m, 10H), 7.35 – 7.12 (m, 11H), 6.90 (d, *J* = 8.5 Hz, 1H), 6.77 (s, 1H), 3.92 (s, 6H),

3.89 (s, 6H), 3.42 – 3.25 (m, 1H), 3.08 (s, 1H), 1.08 (t, *J* = 7.1 Hz, 3H); **^{13}C NMR** (126 MHz, $CDCl_3$) δ 166.9, 166.8, 156.5, 152.4, 141.5, 141.0, 140.9, 140.0, 139.6, 139.1, 138.5, 136.5, 133.9, 133.3, 133.2, 132.5, 131.7, 131.5, 131.4, 130.5, 130.4, 130.3, 129.8, 129.7, 128.7, 128.6, 128.5, 128.5, 128.4, 128.4, 128.2, 128.1, 127.9, 127.3, 127.1, 126.9, 126.8, 124.9, 124.2, 122.2, 120.4, 119.3, 118.4, 116.8, 52.2, 52.1, 44.0, 13.5. **IR** (thin layer film) ν (cm^{-1}) = 3374, 2951, 1721, 1599, 1582, 1551, 1504, 1434, 1287, 1224, 1115, 1085, 988, 865, 816, 754, 693; **MP** 187 – 190 °C; **HRMS** (ESI^+) *m/z* calculated for $C_{68}H_{55}O_{10}N_4$ $[M+H]^+$ 1087.3913, found 1087.3899; **$[\alpha]_D^{25\,°C}$** = –67.5 ° (c = 0.46, $CHCl_3$).

1-isopropyl-3-(3,3'',5,5''-tetrakis(trifluoromethyl)-[1,1':3',1''-terphenyl]-5'-yl)-1-(2'-(3-(3,3'',5,5''-tetrakis(trifluoromethyl)-[1,1':3',1''-terphenyl]-5'-yl)ureido)-[1,1'-binaphthalen]-2-yl)urea (3.28)



(*S*)-**3.28**

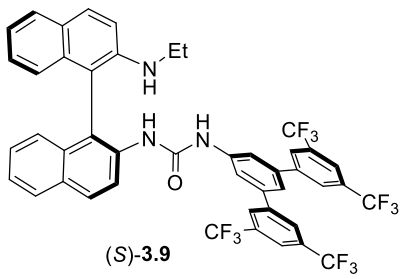
A flame dried Schlenk tube, was loaded with activated 3 Å powdered molecular sieves (20 mg) and isocyanate **3.24** (309 mg, 0.569 mmol, 2 equiv) under inert atmosphere. Anhydrous THF was added (2 mL) and the suspension was cooled to 0 °C. At 0 °C anhydrous pyridine (800 μL) was added, followed by dropwise addition of a solution of (*S*)-*N*^{2}-isopropyl-[1,1'-binaphthalene]-2,2'-diamine **2.29** (100 mg, 0.284 mmol, 1 equiv) in THF (400 μL). The reaction mixture was warmed to rt and stirred for 72 h. After this time, MeOH was added to quench any residual isocyanate and the reaction mixture was stirred for further 15 min, filtered and the solvent removed in *vacuo*. Purification by FCC (pentane: EtOAc = 100% to 90:10, gradient) afforded the title compound as a white solid (188 mg, 45% yield). **^{1}H NMR** (500 MHz, $CDCl_3$) *δ* 8.40 (br s, 1H), 8.15 (d, *J* = 8.7 Hz, 1H), 8.10 (d, *J* = 9.0 Hz, 1H), 8.03 (d, *J* = 8.1 Hz, 1H), 7.96 (d, *J* = 8.2 Hz, 1H), 7.81 (d, *J* = 1.6 Hz, 4H), 7.75 (s, 2H), 7.73 (s, 6H), 7.63 (d, *J* = 8.7 Hz, 1H), 7.59 (ddd, *J* = 8.2, 6.8, 1.2 Hz,

1H), 7.54 (s, 2H), 7.46 (ddd, *J* = 8.1, 6.8, 1.1 Hz, 1H), 7.36 (ddd, *J* = 8.3, 6.8, 1.3 Hz, 1H), 7.32 – 7.27 (m, 4H), 7.23 (d, *J* = 8.5 Hz, 1H), 7.16 (br s, 1H, N**H**), 7.13 (s, 1H), 7.00 (s, 1H), 6.96 (d, *J* = 8.5 Hz, 1H), 6.62 (s, 1H, N**H**), 3.55 (br s, 1H), 1.19 (d, *J* = 6.8 Hz, 3H), 0.74 – 0.61 (m, 3H). **^{19}F NMR** (471 MHz, $CDCl_3$) δ –63.00, –63.02. **^{13}C NMR** (126 MHz, $CDCl_3$) [overlapping signals] δ 155.6 (br), 152.7, 142.1, 141.6, 139.9, 139.8, 139.7, 139.6, 139.5, 134.9 (br), 133.9, 133.4, 133.0, , 132.2 (q, $J_{C–F}$= 33.7 Hz), 132.2, 132.1 (q $J_{C–F}$= 33.5 Hz), 131.0 (br), 130.7, 130.4, 128.8 (br), 128.6, 128.4, 128.0, 127.7, 127.3, 127.1–127.0 (m), 126.9–126.8 (m), 126.7, 125.6, 125.3 (br), 123.1 (q, $J_{C–F}$= 273.0 Hz), 123.0 (q, $J_{C–F}$= 273.0 Hz), 121.6–121.4 (m), 121.4–121.2 (m), 120.8 (br), 120.3 (br), 120.1, 118.3, 54.5 (br), 20.9, 20.0 (br). **IR** (thin layer film) ν (cm^{-1}) = 3327, 365, 2936, 1680, 1623, 1599, 1546, 1508, 1469, 1428, 1367, 1276,1174, 1127, 901, 844, 734, 705, 683, 639; **MP** 196 – 198 °C; **HRMS** (ESI^+) *m/z* calculated for $C_{69}H_{41}F_{24}O_2N_4$ $[M+H]^+$ 1413.2841, found 1413.2780; **$[\alpha]_D^{25\,°C}$** = –133.0 ° (c = 0.5, $CHCl_3$).

*5.3.3.2 Characterisation of the Impurities Contaminating (S)-**2.78***

Characterisation of the impurities obtained in the urea formation step in the synthesis of catalyst (S)-**2.78** according to route 3 (the isocyanate route, Chapter 3, section 3.3.5)

(*S*)-1-(2'-(ethylamino)-[1,1'-binaphthalen]-2-yl)-3-(3,3'',5,5''-tetrakis(trifluoromethyl)-[1,1':3',1''-terphenyl]-5'-yl)urea (3.9)

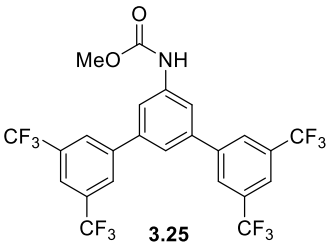


(*S*)-**3.9**

A sample reference of (*S*)-**3.9** was independently synthesised stirring (*S*)-**2.31** (100 mg, 0.32 mmol, 1 equiv) and 5'-isocyanato-3,3",5,5"-tetrakis(trifluoromethyl)-1,1':3',1"-terphenyl **3.24** (174 mg, 0.32 mmol, 1 equiv) in anhydrous CH_2Cl_2 at rt for overnight. After this time, MeOH was added and the reaction

mixture was stirred for further 15 min at rt. Volatiles were removed *in vacuo* and the crude product was purified by FCC on silica gel (eluent pentane:EtOAc = 100:0 to 95:5, gradient) to afford a white solid (218.5 mg, 80% yield). **^{1}H NMR** (500 MHz, $CDCl_3$) δ 8.48 (d, *J* = 9.0 Hz, 1H), 8.01 (d, *J* = 9.1 Hz, 1H), 7.95 (d, *J* = 1.6 Hz, 4H), 7.91 – 7.87 (m, 3H), 7.85 (d, *J* = 9.0 Hz, 1H), 7.75 – 7.70 (m, 1H), 7.53 (d, *J* = 1.6 Hz, 2H), 7.41 (ddd, *J* = 8.1, 6.7, 1.2 Hz, 1H), 7.35 (t, *J* = 1.7 Hz, 1H), 7.28 – 7.13 (m, 4H), 7.08 (d, *J* = 8.4 Hz, 1H), 6.88 – 6.82 (m, 1H), 6.74 (s, 1H), 6.55 (s, 1H), 3.61 (br s, 1H), 3.18 (q, *J* = 7.1 Hz, 2H), 1.00 (t, *J* = 7.1 Hz, 3H); **^{19}F NMR** (471 MHz, $CDCl_3$) δ –62.74; **^{13}C NMR** (126 MHz, $CDCl_3$) [overlapping signals] δ 152.8, 144.2-(br), 142.4, 140.4, 140.0, 135.6, 133.8, 132.8, 132.4 (q, $J_{C–F}$ = 33.5 Hz), 131.2, 130.5, 129.8, 128.4, 128.3, 127.7 (br), 127.5, 127.2, 125.2, 124.6, 123.6, 123.3 (q, $J_{C–F}$ =273.5 Hz), 122.5 (br), 122.1, 121.9 (m), 121.3, 120.7, 120.0, 119.5, 114.3, 38.8, 15.0. **IR** (thin layer film) ν (cm^{-1}) = 3355, 3058, 2972, 1669, 1598, 1504, 1367, 1277, 1176, 1132, 706, 683; **MP** 145–146 °C; **HRMS** (ESI^+) *m/z* calculated for $C_{45}H_{30}F_{12}ON_3$ $[M+H]^+$ 856.2192, found 856.2180; **[α]$_D^{25\,°C}$** = –82.8° (c = 0.6, $CHCl_3$).

methyl (3,3'',5,5''-tetrakis(trifluoromethyl)-[1,1':3',1''-terphenyl]-5'-yl)carbamate (3.25)

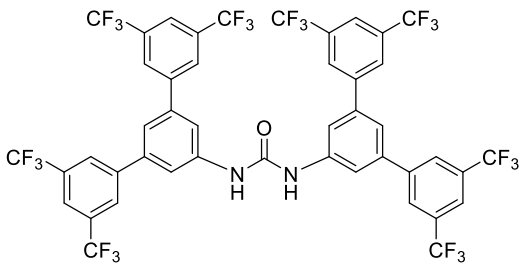


3.25

A sample reference of **3.25** was independently synthesised stirring isocyanate **3.24** (10 mg, 0.018 mmol) in anhydrous MeOH at rt for overnight. Volatiles were removed *in vacuo* to afford a white solid. **^{1}H NMR** (500 MHz, $CDCl_3$) δ 8.06 (s, 4H), 7.94 (s, 2H), 7.76 (s, 2H), 7.46 (d, *J* = 1.8 Hz, 1H), 6.91 (s, 1H), 3.87 (s, 3H). **^{19}F NMR** (470 MHz, $CDCl_3$) δ –62.75. The compound is poorly soluble in $CDCl_3$, so it was not possible to record a ^{13}C NMR spectrum in this solvent. THF-d_8 is a more suitable solvent. **^{1}H NMR** (500 MHz, THF-d_8) δ 9.12 (s, 1H), 8.33 (d, *J* = 1.7 Hz, 4H), 8.10 (s, 2H), 7.99 (d, *J* = 1.6 Hz, 2H), 7.80 (t, *J* = 1.6 Hz, 1H), 3.79 (s, 3H). **^{19}F NMR** (471 MHz, THF-d_8) δ

–63.53. **^{13}C NMR** (126 MHz, THF-d_8) δ 154.0, 143.3, 141.4, 139.8, 131.9 (q, $J_{C–F}$ = 33.1 Hz), 127.6, 123.6 (q $J_{C–F}$ = 273.0 Hz), 121.3–121.0 (m), 120.3, 117.1, 51.4. **IR** (thin layer film) ν (cm^{-1}) 1711, 1605, 1545, 1473, 1367, 1277, 1233, 1173, 1130, 1070, 900, 869, 845, 704, 683. **MP** 324–325 ° C; **HRMS** (ESI^-) *m/z* calculated for $C_{24}H_{12}F_{12}O_2N$ $[M–H]^–$ 574.0682, found 574.0685.

1,3-bis(3,3'',5,5''-tetrakis(trifluoromethyl)-[1,1':3',1''-terphenyl]-5'-yl)urea (3.26)

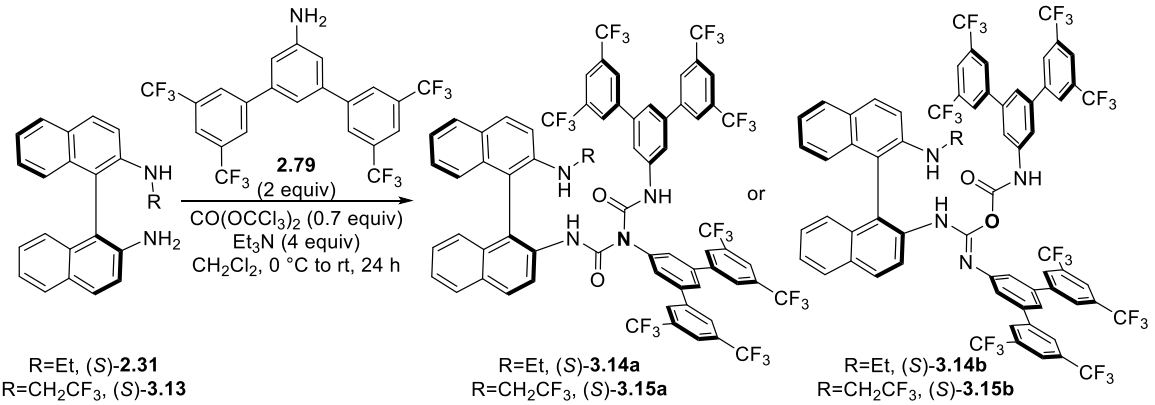


3.26

A sample reference of **3.26** was independently synthesised stirring aniline **2.79** (10 mg, 0.019 mmol, 1 equiv) and isocyanate **3.24** (10.5 mg, 0.019 mmol, 1 equiv) in anhydrous CH_2Cl_2 at rt for overnight. Volatiles were removed *in vacuo* and the crude product was purified by FCC (pentane:EtOAc = 95:5 then Acetone 100%) to afford a white solid. **^{1}H NMR** (400 MHz, Acetone) δ 8.88 (s, 1H), 8.21 (s, 4H), 7.95 (d, *J* = 1.7 Hz, 2H), 7.90 (s, 2H), 7.81 (q, *J* = 1.5 Hz, 1H); **^{19}F NMR** (377 MHz, Acetone) δ -63.28; **^{13}C NMR** (101 MHz, Acetone) δ 152.8, 143.1, 141.6, 139.4, 131.7 (q, $J_{C–F}$ = 33.2 Hz), 127.7, 123.5 (q, $J_{C–F}$ = 271.6 Hz), 121.1, 120.4, 117.9; **IR** (thin layer film) ν (cm^{-1}) 3329, 1660, 1614, 1574, 1392, 1366, 1279, 1177, 1137; **MP** It does not melt below 300 °C; **HRMS** (ESI^+) *m/z* calculated for $C_{45}H_{21}F_{24}ON_2$ $[M+H]^+$ 1061.1265, found 1061.1267.

5.3.3.3 Characterisation of Side-Products (S)-3.14–(S)-3.16

Characterisation of the side-products obtained in the synthesis of catalyst (S)-**2.78** according to the one-pot-two-step protocol involving in situ generation of the isocyanate (Chapter 3, section 3.3.1)



Synthesis: In a flame-dried Schlenk tube under inert atmosphere, triphosgene (0.7 equiv) was dissolved in CH_2Cl_2 (0.1 M with respect to the chiral BINAM-derived aniline). The solution was cooled to 0 °C and **2.79** (2 equiv) was added at this temperature. Then NEt_3 (4 equiv) was added dropwise at 0 °C and the reaction mixture was stirred at rt for 2 h under a flow of nitrogen. After disappearance of **2.79** (monitored by TLC from a sample of the reaction mixture quenched with a drop of MeOH; eluent: pentane/EtOAc), the (*S*)-BINAM-derived aniline (1 equiv) was added as a solid and the reaction stirred at rt for 24 h (until TLC showed no further conversion). An excess of MeOH was added and the reaction mixture stirred for further 5 min. Water was then added and the layers were separated. The aqueous one was extracted twice with CH_2Cl_2. The combined organic layers were washed with brine, dried over $MgSO_4$ and evaporated *in vacuo*. The crude mixture was. then purified by FCC on silica gel.

(*S*)-3.14

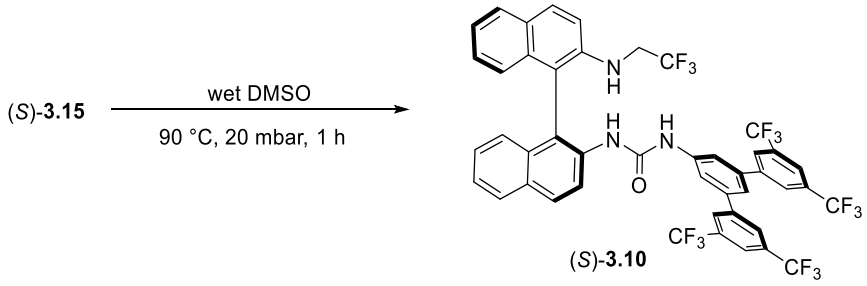
(*S*)-**3.14** is the main product of the reaction between chiral amine (*S*)-**2.31** and 2 equiv of achiral amine **2.79** according to the one-pot-two-step protocol with *in situ* generation of the isocyanate. **^{1}H NMR** (400 MHz, $CDCl_3$) δ 11.93 (s, 1H), 8.57 (d, *J* = 9.1 Hz, 1H), 8.10 (d, *J* = 9.1 Hz, 1H), 8.02 (d, *J* = 1.6 Hz, 4H), 8.00 (br s, 4H), 7.94 (d, *J* = 8.2, 1H), 7.91 – 7.88 (m, 2H), 7.87 (d, *J* = 1.6 Hz, 2H), 7.82 (bs s, 2H), 7.62 (t, *J* = 1.7 Hz, 1H), 7.47 (t, *J* = 1.7 Hz, 1H), 7.44 (td, *J* = 7.6, 1.2 Hz, 1H), 7.39–7.01 (m, 5H), 6.97 – 6.90 (m, 2H), 6.87 (td, *J* = 7.4, 1.3 Hz, 1H), 6.81 (d, *J* = 9.0 Hz, 1H), 6.63 (s, 1H), 6.58 (dd, *J* = 8.5, 1.1 Hz, 1H), 3.25 (br s, 1H), 3.09 – 2.92 (m, *J* = 6.8 Hz, 2H), 0.88 (t, *J* = 7.1 Hz, 3H). **^{19}F NMR** (377 MHz, $CDCl_3$) δ –62.62, –62.71.

(*S*)-3.15

(*S*)-**3.15** is the main product of the reaction between chiral amine (*S*)-**3.13** and 2 equiv of achiral amine **2.79** according to the one-pot-two-step protocol with *in situ* generation of the isocyanate. *Spectra in $CDCl_3$:* **^{1}H NMR** (500 MHz, $CDCl_3$) δ 11.87 (s, 1H, N**H**), 8.45 (d, *J* = 9.1 Hz, 1H), 8.12 (d, *J* = 9.1 Hz, 1H), 8.04 – 7.73 (m, 15H) 7.51 (t, *J* = 1.7 Hz, 1H), 7.50 – 7.43 (m, 2H), 7.29 – 7.23 (m, 2H), 7.18 (d, *J* = 9.0 Hz, 1H), 7.14 – 6.85 (m, 6H), 6.63 (dd, *J* = 8.3, 1H), 6.38 (s, 1H, N**H**), 3.84 (dp, *J* = 16.5, 8.3 Hz, 1H), 3.68 (dd, *J* = 8.6, 6.1 Hz, 1H, N**H**), 3.56 – 3.43 (m, 1H). **^{19}F NMR** (471 MHz, $CDCl_3$) δ –62.67, –62.71, -72.22 (t, *J* = 8.7 Hz). **^{13}C NMR** (126 MHz, $CDCl_3$) [overlapping signals] δ 154.40, 152.22, 142.53, 141.92, 140.65, 140.4 (br), 139.71, 137.30, 133.89, 132.6, 132.5 (q, *J* = 33.6 Hz), 132.4 (q, *J* = 33.6 Hz), 132.3, 131.77, 130.56, 130.12, 128.52, 128.00, 127.94 (br), 127.82, 127.68, 127.63, 127.60, 127.54, 126.36, 126.27, 125.04, 124.8 (q, *J* = 282.3 Hz), 123.3 (q, *J*= 272.9), 123.24, 122.78, 122.30 (br), 122.03, 121.77 (p, *J* = 3.7 Hz), 121.47, 120.87, 119.17, 113.03, 111.31, 45.04 (q, *J* = 33.1 Hz). *Spectra in THF-d_8*

^{1}H NMR (400 MHz, THF) δ 11.63 (s, 1H, N**H**), 8.52 (d, *J* = 9.1 Hz, 1H), 8.19 (s, 4H), 8.08 (s, 4H), 8.02 (s, 2H), 8.00 – 7.95 (m, 3H), 7.93 (s, 2H), 7.91 (d, *J* = 1.7 Hz, 1H), 7.82 (d, *J* = 8.2 Hz, 1H), 7.69 (d, *J* = 1.7 Hz, 1H), 7.38 (d, *J* = 1.7 Hz, 2H), 7.27 (t, *J* = 7.5 Hz, 1H), 7.21 (d, *J* = 8.2 Hz,1H), 7.19 (d, *J* = 9.2 Hz, 1H), 7.07 (t, *J* = 7.7 Hz, 1H), 6.92 (d, *J* = 9.0 Hz, 1H), 6.83 – 6.70 (m, 3H), 6.66 (s, 1H, N**H**), 6.44 (d, *J* = 8.1 Hz, 1H), 4.53 (t, *J* = 7.2 Hz, 1H, N**H**), 3.79 – 3.63 (m, 1H), 3.56 – 3.49 (m, 1H). **HRMS** (ESI^+) *m/z* calculated for $C_{68}H_{36}F_{27}O_2N_4$ $[M+H]^+$ 1453.2402, found 1453.2364.

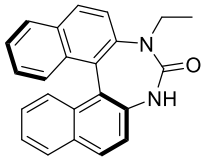
*Degradation product from (S)-**3.15***



(*S*)-**3.15** was dissolved in wet DMSO-d_6. Evaporation of the solvent *in vacuo* (90 °C) led to formation of (*S*)-**3.10**. *Spectra in $CDCl_3$:* **^{1}H NMR** (400 MHz, $CDCl_3$) δ 8.35 (d, *J* = 9.0 Hz, 1H), 7.92 (d, *J* = 8.7 Hz, 1H), 7.84 (d, *J* = 1.6 Hz, 4H), 7.82–7.77 (m, 3H), 7.75 (d, *J* = 9.0 Hz, 1H), 7.61 (d, *J* = 7.4 Hz, 1H), 7.37 (s, 2H), 7.31 (t, *J* = 7.6 Hz, 1H), 7.27 (s, 1H), 7.21 – 7.04 (m, 4H), 6.94 (d, *J* = 8.5 Hz, 1H), 6.81 (d, *J* = 7.8 Hz, 1H), 6.68 (s, 1H), 6.37 (s, 1H), 3.86 (t, *J* = 7.3 Hz, 1H), 3.76 (dd, *J* = 16.0, 7.8 Hz, 1H), 3.50 (dd, *J* = 16.1, 6.3 Hz, 1H). **^{19}F NMR** (377 MHz, $CDCl_3$) δ –62.77 (d, *J* = 2.1 Hz, 12F), –72.35 (t, *J* = 8.8 Hz, 3F). *Spectra in THF-d_8:* **^{1}H NMR** (500 MHz, THF-d_8) δ 8.96 (s, 1H N**H**), 8.91 (d, *J* = 9.1 Hz, 1H), 8.37 (s, 4H), 8.16 (s, 2H), 8.12 (d, *J* = 9.3 Hz, 1H), 8.11 (d, *J* = 9.2 Hz, 1H), 8.01 (d, *J* = 8.1 Hz, 1H), 7.96 (d, *J* = 8.0, 1H), 7.92 (d, *J* = 1.6 Hz, 2H), 7.80 (t, *J* = 1.7 Hz, 1H), 7.63 (d, *J* = 9.0 Hz, 1H), 7.44 (ddd, *J* = 8.1, 6.8, 1.2 Hz, 1H), 7.36 – 7.24 (m, 3H), 7.12 – 7.09 (d, *J* = 8.1 Hz, 1H), 7.08 (s, 1H, N**H**) 7.02 – 6.97 (d, *J* = 8.0 Hz, 1H), 4.99 (t, *J* = 7.2

Hz, 1H, N**H**), 4.15 (m, 1H), 4.01 – 3.88 (m, 1H). **^{19}F NMR** (471 MHz, THF-d_8) δ -63.51 (12F), –72.95 (3F); **^{13}C NMR** (126 MHz, THF-d_8) δ 152.4, 143.5, 143.4, 142.0, 139.6, 137.0, 134.2, 133.1, 131.8 (q, J = 33.1 Hz), 130.8, 129.9, 128.6, 128.2, 128.0, 127.8, 127.6–127.4 (m), 126.9, 126.2, 125.5 (q, J= 281. 3 Hz), 124.8, 124.1, 123.6 (q, J = 273.2 Hz) 123.6, 122.2, 121.25 – 120.94 (m), 120.7, 119.6, 118.4, 117.2, 113.7, 111.4, 44.1 (q, J = 33.0 Hz). **HRMS** (ESI$^+$) *m/z* calculated for $C_{45}H_{27}F_{15}ON_3$ $[M+H]^+$ 910.1909, found 910.1906.

(*S*)-3-ethyl-3,5-dihydro-4H-dinaphtho[2,1-d:1',2'-f][1,3]diazepin-4-one (3.16)



(*S*)-**3.16**

(*S*)-**3.16** was independently synthesised stirring (*S*)-**2.31** (100 mg, 0.32 mmol, 1 equiv) and triphosgene (33 mg, 0.112 mmol, 0.35 equiv) with Et_3N (90 μL, 0.64 mmol, 2 equiv.) in anhydrous CH_2Cl_2 at rt for overnight. After this time, volatiles were removed *in vacuo* and the crude product was purified by FCC on silica gel (eluent pentane:EtOAc = 100:0 to 70:30, gradient) to afford a white solid. **^{1}H NMR** (500 MHz, $CDCl_3$) δ 7.96 (d, J = 9.0 Hz, 1H), 7.93–7.88 (m, 3H), 7.53 (d, J = 8.9 Hz, 1H), 7.47–7.41 (m, 2H), 7.39 (d, J = 8.5 Hz, 1H), 7.32–7.25 (m, 2H), 7.25 – 7.16 (m, 2H), 6.86 (s, 1H, N**H**), 4.18 (dq, J = 14.0, 7.0 Hz, 1H), 3.77 (dq, J = 14.0, 7.0 Hz, 1H), 1.10 (t, J = 7.2 Hz, 3H). **^{13}C NMR** (126 MHz, $CDCl_3$) δ 166.6, 141.8, 141.0, 132.4, 131.8, 131.4, 130.8, 129.4, 129.4, 128.1, 128.0, 128.0, 127.5, 127.2, 126.3, 126.2, 125.5, 124.8, 123.1, 121.2, 120.8, 41.9, 13.6. **HRMS** (ESI$^+$) *m/z* calculated for $C_{23}H_{19}ON_2$ $[M+H]^+$ 339.1492, found 339.1493.

5.3.4 Copy of the NMR Spectra Used in the Assignment of (*S*)-3.14-3.16

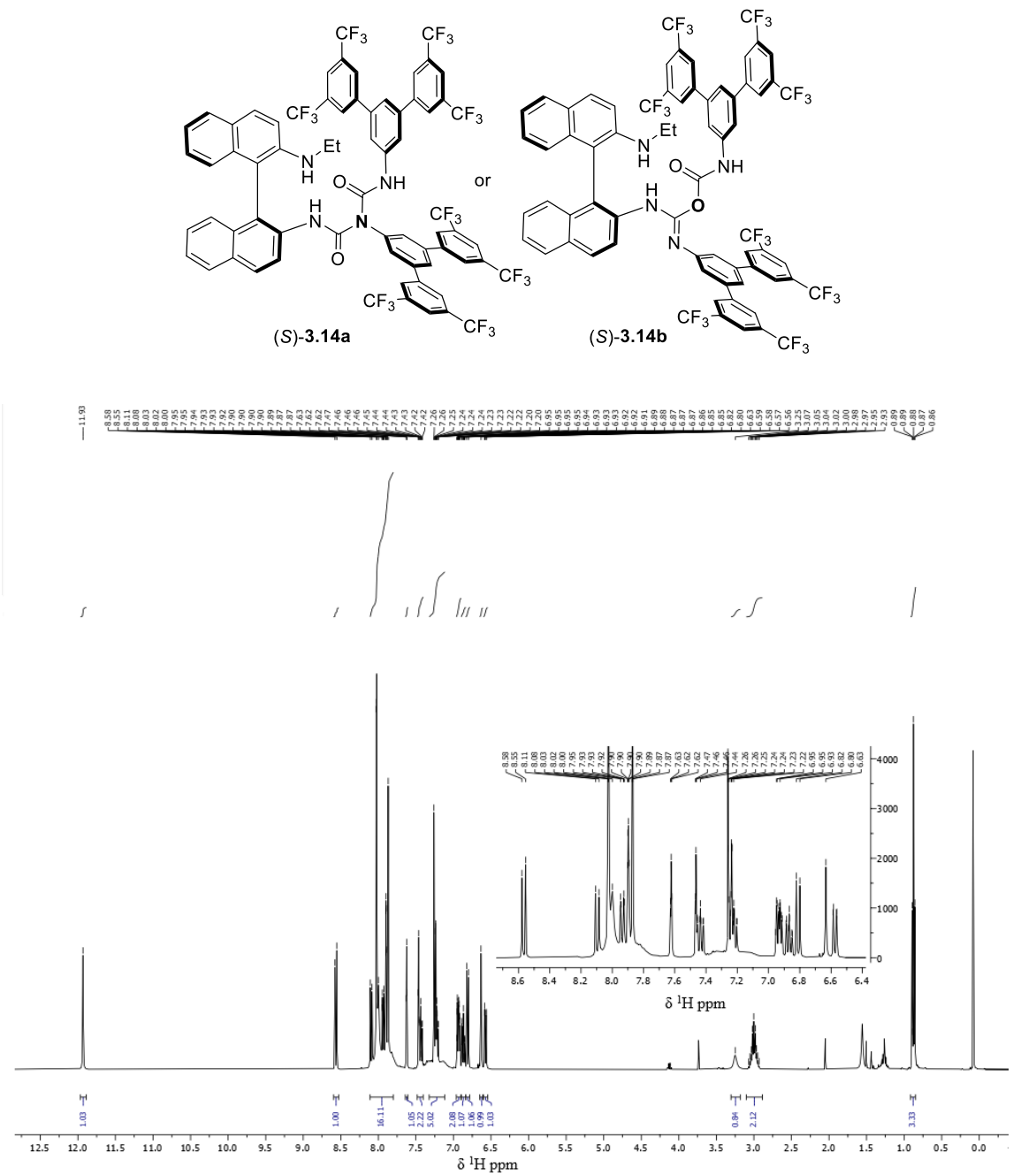


Figure 5.1: ^{1}H NMR spectrum of (*S*)-**3.14** in $CDCl_3$.

Spectra in $CDCl_3$

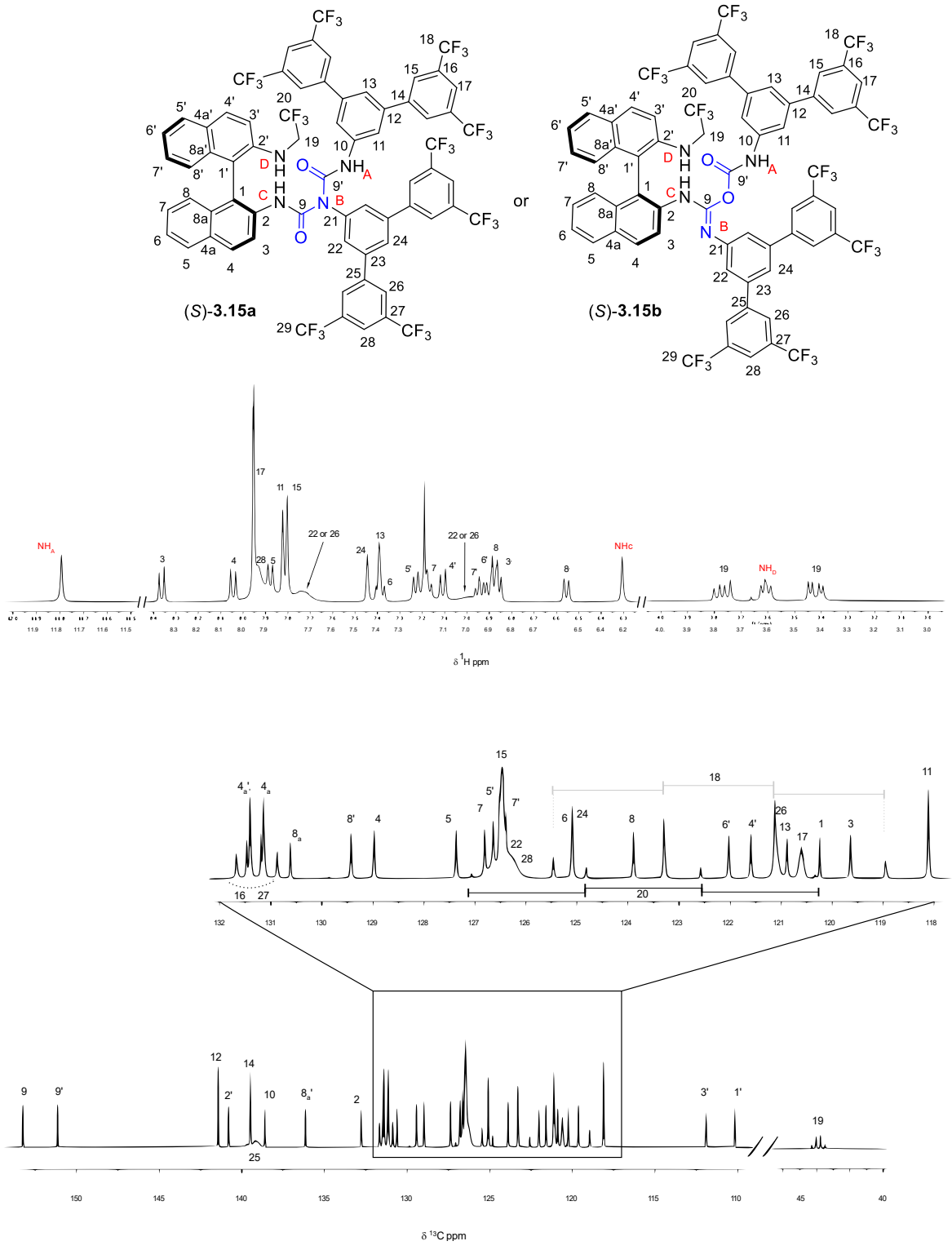


Figure 5.2: ^{1}H NMR and ^{13}C NMR spectra of (*S*)-**3.15** ($CDCl_3$).

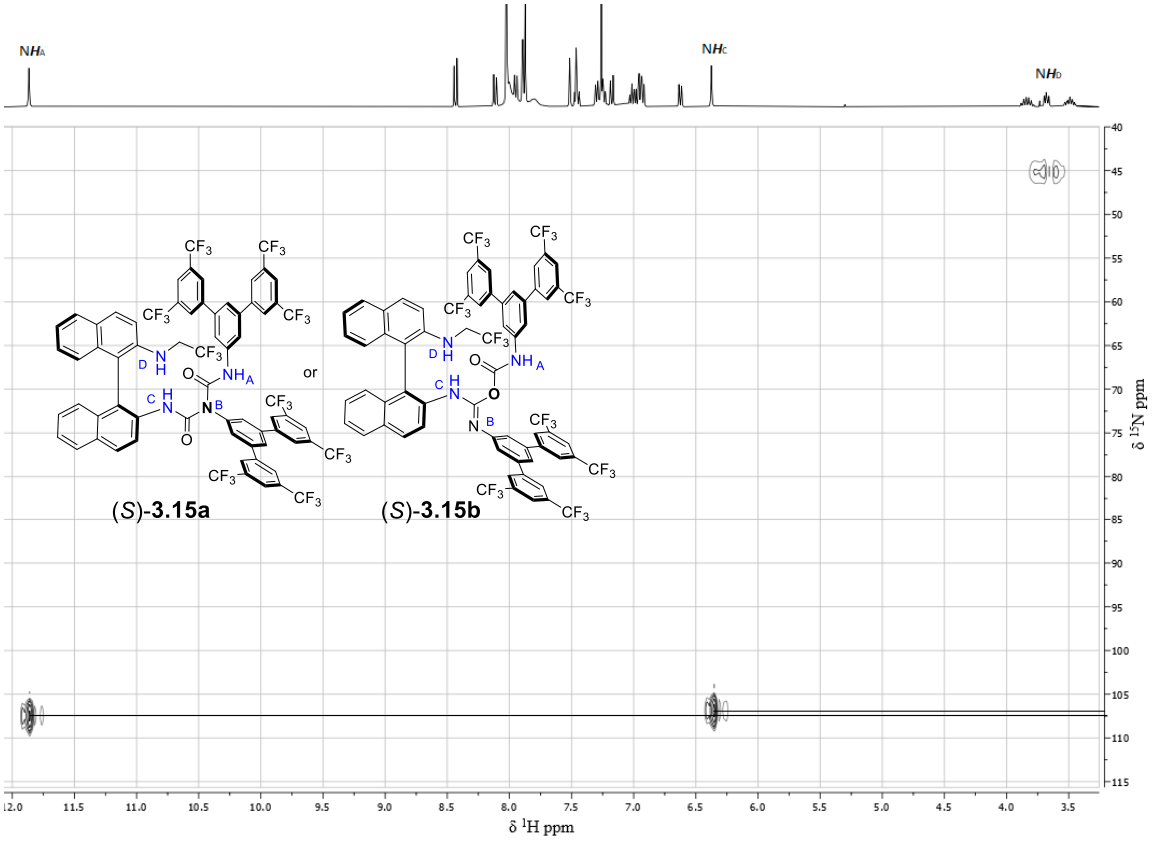


Figure 5.3: ^{1}H-^{14}N HSQC of (*S*)-**3.15** ($CDCl_3$).

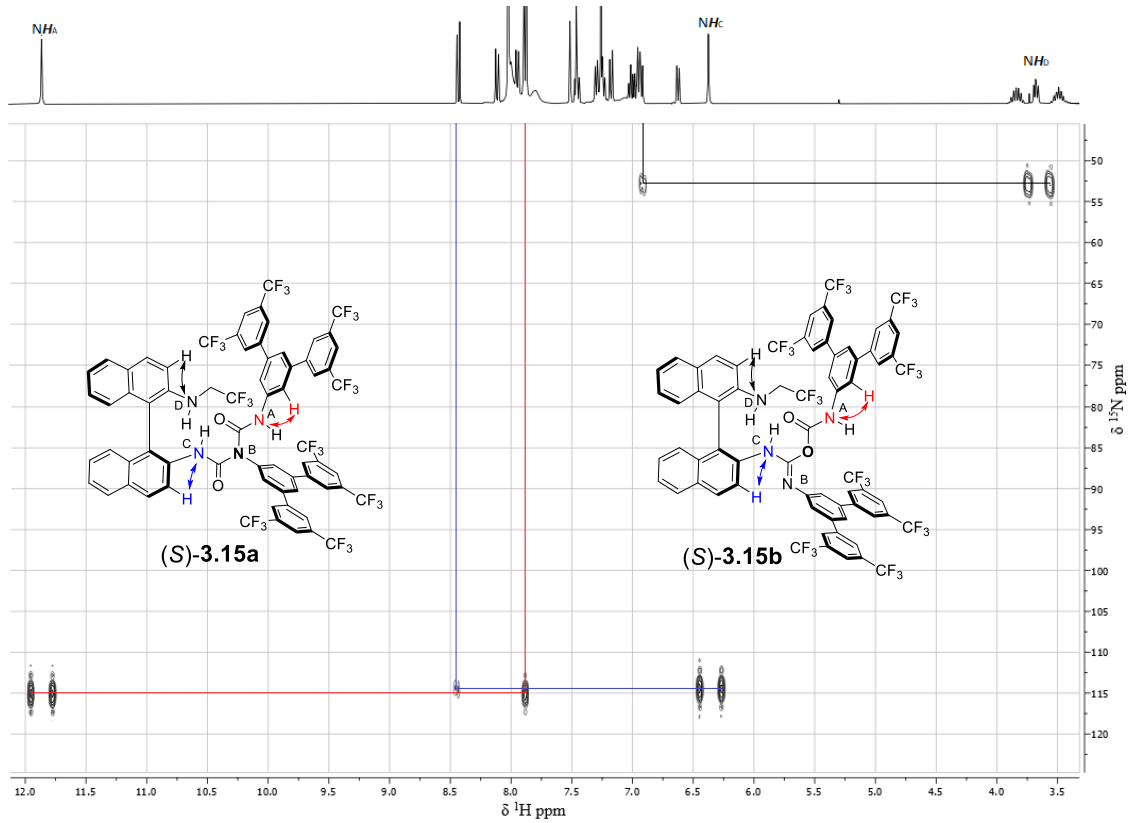


Figure 5.4: ^{1}H-^{14}N HMBC of (*S*)-**3.15** ($CDCl_3$).

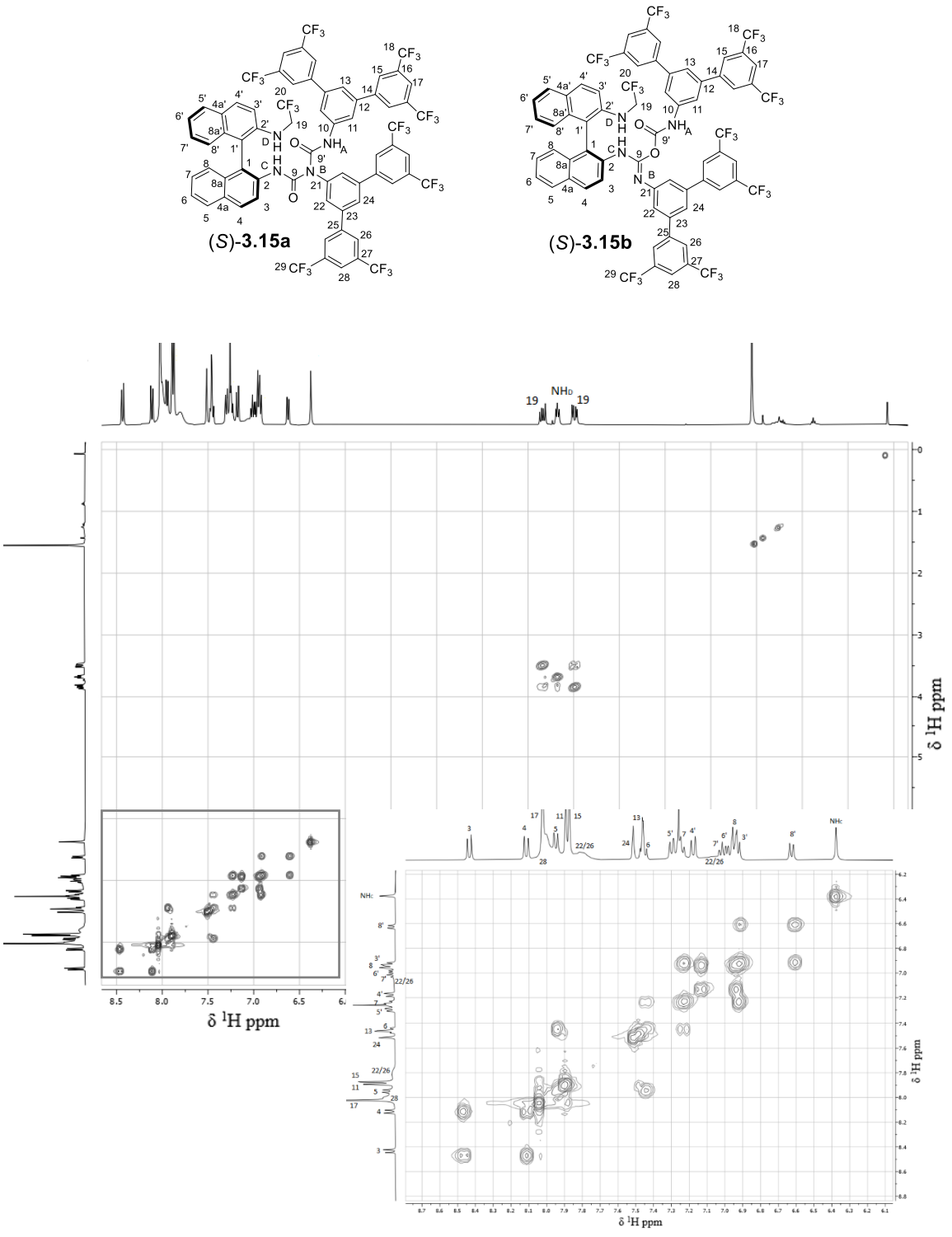


Figure 5.5: COSY of (*S*)-**3.15**($CDCl_3$).

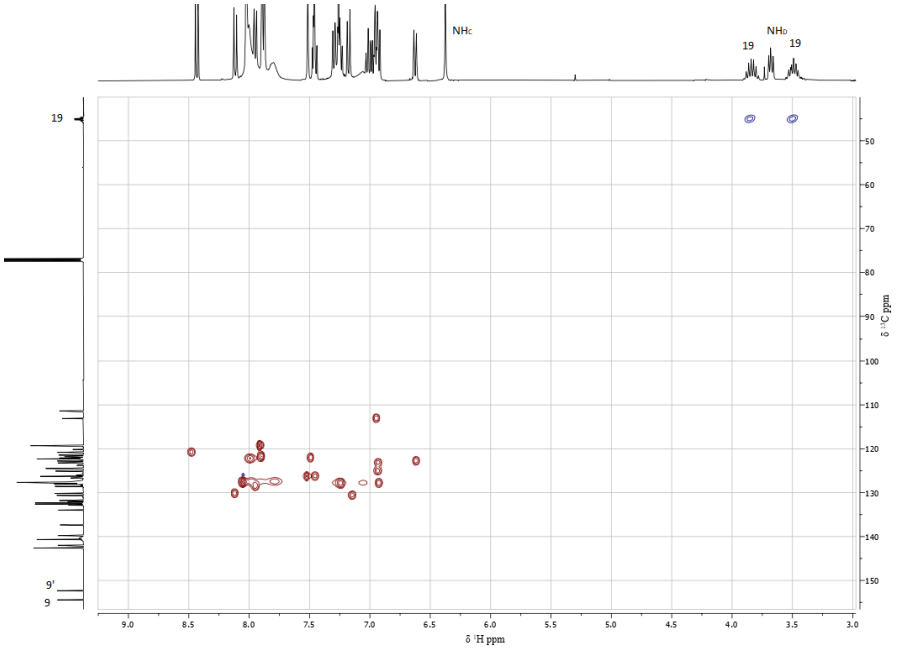


Figure 5.6: ^{1}H-^{13}C HSQC of (*S*)-**3.15** ($CDCl_3$).

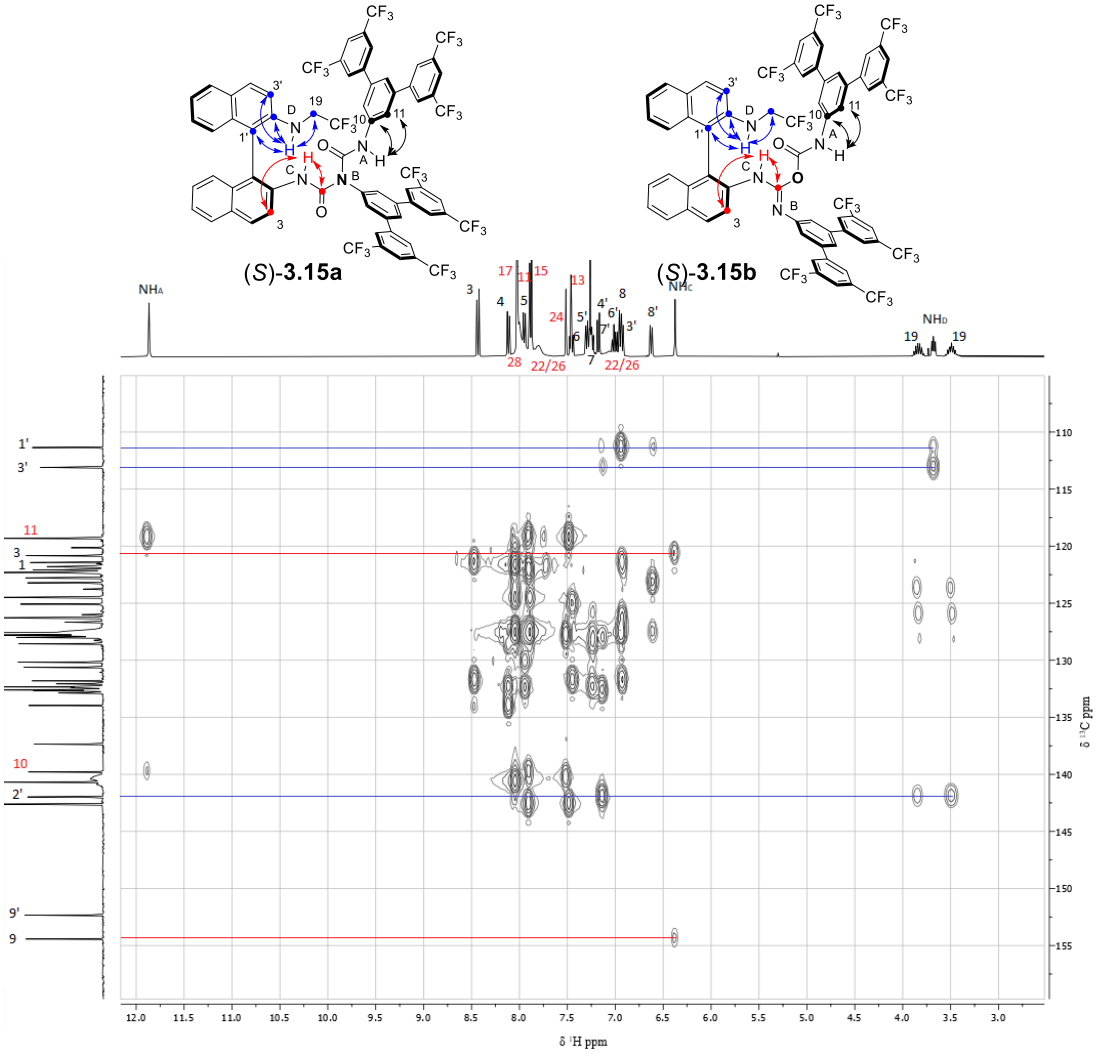


Figure 5.7: ^{1}H-^{13}C HMBC of (*S*)-**3.15** ($CDCl_3$). Black numbering: signals of the BINAM scaffold; red numbering: signals of the terphenyl.

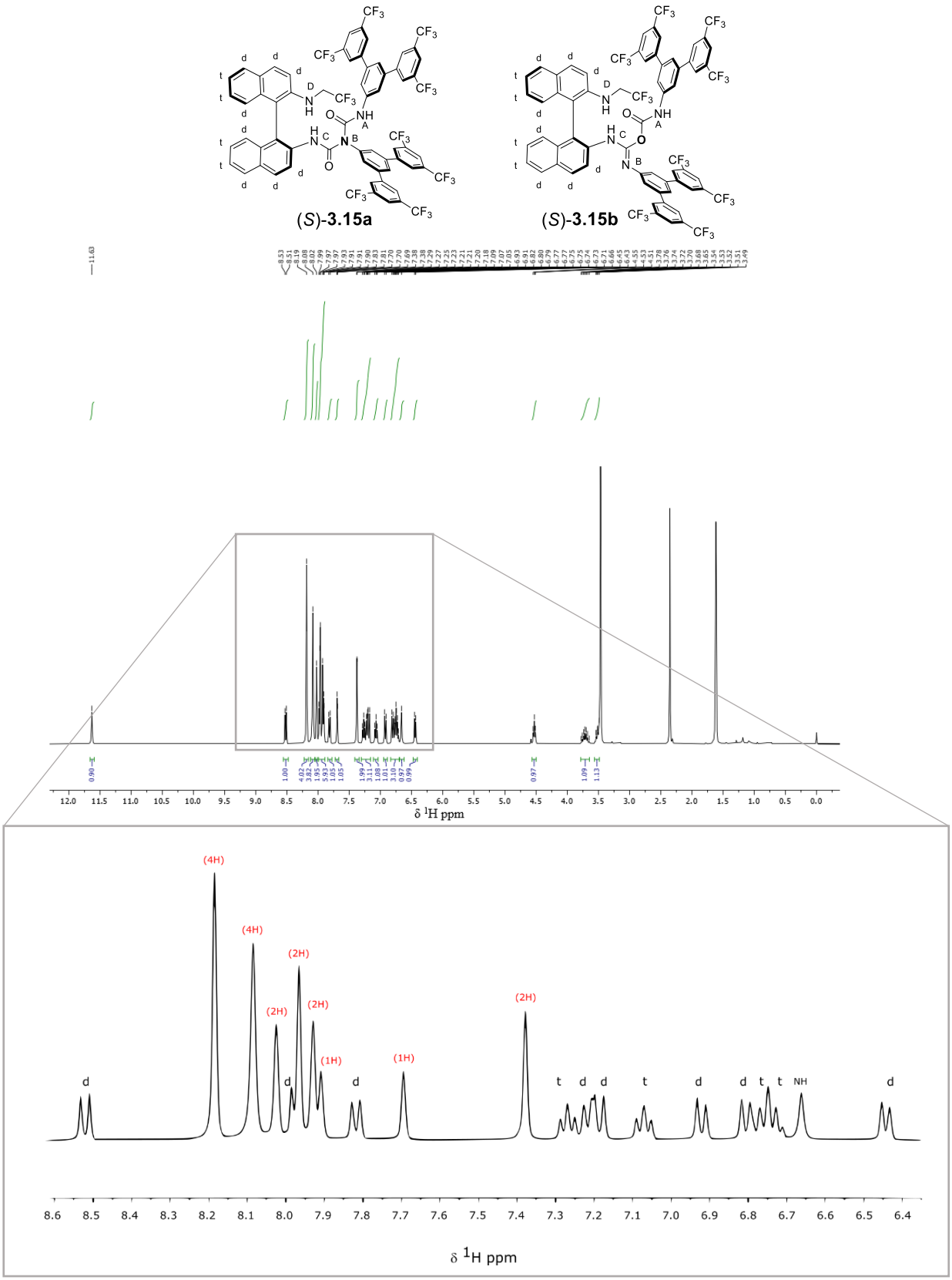


Figure 5.8: ^{1}H NMR of (*S*)-**3.15** in THF-d_8

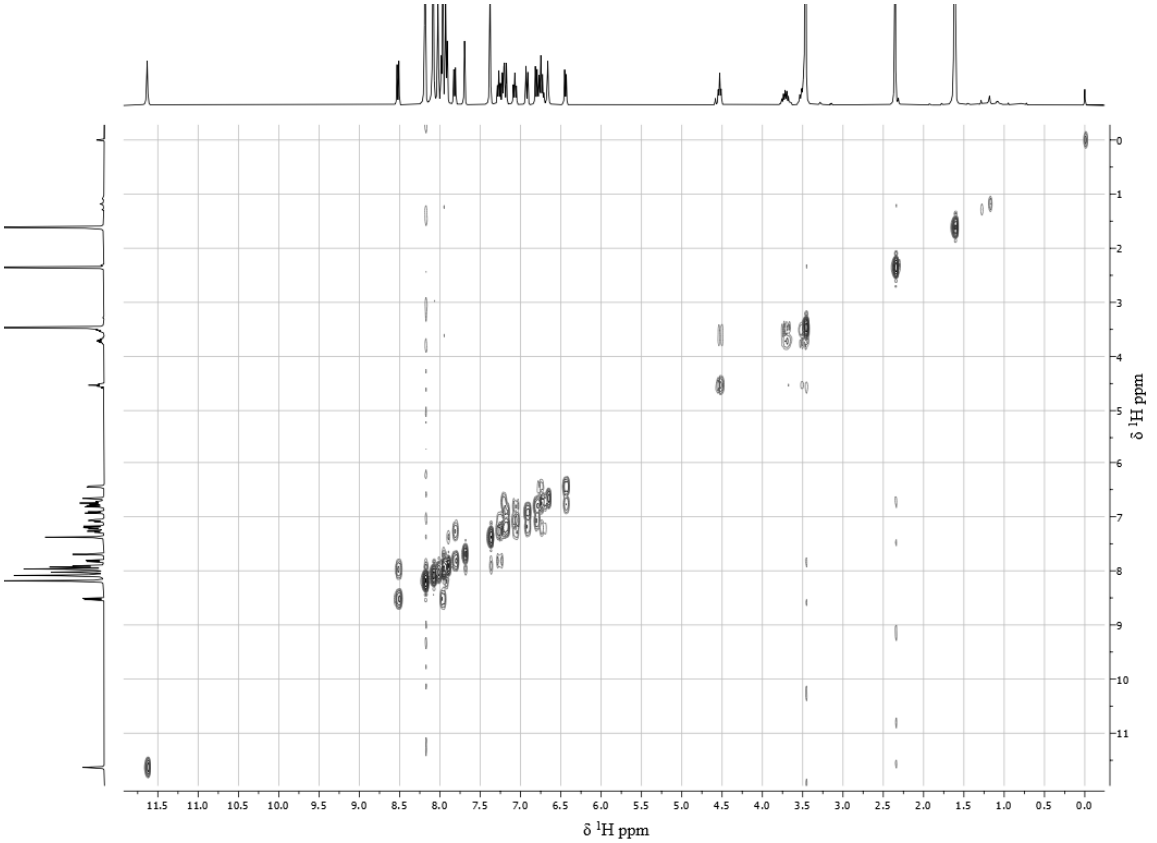


Figure 5.9: COSY of (*S*)-**3.15 (**THF-d_8).

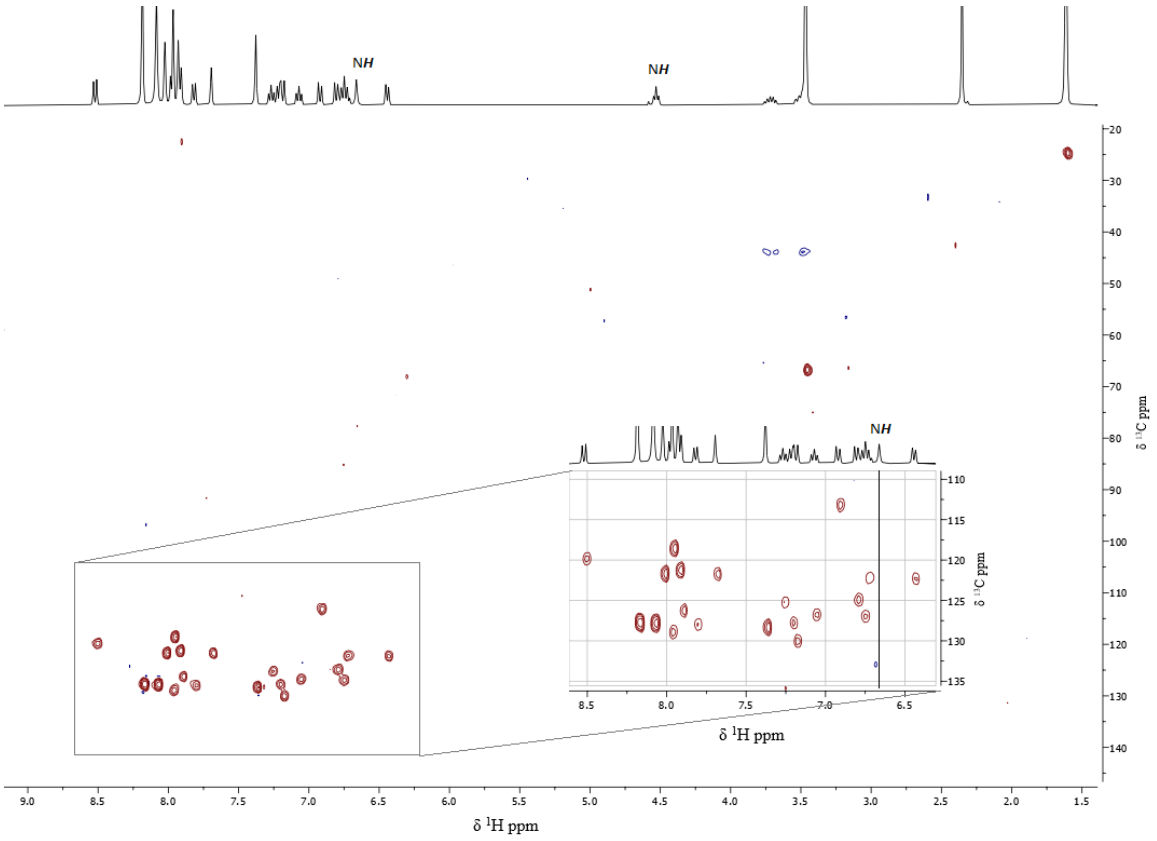


Figure 5.10 ^{1}H-^{13}C HSQC of (*S*)-**3.15 (**THF-d_8).

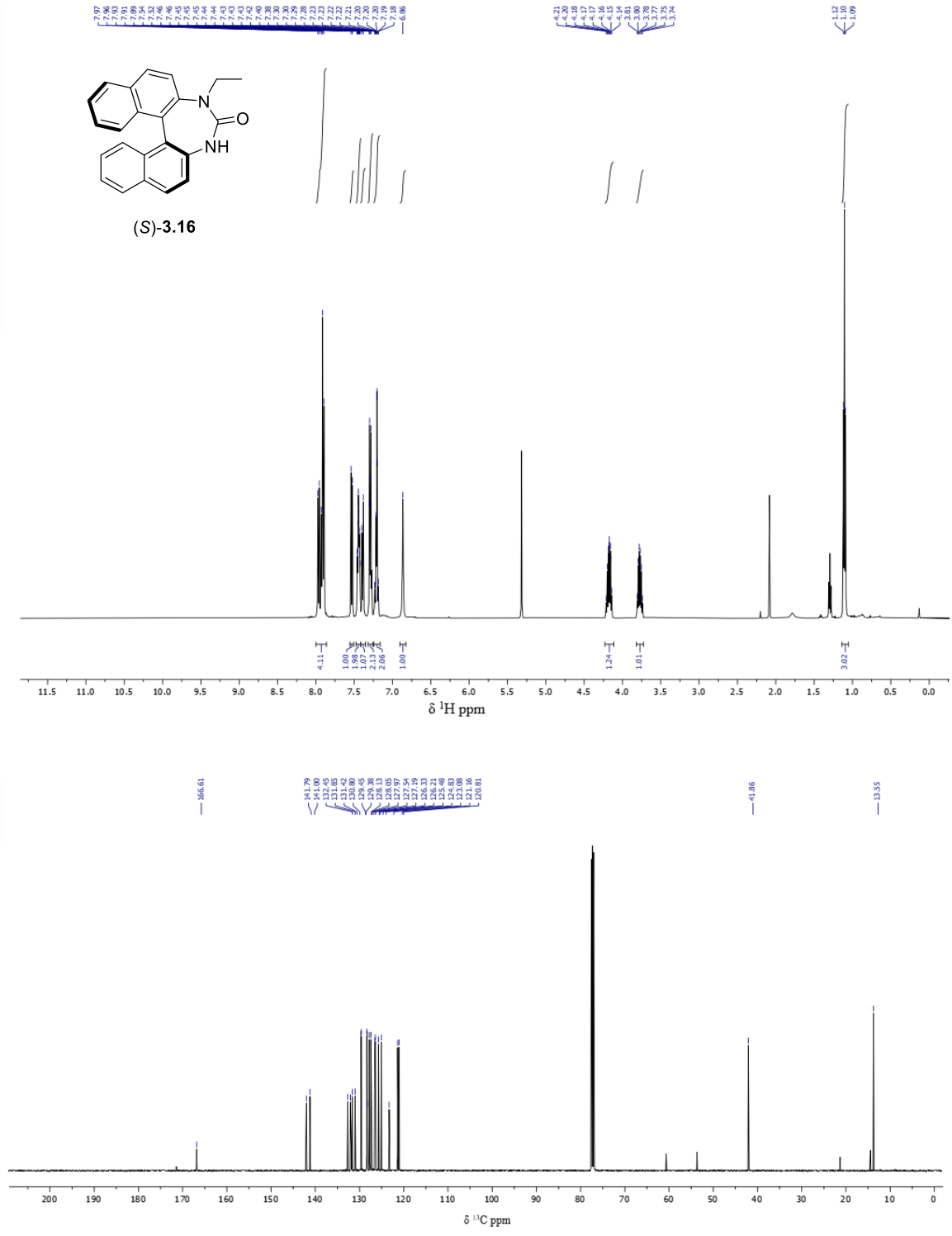


Figure 5.11: ^{1}H NMR and ^{13}C NMR spectra of (*S*)-**3.16** ($CDCl_3$).

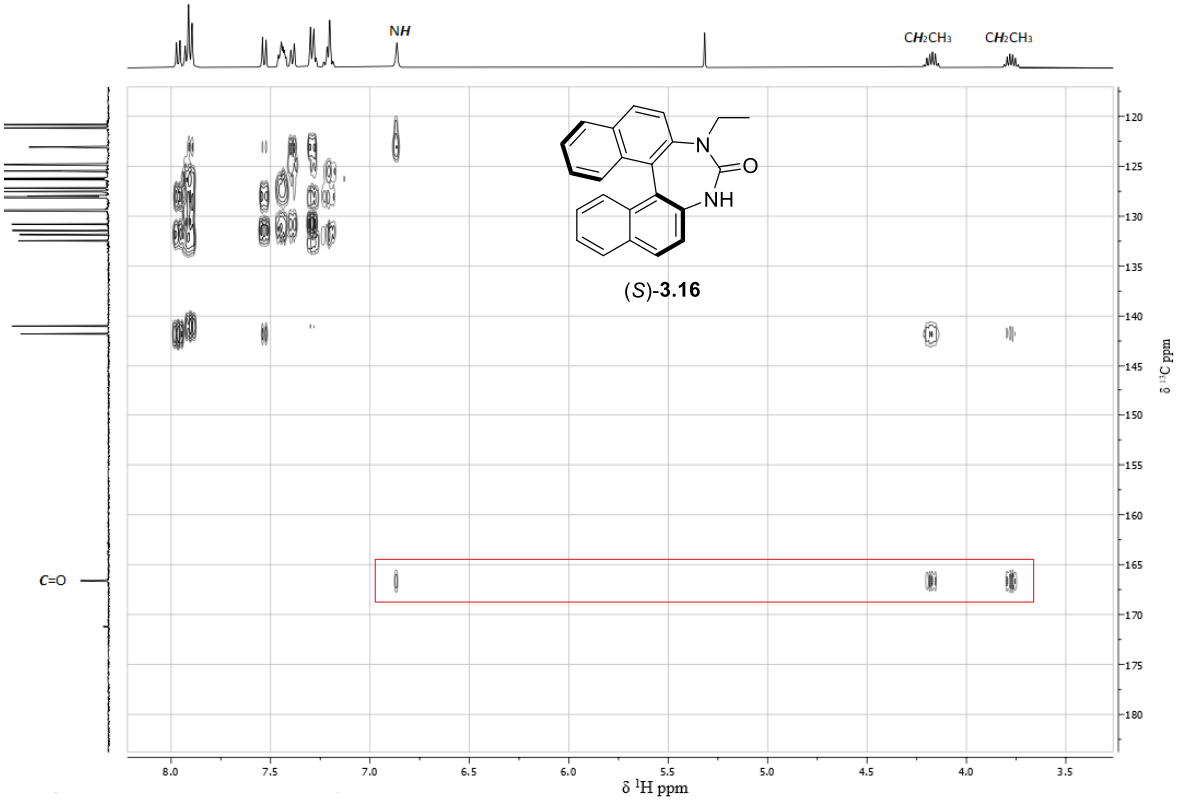


Figure 5.12: ^{1}H-^{13}C HMBC of (*S*)-**3.16** in $CDCl_3$.

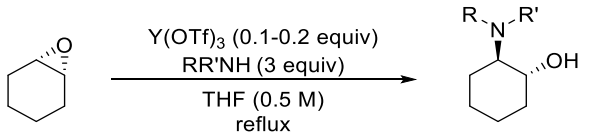
5.4 Additional Data from Chapter 4

5.4.1 Experimental procedures and Characterisation of Compounds from Chapter 4

5.4.1.1 Synthesis and Characterisation of the Starting Materials

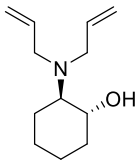
β-Amino alcohol

See the *general procedure D* (section 5.2.2.2)



4.4 *rac*-**4.12–4.14**

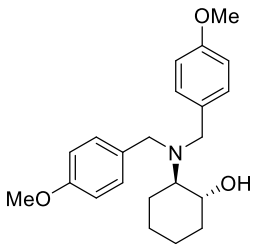
***rac*-2-(diallylamino)cyclohexan-1-ol (4.12)**



rac-**4.12**

Alcohol *rac*-**4.12** was synthesised reacting cyclohexene oxide (1.5 mL, 15 mmol, 1 equiv) with *N*-methyl-1,1-diphenylmethanamine (5.5 mL, 45 mmol, 3 equiv) in EtOH (10 mL) at 100 °C in a pressure tube for 48 h. After disappearance of the starting material, the reaction mixture was diluted in EtOAc and washed with H_2O and brine. The crude product was purified by FCC on silica gel (*n*-hexane:EtOAc 100% to 95:5, gradient) to afford *rac*-**4.12** as a colourless liquid (2.21 g, 75% yield). **^{1}H NMR** (500 MHz, $CDCl_3$) δ 5.78 (dddd, J = 17.1, 10.1, 8.0, 4.7 Hz, 2H), 5.15 (d, J = 17.2, 2H), 5.10 (d, J = 10.2, 2H), 3.82 (br s, 1H), 3.36 (td, J = 9.8, 4.5 Hz, 1H), 3.31 (dd, J = 14.2, 4.7, 1.8 Hz, 2H), 2.90 (dd, J = 14.2, 8.1 Hz, 2H), 2.41 (ddd, J = 11.5, 9.8, 3.3 Hz, 1H), 2.10 (ddt, J = 9.2, 4.7, 2.8 Hz, 1H), 1.85 – 1.58 (m, 3H), 1.30 – 1.03 (m, 4H); **^{13}C NMR** (126 MHz, $CDCl_3$) δ 136.9, 117.0, 69.2, 65.2, 52.5, 33.1, 25.5, 24.1, 22.6; **IR** (thin layer film) ν (cm^{-1}) = 3470, 3078, 2930, 2857, 1642, 1452, 1404, 1357, 1279, 1202, 1155, 1077, 1044, 984, 916, 872, 845; **HRMS** (ESI^+) *m/z* calculated for $C_{12}H_{22}ON^+$ $(M+H)^+$ 196.1696, found 196.1696.

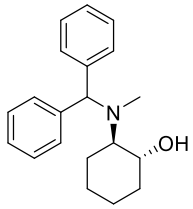
***rac*-2-(bis(4-methoxybenzyl)amino)cyclohexan-1-ol (4.13)**



rac-**4.13**

Alcohol *rac*-**4.13** was prepared following the *general procedure D* (24 h) from cyclohexene oxide (384 µl, 3.8 mmol, 1 equiv) and bis(4-methoxybenzyl)amine[21] (2.00 g, 7.75 mmol, 2 equiv) with 204 mg (0.1 equiv) of $Y(OTf)_3$. Purification by FCC on silica gel (pentane: EtOAc = 95:5 to 80:20, gradient) afforded *rac*-**4.13** as a pale-yellow oil (1.35 g, 99% yield). **^{1}H NMR** (400 MHz, CDCl3) δ 7.17 (d, J = 8.5 Hz, 4H), 6.85 (d, J = 8.5 Hz, 4H), 3.82 – 3.74 (m, 9H), 3.49 (td, J = 10.0, 4.4 Hz, 1H), 3.29 (d, J = 13.2 Hz, 2H), 2.34 (ddd, J = 11.8, 9.7, 3.4 Hz, 1H), 2.13 – 2.02 (m, 1H), 1.98 – 1.90 (m, 1H), 1.82 – 1.74 (m, 1H), 1.72 – 1.62 (m, 1H), 1.34 – 1.03 (m, 4H); **^{13}C NMR** (101 MHz, CDCl3) δ158.8, 131.7, 130.1, 113.9, 69.0, 63.9, 55.3, 52.8, 33.3, 25.6, 24.2, 22.2; **IR** (thin layer film): ν (cm^{-1}) = 2918, 2850, 2361, 1736, 1612, 1512, 1463, 1302, 1248, 1174, 1089, 1036, 808, 617; **HRMS** (ESI^+) *m/z* calculated for $C_{22}H_{30}NO_3^+$ $[M+H]^+$ 356.22202, found 356.22178.

***trans*-2-(benzhydryl(methyl)amino)cyclohexan-1-ol (4.14)**



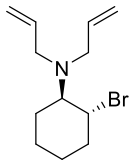
rac-**4.14**

Alcohol *rac*-**4.14** was prepared following the *general procedure D* (18 h) from cyclohexene oxide (1 mL, 10 mmol, 1 equiv) and *N*-methyl-1,1-diphenylmethanamine (3.9 g, 20 mmol, 2 equiv) with 1 g (0.2 equiv) of $Y(OTf)_3$. Purification by FCC on silica gel (pentane: EtOAc = 100% to 96:4, gradient) afforded *rac*-**4.14** as a white solid (1.33 g, 45% yield). **^{1}HNMR** (400 MHz, $CDCl_3$) δ 7.39 – 7.34 (m, 2H), 7.31 – 7.26 (m, 2H), 7.24 – 7.16 (m, 4H), 7.13 – 7.07 (m, 2H), 4.56 (s, 1H), 3.92 (br s, 1H), 3.43 (td, *J* = 10.0, 4.3 Hz, 1H), 2.36 (ddd, *J* = 11.9, 9.7, 3.3 Hz, 1H), 2.08 (s, 3H), 2.04 – 1.95 (m, 1H), 1.71 – 1.45 (m, 3H), 1.20 – 0.92 (m, 3H), 0.83 (qt, *J* = 12.9, 3.5 Hz, 1H); **^{13}C NMR** (101 MHz, $CDCl_3$) δ 143.4, 142.3, 128.7, 128.6,

128.0, 127.6, 127.1, 127.0, 73.3, 69.5, 64.0, 33.4, 33.3, 25.2, 24.1, 21.3; **IR** (thin layer film) ν (cm^{-1}) = 3450, 2928, 2859, 1596, 1488, 1450, 1356, 1287, 1212 1062, 1020, 962, 759, 744, 206, 693; **MP:** 135 – 137 °C; **HRMS** (ESI^+) *m/z* calculated for $C_{20}H_{28}ON^+$ $(M+H)^+$ 2096.2014, found 296.2009.

β-Haloamines

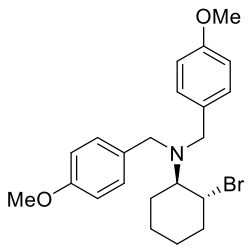
rac-*N*,*N*-diallyl-2-bromocyclohexan-1-amine (4.15)



rac-**4.15**

In a flame-dried round-bottom-flask, alcohol *rac*-**4.12** (1.0 g, 5 mmol, 1 equiv) and PPh_3 (1.6 g, 6.1 mmol, 1.2 equiv) were dissolved in anhydrous $CHCl_3$ (25 mL, 0.2 M). The reaction mixture was cooled to 0 °C and *N*-bromosuccinimide (NBS, 1.09 g, 6.1 mmol, 1.2 equiv) was added portion-wise. The reaction was stirred at rt until disappearance of the starting material (monitored by TLC). The solvent was removed *in vacuo* and the crude product was purified by FCC on silica gel (*n*-hexane: EtOAc = 100:0 to 95:5, gradient) to afford *rac*-**4.15** as a colourless oil (600 mg, 46%). **^{1}H NMR** (500 MHz, $CDCl_3$) δ 5.87 (dddd, *J* = 17.4, 10.2, 7.3, 5.0 Hz, 2H), 5.19 (d, *J* = 17.2, 2H), 5.07 (d, *J* = 10.2, 2H), 4.03 (ddd, *J* = 11.5, 10.6, 4.3 Hz, 1H), 3.32 (ddt, *J* = 14.4, 5.0, 1.8 Hz, 2H), 3.00 (dd, *J* = 14.3, 7.3, 2H), 2.70 (td, *J* = 10.8, 3.8 Hz, 1H), 2.50 – 2.34 (m, 1H), 2.01 – 1.74 (m, 3H), 1.66 (dddd, *J* = 12.0, 8.6, 5.7, 3.2 Hz, 1H), 1.34 – 1.10 (m, 3H); **^{13}C NMR** (126 MHz, $CDCl_3$) δ 136.7, 115.2, 63.4, 55.4, 51.9, 37.7, 26.4, 25.9, 24.2. **IR** (thin layer film) ν (cm^{-1}) = 3077, 2933, 2857, 2807, 1642, 1148, 1416, 1260, 1189, 1155, 1085, 965, 916, 800, 690; **HRMS** (ESI^+) *m/z* calculated for $C_{12}H_{21}BrN^+$ $(M+H)^+$ 258.0852, found 258.0853.

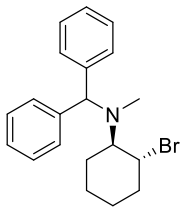
***rac*-2-bromo-*N*,*N*- bis(4-methoxybenzyl)cyclohexan-1-amine (4.16)**



rac-**4.13**

In a flame-dried round-bottom-flask, alcohol *rac*-**4.13** (1.5 g, 4.2 mmol, 1 equiv), CBr_4 (1.39 g, 4.2 mmol, 1 equiv) and PPh_3 (1.10 g, 4.2 mmol, 1 equiv) were stirred in anhydrous CH_3CN at rt for 24 h. Then Et_2O was added, causing the precipitation of a white solid. The mixture was filtered, and the solvent removed *in vacuo*. Purification by FCC on silica gel (pentane:EtOAc = 99:1 to 96:4, gradient) afforded *rac*-**4.16** as a white solid (662 mg, 38% yield). **^{1}H NMR** (400 MHz, $CDCl_3$) δ 7.40 (d, J = 8.6 Hz, 4H), 6.85 (d, J = 8.6 Hz, 4H), 4.14 (td, J = 11.3, 4.3 Hz, 1H), 3.84 – 3.76 (m, 8H), 3.38 (d, J = 13.5 Hz, 2H), 2.65 (td, J = 11.2, 3.6 Hz, 1H), 2.46 – 2.36 (m, 1H), 2.11 – 2.03 (m, 1H), 1.83 – 1.70 (m, 2H), 1.68- 1.60 (m, 1H), 1.37 – 1.07 (m, 3H); **^{13}C NMR** (101 MHz, CDCl3) δ 158.6, 132.1, 130.2, 113.6, 63.0, 56.0, 55.4, 52.8, 38.9, 27.7, 26.2, 25.3; **IR** (thin layer film): ν (cm^{-1}) = 2932, 2856, 2833, 1611, 1509, 1245, 1170, 1035; **MP** 69 – 72 °C; **HRMS** (ESI^+) *m/z* calculated for $C_{22}H_{29}BrNO_2^+$ $[M+H]^+$ 418.13762, found 418.13770.

***trans*-*N*-benzhydryl-2-bromo-*N*-methylcyclohexan-1-amine (4.17)**

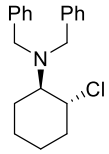


rac-**4.17**

In a flame-dried round-bottom-flask, alcohol *rac*-**4.14** (300 mg, 1 mmol, 1 equiv) and PPh_3 (314.8 mg, 1.2 mmol, 1.2 equiv) were dissolved in anhydrous $CHCl_3$ (5.0 mL, 0.2 M). The reaction mixture was cooled to 0 °C and *N*-bromosuccinimide (NBS, 218 mg, 1.2 mmol, 1.2 equiv) was added portion-wise. The reaction was stirred at rt until disappearance of the starting material (monitored by TLC). The solvent was removed *in vacuo* and the crude product was purified by FCC on silica gel (pentane: Et_2O = 100:0 to 96:4, gradient) to afford *rac*-**4.17** as a white solid (120 mg, 33%). **^{1}H NMR** (400 MHz, $CDCl_3$) δ 7.62 – 7.42 (m, 4H), 7.37 – 7.26 (m, 4H), 7.24 – 7.13 (m, 2H), 4.80 (s, 1H), 4.16 (ddd, J = 11.7, 10.6, 4.3 Hz, 1H), 2.77 (ddd, J = 11.6, 10.6, 3.7 Hz, 1H), 2.51 – 2.36 (m, 1H), 2.19 (s, 3H), 1.97 –

1.82 (m, 1H), 1.81 – 1.67 (m, 2H), 1.61 (dq, *J* = 12.6, 2.9 Hz, 1H), 1.36 (tdd, *J* = 13.0, 11.6, 3.7 Hz, 1H), 1.20 (qt, *J* = 13.2, 3.6 Hz, 1H), 1.05 – 0.89 (m, 1H); **^{13}C NMR** (101 MHz, $CDCl_3$) δ 144.4, 142.8, 128.5, 128.4, 128.4, 127.9, 126.8, 126.7, 73.4, 63.1, 56.4, 38.7, 32.8, 27.5, 25.3, 25.0; **IR** (thin layer film) ν (cm^{-1}) = 3060, 3024, 2933, 2856, 2792, 1597, 1490, 1339, 1219, 1187, 1149, 1021, 761, 745, 705; **MP:** 88–89 °C; **HRMS** (ESI^+) *m/z* calculated for $C_{20}H_{25}NBr^+$ $(M+H)^+$ 358.1170, found 358.1165.

***rac*-*N*,*N*-dibenzyl-2-chlorocyclohexan-1-amine (4.21)**



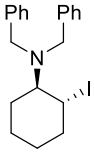
rac-**4.21**

In a flame-dried round-bottom-flask, alcohol *rac*-**4.11** (600 mg, 2.24 mmol, 1 equiv) was dissolved in anhydrous CH_2Cl_2 (9 mL, 0.25 M). The solution was cooled to 0 °C and Et_3N (470 µL, 3.37 mmol, 1.5 equiv) was added via a syringe, followed by dropwise addition of MsCl (260 µL,3.37 mmol, 1.5 equiv) at 0 °C. The reaction was warmed to rt and monitored by ^{1}H NMR: after 2 h the main product was the corresponding mesylate, alongside ~15% of chloride *rac*-**4.21** and no further conversion was observed after further 3 h. The reaction mixture was washed with a saturated aqueous solution of $NaHCO_3$ and brine; the organic layer was dried over $MgSO_4$ and concentrated under reduced pressure. The crude product was re-dissolved in anhydrous CH_2Cl_2 (28 mL) and 363 mg (1 equiv) of $FeCl_3$ were added.[22] The reaction mixture was stirred at rt under inert atmosphere for overnight, then it was washed with H_2O to remove the inorganic salts. Layers were separated and the aqueous one was extracted twice with CH_2Cl_2. The combined organic layers were dried over $MgSO_4$ and concentrate *in vacuo*. The crude product was purified by FCC on silica gel (pentane:Et_2O = 100:0 to 95:5, gradient) to afford *rac*-**4.21** as a white solid (281.5 mg, 43%). **^{1}H NMR** (400 MHz, $CDCl_3$) δ 7.51 – 7.43 (m, 4H), 7.34 – 7.27 (m, 4H), 7.25 – 7.18 (m, 2H), 4.01 (ddd, *J* = 11.4, 10.5, 4.4 Hz, 1H), 3.90 (d, *J* = 13.8 Hz, 2H), 3.54 (d, *J* = 13.8 Hz, 2H), 2.63 (ddd, *J* = 11.8, 10.5, 3.7 Hz, 1H), 2.33 – 2.23 (m, 1H), 2.12 – 2.03 (m, 1H), 1.81 – 1.73 (m, 1H), 1.72 – 1.64 (m, 1H), 1.64 – 1.50

(m, 1H), 1.38 – 1.06 (m, 3H); **^{13}C NMR** (101 MHz, $CDCl_3$) δ 140.2, 128.9, 128.1, 126.8, 77.4, 77.0, 76.7, 63.2, 62.1, 53.7, 37.8, 26.5, 26.4, 25.1; **IR** (thin layer film): ν (cm^{-1}) = 3062, 3026, 2936, 2857, 2801, 1494, 1453, 1375, 1260, 1209, 1148, 1090, 1028, 800, 736, 698; **MP** 85–88 °C; **HRMS** (ESI^+) *m/z* calculated for $C_{20}H_{25}ClN^+$ $[M+H]^+$ 314.1670, found 314.1671.

***rac*-*N*,*N*-dibenzyl-2-iodocyclohexan-1-amine (4.22)**

Synthesised by Jimmy Wang, following the procedure reported by Chong.[14]



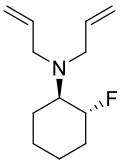
rac-**4.22**

In a flame-dried round-bottom-flask, alcohol *rac*-**4.11** (2.00 g, 6.77 mmol, 1 equiv) and PPh_3 (2.66 g, 10.15 mmol, 1.5 equiv) were dissolved in anhydrous $CHCl_3$ (34 mL, 0.2 M). The reaction mixture was cooled to 0 °C and imidazole (691 mg, 10.15 mmol, 1.5 equiv) was added followed by portion-wise addition of iodide (1.29 g, 10.15 mmol, 1.5 equiv). The reaction was stirred at rt until disappearance of the starting material (2 h, monitored by TLC). The solvent was removed *in vacuo* and the crude product was purified by FCC on silica gel (pentane:Et_2O = 100:0 to 95:5, gradient) to afford *rac*-**4.22** as a white solid (1.40 g, 51%). **^{1}H NMR** (400 MHz, $CDCl_3$) δ 7.46 (d, *J* = 7.4 Hz, 4H), 7.27 – 7.19 (m, 4H), 7.18 – 7.11 (m, 2H), 4.16 (ddd, *J* = 12.1, 10.9, 4.2 Hz, 1H), 3.75 (d, *J* = 13.5 Hz, 2H), 3.29 (d, *J* = 13.5 Hz, 2H), 2.60 – 2.35 (m, 2H), 2.04 – 1.73 (m, 3H), 1.47 – 1.37 (m, 1H), 1.33 – 1.00 (m, 3H); **^{13}C NMR** (101 MHz, $CDCl_3$) δ 139.5, 129.4, 129.3, 128.1, 128.1, 126.9, 63.4, 53.6, 41.2, 37.5, 29.34, 25.5, 25.2. **IR** (thin layer film): ν (cm^{-1}) = 3023, 2922, 2853, 2807, 1493, 1452, 1364, 1208, 1172, 1132, 1068, 1028, 987, 969, 953, 913, 745, 737; **MP**: 131–133. **HRMS** (ESI^+) *m/z* calculated for $C_{20}H_{25}IN^+$ $[M+H]^+$ 406.1026, found 406.1025. Spectroscopic data were in agreement with the ones previously reported in literature.[14]

5.4.1.2 Characterisation of the β-Fluoroamines and Derivatisation Products

The absolute configuration was assigned by derivatizing (*R*,*R*)-**2.109** and (*R*,*R*)-**4.18** to the corresponding β-fluoropicolinamide **2.128** (p.290).[15] The configuration of **4.19** and **4.20** was assigned by analogy.

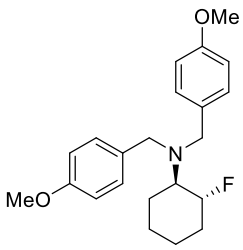
(1*R*,2*R*)-*N*,*N*-diallyl-2-fluorocyclohexan-1-amine (4.18)



(R,R)-**4.18**

In a vial equipped with a magnetic stirring bar were sequentially added *rac*-**4.15** (103 mg, 0.4 mmol, 1 equiv), the catalyst (*S*)-**2.78** (56 mg, 0.04 mmol, 10 mol%), KF (120 mg, 2.0 mmol, 5 equiv) and CF_3Ph (800 μL, 0.5 M). The vial was sealed, and the reaction mixture was stirred at 900 rpm at rt for 72 h. The crude mixture was then filtered through a small plug of silica (and eluted with CH_2Cl_2/EtOAc = 1:1), evaporated to dryness under reduced pressure and directly purified by FCC (*n*-hexane:Et_2O = 100:0 to 99.3:0.7, gradient). Colourless oil, 66 mg, 84% yield, e.r. = 67:33 (determined by derivatization to **2.128**). **^{1}H NMR** (500 MHz, $CDCl_3$) δ 5.85 (ddt, *J* = 16.6, 10.1, 6.2 Hz, 2H), 5.19 (d, *J* = 17.2 Hz, 2H), 5.08 (d, *J* = 10.1 Hz, 2H), 4.50 (dtd, *J* = 50.4, 10.3, 4.9 Hz, 1H), 3.29 (dd, *J* = 14.4, 6.3 Hz, 2H), 3.20 (dd, *J* = 14.5, 6.3 Hz, 2H), 2.75 (dddd, *J* = 12.0, 9.7, 8.2, 4.0 Hz, 1H), 2.18 – 2.07 (m, 1H), 1.87 – 1.76 (m, 1H), 1.75 – 1.62 (m, 1H), 1.50 – 1.37 (m, 1H), 1.29 – 1.09 (m, 4H); **^{19}F NMR** (376 MHz, CDCl3) δ -174.93 (d, *J* = 50.6 Hz); **^{13}C NMR** (126 MHz, $CDCl_3$) δ 137.6, 116.4, 92.8 (d, $J_{C\text{-}F}$ = 177.1 Hz), 62.6 (d, $J_{C\text{-}F}$ = 15.2 Hz), 53.8, 32.6 (d, $J_{C\text{-}F}$ = 17.8 Hz), 27.3 (d, $J_{C\text{-}F}$ = 8.3 Hz), 24.9 (d, $J_{C\text{-}F}$ = 2.2 Hz), 23.9 (d, $J_{C\text{-}F}$ = 11.4 Hz); **IR** (thin layer film) ν (cm^{-1}) = 3652, 2981, 1382, 1260, 1077, 955, 773; **HRMS** (ESI^+) *m/z* calculated for $C_{12}H_{21}FN^+$ $[M+H]^+$ 198.1652, found 198.1654; **$[\alpha]_D^{25\,°C}$** = –12.9 ° (c = 0.4, $CHCl_3$, e.r. = 67:33)

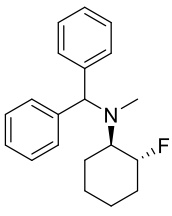
(1*R*,2*R*)-2-fluoro-*N*,*N*-bis(4-methoxybenzyl)cyclohexan-1-amine (4.19)



(R,R)-**4.19**

In a vial equipped with a magnetic stirring bar were sequentially added *rac*-**4.16** (83.6 mg, 0.2 mmol, 1 equiv), the catalyst (*S*)-**2.78** (28 mg, 0.02 mmol, 10 mol%), KF (60 mg, 1.0 mmol, 5 equiv) and CF_3Ph (400 μL, 0.5 M). The vial was sealed, and the reaction mixture was stirred at 900 rpm at rt for 72 h. The crude mixture was then filtered through a small plug of silica (and eluted with CH_2Cl_2/EtOAc = 1:1), evaporated to dryness under reduced pressure and directly purified by FCC (*n*-hexane:toluene = 50:50 to 35:65, gradient). White solid, 45.3 mg, 63% yield, e.r. = 84:16. **^{1}H NMR** (500 MHz, $CDCl_3$) δ 7.38 – 7.32 (m,4H), 6.93 – 6.81 (m, 4H), 4.64 (dddd, J = 50.7, 10.5, 10.5, 5.0 Hz, 1H), 3.82 (s, 6H), 3.77 (d, J = 13.6 Hz, 2H), 3.69 (d, J = 13.6 Hz, 2H), 2.75 – 66 (m, 1H), 2.20 – 2.12 (m, 1H), 1.95 – 1.86 (m,1H), 1.76 – 1.63 (m, 2H), 1.48 – 1.27 (m, 2H), 1.24 – 1.05 (m, 2H); **^{19}F NMR** (377 MHz, CDCl3) δ –174.75 (d, J= 50.7 Hz); **^{13}C NMR** (126 MHz, $CDCl_3$) δ 158.4, 132.8, 129.6, 113.5, 93.3 (d, $J_{C\text{-}F}$ = 177.7 Hz), 60.9 (d, $J_{C\text{-}F}$ = 15.0 Hz), 55.2, 53.6, 32.7 (d, $J_{C\text{-}F}$ = 17.5 Hz), 27.6 (d, $J_{C\text{-}F}$ = 8.8 Hz), 24.9 (d, $J_{C\text{-}F}$ = 2.2 Hz), 24.0 (d, $J_{C\text{-}F}$ = 11.5 Hz); **IR** (thin layer film) ν (cm^{-1}) = 2936, 2834, 1611, 1510, 1245, 823; **MP** 50 – 53 °C; **HRMS** (ESI^+) *m/z* calculated for $C_{22}H_{29}FNO_2^+$ $[M+H]^+$ 358.21768, found 358.21794; **$[\alpha]_D$ $^{25\ °C}$** = –11.9 ° (c = 0.44, $CHCl_3$, e.r. = 85.5:14.5); **HPLC separation:** DAICEL CHIRALPAK® IA-3, heptane:^{i}PrOH = 99:1, 1 mL/min, t_1 = 6.04 min (major), t_2 = 7.01 min (minor).

(1*R*,2*R*)-*N*-benzhydryl-2-fluoro-*N*-methylcyclohexan-1-amine (4.20)

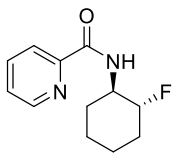


(R,R)-**4.20**

Rac-**4.17** (18 mg, 0.05 mmol), CsF (23 mg, 0.15 mmol, 3 equiv), (*S*)-**2.78** (3.5 mg, 5 mol%) were stirred in CH_2Cl_2 (0.25 M) at rt for 24 h. After this time, the reaction mixture was filtered on a silica plug, evaporated to dryness and

analysed by ^{1}H and ^{19}F NMR (4-fluoroanisole as internal standard) to determine the yield; an aliquot of the reaction mixture was purified by preparative TLC and analysed by HPLC (chiral stationary phase) to determine the e.r. >95% ^{19}F NMR yield, e.r. = 81:19. **^{1}H NMR** (400 MHz, $CDCl_3$) δ 7.49 – 7.42 (m, 4H), 7.29 – 7.22 (td, J = 7.5, 1.9 Hz, 4H), 7.20 – 7.09 (m, 2H), 4.90 (s, 1H), 4.63 (dtd, J = 50.6, 10.2, 4.9 Hz, 1H), 2.78 (dddd, J = 11.9, 9.7, 8.0, 4.0 Hz, 1H), 2.23 (s, 3H), 2.16 – 2.01 (m, 1H), 1.82 (dtt, J = 12.8, 6.3, 3.1 Hz, 1H), 1.71 – 1.54 (m, 2H), 1.42 – 0.77 (m, 4H); **^{19}F NMR** (377 MHz, $CDCl_3$) δ –174.98 (d, J = 50.8 Hz); **^{13}C NMR** (101 MHz, $CDCl_3$) [overlapping signals] δ 144.2, 144.1, 128.4, 128.3, 128.0, 127.9, 126.6, 92.6 (d, $J_{C\text{-}F}$ = 177.3 Hz), 74.2 (d, $J_{C\text{-}F}$ = 2.6 Hz), 61.3 (d, $J_{C\text{-}F}$ = 15.4 Hz), 33.8, 32.5 (d, $J_{C\text{-}F}$ = 17.6 Hz), 27.2 (d, $J_{C\text{-}F}$ = 9.3 Hz), 24.8 (d, $J_{C\text{-}F}$ = 2.2 Hz), 23.9 (d, $J_{C\text{-}F}$ = 11.5 Hz). **IR** (thin layer film) ν (cm^{-1}) 2927, 2854, 1488, 1452, 1381, 1350, 1260, 1120, 1018, 955, 761, 744, 704, 693; **HRMS** (ESI^+) *m/z* calculated for $C_{20}H_{25}FN^+$ $[M+H]^+$ 298.1966, found 298.1966; **$[\alpha]_D^{25\ °C}$** = –2.9 ° (c = 0.7, $CHCl_3$, e.r. = 76.5:23.5); **HPLC separation:** DAICEL CHIRALPAK® IC-3, Heptane:^{i}PrOH = 99.5:0.5, 1 mL/min; t_1 = 3.767 min (major), t_2 = 4.678 min (minor).

***N*-((1*R*,2*R*)-2-fluorocyclohexyl)picolinamide (2.128)**



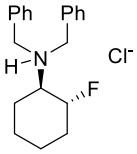
(R,R)-**2.128**

In a Schlenk tube under inert atmosphere, bis(dibenzylideneacetone)palladium(0) ($Pd(dba)_2$, 14.5 mg, 0.025 mmol, 0.1 equiv) and 1,4-Bis(diphenylphosphino)butane (dppb, 11 mg, 0.025 mmol, 0.1 equiv) were stirred in anhydrous and degassed THF (1 mL) for 15 min at rt. Then **4.18** (50 mg, 0.253 mmol, 1 equiv) was added as a solution in THF (1.5 mL), followed by 2-thiosalycilic acid (98 mg, 0.63 mmol, 2.5 equiv). The reaction mixture was stirred at 60 °C for O/N. After this point ^{19}F NMR analysis showed that the intermediate *N*-allylated product was still present and further 0.1 equiv of $Pd(dba)_2$ and dppb were added, and the reaction mixture stirred for further 24 h. The reaction mixture was then passed over a celite

plug, and the solvent removed in vacuo. The residue was dissolved in CH_2Cl_2 and picolinic acid (31 mg, 0.253 mmol, 1 equiv), DMAP (34 mg, 0.278 mmol, 1.1 equiv) and di-isopropyl carbodiimide (DIC, 35 mg, 0.278 mmol, 1.1 equiv) were added. The reaction mixture was stirred at rt for overnight. After this time, an aliquot of the reaction mixture was purified by preparative TLC and analysed by HPLC (chiral stationary phase) to determine the e.r. (67:33 e.r.). **HPLC separation:** DAICEL CHIRALPAK® AS-H, *n*-hexane:^{i}PrOH = 90:10, 1 mL/min; t_1 = 15.5 min (major), t_2 = 17.7 min (minor).

*5.4.1.3 Characterisation of the Salts of **2.109***

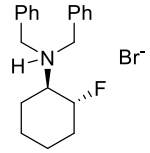
(1*R*,2*R*)-*N*,*N*-dibenzyl-2-fluorocyclohexan-1-ammonium chloride (2.109*HCl)



(R,R)-**2.109***HCl

^{1}H NMR (500 MHz, $CDCl_3$) δ 12.39 (br s, 1H), 7.92 – 7.86 (m, 2H), 7.84 – 7.78 (m, 2H), 7.44 – 7.30 (m, 6H), 4.94 (dtd, *J* = 51.5, 10.5, 4.7 Hz, 1H), 4.55 (dd, *J* = 12.9, 4.9 Hz, 1H), 4.40 (dd, *J* = 12.6, 4.0 Hz, 1H), 4.28 (dd, *J* = 13.0, 6.1 Hz, 1H), 4.12 (dd, *J* = 13.0, 7.8 Hz, 1H), 3.41 – 3.23 (m, 1H), 2.99 – 2.85 (m, 1H), 2.23 – 2.15 (m, 1H), 1.72 – 1.57 (m, 2H), 1.40 – 1.19 (m, 2H), 1.16 – 1.04 (m, 1H), 1.03 – 0.92 (m, 1H); **^{19}F NMR** (471 MHz, $CDCl_3$) δ –174.17 (d, *J* = 52.8 Hz); **^{13}C NMR** (126 MHz, $CDCl_3$) [overlapping signals] δ 132.2, 132.0, 129.9, 129.7, 129.6, 129.2, 129.1, 90.8 (d, $J_{C\text{-}F}$ = 179.6 Hz), 63.9 (d, $J_{C\text{-}F}$ = 14.0 Hz), 59.6 (d, $J_{C\text{-}F}$ = 6.0 Hz), 54.6, 32.27 (d, $J_{C\text{-}F}$ = 17.3 Hz), 27.4 (d, $J_{C\text{-}F}$ = 5.7 Hz), 24.3 (d, $J_{C\text{-}F}$ = 2.0 Hz), 23.1 (d, $J_{C\text{-}F}$ = 11.0 Hz); **IR** (thin layer film) ν (cm^{-1}) = 3395, 2989, 2944, 2870, 2569, 1495, 1455, 1393, 1142, 1083, 1030, 751, 700; **MP** 137 – 140 °C; **$[\alpha]_D^{25\,°C}$** = +14.9 ° (c = 1.1, $CHCl_3$, e.r. = 82:18).

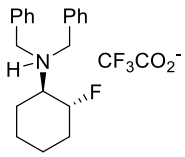
(1*R*,2*R*)-*N*,*N*-dibenzyl-2-fluorocyclohexan-1-ammonium bromide (2.109*HBr)



(R,R)-**2.109***HBr

^{1}H NMR (500 MHz, $CDCl_3$) δ 11.25 (br s, 1H), 7.97 – 7.90 (m, 2H), 7.89 – 7.85 (m, 2H), 7.46 –7.34 (m, 6H), 4.96 (dtd, J = 51.5, 10.5, 4.7 Hz, 1H), 4.61 (dd, J = 13.0, 5.7 Hz, 1H), 4.48 (dd, J = 12.7, 4.7 Hz, 1H), 4.35 (dd, J = 13.0, 6.4 Hz, 1H), 4.21 (ddd, J = 12.8, 8.2, 1.7 Hz, 1H), 3.41 (ddt, J = 14.9, 9.5, 4.4 Hz, 1H), 3.09 – 2.96 (m, 1H), 2.29 – 2.18 (m, 1H), 1.76 – 1.59 (m, 2H), 1.44 – 1.23 (m, 2H), 1.20 – 0.98 (m, 2H); **^{19}F NMR** (471 MHz, $CDCl_3$) δ –174.12 (d, J = 52.9 Hz); **^{13}C NMR** (126 MHz, $CDCl_3$) δ [overlapping signals] 132.4, 132.0, 130.1, 130.0, 129.2, 128.9, 90.7 (d, $J_{C\text{-}F}$ = 180.0 Hz), 64.4 (d, $J_{C\text{-}F}$ = 13.9 Hz), 59.8 (d, $J_{C\text{-}F}$ = 6.1 Hz), 54.8, 32.2 (d, $J_{C\text{-}F}$ = 17.3 Hz), 27.5 (d, $J_{C\text{-}F}$ = 5.5 Hz), 24.3 (d, $J_{C\text{-}F}$ = 2.1 Hz), 23.1 (d, $J_{C\text{-}F}$ = 11.0 Hz); **IR** (thin layer film) ν (cm^{-1}) = 2949, 2592, 1498, 1458, 1216, 1033, 967, 743, 698, 662; **MP** 176 – 180 °C; **[α]$_D^{25\ °C}$** = +8.87 ° (c = 1.1, $CHCl_3$, e.r. = 80.5:19.5).

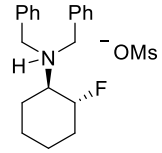
(1*R*,2*R*)-*N*,*N*-dibenzyl-2-fluorocyclohexan-1-ammonium trifluoroacetate (2.109*TFA)



(R,R)-**2.109***CF_3CO_2H

^{1}H NMR (500 MHz, $CDCl_3$) δ 11.66 (br s, 1H), 7.60 – 7.53 (m, 4H), 7.42 – 7.35 (m, 6H), 4.88 (dtd, J = 51.2, 10.5, 4.8 Hz, 1H), 4.43 (d, J = 13.0 Hz, 2H), 4.26 (d, J = 13.0 Hz, 2H), 3.33–3.24 (m, 1H), 2.35–2.27 (m, 1H), 2.26–2.18 (m, 1H), 1.74–1.59 (m, 2H), 1.45–1.34 (m, 1H), 1.29 – 0.95 (m, 4H); **^{19}F NMR** (471 MHz, $CDCl_3$) δ –75.71 (3F), –174.32 (d, J = 52.7 Hz, 1F).); **^{13}C NMR** (126 MHz, $CDCl_3$) δ 161.6 (q, J = 35.4 Hz), 131.9 (br), 131.0, 129.4, 129.1, 116.8 (q, J = 292.5 Hz), 91.4 (d, J = 178.9 Hz), 63.4 (d, J = 14.2 Hz), 56.8 (br), 32.4 (d, J = 17.3 Hz), 27.4 (d, J = 6.6 Hz), 24.5 (d, J = 2.1 Hz), 23.3 (d, J = 11.2 Hz); **IR** (thin layer film) ν (cm^{-1}) =2946, 2868, 2555, 1735, 1671, 1457, 1199, 1132, 1030, 970, 871, 799, 753, 719; **MP** 103 – 105 °C; **[α]$_D^{25\ °C}$** = –2.8 ° (c =1.2, $CHCl_3$, e.r. = 98:2).

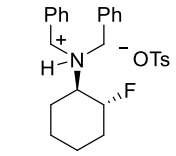
(1*R*,2*R*)-*N*,*N*-dibenzyl-2-fluorocyclohexan-1-ammonium mesylate (2.109*MsOH)



(R,R)-**2.109***MsOH

^{1}H NMR (400 MHz, $CDCl_3$) δ 10.67 (br s, 1H), 7.84 – 7.55 (m, 4H), 7.49 – 7.31 (m, 6H), 4.84 (dtd, *J* = 51.3, 10.4, 4.7 Hz, 1H), 4.64 – 4.22 (m, 4H), 3.48 – 3.26 (m, 1H), 2.83 (s, 3H), 2.49 (br s, 1H), 2.33 – 1.98 (m, 1H), 1.72 – 1.60 (m, 2H), 1.44 – 1.20 (m, 2H), 1.19 – 0.83 (m, 2H); **^{19}F NMR** (376 MHz, $CDCl_3$) δ –174.30 (d, *J* = 53.3 Hz); **^{13}C NMR** (101 MHz, $CDCl_3$) [overlapping signals] δ 131.7, 131.3, 130.0, 129.9, 129.6, 129.5, 129.3, 90.6 (d, *J* = 179.1 Hz), 64.6 (d, *J* = 14.2 Hz), 59.7 (d, *J* = 6.0 Hz), 55.1, 39.7, 32.2 (d, *J* = 17.4 Hz), 27.1 (d, *J* = 5.8 Hz), 23.7 (d, *J* = 119.1 Hz); **IR** (thin layer film) ν (cm^{-1}) = 3673,2981, 2938, 1494, 1454, 1375, 1250, 1159, 1073, 953, 745, 698; **MP** 187–189 °C; **[α]$_D^{25\,°C}$** = +7.4 ° (c = 0.9, $CHCl_3$, e.r. = 84.5:15.5).

(1*R*,2*R*)-*N*,*N*-dibenzyl-2-fluorocyclohexan-1-ammonium tosylate (2.109*TsOH)



(R,R)-**2.109***TsOH

^{1}H NMR (400 MHz, $CDCl_3$) δ 10.49 (br s, 1H), 7.86 – 7.74 (m, 2H), 7.69 – 7.51 (m, 4H), 7.38– 7.27 (m, 6H), 7.16 (d, *J* = 8.0 Hz, 2H), 4.85 (dtd, *J* = 51.3, 10.5, 4.8 Hz, 1H), 4.54 (t, *J* = 14.7 Hz, 2H), 4.47 – 4.24 (m, 2H), 3.37 (tdd, *J* = 9.7, 7.7, 3.8 Hz, 1H), 2.55 – 2.42 (m, 1H), 2.34 (s, 3H), 2.17 (tdd, *J* = 10.0, 4.8, 2.4 Hz, 1H), 1.71 – 1.54 (m, 2H), 1.44 – 1.22 (m, 2H), 1.18 – 0.89 (m, 2H); **^{19}F NMR** (376 MHz, $CDCl_3$) δ –174.25 (d, *J* = 53.1 Hz); **^{13}C NMR** (101 MHz, $CDCl_3$) δ 143.0, 139.7, 131.7, 131.3, 129.8, 129.2, 128.7, 126.1, 90.6 (d, *J* = 179.1 Hz), 64.7 (d, *J* = 14.2 Hz), 59.7 (d, *J* = 6.1 Hz), 55.1, 32.2 (d, *J* = 17.3 Hz), 27.0 (d, *J* = 5.7 Hz), 24.2 (d, *J* = 1.9 Hz), 23.0 (d, *J* = 10.9 Hz), 21.3; **IR** (thin layer film) ν (cm^{-1}) = 3442, 3009,2947, 2640, 2237, 1637, 1498, 1457, 1329, 1212, 1166, 1039, 909, 726, 699; **MP** 127 – 130 °C; **[α]$_D^{25\,°C}$** = –2.6 ° (c = 1.2, $CHCl_3$, e.r. = 82:18).

5.4.2 Experimental Procedure for the Asymmetric Fluorination under HB-PTC in a Mechanically Stirred Reactor

Reaction: A OptiMax^{TM} HFCal Mettler Toledo 1 L glass reactor (diameter 98 mm, dish bottom head) equipped with a 45 mm glass 45 °down-pumping 4-blade PBT (pitched blade turbine), a 4 mm glass baffle, a temperature probe and a calibration probe was charged with 250 mL of CH_2Cl_2 followed by solid *rac*-**2.108** (200 g, 0.558 mol). The jacket temperature was set at 22 °C and the stirring speed at 1100 rpm. Full solubilisation (visually judged, ~10 min) and temperature stabilisation at 22 °C was achieved prior of performing the first calibration. The stirring speed was reduced to 300 rpm and solid catalyst (*S*)-**2.78** (3.9 g, 0.5 mol%) was added followed by further 30 mL of CH_2Cl_2 (to wash the flask and funnel). Full solubilisation (visually jusged, ~ 30 s) was achieved prior to the addition of solid CsF (104 g, 1.2 equiv) as a single charge. The stirring rate was increased to 1100 rpm and the reaction stirred at this speed until full conversion (monitored by ^{1}H and ^{19}F NMR) which was reached after 48 h. A second calibration was performed at this point.

Reaction monitoring (NMR): Samples were taken from the stirred reactor and filtered using a 13 mm syringe filter (0.45 μm PTFE). Exactly 50 μL of filtrate were transferred in a vial and evaporated to dryness. 10 μL of 4-fluoroanisole and 1 mL of $CDCl_3$ were added and both ^{1}H NMR (to estimate the conversion) and quantitative ^{19}F NMR (to obtain the yield) were recorded.

Work-up: The reactor was emptied and washed with 600 mL of CH_2Cl_2: $^{i}Pr_2O$ = 1:1 (2x 300 mL each wash). The combined organic phases were filtered on a plug of Clarcel® filter aid (4 cm high), eluting with further 100 mL of CH_2Cl_2: $^{i}Pr_2O$ = 1:1. The filtrate was evaporated *in vacuo* to obtain 160 g of crude **2.109**. The crude product was dissolved in $^{i}Pr_2O$ (800 mL) and extracted with $HCl_{(aq)}$ 1 M (3x 500 mL). The organic layer was washed with brine (300 mL), dried over $MgSO_4$ and evaporated *in vacuo* to recover the crude

catalyst (see below for its purification). The aqueous phase was neutralised with $NaOH_{(aq)}$ 5 M (300 mL, pH = 8, monitored by pH-paper) and extracted with CH_2Cl_2 (800 mL followed by 3x500 mL). The combined organic layers were washed with brine (500 mL), passed through a plug of $MgSO_4$ and evaporated in *vacuo* to afford (*R*,*R*)-**2.109** as a white solid (157.39 g, 95% yield, >99% purity weight %, 81.5:18.5 e.r.).

Crystallisation: The product was fully solubilised in ^{i}PrOH (500 mL) at 60 °C and trifluoroacetic acid (40.5 mL, 1 equiv) was added dropwise while stirring to form the corresponding salt. Volatiles were removed *in vacuo* to afford a white solid (217.7 g) which was dissolved in refluxing ^{i}PrOH (218 mL). Crystallisation was achieved by slowly (over 2 h) cooling the solution to 35 ° C, temperature that was maintained for further 4 h. (*Note:* control of the crystallisation time is necessary to achieve a good level of enantioenrichment). After this time the solid was filtered and washed twice with cold (+4 °C) ^{i}PrOH to afford 115.7 g of (*R*,*R*)-**2.109***TFA in 98:2 e.r (53% recrystallisation yield).

e.r. determination: All the e.r. were determined on the free base. The e.r. of recrystallised (*R*,*R*)-**2.109***TFA was determined on 5 samples randomly taken and neutralised with $NaOH_{(aq)}$ 5 M, extracted with heptane and analysed by HPLC using a chiral non-racemic stationary phase. HPLC separation: DAICEL CHIRALPAK® IB-3, Heptane:^{i}PrOH = 99:1, 1 mL/min; t_1 = 3.02 min (minor), t_2 = 3.66 min (major).

Catalyst Recovery: crude (*S*)-**2.78** from the work-up was passed through a short silica pad (heptane: EtOAc = 90:10) and recrystallised from refluxing heptane (5 mL/g) and EtOH (1 mL/g). 2.22 g, 57% recovery. Alternatively, crude (*S*)-**2.78** can be directly purified by flash column chromatography (heptane, $^{i}Pr_2O$= 100% to 80:20, gradient). This method was used to recover the catalyst from the small-scale screening reactions (~65% recovery).

5.4.3 Optimisation of the Recrystallisation

The tests were performed on 0.5 g, adding 500 μL (corresponding to 1vol =1 mL/g) of solvent and warming up the mixture to the boiling point. If no dissolution was obtained, the procedure was repeated with addition of further 500 μL of solvent up to 5 ml (10 mL/g). If solubilisation was attained, the system was left at rt for 24 h, after which the crystallisation yield was determined by weigh. In absence of precipitation, the system was transferred in the fridge (+ 4 °C) for further 24 h and the yield determined by weigh. If no precipitation had occurred, the system was transferred in the freezer (–20 °C) for further 24 h. For binary solvent mixtures, the salt was dissolved in the minimum amount of a suitable solvent, as determined in the previous tests, and twice as much of a tested antisolvent was layered on top of it. If crystallisation did not occur within 24 h, the system was cooled first to +4 °C (24 h) and then to – 20 °C (24 h). In all cases, after having determined the yield, the crystallised salt was neutralised with NaOH 5 M and the e.r. was determined on the free base.

Table 5.7: Crystallisation conditions for the free base **2.109**

Entry	*Solvent (mL/g)*	*Note*	*Yield*	*e.r.*
1	MeOH (4)	↓ at rt	62%	82:18
2	EtOH (4)	↓ at rt	62%	82:18
3	^{i}PrOH (4)	↓ at rt	48%	81:19
4	*n*-Octanol (2)	↓ at rt	68%	81:19
5	Acetonitrile (1)	↓ at rt	55%	79.5:20.5
6	Acetone (1)	↓ at rt	19%	73:27
7	$CHCl_3$ (1)	↓ at – 20 °C	24%	75.5:24.5
8	EtOAc (1)	↓ at 4 °C	54%	79:21
9	THF (2)	No ↓	–	–
10	$^{i}Pr_2O$ (1)	↓ at rt	58%	71.5:21.5
11	Toluene (1)	↓ at 4 °C	23%	75:25
12	Heptane (2)	↓ at rt	55%	79.5:20.5
13	Cyclohexane (3)	↓ at rt	24%	74:26
14	α,α,α-trifluorotoluene (1)	↓ at rt	33%	74.5:25.2
15	1,2-difluorobenzene (1)	↓ at 4 °C	45%	76:24

The starting e.r. of (*R*,*R*)-**2.109** was 81.5:18.5 e.r.

Table 5.8: Crystallisation Conditions for the HCl salt of **2.109**

Entry	*Solvent 1 (mL/g)*	*Solvent 2 (mL/g)*	*Note*	*Yield*	*e.r.*
1	H_2O	–	No dissolution	–	–
2	MeOH (1)	–	No ↓	–	–
3	EtOH (1)	–	No ↓	–	–
4	^{i}PrOH (2)	–	↓ at 4 °C	91%	82.5:17.5
5	*n*-Octanol (3)	–	↓ at 4 °C	44%	79.5:20.5
6	Acetonitrile (3)	–	↓ at rt	34%	82:18
7	Acetone (4)	–	↓ at rt	25%	82:18
8	$CHCl_3$ (1)	–	No ↓	–	–
9	EtOAc	–	No dissolution	–	–
10	THF (2)	–	↓ at rt	56%	81:19
11	$^{i}Pr_2O$	–	No dissolution	–	–
12	Toluene	–	No dissolution	–	–
13	Heptane	–	No dissolution	–	–
14	Cyclohexane	–	No dissolution	–	–
15	α,α,α-trifluorotoluene	–	No dissolution	–	–
16	1,2-difluorobenzene (2)	–	↓ at rt	48%	82:18
17	EtOH (1)	Heptane (2)	No ↓	–	–
18	^{i}PrOH (1)	Heptane (2)	↓ at rt	79%	84:16
19	$CHCl_3$ (1)	Heptane (2)	↓ at -20 °C	1%	–
20	EtOH (1)	Cyclohexane (2)	No ↓	–	–
21	^{i}PrOH (1)	Cyclohexane (2)	↓ at rt	64%	84.5:15.5
22	$CHCl_3$ (1)	Cyclohexane (2)	No ↓	–	–
23	EtOH (1)	H_2O (2)	No ↓	–	–
24	MeOH (1)	H_2O (2)	No ↓	–	–

The starting e.r. of (*R*,*R*)-**2.109** was 81.5:18.5 e.r.

Table 8.9: Crystallisation Conditions for the HBr salt **2.109**

Entry	*Solvent (mL/g)*	*Note*	*Yield*	*e.r.*
1	H_2O	No dissolution	–	–
2	EtOH (1)	No ↓	–	–
3	^{i}PrOH (1)	↓ at rt	56%	80.5:19.5
4	Acetonitrile (1)	↓ at rt	24%	76:24
5	Acetone (5)	↓ at rt	49%	75.5:24.5
6	THF (1)	↓ at rt	54%	79:21
7	1,2-difluorobenzene (2)	↓ at rt	46%	76:24

The starting e.r. of (*R*,*R*)-**2.109** was 81.5:18.5 e.r.

Table 5.10: Crystallisation Conditions for the CF_3COOH salt **2.109**

Entry	*Solvent (mL/g)*	*Note*	*Yield*	*e.r.*
1	EtOH (1)	↓ at 4 °C	50%	74:26
2	*^{i}PrOH (1)*	*↓ at rt*	*64%*	*94:6*
3	Acetonitrile (1)	No ↓	–	–
4	Acetone (1)	No ↓	–	–
5	*EtOAc (1)*	*↓ at 4 °C*	*47%*	*96:4*
6	THF (1)	No ↓	–	–
7	Toluene (1)	No ↓	–	–
8	Heptane (1)	↓ at rt	45%	83.5:16.5
9	Cyclohexane (1)	No ↓	–	–
10	α,α,α-trifluorotoluene (1)	No ↓	–	–
11	1,2-difluorobenzene (1)	No ↓	–	–

The starting e.r. of (*R*,*R*)-**2.109** was 81.5:18.5 e.r.

Table 5.11: Crystallisation Conditions for the MsOH salt **2.109**

Entry	*Solvent 1 (mL/g)*	*Solvent (mL/g)*	*Note*	*Yield*	*e.r.*
1	EtOH (2)	-	↓ at rt	48%	83:16
2	^{i}PrOH (2)	-	↓ at rt	83%	84.5:15.5
3	Acetonitrile (2)	-	↓ at rt	72%	82.5:17.5
4	Acetone	-	No dissolution	–	–
5	EtOAc	-	No dissolution	–	–
6	THF	-	No dissolution	–	–
7	Toluene (3)	-	No ↓	–	–
8	Heptane	-	No dissolution	–	–
9	Cyclohexane	-	No dissolution	–	–
10	α,α,α-trifluorotoluene	-	No dissolution	–	–
11	1,2-difluorobenzene		No dissolution	–	–
12	EtOH (1)	Acetone (5)	↓ at rt	61%	84:16
13	EtOH (1)	EtOAc (5)	↓ at rt	69%	83:17
14	EtOH (1)	THF (4)	↓ at rt	65%	83:17
15	EtOH (4)	Heptane (4)	↓ at rt	32%	84.5:15.5
16	EtOH (4)	Cyclohexane (5)	↓ at rt	40%	85.5:14.5
17	EtOH (1)	α,α,α-trifluorotoluene (5)	↓ at rt	38%	85.5:15.5
18	EtOH (1)	1,2- difluorobenzene (4)	No ↓	–	–

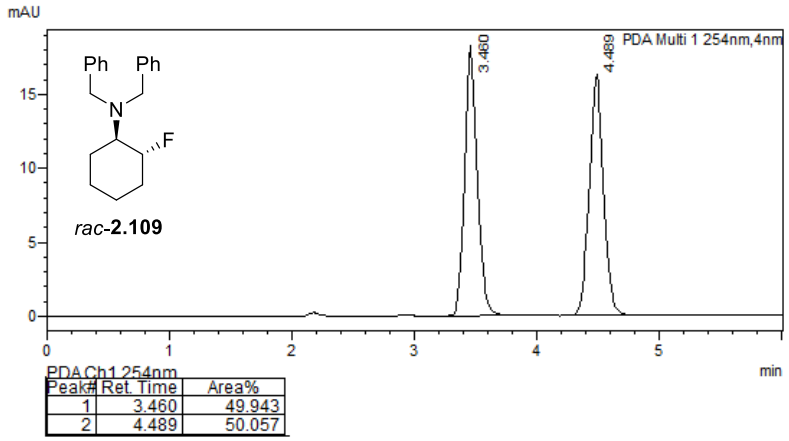
The starting e.r. of (*R*,*R*)-**2.109** was 81.5:18.5 e.r.

Table 5.12: Crystallisation Conditions for the TsOH salt **2.109**

Entry	*Solvent 1 (mL/g)*	*Solvent 2 (mL/g)*	*note*	*yield*	*e.r.*
1	MeOH (1)	–	No ↓	–	–
2	EtOH (1)	–	No ↓	–	–
3	^{i}PrOH (2)	–	No ↓	–	–
4	*n*-Octanol (2)	–	No ↓	–	–
5	Acetone (1)	–	↓ at rt	48%	72:28
6	$CHCl_3$ (1)	–	No ↓	–	–
7	Acetonitrile (1)	–	↓ at rt	16%	66:34
8	EtOAc (1)	–	↓ at 4 °C	45%	61.5:38.5
9	THF (1)	–	↓ at 4 °C	50%	78:22
10	$^{i}Pr_2O$	–	No dissolution	–	–
11	*Toluene (2)*	–	*↓ at 4 °C*	*32%*	*58:42*
12	Heptane	–	No dissolution	–	–
13	Cyclohexane	–	No dissolution	–	–
14	α,α,α-trifluorotoluene (1)	–	↓ at rt	67%	81.5:18.5
15	1,2-difluorobenzene (1)	–	↓ at rt	10%	71.5:28.5
16	EtOH (1)	Heptane (2)	No ↓	–	–
17	^{i}PrOH (2)	Heptane (4)	No ↓	–	–
18	$CHCl_3$ (1)	Heptane (2)	No ↓	–	–
19	MeOH (1)	H_2O (2)	No ↓	–	–

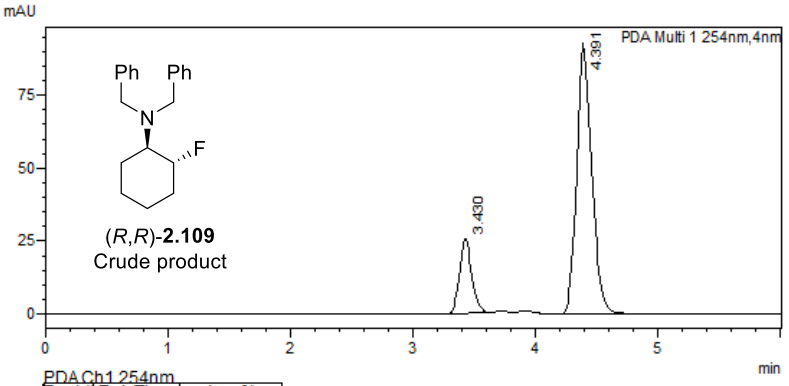
The starting e.r. of (*R*,*R*)-**2.109** was 81.5:18.5 e.r.

5.4.4 HPLC Trace of (*R*,*R*)-2.109



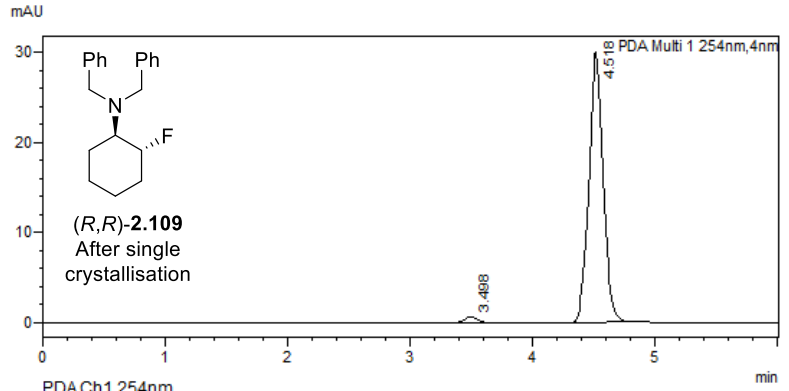
PDA Ch1 254nm

Peak#	Ret. Time	Area%
1	3.460	49.943
2	4.489	50.057



PDA Ch1 254nm

Peak#	Ret. Time	Area%
1	3.430	17.948
2	4.391	82.052



PDA Ch1 254nm

Peak#	Ret. Time	Area%
1	3.498	1.863
2	4.518	98.137

5.4.5 Characterization of 4.23

White solid. **^{1}H NMR** (500 MHz, $CDCl_3$) δ 7.95 – 7.90 (m, 2H, overlapped signals), 7.84 (d, *J* =8.4 Hz, 1H), 7.77 (d, *J* = 8.8 Hz, 1H), 7.73–7.69 (m, 5H), 7.67 (s, 2H), 7.65 –7.62 (m, 6H), 7.53 (t, *J* = 7.5 Hz, 1H), 7.46 – 7.33 (m, 5H), 7.29 (t, *J* = 8.2, 1H), 7.23 – 7.16 (m, 3H), 7.15 – 6.80 (m, 10H), 6.79– 6.77 (m, 2H), 6.74 (d, *J* = 8.6 Hz, 1H), 6.69 (s, 1H, N**H**), 6.52 (s, 1H, N**H**), 5.00 (td, *J* = 11.6, 4.3 Hz, 1H), 4.31 (br s, 1H), 3.48– 3.30 (m, 4H), 2.81 (dq, *J* = 13.7, 6.8 Hz, 1H), 2.63 (td, *J* = 11.0, 3.5 Hz, 1H), 1.77– 1.69 (m, 1H), 1.27 – 1.16 (m, 1H), 1.08 – 0.99 (m, 2H), 0.86 – 0.77 (m, 2H), 0.64 (t, *J* = 6.9 Hz, 3H), -0.03 – -0.23 (m, 2H); **^{19}F NMR** (376 MHz, $CDCl_3$) [overlapping signals] δ –63.11; **^{13}C NMR** (126 MHz, $CDCl_3$) [overlapping signals] δ 155.3, 155.0, 142.6, 142.3, 140.6, 140.2, 139.0, 138.8, 138.6, 134.0, 135.4, 135.2, 134.0, 133.1, 133.0, 132.9, 132.5, 132.6, 132.2 (q, *J* = 33.3 Hz), 132.0 (q, *J* = 33.3 Hz), 130.9, 130.4 (br), 129.6, 129.2, 129.1 (br), 128.7, 128.5, 128.4, 128.2, 128.1, 127.6, 127.4, 127.4, 127.3, 127.2, 127.0, 126.9, 123.3 (q, *J* = 272.9 Hz), 123.4 (q, *J* = 273.0 Hz), 121.4–121.1 (m, 2 signals), 119.1, 119.0, 118.7, 118.2, 58.6, 57.9, 55.2 (br, Ph**C**H_2), 52.4 (br, Ph**C**H_2), 44.8 (**C**H_2CH_3), 33.2, 25.2, 24.2, 24.1, 12.7 (CH_2**C**H_3); **HRMS** (ESI^+) *m/z* calculated for $C_{88}H_{62}O_2N_5F_{24}$ $[M+H]^+$ 1676.4515, found 1676.4432.

5.5 References

(1) Pupo, G.; Ibba, F.; Ascough, D. M. H.; Vicini, A. C.; Ricci, P.; Christensen, K. E.; Pfeifer, L.; Morphy, J. R.; Brown, J. M.; Paton, R. S.; Gouverneur, V. "Asymmetric Nucleophilic Fluorination under Hydrogen Bonding Phase-Transfer Catalysis." *Science* **2018**, *360*, 638–642.

(2) Ibba, F. "Hydrogen Bonding Phase-Transfer Catalysis: A New Approach to Asymmetric Fluorination", University of Oxford, 2020.

(3) Mikláš, R.; Kasák, P.; Devínsky, F.; Putala, M. "Fluoride Anion Sensing Using Colorimetric Reagents Containing Binaphthyl Moiety and Urea Binding Site." *Chem. Pap.* **2009**, *63*, 709–715.

(4) Takasaki, M.; Motoyama, Y.; Yoon, S. H.; Mochida, I.; Nagashima, H. "Highly Efficient Synthesis of Optically Pure 5,5′,6,6′,7, 7′,8,8′-Octahydro-1,1′-Bi-2-Naphthol and -Naphthylamine Derivatives by Partial Hydrogenation of 1,1′-Binaphthyls with Carbon Nanofiber Supported Ruthenium Nanoparticles." *J. Org. Chem.* **2007**, *72*, 10291–10293.

(5) Kano, T.; Tanaka, Y.; Osawa, K.; Yurino, T.; Maruoka, K. "Facile Synthesis of Structurally Diverse 3,3′-Disubstituted 1,1′-Binaphthyl-2,2′-Diamines in Optically Pure Forms." *J. Org. Chem.* **2008**, *73*, 7387–7389.

(6) Juríček, M.; Kasák, P.; Stach, M.; Putala, M. "Potential 1,1′-Binaphthyl NLO-Phores with Extended Conjugation between Positions 2 and 6, and 2′ and 6′." *Tetrahedron Lett.* **2007**, *48*, 8869–8873.

(7) Chen, Y. H.; Qi, L. W.; Fang, F.; Tan, B. "Organocatalytic Atroposelective Arylation of 2-Naphthylamines as a Practical Approach to Axially Chiral Biaryl Amino Alcohols." *Angew. Chemie - Int. Ed.* **2017**, *56*, 16308–16312.

(8) Pu, X.; Qi, X.; Ready, J. M. "Allenes in Asymmetric Catalysis: Asymmetric Ring Opening of *Meso*-Epoxides Catalyzed by Allene-Containing Phosphine Oxides." *J. Am. Chem. Soc.* **2009**, *131*, 10364–10365.

(9) Meguro, M.; Asao, N.; Yamamoto, Y. "Ytterbium Triflate and High Pressure-Mediated Ring Opening of Epoxides with Amines." *J. Chem. Soc. Perkin Trans. 1* **1994**, 2597–2601.

(10) Carter, C.; Fletcher, S.; Nelson, A. "Towards Phase-Transfer Catalysts with a Chiral Anion: Inducing Asymmetry in the Reactions of Cations." *Tetrahedron Asymmetry* **2003**, *14*, 1995–2004.

(11) Ci, X.; Kellett, M. A.; Whitten, D. G. "Oxidative Photofragmentation of α,ß-Amino Alcohols *Via* Single Electron Transfer: Cooperative Reactivity of Donor and Acceptor Ion Radicals in Photogenerated Contact Radical Ion Pairs." *J. Am. Chem. Soc.* **1991**, *113*, 3893–3904.

(12) Schiffers, I.; Rantanen, T.; Schmidt, F.; Bergmans, W.; Zani, L.; Bolm, C. "Resolution of Racemic 2-Aminocyclohexanol Derivatives and Their Application as Ligands in Asymmetric Catalysis." *J. Org. Chem.* **2006**, *71*, 2320–2331.

(13) Hamilton, G. L.; Kanai, T.; Toste, F. D. "Chiral Anion-Mediated Asymmetric Ring Opening of *Meso*-Aziridinium and Episulfonium Ions." *J. Am. Chem. Soc.* **2008**, *130*, 14984–14986.

(14) Chong, H.-S.; Sun, X.; Chen, Y.; Wang, M. "Synthesis, Characterization, and Nucleophilic Ring Opening Reactions of Cyclohexyl-Substituted β-Haloamines and Aziridinium Ions." *Tetrahedron Lett.* **2015**, *56*, 946–948.

(15) Kalow, J. A.; Doyle, A. G. "Enantioselective Fluoride Ring Opening of Aziridines Enabled by Cooperative Lewis Acid Catalysis." *Tetrahedron* **2013**, *69*, 5702–5709.

(16) Duthion, B.; Pardo, D. G.; Cossy, J. "Enantioselective Synthesis of β-Fluoroamines from β-Amino Alcohols: Application to the Synthesis of LY503430." *Org. Lett.* **2010**, *12*, 4620–4623.

(17) Wade, T. N. "Preparation of Fluoro Amines by the Reaction of Aziridines with Hydrogen Fluoride in Pyridine Solution." *J. Org. Chem.* **1980**, *45*, 5328–5333.

(18) Pupo, G.; Vicini, A. C.; Ascough, D. M. H.; Ibba, F.; Christensen, K. E.; Thompson, A. L.; Brown, J. M.; Paton, R. S.; Gouverneur, V. "Hydrogen Bonding Phase-Transfer Catalysis with Potassium Fluoride: Enantioselective Synthesis of β-Fluoroamines." *J. Am. Chem. Soc.* **2019**, *141*, 2878–2883.

(19) Prat, D.; Hayler, J.; Wells, A. “A Survey of Solvent Selection Guides.” *Green Chem.* **2014**, *16*, 4546–4551.

(20) Prat, D.; Pardigon, O.; Flemming, H. W.; Letestu, S.; Ducandas, V.; Isnard, P.; Guntrum, E.; Senac, T.; Ruisseau, S.; Cruciani, P.; Hosek, P. “Sanofi’s Solvent Selection Guide: A Step Toward More Sustainable Processes.” *Org. Process Res. Dev.* **2013**, *17*, 1517–1525.

(21) Martinez-Cuezva, A.; Lopez-Leonardo, C.; Bautista, D.; Alajarin, M.; Berna, J. “Stereocontrolled Synthesis of β-Lactams within [2]Rotaxanes: Showcasing the Chemical Consequences of the Mechanical Bond.” *J. Am. Chem. Soc.* **2016**, *138*, 8726–8729.

(22) Ortega, N.; Feher-Voelger, A.; Brovetto, M.; Padrón, J. I.; Martín, V. S.; Martín, T. “Iron(III)-Catalyzed Halogenations by Substitution of Sulfonate Esters.” *Adv. Synth. Catal.* **2011**, *353*, 963–972.